

Vol 15 No 1 (2011)

Vol 15 No 2 (2011)

Malaysian Journal of Analytical Sciences Vol 15 No 1 2011

		Page
1.	ATMOSPHERIC SURFACTANTS AROUND LAKE ECOSYSTEM OF TASIK KENYIR, TERENGGANU (Surfaktan di Atmosfera di Persekitaran Ekosistem Tasik Kenyir, Terengganu) Norfazrin Mohd Hanif, Mohd Talib Latif, Mohammed Rozali Othman	1
2.	REMOVAL OF Zn(II), Cd(II) AND Mn(II) FROM AQUEOUS SOLUTIONS BY ADSORPTION ON MAIZE STALKS (Penyingkiran Zn(II), Cd(II) Dan Mn(II) Daripada Larutan Akueus Melalui Penjerapan Pada Tangkai Jagung) G. O. El-Sayed, H. A. Dessouki and S. S. Ibrahiem	8
3.	ISOLATION OF CHEMICAL CONSTITUENTS FROM RHIZOMES OF ETLINGERA SPHAEROCEPHALA VAR. GRANDIFLORA (Pemencilan Kandungan Kimia Daripada Rizom Etlingera Sphaerocephala var. Grandiflora) M.A.A. Yahya, W.A. Yaacob and I. Nazlina	22
4.	DISCRIMINATOR SETTING AND COCKTAIL PREPARATION FOR ANALYSIS OF ALPHA AND BETA EMITTERS IN AQUEOUS SOLUTION USING LIQUID SCINTILLATION COUNTER (Penetapan Diskriminator dan Penyediaan Koktil Untuk Analisis Pemancar Alfa dan Beta Didalam Larutan Berakueus Menggunakan Pembilang Sintilasi Cecair) Zaini Hamzah, Masitah Alias and Zaharudin Ahmad	27
5.	SPECTROSCOPIC AND STRUCTURAL STUDY OF A SERIES OF PIVALOYLTHIOUREA DERIVATIVES (Spektroskopi dan Kajian Struktur Satu Siri Terbitan Pivaloiltiourea) Siti Aishah Zakaria, Siti Hajar Muharam, Mohd Sukeri Mohd Yusof, Wan Mohd Khairul, Maisara Abdul Kadir & Bohari M. Yamin	37
6.	IONIC LIQUID SUPPORTED ACID-CATALYSED ESTERIFICATION OF LAURIC ACID (Mangkin Asid Disokong pada Cecair Ionik Sebagai Mangkin dalam Tindak Balas Pengesteran Asid Laurik) Zalita Yaacob, Nor Asikin Mohd Nordin, Mohd Ambar Yarmo	46
7.	A SIMPLE AND COST EFFECTIVE ISOLATION AND PURIFICATION PROTOCOL OF MITRAGYNINE FROM MITRAGYNA SPECIOSA KORTH (KETUM) LEAVES (Satu Protokol Pengasingan Mitragina daripada Daun Mitragyna speciosa Korth (Ketum) yang Mudah dan Kos Efektif) Goh Teik Beng, Mohamad Razak Hamdan, Mohammad Jamshed Siddiqui, Mohd Nizam Mordi and Sharif Mahsufi Mansor	54

8.	A STUDY OF NATURAL RADIONUCLIDE ACTIVITIES AND RADIATION HAZARD INDEX IN SOME GRAINS CONSUMED IN JORDAN (Satu Kajian Mengenai Aktiviti Radionuklida Semulajadi dan Indeks Hazard Sinaran Di Dalam Beberapa Bijirin Yang Di makan di Jordan) A.A. Tawalbeh, K.M. Abumurad, S.B. Samat, M.S. Yasir	61
9.	STRUCTURAL AND SPECTROSCOPIC STUDIES OF NOVEL METHYLBENZOYLTHIOUREA DERIVATIVES (Struktur Dan Kajian Spektroskopi Terbitan Metilbenzoilthiourea) Rabia'tun Hidayah Jusoh, Wan M. Khairul, M. Sukeri M. Yusof, Maisara Abdul Kadir, Bohari M.Yamin	70
10.	IMPROVEMENT OF THE PHOTOSTABILIZATION OF PVC FILMS IN THE PRESENCE OF THIOACETIC ACID BENZOTHIAZOLE COMPLEXES (Peningkatan Ciri-ciri Fotokestabilan Filem PVC dengan Kehadiran Kompleks Asid Thioasetik Benzothiazola) Emad Yousif, Jumat Salimon, Nadia Salih	81
11.	SYNTHESIS, CHARACTERIZATION AND NEUROTOXIC EFFECT OF SCHIFF BASE LIGANDS AND THEIR COMPLEXES (Sintesis, Pencirian dan Pengaruh Nurotoksik Bes Schiff dan Kompleksnya) Ahmad Fauzi Abu Bakar, Hadariah Bahron, Karimah Kassim, Mazatulikhma Mat Zain	93
12.	SYNTHESIS AND CHARACTERIZATION OF YAG:Ce PREPARED BY SOLID STATE REACTION METHOD (Sintesis dan Pencirian YAG:Ce Disediakan Melalui Kaedah Tindak Balas Keadaan Pepejal) Ahmad Saat, Hazimah Harun, Zaini Hamzah	101
13.	SYNTHESIS AND CHARACTERIZATION OF DIPHENYLTIN(IV) DITHIOCARBAMATE COMPOUNDS (Sintesis dan Pencirian Sebatian Difenilstanum(IV) Ditiokarbamat) Amirah Faizah Abdul Muthalib, Ibrahim Baba, Yang Farina, Mohd Wahid Samsudin	106
14.	ANALISIS KROMATOGRAFI GAS×KROMATOGRAFI GAS—SPEKTROMETRI JISIM MASA-PENERBANGAN DAN AKTIVITI ANTIBAKTERIA MINYAK PATI AMOMUM XANTHOPHLEBIUM (Gas Chromatography Gas x Gas Chromatography—Time-of-Flight Mass Spectrometry Analysis and Antibacterial Activity of Essential Oil from Amomum xanthophlebium) A. Masila, I. Aminah, W.A. Yaacob, I. Nazlina	113
15.	EXTRACTION OF Eu (III) IN MONAZITE FROM SOILS CONTAINING 'AMANG' COLLECTED FROM KG GAJAH EX-MINING AREA (Pengekstrakan Eu(III) Dalam Monazit Daripada Tanih Mengandungi Amang Dari Kawasan Bekas Lombong Kg. Gajah) Zaini Hamzah, Nor Monica Ahmad, and Ahmad Saat	122



ATMOSPHERIC SURFACTANTS AROUND LAKE ECOSYSTEM OF TASIK KENYIR, TERENGGANU

(Surfaktan di Atmosfera di Persekitaran Ekosistem Tasik Kenyir, Terengganu)

Norfazrin Mohd Hanif¹, Mohd Talib Latif², Mohammed Rozali Othman^{1*}

¹School of Chemical Sciences and Food Technology, ²School of Environmental and Natural Resource Sciences, Faculty of Science and Technology, Universiti Kebangsaan Malaysia, 43600, UKM Bangi, Selangor.

*Corresponding author: rozali@ukm.my

Abstract

Lake ecosystem is a sources of natural organic matter characteristic by humic-like substances (HULIS) believe to have high amount of surface active agents (surfactants) which capable to influence the cloud and climate. This study determined the concentration of anionic surfactants in the atmosphere around lake ecosystems at Kenyir, Terengganu. Aerosols samples were collected by using a High Volume Air Sampler (HVAS) equipped with high volume impactor (to separate between fine and coarse mode aerosols) and glass-fibre filter paper at flow rate of 1.13 m³min⁻¹ for 24 hours. Several possible sources of natural surfactants in the atmosphere e.g. soils, vegetations and surface water were also collected in order to determine the possible sources and flux of anionic surfactants in the atmosphere. Anionic surfactant was analysed based on colorimetric methods by using methylene blue active substances (MBAS) and UV-visible spectrophotometer at 650 nm. Subsequently, simplified calculations were conducted in estimating the flux of anionic surfactants from various possible sources. The results indicated that the concentration of anionic surfactants in aerosols (coarse and fine mode), soil, vegetation and surface water were $59.17 \pm 2.61 \mu mol/m³$ and $78.10 \pm 9.30 \mu mol/m³$, $0.33 \pm 0.17 \mu molg⁻¹$, $0.28 \pm 0.08 \mu molg⁻¹$ (dry weight) and $0.01 \pm 0.004 \mu molL⁻¹$, respectively. The overall flux of surfactants signified that soils provide the highest amount of surfactants which is $119.39 \mu molg⁻¹$ in comparison to other possible sources (vegetation = $26.88 \mu molg⁻¹$ and surface water = $12.1 \times 10^{-6} \mu molg⁻¹$). Results indicated that soil become a significant natural source of anionic surfactants to the atmosphere which may due to the availability of HULIS.

Keywords: anionic surfactants, lake ecosystems, flux of anionic surfactants, HULIS

Abstrak

Ekosistem tasik yang merupakan sumber bahan organik yang dicirikan sebagai sebatian seperti humik (HULIS) dipercayai mempunyai surfaktan dalam kuantiti yang tinggi dan berupaya mempengaruhi awan dan cuaca. Kajian ini dilakukan untuk menentukan kepekatan surfaktan anion di persekitaran Tasik Kenyir, Terengganu. Sampel aerosol dikutip pada kadar alir 1.13 m³min⁻¹ selama 24 jam menggunakan Pensampel Udara Berisipadu Tinggi (*High Volume Air Sampler, HVAS*) yang dilengkapi dengan impaktor (untuk memisahkan aerosol bersaiz halus dan kasar) dan kertas turas gentian kaca. Beberapa sumber surfaktan di udara seperti tanih, vegetasi dan air di permukaan tasik juga dikutip untuk menentukan sumber dan fluks surfaktan anion di atmosfera. Surfaktan anion dianalisis menggunakan kaedah kolorimetri dengan menggunakan sebatian aktif metilena biru (*methylene blue active substances,MBAS*) dan spektrofotometer UV-Vis pada panjang gelombang 650 nm. Seterusnya pengiraan untuk menganggar surfaktan anion daripada pelbagai sumber dilakukan. Keputusan menunjukkan bahawa kepekatan purata surfaktan anion dalam aerosol (kasar dan halus), tanih, vegetasi dan air permukaan masing-masingnya ialah 59.17 \pm 2.61 μ mol/m³ dan 78.10 \pm 9.30 μ mol/m³, 0.33 \pm 0.17 μ molg⁻¹, 0.28 \pm 0.08 μ molg⁻¹ (berat kering) dan 0.01 \pm 0.004 μ molL⁻¹. Fluks keseluruhan surfaktan mendapati tanih menyumbangkan nilai surfaktan anion terbesar iaitu 119.39 Mmolyr⁻¹ berbanding dengan sumber-sumber lain (vegetasi = 26.88 Mmolyr⁻¹ dan air permukaan = 12.1 x 10⁻⁶ Mmolyr⁻¹). Kesimpulan mendapati tanih adalah merupakan sumber semulajadi surfaktan anion yang utama dan ini mungkin disebabkan kehadiran HULIS.

Kata kunci: surfaktan anion, ekosistem tasik, fluks surfaktan anion, HULIS

Norfazrin Mohd Hanif et al: ATMOSPHERIC SURFACTANTS AROUND LAKE ECOSYSTEM OF TASIK KENYIR, TERENGGANU

Introduction

Surfactants (a contraction of surface active agents) have the potential in influencing the global climate. In environmental context, surfactants play an important role due to their ability to reduce surface tension, which affect the physical properties of cloud droplets and eventually lead to enhancement of cloud albedo [1]. Surfactants can be naturally derived from various possible sources. However, it is hard to differentiate significantly the contribution of each source towards load of surfactants in atmosphere. Thus, estimation of flux might be useful in predicting the contribution of possible sources. For this reason, Lake Kenyir representing the natural ecosystem was chosen where all possible biogenic sources of surfactants were available, for identifying the sources of surfactants.

Surfactants can be naturally generated from various sources. Several studies indicate that some class of compound in atmosphere displayed similar characteristics as humic substances found in soil and therefore this compound is often called humic-like substances. The formation of stable humic substances was resulted from the transformation of soil organic matter comprised of plant and animal residues by microorganism and chemical process [2, 3, 4]. Humic substances are generally classified as humin, humic acid, and fulvic acid [5]. Among all, it was noted that oxidation process has the ability to generate surfactants from humic acid. Solvent extractable (lipophilic) and water soluble products are often caused by the chemical degradation (hydrolysis, oxidation, reduction) of humic acid [6]. Surfactants also can be correlated with HULIS since some characteristics (e.g ability to reduce the surface tension, water solubility etc.) were comparable [7]. Thus it can suggested that HULIS can be categorized as surfactants as it displays similar characters like surfactants.

Apart from that, various vegetation surrounded the lake environment as well can generate surfactants in atmosphere. Earth's vegetation naturally releases huge amounts of organic species into the air [8]. Certain fraction of particulate matter is present in atmosphere due to conversion of volatile organic compound. It was found that these biogenic VOC have the ability to produce condensable products as a result of rapid oxidation by radicals and ozone into less volatile oxygenated organics that have surface-active properties [9, 10]. The lake surface layer able to act as a sink that accumulate various organic substances, hence can be regarded as a source of surfactants. Besides, phytoplankton and algae that accumulate at the surface layer of water bodies can exedute certain organic compounds. Various researcher found out that these compounds comprised functional groups mainly carbonyl compounds and carboxylic acids which might be decomposition products of longer chain fatty acids [11, 12, 13, 14]. And, it was noted that these compounds are known to be surface active.

Taken all into account, lake environments proved to cater an adequate environment for the study of surfactants formation from natural sources. By estimating the flux of surfactants from various sources, it is possible for us to understand the role of surfactants which found to be able to contribute to the changes of global climate.

Experimental

Sampling location

Kenyir Lake which located in the state of Terengganu ($N = 5^012.902'$, $E = 102^038.306'$) is a well-known as artificial lake which surrounded by tropical forest. The lake covers 260 km² and contains 340 small islands, which were once hiltops and highlands, more than 14 waterfalls, numerous rapids and rivers. Besides, it is also home to numerous species of freshwater fishes and exotic wildlife. From studies and observations conducted by the Department of Fisheries, species such as the *big Lampam Sungai* (Barboides), *Kelah* (Malaysian Mahsee), *Toman* (Snakehead), *Kawan* (Friendly Barb), *Kalui* (Giant Gouramy) and *Kelisa* (Green Arowana) are found in waters and around dead trees. Hence, this man-made lake certainly provides a suitable environment in investigating the contribution of natural ecosystem towards the surfactants load in atmosphere.

Sampling and preparation of sample

Aerosol

High volume air sampler equipped with glass fibre filter paper with a flow rate of 1.13 m³min⁻¹ was used collect atmospheric particulate matter for 24 hours. After sampling, filter papers were divided into 4 sections. A quarter of the samples were put in a centrifuge tube containing 50ml of deionised water. Prior to analysis, the solutions were then sonicated for about 45 minutes and were filtered through 0.2um Whatman filter paper 47mm diameter in 100ml volumetric flask.

Surface water

Surface microlayer was collected at several sampling by using rotation drum as suggested elsewhere [15]. The surface collector uses a smooth, rotating cylinder whose surface is readily wet by water. This method results in the collection of thinner and less disturbed surface water. After sampling, samples were stored in vial at 4^oC prior to analysis by colorimetric methods as methylene blue active substances (MBAS) for anionic surfactants.

Soil

The surface of soil (approximately 5cm \sim representing zone A) was collected using a wooden scoop. Soil samples were placed in a sealed plastic bag and labeled before being analysed in laboratory. The samples were dried in an oven for 2 hours at 40° C before being sieved through a 63um sieve. Next, 50mg of samples were weighed and placed in a centrifuge tube filled with 50ml of deionised water. The solutions were then sonicated for about 45minutes and were filtered through 0.2um Whatman filter paper 47mm diameter in 100ml volumetric flask.

Vegetation

Several part of vegetation (leaf, bark and stem) were collected and kept in a sealed plastic bag. Samples were dried in an oven for 2 hours at 40°C before being meshed in a blender. Next, 50mg of grinned samples were weighed and placed in a centrifuge tube filled with 50ml of deionised water. The solutions were then sonicated for about 45 minutes and were filtered through 0.2um Whatman filter paper 47mm diameter in 100ml volumetric flask.

Determination of anionic surfactant as methylene blue active substances (MBAS)

The sample solution (20 mL) was put in 40 mL vial (vial A) equipped with a screw cap and Teflon liner. The alkaline buffer (2 mL) and neutral methylene blue solution (1 mL), followed by chloroform (5 mL), was added to vial A in that order. The vial was closed tightly using a holed screw-cap and Teflon liner before being vigorously shaken using a vortex mixer for two minutes. After shaking, the vial was left awaiting phase separation. The screw-cap was loosened to release the pressure inside. Once the two phases were separated, a separating funnel was used to transfer the chloroform layer into the new vial (vial B) that contained ultra pure water (22 mL) and acid methylene blue solution (1 mL). Vial B was shaken using a vortex mixer for two minutes. The cap was loosened for few seconds and re-tightened. After the chloroform had completely separated from the water (after two minutes), the chloroform layer was collected after using separating funnel and put into the 10 mm quartz cell. The absorbance of chloroform phase was measured by an ultra-violet spectrometer at a wavelength of 650 nm. The limit of detection estimated as blank solution, $0.05~\mu M$ SDS, was analysed using the same method as for the aerosol extracts.

Estimation of MBAS Fluxes Produces from Various Sources

A simplify model was employed for estimating the amount of MBAS produced from various possible sources (e.g. soils, vegetation, and surface water), based on the average concentration of MBAS found in aerosols produced from key sources, and flux of particles (PF) from each source [16, 17, 18, 19, 20] (Table 1). Photo-oxidation factor (POF), the maximum value which able to generate surfactants as MBAS was estimated as four times higher from the concentration surfactants in any substances before photo-oxidation process [21]. This estimation was made by assuming that the concentration of MBAS increases about fourfold after exposure to sunlight and oxidants in the atmosphere.

Table 1: Particle flux of	possible sources of	f atmospheric	surfactants.
---------------------------	---------------------	---------------	--------------

Possible sources	Particle Flux (PF) (Tg yr ⁻¹)
Soil	91
Forest/Vegetation	24
Surface water	4290

Model

Estimation of flux of MBAS based on their production from various sources (mol yr⁻¹)

= MBAS x POF x PF

where

MBAS = Concentration of MBAS from various possible sources (μmol g⁻¹)

POF = Photo-oxidation factor

PF = Particle flux of each source (Tg yr⁻¹)

Results and Discussion

Possible sources of surfactants in lake ecosystem

The concentration of surfactants was found high in soils samples which is $0.328 \pm 0.165 \, \mu \text{molg}^{-1}$, followed by vegetation $(0.28 \pm 0.08 \, \mu \text{molg}^{-1})$ and surface water $(0.01 \pm 0.004 \, \mu \text{molL}^{-1})$, respectively. The high concentration of surfactants presence in soil is corresponding with the hypothesis that surfactants might be originated from humic-like substances (HULIS) [7]. HULIS are ubiquitous may consist of vegetation-derived organic microparticles or may partially be generated from biogenic unsaturated hydrocarbons. Studies carried out by other researchers have shown that organic components in airborne dust were similar to humic substances found in soil and aqueous systems [22, 23]. Thus, it can be suggested that humic acids in soils represent one potential source of HULIS.

There is a possibility that surfactants concentration might be influenced by vegetation as the difference between sources (i.e soil and vegetation) is insignificant (p>0.05). Photochemical oxidation products from volatile organic precursors emitted by vegetation were also detected in the particulate matter [24]. However, spectroscopic measurement by using UV spectrometer verifies the fact that soil is the main source that contributes to the high concentration of surfactants in air (Figure 1). The UV/VIS spectra of aerosol extract exhibit featureless curves of increasing absorbance towards lower wavelength. A study on the existence of HULIS in airborne particulate matter collected in same environment which is forested and agriculturally area (Sauerland, Germany), also observe the similar pattern of spectra [25]. Thus it can be suggested that surfactants can be correlated with HULIS found in soil.

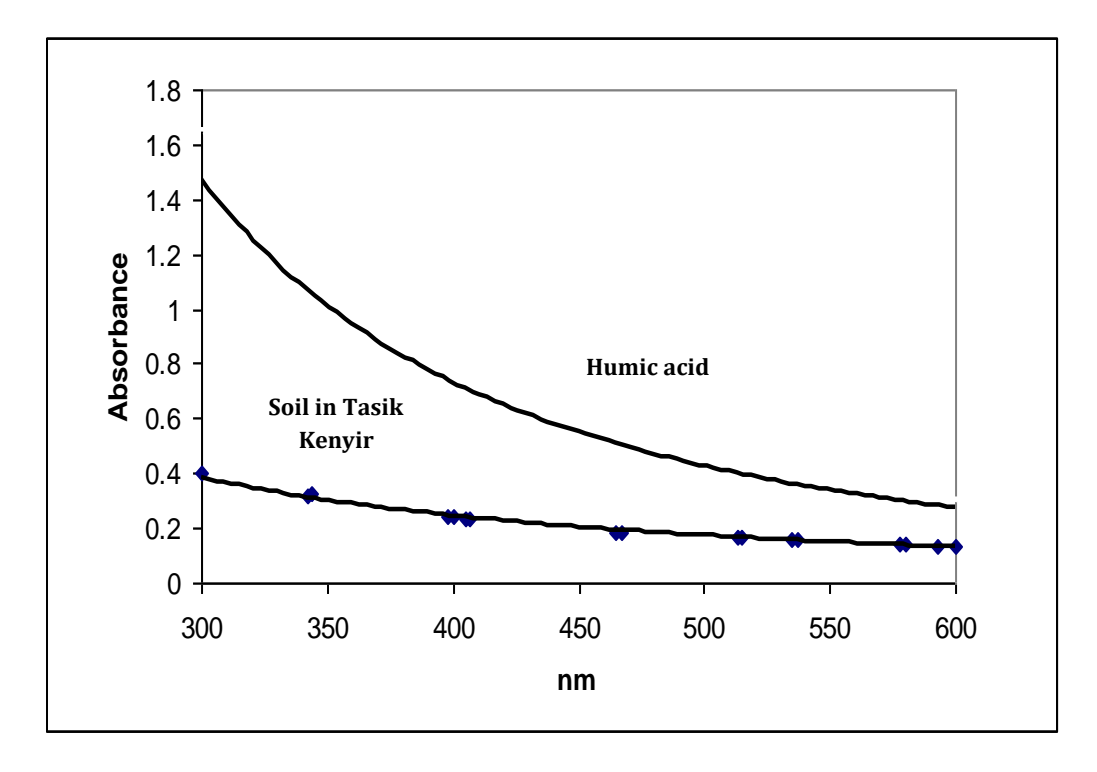


Figure 1: UV/Vis spectra

Flux of surfactants

The flux of MBAS was estimated from the average concentration of MBAS found in aerosols produced from key sources, and flux of particles (PF) from each source [18]. The overall flux of surfactants signified that soils provide the highest amount of surfactants which is 119.39 Mmolyr⁻¹ in comparison to other possible sources (Table 2) (vegetation = 26.88 Mmolyr⁻¹and surface water = 0.21 Mmolyr⁻¹). This result also mirrored those from previous studies by suggest soil particles which are rich in humic substances can act as a major sources of anionic surfactants in atmospheric aerosols [17, 18, 19, 20].

Table 2: Flux of MBAS to the atmosphere based on their possible sources
at Tasik Kenyir, Terengganu

Туре	Possible sources	MBAS Flux (Mmol yr ⁻¹)
Natural resources	Soil Forest/Vegetation Ocean	119.39 26.88 0.21

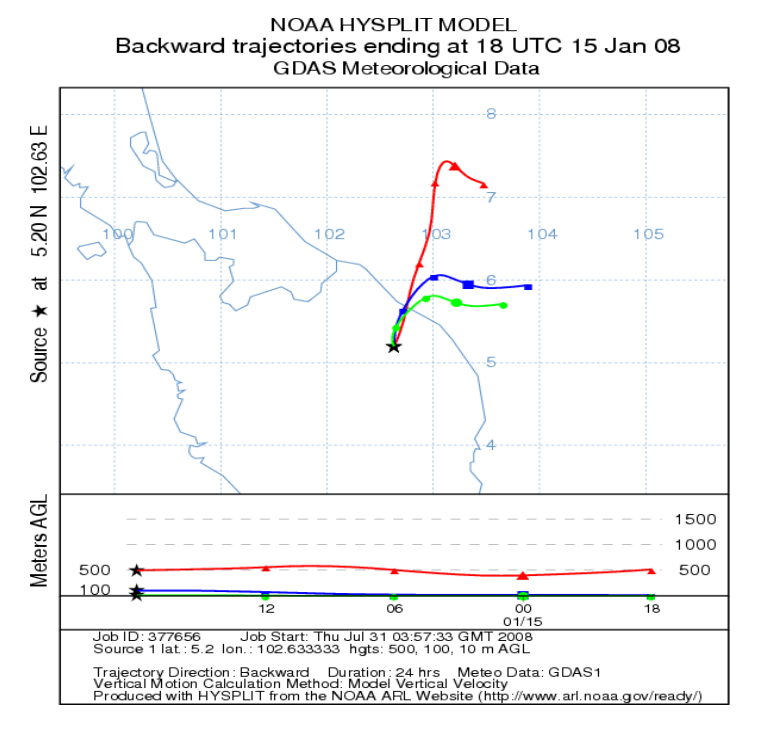


Figure 2: Backward trajectories

Back trajectory

The backward trajectory analysis using HYSPLIT model (*HYbrid Single- Particle Lagrangian Integrated Trajectory Model*) clearly shows that the air parcel was originated from South China Sea (Figure 2). Although the distance between sampling point and sea was considerable, it is interesting to note that sea-surface microlayer can be considered as one of the possible sources surfactants in lake ecosystem. Surfactants in sea surface microlayer generally originated from bubble bursting at the ocean surface [26]. Organic matter can be directly incorporated in

Norfazrin Mohd Hanif et al: ATMOSPHERIC SURFACTANTS AROUND LAKE ECOSYSTEM OF TASIK KENYIR, TERENGGANU

marine particles when gas bubbles burst at the surface. In addition, rising gas bubbles scavenge organic material such as surfactants in the water column when they rise towards the surface. Apart from that, marine phytoplankton was also known to produce surface-active materials as part of their metabolism [27]. However, as mentioned earlier, soil remain to be the dominant source as the aerosol extracts display similar characteristic with humic acid found in soil (Figure 1). Thus, there is a possibility that, wash out and dilution processes from rain water are believed to have reduced the amount of surfactants. Hence explained the fact that the load of surfactants in lake ecosystem were not influenced by surfactants originated from sea surface microlayer.

Conclusion

Emission of surfactants as MBAS to the atmosphere can originate from various possible sources found in lake environment. Hence indicated that natural ecosystem has the potential to contribute to the amount of surfactants in atmosphere. Since surfactants and HULIS merely display similar properties, it can be suggested that surfactants might be a product generated from the oxidation of humic substances found in soil. Thus, apart from biogenic influence, that secondary mechanism also plays an important role in contributing to surfactants load in atmosphere.

Acknowledgement

The funding from the National University of Malaysia (UKM-GUP-ASPL-07-05-138) is gratefully acknowledged.

References

- 1. Facchini, M. C. Mircea, M., Fuzzi, S. & Charlson, R. J. (2001). Comments on "Influence of soluble surfactant properties on the activation of aerosol particles containing inorganic solute". *Journal of the Atmospheric Sciences*, 58, 1465-1467.
- 2. Grasset, L. & Ambles, A. (1998a). Structure of humin and humic acid from an acidic soil as revealed by phase transfer catalyzedhydrolysis. *Organic Geochemistry*, 29, 881-891.
- 3. Grasset, L. & Ambles, A. (1998b). Structural study of soil humic acid and humin using a new preparative thermochemolysis technique. *Journal of Analytical and Applied Pyrolysis*, 47, 1-12.
- 4. Stevenson, F.J. (1994). Humus chemistry: Genesis, composition, reactions. John Wiley & Sons, Inc
- 5. Kiss, G., Tombacz, E., Varga, B., Alsberg, T. & Persson, L. (2003). Estimation of the average molecular weight of humic-like substances isolated from fine atmospheric aerosol. *Atmospheric Environment*, 37, 3783-3794.
- 6. Hanninen, K & Niemela, K. (1992). Alkaline degradation of peat humic acids. Part II. Identification of hydrophilic products. *Acta Chemica Scandinavica*, 46, 459-463.
- 7. Latif, M. T., Brimblecombe, P., Ramli, N. A., Sentian, J., Sukhapan, J. & Sulaiman, N. (2005). Surfactants in South East Asian aerosols. *Environmental Chemistry*, 2, 198-204.
- 8. Williams, J. (2004). Organic trace gases in the atmosphere: An overview. *Environmental Chemistry*, 1, 125-136.
- 9. Andrea, M. O & Crutzen, P. J. (1997). Atmospheric aerosols: Biogeochemical sources and role in atmosphere chemistry. *Science*, 276, 1052-1058.
- 10. Saxena, P. & Hildemann, L. M. (1996). Water-Soluble organics in atmospheric particles: A critical review of the literature and application of thermodynamics to identify candidate compounds, *Journal of Atmospheric Chemistry*, 24, 57-109.
- 11. Cavalli, F., Facchini, M. C., Decesari, S., Mircea, M., Emblico, L., Fuzzi, S., Ceburnis, D., Yoon, Y. J., O'Dowd, C. D., Putaud, J.-P. & Dell'Acqua, A. (2004). Advances in characterization of size resolved organic matter in marine aerosol over the North Atlantic. *Journal of Geophysic Research* 109, 10375-10376.
- 12. Russell, L. M., Maria, S. F. & Myneni, S. C. B. 2002. Mapping organic coatings on atmospheric particles. *Geophysic Research Letter*, 29, 10375-10376.
- 13. Sempere, R. & Kawamura, K. (2003). Trans-hemispheric contribution of C2-C10 alpha omegadicarboxylic acids and related polar compounds to water-soluble organic carbon in the western Pacific aerosols in relation to photochemical oxidation reactions. *Global Biogeochemical Cycles.* 17, 10375-10376.
- 14. Mochida, M., Kitamori, Y., Kawamura, K., Nojiri, Y. & Suzuki, K. (2002). Fatty acids in the marine atmosphere: Factors governing their concentrations and evaluation of organic films on seasalt particles, *Journal of Geophysic Research*, 107, 10376
- 15. Harvey, G.W. (1966). Microlayer collection from the sea surface: A new method and initial results. *Applied Oceanography*, 11(4): 608-613

- 16. Brimblecombe, P. (1996). Air Composition and Chemistry, 2nd Edition/Ed. Cambridge University Press, Cambridge.
- 17. Andreae, M. O. (1991). Global Biomass Burning: Atmospheric, Climatic and Biospheric Implication. MIT Press, Cambridge.
- 18. Andreae, M. O. (1995). Climatic Effects of Changing Atmospheric Aerosol Levels. Elsevier, Amsterdam.
- 19. Alotaibi, Y. (2004). Chemistry of Humic-like Substances in the Atmosphere. PhD Thesis, University of East Anglia, Norwich.
- 20. Seinfeld, J. H. & Pandis, S. N. (1998). Atmospheric Chemistry and Physics: From Air Pollution to Climate Change. John Wiley & Sons, New York.
- 21. Latif, M. T. (2006). Characteristics and distribution of surfactants in the atmosphere., PhD Thesis, University of East Anglia, Norwich.
- 22. Subbalakshmi, Y., Patti, A. F., Lee, G. S. H. & Hooper, M. A. (2000). Structural characterisation of macromolecular organic material in air particulate matter using Py-GC-MS and solid state 13C-NMR. *Journal of Environmental Monitoring*, 2, 561-565.
- 23. Chefetz, B., Tarchitzky, J., Deshmukh, A. P., Hatcher, P. G. & Chen, Y. (2002). Structural characterization of soil organic matter and humic acids in particle-size fractions of an agricultural soil. *Soil Science Society of America Journal*, 66, 129-141.
- 24. Alves, C., Pio, C. & Duarte, A. (1999). The Organic Composition Urban Portuguese Areas of Air Particulate Matter from Rural. *Physical Chemistry of Earth (B)*, 6, 705-709.
- 25. Havers, N., Burba, P., Lambert, J. & Klockow, D. (1998). Spectroscopic characterization of humiclike substances in airborne particulate matter. *Journal of Atmospheric Chemistry*, 29: 45–54.
- 26. Smoydzin, L & von Glasow, R. (2006). Do organic surface films on sea salt aerosols influence atmospheric chemistry? A model study. *Atmos. Chem. Phys. Discuss.*, 6: 10373–10402.
- 27. Botte, V. & Mansutti, D. (2005). Numerical modelling of the Marangoni effects induced byplankton-generated surfactants. *Journal of Marine Systems*. 57, 55–69.



REMOVAL OF Zn(II), Cd(II) AND Mn(II) FROM AQUEOUS SOLUTIONS BY ADSORPTION ON MAIZE STALKS

(Penyingkiran Zn(II), Cd(II) Dan Mn(II) Daripada Larutan Akueus Melalui Penjerapan Pada Tangkai Jagung)

G. O. El-Sayed¹*, H. A. Dessouki ¹ and S. S. Ibrahiem²

¹ Chemistry Department, Faculty of Science, Benha University, Benha, Egypt ² National Water Research Center, Central Lab. for Environ. Qual. Monit., Elganater Elkhayria, Egypt

*Corresponding author: gamaloelsayed@yahoo.com

Abstract

The potential to remove Zn(II), Cd(II) and Mn(II) from aqueous solutions through biosorption using maize stalks as an agriculture waste, was investigated in batch experiments. Different factors influencing metal adsorption such as contact time, initial metal ion concentration (40–1000 mg/L), pH (1–8), ionic strength and temperature (298–328 K) were investigated. The adsorption process was relatively fast and equilibrium was established after about 90 min. The optimum initial pH for zinc, cadmium and manganese adsorption by maize stalks was 7.0, 6.0 and 5.0, respectively. Under optimum conditions, the maximum adsorption capacity of zinc, cadmium and manganese ions was 30.30, 18.05 and 16.61 mg metal/g dry biomass, respectively. In order to investigate the sorption isotherm, three equilibrium models, Langmuir Freundlich and Temkin isotherms, were analyzed. The adsorption process for the three metal ions was found to be exothermic in nature. Free energy of adsorption (ΔG^0), enthalpy (ΔH^0) and entropy (ΔS^0) changes were calculated.

Keywords: maize stalks; metal removal; cadmium; manganese; zinc

Abstrak

Potensi penyingkiran Zn(II), Cd(II) dan Mn(II) daripada larutan akueus melalui bioerapan menggunakan tangkai jagung sebagai buangan pertanian telah dikaji menggunakan kaedah kelompok. Pelbagai factor yang mempengaruhi jerapan logam seperti masa sentuhan, kepekatan awal logam (40–1000 mg/L), pH (1–8), kekuatan ion dan suhu (298–328 K) telah dikaji. Proses penjerapan adalah agak pantas dan keseimbangan dicapai selepas 90 min. pH optimum bagi penjerapan zink, kadmium dan mangan oleh tangkai jagung masing-masingnya ialah 7.0, 6.0 dan 5.0. Pada keadaan optimum, muatan pejerapan maksimum bagi ion zink, kadmium dan mangan, masing-masing adalah 30.30, 18.05 and 16.61 mg logam/g biojisim kering. Bagi kajian isoterma erapan, tiga model keseimbangan iaitu isoterma Langmuir Freundlich dan Temkin dianalisis. Proses jerapan bagi ketiga-tiga ion logam adalah eksotermal. Perubahan tenaga bebas penjerapan (ΔG^0), entalpi (ΔH^0) dan entropi (ΔS^0) telah dikira.

Kata kunci: tangkai jagung; penyingkiran logam; cadmium, mangan; zink

Introduction

Toxic heavy metal contamination of industrial wastewater is an important environmental problem. Many industries such as electroplating, pigments, metallurgical processes, and mining and leather industries release various concentrations of heavy metals. Metal ions such as cadmium, chromium, copper, lead, zinc, manganese and iron are commonly detected in both natural and industrial effluents. The commonly used procedures for removing metal ions from effluents include filtration [1], chemical precipitation [2], chemical coagulation [3], flocculation [4], ion exchange [5], reverse osmosis [6], membrane technologies [7-9] and solvent extraction [10]. These processes may be ineffective or expensive, especially when the heavy metal ions are present in high concentrations. The use of adsorbents of biological origin has emerged in the last decade as one of the most promising alternatives to

conventional heavy metal management strategies. Biosorption is a fast and reversible reaction of the heavy metals with biomass. The by-products obtained from biomaterial production are a cheap source of biosorbents. Several agricultural waste materials have been studied and developed for the effective removal of heavy metals like maize bran [11], coffee husks [12], rice straw [13], sugar peat pulp [14], olive pomace [15], apple wastes [16], palm kernel fibre [17], peanut hull [18], cocoa shell [19], hazelnut husks [20], oak sawdust [21] and grape stalks [22].

Maize is an economical crop in Egypt, large areas are cultivated with it. The aim of the present study is to examine the ability of maize stalks as cheep bio-adsorbent for removal of Zn(II), Cd(II) and Mn(II) ions from aqueous solutions. The different factors affecting adsorption process were evaluated as time of contact, initial concentration of the metal, solution pH, temperature and adsorbent dosage. Furthermore, equilibrium, kinetic and thermodynamic studies on the adsorption of different metal ions onto the maize stalks were also carried out for the design of adsorption process. The advantage of using maize stalks as adsorbent is the ability of using the dry biomass after removal process in the manufacture of a sheep type of artificial wood by special treatment.

Materials and Methods

Biomass preparation

Maize stalks were collected and used as sorbent for the biosorption of Zn(II), Cd(II) and Mn(II) ions. The maize stalks sample was collected from Sharqiya Governorate region of Egypt. Samples were washed several times using deionised water to remove extraneous and dust. They were then dried in an oven at 105 °C for 24 h. The dried biomass was chopped and filtered. The granules were sieved and the particles having sizes less than 150 μ m were used in the tests. The adsorbent was kept dry in a closed container until the time of use.

Determination of point of zero charge

Point of zero charge of an adsorbent surface is the pH at which that surface has a net neutral charge. This value was evaluated by adding 0.1g of maize stalks to 50 mL of water with varying pH from 2 to 11.6 and stirred for 24 h. The initial pH was adjusted by adding either HCl or NaOH solutions and the final pH of the solution was plotted against the initial solution pH (Figure 1). pHZPC for maize stalks is determined as pH 5.2.

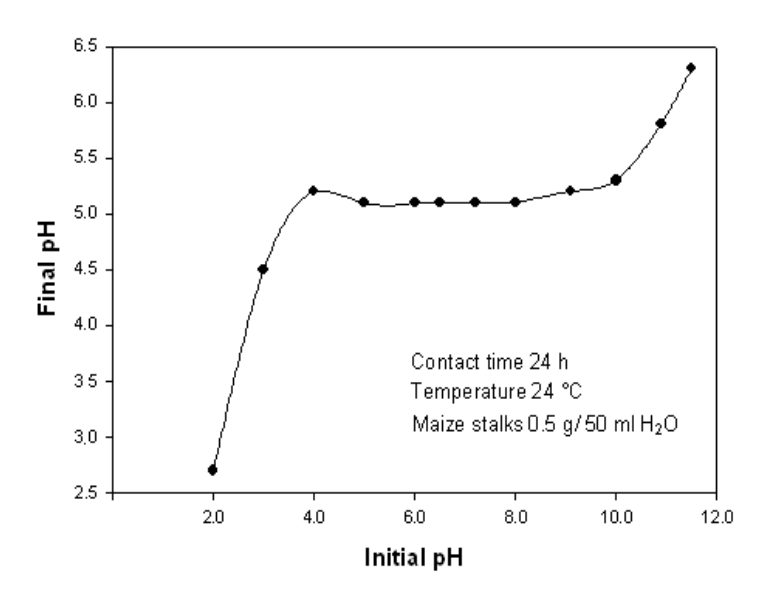


Figure 1: Point of zero charge (pHZPC) of maize stalks used for the adsorption experiments.

Batch sorption experiment

Using definite amount (0.5 g) of adsorbent in a 250 mL stopper conical flask containing 25 mL of metal ion solution, batch sorption studies were carried out at desired pH value, contact time, temperature and ionic strength.

Different initial concentration of Zn(II), Cd(II) or Mn(II) solutions were prepared by proper dilution from stock 1000 mg/L metal ions standard solutions. Standard metal ions solutions were prepared from the following salts: Zn(NO₃)₂, Cd(NO₃)₂ and MnCl₂. pH of the test solution was monitored by adding 0.1M HCl and 0.1M NaOH solution as required. The amount of biosorbent was then added to the metal ion solution in the conical flask and stirred for the desired contact time using a magnetic stirrer at 100 rpm. The time required for reaching equilibrium condition estimated by drawing samples at regular interval of time till the equilibrium was reached. The content of the metal ion in the test flask was separated from biosorbent by filtration through a filter paper and was analyzed by ICP-OES 2010 Serial Optical Emission Spectrometer, Optima (PerkinElmer). The samples were analyzed three times and the mean values were computed. The amount of metal ion adsorbed per unit mass of the biosorbent was evaluated by using following equations:

$$q_{max} = (C_0 - C_e) \frac{v}{w} \tag{1}$$

Where, C_0 is the initial metal ion concentration, and C_e is the metal ion concentration at equilibrium and V is the volume of metal ion solution in milliliters, W is the mass of adsorbent in grams. The percent of metal ion removal was evaluated from the equation:

% Removal =
$$\frac{(c_0 - c_e)}{c_0} \times 100$$
 (2)

Results and Discussion

Effect of pH on metal ion removal

The pH of the metal ion solution is an important parameter for adsorption of metal ions because it affects the solubility of the metal ions, concentration of the counter ions on the functional groups of the adsorbent and the degree of ionization of the adsorbate. To examine the effect of pH on metal ion removal efficiency, the pH was varied from 1.0 to 8.0 for Cd(II) and from 1.0 to 7.0 for Zn(II) and Mn(II) to prevent precipitation of metal hydroxides. As shown in Figure 2 the uptake of free ionic Cd(II) depends greatly on pH, where optimal metal removal efficiency occurs at pH 6.0 and then decreases at higher pH values, this behavior can be detected in other works [23]. Removal efficiency for Cd(II) increased from 7% to 46% over pH range from 1.0 to 6.0. In case of Zn(II), the metal uptake increases from 26% at pH 1.0 to 63% at pH 5.0, then it decreases by increasing the pH. The same figure indicated that the removal of Mn(II) increases from 16% at pH 1.0 to 38% at pH 7.0. This behavior is expected, as the acidity of the medium can affect the metal uptake on a biosorbent because hydrogen ions could compete with metallic ions for active sites on the biosorbent surface.

Effect of contact time and temperature

Figure 3 shows the effect of contact time on the rate of metal ion uptake onto maize stalks. At the beginning of adsorption, the values of % removal increased quickly, and then after 30 min, the change turned slow. Thus, the adsorption of the three metal ions on maize stalks was speedy. After about 90 min, the adsorbed quantity of the three metal ions showed nearly no change. The two stage sorption mechanism with the first rapid and quantitatively predominant and the second slower and quantitatively insignificant, has been extensively reported in literature [24,25]. This behavior gives away a slow approach to equilibrium. The nature of adsorbent and its available sorption sites affected the time needed to reach the equilibrium [26].

The effect of temperature of the adsorbate was also examined for solutions of 1000 mg/L metal ion and 20 g/L adsorbent at optimum pH values. Figure 4 shows the biosorption of Zn(II), Cd(II) and Mn(II) ions as a function of the temperature. The biosorption percentage decreased from 52 to 28% for Zn(II) ions, from 34 to 16% for Cd(II) ions and from 39 to 13% for Mn(II) ions as temperature was increased from 25 to 55 °C for the equilibrium time 90 min. These results indicated the exothermic nature of Zn(II), Cd(II) and Mn(II) biosorption onto maize stalks. A decrease in metal ion biosorption with the rise in temperature may be due to either the damage of active binding sites in the biomass [27] or increasing tendency to metal desorption from the interface to the solution [28] by weakening of adsorptive forces between the active sites of the adsorbent species [29].

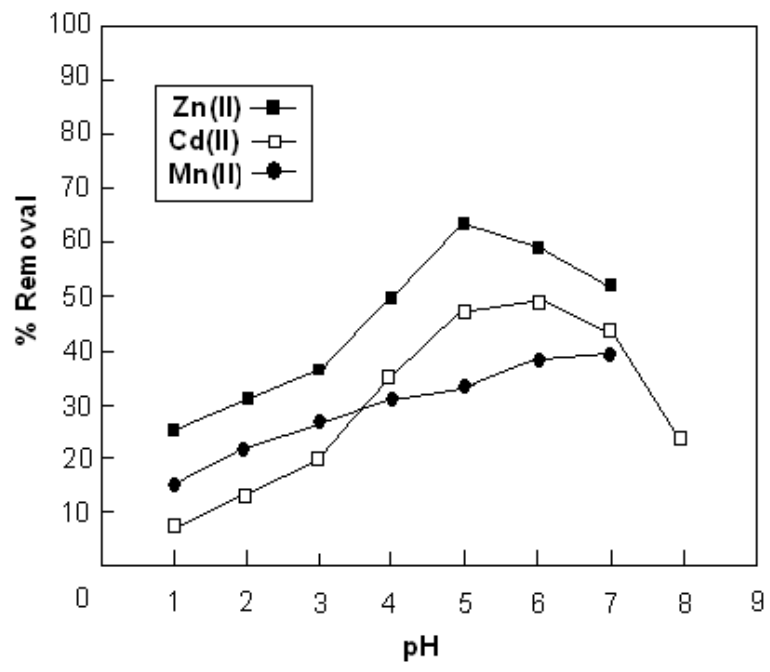


Figure 2: Effect of pH on the percent removal of Zn(II), Cd(II) and Mn(II) using maize stalks as adsorbent

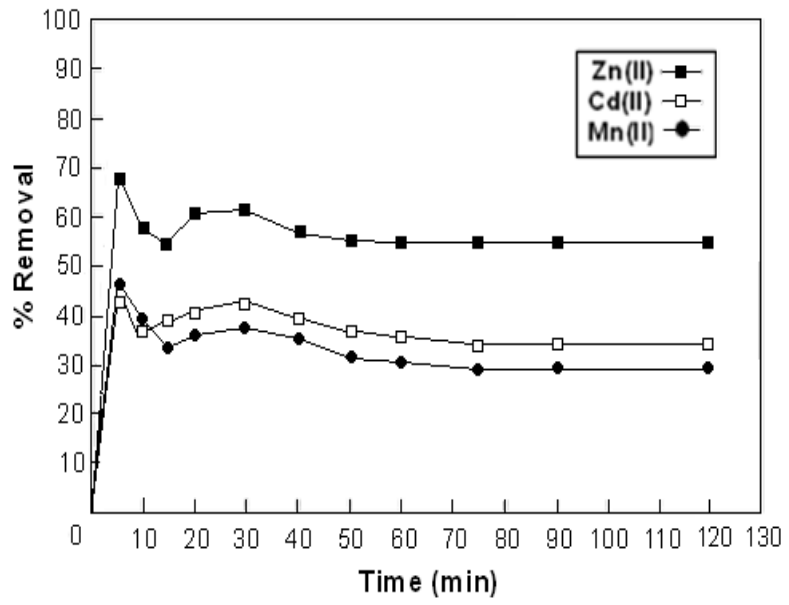


Figure 3: Effect of contact time on metal ion removal at optimum pH value

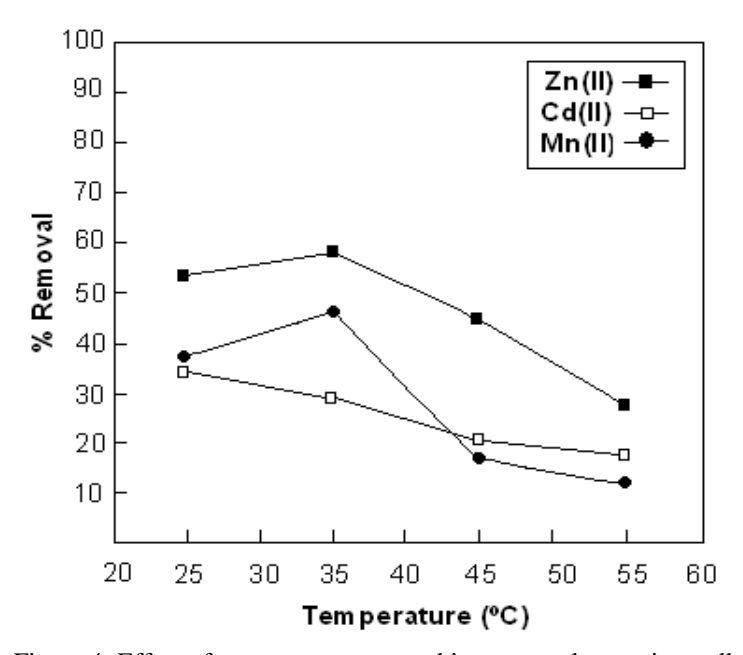


Figure 4: Effect of temperature on metal ion removal on maize stalks

Effect of ionic strength

The Influence of ionic strength I on heavy metal ions sorption by different biosorptions was investigated to determine solution chemistry effects. Different I values (0.1-1.0) were used by adding definite weights of solid KCl to a definite concentration of the metal ion (1000 mg/L). From the results obtained (Figure 5), it can be seen that the increasing of the ionic strength results in a decrease in the amount of the metal ion adsorbed as a result of the competition between the metal ions and the salt ions [30]. The reduction in uptake is probably due to the excess of K^+ ions which inhibit the approach of adsorbed ions to the active sites of the sorbent. Generally, there are two possible ways by which increasing I can influence metal ion sorption on different adsorbents: (1) decrease the solution-phase activity of metal ion and (2) increases concentration of competing ion (K^+). With increasing I, there is a little decrease in metal ion removal which can be attributed to the presence of sorption sites of different affinities.

Effect of initial metal ion concentration

The metal uptake mechanism is particularly dependent on the initial heavy metal concentration; at low concentrations, metal ions are adsorbed by specific active sites, while with increasing metal concentrations the binding sites become more quickly saturated as the amount of biomass concentration remained constant [31]. Figure 6 shows that the amount of metal ion sorbed per unit mass of maize stalks (i.e., sorption capacity) at optimum pH values and after 90 min of contact time was increased with the increase of the initial concentration of metal ion. It was observed also from the same figure that the adsorption capacity decreases in the following manner Zn(II) > Cd(II) > Mn(II). In the same time, the percentage removal was decreased with increasing the initial metal ion concentration for all metal ions studied.

Adsorption isotherms

To describe the adsorption process of Zn(II), Cd(II) and Mn(II) onto maize stalks, the three empirical models of Langmuir, Freundlich and Temkin isotherms were tested. The adsorption studies were conducted at fixed adsorbent dosage (0.5 g) by varying initial concentrations of heavy metals (40-1000 mg/L). These isotherms relate metal uptake per unit weight of adsorbent q_e to the equilibrium metal ion concentration in the bulk phase C_e .

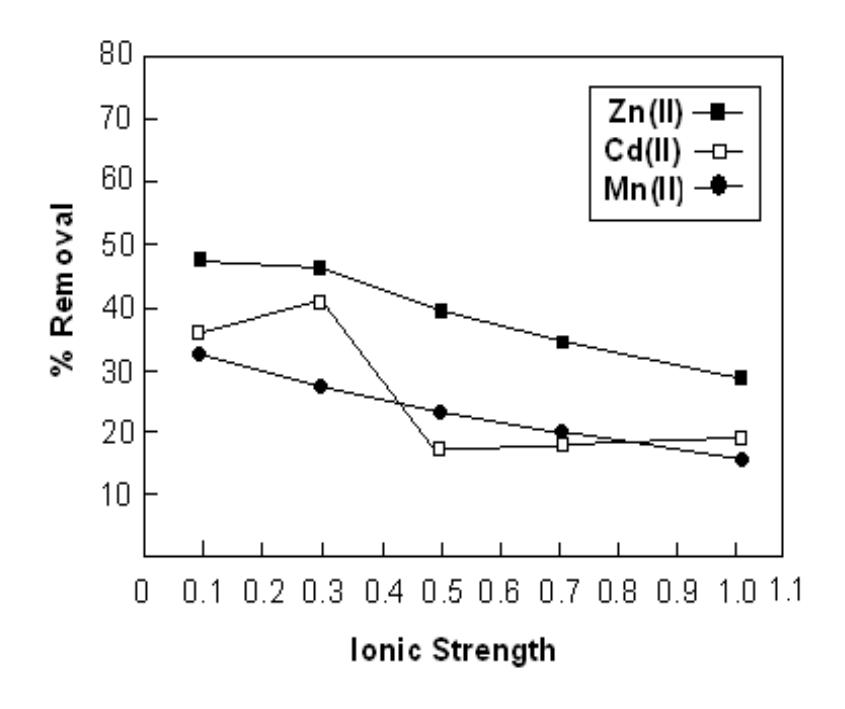


Figure 5: Effect of ionic strength on metal ion removal on maize stalks

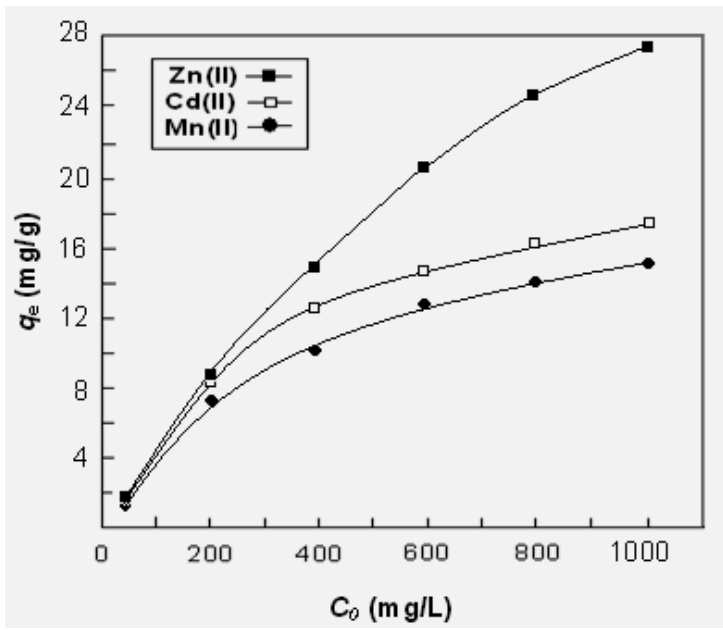


Figure 6: Effect of initial metal ion concentration on sorption capacity using maize stalks as adsorbent

The Langmuir Model

The Langmuir isotherm models is used to describe the relationship between the amount of adsorbed material and its equilibrium concentration in solutions. The Langmuir isotherm is valid for monolayer adsorption on a surface containing finite number of identical sites. The model assumes a uniform adsorption on the surface and transmigration in the plane of the surface. The Langmuir isotherm is expressed as follows [32]:

$$q_{\varepsilon} = (K_L C_{\varepsilon})/(1 + bC_{\varepsilon}) \tag{3}$$

where, q_e is the adsorption capacity at equilibrium in mg/g, C_e is the concentration at equilibrium (mg/L) and K_L is the Langmuir equilibrium constant in (mL/mg) and is expressed as follows:

$$K_L = Q_0 b \tag{4}$$

where, Q_o is the adsorption capacity at saturation in mg/g and b the adsorption coefficient in L/mg; The linear form of Langmuir isotherm model can be represented by using the equation below:

$$\frac{c_g}{q_g} = \frac{1}{Q_0b} + \frac{c_g}{Q_0} \tag{5}$$

The linear plots of Ce/q_e vs C_e show that adsorption follows the Langmuir adsorption model (Figure 7). The values of Q_o and b can be calculated (Table 1) from the slope and intercept of the plot, respectively. The correlation coefficients are 0.932, 0.998 and 0.989 for Zn(II), Cd(II) and Mn(II), respectively. These results reveal that the Langmuir-type sorption isotherm is suitable for equilibrium studies For Cd(II) and Mn(II) only, suggesting the formation of monolayer coverage of the adsorbate on the surface of adsorbent for these metalions [33]. The amount of metal ions adsorbed per unit mass of the adsorbent increased with the metal concentration as expected and the sorption capacities were 30.30, 18.05 and 16.61 for Zn(II), Cd(II) and Mn(II) ions, respectively.

The essential characteristics of the Langmuir isotherm can be explained by the equilibrium separation factor R_L defined as follows:

$$R_L = 1/(1 + bC_0) (6)$$

Depending on the value of R_L , the shape of the isotherm and whether the adsorption is favorable or not can be determined. The calculated R_L values for Zn(II), Cd(II) and Mn(II) at 298 K, were represented in Table 1. It was observed that at these experimental conditions, sorption of the different metal ions by maize stalks was found to be a favorable process [34] as the values of R_L are 0.719, 0.895 and 0.905 for Zn(II), Cd(II) and Mn(II), respectively.

The maximum adsorption capacities (Q_0) of adsorbent calculated from Langmuir isotherm equation which defines the maximum capacity of the adsorbent for metal ions were found to be comparable with other adsorbents reported in the literature for Zn(II), Cd(II) and Mn(II), Table 1.

The Freundlich Model

The Freundlich isotherm assuming that the adsorption process takes place on heterogeneous surfaces and adsorption capacity is related to the concentration of the adsorbent. The Freundlich model is based on the following expression [51]:

$$q_{\varepsilon} = K_F C_{\varepsilon}^{1/n} \tag{7}$$

where, K_F is the Freundlich constant and 1/n is a constant indicating the reaction intensity. The two Freundlich parameters K_F and 1/n can be determined graphically by plotting the experimental data and then using the Freundlich equation in the following form:

$$\ln q_{\varepsilon} = \ln K_F + (1/n) \ln C_{\varepsilon} \tag{8}$$

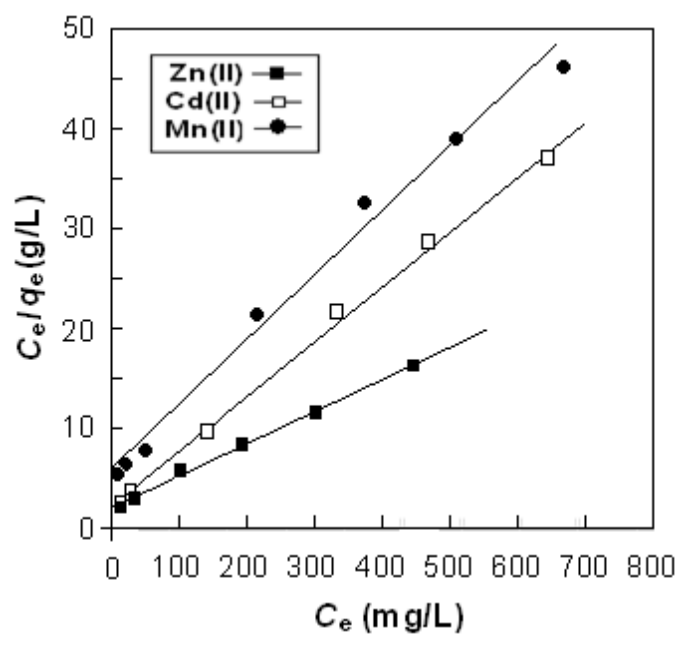


Figure 7: Langmuir isotherm plot for the adsorption of Zn(II), Cd(II) and Mn(II) on maize stalks at optimum pH values.

Table 1: Langmuir constant for different adsorbents

Metal	Adsorbent	Langmuir constant,	Reference
		$Q_{ heta}$ (mg/g)	
Zn(II)	Sunflower stalks	30.7	35
	Black Locust	5.0	36
	Oak saw dust	6.9	36
	Carrot residues	29.6	37
	Saw dust	14.1	29
	Neem bark	13.3	29
	Sugar beat pulp	17.7	38
Cd(II)	Groundnut husk	42.7	39
	Sugar cane bagasse	149.9	40
	Olive cake	65.4	41
	Lignite	40.2	42
	Spent grain	17.3	43
	Maize bran	7.4	44
	Tree fern	16.3	45
Mn(II)	Pseudomonas aeruginosa	22.4	46
	natural zeolitic tuff	10.0	47
	chitin	0.643	48
	kaolinite	0.446	49
	Cyanobacterium Gloeothece	0.473-0.906	50
	Magna		

The variations of $\ln q_e$ with $\ln C_e$ for zinc, cadmium and manganese cations are shown in Figure 8. It can be seen from the linear relationship that the adsorption of the three metals on maize stalks follows the Langmuir model. The values of K_F and n are presented in Table 1. The n values are 2.01, 2.48 and 2.23 for Zn(II), Cd(II) and Mn(II), respectively (greater than 1), indicating that the adsorption is favorable [52].

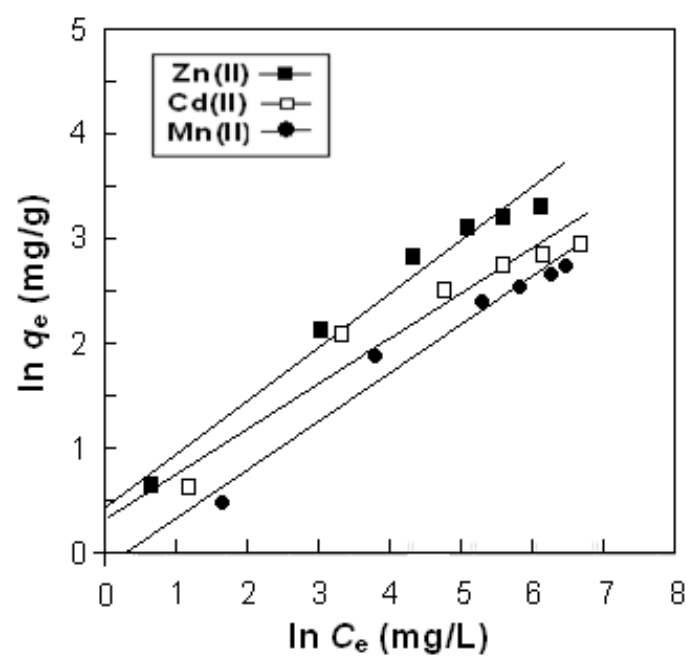


Figure 8. Freundlich isotherm plot of Zn(II), Cd(II) and Mn(II) on maize stalks

It can be observed from the correlation coefficient values (R^2) in Table 2 that Freundlich isotherm model exhibited good fit to the sorption data of Zn(II) and Mn(II).

The Temkin Isotherm

This isotherm was developed by Temkin and Pyzhev [53], and it is based on the assumption that the heat of adsorption decreases linearly with the increase of coverage of adsorbent [54]. Temkin isotherm assumes that the fall in the heat of sorption is linear rather than logarithmic [55]. This model can be shown by the equation:

$$q_{\varepsilon} = \frac{RT}{b_{T}} \ln K_{T} + \frac{RT}{b_{T}} \ln C_{\varepsilon}$$
 (9)

where, K_T (L/g) is Temkin adsorption potential and b_T (kJ/mol) is heat of sorption (Table 1). The linear plot of C_e versus q_e for the three metal ions for Temkin model is shown in Figure 9. From the slope and intercept of the straight line b_T and K_T can be evaluated, respectively.

Table 2: Modeled Langmuir and Freundlich isotherms parameters for zinc(II), cadmium(II) and manganese(II) adsorption on maize stalks

Metal	L	agmuir Is	sotherm		Freundli	Freundlich Isotherm			Temkin Isotherm		
Ion	Q_{0}	\boldsymbol{b}	R_L	R^2	K_F	n	R^2	K_{T}	$oldsymbol{b_{\mathrm{T}}}$	R^2	
	(mg/g)	(L/mg)	(L/mg)		$(L^n mg^{1-n}/g)$			(L/g)	(kJ/mol)	
Zn(II)	30.30	0.017	0.268	0.932	1.517	2.01	0.983	0.47	515.1	0.944	
Cd(II)	18.05	0.023	0.213	0.998	1.509	2.48	0.925	0.64	866.3	0.994	
Mn(II)	16.61	0.009	0.410	0.989	0.842	2.23	0.975	0.64	945.6	0.957	

By comparing the correlation coefficients (R^2) obtained from the three isotherms plots plots (Table 1), it can be concluded that Langmuir model can be applied successfully to Cd(II) and Mn(II) and Freundlich model can be applied to Zn(II) and Mn(II), while Temkin isotherm model appears to be favorable for fitness to the experimental data of Cd(II).

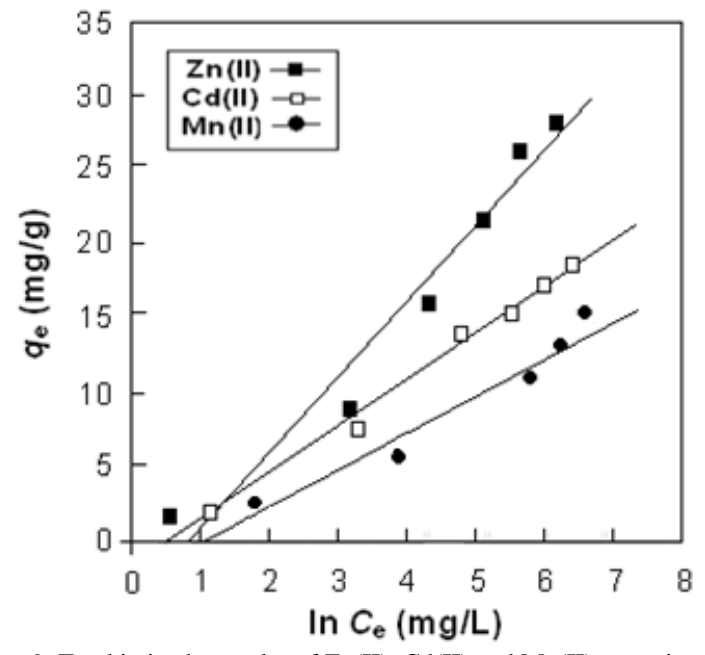


Figure 9. Temkin isotherm plot of Zn(II), Cd(II) and Mn(II) on maize stalks

Thermodynamic Parameters

The temperature dependence of the thermodynamic parameters on the adsorption of Zn(II), Cd(II) and Mn(II) on maize stalks were calculated using equations [56]:

$$\Delta G^{\circ} = -RT \ln K \tag{10}$$

The Gibbs free energy change (ΔG^o) is related to the entropy change (ΔH^o) and enthalpy change (ΔS^o) at constant temperature by the following equation:

$$\Delta G^{o} = \Delta H^{o} - T \Delta S^{o} \tag{11}$$

Combining the above two equations, we get:

$$\ln K = -\frac{\Delta H^o}{RT} + \frac{\Delta S^o}{R} \tag{12}$$

where, R is the universal gas constant (8.314 J/mol K), T is the absolute temperature (K) and K is the Langmuir equilibrium constant. ΔG° was calculated at different temperatures from equation (9). By plotting the values of $\ln K$ versus 1/T (Figure 10) using equation (11), the values of ΔH° and the ΔS° were calculated from the slope and intercept, respectively, Table 3.

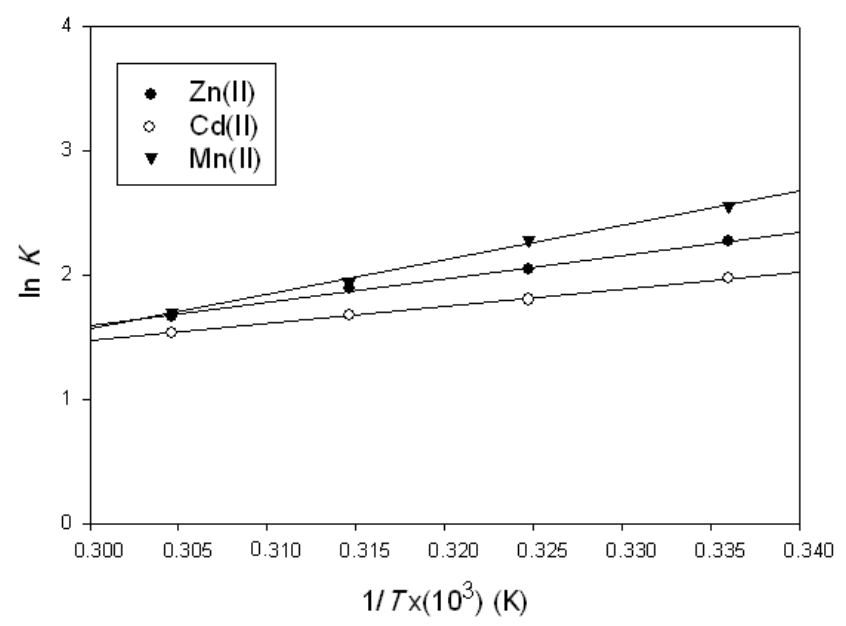


Figure 10. Plot of ln K vs. 1/T for removal of Zn(II), Cd(II) and Mn(II) by maize stalks

Table 3: Thermodynamic parameters of Zn(II),	, Cd(II) and Mn(II) on maize stalks at initial metal ion
concentration 1000 mg/L	

Metal ion	T(K)	ΔG^{o} (KJ/mol)	$\Delta H^{o}(\mathrm{KJ/mol})$	ΔS^{o} (J/mol K)
Zn(II)	298	-3.244		
	308	-3.354	-24.27	-10.97
	318	-3.464]	
	328	-3.573		
Cd(II)	298	-3.800		
	308	-3.928	-14.17	-12.80
	318	-4.056		
	328	-4.184		
Mn(II)	298	-7.406		
	308	-7.656	-25.35	-24.94
	318	-7.905		
	328	-8.155		

The negative values of Gibbs free energy change (ΔG°) indicate that the adsorption process for the three metal ion7s is feasible and spontaneous. It was observed that the values become more negative with increase in temperature. The negative values of ΔH° indicate that the adsorption of metal ions on maize stalks is exothermic. The negative values of ΔS° suggest decreased randomness at the solid/solution interface and no significant changes occur in the internal structure of the adsorbent through the adsorption of metal ions onto maize stalks [57].

Conclusion

The biosorption of Zn(II), Cd(II) and Mn(II) on maize stalks was investigated. Adsorption of the three metal ions is dependent on their initial concentrations and pH of the metal solution and the equilibrium were attained after 90 min of mixing. The results indicate that the optimum pH for maximum removal of Zn(II), Cd(II) and Mn(II) ions are 7.0, 6.0 and 5.0, respectively. The adsorption process was found to be exothermic. Langmuir adsorption model can be

El-Sayed et al: REMOVAL OF Zn(II), Cd(II) AND Mn(II) FROM AQUEOUS SOLUTIONS BY ADSORPTION ON MAIZE STALKS

applied successfully with cadmium and manganese, Freundlich adsorption model fitted well with zinc and manganese, while Temkin model can be applied to cadmium. The sorption capacities were 30.03, 18.05 and 16.61 mg/g for Zn(II),Cd(II) and Mn(II) ions, respectively. Maize stalks which is an agricultural waste material can be used for industrial water treatment to eliminate low concentrations of heavy metal ions as zinc, cadmium and manganese.

References

- 1. Bessbousse, H., Rhlalou, T., Verchère, J.-F. and Lebrun, L. 2008. Removal of heavy metal ions from aqueous solutions by filtration with a novel complexing membrane containing poly(ethyleneimine) in a poly(vinyl alcohol) matrix. Journal of Membrane Science, 307: 249-259.
- 2. Esalah, J.O., Weber, M.E. and Vera, J.H. 2000. Removal of lead from aqueous solutions by precipitation with sodium di-(*n*-octyl) phosphinate. Separation and Purification Technology, 18: 25-36.
- 3. El Samrani, A.G., Lartige, B.S. and Villieras, F. 2008. Chemical coagulation of combined sewer over flow: heavy metal removal and treatment optimization. Water Research, 42: 951-960.
- 4. Ofir, E., Oren, Y. and Adin, A. 2007. Comparing pretreatment by iron of electro-flocculation and chemical flocculation. Desalination, 204: 87-93.
- 5. Lin, L.-C., Li, J.-K. and Juang, R-S. 2008. Removal of Cu(II) and Ni(II) from aqueous solutions using batch and fixed-bed ion exchange processes. Desalination, 225: 249-259.
- 6. Benito, Y. and Ruíz, M.L. 2002. Reverse osmosis applied to metal finishing wastewater. Desalination, 142: 229-234.
- 7. Cooper, C.A., Lin, Y.S. and Gonzalez, M. 2004. Separation properties of surface modified silica supported liquid membranes for divalent metal removal/recovery. Journal of Membrane Science, 229: 11-25.
- 8. Juang, R.-S. and Shiau, R.-C. 2000. Metal removal from aqueous solutions using chitosan-enhanced membrane filtration. Journal of Membrane Science, 165: 159-167.
- 9. Nasef, M.M. and Yahaya, A.H. 2009. Adsorption of some heavy metal ions from aqueous solutions on Nafion 117 membrane. Desalination, 249: 677-681.
- 10. Gupta, S.K., Rathore, N.S., Sonawane, J.V., Pabby, A.K., Janardan, P., Changrani, R.D. and Dey, P.K. 2007. Dispersion-free solvent extraction of U(VI) in macro amount from nitric acid solutions using hollow fiber contactor. Journal of Membrane Science, 300: 131-136.
- 11. Hasan, S.H., Singh, K.K., Prakash, O., Talat, M. and Ho, Y.S. 2008. Removal of Cr(VI) from aqueous solutions using agricultural waste 'maize bran. Journal of Hazardous Materials, 152: 356-365.
- 12. Oliveira, W.E., Franca, A.S., Oliveira, L.S. and Rocha, S.D. 2008. Untreated coffee husks as biosorbents for the removal of heavy metals from aqueous solutions. Journal of Hazardous Materials, 152: 1073-108.
- 13. Gao, H., Liu, Y., Zeng, G., Xu, W., Li, T. and Xia, W. 2008. Characterization of Cr(VI) removal from aqueous solutions by a surplus agricultural waste—Rice straw. Journal of Hazardous Materials, 150: 446-452.
- 14. Altundogan, H.S., Bahar, N., Mujde, B. and Tumen, F. 2007. The use of sulphuric acid-carbonization products of sugar beet pulp in Cr(VI) removal. Journal of Hazardous Materials, 144: 255-264.
- 15. Pagnanelli, F., Mainelli, S., Vegliò, F. and Toro, L. 2003. Heavy metal removal by olive pomace: biosorbent characterisation and equilibrium modeling. Chemical Engineering Science, 58: 4709-4717.
- 16. Maranon, E. and Sastre, H. 1991. Heavy metal removal in packed beds using apple wastes, Bioresources Technology, 38: 39-43.
- 17. Ho, Y-S. and Ofomaja, A.E. 2006. Kinetic studies of copper ion adsorption on palm kernel fibre, Journal of Hazardous Materials B, 137: 1796–1802.
- 18. Zhu, C.-S., Wang, L.-P. and Chen, W.-b. 2009. Removal of Cu(II) from aqueous solution by agricultural by-product: Peanut hull. Journal of Hazardous Materials, 168: 739-746.
- 19. Meunier, N., Laroulandie, J., Blais, J.F. and Tyagi R.D. 2003. Cocoa shells for heavy metal removal from acidic solutions. Bioresources Technology, 90: 255-263.
- 20. Demirbas, O., Karadag, A., Alkan, M. and Dogan, M. 2008. Removal of copper ions from aqueous solutions by hazelnut shell. Journal of Hazardous Materials, 153:677–684.
- 21. Argun, M. E., Dursun, S., Ozdemir, C. and Karatas, M. 2007. Heavy metal adsorption by modified oak sawdust: Thermodynamics and kinetics. Journal of Hazardous Materials, 141: 77-85.
- 22. Fiol, N., Escudero, C. and Villaescusa, I. 2008. Chromium sorption and Cr(VI) reduction to Cr(III) by grape stalks and yohimbe bark. Bioresources Technology, 99: 5030-5036.

- 23. Nadeema, M., Shabbira, M., Abdullahb, M.A., Shahc, S.S. and McKayd, G. 2009. Sorption of cadmium from aqueous solution by surfactant-modified carbon adsorbents. Chemical Engineering Journal, 148: 365–370.
- 24. Saeed, A., Akhter, M.W. and Iqbal, M. 2005. Removal and recovery of heavy metals from aqueous solution using papaya wood as a new biosorbent. Separation and Purification Technology, 45: 25–31.
- 25. Runping, H., Pan, H., Zhaohui, C., Zhenhui, Z. and Mingsheng, T. 2008. Kinetics and isotherms of Neutral Red adsorption on peanut husk. Journal of Environmental Science, 20: 1035–1041.
- 26. Naiya, T. K., Bhattacharya, A. K. and Das, S. K. 2009. Adsorptive removal of Cd(II) ions from aqueous solutions by rice husk ash. Environmental Progress in Chemical Engineering, 28: 535-546.
- 27. Ozer, A. and Ozer, D. 2003. Comparative study of the biosorption of Pb(II), Ni(II) and Cr(VI) ions onto *S. cerevisiae*: determination of biosorption heats. Journal of Hazardous Materials, 100: 219–229.
- 28. Saltal, K., Sar, A. and Aydın, M. 2007. Removal of ammonium ion from aqueous solution by natural Turkish (Yıldızeli) zeolite for environmental quality. Journal of Hazardous Materials, B 141: 258–263.
- 29. Naiya, T.K., Chowdhury, P., Bhattacharya, A.K. and Das, S. K. 2009. Saw dust and neem bark as low-cost natural biosorbent for adsorptive removal of Zn(II) and Cd(II) ions from aqueous solutions. Chemical Engineering Journal, 148: 68-79.
- 30. Cieslak-Golonka, M. 1996. Toxic and mutagenic effects of chromium (VI). A review, Polyhedron, 15: 3667-3918.
- 31. Horsfall, M. and Spiff, A.I. 2005. Equilibrium Sorption Study of Al³⁺, Co²⁺ and Ag⁺ in Aqueous Solutions by Fluted Pumpkin (*Telfairia Occidentalis* HOOK f) Waste Biomass. Acta Chimica Slovinica, 52: 174–181.
- 32. Langmuir, I. 1916. The constitution and fundamental properties of solids and liquids. Journal of American Chemical Society, 38: 2221–2295.
- 33. Pehlivan, E. and Altun, T. 2008. Biosorption of chromium(VI) ion from aqueous solutions using walnut, hazelnut and almond shell. Journal of Hazardous Materials, 155: 378-384.
- 34. Bulut, Y., Gozubenli, N. and Aydın, H. 2007. Equilibrium and kinetics studies for adsorption of direct blue 71 from aqueous solution by wheat shells. Journal of Hazardous Materials, 144: 300–306.
- 35. Sun, G. and Shi, W. 1998. Sunflower stalks as adsorbents for the removal of metal ions from waste water. Industrial and Engineering Chemical Research, 37: 1324–1328.
- Sciban, M., Klasnja, M. and Skrbic, B. 2006. Modified hardwood saw dust as adsorbent of heavy metal ions from water., Wood Science Technology, 40: 217–227.
- 37. Eslamzadeh, T., Nasernejad, B., Pour, B.B., Zamani, A. and Bygi. M.E. 2004. Removal of heavy metals from aqueous solution by carrot residues. Iran, Journal Science and Technology Transaction A, 28A1: 161–167.
- 38. Pehlivan, E., Cetin, S. and Yanik, B.H. 2005. Equilibrium studies for the sorption of zinc and copper from aqueous solutions using sugar beat pulp and fly ash. Journal of Hazardous Materials, 135: 193–199.
- 39. Okieiman, F.E., Okundla, E.V. and Ogbeifun, D.E. 1991. Sorption of cadmium and lead ions on modified groundnut (*Arachis hypogea*) husks. Journal of Chemical Technology and Biotechnology, 51: 97–103.
- Krishnan, K.A. and Anirudhan, T.S. 2003. Removal of cadmium(II) from aqueous solutions by steamactivated sulphurised carbon prepared from sugar-cane bagasse pith: kinetics and equilibrium studies. Water SA 29: 147– 156.
- 41. Al-Anber, Z.A. and Matouq, M.A.D. 2008. Batch adsorption of cadmium ions from aqueous solution by means of olive cake. Journal of Hazardous Materials, 151: 194–201.
- 42. Allen, J.S. and Brown, P.A. 2004. Isotherm analyses for single component and multicomponent metal sorption onto lignite. Journal of Chemical Technology and Biotechnology, 62: 17–24.
- 43. Low, K.S., Lee, C.K. and Liew, S.C. 2000. Sorption of cadmium and lead from aqueous solutions by spent grain. Process Biochemistry, 36: 59–64.
- 44. Singh, K.K., Rupainwar, D.C. and Hasan S.H. 2005. Low cost bio-sorbent "maize bran" for the removal of cadmium from wastewater. Journal of the Indian Chemical Society, 82: 342–346.
- 45. Ho, Y.S. and Wang, C.C. 2004. Pseudo-isotherms for the sorption of cadmium ion onto tree fern. Process Biochemistry, 39: 761–765.
- 46. Silva, R.M.P., Rodriguez, A.A., De, J.M.G.M. and Moreno, D.C. 2009. Biosorption of chromium, copper, manganese and zinc by Pseudomonas aeruginosa AT18 isolated from a site contaminated with petroleum. Bioresources Technology, 100: 1533–1538.

El-Sayed et al: REMOVAL OF Zn(II), Cd(II) AND Mn(II) FROM AQUEOUS SOLUTIONS BY ADSORPTION ON MAIZE STALKS

- 47. Rajic, N., Stojakovic, D., Jevtic, S., Logar, N.Z., Kovac, J. and Kaucic, V. 2009. Removal of aqueous manganese using the natural zeolitic tuff from the Vranjska Banja deposit in Serbia. Journal of Hazardous Materials, 172: 1450–1457.
- 48. Robinson-Lora, M.A. and Brennan, R.A. 2010. Biosorption of manganese onto chitin and associated proteins during the treatment of mine impacted water. Chemical Engineering Journal, 162:565 -572.
- 49. Yavuz, O., Altunkaynak, Y. and Guze, F. 2003. Removal of copper, nickel, cobalt and manganese from aqueous solution by kaolinite. Water Research, 37: 948–952.
- 50. Mohamed, Z.A. 2001. Removal of cadmium and manganese by a non-toxic strain of the freshwater cyanobacterium *gloeothece magna*. Water Research, 35: 4405–4409.
- 51. Freundlich, H.M.F. 1906. Over the adsorption in solution. Journal of Physical Chemistry, 57: 385–470.
- 52. Senturk, H.B., Ozdes, D., Gundogdu, A., Duran, C. and Soylak, M. 2009. Removal of phenol from aqueous solutions by adsorption onto organomodified Tirebolu bentonite: Equilibrium, kinetic and thermodynamic study. Journal of Hazardous Materials, 172: 353–362.
- 53. Temkin, M.J. and Pyzhev, V. 1940. Recent modifications to langmuir isotherms. Acta Physiochimica URRS, 12: 217–222.
- 54. Aharoni, C. and Ungarish, M. 1977. Kinetics of activated chemisorption. Part 2-Theoretical models. Journal of Chemical Society, Faraday Transaction, 73: 456.
- 55. Hosseine, M., Merten, M., Ghorbani, M. and Arshadi, M.R. 2003. Asymmetrical Schiff bases as inhibitors of mild steel corrosion in sulphuric acid media. Materials Chemistry and Physics, 78: 800–807.
- 56. Meena, A.K., Mishra, G.K., Rai, P.K., Rajagopal, C. and Nagar, P.N. 2005. Removal of heavy metal ions from aqueous solutions using carbon aerogel as an adsorbent. Journal of Hazardous Materials, B 122: 161-170.
- 57. Ugurlu, M. 2009. Adsorption of a textile dye onto activated sepiolite. Microporous and mesoporous Materials, 119: 276-283.



ISOLATION OF CHEMICAL CONSTITUENTS FROM RHIZOMES OF ETLINGERA SPHAEROCEPHALA VAR. GRANDIFLORA

(Pemencilan Kandungan Kimia Daripada Rizom Etlingera Sphaerocephala var. Grandiflora)

M.A.A. Yahya¹, W.A. Yaacob^{1*} and I. Nazlina²

¹School of Chemical Sciences and Food Technology, ²School of Bioscience and Biotechnology, Faculty of Science and Technology, Universiti Kebangsaan Malaysia, 43600 Bangi, Selangor, Malaysia.

*Corresponding author: wanyaa@ukm.my

Abstract

A phytochemical investigation was conducted on the rhizomes of *Etlingera sphaerocephala* var. *grandiflora* (Zingiberaceae). Steroids of β -sitosterol and stigmasterol, together with a phenolic compound of paeonol were isolated using several chromatographic means. Their structures were established on the basis of extensive spectroscopic (IR, MS, NMR) data analysis and by comparison of the data obtained with those of the literature.

Keywords: Zingiberaceae, *Etlingera sphaerocephala* var. *grandiflora*, β-sitosterol, stigmasterol, paeonol, NMR

Abstrak

Suatu penyelidikan fitokimia dilakukan ke atas rizom *Etlingera sphaerocephala* var. *grandiflora* (Zingiberaceae). Steroid β-sitosterol dan stigmasterol, berserta sebatian fenolik paeonol dipisahkan menggunakan beberapa cara kromatografi. Struktur mereka dibuktikan berasas kepada analisis data spektroskopi (IM, SJ, RMN) yang ekstensif dan secara membandingkan data tersebut dengan data kepustakaan

Kata kunci: Zingiberaceae, Etlingera sphaerocephala var. grandiflora, β-sitosterol, stigmasterol, paeonol, NMR

Introduction

There are 151 species of Zingiberaceae belonging to 18 genera found in Peninsular Malaysia [1]. The largest genus of Zingiberaceae is *Alpinia* (23 species), followed among others by *Scaphochlamys* (20), *Amomum* (18), *Globba* (15), *Geostachys* (13), *Etlingera* (10) and *Zingiber* (10). The species of *Etlingera* in Peninsular Malaysia has now increased to fifteen [2]. The largest among *Etlingera* species are about 10 m in height. There are more than 100 species of Indo-pacific *Etlingera* growing from sea level to 2500 m [3].

Etlingera sphaerocephala var. grandiflora was described by Holttum [4] as a plant with subterranean, sub-globose, sub-cylindric inflorescence where its flowers appearing at soil level; its stature is 2.5 m; its leaves when young are also suffused red or purple below; its labellum of deep crimson lip, white margins, is 6 cm or more in length and 2.7 cm wide; and the base is red in color. Etlingera sphaerocephala var. grandiflora can be found in many parts of the Peninsular Malaysia and Borneo [5] mainly in lowland forests and at moderate elevation on the mountains. No use has ever been recorded for E. sphaerocephala var. grandiflora [3]. In this paper, we report the isolation and characterization of β-sitosterol, stigmasterol and paeonol from the rhizomes of E. sphaerocephala var. grandiflora. These compounds are reported for the first time from Etlingera.

Yahya et al: ISOLATION OF CHEMICAL CONSTITUENTS FROM RHIZOMES OF *ETLINGERA SPHAEROCEPHALA* VAR. *GRANDIFLORA*

Materials and Methods

Plant Material

Rhizomes of the *Etlingera sphaerocephala* var. *grandiflora* were collected in January 2009 from Genting Peras, Hulu Langat, Selangor, Malaysia. A voucher specimen of WYA 386 for the plant has been deposited at the Universiti Kebangsaan Malaysia Herbarium.

Extraction and Isolation

Air-dried rhizomes (315 g) were ground into a fine powder and soaked in n-hexane (5.0 L) for six days. The solution was filtered, and the combined filtrates were rotary evaporated under reduced pressure to produce 1.5 g (0.48%) of a brown-gummy rhizomes n-hexane extract. The remaining rhizomes powder was soaked in methanol (2.5 L) for another six days. The solution was filtered, and the combined filtrates were concentrated using a rotary evaporator to yield 6.3 g (2.1%) of a brown-oily rhizomes successive methanol extract.

The rhizomes n-hexane extract (1.5 g) was subjected to silica gel column chromatography (CC) (Merck 1.09385) by eluting n-hexane containing increasing percentages of ethyl acetate and the fractions collected was 100 mL each. Fractions 4 and 5 were combined (96 mg) and then subjected to radial chromatography (RC) (Merck 1.07749) by using increasing polarities of n-hexane: ethyl acetate to produce 12.4 mg of β -sitosterol (1). Fractions 6, 7 and 8 were combined (139 mg) and then subjected to silica gel preparative thin layer chromatography (PTLC) (Merck 1.07749) using 100:0 to 10:90 of n-hexane: ethyl acetate to afford 6.6 mg of stigmasterol (2).

The rhizomes successive methanol extract (6.3 g) underwent silica gel flash CC (Merck 1.07747) using 10% polarity increments from 90: 10 chloroform: methanol to 100% methanol whereby 100 mL fractions were collected. The flash CC fractions 5, 6 and 7 were combined (170 mg) and subjected to RC to produce five fractions. The combined fractions 1, 2 and 3 were fractionated over silica gel (Merck 1.07749) on PTLC to give 2.4 mg of paeonol (3).

β-Sitosterol (1; si) /Stigmasterol (2; st)

Colorless needles (12.4 mg)/white powder (6.6 mg). IR cm⁻¹: 3393/3434, 2930/2924, 1611/1639, 1457/1457, 1385/1375, 1171/1179. EIMS for β-sitosterol-C₂₉H₅₀O m/z (rel. int.): 414 [M⁺] (100%), 396 (30.8%), 381 (14.0%), 329 (13.7%), 303 (22.1%), 255 (11.8%), 213 (12.2%), 145 (18.5%), 95 (21.6%), 81 (21.3%), 55 (25.8%), 43 (45.0%). EIMS for stigmasterol-C₂₉H₄₈O m/z (rel. int.): 412 [M⁺] (39.7%), 351 (13.5%), 314 (7.0%), 300 (25.5%), 271 (38.4%), 229 (8.6%), 213 (10.6%), 55 (100%). ¹H NMR (CDCl₃, 400 MHz): 3.53 (1H, m, H-3), 5.36 (1H, d, J = 5.1/7.3 Hz, H-6), 0.69 (3H, s, H-18), 1.02 (3H, s, H-19), 0.93 (3H, d, J = 6.6/6.2 Hz, H-21), 5.16_{st} (1H, dd, J = 15.6, 8.4 Hz, H-22); 5.02_{st} (1H, dd, J = 15.6, 9.2 Hz, H-23), 0.85 (3H, d, J = 7.0/7.3 Hz, H-26), 0.83/0.81 (3H, d, J = 7.0 Hz, H-27), 0.87/0.83 (3H, t, J = 7.7/7.0 Hz, H-29), 1.05-2.32 (others). ¹³C NMR (CDCl₃, 100 MHz): 141.0 (C-5), 121.9 (C-6), 72.0 (C-3), 57.0/57.1 (C-14), 56.3 (C-17), 50.4/50.3 (C-9), 46.1/51.5 (C-24), 42.6/42.3 (C-4, C-13), 40.0 (C-12), 37.5 (C-1), 36.7 (C-10), 36.4/40.7 (C-20), 34.2/138.5 (C-22), 32.2/32.1 (C-8), 32.1_{si} (C-7), 31.9_{st} (C-7, C-25), 31.9/31.7 (C-2), 29.4_{si} (C-25), 28.5/29.3 (C-16), 26.3/129.5 (C-23), 24.5 (C-15), 23.3/25.6 (C-28), 21.3_{si} (C-11), 21.3_{st} (C-11, C-21), 20.1/19.0 (C-27), 19.6 (C-19), 19.3/21.4 (C-26), 19.0_{si} (C-21), 12.2 (C-29), 12.1 (C-18).

Paeonol (3)

White needles (2.4 mg). IR cm⁻¹: 3432, 2925, 1720, 1383, 1246, 1021. EIMS for $C_9H_{10}O_3$ m/z (rel. int.): 166 [M⁺] (31.3%), 151 (100%), 108 (16.5%), 95 (21.0%), 43 (34.6%). H NMR (400 MHz, CDCl₃) δ : 2.56 (3H, s, CH₃), 3.84 (3H, s, OCH₃), 6.42-6.45 (2H, m, H-3, H-5), 7.63 (1H, d, J=8.8 Hz, H-6), 12.75 (1H, s, OH). CDCl₃ δ : 114.1 (C-1), 165.4 (C-2), 101.0 (C-3), 166.3 (C-4), 107.9 (C-5), 132.5 (C-6), 202.8 (C=O), 55.8 (OCH₃), 26.4 (CH₃).

2 (trans-CH=CH across C22--C23; Stigmasterol)

3 (Paeonol)

Results and Discussion

Purification of the Etlingera sphaerocephala var. grandiflora rhizomes extracts produced β-sitosterol (1), stigmasterol (2) and paeonol (3). β-Sitosterol (1) was isolated as colorless needles. Column chromatography of the rhizomes n-hexane extract gave a 139 mg combined fractions, and its preparative thin layer chromatography yielded 6.6 mg of stigmasterol (2) as white powder. Spectral data of stigmasterol differed minimally from those of βsitosterol at and around a trans-C22-C23 double bond in the former. The EIMS of β-sitosterol/stigmasterol showed the molecular ion m/z 414/412 [M⁺] that corresponds to the formula C₂₉H₅₀O/C₂₉H₄₈O and in agreement with other previous spectral data. H NMR spectrum of β-sitosterol/stigmasterol indicated the presence of six methyl peaks of H-18, H-27, H-29, H-26, H-21 and H-19 that appeared at respective δ 0.69, 0.83/0.81, 0.87/0.83, 0.85, 0.93 and 1.02. The hydroxymethine proton H-3 of β -sitosterol/stigmasterol came out at δ 3.53 as a multiplet. One proton appeared at δ 5.36 as a doublet with coupling constants of 5.1/7.3 Hz represents the endocyclic double bond proton H-6 of β-sitosterol/stigmasterol. Stigmasterol showed two doublet-of-doublets for the other olefinic protons H-23 and H-22 at δ 5.02 (1H, dd, J = 9.2, 15.6 Hz) and 5.16 (1H, dd, J = 8.4, 15.6 Hz) respectively. The ¹H NMR spectral data of stigmasterol are in agreement with those of Hussain et al. [6]. The ¹³C NMR spectrum of βsitosterol/stigmasterol showed 28/26 signals for the 29 carbons skeleton with the overlapping of 2/6 carbons. The significant carbon signal for the β-sitosterol/stigmasterol would be the C-3 attached to a hydroxyl group and appeared at δ 72.0. The endocyclic carbon-carbon double bond of β-sitosterol/stigmasterol was represented by two signals at δ 121.9 and 141.0 of C-6 and C-5. Other olefinic carbons of stigmasterol appeared at δ 138.5 and 129.5 for C-22 and C-23. The quaternary C-5 signal is shifted to lower field than those of the tertiary C-6, C-22 and C-23. The similarity of the ¹³C spectral data of β-sitosterol/stigmasterol with those of the published data in [7]/[8]

Yahya et al: ISOLATION OF CHEMICAL CONSTITUENTS FROM RHIZOMES OF *ETLINGERA SPHAEROCEPHALA* VAR. *GRANDIFLORA*

confirmed that both two are of the same structure. β-Sitosterol/stigmasterol has never been reported before from any other *Etlingera*. However β-sitosterol was found in many other plant families including Zingiberaceae such as *Zingiber* [9], *Alpinia* [10], *Globba* [11], *Kaempferia* [12], *Costus* [13], *Renealmia* [14], *Aframomum* [15] and *Hedychium* [16], whereas stigmasterol including Zingiberaceae of *Renealmia* [14], *Alpinia* [17, 18] and *Zingiber* [9].

Paeonol (3) was isolated from the rhizomes successive methanol extract as white needles. Mass spectrum of this compound showed a molecular ion peak at m/z 166, which is in agreement with the molecular formula C₉H₁₀O₃ of paeonol. ¹H NMR spectrum of paeonol showed that there are two singlets at δ 2.56 and 3.84 representing two methyl groups attached to respective quaternary carbonyl, and oxygen. A signal for H-3, H-5 appeared at δ 6.42-6.45 as a multiplet. Proton H-6 showed a doublet which appeared at δ 7.63 with a coupling constant of 8.8 Hz. A hydrogen-bonded, six-membered ring phenolic proton was displayed very down-field at δ 12.75. ¹³C NMR data of this compound showed that there were nine signals which represents nine different carbons. The signal at δ 202.8 was assigned to the carbonyl group of C-1. Moreover, signals at δ 101.0, 107.9 and 132.5 were assigned to respective aromatic carbons of C-3, C-5 and C-6. Signal at δ 165.4 was assigned to C-2 which is known as an aromatic carbon attached to a hydroxyl group whereas the appearance of the aromatic C-4 with the methoxy substitution was seen at δ 166.3 due to the electron donating feature of the oxygen atoms in those groups. Two upfield signals appeared at δ 26.4 and 55.8 for methyl groups of COCH₃ and OCH₃. Comparison of the ¹H and ¹³C NMR data of paeonol with the previously published data in [19] confirmed that both are of the same compound. Paeonol has never been isolated before from any genus of Zingiberaceae. The fact that paeonol was found in the woody plants of Luculia intermedia [20], Rosmarinus officinalis [21], Moutan cortex [22] as well as in the nonwoody plants of Arisaema erubescens [23], Exacum affine [24], Primula auricula [25], Cynanchum paniculatum [25] supports its existence in our non-woody plant of Etlingera sphaerocephala var. grandiflora.

Conclusion

The isolation and identification of β -sitosterol (1), stigmasterol (2) and paeonol (3) from the rhizomes of *Etlingera* sphaerocephala var. grandiflora was the first ever to be reported from this plant. The work was carried out by utilizing several kinds of chromatographic separation techniques and spectroscopic analyses.

Acknowledgements

We wish to extend our gratitude to the School of Chemical Sciences and Food Technology, Universiti Kebangsaan Malaysia for the provision of laboratory facilities and technical assistance. We also wish to thank the Ministry of Higher Education Malaysia and the Universiti Kebangsaan Malaysia for financial support through the Fundamental Research Grant Scheme UKM-ST-06-FRGS0110-2009 and the Operation Fund for Research University UKM-OUP-KPB-31-156/2011.

References

- 1. Turner, I.M. (1995). A catalogue of the vascular plants of Malaya. *Gardens' Bulletin Singapore*. 47(2): 642-655.
- 2. Lim, C.K. (2001). Taxonomic notes on *Etlingera* Giseke (Zingiberaceae) in Peninsular Malaysia: the "*Achasma*" taxa and supplementary notes on the "*Nicolaia*" taxa. *Folia Malaysiana*. 2(3): 141-178, 209-210.
- 3. Poulsen, A.D. (2006). Etlingera of Borneo. Natural History Publications (Borneo). Kota Kinabalu.
- 4. Holttum, R.E. (1950). The Zingiberaceae of the Malay Peninsula. *Gardens' Bulletin Singapore*. 13(1): 1-249.
- 5. Smith, R.M. (1986). New combinations in *Etlingera* Giseke (Zingiberaceae). *Notes Royal Botanic Garden Edinburgh*. 43: 243-254.
- 6. Hussain, M.M., Rahman, M.S., Jabbar, A., Rashid, M.A. (2008). Phytochemical and biological investigations of *Albizzia lebbeck* Benth. *Boletín Latinoamericano y del Caribe de Plantas Medicinales y Aromáticas*. 7(5): 273-278.
- Zhang, X., Geoffroy, P., Miesch, M., Julien-David, D., Raul, F., Aoude-Werner, D., Marchioni, E. (2005). Gram-scale chromatographic purification of β-sitosterol. Synthesis and characterization of β-sitosterol oxides. Steroids. 70(13): 886-895.
- 8. De-Eknamkul, W., Potduang, B. (2003). Biosynthesis of β-sitosterol and stigmasterol in *Croton sublyratus* proceeds via a mixed origin of isoprene units. *Phytochemistry*. 62: 389-398.

- 9. Peng, W., Zhang, Y., Yang, K., Xiao, Y. (2007). Chemical constituents of *Zingiber officinale* (Zingiberaceae). *Yunnan Zhiwu Yanjiu*. 29(1): 125-128.
- 10. Phan, M.G., Le, H.T., Phan, T.S., Otsuka, H. (2007). Chemical constituents of the fruits of *Alpinia conchigera* Griff. (Zingiberaceae). *Tap Chi Hoa Hoc*. 45(4): 509-512.
- 11. Qiao, C., Xu, L., Shen, Y., Hao, X. (1999). Chemical constituents from *Globba racemosa* Smith. *Huaxue Yanjiu Yu Yingyong*. 11(5): 575-576.
- 12. Sukari, M.A., Neoh, B.K., Lajis, N.H., Ee, G.C.L., Rahmani, M., Ahmad, F.B.H., Yusof, U.K. (2004). Chemical constituents of *Kaempferia angustifolia* (Zingiberaceae). *Oriental Journal of Chemistry*. 20(3): 451-456.
- 13. Qiao, C., Li, Q., Dong, H., Xu, L., Wang, Z. (2002). Studies on chemical constituents of two plants from *Costus. Zhongguo Zhongyao Zazhi*. 27(2): 123-125.
- 14. Lognay, G., Marlier, M., Haubruge, E., Trevejo, E., Severin, M. (1989). Study of the lipids from *Renealmia alpinia* (Rott) Maas. *Grasas y Aceites*. 40(6): 351-355.
- 15. Vidari, G., Vita Finzi, P., De Bernardi, M. (1971). Flavonols and quinones in stems of *Aframomum giganteum*. *Phytochemistry*. 10(12): 3335-3339.
- 16. Xiao, P., Sun, C., Zahid, M., Ishrud, O., Pan, Y. (2001). New diterpene from *Hedychium villosum*. *Fitoterapia*. 72(7): 837-838.
- 17. Phan, M.G., Phan, T.S. (2004). Phytochemical investigation of *Alpinia globosa* (Lour.) Horaninov, Zingiberaceae. *Tap Chi Hoa Hoc*. 42(3): 376-378.
- 18. Phan, M.G., Dang, B.T., Phan, T.S. (2005). Flavonoid compounds from the rhizomes of *Alpinia conchigera* Griff., Zingiberaceae. *Tap Chi Hoa Hoc*. 43(1): 105-108.
- 19. Kim, M.Y., Lee, H.S., Bae, K.H., Yun, Y.S., Song, J.Y., Han, Y.S. (2006). Use of paeonol for inhibiting angiogenesis or for enhancing radiosensitization. PCT Int. Appl. WO 2006121263 A1 20061116.
- 20. Zhou, F., Tan, G., Liang, P. (1981). Isolation of paeonol, an analgesic principle from *Luculia intermedia* Hutch. *Zhongcaoyao*. 12(7): 6.
- 21. Cheng, W., Chen, H., Zhang, Y., Gao, S., Tao, Y., Gu, K. (2005). Study on chemical constituents in *Rosmarinus officinalis. Zhongcaoyao*. 36(11): 1622-1624.
- 22. Kitagawa, I., Yoshikawa, M., Tsunaga, K., Tani, T. (1979). Studies on *Moutan cortex*. II. On the chemical constituents. *Shoyakugaku Zasshi*. 33(3): 171-177.
- 23. Ducki, S., Hadfield, J.A., Lawrence, N.J., Zang, X., McGown, A.T. (1995). Isolation of paeonol from *Arisaema erubescens*. *Planta Medica*. 61(6): 586-587.
- 24. Matsumoto, M. (1994). 2'-Hydroxy-4'-methoxyacetophenone (paeonol) in *Exacum affine* cv. *Bioscience*, *Biotechnology*, *and Biochemistry*. 58(10): 1892-1893.
- 25. Weeks, R.A., Dobberstein, R.H., Farnsworth, N.R. (1977). Isolation of paeonol from *Bathysa meridionalis*. *Lloydia*. 40(5): 515-516.



DISCRIMINATOR SETTING AND COCKTAIL PREPARATION FOR ANALYSIS OF ALPHA AND BETA EMITTERS IN AQUEOUS SOLUTION USING LIQUID SCINTILLATION COUNTER

(Penetapan Diskriminator dan Penyediaan Koktil Untuk Analisis Pemancar Alfa dan Beta Didalam Larutan Berakueus Menggunakan Pembilang Sintilasi Cecair)

Zaini Hamzah^{1*}, Masitah Alias¹ and Zaharudin Ahmad²

¹Faculty of Applied Sciences, Universiti Teknologi MARA, 40450 Shah Alam, Selangor, Malaysia ²Radiochemistry and the Environment Group, Malaysian Nuclear Agency, 43000 Bangi, Selangor, Malaysia

*Corresponding author: zainihamzah@live.com

Abstract

Liquid scintillation counting (LSC) is not only being used to measure pure beta emitters, but it can be used to measure both alpha and beta emitters simultaneously. Measurement of alpha and beta emitters in aqueous solution is done using a single sample. For the sample preparation, colorless detergent or emulsifier was used to incorporate the water into an organic based scintillator to produce a clear homogeneous solution, since this is the best form to give the highest count rate and detection efficiency. The instrument also need some attention, where after calibration, the LSC was set for the discriminator level which is suitable for measurement of both alpha and beta radiations. In this study, the focus is on the development of the best scintillation cocktail and establishes the best discriminator setting. From this study the best proportion of scintillation cocktail is 2:4:4 for water, toluene, and Triton-N101 (emulsifier) respectively and the best discriminator setting for alpha and beta counting are 120. Abstract in English

Keywords: alpha emitter, beta emitter, cocktail, LSC, scintillant.

Abstrak

Pembilang sintilasi cecair (PSC) bukan hanya digunakan untuk mengukur pemancar beta tulen, tetapi boleh juga digunakan untuk mengukur kedua-dua pemancar alfa and beta serentak. Pengukuran pemancar alfa dan beta di dalam larutan berair boleh digunakan menggunakan sampel yang sama. Untuk penyediaan sampel, emulsifier tanpa warna telah digunakan bagi mengikat air ke dalam sintilator berasaskan organik untuk menghasilkan larutan homogeneous, kerana ini adalah merupakan bentuk terbaik yang memberikan kadar bilangan dan efisiensi pengesanan yang tertinggi. Peralatan juga memerlukan perhatian, dimana selepas proses kalibrasi, PSC perlu penentuan tahap diskrimanator yang sesuai untuk pengukuran kedua-dua radiasi alfa dan beta. Ini adalah untuk memastikan kadar limpahan dari kedua-dua radiasi rendah. Di dalam kajian ini, fokus ditumpukan kepada membangunkan koktil sintilasi dan menentukan tahap diskriminator yang sesuai. Dari kajian ini didapati kadar terbaik bagi koktil sintilasi adalah 2:4:4 bagi air, toluen dan Triton N-101 (emulsifier) masing-masing dan tahap diskriminator terbaik adalah pada 120 untuk pengukuran zarah alfa dan beta serentak.

Kata kunci: pemancar alfa, pemancar beta, koktil, PSC, sintilan.

Introduction

Measurement of alpha and beta emitters in environment especially water samples are normally carried out using separate method, since both radiations having different properties. Recently, with the advancement of liquid scintillation counting (LSC), the measurement of radionuclides in the natural environment where radionuclide concentrations are low, becoming more feasible since the instrument background is very low. The contribution of instrument background to the precision of the measurement is often important. The "low level" instruments have

Zaini Hamzah et al: DISCRIMINATOR SETTING AND COCKTAIL PREPARATION FOR ANALYSIS OF ALPHA AND BETA EMITTERS IN AQUEOUS SOLUTION USING LIQUID SCINTILLATION COUNTER

their background reduction features that are the efficiency to background (E^2/B) factor is increased or minimum detectable activity (MDA) is decreased [1].

This method is based on the recently available liquid scintillation counting (LSC) systems with the ability of discrimination of alpha and beta emitters by the time distribution of the light emission each generates from scintillators, in the term of pulse shape discrimination (PSD) or pulse decay analysis (PDA). Pulse Shape Analysis (PSA) is a pulse shape discrimination technique that is based on a method that integrates the charge of 'tail' of scintillation pulse and compares it with the total charge in the same pulse. Different settings of the PSA level assign the pulse into either a long (alpha-like) or short (beta-like) category. Thus, different PSA settings allow pulses to be categorized according to their length (shape). Typically, increasing the PSA setting will direct more pulses toward the long or alpha category. However, depending on how the technique is implemented, the reverse can also be true, i.e., increasing the setting may direct more alpha counts into the beta category. There are several methods of accomplishing pulse shape analysis including slow crossover timing, fast crossover timing, and constant fraction of pulse-height trigger [1].

Water quality is an important aspect of environmental studies. Natural waters contain both alpha (such as ²³⁸U) and beta (such as ⁴⁰K) emitters in widely varying concentrations which are responsible for a generally small fraction of the total dose received from natural and artificial radioactivity [2]. For practical purposes, the recommended guideline for activity concentrations are 0.1 BqL⁻¹ for gross alpha and 1 BqL⁻¹ for gross beta in the drinking water [3]. The recommendations do not differentiate between natural and man-made radionuclides. Below these reference levels of gross activity, drinking water is acceptable for human consumption and any action to reduce radioactivity is not necessary. In the last decades, nationwide studies have been performed in practically every developed country, where drinking water is regularly sampled and analyzed. In developing nations, data on the natural radioactivity in water are not always available. According to a UNSCEAR report [4], drinking water is considered to be an important factor in increasing the natural radiation exposure in humans.

The occurrence of natural radionuclides in drinking water poses a problem of health hazard, when these radionuclides are taken into the body by ingestion. Several naturally occurring alpha or beta emitting radionuclides such as ²³⁸U, ²²⁶Ra, ²²²Rn, ²¹⁰Pb, ²²⁸Ra and others are frequently dissolved in domestic water supplies and their concentrations vary over an extremely wide range, mainly depending upon the amount of radio elements present in bedrock and soil with which the water comes in contact [5].

Terlikowska *et. al.* [6], has done some work on the application of alpha/beta discrimination in liquid scintillation counting for the purity control of ^{99m}Tc medical solutions. Shing-Fa Fang *et al.* [7], has worked on the comparison of Alpha/Beta separation performance of Commercially Available Scintillation Cocktails and counting by QuantulusTM 1220 Liquid Scintillation Counter. Maurizio Forte *et. al.* [8], has done some natural radionuclides measurements in drinking water using Ultra-low Level Liquid Scintillation Counting. Cantaloub *et.al.* [9] studied the interaction of sample, cocktail and headspace volume when measuring aqueous radon in small volume sample. The study focused on measurement of radon using commercial cocktail, Ultima Gold F.

In this study, the focus is on the development of the best scintillation cocktail and establishes the best discriminator setting for LSC TRICAB 2700 from Packard that available in Malaysian Nuclear Agency (NM) in Bangi, Malaysia. The scintillation cocktail was developed using emulsifier (Triton N-101) mixed with solvent (toluene) and scintillator (2,5-diphenyloxazole, PPO and 1,4-bis(5-diphenyloxazol-2-yl)-benzene, POPOP).

Experimental

Instrument Calibration

Liquid Scintillation Counter TRICAB 2700 is a Packard instrument which is capable for measuring both alpha and beta radiations in water. Before any samples are counted, the instrument must be calibrated. This is performed automatically with the use of the calibration (SNC) protocol plug and the unquenched ¹⁴C calibration standard.

Alpha/ beta Calibration and Discriminator Setting

Using Packard TRICAB models with alpha/beta discrimination, the optimum setting is the setting where there is equal and minimum spillover of alpha pulses into the beta Multi Channel Analyzer (MCA) and beta pulses into the alpha Multi Channel Analyzer (MCA). The determination of an optimum PDD requires two standards: one of the pure alpha emitter of interest and one of the pure beta emitter of interest. ²⁴¹Am and ³⁶Cl samples in Packard Ultima Gold AB, a cocktail specifically designed for alpha/beta separation were used for setting the percent spillover or percent misclassification of alpha and beta emitters. To achieve this, one need to vary the discriminator setting on the instrument (LSC). The instrument determines it optimum setting that results in the minimum misclassification of alpha and beta activity, and will generate the percent misclassification plot on demand. Several observations can be made by comparing these two curves. The first observation is the obvious shift in the instrument determined optimum PDD to a slightly higher value with TR-PDA than without TR-PDA. The next observation is the flattening of the alpha curve.

Cocktail development

Cocktail development is the method where we attempt to incorporate the water in an organic solvent. A triangular method was used to get the best proportion of water, organic solvent and Triton N-100 with 4.0 g/L PPO and 0.4 g/L POPOP (Figure 1).

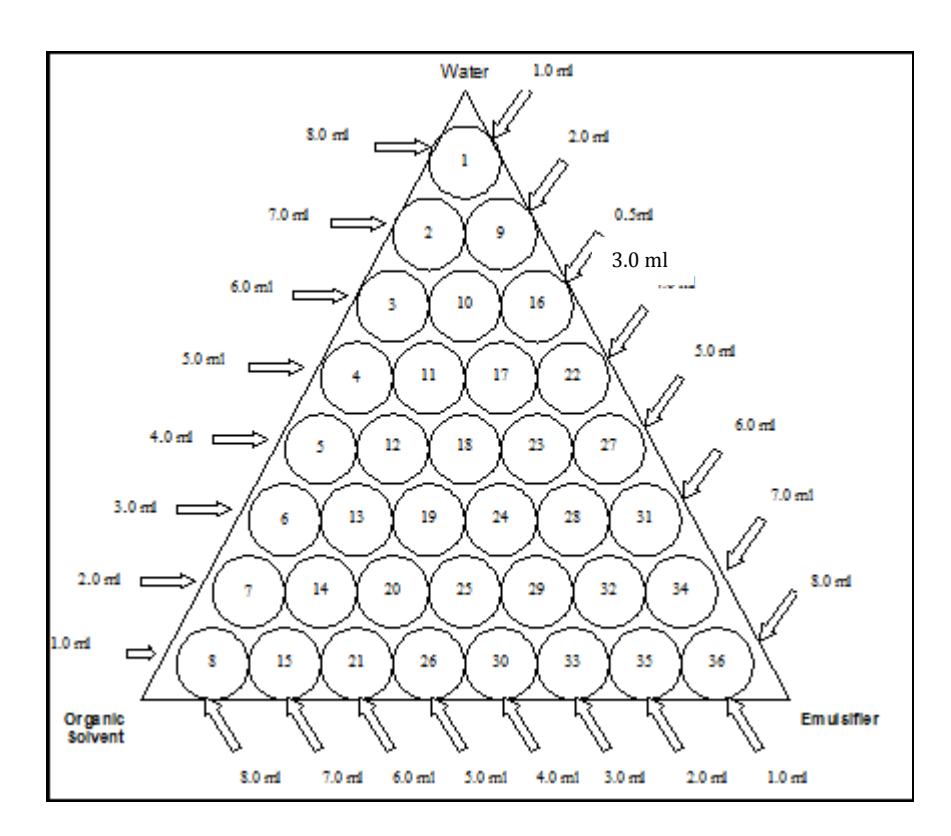


Figure 1: The position of vials for different composition of water, toluene and Triton N-100

Results and Discussion

Instrument Calibration

During the calibration procedure, the high voltage applied to photomultiplier tube (PMT) is adjusted individually until the tubes are normalized (synchronized) in their response to the ¹⁴C calibration standard. Then, the high

Zaini Hamzah et al: DISCRIMINATOR SETTING AND COCKTAIL PREPARATION FOR ANALYSIS OF ALPHA AND BETA EMITTERS IN AQUEOUS SOLUTION USING LIQUID SCINTILLATION COUNTER

voltage to both tubes is adjusted simultaneously until the end point of ¹⁴C spectrum fall in the appropriate position on the spectra analyzer (on-board 400-channel) multi-channel analyzer.

It is highly recommended that the SNS cassette (containing the ¹⁴C calibration standard) be left in the instrument at all time. If the instrument is not IDLE, the calibration procedure is performed once every a 23-hour timer is checked. If 23 hour has elapsed since the previous calibration, the instrument will automatically perform the SNC procedure. If the time has NOT elapsed, the SNC cassette is bypassed. When the calibration is complete, the message SYSTEM NORMALIZED appears on the printout. This indicates that the instrument is ready for counting.

Discriminator Setting

Separate optimum PDD setting should also derived for unique alpha and beta standard pairs. For gross alpha and gross beta measurements where the particular radionuclides may not be known, an alpha and beta standard of similar energy to the alpha and beta in the samples is desirable. To arrive at the optimum setting, each standard is counted individually at range of PDD settings and the percent misclassification of alphas into the beta MCA and vice versa are plotted against PDD on the same graph. When only the beta emitter is of interest, a PDD value below the instrument determined optimum may be used, which minimizes the misclassification of alpha activity into the beta MCA at the expense of reducing the beta efficiency. Similarly, when only the alpha emitter is of interest, a PDD value greater than the optimum, can be used. This minimizes the mis-classification of beta events into the alpha MCA at the expense of reduced alpha counting efficiency.

The effect of Time-Resolved Pulse Decay Analysis (TR-PDA) on the misclassification curve is slightly higher value with TR-PDA and the flattening of alpha curve is the cause of the shift in the intersection of the curves and results in a higher optimum PDD value. The flattened shape of the alpha curve is due to TR-LSC discrimination of misclassified alpha events in the beta MCA. At this higher value, beta misclassification is also reduced. Manual adjustment the discriminator to a higher or lower value than the optimum will further reduce either beta or alpha misclassification at the expense of some loss of alpha or beta counting efficiency, respectively.

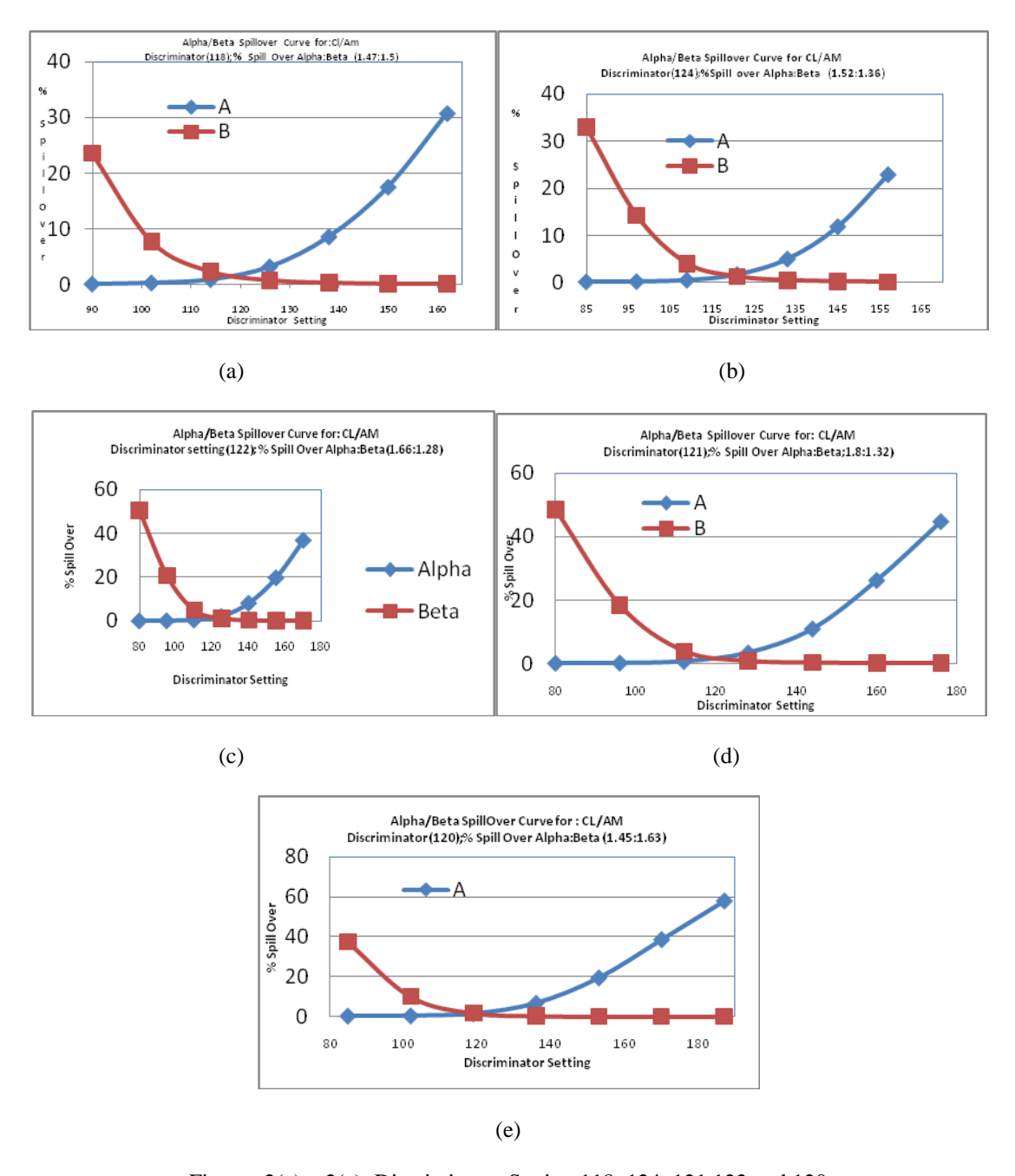
Figures 2(a) to 2(e) show the alpha/beta spillover curve for $^{36}\text{Cl}/^{241}\text{Am}$. From these curves we have chosen the discriminator 120 with the percent spillover alpha:beta (1.45:1.63).

Cocktail development

In this study, the emulsifier used was Triton N-101 and the solvent was toluene scintillation grade. The amount of primary and secondary scintillator was 4.0 g/L and 0.4 g/L of PPO and POPOP respectively. Using the triangular method [10], 36 vials were used to be filled with different proportions of water, toluene and emulsifier (Triton N-100).

Tables 1(a) and 1(b) show the proportion of water, toluene, and triton N-101 in different vials. The appearance of liquid in each vial was recorded as cloudy, clear and opaque. The aim of this cocktail is to get a clear solution and that solution is giving the best count rate. The count rate of ³H (pure beta emitter) and ²²⁶Ra (alpha emitter) are listed in the column 2 of Table 1.

Both ³H and ²²⁶Ra show the same characteristics when mixed with cocktail. The aim of this cocktail preparation is to get the clear stable solution, with the best count rate as well as giving the best merit value. From Tables 1 (a) and (b), the best proportion for the mixture of water:toluene:Triton N-101 is 2:4:4. So, for 20 mL mixture, the amount of water is 4 mL.



Figures 2(a) – 2(e): Discriminator Setting 118, 124, 121,122 and 120

Zaini Hamzah et al: DISCRIMINATOR SETTING AND COCKTAIL PREPARATION FOR ANALYSIS OF ALPHA AND BETA EMITTERS IN AQUEOUS SOLUTION USING LIQUID SCINTILLATION COUNTER

Table 1(a): The proportion of water, toluene, and triton-N100, appearance and the activities for beta emitter (³H)

Vial no.	Count (CPM)	Efficiency	Water	Toulene	Triton	Appearance	Homogenity	Viscosity	% of water in solution	Merit value	% Triton
MA-38	51	0.5	8	1	1	milky	heterogenous	viscous	80	42.8	10
MA-39	140	1.5	7	2	1			viscous	70	103.1	10
MA-40	471	5.0	6	3	1	milky	heterogenous	not viscous	60	297.3	10
MA-41	728	7.7	5	4	1		heterogenous		50	383.0	10
MA-42	1044	11.0	4	5	1	milky	heterogenous	not viscous	40	439.2	10
		8.2	3	6	1	milky	heterogenous	not viscous	30		10
MA-43	780		2	7		milky	heterogenous	not viscous	20	246.1	10
MA-46	968	10.2		_	1	milky	heterogenous	not viscous		203.7	
MA-47	953	10.0	1	8	1	milky 	heterogenous	not viscous	10	100.3	10
MA-51	3096	32.6	1	7	2	milky	heterogenous	viscous	10	325.6	20
MA-52	1748	18.4	2	6	2	opaque	heterogenous	viscous	20	367.7	20
MA-53	1420	14.9	3	5	2	opaque	heterogenous	viscous	30	448.0	20
MA-54	853	9.0	4	4	2	opaque	heterogenous	viscous	40	359.0	20
MA-55	513	5.4	5	3	2	opaque	heterogenous	viscous	50	269.9	20
MA-56	290	3.1	6	2	2	opaque	heterogenous	viscous	60	183.3	20
MA-57	131	1.4	7	1	2	cloudy	heterogenous	viscous	70	96.1	20
MA-58	176	1.8	6	1	3	cloudy	heterogenous	viscous	60	111.0	30
MA-59	435	4.6	5	2	3	clear	homogeneous	not viscous	50	228.6	30
MA-60	694	7.3	4	3	3	clear	homogeneous	not viscous	40	291.8	30
MA-61	1085	11.4	3	4	3	cloudy	heterogenous	viscous	30	342.5	30
MA-62	1739	18.3	2	5	3	cloudy	heterogenous	viscous	20	365.8	30
MA-63	2634	27.7	1	6	3	clear	homogeneous	not viscous	10	277.0	30
MA-64	2298	24.2	1	5	4	clear	homogeneous	not viscous	10	241.7	40
MA-65	1436	15.1	2	4	4	clear	homogeneous	not viscous	20	302.0	40
MA-66	891	9.4	3	3	4	cloudy	heterogenous	viscous	30	281.3	40
MA-67	529	5.6	4	2	4	clear	homogeneous	viscous	40	222.7	40
MA-68	235	2.5	5	1	4	clear	homogeneous	viscous	50	123.7	40
MA-69	310	3.3	4	1	5	clear	homogeneous	viscous	40	130.3	50
MA-70	651	6.8	3	2	5	clear	homogeneous	viscous	30	205.4	50
MA-71	1191	12.5	2	3	5	clear	homogeneous	not viscous	20	250.6	50
MA-72	1847	19.4	1	4	5	clear	homogeneous	not viscous	10	194.3	50
MA-73	1588	16.7	1	3	6	clear	homogeneous	not viscous	10	167.0	60
MA-74	899	9.5	2	2	6	clear	homogeneous	not viscous	20	189.0	60
MA-75	411	4.3	3	1	6	cloudy	homogeneous	not viscous	30	129.8	60
MA-76	541	5.7	2	1	7	clear	homogeneous	viscous	20	113.9	70
MA-77	1126	11.8	1	2	7	c;ear	homogeneous	viscous	10	118.5	70
MA-78	681	7.2	1	1	8	clear	homogeneous	not viscous	10	71.6	80

Note: The best portion of cocktail mixture

Table 1(b): The proportion of water, toluene, and triton-N100, appearance and the activities for alpha emitter (²²⁶Ra)

						Ι		I			
ViaIID	Count (CPM)	Efficiency	Water	Toulene	Triton	Appearance	Homogenity	Viscosity	water in solu		% Triton
MA-79	203	4.9	8	1	1	milky	heterogenous	viscous	80	393.6	10
MA-80	254	6.2	7	2	1	milky	heterogenous	viscous	70	432.2	10
MA-81	471	11.5	6	3	1	milky	heterogenous	not viscous	60	689.8	10
MA-82	334	8.1	5	4	1	milky	heterogenous	not viscous	50	406.8	10
MA-83	478	11.7	4	5	1	milky	heterogenous	not viscous	40	467.2	10
MA-84	503	12.3	3	6	1	milky	heterogenous	not viscous	30	368.4	10
MA-85	529	12.9	2	7	1	milky	heterogenous	not viscous	20	258.2	10
MA-86	575	14.0	1	8	1	milky	heterogenous	not viscous	10	140.4	10
MA-87	719	17.6	1	7	2	milky	heterogenous	viscous	10	175.7	20
MA-88	640	15.6	2	6	2	opaque	heterogenous	viscous	20	312.8	20
MA-89	581	14.2	3	5	2	opaque	heterogenous	viscous	30	426.1	20
MA-90	405	9.9	4	4	2	opaque	heterogenous	viscous	40	395.5	20
MA-91	307	7.5	5	3	2	opaque	heterogenous	viscous	50	373.9	20
MA-92	313	7.6	6	2	2	opaque	heterogenous	viscous	60	457.9	20
MA-93	405	9.9	7	1	2	cloudy	heterogenous	viscous	70	691.7	20
MA-94	326	7.9	6	1	3	cloudy	heterogenous	viscous	60	476.0	30
MA-95	336	8.2	5	2	3	clear	homogeneous	not viscous	50	408.7	30
MA-96	357	8.7	4	3	3	clear	homogeneous	not viscous	40	348.4	30
MA-97	415	10.1	3	4	3	cloudy	heterogenous	viscous	30	304.0	30
MA-98	494	12.1	2	5	3	cloudy	heterogenous	viscous	20	241.1	30
MA-99	637	15.6	1	6	3	clear	homogeneous	not viscous	10	155.7	30
MA-100	574	14.0	1	5	4	clear	homogeneous	not viscous	10	140.1	40
MA-101	379	9.2	2	4	4	clear	homogeneous	not viscous	20	184.6	40
MA-102	351	8.5	3	3	4	cloudy	heterogenous	viscous	30	256.4	40
MA-103	378	9.2	4	2	4	clear	homogeneous	viscous	40	369.0	40
MA-104	359	8.7	5	1	4	clear	homogeneous	viscous	50	437.1	40
MA-105	327	8.0	4	1	5	clear	homogeneous	viscous	40	318.8	50
MA-106	397	9.7	3	2	5	clear	homogeneous	viscous	30	290.5	50
MA-107	400	9.7	2	3	5	clear	homogeneous	not viscous	20	194.9	50
MA-108	578	14.1	1	4	5	clear	homogeneous	not viscous	10	141.2	50
MA-109	502	12.3	1	3	6	clear	homogeneous	not viscous	10	122.6	60
MA-110	359	8.8	2	2	6	clear	homogeneous	not viscous	20	175.1	60
MA-111	322	7.9	3	1	6	cloudy	homogeneous	not viscous	30	235.6	60
MA-112	321	7.8	2	1	7	clear	homogeneous	viscous	20	156.6	70
MA-113	614	15.0	1	2	7	c;ear	homogeneous	viscous	10	150.1	70
MA-114	441	10.8	1	1	8	clear	homogeneous	not viscous	10	107.5	80

Note: The best portion of cocktail mixture

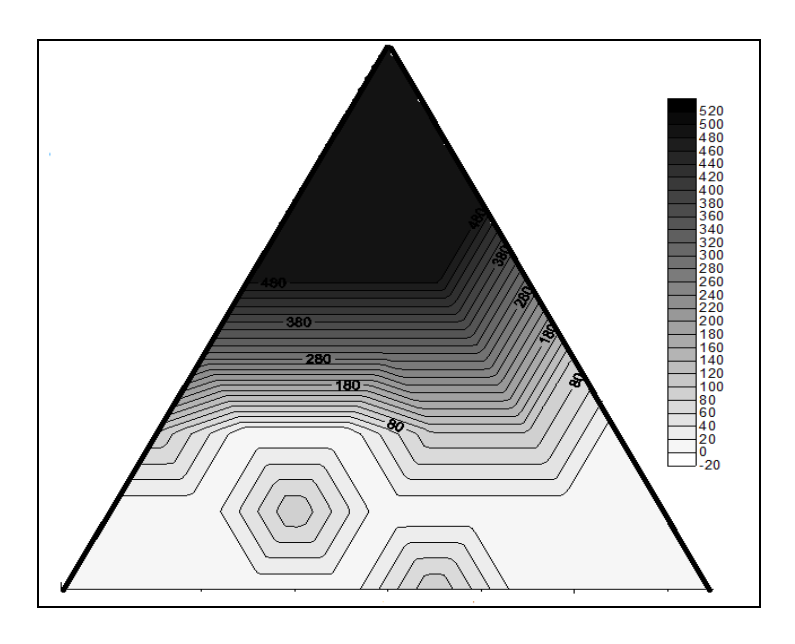


Figure 2(a): Appearance

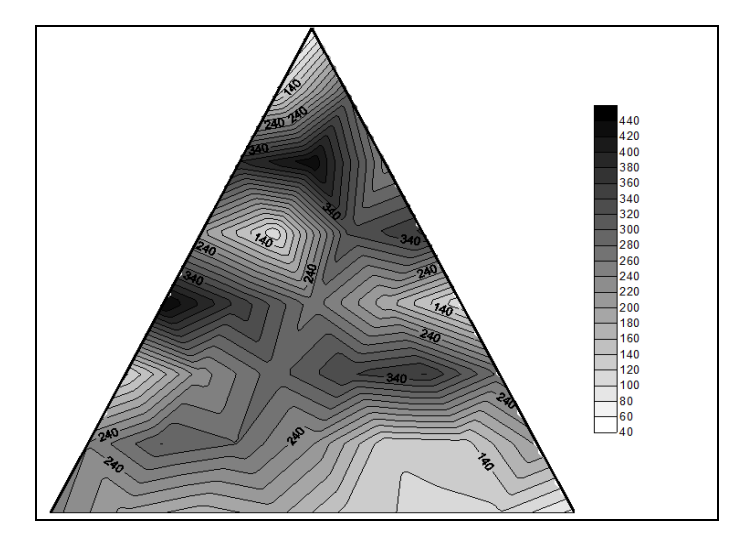


Figure 2(b): Merit Value

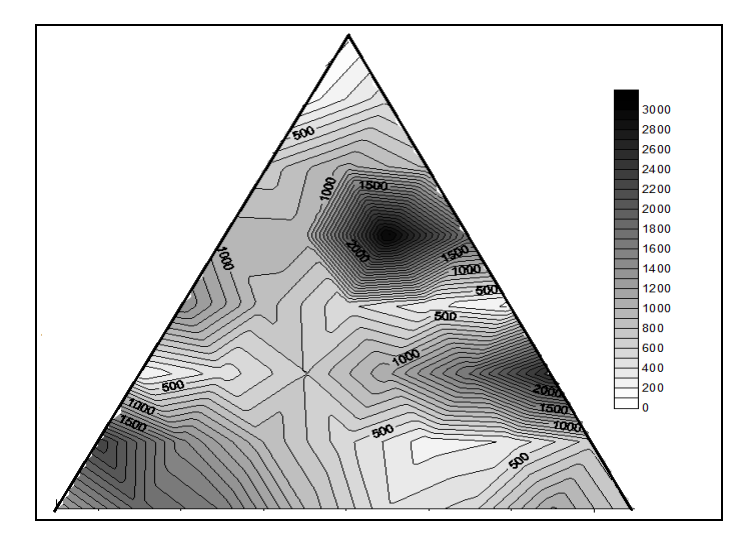


Figure 2(c): Count Rates of ³H

From Figures 2(a), (b) and (c) are the contour for appearance, merit value and count rate of ³H for 36 vials. It gives clear indication of the best appearance, merit value and count rate.

Conclusion

This instrument, LSC Packard TRICAB 2700 used ¹⁴C for its calibration. The best discriminator setting for alpha/beta counting obtained in this study is 120 with 1.45:1.63 percentage ratio of alpha/beta spillover. The best proportion for the scintillation cocktail is found to be 2:4:4 for water, toluene, and triton N-100 with 4 g/L PPO and 0.4 g/L POPOP.

Acknowledgement

The authors would like to thank Malaysian Nuclear Agency for allowing the project to be carried out at Malaysian Nuclear Agency (NM) laboratory in Bangi.

References

- 1. Packard, (1994) Liquid Scintillation Counter (TRICAB 2700) Manual.
- 2. UNSCEAR (1993) Ionizing Radiation: Sources and Effects of Ionizing Radiation. United Nations Scientific Committee on the Effects of Atomic Radiation. Report to the General Assembly, with Scientific Annexes. United Nations Sales Publication E.94.IX.2.United Nations, New York.
- 3. WHO, (1993). Guidelines for Drinking Water Quality. Second ed., Recommendations, vol. 1, World Health Organization, Geneva, Switzerland, pp. 114–121.
- 4. UNSCEAR (United Nations Scientific Committee on the Effects of Atomic Radiations), (2000). Sources and effects of ionizing radiation. Report to the General Assembly, United Nations, New York.
- 5. Malanca, A., Repetti, M., Macedo, H.R., (1998). Gross alpha and beta-activities in surface and ground water of Rio Grando do Norte, Brazil. *Inter J. Appl. Radiat.and Isotopes.* **49** (7), 893–898.
- 6. Terlikowska T, D Hainos, P Cassette and T Radoszewski (2000). 'Application of alpha/beta discrimination in liquid scintillation counting for the purity control of ^{99m}Tc medical solutions'. *Appl. Radiat and Isotopes*, **52**, 627-632.

Zaini Hamzah et al: DISCRIMINATOR SETTING AND COCKTAIL PREPARATION FOR ANALYSIS OF ALPHA AND BETA EMITTERS IN AQUEOUS SOLUTION USING LIQUID SCINTILLATION COUNTER

- 7. Shing-Fa Fang *et al* (2006). 'Comparison of Alpha/Beta Separation Performance of Commercially Available Scintillation Cocktails Counting by QuantulusTM 1220 Liquid Scintillation Counter' Division of Health Physics, Institute of Nuclear Energy Research, 1000 Wen-Hua Road, Chiaan Village, Lungtan, Taoyuan, Taiwan, R.O.C.
- 8. Maurizio Forte, Rosella Rusconi, Elisabetta Di Caprio, Silvia Bellinzona and Giuseppe (2000) 'Natural Radionuclides Measurements in Drinking Water by Liquid Scintillation Counting'. ARPA Loambardia, Italy.
- 9. Cantaloub, M. J. Higginbothram, J. Istok and L semprini. (2008) 'Interaction of sample, cocktail and headspace volume when measuring aqueous Radon in small volume. Nuclear Engineering Dept., Oregon State University.
- 10. Van Der Laarse, J.D, (1967) Experience with emulsion counting of tritium, *Inter.J.Appl.Radiat. Isotopes*, 18, 485



SPECTROSCOPIC AND STRUCTURAL STUDY OF A SERIES OF PIVALOYLTHIOUREA DERIVATIVES

(Spektroskopi dan Kajian Struktur Satu Siri Terbitan Pivaloiltiourea)

Siti Aishah Zakaria¹, Siti Hajar Muharam¹, Mohd Sukeri Mohd Yusof^{1,3*}, Wan Mohd Khairul¹, Maisara Abdul Kadir¹ & Bohari M. Yamin²

¹Department of Chemical Sciences, Faculty of Science and Technology, Universiti Malaysia Terengganu, 21030 Kuala Terengganu, Terengganu. ²School of Chemical Sciences and Food Technology, Faculty of Science and Technology, Universiti Kebangsaan Malaysia, 43650 Bangi, Selangor. ³Institue of Marine Biotechnology, Universiti Malaysia Terengganu, 21030 Kuala Terengganu, Terengganu.

*Corresponding author: mohdsukeri@umt.edu.my

Abstract

A series of pivaloylthiourea derivatives, N-(2-nitrophenyl)-N'-(pivaloyl)thiourea (II) and N-(4-nitrophenyl)-N'-(pivaloyl)thiourea (III) were synthesised and characterised by typical spectroscopic methods and single crystal X-ray diffraction. The IR spectra show the important stretching bands for v(N-H), v(C=O), v(C-N) and v(C=S) at around 3300 cm⁻¹, 1600 cm⁻¹, 1300 cm⁻¹ and 700 cm⁻¹, respectively. There are two vital chromophores, C=O and C=S were observed in the UV spectra with maximum absorption at 230 nm and 290 nm, respectively. The crystal structures of (II) and (III) have been determined by single crystal X-ray diffraction analysis. Both of the molecules adopt *cis-trans* configuration with respect to the position of the phenyl and pivaloyl groups relative to the thiono S atom, across their C-N bonds. There is an intramolecular hydrogen bond, N-H⁻⁻O in both molecules that lead to the formation of a pseudo-six-membered ring. In the crystal lattice, the molecules are linked by intermolecular hydrogen bonds N-H⁻⁻S, C-H⁻⁻S and N-H⁻⁻O forming dimer (II) and 3-dimensional network (III). H NMR spectra show chemical shift at δ_H 12.70 – 12.88 ppm and δ_H 10.84 – 10.94 ppm were assigned for both NH proton. Whereas, the chemical shift for ¹³C NMR analysis for C=O and C=S presence at δ_C 179-180 ppm.

Keywords: Thiourea derivatives, Pivaloylthiourea, Crystal structure.

Abstrak

Satu siri terbitan pivaloiltiourea iaitu N-(2-nitrofenil)-N'-(pivaloil)tiourea (**II**) N-(3-nitrofenil)-N'-(pivaloil)tiourea (**III**) telah berjaya disintesis dan dilakukan pencirian dengan menggunakan kaedah spektroskopi dan kristalografi hablur tunggal sinar-X. Spektra IR menunjukkan regangan penting bagi v(N-H), v(C=O), v(C-N) dan v(C=S) masing-masing pada julat 3300 cm⁻¹, 1600 cm⁻¹, 1300 cm⁻¹ dan 700 cm⁻¹. Terdapat dua kromofor penting dapat diperhatikan di dalam spektra UV iaitu merujuk kepada C=O dan C=S dengan penyerapan maksimum pada 230 nm dan 290 nm setiap satunya. Struktur hablur (**I**) dan (**III**) telah ditentukan dengan analisis kristalografi hablur tunggal sinar-X. Kedua-dua molekul menunjukkan konfigurasi cis-trans bagi kedudukan kumpulan fenil dan pivaloil terhadap kumpulan tiono C=S pada ikatan C-N masing-masing. Terdapat ikatan hidrogen intramolekul N-H $^{--}$ O pada kedua-dua molekul yang membentuk pseudo gelang berahli enam. Pada kekisi hablur, molekul-molekul dihubungkan dengan ikatan-ikatan hidrogen N-H $^{--}$ S, N-H $^{--}$ S dan N-H $^{--}$ O yang membentuk dimer (**II**) dan rangkaian 3-dimensi (**III**). Spektra 1 H NMR menunjukkan anjakan kimia pada δ _H 12.70 – 12.88 ppm dan δ _H 10.84 – 10.94 ppm bagi kedua-dua NH proton. Manakala, anjakan kimia untuk analisis 13 C 13 Po 13 Po

Kata kunci: Terbitan thiourea, Pivaloiltiourea, Struktur hablur

Introduction

The studies on chemical and structural properties of thiourea derivatives have received much attention due to the their wide potential application in pharmaceutical, agriculture and industrial [1-4]. The group N-C=S itself is considered as chemotherapeutic interest and responsible for the pharmacological activity [5]. The thiourea derivatives have been shown to exhibit antitubercular, antithroid, anthelmintic, antibacterial, antifungal, antioxidant, antimalaria, anticorrosion, insecticidal and rodenticidal properties [6-10]. In addition, some derivatives are biologically active, denature proteins and inhibit the formation of micelles [11].

Therefore, the structural and some spectral properties of the title compounds; N-(2-nitrophenyl)-N'-(pivaloyl)thiourea (II) and N-(4-nitrophenyl)-N'-(pivaloyl)thiourea (III) (Figure 1) are discussed in this paper.

Figure 1: Molecular structural representations of N-(2-nitrophenyl)-N'-(pivaloyl)thiourea (**I**), N-(3-nitrophenyl)-N'-(pivaloyl)thiourea (**II**) and N-(4-nitrophenyl)-N'-(pivaloyl)thiourea (**III**).

Materials and Methods

All chemicals and solvents are in analytical grade and were used without further purification as received. Infrared spectra were recorded with Perkin Elmer 100 spectrometer in the region of $400 - 4000 \text{ cm}^{-1}$ using the conventional KBr pellet method for solid samples. UV spectra were recorded using UV-Visible Spectrophotometer Shimadzu model 1601PC and methanol as a solvent in the concentration 10^{-6}M . The wavelength range lies at 200-400 nm. Single crystals data were collected using Bruker SMART APEX 4K CCD with a graphite monochromated Mo K α radiation source. ^{1}H and ^{13}C NMR spectra in DMSO- d_{6} as solvent were measured with a Bruker AVANCE III 400 MHz spectrometer (400.11 MHz for ^{1}H and 100.61 MHz for ^{13}C) at room temperature.

Synthesis of (I), (II) and (III).

A solution of pivaloyl chloride (5.0 g, 4 mmol) and ammonium thiocyanate (3.15 g, 4 mmol) in acetone (10 ml) were stirred for ca. 10 minutes. o-nitroaniline (I) / m-nitroaniline (II) / p-nitroaniline (III) (2.37 g, 2 mmol) in 10 ml of acetone was added dropwise. The solution mixture was put at reflux for 1 h. The resulting solution was poured into a beaker containing some ice cubes. The yellow precipitate was filtered off and underwent product isolation.

N-(2-nitrophenyl)-N'-(pivaloyl)thiourea (I) ($C_{12}H_{15}N_3O_3S$)

Yield 73%; m.p. : 58.4-59.2 °C; ¹H NMR (DMSO- d_6 , 400.11 MHz): $\delta_{\rm H}$ 1.28 (s, 9H, CH₃), $\delta_{\rm H}$ 7.03 (d, 1H, $J_{\rm HH}$ = 8.40 Hz, Ar), $\delta_{\rm H}$ 7.53-7.57 (m, 1H, $J_{\rm HH}$ = 7.80 Hz, Ar), $\delta_{\rm H}$ 7.76-7.79 (m, 1H, $J_{\rm HH}$ = 7.60 Hz, Ar), $\delta_{\rm H}$ 8.079 (d, 1H, $J_{\rm HH}$ = 8.00 Hz, Ar), $\delta_{\rm H}$ 10.94 (s, 1H, NH), $\delta_{\rm H}$ 12.79 (s, 1H, NH). ¹³C NMR (DMSO- d_6 , 100.61MHz): $\delta_{\rm C}$ 26.61 (CH₃), $\delta_{\rm C}$ 40.41 (C), $\delta_{\rm C}$ 125.26, 125.83, 128.27, 130.82, 144.61, 146.65 (Ar), $\delta_{\rm C}$ 180.67 (CS), $\delta_{\rm C}$ 181.59 (CO). Anal. Calcd : C, 57.23; H, 5.37; N, 14.94 %. Found : C, 57.21; H, 5.33; N, 14.89 % .

N-(3-nitrophenyl)-N'-(pivaloyl)thiourea (II) ($C_{12}H_{15}N_3O_3S$)

Yield 78%; m.p. : 68.7-69.1 °C; ¹H NMR (DMSO- d_6 , 400.11 MHz): $\delta_{\rm H}$ 1.27 (s, 9H, CH₃), $\delta_{\rm H}$ 7.67 - 7.71 (m, 1H, $J_{\rm HH}$ = 8.20 Hz, Ar), $\delta_{\rm H}$ 7.97 (d, 1H, $J_{\rm HH}$ = 8.00 Hz, Ar), $\delta_{\rm H}$ 8.10 (d, 1H, $J_{\rm HH}$ = 7.60 Hz, Ar), $\delta_{\rm H}$ 8.74 (s, 1H, Ar), $\delta_{\rm H}$ 10.84 (s, 1H, NH), $\delta_{\rm H}$ 12.70 (s, 1H, NH). ¹³C NMR (DMSO- d_6 , 100.61MHz): $\delta_{\rm C}$ 26.61 (CH₃), $\delta_{\rm C}$ 40.40 (C), $\delta_{\rm C}$ 119.58, 121.29, 130.40, 131.61, 139.66, 148.0065 (Ar), $\delta_{\rm C}$ 180.50 (CS), $\delta_{\rm C}$ 180.63 (CO). Anal. Calcd : C, 57.23; H, 5.37; N, 14.94 %. Found : C, 57.27; H, 5.29; N, 14.92 % .

N-(4-nitrophenyl)-N'-(pivaloyl)thiourea (III) (C₁₂H₁₅N₃O₃S)

Yield 77%; m.p. : 142.9-143.6 °C; ¹H NMR (DMSO- d_6 , 400.11 MHz): $\delta_{\rm H}$ 1.27 (s, 9H, CH₃), $\delta_{\rm H}$ 8.04 (d, 2H, $J_{\rm HH}$ = 8.80 Hz, Ar), $\delta_{\rm H}$ 8.25 (d, 2H, $J_{\rm HH}$ = 8.80 Hz, Ar), $\delta_{\rm H}$ 10.88 (s,1H, NH), $\delta_{\rm H}$ 12.88 (s,1H, NH). ¹³C NMR (DMSO- d_6 , 100.61MHz): $\delta_{\rm C}$ 26.57 (CH₃), $\delta_{\rm C}$ 40.43 (C), $\delta_{\rm C}$ 124.62, 124.67 (Ar), $\delta_{\rm C}$ 179.97 (CS), $\delta_{\rm C}$ 180.75 (CO). Anal. Calcd : C, 57.23; H, 5.37; N, 14.94 %. Found : C, 57.20; H, 5.35; N, 14.98 % .

Results and Discussion

Infrared spectra

The IR spectra show important stretching bands for v(N-H), v(C=O), v(C-N) and v(C=S) in all compounds. A medium intensity bands presence at 3347.58 (I), 3273.25 (II) and 3303.91 cm⁻¹ (III) which corresponds to stretching v(N-H) (Figure 2). The stretching band of v(N-H) (I) has higher frequency compared to compounds (II) and (III) due to the position of electron withdrawing group near to the NH moiety. The strong absorption bands around 1690 cm⁻¹ attributes to the stretching of v(C=O) and it is decreasing in frequencies compared with typical carbonyl absorption (1700 cm⁻¹) [12]. This is resulting from a conjugated resonance of phenyl ring and the formation of intramolecular hydrogen bonding with N-H [13]. The medium stretching vibration of v(C-N) bands are at 1345.88 (I), 1342.19 (II) and 1317.85 cm⁻¹ (III). The medium bands around 740 cm⁻¹ are assigned for stretching v(C=S) modes. From the infrared spectra analysis (Table 1) show that the thiourea moieties were formed for compounds (I), (II) and (III) and in good agreement with previous studies [14-15].

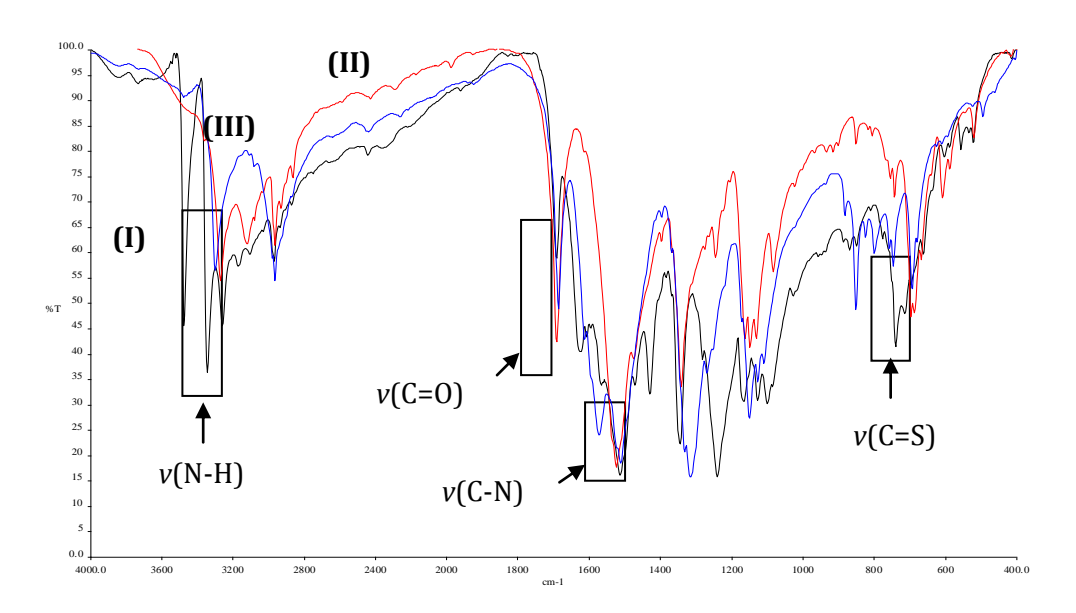


Figure 2: The FTIR spectra of compounds (I), (II) and (III).

Table 1: IR absorption data for compounds (I), (II) and (III).

Compounds	Wavenumber (cm ⁻¹)				
•	v(N-H)	v(C=O)	v(C-N)	v(C=S)	
(I)	3347.58	1692.94	1345.88	741.57	
(II)	3273.25	1692.58	1342.19	744.34	
(III)	3303.91	1686.45	1317.85	747.62	

Ultraviolet spectra

UV absorption for compounds (I), (II) and (III) exhibit $n \to \pi^*$ and $\pi \to \pi^*$ transition (HUMO \to LUMO). The UV spectra show two important bands for chromophores carbonyl (C=O) and thione (C=S) groups. All compounds show maximum absorption bands at 230 nm and 290 nm were assigned for chromophores C=O and C=S respectively. There is a presence of NO₂ band in *para* position (III) with maximum absorption 330 nm (Figure 3). Table 2 shows the maximum absorption for each compounds; (I), (II) and (III) from the UV spectra analysis.

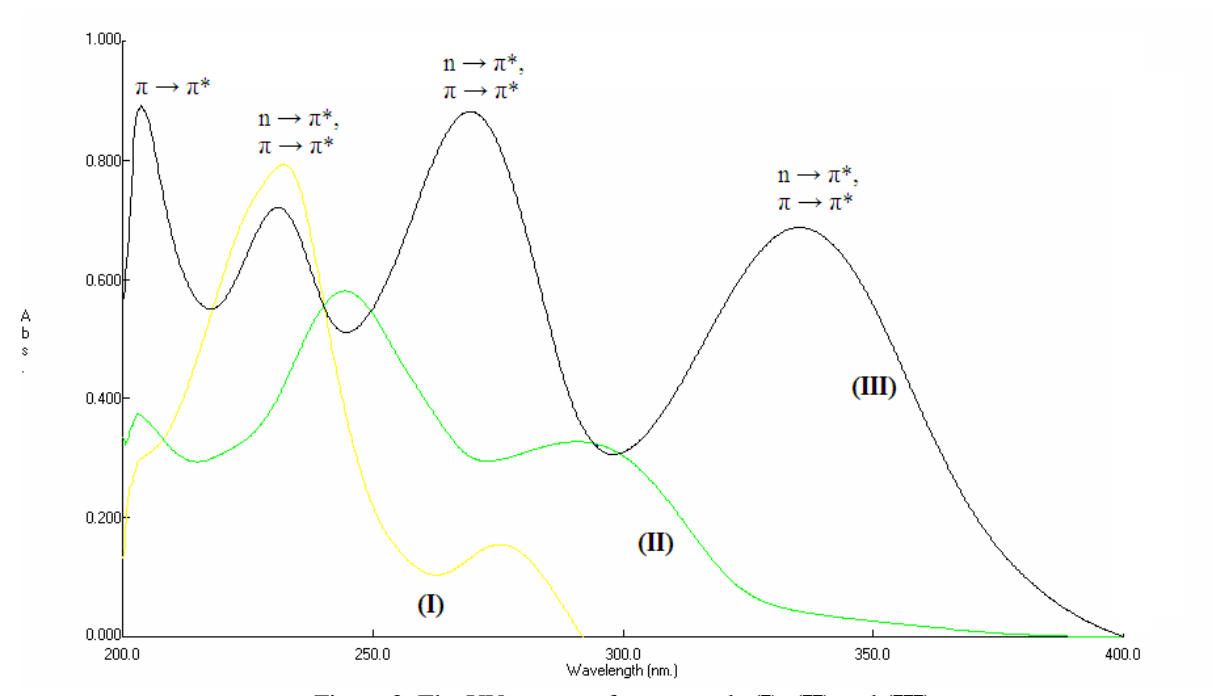


Figure 3: The UV spectra of compounds (I), (II) and (III).

Table 2: UV absorption maximum of compounds (I), (II) and (III).

Compounds	λ^{\max} (nm)			Transition
_	C=O	C=S	NO_2	
(I)	232.2	275.2	-	$n \to \pi^*, \pi \to \pi^*$
(II)	244.4	290.6	-	$n \to \pi^*, \pi \to \pi^*$
(III)	231.6	269.4	335.4	$n \to \pi^*, \pi \to \pi^*$

X-ray Crystallographic Studies

Compounds (**II**) and (**III**) were obtained as a single crystal and suitable for single crystal X-ray diffractometer analysis (Table 3). Both of the molecules are discret and adopt *cis-trans* configuration with respect to *cis* position for phenyl and *trans* position for pivaloyl groups relative to the thiono S atom, across their C-N bonds (Figures 4 & 5). Compound (**II**) shows the plane of carbonyl-thiourea S1/C6/N1/N2/O1/C5 and 3-nitrophenyl are nearly planar with maximum deviation 0.077Å at O2 atom. The dihedral angle of this two plane is 85.64(7)°. However, the plane of carbonyl-thiourea S1/C6/N1/N2/O1/C5 and 4-nitrophenyl of compound (**III**) are more planar with maximum deviation of 0.045 Å at C6 atom. The dihedral angle between these plane is 28.32(8)°.

Table 3: Crystal data for compounds (II) and (III).

Compound	(II)	(III)
Empirical formula	$C_{12}H_{15}N_3O_3S$	$C_{12}H_{15}N_3O_3S$
Formula mass (g mol ⁻¹)	281.33	281.33
Crystal system	Ortorhombic	Monoclinic
Space group	Pna2 ₁	$P2_1/c$
a(Å)	20.400(5)	6.258(2)
$b(ext{Å})$	10.886(3)	10.959(4)
c(Å)	6.2120(15)	20.421(7)
α (°)	90	90
β (°)	90	99.697(10)
γ(°)	90	90
Volume (Å ³)	1379.5(6)	1380.5(8)
Z, density (calculated)	4, 1.355	4, 1.354
(mg/m^3)	,	,
Absorption coefficients	0.242	0.242
(mm^{-1})		
F(000)	592	592
Crystal size (mm)	0.48 x 0.18 x 0.12	0.38 x 0.33 x 0.12
Crystal description	Slab	Slab
Crystal colour	Colourless	Colourless
θ Range (°)	2.00 - 27.48	2.02 - 27.49
Index ranges	$-21 \le h \le 26$	$-8 \le h \le 8$
	$-13 \le k \le 14$	$-14 \le k \le 14$
	$-7 \le 1 \le 7$	$-26 \le 1 \le 26$
Independent reflections	8152 / 3020	15257 / 3157
-	[R(int) = 0.0318]	[R(int) = 0.0401]
Maximum and minimum	0.9715 and 0.8926	0.9715 and 0.9136
transmissions		
Procession method	Full-matrix least-	Full-matrix least-
	squares on F ²	squares on F ²
Data/ restrains/ parameters	3020 / 1 / 172	3157 / 0 / 175
Goodness-of-fit on F ²	1.070	0.905
Largest diff. peak (eÅ ⁻³)	0.281	0.490
Largest diff. hole (eÅ ⁻³)	-0.145	-0.027
R, wR	0.0416, 0.0945	0.0548, 0.1183
R, wR (all reflection)	0.0617, 0.1029	0.0886, 0.1314

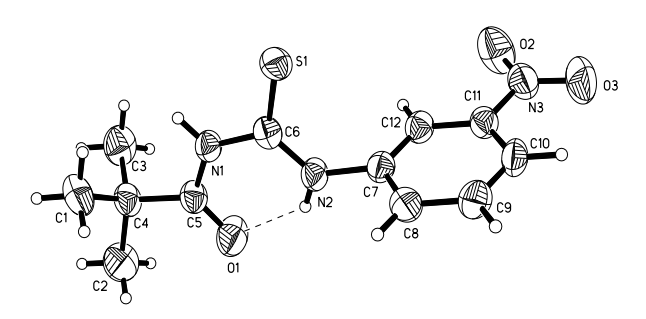


Figure 4: ORTEP drawing for (II) (ellipsoids are plotted at the 50% probability) with intramolecular hydrogen bond.

Siti Aishah Zakaria et al: SPECTROSCOPIC AND STRUCTURAL STUDY OF A SERIES OF PIVALOYLTHIOUREA DERIVATIVES

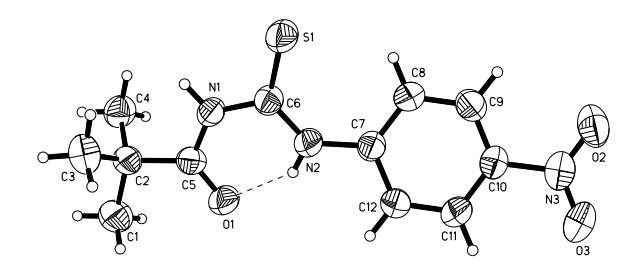


Figure 5: ORTEP drawing for compound (III) (ellipsoids are plotted at the 50% probability) with intramolecular hydrogen bonds.

The bond length and angles (Table 4) are in normal ranges [16] and comparable with other pivaloyl thiourea derivative compounds [17-22]. However, N1-C6 is longer than N2-C6 by 0.053 Å (II) and 0.059 Å (III), similar to the other benzoylthiourea [23-25]. This differences are probably due to the intramolecular hydrogen bonding interaction [13]. The C=S and C=O bond distances for both compounds show the expected full double bond character, while the values of N1-C5, N1-C6, N2-C6 and N2-C7 bond lengths indicate partial double-bond character [26-27]. Thus, the position (i.e., *meta* or *para*) of nitro group on the aryl ring has no significant effect on the bond and angles of the thiourea moiety [28].

Table 4: Selected bond lenght (Å) and angles (°) for compounds (II) and (III).

Compounds	Distances	Bond distances, (Å)	Distances	Angles distances,
(II)	S1-C6	1.668(2)	C6-N2-C7	123.2(2)
. ,	O1-C5	1.222(3)	C5-N1-C6	128.0(2)
	N1-C5	1.377(3)	O2-N3-O3	123.7(3)
	N1-C6	1.386(3)	O2-N3-C11	118.3(2)
	O3-N3	1.217(3)	O3-N3-C11	118.0(3)
	N2-C6	1.327(3)	N2-C6-S1	124.6(2)
(III)	S1-C6	1.652(2)	C5-N1-C6	128.9(2)
	O1-C5	1.222(2)	C6-N2-C7	130.9(2)
	N1-C5	1.382(3)	O2-N3-O3	123.1(2)
	N1-C6	1.390(2)	O2-N3-C10	118.6(2)
	N2-C6	1.337(2)	N1-C6-S1	119.1(2)
	N2-C7	1.413(2)	O1-C5-C2	122.3(2)

There is an intramolecular hydrogen bond in both molecules, NH^{...}O forming a pseudo-six-membered ring (Table 5). Compound (II) has longer distance of N2-H2^{...}O1, 2.605(3) Å compare to (III), the distance of N2-H2^{...}O1 is 2.589(2) Å. This difference indicates an electronic effect and steric effect of the molecules (Valdés-Martínez *et al.*, 1999).

		101 00111	0001100 (11)	(222)*		
Compounds	D	A	D-H	HA	D-H···A	D-H···A
Intramolecular						_
(II)	N2	O1	0.86	1.92	2.605(3)	135°
(III)	N2	O1	0.86	1.85	2.589(2)	143°
Intermolecular						
(II)	N1	S 1	0.86	2.76	3.582(2)	160°
	N2	O2	0.86	2.52	3.197(3)	137°
	C3	S 1	0.96	2.83	3.742(3)	159°
(III)	N1	S 1	0.86	2.87	3.727(2)	174°
	C4	S1	0.96	2 79	3 659(3)	151°

Table 5: Intramolecular and intermolecular hydrogen bond distances (Å) and angles (°) for compounds (II) and (III).

In the crystal lattice, the molecules are linked by intermolecular hydrogen bonds N1-H1⁻⁻⁻S1, N2-H2⁻⁻⁻O2 and C3-H3⁻⁻⁻S1 (**II**) forming a dimer. Whereas for compound (**III**), the intermolecular hydrogen bonds are N1-H1⁻⁻⁻S1 and C4-H4⁻⁻⁻S1 which formed a 3-dimensional network (Figures 6 & 7).

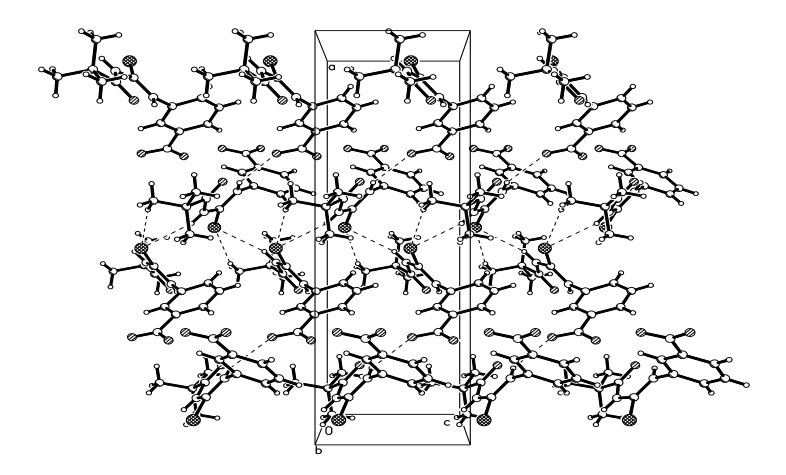


Figure 6: Packing diagram of (\mathbf{II}) , viewed down the b axis. Dashed line denote the intermolecular hydrogen bonds.

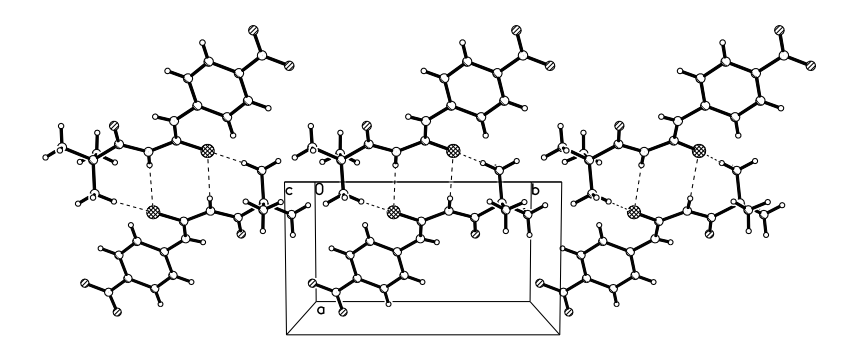


Figure 7: Packing diagram of (III), viewed down the c axis. Intermolecular hydrogen bonds are indicated by the dashed line.

Siti Aishah Zakaria et al: SPECTROSCOPIC AND STRUCTURAL STUDY OF A SERIES OF PIVALOYLTHIOUREA DERIVATIVES

Nuclear Magnetic Resonance

The ¹H NMR and ¹³C NMR spectra are similar and consistent with the structures obtained from single crystal X-ray analysis. The ¹H NMR spectra data showed a sharp singlet peak at $\delta_{\rm H}$ 1.27 ppm (II), (III) and 1.28 ppm (I) correspond to protons of –CH₃. There are multiplet signal at $\delta_{\rm H}$ 7.03 – 8.74 ppm which corresponds to the aromatic protons on phenyl ring in (I), (II) and (III). The two most de-shielded signals are broad and is assigned to NH proton at $\delta_{\rm H}$ 10.94, $\delta_{\rm H}$ 12.79 ppm (I), $\delta_{\rm H}$ 10.84, $\delta_{\rm H}$ 12.70 ppm (II) and $\delta_{\rm H}$ 10.88, $\delta_{\rm H}$ 12.88 ppm (III). These signals are comparable to those found in the similar molecules as reported in previous occasions (Yang *et al.* 2007; Weiqun *et al.* 2004).

The 13 C NMR spectra show a signal for carbon methyl which was observed at $\delta_{\rm C}$ 26.61 ppm (I),(II) and $\delta_{\rm C}$ 26.57 ppm (III). Another signal for carbon bound to methyl group can be seen at $\delta_{\rm C}$ 40.41 ppm (I), $\delta_{\rm C}$ 40.40 ppm (II) and $\delta_{\rm C}$ 40.43 ppm (III). Whereas, the aromatic carbons of the phenyl ring appear around $\delta_{\rm C}$ 119-147 ppm for all compounds. The chemical shift of carbon atom for thione presence at $\delta_{\rm C}$ 180.67 ppm (II), $\delta_{\rm C}$ 180.63 ppm (II) and $\delta_{\rm C}$ 179.97 ppm (III). In addition, carbonyl carbon exhibits as singlet at $\delta_{\rm C}$ 181.59 ppm (II), $\delta_{\rm C}$ 180.63 ppm (II) and $\delta_{\rm C}$ 180.75 ppm (III). In general a chemical shifts for compounds (I), (II) and (III) show no significant difference in proton and carbon NMR analysis.

Conclusion

In this report, the synthesis of three new pivaloyl thiourea compounds (I), (II) and (III) have been carried out and characterised by spectroscopic methods namely infrared (IR), ultraviolet (UV-vis) and nuclear magnetic resonance analysis (NMR). The IR spectra show the important stretching bands for v(N-H), v(C=O), v(C-N) and v(C=S) for (I), (II) and (III). There are two vital chromophores identified as C=O and C=S which are believed responsible to the $n \to \pi^*$ and $\pi \to \pi^*$ transition were observed in the UV spectra for all compounds. The structures of molecules (II) and (III) were determined by single crystal X-ray diffraction analysis. From the analysis, it is obvious that the position *meta* or *para* of nitro group on the aryl ring has no significant effect on the bond and angles of the thiourea moiety.

Acknowledgement

The authors would like to acknowledge the financial support from the Ministry of Science, Technology and Innovation (MOSTI) for the research grants e-science fund 52022 and HRD (S&T) National Science Fellowship (NSF) for postgraduate scholarship.

References

- 1. Kelman, D.R., L.F. Szczepura, K.I. Goldberg, W. Kaminsky, A.K. Hermetet, L.J. Ackerman, J.K. Swearingen, D.X. West. (2002) Structural, spectral and thermal studies of *N*-2-(4-picolyl)- and *N*-2-(6-picolyl)-*N*'-(2-bromophenyl)thiourea. J. Mol. Struct. 610: 143-150.
- 2. Zhong, Z., R. Xing, S. Liu, L. Wang, S. Cai, P. Li. (2008) Synthesis of acylthiourea derivatives of chitosan and their antimicrobial activities in vitro. Carbohydrate Research. 343: 566-570.
- 3. Fontàs, C., M. Hidalogo, V. Salvadó, E. Anticó. (2005) Selective recovery and preconcentration of mercury with a benzoylthiourea-solid supported liquid membrane system. Analytica. Chim. Acta. 547: 225-261.
- 4. Zhang, Y-M., L. Xian, T-B. Wei, L-X. Cai. (2003) *N*-Benzoyl-*N*'-(2-hydroxyethyl)thiourea. Acta. Cryst. E59: o817-o819.
- 5. Bergendorff, O., C.M.L. Persson, C. Hansson. (2004) HPLC analysis of alkyl thioureas in an orthopaedic brace and patch testing with pure ethylbutylthiourea. Contact Dermatitis. 51: 273-277.
- 6. Joseph, M., V. Suni, C.R. Nayar, M.R.P. Kurup, H.-K. Fun. (2004) Synthesis, spectral characterization and crystal structure of 2-benzoylpyridine *N*(4)-cyclohexylthiosemicarbazone. J. Mol. Struct. 705: 63-70.
- 7. Campo, R.D., J.J. Criado, R. Gheorghe, F.J. González. (2004) *N*-benzoyl-*N*'-alkylthioureas and their complexes with Ni(II), Co(III) and Pt(II) crystal structure of 3-benzoyl-1-butyl-1-methyl-thiourea: activity against fungi and yeast. J. Inorg. Biochem. 98: 1307-1314.
- 8. Dong, Y., T.K. Venkatachalam, R.K. Narla, V.N. Trieu. (2004) *N*-Benzoyl-*N'*-(3-pyridyl)thiourea. Bioorg. Med. Chem. Lett. 10: 87-90.

- 9. Mahajan, A., S. Yeh, M. Nell, C.E.J.V. Rensburg, K. Chilale. (2007) Synthesis of new 7-chloroquinolinyl thioureas and their biological investigation as potential antimalaria and anticancer agents. Bioorg. Med. Chem. Lett. 17: 5683-5685.
- 10. Shen, C.B., D.Y. Han, Z.M. Ding. (2007) The inhibition effect of thiourea on bulky nanocrystallized ingot iron in acidic sulfate solution. Mater. Chem. Phys. 109: 417-421.
- 11. Yang, W., W. Zhou, Z. Zhang. (2007) Structural and spectroscopic study on *N*-2-fluorobenzoyl-*N*'-4-methoxyphenylthiourea. J. Mol. Struct. 828: 46-53.
- 12. Rode, J.E., J.C. Dobrowolski., Z. Rzączyńska. (2002) DFT conformation and IR spectra of 1,1-dicarboxycyclobutane. J. Mol. Struct. 642: 147-156.
- 13. Weiqun, Z., L. Baolong, L. Zhu, D. Jiangang, Z. Yong, L. Lude, Y. Xujie. (2004) Structural and spectral studies on *N*-(4-chloro)benzoyl-*N*'-(4-tolyl)thiourea. J. Mol. Struct. 690: 145-150.
- 14. Gambino, D., E. Kremer, E.J. Baran. (2002) Infrared spectra of new Re(III) complexes with thiourea derivatives. Spectrochim. Acta A. 58: 3085-3085.
- 15. Fernández, E.R., J.L. Manzano, J.J. Benito, R. Hermosa, E. Monte, J.J. Criado. (2005) Thiourea, triazole and thiadiazine compounds and their metal complexes as antifungal agents. J. Inorg. Biochem. 99: 1558-1547.
- 16. Allen, F.H., O. Kennard, D.G. Watson, L. Brammer, A.G. Orpen, R. Taylor. (1987) Table of body length determined by X-ray and neutron diffraction. Part I. Body length in organic compounds. J. Chem. Soc. Perkin Trans ii. 1-9.
- 17. Shoukat, N., M.K. Rauf, M. Bolte, A. Badahah. (2007) 1-(2-Chlorophenyl)-3-pivaloylthiourea. Acta Cryst. E63: o920-o922.
- 18. Sultana, S., M.K. Rauf, M. Ebihara, A. Badshah. (2007a) *N*-(3-Bromofenil)-*N*'-pivaloylthiourea. Acta Cryst. E63: o2602.
- 19. Sultana, S., M.K. Rauf, M. Ebihara, A. Badshah. (2007b) *N*-(pyrimindin-2-il)-*N*'-pivaloylthiourea. Acta Cryst. E63: o2674.
- Sultana, S., M.K. Rauf, M. Ebihara, A. Badshah. (2007c) 1-(4-Nitrophenyl)-3-pivaloylthiourea. Acta Cryst. E63: o2801.
- 21. Yusof, M.S.M., N.I.A. Ramadzan, B.M. Yamin. (2006) *N*-(3-phenylthiourea)-*N*'-pivaloylthiourea. Acta Cryst. E62: o5513-o5514.
- 22. Dillen, J., M.G. Woldu, K.R. Koch. (2006a) *N,N*-Di-*n*-butil-*N*'-pivaloylthiourea. Acta Cryst. E62: o4819-o4820.
- 23. Dillen, J., W. Ghebreysus, K.R. Koch. (2006b) N,N-(Heptane-2,6-diyl)-N'-(3,4,5-methoxy-benzoyl)thiourea. Acta. Cryst. E62: o5225-o5227.
- 24. Rauf, M.K., A. Badshah, U. Flörke, (2006a) 1-Benzoyl-3-[3-(trifluoromethyl)phenyl]thiourea. Acta. Cryst. E62: o2452-o2453.
- 25. Saeed, A., U. Flörke. (2006) 1-(2-Chlorophenyl)-3-(4-methylbenzoyl)thiourea. Acta. Cryst. E62: o2403-o2405.
- 26. Rauf, M.K., A. Badshah, M. Bolte. (2006b) 1-(3-Chlorobenzoyl)-3-(2,4,6-trichlorophenyl)-thiourea. Acta. Cryst. E62: 02444-02445.
- 27. Borowiak, T., Dutkiewicz, J.G. Sośnicki, T.S. Jagodziński, P.E. Hansen. (2008) Secondary thioamide group deformations in different surroundings: The case of intramolecular N-H⁻⁻N hydrogen bond An X-ray study combined with theoretical calculations. J. Mol. Struct. 892: 438-445.
- 28. Valdés-Martínez, J., S. Hernández-Ortega, D.X. West, L.J. Ackerman, J.K. Swearingen, A.K. Hermetet. (1999) Structural and spectral studies of *N*-(2-pyridyl)-*N*'-tolylthioureas. J. Mol. Struct. 4278: 219-226.



IONIC LIQUID SUPPORTED ACID-CATALYSED ESTERIFICATION OF LAURIC ACID

(Mangkin Asid Disokong pada Cecair Ionik Sebagai Mangkin dalam Tindak Balas Pengesteran Asid Laurik)

Zalita Yaacob^{1*}, Nor Asikin Mohd Nordin², Mohd Ambar Yarmo¹

¹School of Chemical Science and Food Technology, Faculty of Science and Technology, Universiti Kebangsaan Malaysia, 43600 Bangi, Selangor Darul Ehsan, Malaysia. ²Department of Science, UTM SPACE, Universiti Teknologi Malaysia International Campus Jalan Semarak, 54100 Kuala Lumpur, Malaysia.

*Corresponding author: zalita_y@yahoo.com

Abstract

Ionic Liquid (IL) based on 1-n-butyl-3-methylimidazolium bis(trifluoromethylsulfonyl)imide (BMI.NTf₂) under acidic condition was used as catalyst for the esterification reaction of fatty acid. Various acids namely sulphuric acid, perchloric acid, p-toulene sulphonic acid and various chloride salts such as zinc chloride (ZnCl₂) and iron(III) chloride (FeCl₃) immobilized in ionic liquid BMI.NTf₂ gave acidic ILs. These acidic ILs were tested as catalysts for esterification reactions. Esterification of alcohol (methanol) with fatty acid (lauric acid) using ionic liquid BMI.NTf₂ combined with H_2SO_4 (BMI.NTf₂(H_2SO_4)) gave high activity (>85%) and selectivity (100%) observed over a period of 2 hours reaction with reaction temperature 70° C. The ester became easily separated due to IL forming biphasic with product after the reaction where ester accumulated as the upper phase and IL with water produced after reaction at lower phase. Catalytic activities comparison also be studied between acidic ionic liquid BMI.NTf₂ with acidic ionic liquid ChCl·2ZnCl₂ and conventional acid catalyst. These ILs were characterised by using FTIR, NMR and TGA. Results from FTIR were showed no significant difference between ILs with ILs in acidic condition. The TGA curve show BMI.NTf₂ thermal's decomposition is \geq 400°C but when BMI.NTf₂ combination with H_2SO_4 , TGA curve show weight loss increase and becomes unstable. The advantages of ILs as catalyst are "clean process" and "green chemistry" due to its behaviour such as non-volatile, no loss of solvent through evaporation and reduced environmentally impact. This ILs-catalyst system can be recycle for futher reaction.

Keywords: 1-n-butyl-3-methylimidazolium bis(trifluoromethylsulfonyl)imide; Choline chloride; Ionic liquids; Acidic condition; Esterification; Fatty acid

Abstrak

Cecair ionik (IL) berdasarkan 1-n-butil-3-metilimidazolium bis(triflorometilsulfonil)imida (BMI.NTf₂) dalam keadaan berasid digunakan sebagai mangkin dalam tindak balas pengesteran asid lemak. Pelbagai asid seperti asid sulfurik, asid perklorik, asid ptoulena sulfonik dan pelbagai garam klorida seperti zink klorida (ZnCl₂) dan ferum klorida (FeCl₃) dipegunkan pada cecair ionik BMI.NTf₂ menjadikannya ILs berasid. ILs berasid ini diuji sebagai mangkin dalam tindak balas pengesteran. Tindak balas pengesteran alkohol (metanol) dengan asid lemak (asid laurik) menggunakan cecair ILs BMI.NTf₂ kombinasi bersama H₂SO₄ memberikan aktiviti yang tinggi (>85%) dan selektiviti yang tinggi (100%) yang mana diperhatikan pada 2 jam tindak balas pada suhu tindak balas 70°C. Produk ester yang terhasil dapat dipisahkan dengan mudah kerana ILs membentuk bifasa dengan produk selepas tindak balas di mana ester terkumpul pada fasa atas manakala cecair ionik dan air yang terhasil pula terkumpul pada fasa bawah. Perbandingan aktiviti-aktiviti mangkin juga dikaji antara IL BMI.NTf₂ berasid dengan IL ChCl'2ZnCl₂ berasid dan mangkin asid konvensional. ILs ini kemudiannya dicirikan dengan menggunakan FTIR, NMR dan TGA. Keputusan yang didapati daripada FTIR menunjukkan tiada perbezaan antara ILs dengan ILs dalam keadaan berasid. Keluk TGA menunjukkan penguraian terma BMI.NTf₂ adalah ≥400°C tetapi apabila kombinasi BMI.NTf₂ bersama H₂SO₄, keluk TGA menunjukkan kehilangan berat meningkat dan menjadi tidak stabil. Kelebihan menggunakan ILs sebagai mangkin adalah kerana ILs ini

Zalita Yaacob et al: IONIC LIQUID SUPPORTED ACID-CATALYSED ESTERIFICATION OF LAURIC ACID

merupakan "proses bersih" dan "kimia hijau" kerana sifatnya yang tidak meruap, tiada kehilangan pelarut melalui penyejatan dan mengurangkan kesan kepada alam sekitar. Sistem mangkin-ILs ini boleh diguna semula untuk tindak balas berikutnya.

Kata kunci: 1-n-butil-3-metlimidazolium bis(trifluorometilsulfonil)imida; Kolin klorida; Cecair ionik; Keadaan berasid; Pengesteran; Asid lemak

Introduction

Esterification of alcohol with fatty acid is the most important reaction in oleochemical industry. The products, fatty acid esters are used as raw material for emulsifiers or as oiling agents for foods, lubricants for plastics; spin finishes and textiles; paints and ink additives and for mechanical processing; surfactants; personal care emollients and base materials for perfume; Japanese candles, etc [1,2]. Esterification reaction usually uses conventionally homogeneous catalyst such as sulphuric acid, *p*-toulene sulphonic acid or phosphoric acid. There are problems when using conventional catalyst where these acid catalysts are toxic, corrosive, involve expensive separation, hard to remove from product, require large volumes of salt waste during neutralization of homogeneous acid and gave environmentally effect [1,2,3,10].

Ionic liquids (ILs) are liquids referred to a new class of solvents that consists only of ions. Ionic liquids also a green reaction media (catalyst + solvent) [3,4,5]. The using of ILs as a catalyst in esterification reaction will solve the problems of using conventionally homogeneous catalysts. This is because, the special characteristics of ionic liquids which are non-volatile, negligible vapour pressure, hence are not volatile to the environment after evaporation ensure ionic liquids to be more environmentally friendly or clean process (green chemistry) [3,5,6]. Ionic liquids are also non corrosive and an interesting aspect here is that the special solubility characteristic of ionic liquids enables a biphasic with product after reaction [4,10,11]. The catalyst can be easily to be isolated effectively from product and can be reused several times [4,10,11].

In recent years the application of ionic liquids as catalyst in esterification reaction has been widely studied especially imidazolium based ILs, also knowing the modern era of ILs [12]. Esterification reaction commonly uses imidazolium based ILs in acidic condition [7,8]. The classical ionic liquids such as 1-n-butyl-3-methylimidazolium tetrafluoroborate and hexafluorophosphate (BMI.BF₄ and BMI.PF₆) are common ionic liquids used in esterification reaction as catalysts. However, these ionic liquids are not stable under acidic condition and are easily decomposed [8]. In our study, we used ionic liquid 1-n-butyl-3-methylimidazolium bis(trifluoromethylsulfonyl)imide (BMI.NTf₂) under acidic condition after combination with Bronsted or Lewis acids. We also employ ChCl-based ILs or ChCl²ZnCl₂ as catalyst in the esterification reaction of fatty acid. We then make activity comparison of this catalyst with that of ILs BMI.NTf₂ under acidic condition by increasing reaction times. The use of ionic liquid ChCl²ZnCl₂ is being investigated to find what extent is effectiveness when choline chloride based ionic liquids as catalyst in the esterification of lauric acid. This rational is taken because imidazolium based ionic liquids is more expensive than that based on choline chloride [7].

Previous work by Lapis et al. [8] and Sunitha et al. [7] deal with the application of ionic liquid BMI.NTf₂ with choline chloride. While the study involving the use of Lewis acid (chloride salt) combined with an ionic liquid has been carried out by Abbott et al. and Angueira et al. [9,13]. The work done by Lapis et al. reported the application of ionic liquid BMI.NTf₂ in acidic and basic condition on transesterification reaction of soybean oil. They found that, in this process, the acid is almost completely retained in ionic liquid phase and the biodiesel separates from the ionic liquid and the aqueous phase [8]. While Sunitha et al. study about the using of acidic ionic liquid ChCl²ZnCl₂ as catalyst for esterification of long chain carboxylic acids and long chain alcohols typically referred to as 'wax ester' [7]. However, no report has been made regarding the use of ionic liquid BMI.NTf₂ and ChCl²ZnCl₂ in acid or base as catalyst in the esterification reaction of fatty acid.

Experimental

Materials

1-n-butyl-3-methylimidazolium bis(trifluoromethylsulfonyl)imide (BMI.NTf₂) and zinc chloride (98%) were obtained from Merck. Choline chloride (ChCl) (>97%), iron(III) chloride anhydrous and lauric acid (98%) were obtained from Fluka. Sulphuric acid (95-98%) was obtained from ChemAr, perchloric acid (70%) was obtained

from Riedel de Hëin, *p*-toulene sulphonic acid (98.5%) was obtained from Aldrich, stannous chloride anhydrous was obtained from Ajax Chemical and methanol (99.99%) was obtained from Fisher Scientific.

Preparation of Catalysts

BMI.NTf₂ (1.79 ml, 6.17 mmol) was mixed with concentrated sulphuric acid (0.34 ml, 6.17 mmol) with stirring until ionic liquid dissolved in sulphuric acid. Combination BMI.NTf₂ with another acid was carried out the same method. Choline chloride (20 mmol) was mixed with zinc chloride (40 mmol) and heated to 150°C with stirring until a clear colourless solution was obtained.

Characterization Procedures

Ionic liquids were characterized for ionic liquid $BMI.NTf_2$ and the combination H_2SO_4 with $BMI.NTf_2$ by FTIR, 1H NMR and also TGA. The FTIR spectra of ionic liquids were recorded on Perkin Elmer model gx 1605. The 1H NMR spectra of the ionic liquids were recorded after dissolution of the complex in $CDCl_3$ for $BMI.NTf_2$ and D_2O for ChCl with TMS as reference (400 MHz). TGA was performed by Mettler Toledo thermal analyzer. Weights of the samples used were between 20-30 mg and all the samples were heated at $10^{\circ}C/min$ in nitrogen from room temperature up to $500^{\circ}C$.

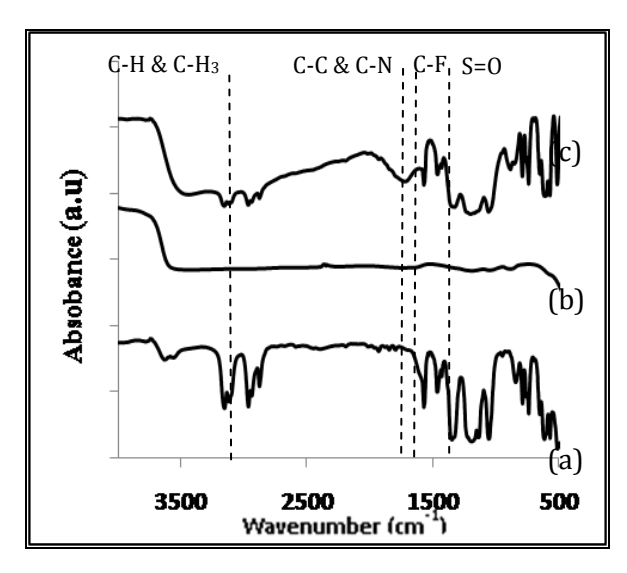
Esterification Procedures

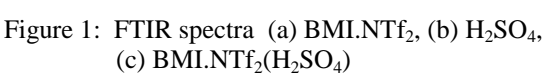
Esterification of lauric acid with methanol was performed in a three-neck flask at atmospheric pressure equipped with a magnetic stirrer bar, thermometer, Dean-Stark receiver, aluminium foil and reflux condenser. The mole ratios for methanol, lauric acid, ILs BMI.NTf₂ and H_2SO_4 are 4:1:0.1:0.1. While the mole ratios for methanol, lauric acid, ChCl and ZnCl₂ are 4:1:1:2 [7]. The reaction temperature was 70° C. The products were determined by gas chromatography (GC-FID, Agilent 6890) using DB-Wax column (30 m) with added internal standard. The parameter for the temperature program is the starting temperature is 100° C (3 min), ramp at 5° C min⁻¹ to 250 (10 min).

Results and Discussion

Characterization using FTIR Technique

Figure 1. shows the FTIR spectra of BMI.NTf₂, H_2SO_4 and BMI.NTf₂(H_2SO_4). While, Figure 2. shows the FTIR spectra of ChCl, $ZnCl_2$ and ChCl 2ZnCl_2 .





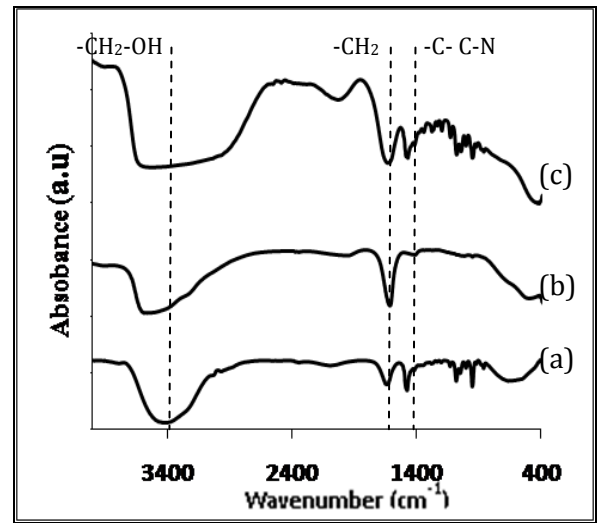


Figure 2: FTIR spectra (a) ChCl, (b) ZnCl₂, (c) ChCl 2ZnCl₂

From Figures 1. and 2. no significant difference was shown, can see that when acids were added to BMI.NTf₂ or choline chloride it is just physical mixture between combined acids and ionic liquids. FTIR spectra from Figure 1. shows a band near 2970 cm⁻¹, indicating C-H and CH₃ stretching (C-H, C-H₃ = 2850 - 2980 cm⁻¹), a band near 1590 cm⁻¹ showing the C-C and C-N stretching (C-C, C-N = 1650 - 1590 cm⁻¹), a band near 1400 cm⁻¹ shows C-F stretching (C-F = 1000 - 1400 cm⁻¹) and a band near 1140 cm⁻¹ shows that the S=O stretching in sulphonamides group (1140 - 1350 cm⁻¹). In Figure 1. when sulphuric acid was added to BMI.NTf₂ a band near 1140 cm⁻¹ is getting broad. This might indicate the presence of sulphuric acid. In Figure 2., FTIR spectra show a band near 3420 cm⁻¹ showing the -CH₂-OH stretching (-CH₂OH = 3250 - 3420 cm⁻¹), a band near 1475 cm⁻¹ showing -C-H₂ stretching (-C-H₂ = 1450 - 1475 cm⁻¹) and a band near 1230 cm⁻¹ shows the presence -C-C-N in amine group (-C-C-N = 1100 - 1230 cm⁻¹).

Characterization using ¹H NMR Measurement

Figure 3. Figure 4. show the 1H NMR (400 MHz, CDCl₃ and D₂O, TMS) spectrum of BMI.NTf₂ and choline chloride respectively. Figure 3. shows the chemical shift at 0.99 ppm (-CH₂-CH₃), 1.40 ppm (-CH₂-CH₃), 1.66 ppm (HOD), 1.90 ppm (-CH₂-CH₂-), 3.97 ppm (CH₃-N-), 4.20 ppm (-CH₂-CN-), 7.29 ppm (CDCl₃ solvent) 7.32 ppm (-N-CH-CH-) and 8.79 ppm (-N=CH-N), respectively. Figure 4., the chemical shifts occured at 3.20 ppm (3CH₃'s in N-CH₃), 3.53 ppm (-N-CH₂-CH₂-), 4.06 ppm (-CH₂-CH₂-OH) and 4.80 ppm (D₂O solvent).

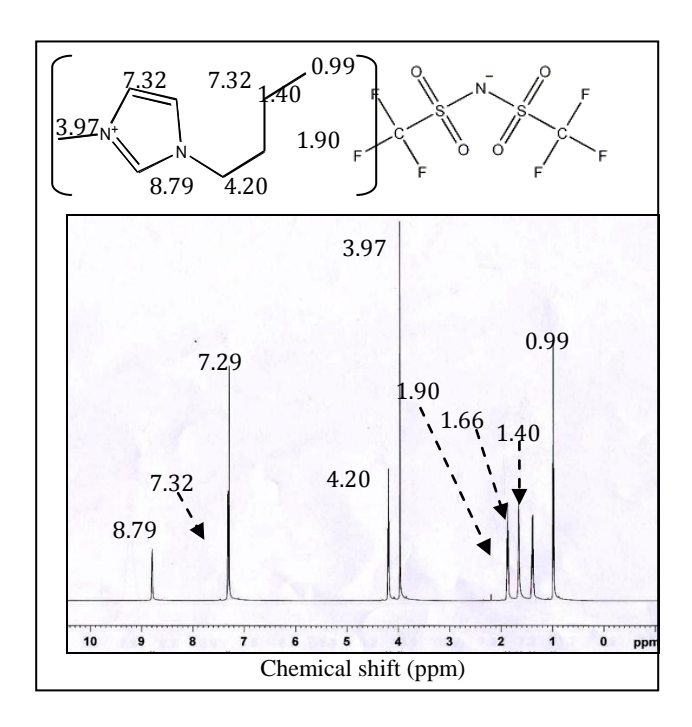


Figure 3. ¹H NMR spectrum of BMI.NTf₂

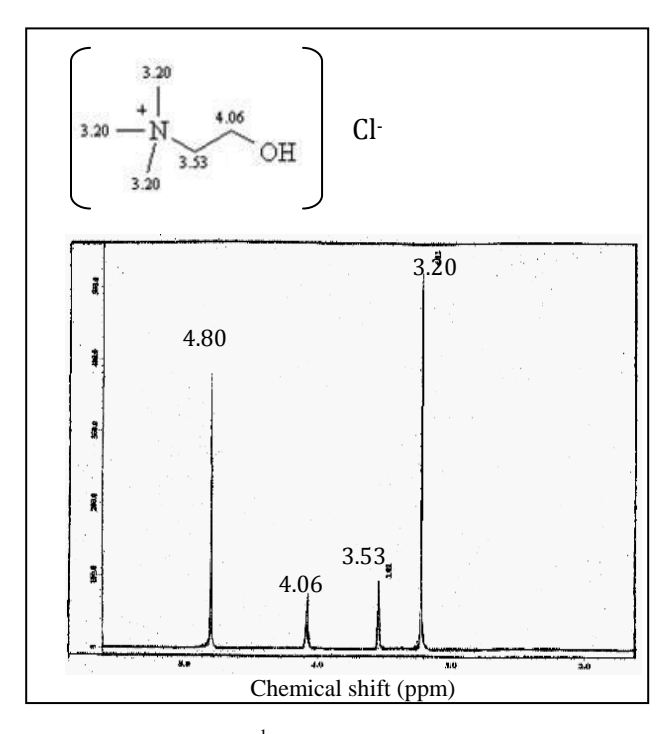


Figure 4: ¹H NMR spectrum of ChCl

Characterization using TGA Technique

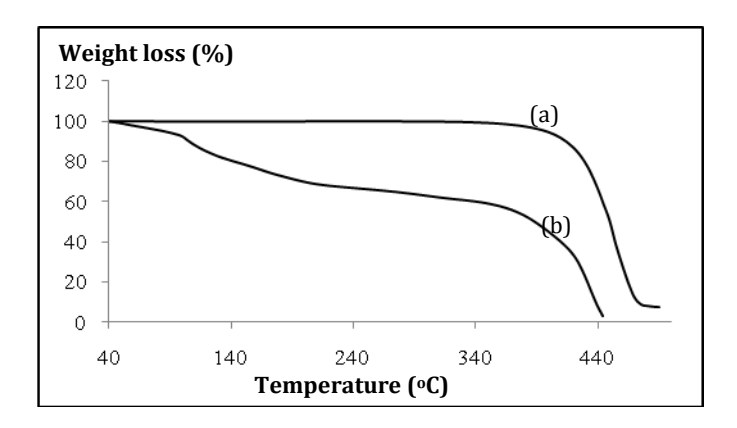


Figure 5: TGA curves of (a) BMI.NTf₂ and (b) BMI.NTf₂(H₂SO₄)

Base of Figure 5. the TGA curves show that the thermal stability of BMI.NTf $_2$ (Figure 5.(a)) is \geq 400°C. This is prove from literature review before that the using ionic liquids immidazolium with anion NTf $_2$ which gives ionic liquids salts with thermal stability of up to 400°C. This occured because of delocalization of the negative charge, the anion and cation is probably less associated and more mobile than triflate anion. However when combining BMI.NTf $_2$ with H_2SO_4 the weight loss slowly increase and making it less stable than pure BMI.NTf $_2$. This is so maybe due to the presence of H_2SO_4 which causes the ionic liquid BMI.NTf $_2$ to be less stable.

Esterification Reaction

Table 1: Esterification of lauric acid with methanol using BMI.NTf₂ combined with H₂SO₄ and ChCl·2ZnCl₂

Entry	Reaction Time [h]	Catalyst (ILs)	Conversion [%]
1	5	BMI.NTf ₂	24.9
2	2	$BMI.NTf_2(H_2SO_4)$	86.8
3	4	$BMI.NTf_2(H_2SO_4)$	88.9
4	5	$BMI.NTf_2(H_2SO_4)$	89.2
5	6	$BMI.NTf_2(H_2SO_4)$	92.2
6	8	$BMI.NTf_2(H_2SO_4)$	90.0
7	5	ChCl	9.0
8	2	ChCl ² ZnCl ₂	9.9
9	4	ChCl ² ZnCl ₂	23.4
10	5	ChCl ² ZnCl ₂	19.5
11	6	ChCl ² ZnCl ₂	36.8
12	8	ChCl ⁻ 2ZnCl ₂	46.3

Reaction condition: Methanol:lauric acid, 4:1, temperature = 70°C

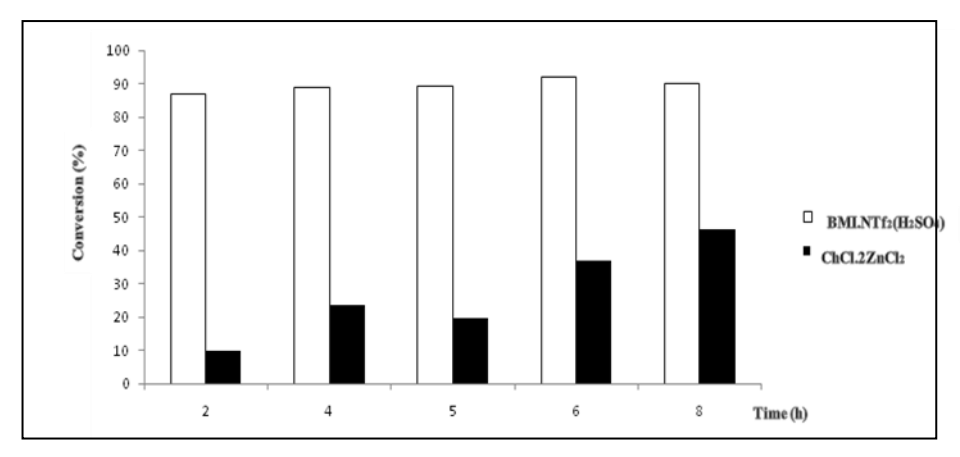


Figure 6. Catalytic activity of BMI.NTf₂(H₂SO₄) and ChCl⁻2ZnCl₂ for esterification of lauric acid

Table 2 Esterification of lauric acid with methanol in combination with various acids to BMI.NTf₂

Entry	Catalyst	Ratio ^a	Conversion [%]
1	H_2SO_4	=	97.8
2	$BMI.NTf_2(H_2SO_4)$	1:1	89.2
3	$HClO_4$	-	97.8
4	BMI.NTf ₂ (HClO ₄)	1:1	71.9
5	PTSA	-	95.9
6	$BMI.NTf_2(PTSA)$	1:1	98.3
7	$ZnCl_2$	-	66.7
8	$BMI.NTf_2(ZnCl_2)$	1:2	84.2
9	$FeCl_3$	-	94.1
10	BMI.NTf ₂ (FeCl ₃)	1:2	76.8

Reaction condition: Methanol:lauric acid, 4:1, temperature= 70°C, 5 hours reaction

^aThe mole ratios of BMI.NTf₂ to Lewis acid/Bronsted acid

Esterification of lauric acid with methanol was carried out using BMI.NTf $_2$ combined with H_2SO_4 (BMI.NTf $_2(H_2SO_4)$) and ChCl $_2ZnCl_2$ (Table 1) with increasing time of reaction and when using conventional homogenous catalyst (Table 2). All selectivity using these catalysts show high selectivity (100%). In Table 1, all BMI.NTf $_2(H_2SO_4)$ show good catalytic activity, (>85%) conversion except BMI.NTf $_2$ without any combination with acid showing result 24.9% conversion. This means H_2SO_4 influenced catalytic activity. From catalytic activity combination of BMI.NTf $_2$ and H_2SO_4 , conversion increased with number of hours of reaction. Catalytic activity of ChCl $_2ZnCl_2$ also increases with time of reaction. Without any combination with $ZnCl_2$, it gives only 9.0% conversion. However, catalytic activity of ChCl $_2ZnCl_2$ for esterification of lauric acid is very low (conversion, 9.0-46.3%) than BMI.NTf $_2(H_2SO_4)$ (conversion, >85%) (see Figure 6). As observed here, catalytic activity using BMI.NTf $_2(H_2SO_4)$ is better than using ChCl $_2ZnCl_2$ in the esterification of lauric acid.

Catalytic activity of combination ionic liquid BMI.NTf₂ with other acid was also carried out (Table 2). When combination BMI.NTf₂ with Bronsted acid and Lewis acid, the catalytic activity shows small decrease compared to using homogeneous acid catalyst without combination with BMI.NTf₂ except combination BMI.NTf₂ with PTSA and FeCl₃, where the conversion increased. As explained here, all acids increase catalytic activity in the esterification reaction compared to catalytic activity using BMI.NTf₂ without any combination.

Conclusion

As conclusion the esterification using ionic liquid BMI.NTf₂ in combination with Bronsted acid and Lewis acid gave high conversion and selectivity. Although these combination ionic liquids showed nearly similar activity as homogeneous acid catalysts, these ionic liquids have their own advantage such as the acid was retained in the ionic liquid phase and easily to separated out because ionic liquid has different phase with product but different with conventional homogeneous acid catalysts. This is because conventional homogeneous acid catalysts are difficult to separate and needs high cost for separation and neutralization. Using these combination ionic liquids has some advantages such as high activity and selectivity like homogeneous catalyst, non-corrosive, ease to separate, easy to prepare, low cost and eco-friendly as these ionic liquids are non-volatile.

Acknowledgements

The authors wish to thank the Ministry of Science, Technology and Innovation (MOSTI) for a fellowship to Zalita Yaacob and research grant UKM-GUP-BTK-08-14-306 to support this research.

References

- 1. Juan, Joon Ching., Zhang, Jingchang & Mohd Ambar Yarmo. 2007. Structure and reactivity of silica supported zirconium sulfate for esterification of fatty acid under solvent-free condition. Applied Catalysis, 332: 209-215.
- 2. Mantri, K., Komura, K. & Sugi, Y. 2005. ZrOCl₂.8H₂O catalysts for the esterification of long chain aliphatic carboxylic acids and alcohols. the enhancement of catalytic performance by supporting on ordered mesoporous silica. Green Chemistry, 7: 677-682.
- 3. Joseph, T., Sahoo, S. & Halligudi, S.B. 2005. Bronsted acidic ionic liquids: a green, efficient and reusable catalyst system and reaction medium for fischer esterification. Journal of Molecular Catalysis, 234: 107-110.
- 4. Wasserscheid, P. & Keim, W. 2000. Ionic liquids new "solutions" for transition metal catalysis. Angew. Chem. Int. Ed, 39:3772 3789.
- 5. Duan, Z., Gu, Y and Deng, Y. 2006. Neutral ionic liquid [BMIm]BF₄ promoted highly selective esterification of tertiary alcohols by acetic anhydride. Journal of Molecular Catalysis A: Chemical, 246: 70-75.
- 6. Wassercheid, P. & Welton, T. 2008. Ionic Liquids in Synthesis. Ed. 2. Vol. 1 & 2. Weinheim: WILEY-VCH Verlags GmbH & Co. KGaA.
- 7. Sunitha, S., Kanjilal, S., Reddy, P.S and Prasad, R.B.N. 2007. Liquid-liquid biphasic synthesis of long chain wax esters using the Lewis acidic ionic liquid choline chloride 2ZnCl₂. Tetrahedron Letters, 48: 6962-6965.
- 8. Lapis, A.A.M., Oliveira, L.F.d., Neto, B.A.D and Dupont, J. 2008. Ionic liquid supported acid/base-catalyzed production of biodiesel. ChemSusChem, 1:759-762.
- 9. Abbott, A.P., Capper, G., Davies, D.L. & Rasheed, R. Ionic liquid based upon metal halide/substituted quaternary ammonium salt mixtures. Inorg. Chem, 43: 3447-3452.
- 10. Zhang, Z.C. 2006. Catalysis in ionic liquids. Adv. Catal, 49: 153-237.
- 11. Welton, T. 2004. Ionic liquids in catalysis. Coordination Chemistry Reviews, 248: 2459-2477.
- 12. Johnson, K.E. 2007. What's an ionic liquid. The Electrochemical Society Interface, Spring, 16: 38-41.

Zalita Yaacob et al: IONIC LIQUID SUPPORTED ACID-CATALYSED ESTERIFICATION OF LAURIC ACID

13. Angueira, E.J and White, M.G. 2007. Super acidic ionic liquids for arene carbonylation derived from dialkylimidazolium chlorides and MCl_3 (M = Al, Ga, or In). Journal of Molecular Catalysis A: Chemical, 277 : 164-170.



A SIMPLE AND COST EFFECTIVE ISOLATION AND PURIFICATION PROTOCOL OF MITRAGYNINE FROM *MITRAGYNA SPECIOSA* KORTH (KETUM) LEAVES

(Satu Protokol Pengasingan Mitragina daripada Daun *Mitragyna speciosa* Korth (Ketum) yang Mudah dan Kos Efektif)

Goh Teik Beng^{1*}, Mohamad Razak Hamdan¹, Mohammad Jamshed Siddiqui², Mohd Nizam Mordi¹ and Sharif Mahsufi Mansor¹

¹Centre of Drug Research, ² School of Pharmaceutical Science, Universiti Sains Malaysia, Minden 11800, Penang, Malaysia.

*Corresponding author: gtb.dd04@student.usm.my

Abstract

The objective of the present study was to develop a simple and cost effective method for the isolation of mitragynine from *Mitragyna speciosa* Korth leaves. The results of our study showed that around 0.088 % (w/w) pure mitragynine was obtained by this newly developed method with a purity of 99.0 % (w/w) based on GC-MS analysis. Moreover, the recovery of the pure mitragynine from the chloroform extract was also more than 95.0 %. Advantages of this new method were simpler, faster and more economical. In conclusion this simple and cost effective method helps to isolate mitragynine with higher purity in comparison with the published methods.

Keywords: Mitragynine speciosa Korth, mitragynine, mitragynine extraction

Abstrak

Objektif kajian ini adalah untuk membangunkan satu kaedah yang mudah dan kos efektif untuk pengasingan mitraginina daripada daun *Mitragyna speciosa* Korth. Keputusan kajian menunjukkan bahawa lebih kurang 0.088 % (w/w) mitraginina tulen telah diperolehi dengan menggunakan kaedah baru yang dibangunkan ini dengan ketulenan 99.0 % (w/w) berdasarkan analysis GC-MS. Malahan, hasil pemerolehan semula mitraginina tulen daripada ekstrak kloroform juga melebihi 95.0 %. Faedah kaedah baru ini adalah lebih mudah, cepat dan ekonomikal. Kesimpulannya, kaedah yang lebih mudah dan kos efektif ini membantu mengasingkan mitraginina dengan ketulenan yang lebih tinggi berbanding dengan kaedah yang telah pun diterbitkan.

Kata kunci: Mitragynine speciosa Korth, mitragina, pengekstrakan mitragina

Introduction

Mitragynine is the main alkaloid present in *Mitragyna speciosa* leaf with opioid agonistic activity [1,2,3,4]. The mitragynine content in *M. speciosa* leaves varied from place to place depending on the geographical location and season [4]. The mitragynine content of Thai *M. speciosa* was 66% of the total alkaloids while the Malaysian species contained only 12% of the total alkaloids [5]. This necessitates finding a simple, fast and reproducible method to obtain mitragynine from Malaysian species of *M. speciosa*.

Currently, several methods are available for the extraction and isolation of mitragynine from *Mitragyna speciosa* leaf. These extraction and isolation methods published have their own advantages and disadvantages. Most of these methods commonly employs soxhlet extraction method using methanol as solvent to obtain the crude extract of *M. speciosa* leaves [6,7,8]. However, these methods were very slow and require days to obtain crude extract of *M. Speciosa*. The extract obtained by these methods were sticky, agglutinated and might need sonication to facilitate the extraction of mitragynine from the crude extracts. Moreover, the process required to obtain pure mitragynine

Goh et al: A SIMPLE AND COST EFFECTIVE ISOLATION AND PURIFICATION PROTOCOL OF MITRAGYNINE FROM *MITRAGYNA SPECIOSA* KORTH (KETUM) LEAVES

from the crude extract was too lengthy and laborious which involves acidification, neutralisation followed by liquid-liquid extraction and finally column chromatography with a series of mobile phase with increasing polarity [6,7,8]. Hence, our main objective of this study is to find a simple and rapid method with maximum output of pure mitragynine from dried leaves of *M. speciosa* as it is not commercially available at cheaper price.

Experimental

Chemicals and solvents

Picric acid, potassium bromide (KBr) and acetanilide were obtained from Sigma-Aldrich, St. Louis, USA. Pure mitragynine standard was obtained from IMR (Institute of Medical Research, Kuala Lumpur, Malaysia). Commercial pure mitragynine standard (ASB-00013890-025) was obtained from Chromadex, Irvin, USA. Solvents hexane, petroleum ether, methanol, acetone, chloroform, ethyl acetate and HCL used were of analytical grade purchased from Fischer Scientific, Loughborough, U.K.

Plant material identification

Leaves of *M. speciosa* were collected from Perlis, Malaysia and were identified by a botanist in the School of Biological Science, Universiti Sains Malaysia (USM). A voucher specimen (No 11074) was deposited at the Herbarium of the School of Biological Science, USM for further references.

Extraction and isolation of mitragynine

Fresh *Mitragyna speciosa* Korth leaves (1.0 kg) were washed with water to remove dirt and adhering material, oven dried at 45-50 °C for three days and milled into fine powder using a blender to get the dry powder (297.0 g). Soxhlet extraction was carried out using 297.0 g powdered leaves with 4 L petroleum ether (40-60 °C) for 8 hour, then petroleum ether solution was discarded and the defatted powdered leaves were dried and the extraction was repeated with 4 L chloroform for 8 hour. The chloroform solution obtained was filtered, concentrated, evaporated to dryness under the reduced pressure using rotary evaporator and was kept in a refrigerator (-20°C). The dried crude chloroform extract was subjected for flash chromatography according to the method of Still *et al.*[10]. Crude fraction containing mitragynine was obtained by eluting with hexane and ethyl acetate (80:20 v/v) and this fraction (100 mL) was subjected to liquid-liquid fractionation using petroleum ether (100 mL X 3 times) for further purification. The petroleum ether layer was discarded and the remaining solution was concentrated under the reduced pressure using a Buchi R215 Rotavapor (Flawil, Switzerland) to obtain crude mitragynine.

Purification of mitragynine by crystallization

Approximately 0.80 g of the isolated crude mitragynine was dissolved in minimum quantity of methanol and this solution was added to a 5 mL saturated methanolic picric acid solution. Side of test tube was scratched and this solution was kept in refrigerator for 20 minutes to obtain orange colored mitragynine picrate crystals. These crystals were filtered, washed with methanol followed by acetone and the melting point of these crystals was determined. The mitragynine picrate crystals were converted to mitragynine free base by dissolving them in hot saturated acetone solution and by adding this solution to an excess of dilute ammonia solution lead to the liberation of free base which was extracted with diethyl ether. This solution was dried to obtain a pale brown, amorphous compound. This compound along with IMR pure standard was subjected for TLC for the comparison of hR_f value.

Qualitative characterisation of mitragynine free base

Various analytical methods such as UV-Visible, IR, NMR, mass spectroscopy, CHN analysis, HPTLC, melting point and determination of dissociation constant were carried out to characterize the isolated pure mitragynine free base. UV-Visible spectroscopy was carried out using Shimadzu UV 160-A double beam spectrophotometer (Kyoto, Japan), the UV spectra of 0.015 ppm pure mitragynine in methanol was obtained against a blank containing methanol. FTIR spectra were recorded using KBr pellets by a Thermal Scientific Nicolet 6700 spectrophotometer with Omnic software (Franklin, USA). ¹H-NMR and ¹³C –NMR were performed using 400 MHz and 100 MHz Bruker spectrometer (Karlsruhe, Germany), respectively. GC-MS spectra were taken using HP 6890A GC system (Santa Clara, USA) with HP-5MS Polyimide coated capillary column (30 m x 0.25 mm i.d. x 0.1 μm), heated from 100°C to 280°C at 10°C / min, 10 Kpa helium at 1.00 mL/min flow rate and an injection volume of I μL with split ratio of 5 : 1. CHN elemental analysis was conducted using Perkin Elmer CHN Analyzer Model 2400-2 (Massachusetts, USA). HPTLC study was performed on a 0.50 mm thick Silica gel 60 G₂₅₄ (10 cm x 20 cm) using a

mobile phase hexane:ethyl acetate (80:20 v/v). TLC plates were then visualized under UV light (254 and 366 nm). Melting point was measured by Koffler Block Electrothermal Melting Point (London, UK) with Acetanilide (113-114°C) as calibration standard. pKa of isolated and purified mitragynine free base was determined by titration method using 0.0001 N HCL with Cyberlab 14 L pH meter (Millbury, USA) in pH modes. In this procedure, 50 mg pure mitragynine in 30 mL methanol was used. The long term stability of the stock solution of mitragynine (1000 ng mL $^{-1}$) refrigerated at -20 °C was tested after storage period of 60 days. The stock was diluted to 1 ng mL $^{-1}$ with pure methanol in three replicates prior to the analysis. The result was expressed as the difference from time t = 0 day. The percentage difference from time t=0 day not exceeded ±15% indicating that the stock solution of mitragynine was stable [11].

Statistical analysis

Results were expressed as the mean \pm S.E.M of three independent experiments. Student's *t*-test was used for statistical analysis; P values < 0.05 were considered to be significant [12]. Statistical calculations were carried out with the Minitab 15.0 English for windows software package.

Results and Discussion

Extraction is an important step involved in the isolation of bioactive compounds from the plants with medicinal value. In our study we followed simple soxhlet extraction method to defat *Mitragyna speciosa* Korth leaves using petroleum ether followed by extraction with chloroform which yielded 7.22 g of crude chloroform extract. It was evident from Table 1 that chloroform extract obtained was pure and rich in mitragynine content (70.0 %) than the methanol extract of the first stage from the published method [6,7,8] with a mitragynine content of only 19.0%. Approximately 0.80 g of crude mitragynine was obtained by flash chromatography of the crude extract followed by liquid-liquid fractionation and the mitragynine in this extract appeared as one single peak in GC-MS with relative purity of 98.0 %. This newly developed method even employed only one step flash chromatography to obtain 98.0 % pure mitragynine (Table. 1) whereas the published methods followed a series of mobile phase to obtain the same result [7]. Thus, this newly developed method required less solvent, incurred less steps and more economical.

Table 1: Comparison of GC-MS purity of mitragynine extracts at various stage between our method and published methods

Stage of	GC-MS Purity	of Mitragynine
Extraction	Using Our Method	Using Published Method [6, 7, 8]
Methanol	-	*19.0
Acid solubilisation	-	
Filtration	-	
Base	-	
neutralization		
Chloroform	70.0	*43.0
First column	92.0	*76.0
Second column	-	96.0
Petroleum ether	98.0	-
washing		
Crystallization	99.0	-

The data is the percentage area of GC-MS based on ca.300.0 g M. speciosa dried leaves at each stage

Results of crystallisation showed that orange colored crystals of mitragynine picrate salt ($ca.\ 0.60\ g.$) obtained from crude mitragynine have a melting point of 220-225 °C. Precipitation of these orange colored crystals leads to the formation of a pale brown, amorphous mass of mitragynine free base ($ca.\ 0.26\ g$). It was very soluble in methanol and gives a very strongly fluorescent solution. The result of TLC study shown that the hR_f (81.9 cm) value of the isolated and purified free base of mitragynine was in accordance with that of IMR pure mitragynine standard

^{*} Results obtained in our lab using published method [6,7,8]

Goh et al: A SIMPLE AND COST EFFECTIVE ISOLATION AND PURIFICATION PROTOCOL OF MITRAGYNINE FROM MITRAGYNA SPECIOSA KORTH (KETUM) LEAVES

(Table 5). Moreover, the purity of the mitragynine obtained by this newly developed method was approximately 99.0 %. In addition, the purified mitragynine showed a single chromatographic peak upon spectroscopic analysis by GC-MS. The spectrum of purified mitragynine ($C_{23}H_{30}N_2O_4$, exact molecular mass = 398.2207) was confirmed with the IMR pure standard and to the NIST 98 mass spectral library. Mitragynine obtained from this newly developed method was 99% pure, when peak area of mitragynine was compared to other minor impurities in the GC-MS analysis (Table 2), and was used as the analytical standard to build the calibration curve (Figure 1) for quantitative analysis.

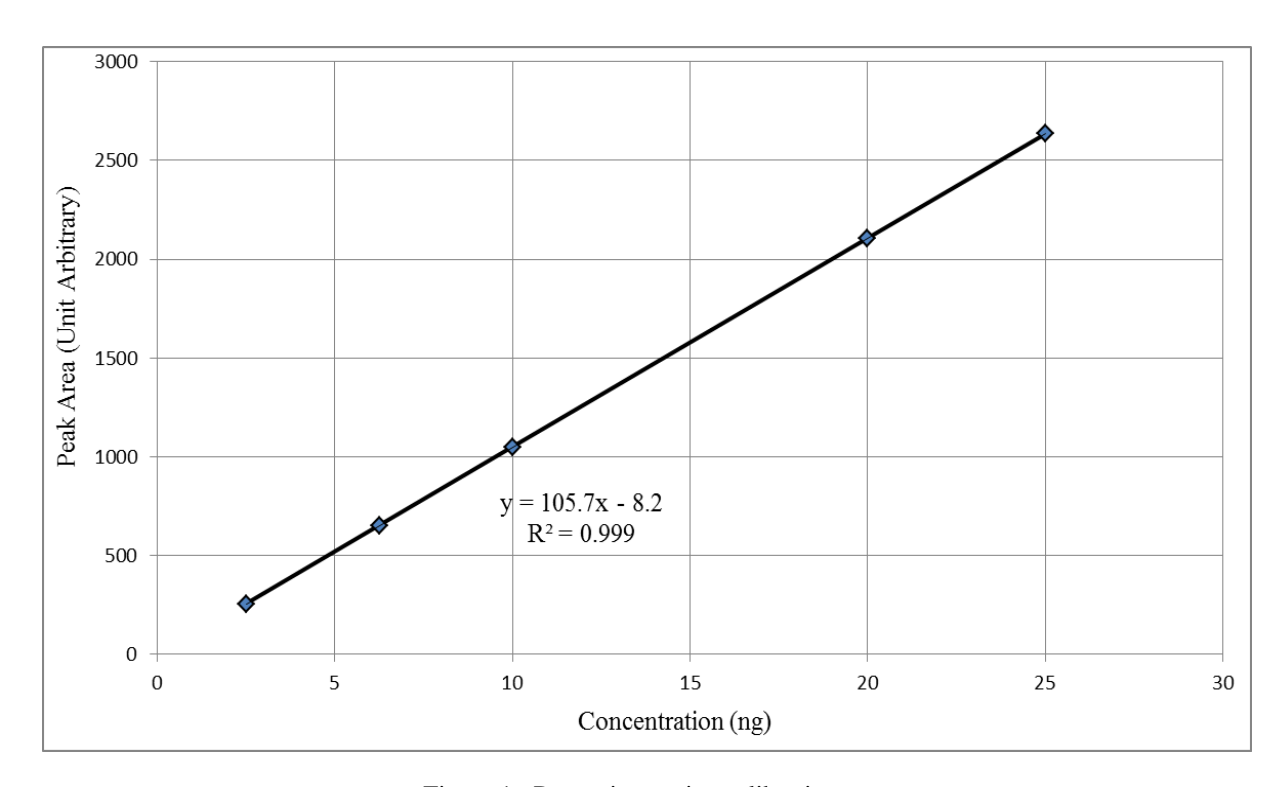


Figure 1: Pure mitragynine calibration curve

The pure mitragynine standard calibration curve was linear with the equation of y=105.7x-8.2 over the range of 0.5-50 ng (n=5, $r^2=0.999\pm0.002$) (Figure 1). The mean coefficients of variation for within day assay precision was 2.33 ± 0.25 % at a concentration range of 0.5-50 ng. For the day to day variation, the mean coefficient of variation was 4.90 ± 0.60 % for the same concentration range. The detection limit (LOD) and quantification limit (LOQ) of assay for mitragynine was 0.50 ng and 2.00 ng respectively. The concentrations giving signal-to-noise ratios of 3:1 and 10:1 were considered to be the LOD and the LOQ respectively.

It is clear from Table 2 that the pure mitragynine obtained (99.0 %) by this newly developed method was stable for six months and its strength was 100 % comparable with that of IMR pure mitragynine standard (Table. 2). The recovery of pure mitragynine from chloroform extract of *M. speciosa* leaves from Perlis, Malaysia by this method was more than 95.0 % at each stage (Table. 3).

Table 2: Comparison of purity and stability of mitragynine obtained by our method and standard mitragynine (Chromadex, Irvin, USA)

Characteristic of	Isolated	Standard mitragynine	
Pure Mitragynine	mitragynine		
Purity (%)	99.0	96.0	
*Purity strength (%)	100.0	98.0	
Stability, 1000 ngmL ⁻¹	0.40	0.30	
Difference from t=0 (ngmL ⁻¹)	,		
after 6 months at -20°C			

^{*}Purity strength (%) was in comparison with IMR standard

Table 3: Recovery (%) of mitragynine from chloroform extract of *M. speciosa* leaves from Perlis, Malaysia by our method.

Type of extract	Actual yield (g)	Theoretical yield (g)	Recovery from chloroform extract (%)
Chloroform	7.22 ± 0.33	-	-
Column chromatography	1.54 ± 0.09	1.55	99.35 ± 0.10
Petroleum ether Washing	0.78 ± 0.06	0.80	97.50 ± 0.12
Crystalization	0.26 ± 0.01	0.27	96.29 ± 0.15

Values are the means of three replicates \pm standard error of the mean (S.E.M.).

From Table 3, it was confirmed that our method is feasible to isolate pure mitragynine. The pure mitragynine (99.0 %) yield obtained by this method was 0.26 ± 0.01 g from ca.300.0 g of M. speciosa dry leaves (Table. 4) and the content of mitragynine we obtained from the M. speciosa leaves of Perlis, Malaysia was 0.088 % w/w (0.88 mg/g of dried leaves). This was within the range of 0.08-0.10% as reported in the literature for leaves extracts of M. speciosa [6, 9].

Table 4: Yields (%) and GC-MS purity (%) of mitragynine obtained from *M. speciosa* leaves of Perlis by our method at each stage.

Stage of extraction	Actual yield (g)	Actual yield (%)	GC-MS Purity (%)
Chloroform	7.22±0.33 ^a	2.60	$70.0 \pm 0.20^{\rm e}$
Column	1.54 ± 0.09^{b}	0.56	$92.0 \pm 0.54^{\rm f}$
Chromatography			
Hexane washing	0.78 ± 0.06^{c}	0.26	98.0 ± 0.32^{g}
Crystallization	0.26 ± 0.01^{d}	0.088	$99.0 \pm 0.25^{\rm h}$

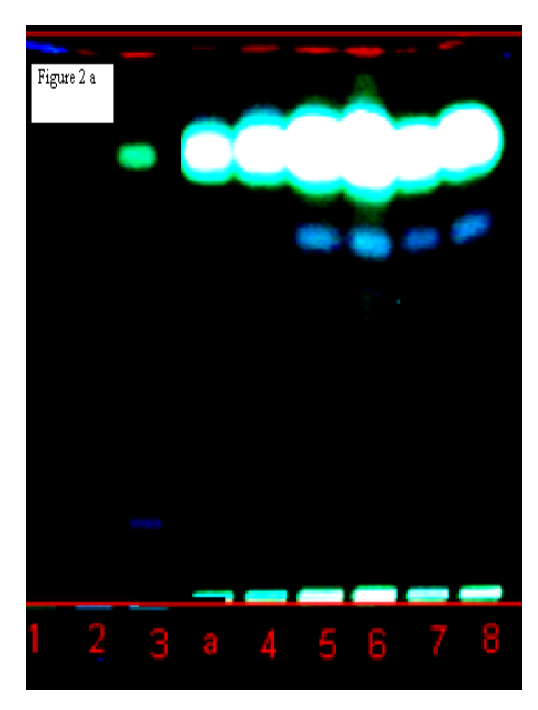
Values are the means of three replicates \pm standard error of the mean (S.E.M). The different alphabet of a,b,c and d represents the values different significantly for the yield obtained whereas the different alphabet e,f,g and h represents the values different significantly for the GC-MS purity at P<0.05 based on Student t-Test Minitab (Illinois USA) (a,b P< 0.05 and e,f P<0.05 in comparison between chloroform extraction and column chromatography, b,c P<0.05 and f,g P<0.05 in comparison between chloroform extraction and column chromatography and hexane washing, c,d P< 0.05 and g,h P<0.05 in comparison between hexane washing and crystallization for both yields and GC-MS purity respectively.

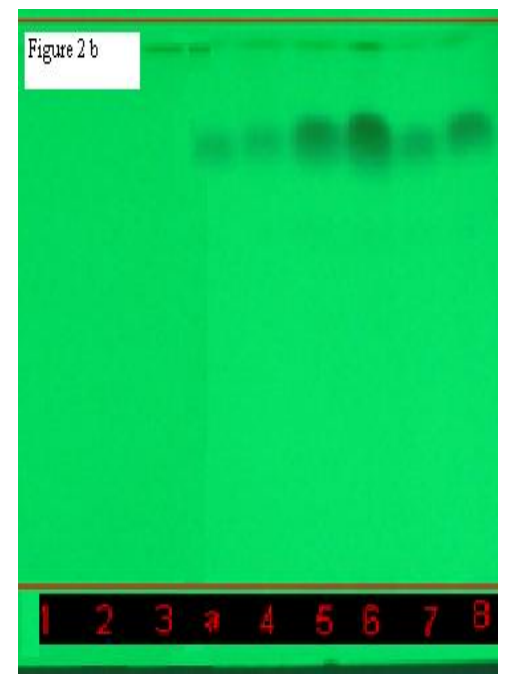
Goh et al: A SIMPLE AND COST EFFECTIVE ISOLATION AND PURIFICATION PROTOCOL OF MITRAGYNINE FROM *MITRAGYNA SPECIOSA* KORTH (KETUM) LEAVES

The details about the HPTLC results of isolated and pure mitragynine are given in Table 5. The hR_f of isolated mitragynine (81.9) was comparable with the hR_f of IMR standard (82.0) which shows that the isolated compound is mitragynine. Figure 2a, 2b shows the HPTLC profile of fractions collected (1-8) from flash chromatography as well as IMR mitragynine standard under UV 365 and 254 nm. It is noted from the Figure 2a and 2b that fractions 1-3 does not contain mitragynine whereas fractions 4-8 containing mitragynine. The hR_f of mitragynine (81.6) present in the fractions 4-8 were in comparison with the hR_f of IMR standard (82.0).

Table 5: HPTLC fingerprint of isolated mitragynine and the standard mitragynine (IMR)

Parameters	TLC conditions / results		
	Isolated mitragynine	Standard mitragynine (IMR)	
Quantity sample applied	2 ul	2 ul	
Detector	12 W VL. 6.1C UV detector	12 W VL. 6.1C UV detector	
	6 W : 254 nm	6 W : 254 nm	
	6 W : 365 nm	6 W : 365 nm	
Stationary Phase	Silica Gel 60G ₂₅₄	Silica Gel 60G ₂₅₄	
Mobile Phase	Hexane: Ethyl acetate (80:20)	Hexane: Ethyl acetate (80:20)	
Applied Concentration, mg/ml	0.03	0.03	
Elution Length, cm	8.0-10.0	8.0-10.0	
hR _{f.} cm	81.9	82.0	
Visual appearance of Band:			
White light	Reddish brown	Reddish brown	
UV 365	Greenish brown	Greenish brown	
UV 254	Brownish	Brownish	
Iodine	Yellowish brown	Yellowish brown	
Dragendorff reagent	Orange	Orange	





Figures 2a and 2b: HPTLC profile of different fractions (1-8) of flash chromatography and standard mitragynine (a) under UV 365 and UV 254 nm.

Mitragynine free base: Yellow amorphous solid. m.p.: $103-105^{0}$ C. pKa = 5.5. UV/Vis λ_{max} (MeOH) nm (log ε): 225 (4.76),290 (3.94). IR (KBr): 1567.2, 1704.5, 3439.3 cm⁻¹. hR_f: 0.82 (C₆H₁₄: EtOOCMe, 80:20). GCMS (EI, 70 eV): m/z (%) = 398 [M $^{+}$] (92), 214. (100),383 (44), 200 (26). CHN: Calcd for C₂₃H₃₀N₂O₄: C, 69.35; H, 7.54; N,7.04. Found C, 69.35; H, 7.50; N, 7.00. 1 H NMR (400 MHz, MeOD): δ 7.68 (1H, br-s, N-H), 7.53 (1H, s, H-17), 6.91 (1H, dd, J=7.9, 7.9 Hz, H-11), 6.89 (1H, d, J=7.9 Hz, H-12), 6.41 (1H, d,J=7.9, H-10), 3.84 (3H, s, 9-OCH₃), 3.78 (3H, s, 17-OCH₃), 3.68 (3H, s, 22-OCH₃), 3.15 (1H, br-d, J=9.8 Hz, H3), 3.07 (1H, m, H-6), 3.04-3.07 (2H, overlapped, H-15, H-21), 2.90-3.00 (2H, overlapped, H-5 and H-6), 2.40-2.55 (3H, overlapped, H-5, H-14, H-21), 1.75-1.80 (2H, overlapped, H-14, H-19), 1.64(1H, br-d,J=11.3, H-20), 1.30(1H, m, H-19), 0.87 (3H, dd, H-18). 13 C NMR (100 MHz, MeOD): 169.36 (C-22), 160.65 (C-17), 154.49 (C-9), 137.33 (C-13), 133.69 (C-2), 121.91 (C-11), 117.72 (C-8), 111.55 (C-16), 107.91 (C-7), 104.26 (C-10), 99.80 (C-12), 61.65 (17-OCH₃), 61.20 (C-3), 57.77 (C-21), 53.85 (C-5), 51.45 (22-COOCH₃), 55.40 (9-OCH₃), 39.95 (C-20), 31.99 (C-15), 29.78 (C-14), 22.78 (C-6), 14.22 (C-19), 12.95 (C-18).

Conclusion

In conclusion, we have developed an alternative method to isolate and purify the mitragynine from *M. speciosa* leaves. The main advantage of this method was simple, fast and cost effective with high reproducibility for the extraction of mitragynine. Morover this method give improved yield of mitragynine (0.088 % w/w) with purity of 99.0 % based on GCMS analysis which was better than the purity of the mitragynine obtained from the other published methods.

Acknowledgements

This work was supported by USM Research University Grant and R&D Initiative Fund, Ministry of Science, Technology and Innovation, Malaysia (MOSTI).

References

- Takayama, H., Ishikawa, H., Kurihara, M., Kitajima, M., Aimi, N., Ponglux, D., Koyama, F., Matsumoto, K., Moriyama, T., Yamamoto, L.T., Watanabe, K., Horie, K. 2002. Studies on the synthesis and opioid agonistic activities ofmitragynine-related indole alkaloids: Discovery of opioid agonists structurally different from other opioid ligands. *Journal of Medicinal Chemistry*, 45: 1949-1956.
- 2. Grewal, K.S. 1932. Observations on the pharmacology of mitragynine. *Journal of Pharmacology and Experimental Therapeutics*, **46**: 251-271.
- 3. Suwanlert, L.S. 1975. A study of Kratom eaters in Thailand. Bulletine on Narcotics, 27: 21-27.
- 4. Shellard, E.J. 1989. Enthnopharmacology of Kratom and the Mitragyna alkaloids. *Journal of Ethnopharmacology*, **25**(1): 123-124.
- 5. Takayama, H. 2004. Chemistry and pharmacology of analgesic indole alkaloids from the Rubiaceous plant, *Mitragyna speciosa. Chemical and Pharmaceutical Bulletin*, **52**(8): 916-928.
- Houghton, P.J., Latiff, A., and Said, I.M. 1991. Alkaloids from *Mitragyna Speciosa*. Phytochemistry, 30: 347-350.
- 7. Ponglux, D., Wongseripipatana, S., Takayama, H., Kikuchi, M., Aimi, M. and Sakai, S. 1994. A new indole alkaloid, 7 hydroxy-7H mitragynine, from *Mitragyna Speciosa* in Thailand. *Planta Medica*, **60**: 580-581.
- 8. Jansen, K.L.R. and Prast, C.J. 1988b. Enthnopharmacology of kratom and the Mitragyna alkaloids. *Journal of Enthnopharmacology*, **23**: 115-119.
- Takayama, H. and Maruyama, T. (2009). Simultaneous analysis of mitragynine, 7-hydroxymitragynine, and other alkaloids in the psychotropic plant "kratom" (Mitragyna speciosa) by LC-ESI-MS. Forensic Toxicology, 27: 67-74.
- 10. Still, W. C.; Kahn, M. and Mitra, A. (1978). Rapid chromatographic techniques for preparative separation with moderate resolution. *Journal of Organic Chemistry*, **43**(14): 2923-2925.
- 11. Janchawee, B., Keawpradub, N., Chittrakarn, S., Prasettho, S., Wararatananurak, P., Sawangjareon, K. 2007. A high performance liquid chromatographic method for determination of mitragynine in serum and its application to a pharmacokinetic study in rats. *Biomedical Chromatography*, **21** (2): 176-183.
- 12. James A. D., John M. F., Graeme A.P., Catherine E. S., Nigel B. P. and Ray A. L. 2010. Seasonal variation of biomass and bioactive alkaloid content of goldenseal, *Hydrastis Canadensis*. *Fitoterapia*, **81**: 925-928.



A STUDY OF NATURAL RADIONUCLIDE ACTIVITIES AND RADIATION HAZARD INDEX IN SOME GRAINS CONSUMED IN JORDAN

(Satu Kajian Mengenai Aktiviti Radionuklida Semulajadi dan Indeks Hazard Sinaran Di Dalam Beberapa Bijirin Yang Di makan di Jordan)

A.A. Tawalbeh^{1*}, K.M. Abumurad², S.B. Samat¹, M.S. Yasir¹

¹ School of Applied Physics, Faculty of Science and Technology, Universiti Kebangsaan Malaysia, 43600 UKM Bangi, Selangor, Malaysia ²Department of Physics, Faculty of Science, Yarmouk University, Irbid, Jordan

*Corresponding author: flower77alaa@yahoo.com

Abstract

Forty samples of different types of imported and locally produced grains consumed in Jordan were analyzed using gamma-ray spectroscopy system with a high Purity germanium (HPGe) detector. The concentrations of the natural radionuclides 238 U, 232 Th and 40 K present in the studied samples were measured, and the radium equivalent activities Ra_{eq} , were calculated. In addition to that, the hazard index HI, was calculated. The average concentrations of 238 U, 232 Th and 40 K were in the range of $(2.0 \pm 0.5) \times 10^{-3}$, $(7.0 \pm 2) \times 10^{-3}$ and 49.93 ± 1.69 ppm, respectively. The values of Ra_{eq} ranged between 17.70 - 245.64 Bq/kg. The HI were ranged between 0.05 - 0.66, which is less than one (the higher limit of HI). The obtained results were compared with the standard accepted international values, and found to be within the acceptable limits.

Keywords: ²³⁸U, ²³²Th and ⁴⁰K, NORM, Grains, Activity concentration, Radium equivalent, Hazard index

Abstrak

Empat puluh sampel daripada pelbagai jenis bijirin tempatan dan yang di import yang di makan di Jordan dianalisis menggunakan sistem spektroskopi sinar gamma dengan pengesan germanium berketulinan tinggi (HPGe). Kepekatan radionuklida, tabii 238 U, 232 Th dan 40 K dalam sampel diukur dan setara radium Ra_{eq} dikira. Selain itu, indeks hazard HI juga dikira. Kepekatan 238 U, 232 Th dan 40 K masing-masing berada dalam julat $(2.0 \pm 0.5) \times 10^{-3}$, $(7.0 \pm 2) \times 10^{-3}$ dan 49.93 ± 1.69 ppm. Nilai Ra_{eq} berkisar antara 17.70 - 245.64 Bq/kg. Indeks HI berkisar antara 0.05 - 0.66, kurang daripada satu (had atas HI). Keputusan yang diperolehi dibandingkan dengan standard di periugkat antarabangsa dan didapati berada dalam julat yang dapat diterima.

Kata kunci: ²³⁸U, ²³²Th dan ⁴⁰K, NORM, Bijirin, Kepekatan aktiviti, Kesetaraan Radium, Indeks Hazard

Introduction

Ionizing Radiation is dangerous to the health, especially the charged particles and the high energy photon [1]. The main natural radioactive sources of ionizing radiation are the long lived ²³⁸U, ²³²Th and their decay series and the ⁴⁰K. The radiological hazard can be the consequence of external or internal exposure. Radionuclides can enter human body through inhalation and ingestion. The ingested radionuclides could be concentrated in certain parts of the body. For examples, ²³⁸U accumulated in human lungs and kidney, ²³²Th in lungs, liver and skeleton tissues and ⁴⁰K in muscles. Depositions of large quantities of these radionuclides in particular organs will affect the health condition of the human such as weakening the immune system, induce various types of diseases, and finally increase in mortality rate. Grain and its products, which is the main component of daily serving such as breads, rice, and pasta, are considered as staple food. Generally, Jordan consumes a large amount of grains (789 × 10³ ton in one year) [2]. Since naturally occurring radioactive materials (NORM) are present in all food commodities, the levels in some grains consumed in Jordan need to be established in order to forecast any possible radiological risk associated

Tawalbeh et al: A STUDY OF NATURAL RADIONUCLIDE ACTIVITIES AND RADIATION HAZARD INDEX IN SOME GRAINS CONSUMED IN JORDAN

with the consumption of the grains. Thus, the main objectives of this research are to quantify the presence of natural radionuclides in some important grains consumed in Jordan, and to estimate the radium equivalent index (Ra_{eq}) and hazard index (HI).

Experimental

Materials

Thirteen types of grains were taken as the sample. All samples used were both local and imported grains and were obtained from local markets. The name of the samples and their number are as follows: rice (9), starch (5), bulgur (4), beans (4), peas (1), lentil (4), chickpea (3), corn (3), lupine (2), fava beans (2), wheat (1), sesame seeds (1) and black seeds (1). This makes the total number of samples collected as forty as shown in Table 1.

Sample Preparation

The samples were prepared for the natural radioactivity measurement. Each dried sample weighing between (300-500 g) was sealed in 500 ml marinelli bottles and kept at room temperature (25 °C) for at least 30 days before counting in to allow reaching the secular equilibrium of ²³²Th and ²³⁸U with their respective decay products, in which the activities of all radionuclide within each series are nearly equal. Each sample was given a code as shown in Table 1.

Natural radioactivity measurement

For each grain Type, a total of 40 samples were prepared for the natural radioactivity measurement. The measurement was conducted for 24 hours using a Ray HPGe – APTEK counting system. The system was calibrated using ⁵⁷Co, ²¹²Pb, ¹⁹²Ir, ²³⁸U, ¹³⁷Cs, ⁶⁰Co and ⁴⁰K, for their known energy (which covers the energy range from 122 keV to 1461 keV) and peak width of gamma-ray emission. The counting efficiency was determined previously for all of its counting geometry. The redionuclides were identified according to their individual photopeak, which are 609 keV (²¹⁴Bi) and 351.9 keV(²¹⁴Pb) for ²³⁸U, 238 keV (²¹²Pb), 583.191 and 510.80 keV, (²⁰⁸Tl) for ²³²Th. And 1460 keV for ⁴⁰K. The activity of ²²⁶Ra during the equilibrium was assumed to be the same as its parent, ²³⁸U. The specific activity for each radionuclide was calculated using equation proposed by Jibiri and Ajao, 2005[3]:

$$A_{s} = {^{C_{n}}}/_{\eta} \gamma_{d} M_{s}$$
 (1)

where A_5 is the specific activity of each radionuclide in the grains in Bq/kg, C_n the count rate in cps, η is the detection efficiency, Y_d is the number of gammas per disintegration of nuclide for a transition and M_s is the mass of the sample in kg.

Using the equation of $A_{R_n} = A_{R_a}$ at secular equilibrium, the daughter activity is equal to that of the parent. In terms of the numbers of atoms of the parent (N_P) and daughter (N_D) , secular equilibrium can be also expressed as [1]:

$$N_p \lambda_p = N_D \lambda_D \tag{2}$$

where λ_{P} are the decay constant of the parent and daughter respectively.

Thus, the concentration of the parent m can be calculated in the sample from the relation [4].:

$$m = \frac{N_p}{N_{av}} \times M \tag{3}$$

where N_{av} is the Avogadro's number (6.022 x 10^{23} atom/ mol), M is the mass number of the parent nucleous.

From above two equations 2 and 3, and substitution the values of half- lives we get the concentrations of the radioisotopes in the unit of mg/kg = 1 part per million (ppm), as follows:

$$m (^{238}\text{U}) = 0.08 \times A_U$$
 (4)
 $m (^{232}\text{Th}) = 0.246 \times A_{Th}$ (5)
 $m (^{40}\text{K}) = 0.038 \times A_K$ (6)

where m is the concentration of the parent nuclides in the unit of ppm, A is the specific activity in the unit of Bq/kg. The specific activity of 40 K for example is well documented [5].

Radium equivalent index (Ra_{eq})

The radium equivalent activity (Ra_{eq}) concept allows a single index or number to describe the gamma output from different mixtures of 238 U (i.e., 226 Ra) 232 Th, and 40 K in a Material [6]. Ra_{eq} for each sample in Bq/kg, is calculated using the following formula proposed by UNSCEAR [7] in Bq/kg.

$$Ra_{eq} = A_{Ra} + 1.43 A_{Th} + 0.077 A_{K}$$
 (7)

where $A_{R\alpha}$, A_{Th} and A_{K} in Bq/kg are the activity concentration of 226 Ra, 232 Th, and 40 K, respectively.

Table1: List of the collected samples and their codes

Sample	Name	Symbol	Sample	Name	Symbol
1	U.S.A Rice ₁	UsRi ₁	21	Lebanese Beans	LeBe
2	U.S.A Rice ₂	$UsRi_2$	22	Argentina Beans	ArBe
3	U.S.A Rice ₃	UsRi ₃	23	Brazilian Peas	BrPe
4	U.S.A Rice ₄	UsRi ₄	24	Jordanian Lentil	JoLe
5	Italian Rice ₅	It Ri	25	Turkish Lentil	TuLe
6	Australian Rice	AuRi	26	Lebanese Lentil	LeLe
7	Pakistani Rice	PaRi	27	Canadian Lentil	Ca Le
8	Indian Rice	InRi	28	Jordanian Chickpea	JoCh
9	Egyptian Rice	EgRi	29	Turkish Chickpea	TuCh
10	Jordanian Starch	JoSt	30	Lebanese Chickpea	LeCh
11	Qatari Starch	QaSt	31	Jordanian Corn	JoCo
12	Lebanese Starch	LeSt	32	Lebanese Corn	LeCo
13	Turkish Starch	TuSt	33	Argentina Corn	ArCo
14	Italian Starch	ItSt	34	Jordanian Lupine	JoLu
15	Jor/ Bulgur/ White	$JoBu_1$	35	Turkish Lupine	TuLu
16	Jor/Bulgur/ Red	$JoBu_2$	36	Jor/Fava beans	JoFa
17	Leb/Bulgur/ White	$LeBu_1$	37	Syrian Fava beans	SyFa
18	Leb/Bulgur/Red	$LeBu_2$	38	Jordanian Wheat	JoWh
19	Jordanian Beans	JoBe	39	Jor/Sesame Seeds	JoSe
20	Brazilian Beans	BrBe	40	Jor/ Black Seeds	JoB1

Hazard index

This index is used to estimate the level of Υ - radiation hazard associated with the natural radionuclides in grains samples. The hazard index (HI) is calculated from the equation [8]:

$$HI = A_{Ra}/370 + A_{Th}/259 + A_{K}/4810 \le 1.$$
 (8)

and Fig. 3 respectively. In Fig. 4, Fig. 5 and Fig. 6 the concentration of the parent nuclides of the natural radioactive series for each sample had been calculated in the unit of ppm. The average concentrations of ²³⁸U, ²³²Th and ⁴⁰K were in the range of $(2.0 \pm 0.5) \times 10^{-3}$, $(7.0 \pm 2) \times 10^{-3}$ and 49.93 ± 1.69 ppm, respectively. The concentration of 238 U ranged from 0.0033± 0.0006 to 0.0012± 0.0002 ppm. In general the measured concentration values of ²³⁸U lies within the acceptable values $8 \times 10^{-5} - 3.3 \times 10^{-2}$ ppm as was reported in [9] except in Jordanian sesame seed sample in which the concentration of 238 U was found to be 0.0033 ± 0.0006 ppm, which is the highest permissible limit allowed. The highest concentration of 232 Th (0.010 ± 0.002) ppm was found in JoBe sample, while the lowest concentration (0.002±0.001) ppm was found in ArBe sample. A result of the ²³²Th concentration measurements in all samples lies within the acceptable value, which should be less than 0.02 ppm for safe use[9]. The maximum value of ⁴⁰K concentration was found in ArBe with a value of 123.57±2.56 ppm. The lowest concentration was found in ItRi with a value of 8.90±0.89 ppm. ⁴⁰K concentration is comparable with the results of other researchers and lies within the acceptable value, which is less than 133 ppm for safe consumption.[7].

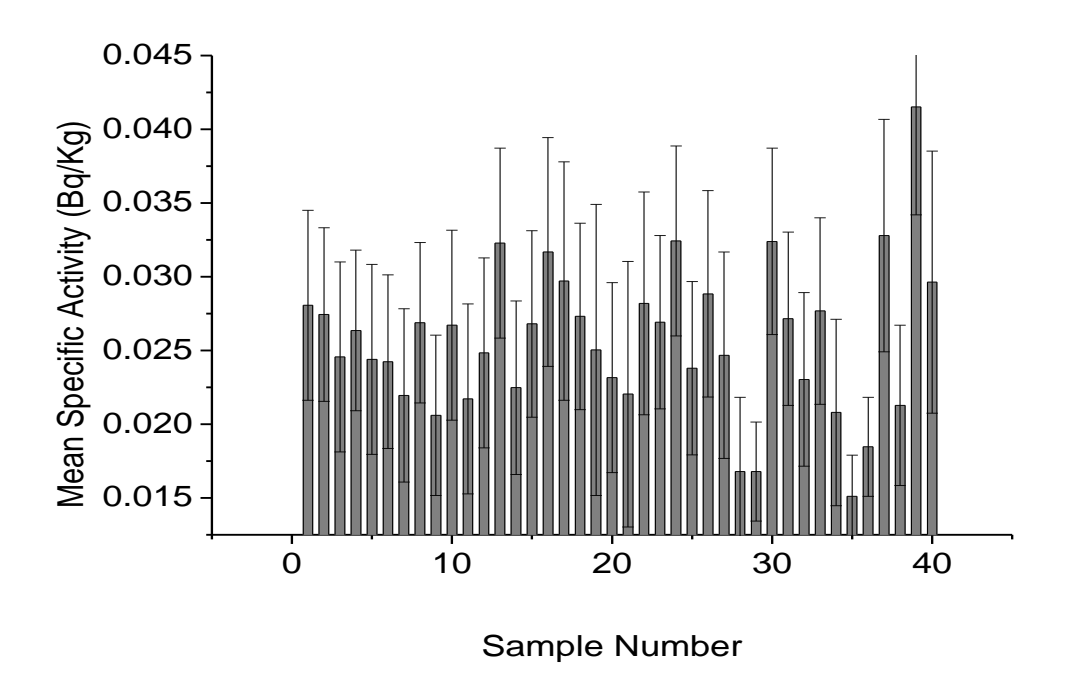


Figure 1: ²³⁸U mean specific activity of the studied samples in the units of Bq/kg.

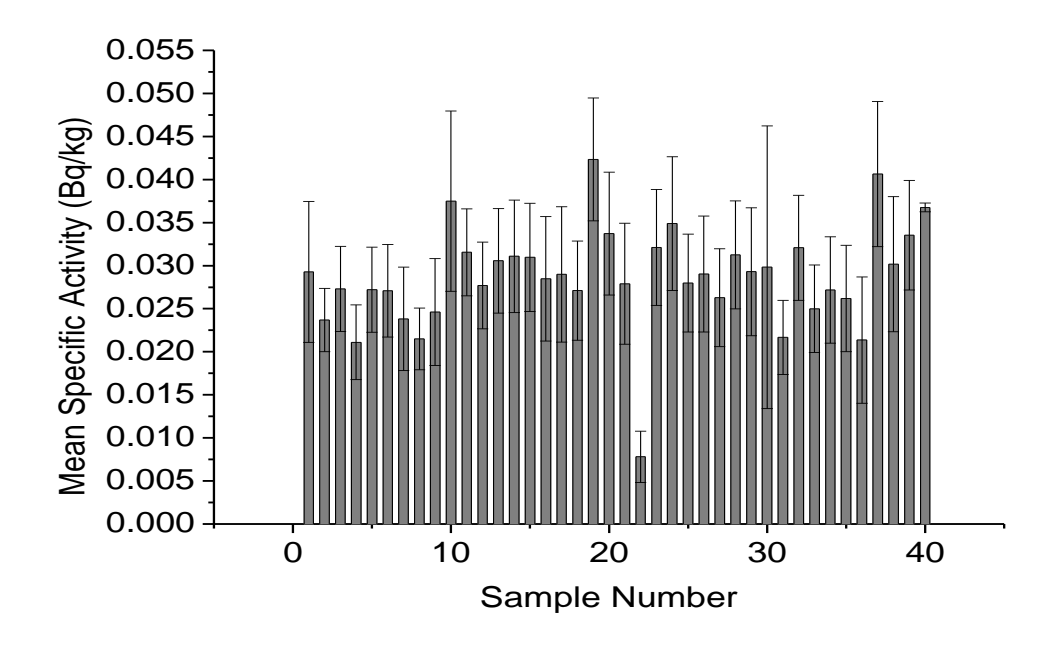


Figure 2: ²³⁸Th mean specific activity of the studied samples in the units of Bq/kg.

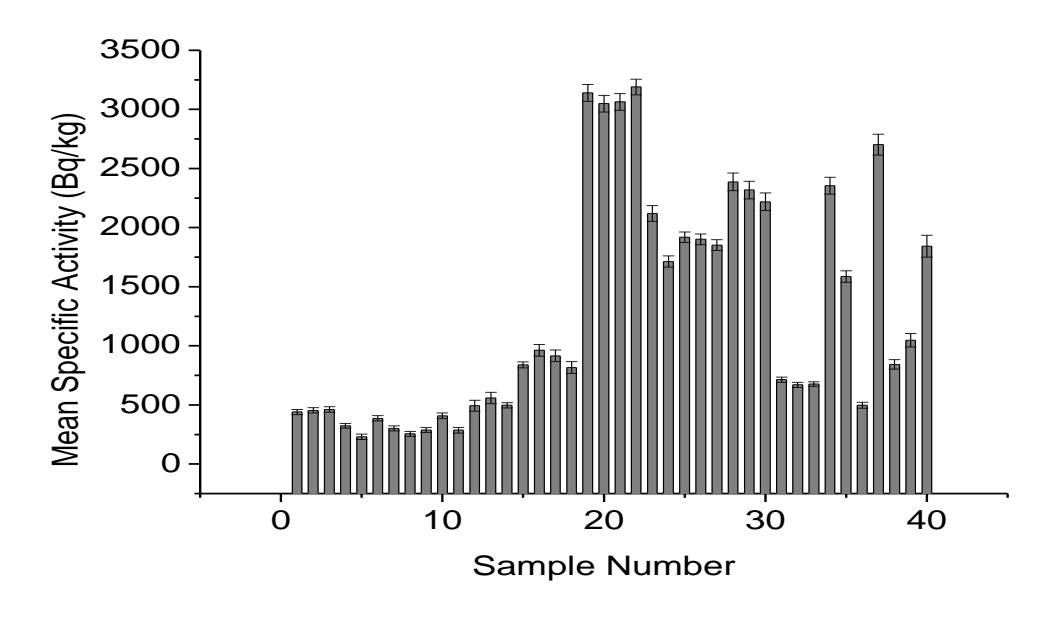


Figure 3: ⁴⁰K means specific activity of the studied samples in the units of Bq/kg.

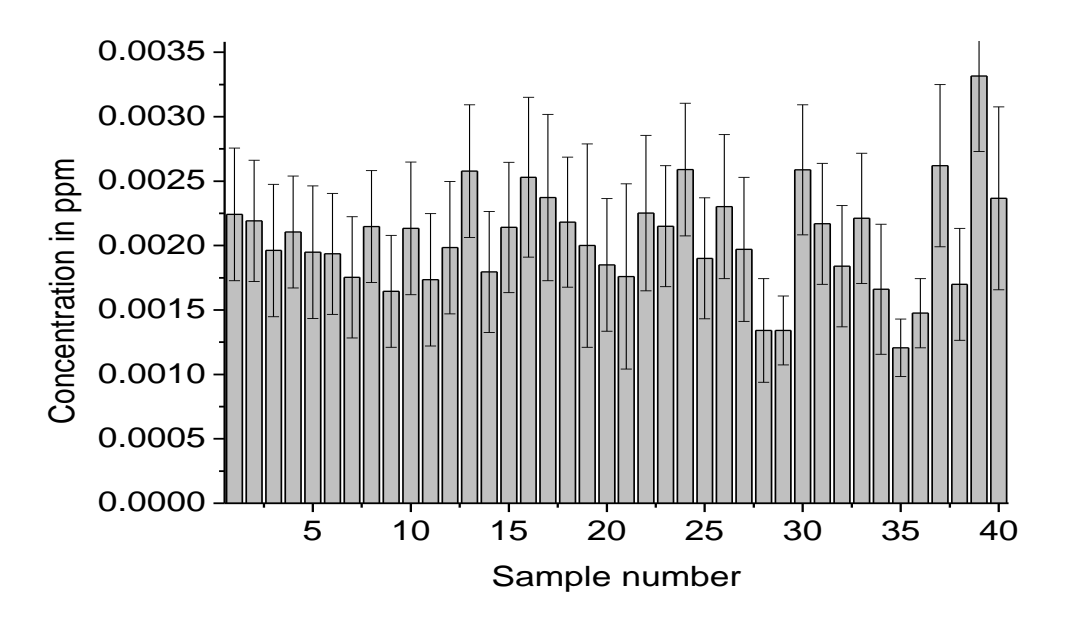


Figure 4: ²³⁸U concentration of the studied samples in the unit of ppm.

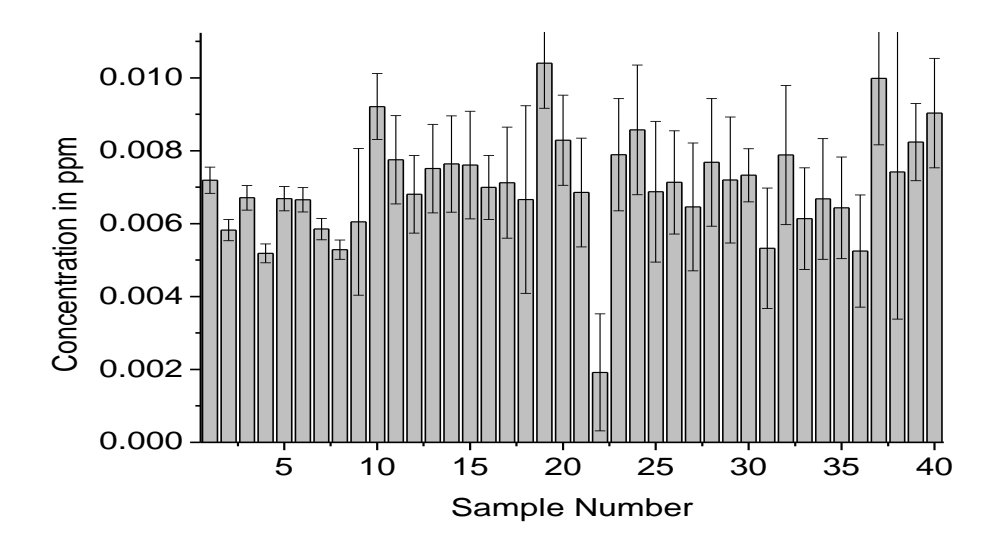


Figure 5: ²³⁸Th concentration of the studied samples in the unit of ppm.

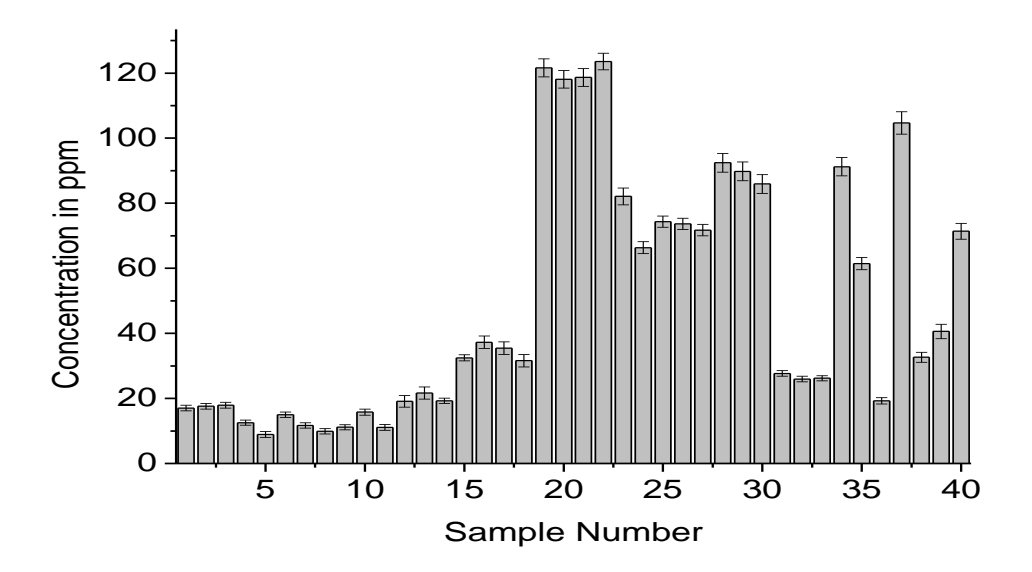


Figure 6: 40K concentration of the studied samples in the unit of ppm

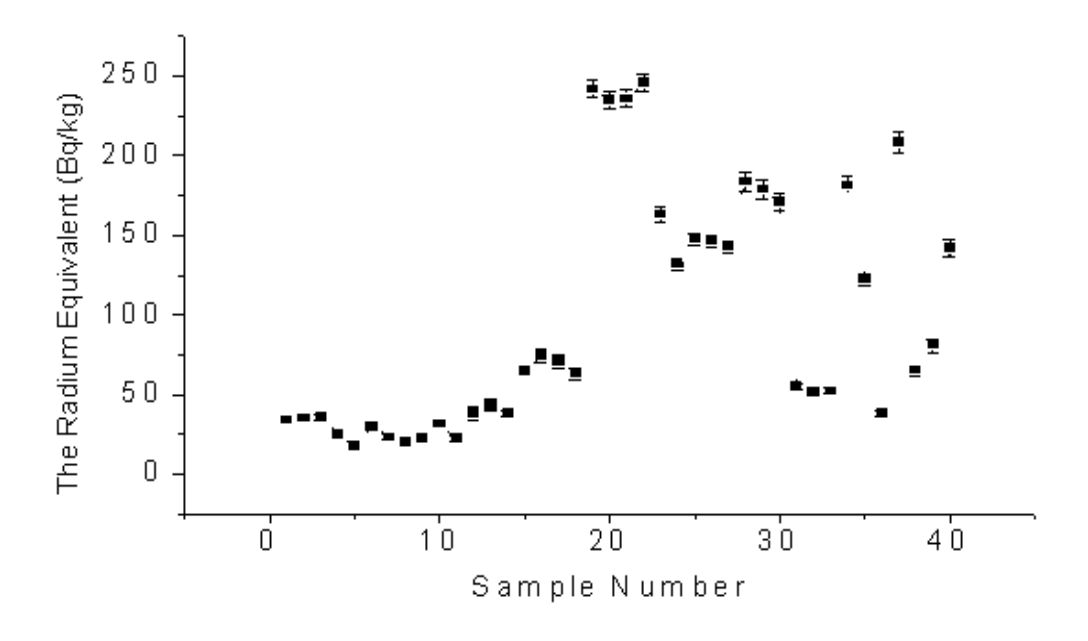


Figure 7: The radium equivalent (Ra_{eq}) of the studied samples.

Radium equivalent index (Ra_{eq})

Fig. 7 illustrates the calculated values of Ra_{eq} corresponding to sample number, the values of Ra_{eq} ranged between 17.70 and 245.64Bq/kg. Of all the 40 samples measured in this study, Argentina beans and all the other samples of beans, Jordanian, Lebanese and Brazilian kinds appeared to have the highest concentrations of Ra_{eq} 245.64, 241.79, 235.90 and 234.75 Bq/kg respectively. Whereas Italian, Indian and Egyptian rice showed the lowest concentration 17.70, 19.64 and 22.17 Bq/kg respectively. The average radioactivity concentration of Ra_{eq} was found to be 99.26 Bq/kg, it is clear that the values of Ra_{eq} in all samples were much less than the safe value 370Bq/kg [8].

Hazard index (HI)

As shown in Fig. 8, the HI ranged between 0.05 and 0.66. It is obviously clear that the values of HI were much less than the safe value, which should be less than one [8].

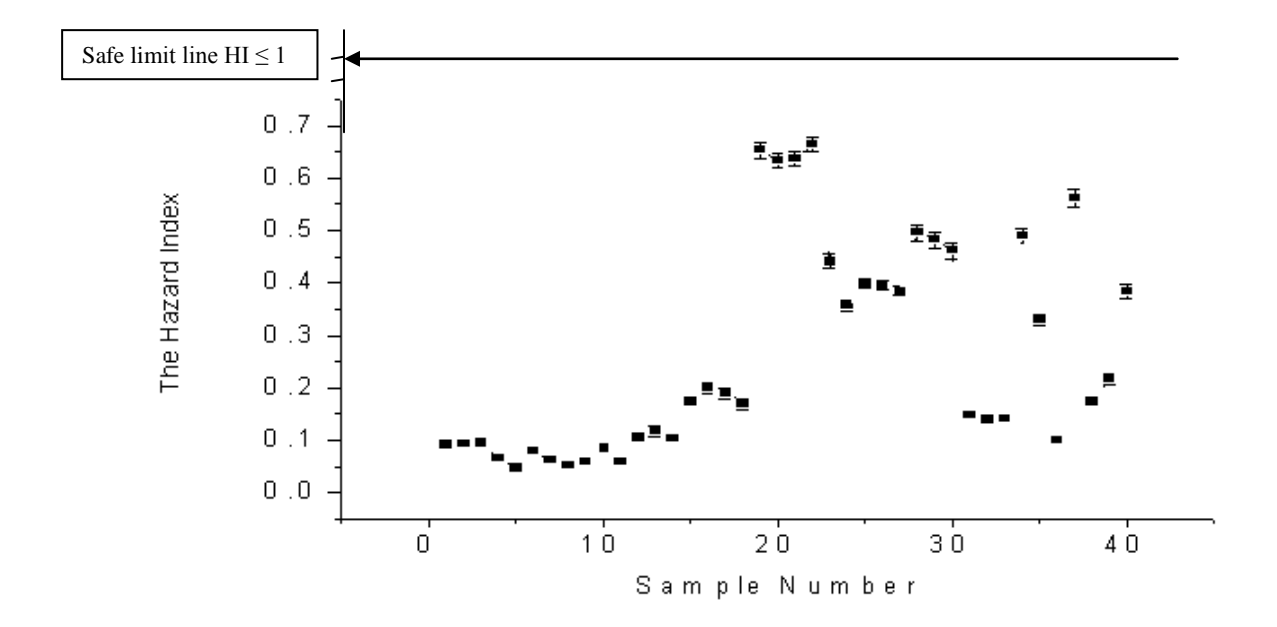


Figure 8: The hazard index (HI) of the studied samples.

Conclusion

The results have shown that the concentration of natural radionuclides of ²³⁸U, ²³²Th, and ⁴⁰K In grain samples studied are relatively lower than the world recommended limits. Except Jordanian sesame seed sample the concentration of ²³⁸U was found to be 0.0033±0.0006 ppm, which is the highest permissible limit allowed. The calculated Radium equivalent and hazard index (HI) are also not exceeding the maximum suggested values. Thus, the grains in Jordan are not supposed to acquire any radiological complication.

Acknowledgement

This project is funded by Yarmouk University. This project also used various facilities provided by Hashemite University, Jordan. The author would like thank Dr. Jamal Al-Jundi, Ms. Nadia AL-Ahmad and Ms Ghada Assayed for their help in preparation and analysis of the samples.

References

- 1. Turner, J.E., 1995. Atoms, Radiation, and Radiation Protection. 2nd ed., John Wiley &Sons.
- 2. FAO, 1999. The Impact Population Growth and Urbanization on Food Consumption Patterns in Jordan. United Nation. New York .
- 3. Jibiri, N. N. and Ajao, A.O., 2005. Natural Activities of ⁴⁰K, ²³⁸U and ²³²Th in Elephant Grass in Ibadan Metropolis, Nigeria. Journal of environmental Radioactivity.78, pp. 105-111.
- 4. Zaiadi J. H., Arif M., Ahmad S., Fatima I., and Qureshi I. H., 1999. Radiation Protection Dosimetry Vo.51 pp.559-564.
- 5. Samat,S.B., Green, S. and Beddoe, A.H., 1997, The ⁴⁰K Activity of One Gram of Potassium, Phys. Med. Biol. Vo 42, pp.407-413.
- 6. Frame, P., 2006. Radium Equivalent Health Physics Society: http://hps.org/.
- 7. Yasir, M.S., Ab Majid A., Yahaya, R., 2007. Study of Natural Radionuclides and its Radiation Hazard Index in Malaysia Building Materials. Radioanalytical and Nuclear Chemistry 273, No.3 pp. 539-541.
- 8. Tufail, M Radioprotection. Iqbal, M., and Mirza, S.M., 2000. Radiation Doses Due to the Natural Radioactivity in Pakistan Marble. Vo 35, No.3 pp. 299-310.
- 9. UNSCEAR, 2000. Sources and Effects of Ionizing radiation. Report to General Assembly, With Scientific Annexes, United Nation, New York



STRUCTURAL AND SPECTROSCOPIC STUDIES OF NOVEL METHYLBENZOYLTHIOUREA DERIVATIVES

(Struktur Dan Kajian Spektroskopi Terbitan Metilbenzoilthiourea)

Rabia'tun Hidayah Jusoh¹, Wan M. Khairul ¹, M. Sukeri M. Yusof^{1*}, Maisara Abdul Kadir¹, Bohari M.Yamin²

¹Department of Chemical Sciences, Faculty of Science and Technology, Universiti Malaysia Terengganu, 21030 Kuala Terengganu, Malaysia. ²School of Chemical Sciences and Food Technology, Faculty of Science and Technology, Universiti Kebangsaan Malaysia, 43650 Bangi, Selangor, Malaysia.

*Corresponding author: mohdsukeri@umt.edu.my

Abstract

Three new compounds, N-(2-methybenzoyl)-N'-(3-methyl-2-pyridyl)thiourea (II) are isomers and N-(2-methylbenzoyl)-N'-(6-methylpyridine-2-yl)thione (III) have been successfully synthesised and characterised by typical spectroscopic techniques, IR, UV-Visible, 1 H and 13 C Nuclear Magnetic Resonance (NMR) and CHNS analysis. The molecular structures were confirmed by single crystal X-ray diffractometer analysis. The Infrared spectra of these compounds showed four significant stretching vibrations, v(N-H), v(C=O), v(C-N) and v(C=S) at 3187-3375 cm⁻¹, 1683-1713 cm⁻¹, 1326-1384 cm⁻¹ and 666-785 cm⁻¹, respectively. The UV-Visible spectra of all compounds show three bands obtained in the range of 205-287 nm, which may be due to $n \rightarrow \pi^*$ and $\pi \rightarrow \pi^*$ transitions. In 13 C NMR spectra, the signal of carbon carbonyl for (I) and (II) can be observed at ca. &c 170 ppm. Whilst, chemical shift of the carbon thione groups for (I) and (II) appeared at ca. 180 ppm. Molecule (I), (II) and (III) crystallise in the monoclinic crystal system with space group $P2_1/n$. Molecule (I) adopts trans-cis configuration in comparison with II which adopts cis-trans configuration of the pyridine and methylbenzoyl groups with respect to the thione S atom across the thiourea C-N bonds. However, (III) is planar due to cyclisation forming two five-membered rings. All molecules are stabilised by intra-molecular hydrogen bonds, N-H $^{-1}$ O, C-H $^{-1}$ N, N-H $^{-1}$ N and C-H $^{-1}$ O lead to the formation of pseudo seven-membered rings (I) and pseudo six-membered (II & III) rings. In the crystal lattice, molecule (I) are linked by the N-H $^{-1}$ O, C-H $^{-1}$ S and N-H $^{-1}$ S (II) inter-molecular hydrogen bonds, whilst for (III), there are no inter-molecular hydrogen bond was observed.

Keywords: Methylbenzoylthiourea, carbonylthiourea, thiourea, spectroscopic studies

Abstrak

Sebanyak tiga sebatian baru, N-(2-metilbenzoil)-N'-(3-metil-2-piridil)tiourea (**II**) telah berjaya disintesis dan dicirikan dengan teknik spektroskopi iaitu spektroskopi infra merah (**IR**), ultralembayung (UV-Vis), 1 H dan 13 C resonans magnet nukleus (NMR) dan analisis unsur CHNS. Struktur hablur yang diperolehi dikaji dengan kristalografi sinar-X hablur tunggal. Analisis IR menunjukkan kehadiran empat puncak utama serapan, iaitu v(N-H), v(C=O), v(C-N) and v(C=S) masing-masing berada pada julat 3187-3375 cm⁻¹, 1683-1713 cm⁻¹, 1326-1384 cm⁻¹ dan 666-785 cm⁻¹. Analisis spektroskopi ultralembayung bagi kesemua sebatian mempunyai tiga puncak maksimum pada panjang gelombang 205-287 nm disebabkan pencampuran peralihan elektronik $n \rightarrow \pi^*$ dan $\pi \rightarrow \pi^*$. Dalam spektra 13 C NMR, kehadiran isyarat bagi karbon karbonil (**I**) dan (**II**) dapat diperhatikan pada sekitar δ_H 170 ppm. Manakala, anjakan kimia pada sekitar 180 ppm adalah menunjukkan kehadiran karbon tion. Molekul (**I**), (**II**) dan (**III**) mempunyai sistem hablur monoklinik dan kumpulan ruang $P2_1/n$. Molekul (**I**) mempunyai konfigurasi *trans-cis* berbanding molekul (**II**) yang mempunyai *cis-trans* merujuk kepada kedudukan kumpulan piridina dan metilbenzoil terhadap kumpulan tion, S pada paksi C-N masing-masing. Namun begitu, molekul (**III**) adalah planar disebabkan pensiklikan dua gelang lima ahli. Kesemua molekul ini distabilkan oleh ikatan hidrogen intermolekul N-H⁻⁻O, C-H⁻⁻N, N-H⁻⁻N dan C-H⁻⁻O yang membentuk satu gelang pseudo tujuh ahli (**I**) dan pseudo enam ahli (**II** & **III**). Dalam kekisi hablur, molekul (**I**) distabilkan oleh ikatan hidrogen inter-molekul.

Kata kunci: Metilbenzoiltiourea, karboniltiourea, tiourea, kajian spektroskopi

Introduction

Since it was synthesised and found by Nencki in 1873 [1], there has been a great interest on thiourea derivatives as a versatile ligand and have been used in numerous applications such as in agriculture, pharmaceutical, materials and catalysis [2-10]. In addition, there a lot of current studies discussing on the ability of these derivatives which are able to possess antitumor [11] antimalarial and anticancer [12], anti-Hiv [13] as well as antituberculosis properties [14]. Many researchers also propose that thiourea derivatives show promising potential in laser technology, optical communication and optical data storage owing to their non-linear properties and ease of coordination with metals [5, 15-16]. In the environmental aspect, thiourea also can act as an organic reagent to identify Cu²⁺ in aqueous solution to control pollution especially in industrial waste [17]. Domínguez *et al.*, (2002) have recently synthesised *N*-benzoyl-*N'*,*N'*-diethylthiourea which have great potential interest to be used as a highly selective reagent for the liquid-liquid extraction of metal cations namely palladium(II) and gold(III) [18].

In this contribution, three new types of N^1N^2 -diarylthioureas have been prepared with o,m-methyl substitution to the aromatic rings at N^1 and 3-methyl and 6-methyl pyridine substituents at N^2 as shown in Figure 1. Their solid state properties were fully investigated by typical spectroscopic methods to give wide electronic variations and the structures were confirmed with X-ray diffraction. The isomers molecular conformations of (I) and (II) can be found in *trans-cis* and *cis-trans* which depend on their position –NHCSNH- grouping. As shown in Figure 1, (III) underwent cyclisation that have some partial double bond characters of the C-N due to delocalisation of the nitrogen lone pair electron to the C=S and C=O groups.

Figure 1: The molecular structures of N-(2-methybenzoyl)-N'-(3-methyl-2-pyridyl)thiourea (**I**), N-(3-methylbenzoyl)-N'-(6-methyl-2-pyridyl)thiourea (**II**) and N-(2-methylbenzoyl)-N'-(6-methyl pyridine-2-yl)thione (**III**).

Experimental

All reactions were carried out under an ambient atmosphere and no special precautions were taken to exclude air or moisture during work-up. All chemicals were purchased from Sigma Aldrich, E. Merck and Fluka and used as received. Infrared spectra of the synthesised compounds were recorded from KBr pellets using FTIR Perkin Elmer 100 Spectrophotometer in the spectral range of 4000 cm⁻¹ to 400 cm⁻¹. The absorption spectra were recorded in cells of quartz 1 cm using a Shimadzu UV-Vis spectrophotometer 1601 series. All compounds were dissolved in pure methanol with concentration in the range of 10⁻⁵ M. The spectra of methylbenzoylthiourea derivatives were recorded at wavelength of 200 nm to 400 nm where there were two distinctive chromophores can be identified.

While the 1 H 400.11 MHz and 13 C 100.61 MHz NMR spectra were recorded using Bruker Avance III 400 Spectrometer in DMSO-d₆ as solvent at room temperature in the range between δ_H 0-15 ppm and δ_C 0-200 ppm. In the experiment, trimethylsilyl (TMS) was used as an internal standard. Whilst for crystallographic structure determination, diffraction data were collected on a Bruker SMART APEX 4K CCD with Mo K α (λ = 0.71073 Å) radiation.

Preparation of (C₅H₃N)NHC(S)NHC(O)C₆H₄(Me)₂ (I)

A solution of 2-methylbenzoyl chloride (1.5 g, 10 mmol) in acetone (25 ml) was added dropwise to ammonium thiocyanate (0.74 g, 10 mmol) in acetone (25 ml) followed by stirring at room temperature for *ca.* 10 minutes. A solution of 2-amino-3-methylpyridin (1.05 g, 10 mmol) in acetone (20 ml) was added dropwise to the stirring mixture. The reaction mixture was heated under reflux for 2 hours and the solution was filtered and cooled to room temperature. The solid product was then recrystallised by methanol to give colourless crystals of the title compound (1.77 g, 62%). IR (KBr pellets): v(N-H) 3375 cm⁻¹ s, v(C=O) 1683 cm⁻¹ s, v(C-N) 1326 cm⁻¹ m, v(C=S) 666 cm⁻¹ s. ¹H NMR (DMSO-d₆, 400.11 MHz): δ 2.32, 2.44 (2 x s, 6H, Me); 7.30-7.34 (m, 3H, C₆H₄); 7.45 (t, J_{HH} = 7 Hz, 1H, C₅H₃); 7.53 (d, J_{HH} = 8 Hz, 1H, C₆H₄); 7.76 (d, J_{HH} = 7 Hz, 1H, C₅H₃); 8.34 (d, J_{HH} = 4 Hz, 1H, C₅H₃); 11.85, 12.17 (2 x s, 1H, NH). ¹³C NMR (DMSO-d₆, 100.61 MHz): δ 17.7, 19.9 (2 x s, Me); 123.5, 123.8, 126.1, 128.5, 131.1, 131.4, 134.6, 136.5, 139.9, 146.7, 150.7 (11 x s, Ar); 170.8 (s, C=O); 180.6 (s, C=S). UV-Vis (MeOH): λ_{max} , nm; (ϵ , L mol⁻¹ cm⁻¹) 206 (92240), 237 (54140), 276 (61600).

Preparation of (C₅H₃N)NHC(S)NHC(O)C₆H₄(Me)₂ (II)

In a manner similar to that described above, (II) was obtained as yellowish crystals by recrystallisation from methanol (2.73 g, 67 %). IR (KBr pellets): v(N-H) 3187 cm⁻¹ s, v(C=O) 1713 cm⁻¹ s, v(C-N) 1329 cm⁻¹ m, v(C=S) 785 cm⁻¹ s. ¹H NMR (DMSO-d₆, 400.11 MHz): δ 2.33, 2.41 (2 x s, 6H, Me); 7.43-7.59 (m, 3H, C₆H₄); 7.79-7.81 (m, 1H, C₅H₃); 7.86 (s, 1H, C₆H₄); 7.96 (d, J_{HH} = 8 Hz, 1H, C₅H₃); 8.11 (d, J_{HH} = 8 Hz, 1H, C₅H₃); 11.79, 12.85 (2 x s, 1H, NH). ¹³C NMR (DMSO-d₆, 100.61 MHz): δ 21.3, 23.9 (2 x s, Me); 125.4, 126.4, 128.4, 128.9, 129.7, 130.5, 132.3, 132.6, 134.3, 134.4, 138.4 (11 x s, Ar); 168.8 (s, C=O); 181.4 (s, C=S). UV-Vis (MeOH): λ_{max} , nm; (ϵ , L mol⁻¹ cm⁻¹) 205 (83200), 234 (55530), 287 (43420).

Preparation of (C₅H₃N)NCSNCOC₆H₄(Me)₂ (III)

In a manner similar to that described above, (III) was obtained as colourless crystals by recrystallisation from methanol (1.5 g mg, 48 %). IR (KBr pellets): v(C=O) 1683 cm⁻¹ w, v(C=N) 1384 cm⁻¹ s, v(C=S) 735 cm⁻¹ s. ¹H NMR (DMSO-d₆, 400.11 MHz): δ 2.67, 2.85 (2 x s, 6H, Me); 7.33-7.39 (m, 3H, C₅H₃); 7.49 (d, J_{HH} = 8 Hz, 1H, C₆H₄); 7.78 (d, J_{HH} = 9 Hz, 1H, C₆H₄); 8.07 (t, J_{HH} = 8 Hz, 1H, C₆H₄); 8.19 (d, J_{HH} = 8 Hz, 1H, C₆H₄). ¹³C NMR (DMSO-d₆, 100.61 MHz): δ 20.6, 22.1 (2 x s, Me); 31.2 (s, C=O); 116.6, 117.7, 126.4, 130.9, 132.1, 132.2, 133.0, 139.3, 139.6, 146.3, 155.9 (11 x s, Ar); 179.0 (s, C=S). UV-Vis (MeOH): λ_{max} , nm; (ϵ , L mol⁻¹ cm⁻¹) 205 (84530), 229 (48470), 281(43440).

Results and Discussion

Syntheses

The title compounds were prepared by methods as shown in Scheme 1, (I) and (II) were produced from the synthesis of o,m-methylbenzoyl chloride with 2-amino-3-methylpyridine and 2-amino-6-methylpyridine. Here, the cyclisation of (III) was obtained from the reaction of o-methylbenzoyl chloride with 2-amino-6-methylpyridine in the refluxing acetone with constant stirring (Scheme 1).

$$\begin{array}{c} & & & & \\ & & & \\ & & & \\ & & & \\ & & & \\ & & & \\ & & & \\ & & & \\ & & & \\ & &$$

Scheme 1: The preparation of (I), (II) and (III).

Infrared spectroscopy

The FTIR spectra and absorption bands data of all the synthesised compounds are shown in Figure 2 and Table 1. Infrared spectra of these compounds have been analysed in the expected frequency region of the v(N-H), v(C=O), v(C-N) and v(C=S). The IR spectra of (I) and (II) show strong absorption bands at 3375 cm⁻¹ and 3187 cm⁻¹ which is due to the v(N-H) and indicate the existence of intra-molecular hydrogen bond. However, the band of v(N-H) of (III) is not observed in the IR spectrum, this is probably due to the electron delocalisation has taken place between C-S and C-N fragment caused by deprotonated of hydrogen at the N atom. The strong absorption of (I) and (II) are observed at the 1683 cm⁻¹ and 1713 cm⁻¹, respectively, which can be attributed to the v(C=O). Whilst in (III), it shows the v(C=O) as a weak carbonyl-like band with the double bond character is presence at 1683 cm⁻¹. Molecule (I), (II) and (III) exhibit vibration of v(C-N) at 1326 cm⁻¹, 1329 cm⁻¹ and 1384 cm⁻¹, respectively. The strong bands of (I) and (II) at 666 cm⁻¹, 785 cm⁻¹ can be assigned to the stretching vibration of v(C=S) assignable to literature [10, 19-20]. While the stretching vibration of v(C=S) indicates some double bond character for (III) which clearly can be observed at 735 cm⁻¹.

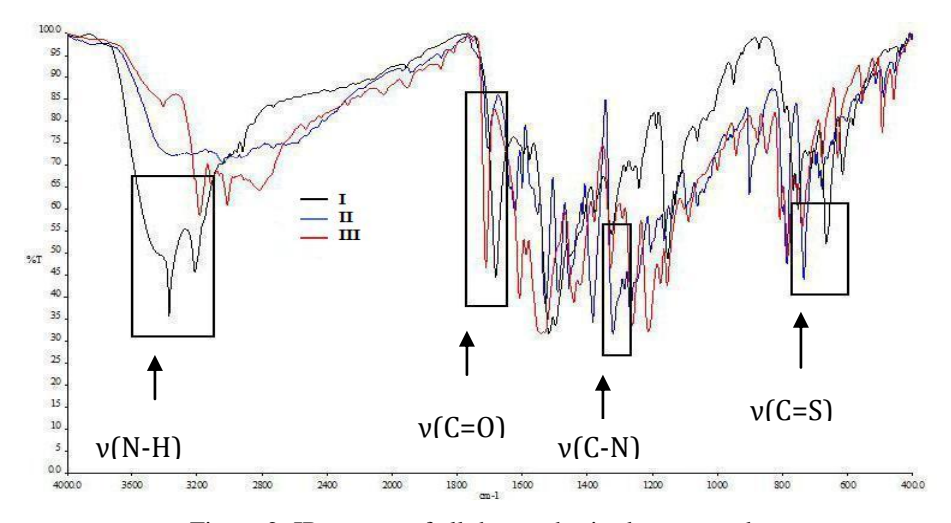


Figure 2: IR spectra of all the synthesised compounds.

Table 1:	Infrared	absorption	bands for	molecule	(I).	(II)	and (TII).

Molecule/ cm ⁻¹	ν (N-H)	ν (C=O)	v (C-N)	ν C=S
		ν (C===O)*	ν (C===N)*	ν (C===S)*
I	3375 s	1683 s	1326 m	666 s
II	3187 s	1713 s	1329 m	785 s
III	-	1683 w*	1384 s*	735 s*

s strong, m medium, w weak

UV-Vis spectroscopy

All the absorption bands of these compounds are shown in Figure 3 and Table 2. The electronic absorption spectra of the ligands (I), (II) and (III) showed three absorption peaks and were recorded in methanol (10^{-5} M). These spectra have three distinctive bands that is due to a mixture of $n\rightarrow\pi^*$ and $\pi\rightarrow\pi^*$ transitions. The absorption bands at 205-237 nm (ϵ = 48470 to 92240 M⁻¹ cm⁻¹) can be assigned to $\pi\rightarrow\pi^*$ transition of the aromatic systems. However, the band observed in the range of 205 to 237 nm is due to perturbation of solvent and overlapping of carbonyl's compounds chromophores in these compounds. These compounds exhibit broad band in the range 229-237 nm (ϵ = 48470 to 54140 M⁻¹ cm⁻¹) and 276-287 nm (ϵ = 43420 to 61600 M⁻¹ cm⁻¹) which can be assigned to $n\rightarrow\pi^*$ and $\pi\rightarrow\pi^*$ transitions which arise from the lone pair of electrons on the oxygen and sulphur of C=O and C=S. The introduction of auxochromes methyl substituent groups at the o and m- position and the electron conjugated π bond in phenyl ring and NH groups produces bathochromic shift in the spectra.

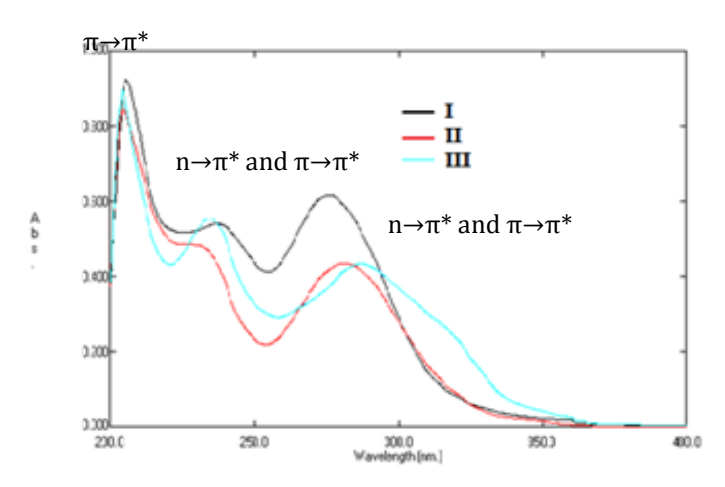


Figure 3: The UV spectra of the (I), (II) and (III).

Table 2. The principal UV absorption bands observed for (I), (II) and (III).

Compounds No.			Absorption λ / nction Coefficient		
	Peak 1	Assignment	Peak 2	Peak 3	Assignments
(1)	206 (92240)	$\pi \rightarrow \pi^*$	237 (54140)	276 (61600)	Mixed $n \rightarrow \pi^*$, $\pi \rightarrow \pi^*$
(II)	205 (83200)	$\pi{ ightarrow}\pi^*$	234 (55530)	287 (43420)	Mixed $n \rightarrow \pi^*$, $\pi \rightarrow \pi^*$
(III)	205 (84530)	$\pi { ightarrow} \pi^*$	229* (48470)	281* (43440)	Mixed $n \rightarrow \pi^*$, $\pi \rightarrow \pi^*$

^{*}indicates the partial double bond

^{*}indicates the partial double bond

NMR spectroscopy

The NMR spectroscopic data of all the synthesised compounds are shown in Table 3. The 1H NMR spectra of compounds (I), (II) and (III) showed the expected methyl resonance between δ_H 2.32-2.85 ppm. In addition, the overlapping unresolved signal of the aromatic protons of (I), (II) and (III) can be observed as distinctive multiple resonances between δ_H 7.30-8.34 ppm. These characteristic resonances are strongly influenced by the o and m-substituents positions of methyl groups at the phenyl and pyridine rings. Compounds (I) and (II) showed the presence of the N(2)H at δ_H 11.85 ppm and 11.79 ppm. For N(1)H attached to the methylbenzoyl substituents, the resonance can be seen at δ_H 12.17 ppm and δ_H 12.85 ppm. Surprisingly, there is no expected N-H signal observed for (III) which are due to the electrons are localised over the C-N moiety. In 13 C NMR spectra, the methyl resonance can be observed between δ_C 17.7-23.9 ppm. Meanwhile the aromatic carbon resonances can be found between δ_C 116.5-155.9 ppm which are corresponding to phenyl rings in the compounds. In addition, one resonance is observed at between δ_C 168.8-170.8 ppm and in between δ_C 180.6-181.4 ppm which is due to the carbon of C=O and C=S for (I) and (II). Whilst, in the case of (III) which showed the partial double bond character C=O and C=S, the resonances can be found at ca. δ_C 31 ppm and δ_C 179.0 ppm which due to its high delocalisation on the cyclisation formed in the molecule.

Table 3: Selected NMR spectroscopic data for the compounds.

	_	1
Compounds No.	1 H NMR/ δ_{H} (ppm)	13 C NMR/ $\delta_{\rm C}$ (ppm)
(I)	2.32, 2.44 (2 x s, 6H, Me), 7.30- 7.34 (m, 3H, C_6H_4), 7.45 (t, $J_{HH} = 7$ Hz, 1H, C_5H_3), 7.53 (d, $J_{HH} = 8$ Hz, 1H, C_6H_4), 7.76 (d, $J_{HH} = 7$ Hz,1H, C_5H_3), 8.34 (d, $J_{HH} = 4$ Hz,1H, C_5H_3),11.85, 12.17 (2 x s, 1H, NH)	17.7, 19.9 (2 x s, Me), 123.5, 123.8, 126.1, 128.5, 131.1, 131.4, 134.6, 136.5, 139.9, 146.7, 150.7 (11 x s, Ar), 170.8 (s, C=O), 180.6 (s, C=S)
(II)	2.33, 2.41 (2 x s, 6H, Me), 7.43-7.59(m, 3H, C ₆ H ₄), 7.79-7.81 (m, 1H, C ₅ H ₃), 7.86 (s, 1H, C ₆ H ₄), 7.96 (d, J _{HH} = 8 Hz, 1H,C ₅ H ₃), 8.11 (d, J _{HH} = 8 Hz, 1 H,C ₅ H ₃), 11.79, 12.85 (2 x s, 1H, NH)	21.3, 23.9 (2 x s, Me), 125.4, 126.4, 128.4, 128.9, 129.7, 130.5, 132.3, 132.6, 134.3, 134.4, 138.4 (11 x s, Ar), 168.8 (s, C=O), 181.4 (s, C=S)
(III)	2.67, 2.85 (2 x s, 6H, Me), 7.33-7.39 (m, 3H, C_5H_3), 7.49 (d, $J_{HH} = 7$ Hz, 1H, C_6H_4), 7.78 (d, $J_{HH} = 9$ Hz, 1H, C_6H_4), 8.07 (t, $J_{HH} = 8$ Hz, 1H, C_6H_4), 8.19 (d, J_{HH} = 8 Hz, 1H, C_6H_4)	20.6, 22.1 (2 x s, Me), 31.2 (s, C=O), 116.6, 117.7, 126.4, 130.9, 132.1, 132.2, 133.0, 139.3, 139.6, 146.3, 155.9 (11 x s, Ar), 179.0 (s, C=S)

Molecular Structural Analysis

All these compounds have been analysed by single crystal X-ray diffraction and exhibit monoclinic crystal system, P2₁/n space group. The crystallographic data and refinement of methylbenzoylthiourea derivatives are shown in Table 4. The thiourea moieties in the compounds are essentially planar. Molecule (III) is planar compared to (I) and (II) due to the formation of bonding between N3-S1 and S1-O1. The planarity conformation of thiourea moieties in (I) and (II) also influenced by intra-molecular N2-H2A···O1 and N1-H1A···N3 hydrogen bonds. Molecule (I) adopts a *trans-cis* configuration with respect to the positions of the 2-methylbenzoyl and 3-methyl-2-pyridiyl groups,

whilst **II** adopts a *cis-trans* configuration with respect to the positions of the 3-methylbenzoyl and 6-methyl-2-pyridyl groups which is relative to the thione S atom across the thiourea C-N bonds (Figure 4).

Table 4: Crystallographic data and refinement of the structures of (I), (II) and (III).

Parameter	(I)	(II)	(III)
Empirical formula	$C_{15} H_{15} N_3 OS$	$C_{15}H_{15}N_3OS$	$C_{15}H_{13}N_3OS$
Formula weight	285.36	285.36	283.34
Crystal system	monoclinic	monoclinic	monoclinic
Space group	P2(1)/n	P2(1)/n	P2(1)/n
Unit cell dimension	a = 7.955 (3) Å, $b = 7.811$	a = 7.1981(19) Å, b =	a = 8.117(3) Å, b =
	(3)Å, c = 23.414 (8) Å,	10.092(3) Å, c =	14.545(5) Å,
	$\beta = 90.827 (6)$ °	19.372(5) Å, β	$c = 11.125(4) \text{ Å}, \beta =$
	A 2	=95.826(5) °	98.782(8) °
Volume	$1454.6 (9) \text{ Å}^3$	$1399.9(6) \text{ Å}^3$	$1298.1(8) \text{ Å}^3$
z, Calculated density	$4, 1.303 \text{ Mg/m}^3$	4, 1.354 Mg/m^3	4, 1.450 Mg/m^3
F (000)	600	600	592
Crystal size	0.49 x 0.46 x 0.17 mm	0.50 x 0.32 x 0.28 mm	0.43 x 0.14 x 0.12 mm
Theta range for data	1.74 to 24.99°	2.11 to 25.00°	2.32 to 24.99°
collection			
Limiting indices	-9<=h<=9,	-8<=h<=8,	-9<=h<=9,
	9<=k<=9,	-8<=k<=12,	17<=k<=17,
	-16<=1<=27	-20<=l<=23	-10<=l<=13
Reflections collected/	7218/2560 [R(int)= 0.0182]	6913/2459 [R(int) =	6574/2266 [R(int)=
unique		0.0201]	0.0575]
Completeness of theta	99.7%	99.9 %	99.2 %
Max and min transmission	0.9633 and 0.8993	0.9384 and 0.8936	0.9709 and 0.9010
Refinement method	Full-matrix least-squares on	Full-matrix least-squares	Full-matrix least-
5	F^2	on F^2	squares on F ²
Data/ restraints/ parameters	2560 / 0/ 183	2459 / 0 / 183	2266 / 0 / 181
Goodness-of-fit on F ²	1.029	1.045	0.980
Final R indices	R1 = 0.0410,	R1 = 0.0453,	R1 = 0.0726,
[I>2sigma(1)]	wR2 = 0.1072	wR2 = 0.1245	wR2 = 0.1905
R indices (all data)	R1 = 0.0542, $wR2 = 0.1148$	R1 = 0.0574, wR2 = 0.1220	
Largest different peak and hole	0.229 and -0.150 e.A ⁻³	0.1328 0.263 and -0.143 e.A ⁻³	0.2259 0.465 and -0.297 e.A ⁻³

The bond lengths and angles of all compounds are in agreement with the anologues of 1-Benzoyl-3-(6-methylpyridin-2-yl)thiourea [21] and 4-Chloro-N-[N-(6-methyl-2-pyridyl)-carbamothioyl]benzamide [1]. The selected bond lengths (Å) and angles (°) are listed in Table 5.

Bond lengths		Bond angles	
(I)			
S1-C9	1.655(2)	O1-C8-C6	122.96(16)
O1-C8	1.214(2)	N1-C8-C6	114.88(15)
N1-C8	1.373(2)	N2-C9-N1	116.11(16)
N1-C9	1.394(2)	N2-C9-S1	126.01(14)
N2-C9	1.327(2)	N1-C9-S1	117.88(14)
(II)			
S1-C8	1.665 (2)	C8-N1-C7	129.14 (17)
O1-C7	1.211(2)	N2-C8-N1	115.07 (17)
N1-C8	1.363 (2)	N2-C8-S1	119.47 (14)
N1-C7	1.388(2)	C8-N2-C9	131.45(16)
N2-C8	1.359(3)	N1-C8-S1	125.46 (15)
(III)			
S1-C9	1.766(4)	C9-S1-N3	85.80(18)
S1-N3	1.783(4)	C9-S1-O1	79.87(17)
S1-O1	2.123(3)	N3-S1-O1	165.66(14)
O1-C8	1.248(5)	C8-O1-S1	105.7(3)
N2-C9	1.329(5)	C9-N2-C10	112.6(4)
N2-C10	1.331(5)	C9-N1-C8	113.0(4)
N1-C9	1.321(5)	N1-C9-N2	124.9(4)
N1-C8	1.337(6)	N1-C9-S1	119.8(3)

Table 5: Selected the bond lengths (Å) and angles (°) for (I), (II) and (III).

The molecular structure of (I), (II) and (III) and their packing diagrams are illustrated in Figure 4 and 5, respectively. The central thiourea moiety, S1/N1/N2/C9, 3-methylpyridine N3/(C10-C15), and 2-methylphenyl, (C1-C6) rings in (I) are essentially planar with maximum deviation of 0.032 (2)Å for N2 atom from the least square plane. The central thiourea moiety makes dihedral angle with the pyridine and 2-methylphenyl rings of 65.53(7)° and 61.82(8)°, respectively. The inclination angle between the pyridine and benzene rings is 12.63(8)° are smaller if compared to (II) 26.06°. The molecular structure of (II) is closely related to (I) with relatively identical in bond lengths and angles. The (6-methyl-2-pyridyl)thiourea fragment (C7/C8/S1/N1/N2/N3/C9-C13/C15) in (II) is essentially planar with maximum deviation of 0.066(1)Å for atom N1 from the least square plane. This fragment makes dihedral angles of 30.29(8)° with respect to the benzene ring (C1-C6) plane. The inclination angle between the two aromatic rings is 26.06°.

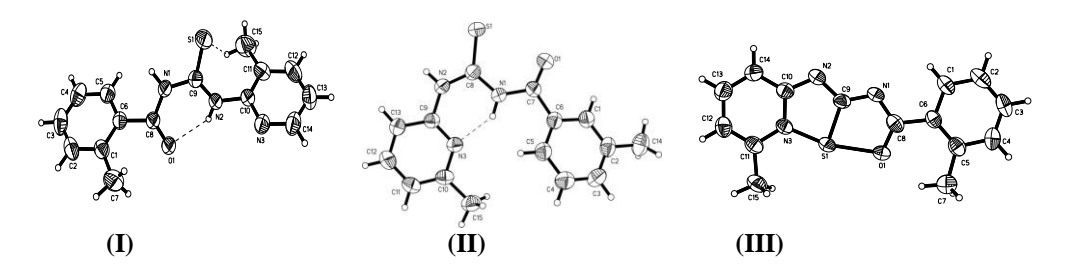


Figure 4: The molecular structures of (I), (II) and (III) with displacement ellipsoids drawn at 50% probability level. The dashed lines indicate the existence of intramolecular hydrogen bonds.

The molecular structural analysis of these compounds show the cyclisation of (III) (Figure 4) through the nitrogen at pyridine, N3 and carbonyl oxygen atom, O1 bonded to the sulphur atom forming two planar five-membered ring structures. This cyclisation is believed as a result of transfer of electron density between nitrogen atom in pyridine and carbonyl oxygen to sulphur form two chelate rings. The bond length of the C-S, C-O and C-N indicate of some partial double bond character whereas it shows that the C=S bond is longer 1.766 Å than in (I) and (II), and comparable by previous reported that the C-S lies at 1.74 Å [22]. These result occur due to the conjugation of lone electron pairs of nitrogen atoms with π -electron of the C=S.

Molecule (I) maintains the *trans-cis* configuration of the thiourea moiety is stabilised by the intra-hydrogen bond between the carbonyl oxygen atom O1 and the thioamide hydrogen atom, H15A (Figure 4). In the crystal lattice, the molecules are linked by the N2-H2···O1 and C13-H13···S1 inter-molecular hydrogen bonds forming two-dimensional (Figure 5). Similar case in (II), there is an intra-molecular hydrogen bond, N1-H1···N3 (Figure 4) and resulting a pseudo-six-membered ring, N3···H1-N1-C8-N2-C9, is formed. In the crystal lattice, the molecules are linked to form centrosymmetric dimers through N2-H2···S1 inter-molecular interactions (Figure 5). Whilst, in (III) it is stabilised by the intra-hydrogen C7-H7···O1 resulting a pseudo-six-membered ring. However, in crystal lattice the case of (III) there is no intermolecular hydrogen interaction bonding involves (Figure 5). Hydrogen-bond geometry of all the synthesised compounds is listed in Table 6.

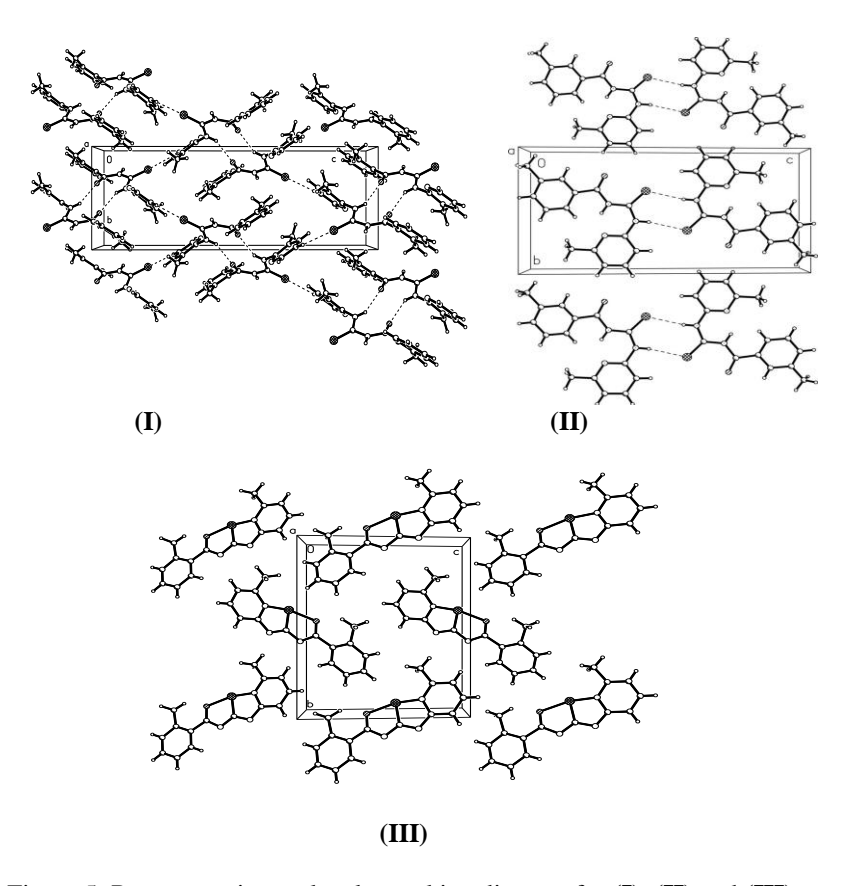


Figure 5: Representative molecular packing diagram for (I), (II) and (III).

0.86 2.06 2.698(2) 130 0.96 2.56 2.962(3) 105 0.86 2.27 3.021(2) 146 0.93 2.84 3.701(3) 154	D-H	HA	DA	D-H A
0.96 2.56 2.962(3) 105 0.86 2.27 3.021(2) 146	0.06	2.06	2 (09/2)	120
0.86 2.27 3.021(2) 146			` '	
· ·	0.96	2.56	` '	105
0.93 2.84 3.701(3) 1.54	0.86	2.27	3.021(2)	146
2.01 2.701(3) 151	0.93	2.84	3.701(3)	154

1.94

2.60

1.99

2.657 (2)

3.4478 (19)

2.764(6)

140

169

136

Table 6: Hydrogen-bond geometry (Å).

D-H···A

Symmetry code: (i) -x + 1, -y, -z.

(I)

(II)

(III)

N2-H2A···O1 C15-H15A···N2 N2-H2A···O1ⁱ C13-H13···S1ⁱⁱ

N1-H1A...N3

N2-H2A···S1i

C7-H7A "O1

Symmetry codes: (i)1-

Conclusion

0.86

0.86

0.96

To conclude, two isomers of methylbenzoylthiourea derivatives and the unexpected secondary amide have been successfully prepared and fully characterised via IR, UV-Visible, 1H and ^{13}C Nuclear Magnetic Resonance (NMR) as well as single crystal X-ray diffractometer. Infrared spectra showed four significant absorptions within the range. The UV-Visible spectra of the compounds were assigned as a mixture of $n\rightarrow\pi^*$ and $\pi\rightarrow\pi^*$ transitions which could be contributed by phenyl rings, C=O and C=S chromophores. In the NMR spectroscopy, the NH group acts as hydrogen-bond donor for compounds (I) and (II) and the presence of C=S plays an important role in the identification of the proposed structures. The crystal structure of the title compounds showed intra- and intermolecular interaction which may increase the hydrogen-bond donors and hydrogen-bond acceptors. Indeed, the presence of S, N and O electron donors in these derivatives have attracted great opportunity in the near future as polydentate ligands to bind with wide range of metal ions in the interest of coordination chemistry.

Acknowledgement

The authors gratefully acknowledge Ministry of Higher Education Malaysia for FRGS research grant No:59001, Ministry of Science Technology and Innovation (MOSTI), HRD (S&T) National Science Fellowship (NSF) for the postgraduate scholarship, Universiti Malaysia Terengganu and Universiti Kebangsaan Malaysia for providing research facilities.

References

- 1. Binzet, G., Emen, F. M., Flörke, U., Ilkaynak, T., Külcü, N. and Arslan, H. 2009. 4-Chloro-*N*-[*N*-(6-methyl-2-pyridyl)-carbamothioyl]benzamide. Acta Cryst. E65. 081-082.
- 2. Xue, S. J., Zou, J. S. and Yang, H. J. 2000. Synthesis and Herbicidal Activities of *N*'-(substituted pyrimidin-2-yl)-*N*-Substituted Phenoxyacetyl Thiourea Derivatives. Chinese Chemical Letters 11(1): 19-20.
- 3. Ranise, A., Spallarossa, A., Bruno, O., Schenone, S., Fossa, P., Menozzi, G., Bondavalli, F., Mosti, L., Capuano, A., Mazzeo, F., Falcone, G. and Filippelli, W. 2003. Synthesis of *N*-substituted-*N*-acylthioureas of 4-substituted piperazines endowed with local anaesthetic, antihyperlipidemic, antiproliferative activities and antiarrythmic, analgesic, antiaggregating actions. IL Farmaco 58: 765-780.
- 4. Xu, X., Qian, X., Li, Z., Huang, Q. and Chen, G. 2003. Synthesis and insecticidal activity of new substituted *N*-aryl-*N*'-benzoylthiourea compounds. Journal of Fluorine Chemistry 121: 51-54.
- 5. Weiqun, Z., Kuisheng, L., Yong, Z. and Lu, L. 2003. Structural and spectral studies of *N*-(4-chloro)benzoyl-*N*'-2-Tolylthiourea. Journal of Molecular Structure 657: 215-223.
- 6. Weiqun, Z., Baolong, L., Liming, Z., Jiangang, D., Yong, Z., Lude, L. and Xujie, Y. 2004. Structural and spectral studies on *N*-(4-chloro)benzoyl-*N*'-(4-tolyl)thiourea. Journal of Molecular Structure 690: 145-150.

- 7. Ke, S.-Y. and Xue, S.-J. 2006. Synthesis and herbicidal activity of *N*-(*o*-fluorophenoxyacetyl)thioureas derivatives and related fused heterocyclic compounds. ARKIVOC (x): 63-68.
- 8. Liu, B. and Tian, L. 2006. 1-Cyclopropylcarbonyl-3-(2-pyridyl)thiourea. Acta Cryst. E62, 04280-04281.
- 9. Selvaraju, K., Valluvan, R. and Kumararaman, S. 2007. A new metal-organic crystal: Potassium thiourea chloride. Material Letters 61:751-753.
- 10. Yang, W., Weiqun, Z. and Zhang, Z. 2007. Structural and spectroscopic study on *N*-2-fluorobenzoyl-*N*'-4-methoxyphenylthiourea. Journal of Molecular Structure 828: 46-53.
- 11. Li, J., Tan, J.-Z., Chen, L.-L., Zhang, J., Shen, X., Mei, C.-L., Fu, L.-L., Lin, L.-P., Ding, J., Xiong, X.-S., Liu, H., Luo, X.-M. and Jiang, H.-L. 2006. Design, synthesis and antitumor evaluation of a new series of *N*-substituted-thiourea derivatives *N*-(2-oxo-1,2-dihydroquinolin-3-yl-methyl)-thiourea. Acta Pharmacologica Sinica 27 (9): 1259.
- 12. Mahajan, A., Yeh, S., Nell, M., Van Rensburg, C. E. J. and Chibalea, K. 2007. Synthesis of new 7-chloroquinolinyl thioureas and their biological investigation as potential antimalarial and anticancer agents. Bioorganic & Medicinal Chemistry Letters 17: 5683-5685.
- 13. Dong, Y., Venkatachalam, T. K., Narla, R. K., Trieu, V. N., Sudbeck, E. A. and Uckun, F. M. 2000. Antioxidant Function of Phenethyl-5-bromo-pyridyl Thiourea Compounds with Potent Anti-HIV Activity. Bioorganic & Medicinal Chemistry Letters 10: 87-90.
- 14. Karakus, S. and Rollas, S. 2002. Synthesis and antituberculosis activity of new *N*-phenyl-*N*-[4-(5-alkyl/arylamino-1,3,4 thiadiazole-2-yl)phenyl]thioureas. IL Farmaco 57: 577-581.
- 15. Raj, S. S. S., Puviarasan, K., Velmurugan, D., Jayanthi, G. and Fun, H.-K. 1999. N-H⁻⁻S hydrogen bonding in *N*-benzoyl-*N*'-methyl-*N*'-phenylthiourea and *N*-benzoyl-N''-(3,4 dimethylphenyl)thiourea. Acta Cryst. C55: 1318-1320.
- 16. Caroline, M. L. and Vasudevan, S. 2009. Growth and characterization of pure and doped bis thiourea zinc acetate: Semiorganic nonlinear optical single crystals. Current Applied Physics 9: 1054-1061.
- 17. Ma, D. L., Xia, D. S., Cui, F. L., Li, J. P. and Wang, Y. 1999. A new sensitive reagent for identifying and determining Cu²⁺. Talanta 48: 9-13.
- 18. Domínguez, M., Anticó, E., Beyer, L., Aguirre, A., Garcià-Granda, S. and Salvadó, V. 2002. Liquid/liquid extraction of palladium(II) and gold(III) with *N*-benzoyl-*N'*, *N'*-diethylthiourea and the synthesis of a palladium benzoylthiourea complex. Polyhedron 21: 1429-1437.
- 19. Bencivenni, L., Cesaro, S. N. and Pieretti, A. 1998. Matrix and ab initio infrared spectra of thiourea and thiourea-d₄ Vibrational Spectroscopy 18: 91–102.
- 20. Dillen, J., Woldu, M. G. and Koch, K. R. 2006. *N,N*-(Heptane-2,6-diyl)-*N*'-(3,4,5-methoxybenzoyl)thiourea. Acta Cryst. E62: 05225-05227.
- 21. Yusof, M. S. M., Soh, S. K. C., Ngah, N. and Yamin, B. M. 2006. 1-Benzoyl-3-(6-methylpyridin-2-yl)thiourea. Acta Cryst. E62: 01446-0144.
- 22. Allen, F. H., Bird, C. M., Rowland, R. S. and Raithby, P. R. 1997. Resonance-Induced Hydrogen Bonding at Sulfur Acceptors in R₁R₂C=S and R₁CS₂ Systems. Acta Cryst. B53: 680-695.



IMPROVEMENT OF THE PHOTOSTABILIZATION OF PVC FILMS IN THE PRESENCE OF THIOACETIC ACID BENZOTHIAZOLE COMPLEXES

(Peningkatan Ciri-ciri Fotokestabilan Filem PVC dengan Kehadiran Kompleks Asid Thioasetik Benzothiazola)

Emad Yousif^{1*}, Jumat Salimon², Nadia Salih²

¹Department of Chemistry, College of Science, Al-Nahrain University, Baghdad, Iraq ²School of Chemical Sciences and Food Technology, Faculty of Science and Technology, Universiti Kebangsaan Malaysia, 43600 Bangi, Selangor, Malaysia

*Corresponding author: emad_yousif@hotmail.com

Abstract

The photostabilization of poly(vinyl chloride) (PVC) films by 2-thioacetic acid benzothiazol with Sn(II), Cd(II), Ni(II), Zn(II) and Cu(II) complexes was investigated. The PVC films containing concentration of complexes 0.5% by weight were produced by the same casting method from tetrahydrofuran (THF) solvent. The photostabilization activities of these compounds were determined by monitoring the carbonyl, polyene and hydroxyl indices with irradiation time. The changes in viscosity average molecular weight of PVC with irradiation time were also tracked (using THF as a solvent). The quantum yield of the chain scission (ϕ_{cs}) of these complexes in PVC films was evaluated and found to range between 4.71×10^{-8} and 8.98×10^{-8} . Results obtained showed that the rate of photostabilization of PVC in the presence of the additive follows the trend:

$$Sn(L)_2 > Cd(L)_2 > Ni(L)_2 > Zn(L)_2 > Cu(L)_2$$

According to the experimental results obtained, several mechanisms were suggested depending on the structure of the additive. Among them HCl scavenging, UV absorption, peroxide decomposer and radical scavenger for photostabilizer additives mechanisms were suggested.

Keywords: Photostabilizer, PVC, 2-Thioacetic benzothiazol acid.

Abstrak

Proses fotokestabilan filem poli(vinil klorida) (PVC) oleh asid 2-thioasetik benzothiazol dengan kompleks Sn(II), Cd (II), Ni(II), Zn(II) dan Cu(II) telah dikaji. Filem PVC yang mengandungi kompleks berkepekatan 0.5% berat telah dihasilkan dengan kaedah acuan yang sama menggunakan pelarut THF. Aktiviti fotokestabilan unsur-unsur ini ditentukan dengan mengkaji indeks karbonil, poliena dan hidroksil dengan masa iradiasi. Perubahan dalam kelikatan berat molekul purata bagi PVC dengan masa iradiasi juga turut dikesan dengan menggunakan THF sebagai pelarut. Hasil kuantum pengguntingan rantai (Φ_{cs}) kompleks-kompleks ini di dalam filem-filem PVC didapati berada dalam julat antara 4.71×10^{-8} and 8.98×10^{-8} . Keputusan yang diperolehi menunjukkan bahawa kadar fotokestabilan PVC dengan kehadiran aditif adalah mengikut turutan berikut:

$$Sn(L)_2 > Cd(L)_2 > Ni(L)_2 > Zn(L)_2 > Cu(L)_2$$

Berdasarkan keputusan eksperimen yang diperolehi, beberapa mekanisme telah dicadangkan bergantung kepada struktur aditif yang digunakan. Empat mekanisme aditif fotokestabilan yang telah dicadangkan termasuklah HCl penguraian, penyerapan UV, pengurai peroksida dan pengautan radikal.

Kata kunci: Fotokestabilan, PVC, Asid 2-thioasetik benzothiazol.

Introduction

Poly(vinyl chloride), better known by its abbreviation PVC, is one of the most versatile plastics. It is the second largest manufactured resin by volume worldwide [1]; currently, its production per annum exceeds 31 million tons. Braun [2] described the most remarkable milestones in PVC history, their importance to the development of macromolecular chemistry, and some PVC research and industrial applications, with respect to polymerization, stabilization, bulk property modification, and chemical and material recycling of PVC waste [3]. The low cost and the good performance of poly(vinyl chloride) products have increased the utilization of this polymer in building, mainly in exterior application, such as window profiles, cladding structure and siding [4]. However, ultimate user acceptance of the PVC products for outdoor building applications will depend on their ability to resist photodegradation over long periods of sunlight exposure. To ensure weather ability, the PVC resin needs to be compounded and processed properly, using suitable additives, leading to a complex material whose behavior and properties are quite different from the PVC resin by itself [5]. On the other hand, it is important to perform reliable accelerated weathering test methods. In this regard, factors that influence the degradation of PVC based materials in the service condition, like light and temperature are accelerated. As part of our on-going research in the photostabilization of poly (vinyl chloride), the photostabilization of PVC was studied using 2-thioacetic benzothiazol complexes

Experimental

Materials

The following complexes were all prepared by the method described in reference [6].

Bis(2-thioacetic acid benzothiazol) tin(II)	$Sn(L)_2$
Bis(2-thioacetic acid benzothiazol) cadmium(II)	$Cd(L)_2$
Bis(2-thioacetic acid benzothiazol) nickel(II)	$Ni(L)_2$
Bis(2-thioacetic acid benzothiazol) zinc(II)	$Zn(L)_2$.
Bis(2-thioacetic acid benzothiazol) copper(II)	$Cu(L)_2$

where M = Sn(II), Cd(II), Ni(II), Zn(II) or Cu(II)

Experimental techniques

Films preparation:

Commercial poly(vinyl chloride) supplied by Petkim company (Turkey) was re-precipitated from THF solution by alcohol several times and finally dried under vacuum at room temperature for 24 hours. Fixed concentrations of poly(vinyl chloride) solution (5 g/100 ml) in tetrahydrofuran were used to prepare polymer films with 30 µm thickness (measured by a micrometer type 2610 A, Germany). The prepared complexes (0.5% concentrations) were added to the films starting at 0 concentrations (control). The films were prepared by evaporation technique at room temperature for 24 hours. To remove the possible residual tetrahydrofuran solvent, film samples were further dried at room temperature for three hours under reduced pressure. The films were fixed on stands especially used for irradiation. The stand is provided with an aluminum plate (0.6 mm in thickness) supplied by Q-panel company.

Irradiation experiments

Accelerated testing technique:

Accelerated weatherometer Q.U.V. tester (Q. panel, company, USA), was used for irradiation of polymers films. The accelerated weathering tester contains stainless steel plate, which has two holes in the front side and a third one behind. Each side contains a lamp (type Fluorescent Ultraviolet Lights) 40 Watt each. These lamps are of the type UV-B 313 giving spectrum range between 290-360 nm with a maximum at wavelength 313 nm. The polymer film samples were vertically fixed parallel to the lamps to make sure that the UV incident radiation is perpendicular on the samples. The irradiated samples are rotated from time to time to ensure that the intensity of light incident on all samples is the same.

Photodegradation measuring methods

Measuring the photodegradation rate of polymer films using infrared spectrophotometery:

The degree of photodegradation of polymer film samples was followed by monitoring FTIR spectra in the range 4000-400 cm⁻¹ using FTIR 8300 Shimadzu Spectrophotometer. The position of carbonyl absorption is specified at 1722 cm⁻¹, polyene group at 1602 cm⁻¹ and the hydroxyl group at 3500 cm⁻¹ [7]. The progress of photodegradation during different irradiation times was followed by observing the changes in carbonyl and polyene peaks. Then carbonyl (I_{co}), polyene (I_{po}) and hydroxyl (I_{OH}) indices were calculated by comparison of the FTIR absorption peak at 1722, 1602 and 3500 cm⁻¹ with reference peak at 1328 cm⁻¹ attributed to oscissoring and bending of CH₂ group, respectively. This method is called band index method which includes [7]:

$$I_s = \frac{A_s}{A_r} \tag{1}$$

As = Absorbance of peak under study

Ar = Absorbance of reference peak

Is = Index of group under study

Actual absorbance, the difference between the absorbance of top peak and base line (a Top Peak - a base line) is calculated using the base line method [8].

Determination of average molecular weight $(\overline{M}_{_{\mathrm{V}}})$ using viscometry method:

The viscosity property was used to determine the average molecular weight of polymer, using the Mark-Houwink relation [9].

$$[\eta] = K\bar{M}_{\nu}^{\alpha} \tag{2}$$

 $[\eta]=$ the intrinsic viscosity

K, α are constants depend upon the polymer-solvent system at a particular temperature.

The intrinsic viscosity of a polymer solution was measured with an Ostwald U-tube viscometer. Solutions were made by dissolving the polymer in a solvent (gm/100ml) and the flow times of polymer solution and pure solvent are t and t_0 respectively. Specific viscosity (η_{sp}) was calculated as follows:

$$\eta_{re} = \frac{t}{t_o}$$

$$\eta_{re} = \text{Relative viscosity}$$
(3)

Emad Yousif et al: IMPROVEMENT OF THE PHOTOSTABILIZATION OF PVC FILMS IN THE PRESENCE OF THIOACETIC ACID BENZOTHIAZOLE COMPLEXES

$$\eta_{sp} = \eta_{re} - 1 \tag{4}$$

The single – point measurements were converted to intrinsic viscosities by the relation 2.

$$[\eta] = (\sqrt{2}/c)(\eta_{sp} - \ln \eta_{re})^{1/2} \tag{5}$$

c = Concentration of polymer solution (g /100 ml).

By applying Equation 5, the molecular weight of degraded and the virgin polymer polymer can be calculated. Molecular weights of PVC with and without additives were calculated from intrinsic viscosities measured in THF solution using the following equation:

$$[\eta] = 1.38 \times 10^{-4} \text{Mv}^{0.77} \tag{6}$$

The quantum yield of main chain scission (ϕ_{cs}) [10] was calculated from viscosity measurement using the following relation 7.

$$\phi_{cs} = (CA/\bar{M}_{v,0}) \left[([\eta_0]/[\eta])^{1/\alpha} - 1 \right] / I_0 t \tag{7}$$

where: C = concentration; A = Avogadro's number; $(\overline{M}_{v,o}) = \text{the initial viscosity-average molecular weight}$; $[\eta_o] = \text{Intrinsic viscosity of PVC before irradiation}$; $I_o = \text{Incident intensity and } t = \text{Irradiation time in second.}$

Results and Discussion

The 2-thioacetic acid benzothiazol complexes with Sn(II), Cd(II), Ni(II), Zn(II) and Cu(II) were used as additives for the photostabilization of PVC films. In order to study the photochemical activity of these additives for the photostabilization of PVC films, the carbonyl and polyene indices were monitored with irradiation time using IR spectrophotometry. The irradiation of PVC films with UV light of wavelength, $\lambda = 313$ nm led to a clear change in the FTIR spectrum, as shown in Figure 1. Appearance of bands in 1772 cm⁻¹ and 1724 cm⁻¹, were attributed to the formation of carbonyl groups related to chloroketone and to aliphatic ketone, respectively. A third band was observed at 1604 cm⁻¹, related to polyene group. The hydroxyl band appeared at 3500 cm⁻¹ was annotated to the hydroxyl group [11].

The absorption of the carbonyl, polyene and hydroxyl groups was used to follow the extent of polymer degradation during irradiation. This absorption was calculated as carbonyl index (I_{co}), polyene index (I_{PO}) and hydroxyl index (I_{OH}). It is reasonable to assume that the growth of carbonyl index is a measure to the extent of degradation. However, in Figure 2, the I_{co} of $Cu(L)_2$ $Zn(L)_2$, $Ni(L)_2$, $Cd(L)_2$ and $Sn(L)_2$ showed lower growth rate with irradiation time with respect to the PVC control film without additives. Since the growth of carbonyl index with irradiation time is lower than PVC control, as seen in Figure 2, it is suitable to conclude that these additives might be considered as photostabilizers of PVC polymer. Efficient photostabilizer shows a longer induction period. Therefore, the $Sn(L)_2$ is the most active photostabilizer, followed by $Cd(L)_2$, $Ni(L)_2$, $Zn(L)_2$ and $Cu(L)_2$ which is the least active. Just like carbonyl, polyene compounds are also produced during photodegradation of PVC. Therefore, polyene index (I_{PO}) could also be monitored with irradiation time in the presence and absence of these additives. Results are shown in Figure 3.

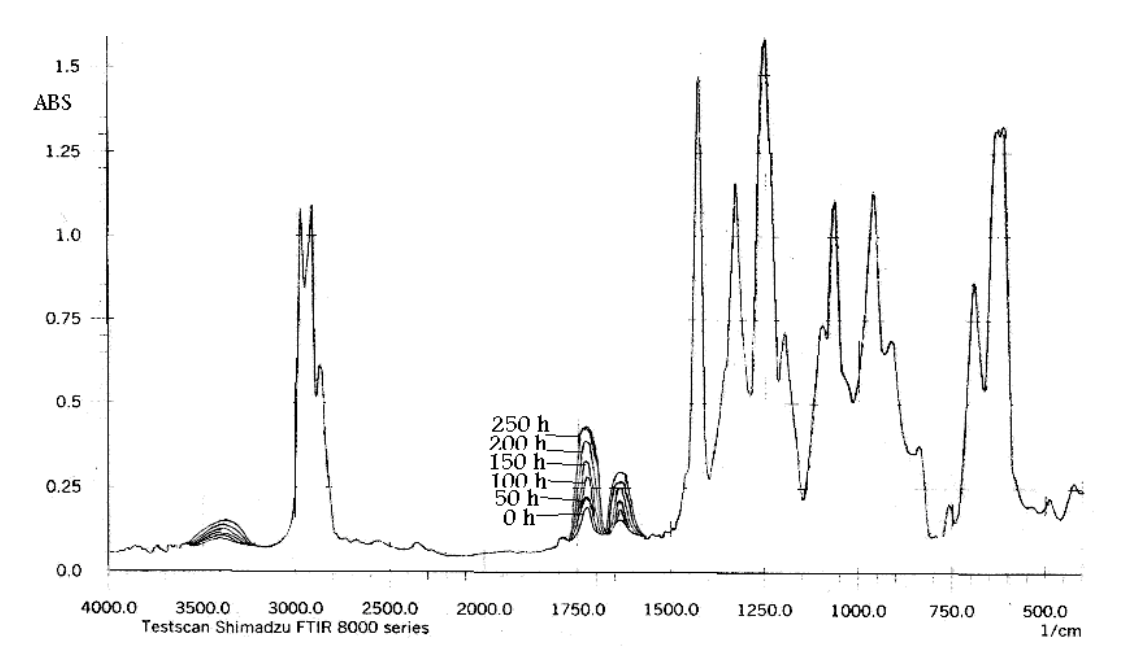


Fig. 1: Change in IR spectrum of PVC film (30 μm) in the presence of Cd(L)₂ complex.

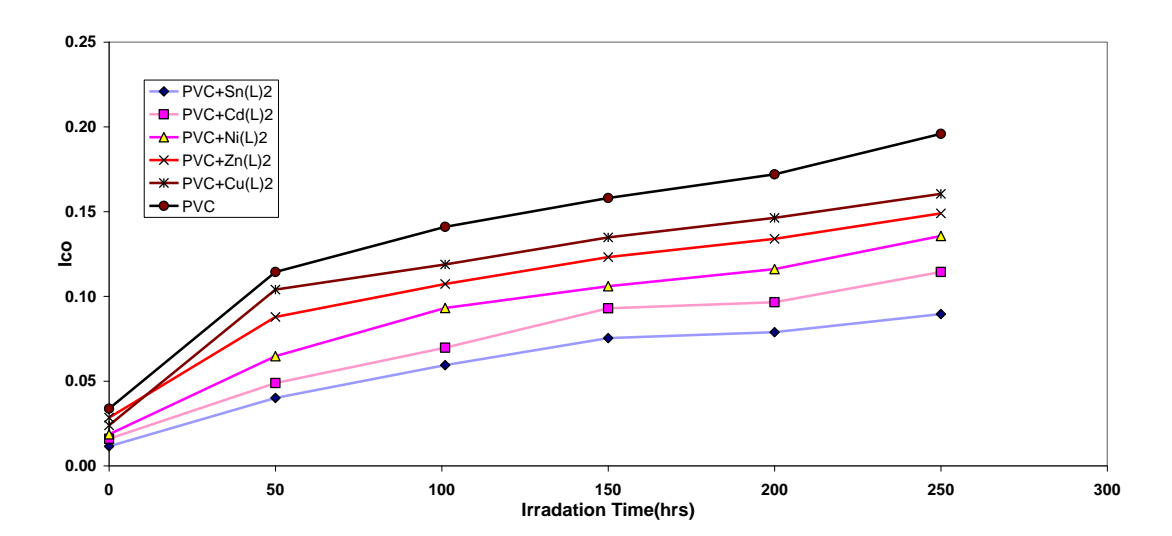


Fig. 2: The relationship between the carbonyl index and irradiation time for PVC films (30 μ m thickness) containing different additives. Concentration of additives is fixed at 0.5% by weight.

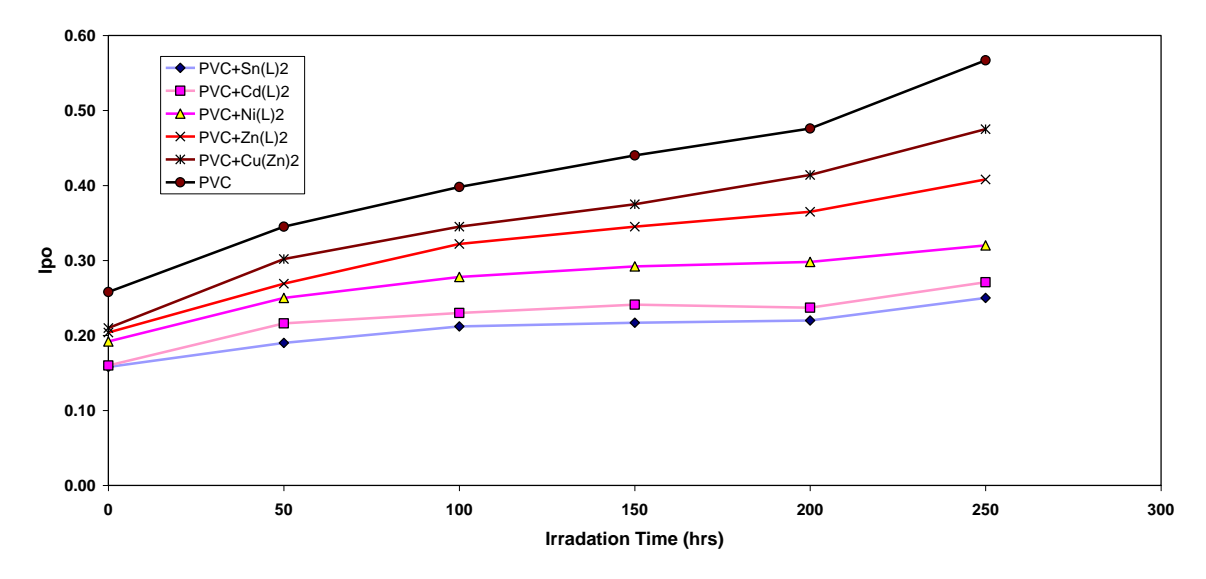


Fig. 3: The relationship between the polyene index and irradiation time for PVC films (30 μ m thickness). Containing different additives, concentration of additives are fixed at 0.5% by weight.

Hydroxyl species were produced during photodegradation of PVC. Therefore, hydroxyl index (I_{OH}) was monitored with irradiation time for PVC and with additives. From Figure 4, the $Cu(L)_2$, $Zn(L)_2$, $Ni(L)_2$, $Cd(L)_2$ and $Sn(L)_2$ showed lower growth rate of hydroxyl index with irradiation time compare to PVC film without modification.

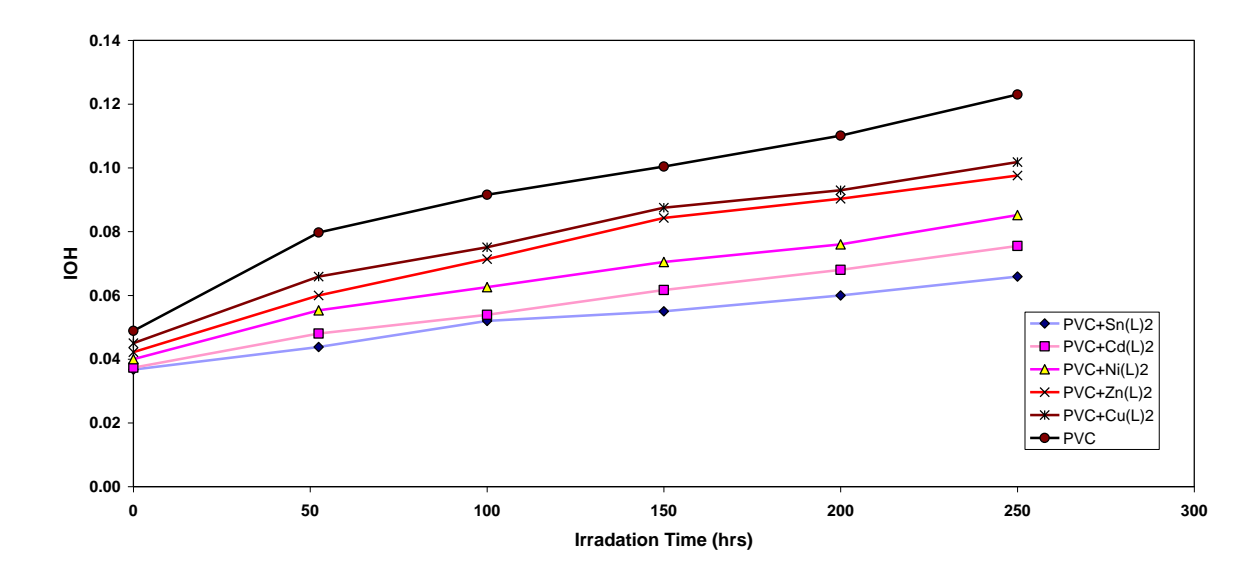


Fig. 4: The relationship between the hydroxyl index and irradiation time for PVC films (30 μm thickness). Containing different additives, concentration of additives are fixed at 0.5% by weight.

Variation of PVC molecular weight during photolysis in the presence of by 2-thioacetic acid benzothiazol complexes

Analysis of the relative changes in viscosity average molecular weight (\overline{M}_v) , has been shown to provide a versatile test for random chain scission. Figure 5 shows the plot of $\overline{M}v$ versus irradiation time for PVC film with and without 0.5% (wt/wt) of the selected additives, with absorbed light intensity of 1.052 x 10^{-8} ein. dm⁻³. s⁻¹. $\overline{M}v$ is measured using Equation 4 with THF as a solvent at 25 °C.

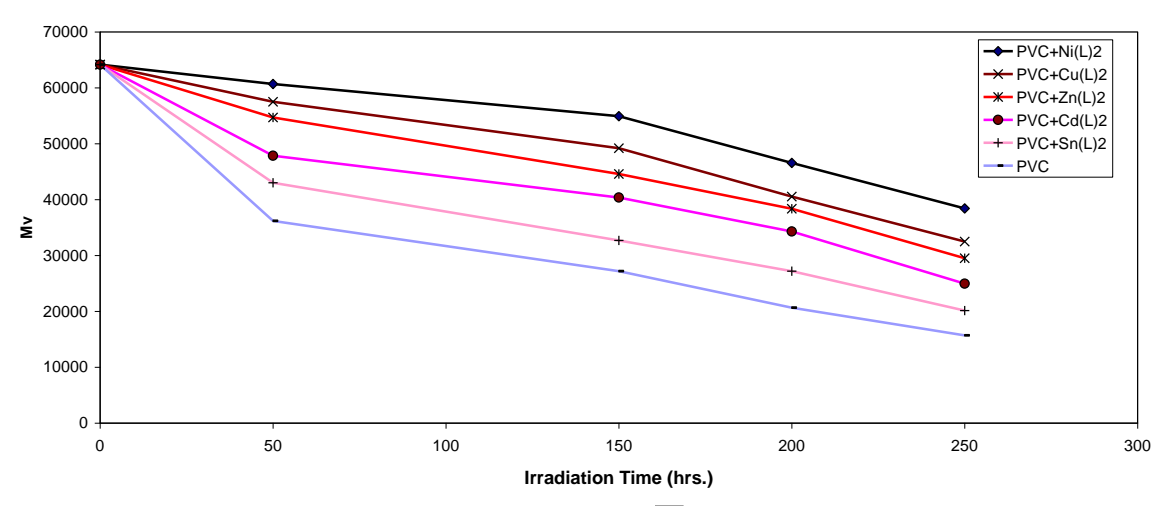


Fig. 5: Changes in the viscosity-average molecular weight (\overline{M}_v) during irradiation of PVC films (30 μ m) (control) and with 0.5 wt% of additives.

It is worth mentioning that traces of the films with additives are not soluble in THF indicating that cross-linking or branching in the PVC chain does occur during the course of photolysis [12]. For better support of this view, the number of average chain scission (average number cut per single chain) (S) [13] was calculated using the relation 8:

$$S = \frac{\overline{M}_{v,o}}{\overline{M}_{v,t}} - 1 \tag{8}$$

where $\overline{M}_{v,o}$ and $\overline{M}_{v,t}$ are viscosity average molecular weights at initial (o) and t irradiation time respectively.

The plot of S versus time is shown in Figure 6. The curve indicates an increase in the degree of branching such as that might arise from cross-linking occurrence. It is observed that insoluble material was formed during irradiation which provided an additional evidences to the idea that cross-linking does occur.

For randomly distributed weak bond links, which break rapidly in the initial stages of photodegradation, the degree of deterioration α is given as:

$$\alpha = \frac{\text{m.s}}{\overline{M}_{v}} \tag{9}$$

where m is the initial molecular weight.

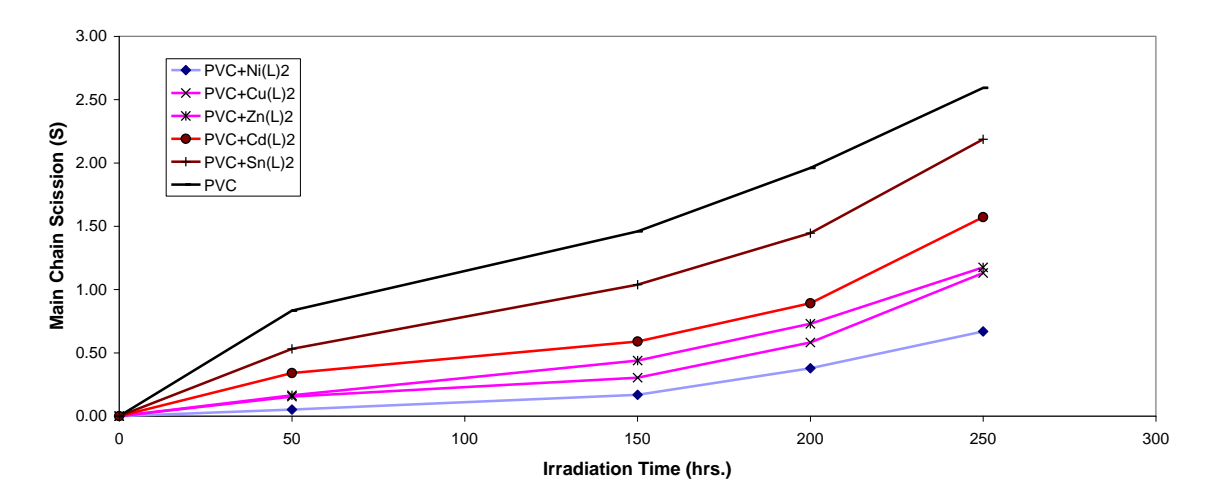


Fig. 6: Changes in the main chain scission (S) during irradiation of PVC films (30 μm) (control) and with 0.5 wt% of additives.

The plot of α as a function of irradiation time is shown in Figure 7.

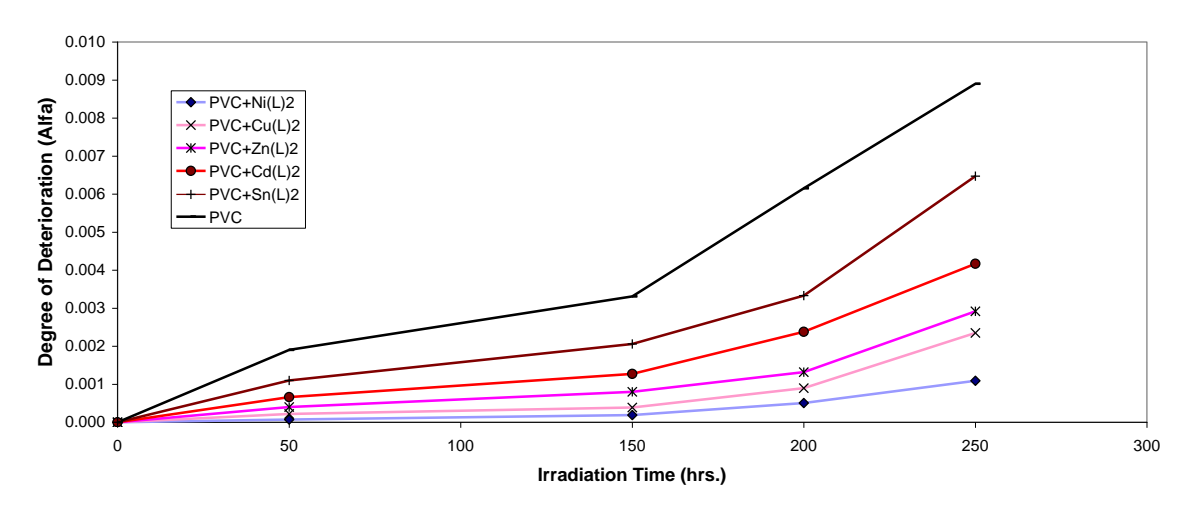


Fig. 7: Changes in the degree of deterioration (α) during irradiation of PVC films (30 μ m) (control) and with 0.5 wt% of additives.

The values of α of the irradiated samples are higher when additives are absent and lower in the presence of additives compared to the corresponding values of the additive free PVC. In the initial stages of photodegradation of PVC, the value of α increases rapidly with time, these indicators indicates a random breaking of bonds in the polymer chain. Another way of degradation reaction characterization is the measurement of the quantum yield of the chain scission (Φ_{cs}). The quantum yield for chain scission was calculated for PVC films with and without 0.5% (wt/wt) of additive mentioned above using relation 5. The Φ_{cs} values for complexes are tabulated in Table 1.

Table 1: Quantum yield (Φcs) for the chain scission for PVC films (30μm) thickness with and without 0.5 (wt/wt) additive after 250 hrs. irradiation time.

Additive (0.5%wt)	Quantum yield of main chain scission (Φ_{cs})
PVC+Sn(L) ₂	4.71E-08
$PVC+Cd(L)_2$	5.23E-08
$PVC+Ni(L)_2$	6.63E-08
$PVC+Zn(L)_2$	7.54E-08
$PVC+Cu(L)_2$	8.98E-08
PVC(control)	8.54E-05

The Φ_{cs} values for PVC films in the presence of additive are less than that of additive free PVC (control), which increase in the order:

$$Sn(L)_2$$
, $Cd(L)_2$, $Ni(L)_2$, $Zn(L)_2$, $Cu(L)_2$ and PVC

It is well established that the quantum yield (Φ_{cs}) increases with increasing temperature [14] around the glass transition temperature, (Tg) of the amorphous polymer, and around the melting temperature of crystalline polymers. In the study presented in this work, the photolysis of PVC film is carried out at a temperature 35 – 45 °C well below the glass transition temperature (Tg of PVC = 80 °C). Therefore, the Φ_{cs} dependency on temperature is not expected to be observed.

Suggested mechanisms of photostabilization of PVC by 2-thioacetic acid benzothiazol complexes

Depending on the overall results obtained, the efficiency of 2-thioacetic acid benzothiazol complexes as stabilizer for PVC films can be arranged according to the change in the carbonyl, polyene and hydroxyl concentration as a reference for comparison as shown in Figures 2 to 4, as follows:

$$Sn(L)_2 > Cd(L)_2 > Ni(L)_2 > Zn(L)_2 > Cu(L)_2$$

Metal carboxylates stabilize PVC by two mechanisms, depending on the metal. Strongly basic carboxylates derived from metals such as Ca and Ba, which have little or no Lewis acidity are mostly HCl scavengers, Scheme 1. Metals such as Sn, Zn, Cd and Cu which are stronger Lewis acids and form covalent carboxylates, not only scavenge HCl, but also substitute carboxylate for the allylic chlorine atoms. These stabilizers provide very good long-term stability and are usually referred to as secondary stabilizers, Scheme 1. Similar mechanism was suggested by Yousif et.al (2009) for photostabilizing of PVC using of 2-thioacetic acid -5-phenyl-1,3,4-oxadiazole complexes [15].

IR spectroscopy has shown that metals carboxylates associate with PVC molecules at the surface of primary particles and are, consequently, very effective in the substitution of allylic chlorine. In this mechanism, the stabilizer is classified as a primary stabilizer. It has been postulated that metals stabilizers associate with chlorine atoms at the surface of PVC primary particles which explains their high efficiency in PVC stabilization [16], Scheme 2.

Emad Yousif et al: IMPROVEMENT OF THE PHOTOSTABILIZATION OF PVC FILMS IN THE PRESENCE OF THIOACETIC ACID BENZOTHIAZOLE COMPLEXES

Scheme 1: Suggested mechanism of photostabilization of complexes as HCl scavengers.

Scheme 2: Suggested mechanism of photostabilization of complexes as primary stabilizers.

Metal chelate complexes generally known as photostabilizers for PVC through both peroxide decomposer and excited state quencher. Therefore, it is expected that these complexes act as peroxide decomposer through the following proposed mechanism, Scheme 3 below. This mechanism is in agreement with that reported by Adil [17].

Scheme 3: Suggested mechanism of photostabilization of complexes as peroxide decomposer.

These metal chelate complexes also function as radical scavengers through energy transfer and by forming unreactive charge transfer complexes between the metal chelate and excited state of the chromophore (POO) and stabilize through resonating structures as shown in Scheme 4. This mechanism is adopted by Adil [17].

Scheme 4: Suggested mechanism of photostabilization of carboxylates complexes as radical scavengers through energy transfer and forming unreactive charge transfer and stabilize through resonating structure.

The ring of benzothiazol in this compound plays an important role in the mechanism of stabilizing process by acting as UV absorber. The UV light absorption by these additives containing benzothiazol dissipates the UV energy to harmless heat energy, Scheme 5. Further more this ring plays a role in resonating structures conjugation of radical in peroxide decomposer, Scheme 5, which supports this compound as a photostabilizer [18].

$$\frac{h_{\nu}}{s}$$
 + heat

Scheme 5: Suggested mechanism of photostabilization of benzothiazole as UV absorber.

Conclusion

In the work described in this paper, the photostabilization of poly(vinyl chloride) (PVC) films using 2-thioacetic acid benzothiozol complexes were studied. These additives behave successfully as photostabilizer for PVC films. The additives take the following order in photostabilization activity according to their decrease in carbonyl, polyene and hydroxyl indices for PVC films.

$$Sn(L)_2 > Cd(L)_2 > Ni(L)_2 > Zn(L)_2 > Cu(L)_2$$

These additives stabilize the PVC films through HCl scavenging, UV absorption or screening, peroxide decomposer and radical scavenger mechanisms. The tin complexes were found to be the more efficient in photostabilization process according to the photostability and mechanisms mentioned above. These mechanisms support the idea of using tin complexes as commercial stabilizer for PVC.

Acknowledgements

We are grateful to Universiti Kebangsaan Malaysia for funding ("Code UKM-GUP-NBT-08-27-113", "UKM-GGPM-NBT-164-2010" and "UKM-OUP-NBT-29-150/2011"), and Department of Chemistry, College of Science, Al-Nahrain University. Special thank to SRF, IIE.

Emad Yousif et al: IMPROVEMENT OF THE PHOTOSTABILIZATION OF PVC FILMS IN THE PRESENCE OF THIOACETIC ACID BENZOTHIAZOLE COMPLEXES

References

- 1. Saeki, Y., Emura, T. 2002. Technical progresses for PVC production. Prog. Polym. Sci. 27: 2055–131.
- 2. Braun, D., 2004. Poly(vinyl chloride) on the way from the 19th century to the 21st century. J. Polym. Sci. A Polym. Chem. 2004;42: 578–586.
- 3. Moulay, S., 2010. Chemical modification of poly(vinyl chloride)-Still on the run. Progress in Polymer Science. 35: 303-331.
- 4. Andrady, A., Hamid, S., Hu, X. & Torikai, A. 1998. Effects of increased solar ultraviolet radiation on materials. Journal of Photochemistry and photobiology B-Biology. 46: 96-103.
- 5. Gardette, J., Gaumet, S. & J. L. Philippart, J. 1993. Influence of the experimental conditions on the photooxidation of poly(vinyl chloride). Journal of Applied Polymer Science. 48(11): 1885-1895.
- 6. Yousif, E., Farina, Y., Kasar, K., Graisa, A. & Ayid. K. 2009. Complexes of 2-thioacetic acid benzothiazole with Some Metal Ions. American Journal of Applied Sciences. 6(4): 605-608.
- 7. Rasheed, R., Mansoor H., Yousif E., Hameed A. FarinaY. & Graisa A., 2009. Photostabilizing of PVC films by 2-(aryl)-5-[4-(aryloxy)-phenyl]-1,3,4-oxadiazole compounds. European Journal of Scientific Research. 30(3): 464-477.
- 8. Rabek, J. & Ranby, B. 1975. Photodegradation, photooxidation and photostabilization of Polymers, John Wiley, New York.
- 9. Mark, J. 2007. Physical properties of polymers handbook. Springer, New York.
- 10. Nakajima, N., Sadeghi, M., Kyu, T. 1990. Photodegradation of poly(methyl methacrylate) by monochromatic light: quantum yield, effect of wavelengths, and light intensity. Journal of Applied Polymer Science. 41: 889 1363.
- 11. Andrady, A., Searle, N. 1989. Photodegradation of rigid PVC formulations. II. Spectral sensitivity to light-induced yellowing by polychromatic light. Journal of Applied Polymer Science. 37:2789-2802.
- 12. Mori, F., Koyama, M. & Oki, Y. 1977. Studies on photodegradation of poly(vinyl chloride) (part 1). Die Angewandte Makromolekulare Chemie. 64(1): 89-99.
- 13. Shyichuk, A. & White, J. 2000. Analysis of chain-scission and crosslinking rates in the photo-oxidation of polystyrene. Journal of Applied Polymer Science. 77(13): 3015-3023.
- 14. Jellinek, H. 1978. Aspects of degradation and stabilization of polyolefines, Elsevier, Amsterdam.
- 15. Yousif, E., Aliwi, S., Ameer, Ukal, J. 2009. Improved photostability of PVC films in the presence of 2-thioacetic acid -5-phenyl-1,3,4-oxadiazole complexes. Turkish Journal of Chemistry. 33: 399-410.
- 16. Yousif, E., Salih, N., Salimon, J. 2011. Improvement of the "Improvement of the Photostabilization of PVC Films in the Presence of 2N-Salicylidene-5-(Substituted)-1,3,4-Thiadiazole. Journal of Applied Polymer Science, 120: 2207–2214.
- 17. Adil, H., Emad Yousif, E., Salimon, J. 2011. New Stabilizers For PVC Based On Benzothiazole Complexes. LAMBERT Academic Publishing, Germany.
- 18. Yousif, E., Hameed, A., Rasheed, R., Mansoor, H., Farina, Y., Graisa, A., Salih, N., Salimon, J. 2010. Synthesis and Photostability Study of Some Modified Poly(vinyl chloride) Containing Pendant Benzothiazole and Benzimidozole Ring. International Journal of Chemistry, 2(1): 65-80.



SYNTHESIS, CHARACTERIZATION AND NEUROTOXIC EFFECT OF SCHIFF BASE LIGANDS AND THEIR COMPLEXES

(Sintesis, Pencirian dan Pengaruh Nurotoksik Bes Schiff dan Kompleksnya)

Ahmad Fauzi Abu Bakar¹*, Hadariah Bahron¹, Karimah Kassim¹, Mazatulikhma Mat Zain²

¹Department of Chemistry, Faculty of Applied Sciences, ²Institute of Science (IOS), Universiti Teknologi MARA 40450 Shah Alam, Selangor, Malaysia

*Corresponding author: fauzi_charming@yahoo.com

Abstract

Two ligands and eight complexes are successfully synthesized by reacting 1,8-diaminonapthelene with aldehyde/ketone derivatives in 1:2 ratio for ligand formation and 1:1 ratio for complex formations. The compounds are characterized through CHN elemental analysis, IR spectroscopy, ¹H NMR spectroscopy, melting point and magnetic susceptibility determination. The neurotoxicity of compounds is evaluated using neuroblastoma SH-SY5Y cell lines and it was indicate the cells were non-toxic either for ligands and complexes after 24 hours exposure.

Keywords: Schiff base, 1,8-diaminonaphthalene, neurotoxicity, SH-SY5Y cell lines

Abstrak

Dua ligan dan lapan kompleks berjaya disintesis dengan tindakbalas 1,8-diaminonapthelene dengan keton/aldehid terbitan dengan nisbah 1:2 untuk pembentukan ligan dan nisbah 1:1 untuk pembentukan kompleks. Sebatian dicirikan melalui analisis unsur, spektroskopi IR, spektroskopi ¹H NMR, takat lebur dan penetapan suseptibiliti magnet. Neurotoksisiti sebatian dinilai menggunakan baris sel neuroblastoma SH-SY5Y yang mendedahkan bahawa ligan dan kompleks tidak toksik ke atas sel-sel selepas 24 jam pendedahan.

Kata kunci: Bes Schiff, 1,8-diaminonaftalena, neurotoksisiti, baris sel SH-SY5Y

Introduction

Schiff base formed by condensation of a primary amine and aldehyde/ketone resulting R¹HC=N-R²/R¹H₃C=N-R₂. it is particularlyfor binding metal ion through N atom that has lone pair on it. It usually used for combining one or more donor atom to form polydentate or macrocyclic ligand [1]. Schiff bases also are characterized by the presence of –N=C– (imine) functional group [3] that can be derived from a large number of carbonyl compounds and amines which is important in biological systems [8]. It was found that Schiff bases produced from salicyldehyde and its derivatives yield polydentate ligands mostly which can form stable complexes with transition metals [8]. Most of the matel make the ration 1:1 to the metal formed complexes with Schiff base. [7]. Schiff base and their first row transition metal complexes [(Cu(II), Co(II), Ni(II) and etc.)] were reported to exhibit fungicidal, bactericidal, antiviral and antitubucular activity [1]. Metal complexes with Schiff base as ligand played an important role in development of coordination chemistry [1]. The antifungal and antibacterial properties of a range of Cu(II) complexes have been evaluated against several phatogenic and the bacterial [5]. Co(II) complexes with N-donor ligands containing binding units suitable either for coordination of single metal ion or for assembling dimetallic center [6].

The research investigation concerns on Schiff base compounds synthesized from the condensation reaction of 1,8-diaminonaphthalene, an aromatic amine containing two fused benzene rings, with aldehydes and ketones containing

electron donating and electron withdrawing substituents in the benzene ring. The compounds investigated are illustrated in Table 1. In this study, we prepared a variety of Schiff base ligands (L) and copper(II), cobalt(II), nickel(II) and zink(II). These compounds are then evaluated for their toxicity on SH-SY5Y neuroblastoma cell lines.

Table 1: Expected Schiff base ligands (L) and its complexes.

	OH HO N CH ₃ L1	OH HO N L2
CuCl ₂ .2H ₂ O	H ₃ C CuL1	CuL2
CoCl ₂ .6H ₂ O	H ₃ C C _O L ₁	CoL2
NiCl ₂ .6H ₂ O	NiL1	NiL2
ZnCl ₂	N=CH ₃	ZnL2

Experimental

Physical measurements

The elemental analysis was carried out on Thermo Finnigan Flash EA 110 Elemental Analyzer. ¹H and ¹³C NMR spectra were recorded on Bruker Varian 300 Hz. Infrared spectra were obtained on Perkin Elmer 1750X FTIR spectrophotometer on KBr discs in the range 4000–350 cm⁻¹ and melting points were measured using BÜCHI Melting Point B-545. Magnetic susceptibility balances of compounds were measured on Sherwood Auto Magnetic susceptibility balance.

Materials

The starting materials used in this work were 1,8-diaminonaphthalene, 2-hydroxyacetophenone, salicyldehyde, copper(II) chloride dihydrate, cobalt(II) chloride hexahydrate, nickel(II) chloride hexahydrate and zinc(II) chloride purchased from Sigma Aldrich. All chemicals and solvents were of analytical grade and used as received without prior purification.

Synthesis of L1

Ethanolic solution of 2-hydroxyacetophenone (2 mmol) was added dropwise to a stirred ethanolic solution of 1,8-diaminonaphthalene (1 mmol). The reaction mixture was refluxed for 8 hours. Then the solution was allowed to slowly evaporate at room temperature, upon which a precipitate was obtained. The product was filtered off, washed with cold ethanol and vacuum dried.

Synthesis of CuL1

Complex CuL1 was prepared by the *in-situ* method. Ethanolic solution of salicyldehyde (2 mmol) was added dropwise to a stirred ethanolic solution of 1,8-diaminonaphthalene (1 mmol). The reaction mixture was refluxed for about 3 hours. Then ethanolic of copper(II) chloride dehydrate (1 mmol) was added into the mixture. After all mixture was completed the mixture was heated under reflux for 5 hours. Then the solution was allowed to slowly evaporate at room temperature, upon which a precipitate was obtained. The product was filtered off, washed with cold ethanol and vacuum dried.

Synthesis of CoL1

Complex CoL1 was prepared by the *in-situ* method. Ethanolic solution of salicyldehyde (2 mmol) was added dropwise to a stirred ethanolic solution of 1,8-diaminonaphthalene (1 mmol). The reaction mixture was refluxed for about 3 hours. Then ethanolic of cobalt(II) chloride hexahydrate (1 mmol) was added into the mixture. After all mixture was completed the mixture was heated under reflux for 5 hours. Then the solution was allowed to slowly evaporate at room temperature, upon which a precipitate was obtained. The product was filtered off, washed with cold ethanol and vacuum dried.

Synthesis of NiL1

Complex CuL1 was prepared by the *in-situ* method. Ethanolic solution of salicyldehyde (2 mmol) was added dropwise to a stirred ethanolic solution of 1,8-diaminonaphthalene (1 mmol). The reaction mixture was refluxed for about 3 hours. The nickel(II) chloride hexahydrate (1 mmol) solution was added into the mixture. After all mixture was completed the mixture was heated under reflux for 5 hours. Then the solution was allowed to slowly evaporate at room temperature, upon which a precipitate was obtained. The product was filtered off, washed with cold ethanol and vacuum dried.

Synthesis of ZnL1

Complex CuL1 was prepared by the *in-situ* method. Ethanolic solution of salicyldehyde (2 mmol) was added dropwise to a stirred ethanolic solution of 1,8-diaminonaphthalene (1 mmol). The reaction mixture was refluxed for about 3 hours. Then ethanolic of zink(II) chloride (1 mmol) was added into the mixture. After all mixture was completed the mixture was heated under reflux for 5 hours. Then the solution was allowed to slowly evaporate at room temperature, upon which a precipitate was obtained. The product was filtered off, washed with cold ethanol and vacuum dried.

Ahmad Fauzi et al: SYNTHESIS, CHARACTERIZATION AND NEUROTOXIC EFFECT OF SCHIFF BASE LIGANDS AND THEIR COMPLEXES

Synthesis of L2

Ethanolic solution of salicyldehyde (2 mmol) was added dropwise to a stirred ethanolic solution of 1,8-diaminonaphthalene (1 mmol). The reaction mixture was refluxed for 8 hours. Then the solution was allowed to slowly evaporate at room temperature, upon which a precipitate was obtained. The product was filtered off, washed with cold ethanol and vacuum dried.

Synthesis of CuL2

Complex CuL1 was prepared by the *in-situ* method. Ethanolic solution of salicyldehyde (2 mmol) was added dropwise to a stirred ethanolic solution of 1,8-diaminonaphthalene (1 mmol). The reaction mixture was refluxed for about 3 hours. Then ethanolic of copper(II) chloride dehydrate (1 mmol) was added into the mixture. After all mixture was completed the mixture was heated under reflux for 5 hours. Then the solution was allowed to slowly evaporate at room temperature, upon which a precipitate was obtained. The product was filtered off, washed with cold ethanol and vacuum dried.

Synthesis of CoL2

Complex CoL1 was prepared by the *in-situ* method. Ethanolic solution of salicyldehyde (2 mmol) was added dropwise to a stirred ethanolic solution of 1,8-diaminonaphthalene (1 mmol). The reaction mixture was refluxed for about 3 hours. Then ethanolic of cobalt(II) chloride hexahydrate (1 mmol) was added into the mixture. After all mixture was completed the mixture was heated under reflux for 5 hours. Then the solution was allowed to slowly evaporate at room temperature, upon which a precipitate was obtained. The product was filtered off, washed with cold ethanol and vacuum dried.

Synthesis of NiL2

Complex NiL1 was prepared by the *in-situ* method. Ethanolic solution of salicyldehyde (2 mmol) was added dropwise to a stirred ethanolic solution of 1,8-diaminonaphthalene (1 mmol). The reaction mixture was refluxed for about 3 hours. Then ethanolic of nickel(II) chloride hexahydrate (1 mmol) was added into the mixture. After all mixture was completed the mixture was heated under reflux for 5 hours. Then the solution was allowed to slowly evaporate at room temperature, upon which a precipitate was obtained. The product was filtered off, washed with cold ethanol and vacuum dried.

Synthesis of ZnL2

Complex ZnL1 was prepared by the *in-situ* method. Ethanolic solution of salicyldehyde (2 mmol) was added dropwise to a stirred ethanolic solution of 1,8-diaminonaphthalene (1 mmol). The reaction mixture was refluxed for about 3 hours. Then ethanolic of zink(II) chloride (1 mmol) was added into the mixture. After all mixture was completed the mixture was heated under reflux for 5 hours. Then the solution was allowed to slowly evaporate at room temperature, upon which a precipitate was obtained. The product was filtered off, washed with cold ethanol and vacuum dried.

Cytotoxicity effect

Human neuroblastoma SH-SY5Y cell lines were given as a gift from cell culture laboratory of Universiti Teknologi MARA (UiTM). The cells differentiated to neutral phenotype with addition of retinoic acid (RA). Incubation of cells in humidified atmosphere at 37°C in 5% of CO₂ conducted in 6 days before testing. Media changed after 3 days.

Small volumes of ligands were added to each well to make the dilution 10nM, 100nm, 1μ M, 10μ M, 100μ M and 1mM. Cultures incubated in humidified atmosphere at 37°C in 5% of CO_2 for 24 hours.

After incubated for 24 hours, 20μ l of MTS solution added to each well and incubated in humidified atmosphere 37°C in 5% of CO₂ for 2-4 hours in the dark. The quantity of formazan product present was determined by measuring its absorbance at 490nm using GloMax Multi Detection System. Cell viability was determined. Compound will be considered as non toxic if the viability of cells is above 50% [4].

Results and Discussion

The Schiff bases were synthesized by condensation reaction between ketone/aldehyde derivatives and 1,8-diaminonaphthalene in 2:1 molar ratio in ethanol and in 1:1 molar ratio between ligand and metal salt. All the Schiff bases are stable at room temperature and soluble in DMSO.

Elemental Analysis (C, H, N)

From the Table 2, comparing the experimental and theoretical values of the C, H and N percentages, it could be seen that the two sets of Schiff base compounds (L1 and L2 with metal complexes) that reported are acceptable. Therefore it could be suggested that the intended Schiff bases have been successfully isolated. The melting point of each ligands were found below 200°C while for complexes were all found above 200°C. This suggested that the compound were stable in air.

G	Calaa	M.P		C]	H	l l	1
Comp.	Color	(° C)	Theo	Expt	Theo	Expt	Theo	Expt
L1	Reddish Brown	150	79.16	80.91	5.62	5.82	7.10	7.58
CuL1	Grey	265	68.48	67.31	4.42	4.06	6.14	5.32
CoL1	Dark Brown	268	69.18	68.76	4.47	3.41	5.80	5.45
NiL1	Dark Brown	260	69.22	68.75	4.47	4.67	6.21	6.02
ZnL1	Dark Brown	274	68.21	68.35	4.40	4.22	6.12	6.77
L2	Light Brown	179	78.67	77.66	4.95	5.34	7.65	7.45
CuL2	Grey	257	67.36	65.79	3.77	3.19	6.55	7.14
CoL2	Black	267	68.09	68.66	3.81	3.11	6.62	6.51
NiL2	Dark Brown	262	68.13	67.65	3.81	3.59	6.62	5.16
ZnL2	Black	267	67.07	66.14	3.75	3.83	6.52	6.71

Table 2: Data of Elemental Analysis

Infrared Spectroscopy

Using Perkin Elmer 1750X FTIR spectrophotometer on KBr discs, Table 3 show the data of infrared spectroscopy investigation of the Schiff bases revealed strong bands in the region 1600 cm $^{-1}$ due to $\nu(C=N)$ [8]. Due to $\nu(-OH)$, IR peaks appear in the spectra of each Schiff bases in the region 2800 cm $^{-1}$ [2]. The peaks of $\nu(-H_2O)$ appear around 3500 cm $^{-1}$. Peak at $\nu(-OH)$ will be disappeared when it formed complexes.

¹H Nuclear Magnetic Resonance Spectroscopy

By using ¹H NMR spectroscopy, the number of hydrogen can be quantified in the Schiff base compounds. The results obtained compared positively with the predicted ¹H NMR from ChemDraw Ultra 7.0.

From ¹H NMR spectrum data for the free ligand L1 shows the multiplet in the range 7.38- 8.10 ppm due to the aromatic proton. Singlet O-H proton will appeared at 12.98 ppm. Singlet methyl proton will appear at around 1.82 ppm while free lidand L2 shows the multiplet in the range 7.00- 8.20 ppm due to the aromatic proton. Singlet O-H proton will appear around 10.66 ppm.

For the complexes L1, the multiplet spectrum that represent aromatic proton will appear at range 6.73-7.84. Singlet methyl proton will appear around 1.65 ppm while complexes L2, the multiplet in the range 7.24-8.22 ppm that indicates aromatic proton and the azomethine proton will appear around 8.54 ppm.

Peaks	L1	CuL1	CoL1	NiL1	ZnL1	L2	CuL2	CoL2	NiL2	ZnL2
Broad v (-OH)	3376.81	3446.53	3367.97	3260.22	3134.32	3424.35	3467.11	3400.49	3400.03	3544.17
v (-OH)	2846.79	-	-	-	-	2848.70	-	-	-	ı
v (C=N)	1600.69	1628.13	1628.11	1618.11	1631.33	1601.38	1621.21	1621.31	1638.52	1618.54
v (M- O)	-	535.12	576.22	521.52	524.47	ı	563.11	574.45	568.06	523.66
v (M-N)	-	443.86	463.13	458.54	476.36	-	446.48	471.22	436.75	451.49

Table 3: Data of Infrared Spectroscopy

Magnetic susceptibility determination

Magnetic susceptibility was determined using Sherwood Auto Magnetic susceptibility balance and the data was shown at Table 4. This data indicated that Cu(II) [Ar]d⁹ are found to have 1.62-1.69 B.M and its correspond to the one unpaired electron. The paramagnetic properties agree that the Cu(II) will be formed tetrahedral or square planar geometry. Co(II) [Ar]d⁷ are found to have 3.23-3.64 B.M and shows as paramagnetic property because it has three lone pair in splitting diagram. From the splitting diagram it shows the Co(II) complexes has tetrahedral geometry. Since Ni(II) [Ar]d⁸ has diamagnetic property and it will formed square planar geometry because the splitting diagram shows the electron are filling in all stage while Zn(II) [Ar]d¹⁰ has diamagnetic property to formed either tetrahedral or square planar geometry.

Complexes	μ _{eff} (Β.Μ.)	$d^{\rm n}$	Suggested Geometry
CuL1	1.62	d^9	Tetrahedral/square planar
CoL1	3.64	d^7	Tetrahedral
NiL1	Diamagnetic	d^8	Square planar
ZnL1	Diamagnetic	d^{10}	Tetrahedral/square planar
CuL2	1.69	d^9	Tetrahedral/square planar
CoL2	3.23	d^7	Tetrahedral
NiL2	Diamagnetic	d^8	Square planar
ZnL2	Diamagnetic	d^{10}	Tetrahedral/square planar

Table 4: Data of Magnetic susceptibility determination

Neurotoxic Effect

The percentages of viability of neuroblastoma SH-SY5Y cell lines after treatment with 2 Schiff bases and 8 complexes are illustrated in Figure 1. The results revealed that all the percentages of viable cells were well above 50% with the minimum cell viability (most toxic) just below 60% for the NiL1 and NiL2. This observation indicated that the Schiff bases ligands and its complexes under study were all considered as non-toxic to the neuroblastoma SH-SY5Y cell lines [4]. It is also interesting to note that L1 seemed to enhance the growth of these cells.

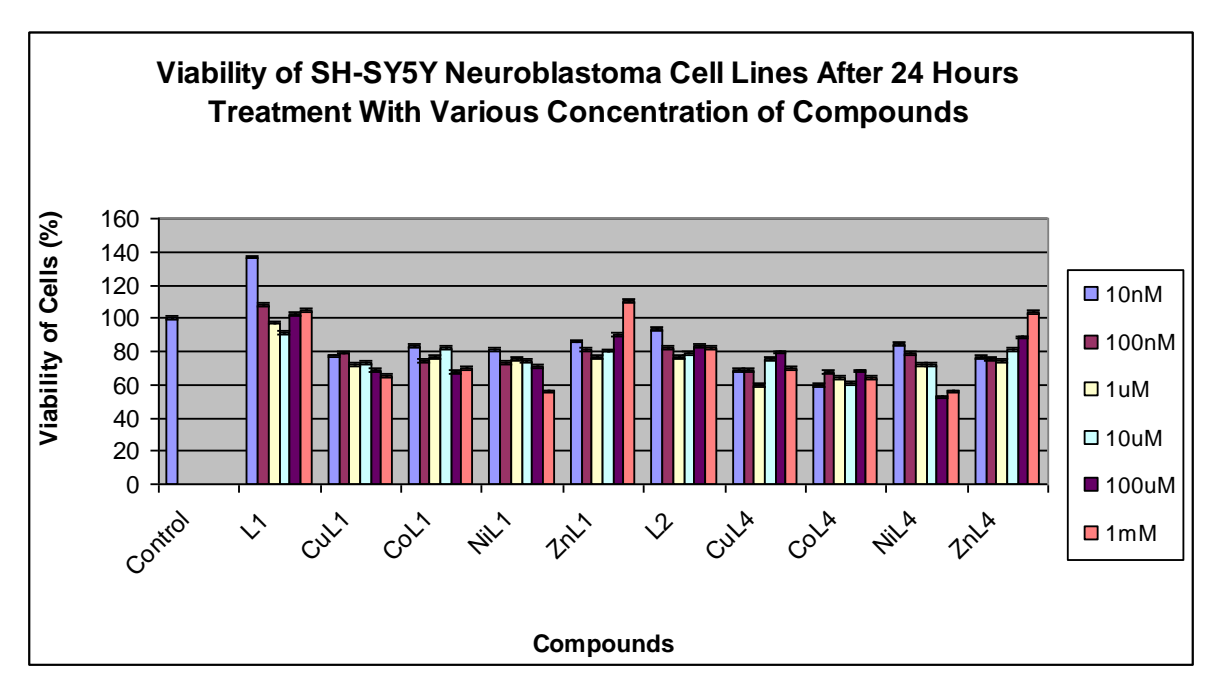


Figure 1: Viability of SH-SY5Y neuroblastoma cell lines after a 24-hour treatment with various concentrations of compounds.

Conclusion

The Schiff bases and their complexes were successfully synthesized and characterized. The compounds were found to be non-toxic to the SH-SY5Y neuroblastoma cell lines after a 24-hour treatment with L1 being the best compound that enhanced the cell growth.

Acknowledgement

This research was supervised by Prof. Madya Dr. Hadariah Bahron, Dr. Karimah Kassim and Pn. Mazatulikhma Mat Zain. We express our sincere appreciation to the Ministry of Higher Education of Malaysia for the research grant FRGS UiTM 5/3/FST/(12/2008), the Department of Chemistry and the Tissue Culture Laboratory of Institute of Science (IOS), UiTM, Shah Alam for the facilities.

References

- 1. Dolaz, M., McKee, V., Gölcu, A. and Tumer, M. (2009) Synthesis, characterization, thermal and electrochemical studies of the N,N'-bis[(3,4-dichlorophenyl)methylidine]cyclohexane-1,4,diamine and its Cu(II), Co(II) and Ni(II).
- 2. El-Ayaan, U. and Aziz, A.A.M.A., (2005) Synthesis, antimicrobial activity and molecular modeling of cobalt and nickel complexes containing the bulky ligand: bis[N-(2,6-diidpropylphenyl)imino] acenaphthene, *European Journal of Medical Chemistry*, 40, 1214-1221.
- 3. Golcu, A., Tumer, M., Demirelli, H. and Wheatley R.A., (2005) Cd(II) and Cu(II) complexes of polydentate Schiff base ligand: synthesis, characterization, properties and biological activity, *Inorg. Chim. Acta.*, 358, 1785-179.
- 4. Lin, Y.C., Huang., Chen, S.C., Liaw C.C., Kuo, S.C., Huang, L.Y. and Gean, P.W., (2009) *Neuroprotective Effecs of Ugonin K on Hydrogen Peroxide-Induced Cell Death in Human Neuroblastoma SH-SY5Y Cells*. Neurochem Res, 34:923-930.
- 5. Lv, J., Liu, T., Cai, S., Wang, X., Liu, L. and Wang, Y., (2006) Synthesis, structure and zbiological activity of cobalt(II) and copper(II) complexes of valine-derived Schiff base, *Journal of Inorganic Biochemistry*, 100, 1888-1896

Ahmad Fauzi et al: SYNTHESIS, CHARACTERIZATION AND NEUROTOXIC EFFECT OF SCHIFF BASE LIGANDS AND THEIR COMPLEXES

- 6. Nasrabadi, M.R., Ganjali, M.R., Gholivand, M.B., Ahmadi, F., Norouzi, P. and Niasari, M.S., (2008) A cyclic voltammetry investigation of the complex formation between Cu²⁺ and some Schiff base in binary acetonitrile/dimethylformamide mixture, Journal of Molecular Structure, 885, 76-81.
- 7. Shakir, M., Azam, M., Parveen, S., Khan, A.U. and Firdaus, F., (2009) *Synthesis and spectroscopic studies on complexes of N,N-bis*(2-pyridinecarboxaldimine)-1,8-diaminonaphthalene (L); DNA binding studies on Cu(II) complexes, Spectrochimica Acta Part A, 71, 1851-1856.
- 8. Rouhollahi, A., Zolfonoun, E. and Niasari, M.S. (2007) *Effect on ionic surfactant on transport of copper (II) through liquid membrane containing a new synthesis Schiff base*. Saperation and Purification Technology, 54, 28-33.



SYNTHESIS AND CHARACTERIZATION OF YAG:Ce PREPARED BY SOLID STATE REACTION METHOD

(Sintesis dan Pencirian YAG:Ce Disediakan Melalui Kaedah Tindak Balas Keadaan Pepejal)

Ahmad Saat^{1*}, Hazimah Harun², Zaini Hamzah²

¹Institute of Science, ²Faculty of Applied Sciences, Universiti Teknologi MARA, 40450 Shah Alam, Selangor, Malaysia.

*Corresponding author: ahmad183@salam.uitm.edu.my

Abstract

Yttrium aluminum garnet (YAG) powder doped with Cerium (Ce) was successfully synthesized by solid-state reaction method. In our work, we investigated YAG and YAG:Ce phase formation by X-ray diffraction (XRD) technique and the result showed that YAG and YAG:Ce were crystallized at 1000° C for 6 h. In all samples, small peak of Ce_2O_3 appeared at $2\theta = 28.572^{\circ}$ and 47.51° . The intensity of these peaks increased with increasing doping concentration of dopant. Field emission scanning electronic microscope (FESEM) images showed that the resultant YAG:Ce powders were basically spherical. Particle size, estimated by XRD using Scherrer's equation, was found to be 53 - 82 nm while by FESEM image the average sizes of the grains were in the range 45 – 50 nm. All the samples have pure YAG phase and the TAG intensity decreases on increasing the doping concentration.

Keywords: YAG:Ce, X-ray diffraction, field emission scanning electronic microscope

Abstrak

Serbuk YAG dengan Cerium (Ce) telah berjaya disintesis dengan menggunakan kaedah tindak balas keadaan pepejal. Dalam kajian ini YAG dan fasa pembentukan YSG:Ce diselidik dengan menggunakan kaedah XRD, dan hasil kajian menunjukkan YAG dan YAG:Ce membentuk hablur pada suhu 1000 °C selepas 6 jam. Dalam semua sampel puncak kecil Ce_2O_3 muncul di $2\theta = 28.572^{\circ}$ dan 47.51° . Keamatan puncak ini meningkat dengan peningkatan kepekatan dopan yang digunakan. Imej-imej mikroskop imbasan elektron pancaran medan (FESEM) menunjukkan serbuk YAG:Ce yang terhasil berbentuk sfera. Saiz zarahzarah yang dianggarkan menggunakan persamaan Scherrer ailah 53 - 82 nm namun menggunakan imej FESEM saiz zarah-zarah berada dalam julat 45 – 50 nm. Semua sampel mengandungi fasa YAG tulen, dan keamatan TAG berkurang dengan peningkatan kepekatan dopan.

Kata kunci: YAG:Ce, pembelauan sinar –X, mikroskop imbasan elektron pancaran medan

Introduction

Recently, inorganic phosphors have been extensively investigated for the application for various types of display panels. To improve the brightness and resolution of these displays, much effort has been made to develop phosphors with controlled morphology, high efficiency and fine size particles [1]. Yttrium Aluminum Garnet (Y₃Al₅O₁₂, YAG) is a well-known inorganic compound which has excellent chemical, physical and optical properties. YAG base phosphors have been widely studied in the application of displays because of their stability at the conditions of high irradiance with an electron beams [2]. Besides, the YAG phosphors doped with various rare earth elements are useful in a variety of display applications including cathode ray tube, low voltage field emission display and backlight source [3]. Among them, cerium-doped YAG (YAG:Ce) is a comprehensively studied phosphor which is used as a yellow-emitting component for the production of white light in the liquid crystal display (LCD) backlighting and the illumination light sources. YAG is used as the host materials of full-color phosphors by changing of the doping material. Previous study, more researchers conducted wet-chemical process, i.e. the sol-gel

Hazimah et al: SYNTHESIS AND CHARACTERIZATION OF YAG:Ce PREPARED BY SOLID STATE REACTION METHOD

process [1, 4-7] co-doping/substitution [8] solvo-thermal method [9] and combustion method [10, 11] have been reported. Although YAG particles synthesized by chemical methods have some advantages, i.e. high purity, homogeneous composition and fine grain size. In this work, we reported preparation of spherical and fine size particles of Ce doped YAG by solid state reaction.

Experimental

Synthesis of YAG:Ce by solid-state reaction method

The powder samples were prepared by solid-state reaction. The starting materials Yttrium Aluminum Garnet, $Y_3Al_5O_{12}$ with grade 99.99% and rare earth element Cerium Oxide, Ce_2O_3 99.99% were weighted separately at various percentage (wt%) on analytical balance. Both sources were mixed together by grinding in an agate mortar. 5 ml of acetone was added into the samples to obtain homogeneous mixtures. Samples, in covered crucibles were transferred into a furnace for crystallization at 1000° C for 6 hours. The temperature was slowly reduces to room temperature by switching off the furnace. Finally, the cooled samples were pounded into a fine powder by using an agate mortar.

Characterization

The products were characterized by using powder X-ray diffraction (XRD) machine a XRD Xpert Pro with graphite monochromator and Cu K α radiation (λ = 0.1540598 nm) in the scanning range of 2 θ between 10° and 80°, with a rate of 0.04° per second. The average crystallite sizes, D were estimated from the broadening of the XRD peaks according to Scherrer's equation [5]:

$$D = \frac{0.89\lambda}{\beta\cos\theta} \tag{1}$$

where λ is the XRD wavelength that is 0.1540598 nm, β is the corrected half-width of the strongest diffraction peak and θ is the diffraction angle. Morphologies of the samples were examined using Zeiss Gemini FESEM scanning electron microscope. The instrument is fully automated and the SmartSEM software is operated via a graphical user interface that can be used intuitively.

Results and Discussion

X-ray diffraction

Figure 1 shows the graph of XRD pattern with various high amount of Ce_2O_3 . In all the samples, small peaks of Ce_2O_3 appeared at $2\theta = 28.572^\circ$ and 47.51° . The spectra show that the intensity of peaks increased with increasing doping concentration of dopant. Although, pure YAG phase in samples and observed the peak intensity decreases on increasing the doping concentration. At high doping concentrations, activation of Ce_2O_3 did not completely occur in the matrix of the YAG host material. So, the samples with low Ce_2O_3 concentrations have crystallites with bigger sizes than that with high concentrations. Figure 2 shows the graph of XRD pattern with various small amount of Ce_2O_3 . The diffraction peaks of samples spectra are indexed as Ce_2O_3 phase and no impurity peaks are detected. From XRD patterns the average size of particles, calculation by Scherrer's equation were between 53 - 82 nm. The YAG:Ce particle size estimated by FESEM photograph as between 45 - 50 nm and it is different in size by Scherrer's equation since Scherrer's equation calculated form XRD patterns while FESEM photographs calculated form selected area in sample. The sizes of particles are consistent with the results estimated by the XRD patterns and FESEM image. In general, similar morphological characteristics were observed in these powders in term of agglomerated and basically spherical in shape.

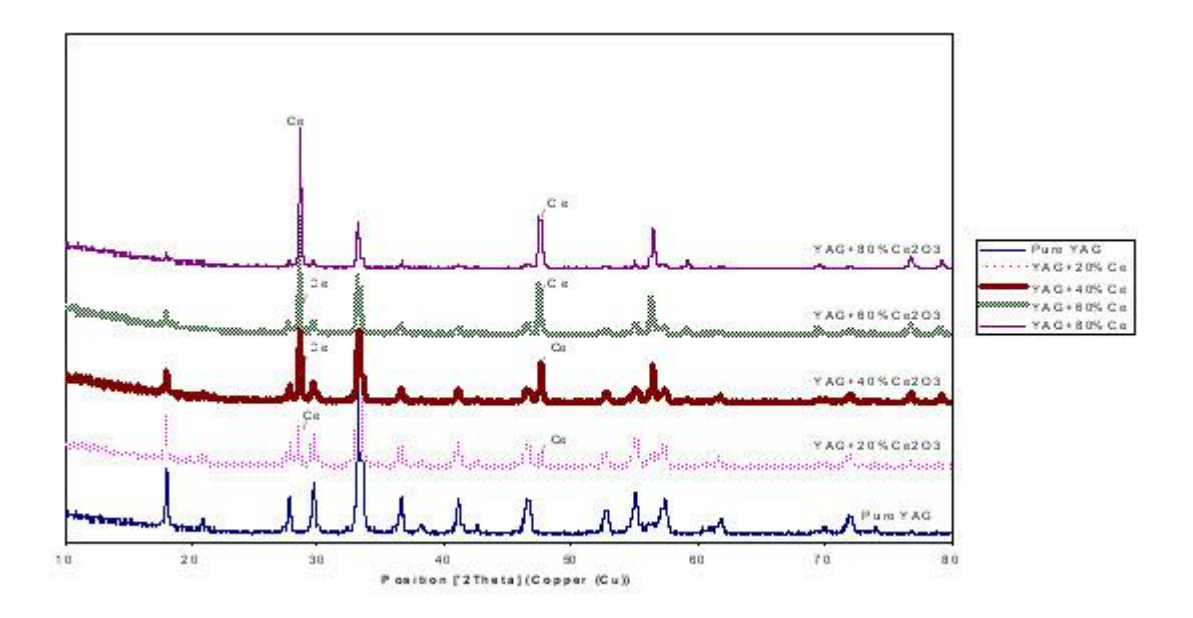


Figure 1: XRD patterns of YAG:Ce particles prepared with different high doping concentrations of Ce₂O₃

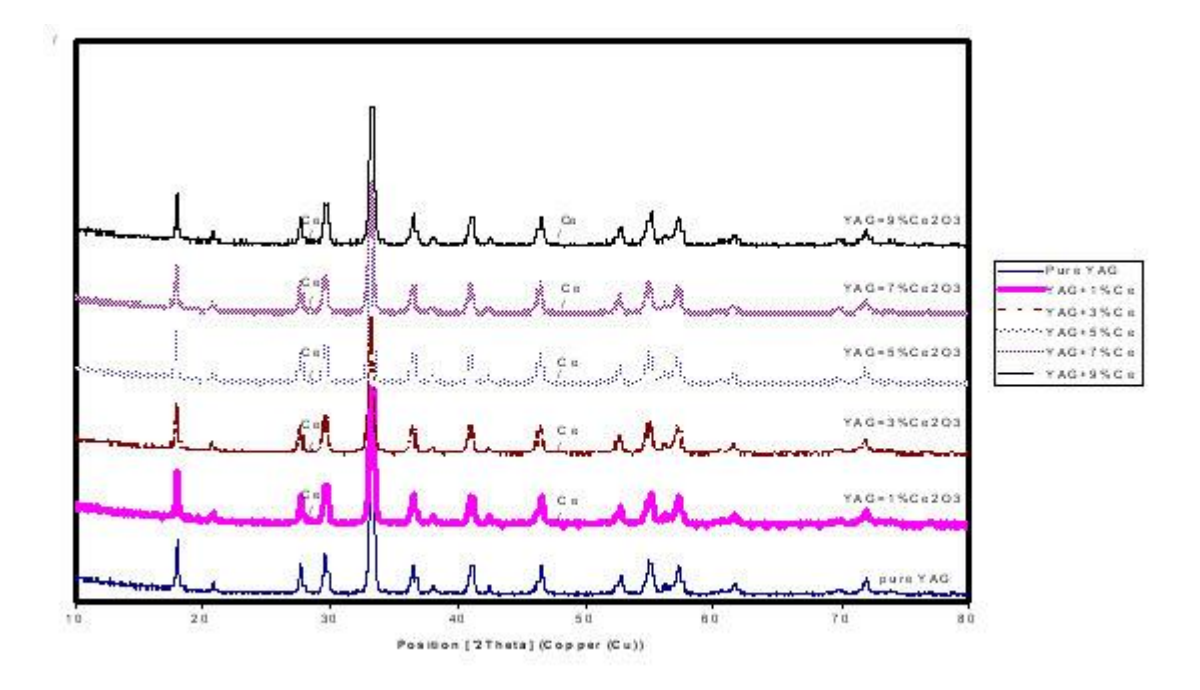


Figure 2: XRD patterns of YAG:Ce particles prepared with different low doping concentrations of Ce₂O₃

Hazimah et al: SYNTHESIS AND CHARACTERIZATION OF YAG:Ce PREPARED BY SOLID STATE REACTION METHOD

Morphology and size of YAG:Ce

FESEM micrograph given in Figure 3 shows the morphology of the YAG:Ce product synthesized at a sintering temperature 1000° C with Ce_2O_3 concentration of 5%. The average size and shape of the particles measured from FESEM photographs were estimated to be between 45-50 nm and spherical, respectively. In this study, we expected the doping concentrations of Ce_2O_3 below 5% were good used as phosphors materials. It is because the lower doping of Ce_2O_3 does not disturb the crystalline structure of samples compared to higher doping of Ce_2O_3 . The luminescence efficiency of phosphors depends on the morphology of the powder particles such as grain size, shape, crystallinity, defects, grain boundary and so on. The grains are monocrystalline, which must be considered a very good property of the phosphor powder.

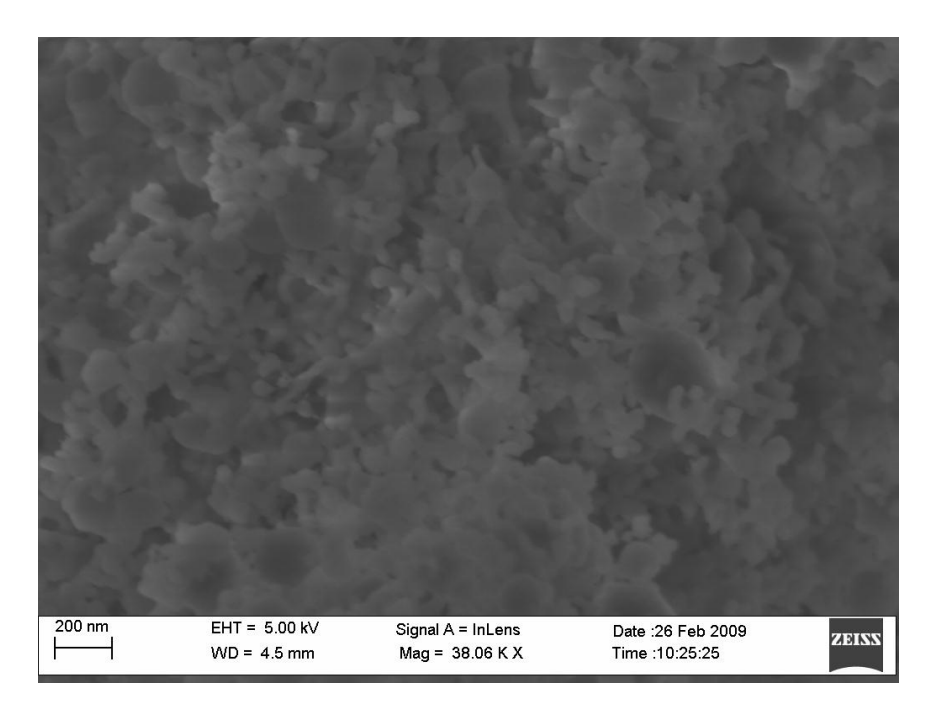


Figure 3. FESEM image of YAG:Ce sample annealed at 1000°C for 6h with Ce₂O₃ concentration of 5%

Conclusion

We have synthesized YAG:Ce by solid-stae reaction. Through this method, the YAG:Ce particle size estimated by FESEM photographs as between 45 - 50 nm, whole from XRD patterns were obtained average size of particle, calculation by Scherrer's equation, between 53-82 nm. Increasing the doping materials could affect the YAG phase as shown by the decreases in peak intensities. In further study, we would concentrate on photoluminescence study for better understanding in analysis.

Acknowledgement

The authors gratefully acknowledge the financial supports for this project from E-science Fund (03-01-01-SF0084) for the Ministry of Science, Technology and Innovation (MOSTI), Malaysia.

References

1. H. M. H. Fadlalla, C. C. Tang, E. M. Elssfah, J. Zhang, E. Ammar, J. Lin, X. X. Ding, (2008). "Synthesis and characterization of photoluminescent cerium-doped yttrium aluminum garnet,". *Materials Research Bulletin*. **43**. 3457-3462.

- 2. Y. C. Kang, I. Wuled Lenggoro, S. B. Pak, K. Okuyama, (2000). "YAG:Ce phosphor particles prepared by ultrasonic spray pyrolysis,". *Materials Research Bulletin*. **35**. 789-798.
- 3. Mikrajuddin Abdullah, Kikuo Okuyama, I. Wuled Lenggoro, Syuichi Taya, (2005). "A polymer solution process for synthesis of (Y, Gd)₃Al₅O₁₂:Ce phosphor particles,". *Journal of Non-Crystalline Solids.* **351**. 697-704.
- 4. H. M. H. Fadlalla, C. C. Tang, S. Y. Wei, X. X. Ding, (2008). "Preparation and properties of nanocrystalline powder in (Y_{1-x} Ce_x)₃Al₅O₁₂ system,". *Journal of Luminescence*. **128**. 1655-1659.
- 5. Kiranmala Devi, Rekha Coudhary, A. K. Satsangi, Ravi Kumar Gupta, (2008). "Sol-gel synthesis and characterization of nanocrystalline yttrium aluminum garnet nanopowder,". *Defense Science Journal*. Vol. **58**, no. 4, pp.545-549.
- 6. Zhang Na, Wang Dajian, Li Lan, Meng Yanshuang, Zhang Xiaosong, Ming Nan, (2006). "YAG:Ce phosphors for WLED via nano-psedoboehmite sol-gel route,". *Journal of Rare Earths*. **24**. 294-297.
- 7. J. Y. Choe, D. Ravichandran. S. M. Blomquist, K. W. Kirchner, E. W. Forsythe, D. C. Morton, (2001). "Catholuminescence study of novel sol-gel derived Y_{3-x}Al₅O₁₂:Tb_x phosphors,". *Journal of Luminescence*. **93**. 119-128.
- 8. Heesun Yang, Dong-Kyoon Lee, Yong-Seong Kim, (2009). "Spectral variations of nano-sized Y₃Al₅O₁₂:Ce phosphors via codoping/substitution and their white LED characteristics,". *Material Chemistry and Physics*. **114.** 665-669.
- 9. Xia Li, (2009). "Fabrication of transparent Yttrium Aluminum Garnet Ceramic,". *Journal of Physics: Conference Series.* **152**.
- 10. Sukumar Roy, Liwu Wang, Wolfgang Sugmund, Fritz Aldinger, (1999). "Synthesis of YAG phase by a citrate-nitrate combustion technique,". *Material Letters*. **39**. 138-141.
- 11. Zhiping Yang, Xu Li, Yong Yang, Xingmin Li, (2007). "The influence of different conditions on tha luminescent properties of YAG:Ce phosphor formed by combustion,". *Journal of Luminescence*. **122-123**. 707-709.



SYNTHESIS AND CHARACTERIZATION OF DIPHENYLTIN(IV) DITHIOCARBAMATE COMPOUNDS

(Sintesis dan Pencirian Sebatian Difenilstanum(IV) Ditiokarbamat)

Amirah Faizah Abdul Muthalib, Ibrahim Baba*, Yang Farina, Mohd Wahid Samsudin

School of Chemical Sciences & Food Technology, Faculty of Science & Technology, Universiti Kebangsaan Malaysia, 43600 Bangi, Malaysia

*Corresponding author: aibi@ukm.my

Abstract

Ten compounds of diphenyltin(IV) with *N*-dialkyldithiocarbamate were successfully prepared using *in situ* methods. Elemental analysis data (C, H, N and S) showed an agreement with the general formula of $(C_6H_5)_2Sn[S_2CNR_1R_2]$ ($R_1 = CH_3$, C_2H_5 , C_7H_7 ; $R_2 = C_2H_5$, C_4H_9 , C_6H_{11} , iC_3H_7 , C_7H_7). The structures of these compounds have been examined by infrared spectroscopy, ultraviolet, 1H , ^{13}C & ^{19}Sn NMR spectroscopy and X-ray crystallography. The infrared spectra of these compounds showed three important peaks for $v(C \xrightarrow{\dots} S)$ and $v(C \xrightarrow{\dots} S)$ bands that appeared in the region of 1474 -1499, 969 - 995 and 324 - 335 cm⁻¹ respectively. Data for ^{13}C NMR spectroscopy showed an important peak in the region of 198 – 200 ppm that corresponded to the NCS₂ group. Single crystal X-ray diffraction studies showed $(C_6H_5)_2Sn[S_2CN(C_2H_5)(CH_3)]_2$ (1) is six coordinated and adopted a *monoclinic* system with space group C_2/c , while $(C_6H_5)_2SnC[S_2CN(C_7H_7)(iC_3H_7)]$ (2) is five coordinated, crystallized in *monoclinic* system with space group P_2/n . Meanwhile, six coordinated $(C_6H_5)_2Sn[S_2CN(CH_3)(iC_3H_7)]_2$ (3) adopted a *orthorhombic* system with a space group P_2/n .

Keywords: diphenyltin(IV), dithiocarbamate.

Abstrak

Sepuluh kompleks daripada difenilstanum(IV) dengan N-dialkilditiokarbamat telah berjaya disediakan menggunakan cara $in\ situ$. Data analisis unsur (C, H, N dan S) terhadap semua kompleks telah menunjukkan persetujuan dengan formula umum (C_6H_5) $_2Sn[S_2CNR_1R_2]$ ($R_1=CH_3$, C_2H_5 , C_7H_7 ; $R_2=C_2H_5$, C_4H_9 , C_6H_{11} , iC_3H_7 , C_7H_7). Struktur kesemua sebatian dapat ditentukan dengan menggunakan spektroskopi inframerah, ultralembayung, 1H , ^{13}C dan ^{119}Sn RMN dan kristalografi sinar-X. Spektrum inframerah bagi sebatian ini menunjukkan tiga jalur penting, iaitu jalur $v(C^{----}N)$, $v(C^{-----}S)$ dan v(Sn-S) yang wujud masing-masing pada julat 1474 -1499, 969 - 995 dan 324 - 335 cm $^{-1}$. Data daripada ^{13}C RMN menunjukkan puncak pada julat 198 - 200 ppm yang menandakan wujudnya kumpulan NCS_2 . Struktur hablur tunggal (C_6H_5) $_2Sn[S_2CN(C_2H_5)(CH_3)]_2$ (1) dan (C_6H_5) $_2SnCl[S_2CN(C_7H_7)(iC_3H_7)]$ (3) mempunyai sistem monoklinik dengan masing-masing mempunyai kumpulan ruang C2/c dan $P2_1/n$ dengan sebatian pertama mempunyai struktur enam koordinatan dan struktur kedua membentuk lima koordinatan. Manakala (C_6H_5) $_2Sn[S_2CN(CH_3)(iC_3H_7)]_2$ (2) menunjukkan sistem ortorombik dengan kumpulan ruang Pbcn dengan membentuk struktur enam koordinatan.

Kata kunci: difenilstanum(IV), ditiokarbamat.

Introduction

Organotin(IV) compounds have received tremendous attention for their synthesis, characterization and biological activities and their ability to bind with sulfur ligand such as thione or dithiocarbamate [1]. Furthermore, tin compound has an ability to form stable bonds with carbon as well as heteroatoms that have received much attention both in academic and applied research [2]. X-ray crystallographic studies of the dithiocarbamate compounds of diorganotin(IV) have shown a variety of coordination environments around the central tin atoms such as molecular geometry, ranging from tetrahedral to distorted octahedral [3]. The ligands coordinated to the tin atom may also display interesting bonding capabilities as two sulfur atoms can act as an S,S-bridging ligand [4]. Organotin compounds are widely used in chemical industries such as antifouling agents, plastic stabilizers, wood

preservatives, bactericides, fungicides and insecticides [5]. Furthermore, organotin(IV) dithiocarbamate compounds have been used in chemical vapour deposition processes, flame retardants, polymer stabilizers and non-linear optical materials [6]. In this paper we report the synthesis and structure determination of ten diphenyltin(IV) dithiocarbamates compounds of the type $(C_6H_5)_2Sn[S_2CNR_1R_2]$ $(R_1 = CH_3, C_2H_5, C_7H_7; R_2 = C_2H_5, C_4H_9, C_6H_{11},$ iC_3H_7 C_7H_7). The crystal structures of diphenyltin(IV) methylisopropyldithiocarbamate, $(C_6H_5)_2Sn[S_2CN(CH_3)(iC_3H_7)]_2(1),$ (N-benzyl-N-isopropyldithiocarbamato)chlorido diphenyltin(IV) diphenyltin(IV) ethylmethyldithiocarbamate, $(C_6H_5)_2SnCl[S_2CN(C_7H_7)(iC_3H_7)](2)$ and (C₆H₅)₂Sn[S₂CN(CH₃CH₂)(CH₃)]₂(3) have also been determined and will be briefly discussed.

Material and Method

Material

All chemicals and solvents that have been used in this experiment were purchased from Merck and used without purification due to their high purity as follows: *N*-methylethylamine, *N*-methylcyclohexylamine, *N*-ethylcyclohexylamine, *N*-ethylisopropylamine, diphenyltin(IV) dichloride, carbon disulphide, chloroform and ethanol.

Instrumentation

The melting point was measured by using the Electrothermal IA 9100. Elemental analysis had been carried out on a Fison EA 1108. Perkin Elmer Model GX Spectrophotometer was used to record the infrared spectra by using KBr disc in the spectral range of 400-4000 cm⁻¹ and nujol in polyethylene tablets in the range of 400-250 cm⁻¹. The ¹H, ¹³C and ¹¹⁹Sn NMR spectra were also recorded in CDCl₃ as solvent using JOEL JNM-LA 400 Spectrometer and tetramethylsilane (TMS) as an internal standard. Bruker SMART APEX diffractometer and Oxford Diffraction Xcaliber Eos Gemini were used to determine X-ray structure and carried out at the Department of Chemistry, University of Malaya and University Putra Malaysia respectively.

General Synthetic Procedure

The compounds (Table 1) were prepared by using direct reaction between 0.005 mol carbon disulphide and an ethanolic solution of amines (0.005 mol). The mixture was stirred for one hour at 277 K and added dropwise to diphenyltin(IV) dichloride (0.0025 mol) in 20 mL of ethanol. The white precipitate that was formed, filtered and washed with cold ethanol and dried in desiccators. Suitable crystals were afforded by slow crystallization from a ethanol:chloroform (1:2) mixture.

Results and Discussion

Ten diphenyltin(IV) dithiocarbamate compounds have been prepared by using the insertion technique [7], which are the reaction between diphenyltin(IV) dichloride, amines and carbon disulphide at 277 K in ethanol to give stable compounds. General scheme for the reaction involved in the synthesis is shown in Figure 1. All compounds exhibit as solids either white or yellowish in colour. Elemental analysis (C, H, N and S) showed that the experimental values are in agreement with theoretical values based on their general formula (Table 1).

Figure 1: General reaction scheme between amines, carbon disulphide and diphenyltin(IV) dichloride.

Table 1: Physical and elemental analysis data for diphenyltin(IV) dithiocarbamate compounds.

Compound	Yield	Melting		Elemen	tal analy	vsis (%)	
	(%)	point (°C)	\mathbf{C}	H	N	\mathbf{S}	Sn
$(C_6H_5)_2Sn[S_2CN(CH_3)(C_2H_5)]_2$	89	164-165	43.22	4.42	4.90	22.51	20.42
			44.37	4.84	5.17	23.69	21.93
$(C_6H_5)_2Sn[S_2CN(CH_3)(C_6H_{11})]_2$	92	141-143	49.27	450	4.17	18.84	17.72
			51.77	5.90	4.31	19.74	18.28
$(C_6H_5)_2Sn[S_2CN(C_2H_5)(C_6H_{11})]_2$	83	117-119	52.99	5.71	3.80	17.57	17.13
			53.17	6.25	4.13	18.93	17.52
$(C_6H_5)_2Sn[S_2CN(CH_3)(iC_3H_7)]_2$	87	179-181	45.37	5.11	4.69	21.14	20.96
			46.40	5.31	4.92	22.52	20.85
$(C_6H_5)_2Sn[S_2CN(C_2H_5)(iC_3H_7)]_2$	90	116-118	48.24	5.74	4.69	21.47	18.53
			48.50	5.30	4.51	21.65	19.86
$(C_6H_5)_2SnCl[S_2CN(C_7H_7)(iC_3H_7)]$	72	197-199	51.41	4.55	2.64	10.63	20.41
			51.85	4.54	2.63	12.04	22.28
$(C_6H_5)_2SnCl[S_2CN(CH_3)(C_7H_7)]$	76	173-175	49.80	3.42	2.86	11.04	22.56
			49.98	3.99	2.78	12.71	23.52
$(C_6H_5)_2Sn[S_2CN(CH_3)(C_4H_9)]_2$	88	85-87	46.48	5.76	4.60	19.83	20.13
			48.24	5.74	4.69	21.47	19.87
$(C_6H_5)_2SnCl[S_2CN(C_7H_7)_2]$	70	218-220	56.29	4.74	2.69	10.12	19.32
			55.84	4.17	2.41	11.04	20.44
$(C_6H_5)_2SnCl[S_2CN(C_2H_5)(C_7H_7)]$	74	187-189	50.53	4.49	3.03	11.17	11.45
			50.94	4.27	2.70	12.36	12.89

Bold = experimental value

Important infrared of diphenyltin(IV) dithiocarbamate bands are listed in Table 2. Based on the spectral data, diphenyltin(IV) dithiocarbamates compounds exhibited peaks that can be assigned to thioureida band, $v(C^{----}N)$ found in the region of 1470 - 1500 cm⁻¹ [6]. By the introduction of more electronegative substituents, the band will move to higher frequency due to the sensitivity towards substitution on the tin atom. Meanwhile, peaks in the region of 970 - 995 cm⁻¹ are attributed to $v(C^{----}S)$ [8]. Existence of a single v(C=S) band at 960 – 1005 cm⁻¹ inferred that the ligand chelated as a bidentate entity [9]. Strong absorption bands which appeared in the region of 325 - 384 cm⁻¹ was attributed to Sn-S stretching frequency that indicated the existence of metal-ligand bond [10].

Table 2: The infrared absorption bands of diphenyltin(IV) dithiocarbamate (cm⁻¹).

Compound	Wavenumber (cm ⁻¹)					
	<i>v</i> (C-H)	$v(\mathbf{C} - \mathbf{N})$	v(C - S)	v(Sn-S)		
$(C_6H_5)_2Sn[S_2CN(CH_3)(C_2H_5)]_2$	2976, 2931	1493	985	354		
$(C_6H_5)_2Sn[S_2CN(CH_3)(C_6H_{11})]_2$	2929, 2854	1478	970	384		
$(C_6H_5)_2Sn[S_2CN(C_2H_5)(C_6H_{11})]_2$	2933, 2856	1474	995	358		
$(C_6H_5)_2Sn[S_2CN(CH_3)(i-C_3H_7)]_2$	2973, 2929	1478	969	354		
$(C_6H_5)_2Sn[S_2CN(C_2H_5)(i-C_3H_7)]_2$	2977, 2933	1475	993	386		
$(C_6H_5)_2SnCl[S_2CN(C_7H_7)(iC_3H_7)]$	2979s, 2980s	1478s	964s	325s		
$(C_6H_5)_2SnCl[S_2CN(CH_3)(C_7H_7)]$	2849s, 2928s	1495m	995s	326s		
$(C_6H_5)_2Sn[S_2CN(CH_3)(C_4H_9)]_2$	2929s, 2954s	1499s	975m	326s		
$(C_6H_5)_2SnCl[S_2CN(C_7H_7)_2]$	2930m	1496m	997w	326s		
$(C_6H_5)_2SnCl[S_2CN(C_2H_5)(C_7H_7)]$	2910s, 2789m	1496m	995s	327s		

Amirah Faizah et al: SYNTHESIS AND CHARACTERIZATION OF DIPHENYLTIN(IV) DITHIO-CARBAMATE COMPOUNDS

The protons for the phenyl groups exhibited chemical shifts in the range 7.27-8.07 ppm (Table 3) as multiplets due to deshielding on complexation similar to what has been reported by Yin et al. (2004) [11]. The -CH₂- protons from the ethyl group resonated as a quartet at 3.69-3.83 ppm, while -CH₃ protons resonated as a triplet at 1.22 - 1.29 ppm [12]. The *N*-methyl protons signal was observed as a singlet at 3.19 - 3.34 ppm, while mutiplets at 1.12 - 1.95 ppm and 4.50 - 4.65 ppm were attributed to *N*-cyclohexyl protons [13]. While for the isopropyl group, the multiplet signal at 5.08 - 5.10 ppm and doublet signal at 1.21-1.26 ppm were attributed to methyne and methyl proton respectively [14]. The important data of ¹³C NMR of the compounds are depicted in Table 4. The assignment of ¹³C signal for NCS₂ group for all compounds appeared in the region of 198 – 200 ppm and indicated the coordination between sulfur and tin atom [15].

Table 3: ¹H NMR spectra data of organotin(IV) dithiocarbamate compounds (δ, ppm).

Compound	Chemical shift, δ (ppm)					
_	Sn-C ₆ H ₅	-NR'; R' = CH_3 , C_2H_5	-NR''; R'' = C_2H_5 , C_6H_{11} , iC_3H_7			
$(C_6H_5)_2Sn[S_2CN(CH_3)(C_2H_5)]_2$	7.27-	3.34(s)	3.83(qt), 1.28(t)			
	7.89(m)					
$(C_6H_5)_2Sn[S_2CN(CH_3)(C_6H_{11})]_2$	7.27-	3.22(s)	4.65(m), 1.91(m), 1.39(m), 1.12(m)			
	7.88(m)					
$(C_6H_5)_2Sn[S_2CN(C_2H_5)(C_6H_{11})]_2$	7.33-	3.72(qt), 1.29(t)	4.50(m), 1.95(m), 1.83(m), 1.65(m)			
	8.07(m)					
$(C_6H_5)_2Sn[S_2CN(CH_3)(iC_3H_7)]_2$	7.34-	3.19(s)	5.10(m), 1.21(d)			
	7.86(m)					
$(C_6H_5)_2Sn[S_2CN(C_2H_5)(iC_3H_7)]_2$	7.30-	3.69(qt), 1.22(t)	5.08(m), 1.26(d)			
	7.85(m)					
$(C_6H_5)_2SnCl[S_2CN(C_7H_7)(iC_3H_7)]$	7.24-	5.03(s), 7.45-7.54(m)	5.08(m), 1.25(d)			
	7.38(m)					
$(C_6H_5)_2SnCl[S_2CN(CH_3)(C_7H_7)]$	7.27-	3.29(s)	5.05(s), 7.39-7.44(m)			
	7.35(m)					
$(C_6H_5)_2Sn[S_2CN(CH_3)(C_4H_9)]_2$	7.27-	3.34(s)	0.95(t), 1.36(m), 1.70(m), 3.75(t)			
	7.49(m)					
$(C_6H_5)_2SnCl[S_2CN(C_7H_7)_2]$	7.27-	5.02(s), 7.41-7.54(m)	5.02(s), 7.41-7.54(m)			
	7.40(m)					
$(C_6H_5)_2SnCl[S_2CN(C_2H_5)(C_7H_7)]$	7.27-	3.75(qt), 1.28(t)	5.06(s), 7.45-7.52(m)			
	7.41(m)					

The coordination number of organotin(IV) dithiocarbamate compounds can be identified by using ¹¹⁹Sn NMR spectroscopy [16]. The R substitute from dithiocarbamate groups that bind to the Sn atom affects the ¹¹⁹Sn chemical shifts even though each compound have the same coordination due to the sensitivity of the chemical environment of the tin atom [17]. Only five compounds were afforded for ¹¹⁹Sn NMR and the chemical shift for the compounds are tabulated in Table 5. This chemical shifts indicated those compounds having a six coordination environment around the tin atom with octahedral structure [16].

Table 4: ¹³ C NMR data of diphenyltin(IV) of	dithiocarbamate compounds (δ , ppm).

Compound	Chemical shift, δ (ppm)					
•	$N^{13}CS_2$	Sn-C ₆ H ₅	-NR'; R' =	-NR'; R' = C_2H_5 ,		
	_		CH_3 , C_2H_5	C_6H_{11}, iC_3H_7		
$(C_6H_5)_2Sn[S_2CN(CH_3)(C_2H_5)]_2$	199.0	128.4, 134.5, 128.6	42.9	53.5, 12.0		
$(C_6H_5)_2Sn[S_2CN(CH_3)(C_6H_{11})]_2$	198.6	129.0, 134.4, 128.4	36.6	65.2, 30.2, 25.5, 25.6		
$(C_6H_5)_2Sn[S_2CN(C_2H_5)(C_6H_{11})]_2$	198.4	129.0, 134.4, 130.3	44.9, 14.2	65.7, 30.9, 25.6, 30.7		
$(C_6H_5)_2Sn[S_2CN(CH_3)(i-C_3H_7)]_2$	198.6	128.5, 134.5, 128.3	35.3	56.9, 19.9		
$(C_6H_5)_2Sn[S_2CN(C_2H_5)(i-C_3H_7)]_2$	198.4	128.2, 134.4, 128.3	43.8, 14.2	57.4, 20.5		
$(C_6H_5)_2SnCl[S_2CN(C_7H_7)(iC_3H_7)]$	198.0	128.5, 135.9, 129.1	58.67, 135.5, 130.1, 128.8, 126.5	53.0, 20.4		
$(C_6H_5)_2SnCl[S_2CN(CH_3)(C_7H_7)]$	201.1	128.1, 134.3, 128.9	42.5	61.4, 135.7, 127.6, 128.9, 128.5		
$(C_6H_5)_2Sn[S_2CN(CH_3)(C_4H_9)]_2$	199.2	134.3, 128.4, 128.2	43.35	13.8, 19.9, 28.9, 58.4		
$(C_6H_5)_2SnCl[S_2CN(C_7H_7)_2]$	199.0	128.8, 133.4, 128.1	57.4, 135.8, 129.2, 128.9, 127.9	57.4, 135.8, 129.2, 128.9, 127.9		
$(C_6H_5)_2SnCl[S_2CN(C_2H_5)(C_7H_7)]$	197.1	135.7, 129.2, 128.9,	50.1, 11.7	58.8, 133.6, 128.7, 128.8, 127.9		

Table 5: 119 Sn NMR data of diorganotin(IV) dithiocarbamate compounds (δ , ppm).

Compound	δ(¹¹⁹ Sn), ppm	Coordination No.
$(C_6H_5)_2Sn[S_2CN(CH_3)(C_2H_5)]_2$	-324.2	6
$(C_6H_5)_2Sn[S_2CN(CH_3)(C_6H_{11})]_2$	-318.0	6
$(C_6H_5)_2Sn[S_2CN(C_2H_5)(C_6H_{11})]_2$	-316.8	6
$(C_6H_5)_2Sn[S_2CN(CH_3)(i-C_3H_7)]_2$	-317.8	6
$(C_6H_5)_2Sn[S_2CN(C_2H_5)(i-C_3H_7)]_2$	-316.9	6

Only three compounds, bis(N-ethyl-N-methyldithiocarbamato- κ^2 S,S')diphenyltin(IV) (1), (N-benzyl-Nisopropyldithiocarbamato)chlorido diphenyltin(IV) **(2)** and bis(N-isopropyl-N-methyldithiocarbamato- κ^2 S,S')diphenyltin(IV) (3) produced single crystals by slow evaporation of ethanol:chloroform 1:2 mixture. The ORTEP plots are shown in Figure 3. The single crystal studies of bis(N-ethyl-N-methyldithiocarbamato- κ^2 S,S')diphenyltin(IV) (1) [18] and bis(N-isopropyl-N-methyldithiocarbamato- κ^2 S,S')diphenyltin(IV) (3) [19] adopted monoclinic system with a space groups C2/c and P2i/n respectively, both with six-coordinated in a skewtrapezoidal-bipyramidal geometry. Both structures (1 and 3) have short thioureide C-N distance, 1.336(2) and 1.323(3) Å respectively, suggesting partial double bond character [6]. The compound (N-benzyl-Nisopropyldithiocarbamato)chlorido diphenyltin(IV) (2) adopted a orthorhombic system with space group Pbcn, the Sn atom is penta-coordinated by an asymmetrically coordinating dithiocarbamate ligand, a Cl and two ispo-C atoms of the Sn-bound phenyl groups [20]. The resulting C₂ClS₂ donor set defines a coordination geometry intermediate between square-pyramidal and trigonal-bipyramidal with a slight tendency towards the latter.

Amirah Faizah et al: SYNTHESIS AND CHARACTERIZATION OF DIPHENYLTIN(IV) DITHIO-CARBAMATE COMPOUNDS

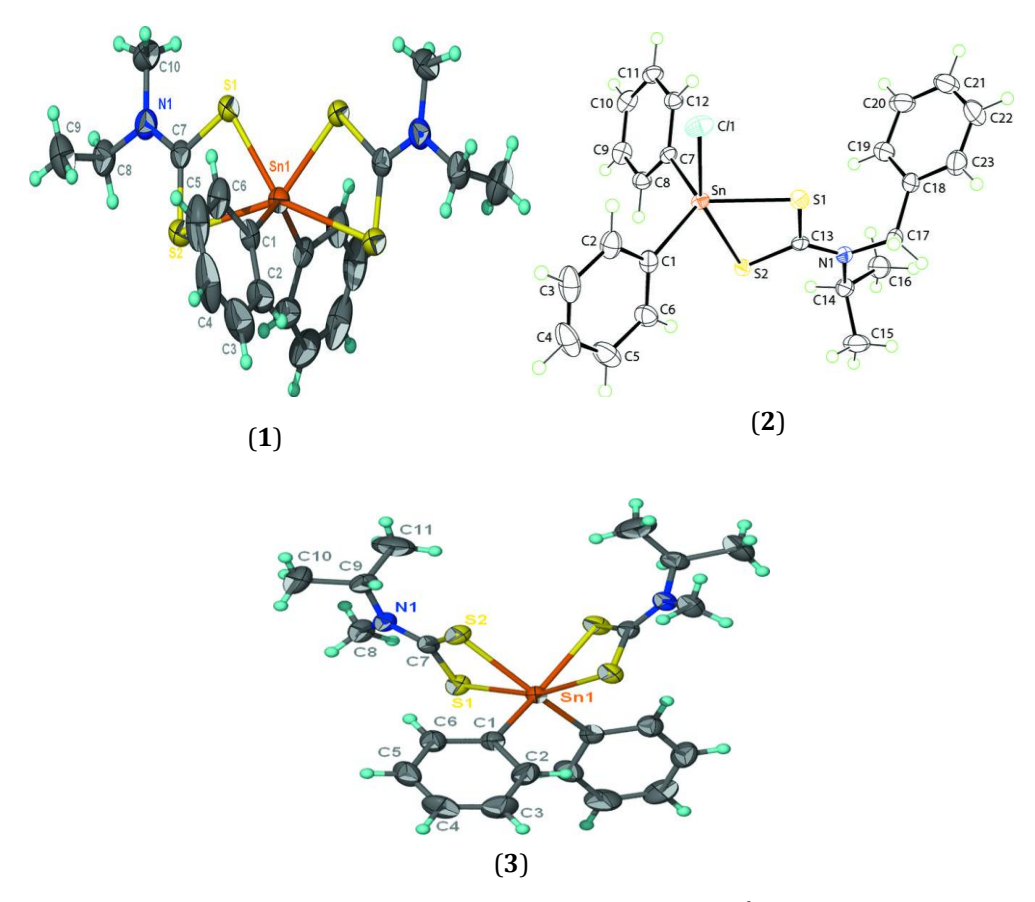


Figure 3. ORTEP plot of (1) bis(*N*-ethyl-*N*-methyldithiocarbamato- κ^2 S,S')diphenyltin(IV), (2) (*N*-benzyl-*N*-isopropyldithiocarbamato)chlorido diphenyltin(IV) and (3) bis(*N*-isopropyl-*N*-methyldithiocarbamato- κ^2 S,S')diphenyltin(IV) at the 50% probability level.

Conclusion

The elemental and spectroscopic data showed that ten diphenyltin(IV) dithiocarbamate compounds are successfully synthesized and pure compounds were obtained. Further, the crystallographic studies of bis(N-isopropyl-Nmethyldithiocarbamato- κ^2 S,S')diphenyltin(IV) bis(N-isopropyl-N-methyldithiocarbamato- κ^2 S,S') and diphenyltin(IV) showed that the dithiocarbamate ligands are bonded to the tin atom in six coordinate symmetry with skew bipyramidal geometry. bidentate manner having trapezoidal While (N-benzyl-Nisopropyldithiocarbamato)chlorido diphenyltin(IV) is penta-coordinated by an asymmetrically coordinating dithiocarbamate ligand, a Cl and two ispo-C atoms of the Sn-bound phenyl groups.

Acknowledgement

We would like to thank Universiti Kebangsaan Malaysia for UKM-GUP-NBT-08-27-111 and the Government of Malaysia for the Science Fund 06-01-02-SF0539 grants. Thank you also to Prof Ng Seik Weng and Prof E. R. T. Tiekink, UM and Dr Mohamed Ibrahim Mohamed Tahir, UPM for the crystal structures. We would also like to thank all faculty members that have contributed to this research.

References

- 1. Shahzadi, S., Ahmad, U.S., Alia, S., Yaqub, S. & Ahmed, F. 2006a. Chloro-diorganotin(IV) Compounds of Pipyridyl Dithiocarbamate: Syntheses and Determination of Kinetic Parameters, Spectral Characteristics and Biocidal Properties. *Journal of the Iranian Chemical Society* 3: 38-45.
- Ali, A.M., Mirza, H.A., Hamid, A.S.H.M. & Bernhardt, V.P. 2005. Diphenyltin(IV) complexes of the 2quinolinecarboxaldehyde Schiff bases of S-methyl- and S-benzyldthiocarbazate (Hqaldsme and Hqaldsbz): Xray crystal structures of Hqaldsme and two conformers of its diphenyltin(IV) complex. *Polyhedron* 24: 383– 390.
- Sharma, J., Singh, Y., Bohra, R. & Rai, K.A. 1996. Synthesis and spectral studies of diorganotin heterocyclic dithiocarbamate complexes: The crystal structure of (CH₃)₂Sn[S₂CNCH₂CH₂CH₂CH₂CH₂CH₂]₂. Polyhedron 15: 1097-1102
- Shahzadi, S., Ali, S., Bhatti, M.H., Fettouhi, M. & Athar M. 2006b. Chlorodiorganotin(IV) complexes of 4-methyl-1-piperidine carbodithioic acid: Synthesis, X-ray crystal structures, spectral properties and antimicrobial studies. *J. Organometal. Chem.* 691: 1797–1802.
- 5. Jang, S.M., Park, J.S., Pyo, S.H., Hong, E.J. & Lee, W. 2001. Improvement of extraction recovery for the organotin compounds in sediment. *Anal. Sci.* 17: 405-408.
- 6. Fuentes-Martinez, P.J., Toledo-Martiez, I., Roman-Bravo, P., Garcia, Y.G.P., Godoy-Alcantar, C., Lopez-Cardoso, M. & Morales-Rojas, H. 2009. Diorganotin(IV) dithiocarbamate complexes as chromogenic sensors of anion binding. *Polyhedron* 28: 3953–3966.
- 7. Jung, O.S. & Sohn, S.Y. 1988. Coordination chemistry of organotin(IV) dithiocarbamate complexes. *Bulletin of the Korean Chemical Society* 9: 356-368.
- 8. Brown, D.A., Glass, W.K & Burke, M.A. 1976. The general use of I.R. spectral criteria in discussions of the bonding and structure of metal dithiocarbamates. *Spectrochim. Acta* 32A: 137-143.
- 9. Criado, J.J, Fernandez, I. & Macias, B. 1990. Novel chelates of Pd(II) dithiocarbamates. Spectroscopic studies and termal behavior. *Inorganica Chimica Acta* 174: 67-75.
- 10. Rodarte de Moura, C.V., de Sousa, A.P.G., Silva, R.M., Abras, A., Horner, M., Bortoluzzi, A.J., Filgueiras, C.A.L. & Wardell, J.L. 1999. Syntheses and spectra of triphenyltin heteroarenethiolates Crystal structures of triphenyltin 1-methyltetrazole-5-thiolate and triphenyltin benzoxazole-2-thiolate. *Polyhedron* 18: 2961-2969.
- 11. Yin, H., Wang, C. & Xing, Q. 2004. Synthesis and characterization of triphenyltin esters of heteroaromatic carboxylic acids and the crystal structure of [Ph₃SnO₂CC₅H₄N·0.5H₂O]. *Polyhedron* 23(10): 1805-1810.
- 12. Damian, C., Onwudiwe, Ajibade, P.A. 2010. Synthesis and characterization of metal complexes of N-alkyl-N-phenyl dithiocarbamates. *Polyhedron* 29: 1431-1436.
- 13. Shaheen, F., Badshah, A., Gielen, M., Dusek, M., Fejfarova, K., Vos, D. & Mirza, B. 2007. Synthesis, characterization, antibacterial and cytotoxic activity of new palladium(II) complexes with dithiocarbamate ligands: X-ray structure of bis(dibenzyl-1-S:S'-dithiocarbamato)Pd(II). *J. Organometal. Chemistry* 692(14): 3019-3026.
- 14. Oliveira, M.M., Pessoa, G.M., Carvalho, L.C., Peppe, C., Souza, A.G. & Airoldi, C. 1999. *N,N'*-Dialkyldithiocarbamate chelates of indium(III): alternative synthetic routes and thermodynamics characterization. *Thermochimica Acta* 328(1-2): 223-230.
- 15. Van Gaal, H.L.M., Diesveld, J.W., Pijpers, F.W & Vander Linden, J.G.M. 1979. ¹³C NMR spectra of dithiocarbamates. Chemical shift, carbon-nitrogen stretching vibration frequencies and *p* bonding in the NCS₂ fragment. *Inorg. Chem.* 18(11): 3251-3260.
- 16. Holecek, J., Nadvornik, M., Handlir, K. & Lycka, A. 1986. ¹³C and ¹¹⁹Sn NMR spectra of Di-n-butyltin(IV) compounds. *J. Organometal. Chemistry* 315: 299-308.
- 17. Jung, O.S., Jeong, H.J. & Sohn, S.Y. 1989. Preparation, properties and structures of estertin(IV) sulphides. *Polyhedron* 8: 2557-2563.
- 18. Amirah Faizah Muthalib, Ibrahim Baba & Ng, S.W. 2010a. Bis(N-ethyl-N-methyldithiocarbamato-κ²S,S')diphenyltin(IV). *Acta Cryst*. E66:m355.
- 19. Amirah Faizah Muthalib, Ibrahim Baba, Yang Farina & Ng, S.W. 2010b. Bis(N-isopropyl-N-methyldithiocarbamato- κ^2 S,S')diphenyltin(IV). *Acta Cryst*. E66:m354.
- 20. Amirah Faizah Muthalib, Ibrahim Baba, Mohamed Ibrahim Mohamed Tahir, Ng, S.W. & Tiekink, E.R.T. 2010c. (*N*-Benzyl-*N*-isopropyldithiocarbamato)-chloridodiphenyltin(IV). *Acta Cryst.* E66:m1087.



ANALISIS KROMATOGRAFI GAS x KROMATOGRAFI GAS-SPEKTROMETRI JISIM MASA-PENERBANGAN DAN AKTIVITI ANTIBAKTERIA MINYAK PATI *AMOMUM XANTHOPHLEBIUM*

(Gas Chromatography x Gas Chromatography—Time-of-Flight Mass Spectrometry Analysis and Antibacterial Activity of Essential Oil from *Amomum xanthophlebium*)

A. Masila¹, I. Aminah¹, W.A. Yaacob¹, I. Nazlina²

¹Pusat Pengajian Sains Kimia dan Teknologi Makanan, ²Pusat Pengajian Biosains dan Bioteknologi, Fakulti Sains dan Teknologi, Universiti Kebangsaan Malaysia, 43600 Bangi, Selangor, Malaysia.

*Corresponding author: wanyaa@ukm.my

Abstrak

Minyak pati daun, batang, rizom dan seluruh tumbuhan beraroma segar bagi *Amomum xanthophlebium* (Zingiberaceae) diperolehi secara penyulingan-air. Peratus hasil minyak daun, batang dan seluruh tumbuhan adalah 0.0032, 0.0074 dan 0.0021% manakala minyak rizom yang diperolehi adalah terlalu sedikit. Komponen kimia bagi setiap minyak dan peratus mereka ditentukan dengan Kromatografi Gas x Kromatografi Gas–Spektrometri Jisim Masa-Penerbangan (KGxKG-SJMP). Analisis minyak *A. xanthophlebium* menunjukkan bahawa mereka didominasi oleh terpena. Komponen utama dalam daun ialah *alo*-aromadendrena (3.41%), (±)-globulol (2.58%) dan rosifoliol (2.55%); batang, α-terpineol (4.25%), rosifoliol (2.41%) dan bingpian (2.27%); rizom, viridiflorol (5.72%), (±)-globulol (5.23%) dan α-kadinol (4.81%); seluruh tumbuhan, eukaliptol (4.11%), *l*-α-terpineol (2.88%) dan rosifoliol (2.82%). Minyak batang *A. xanthophlebium* menunjukkan aktiviti antibakteria terhadap Gram-negatif *Escherichia coli* dan Gram-positif *Staphylococcus aureus* rintang-metisilin pada kepekatan perencatan minimum 80 mg/ml.

Kata kunci: Amomum xanthophlebium, minyak pati, KGxKG-SJMP.

Abstract

Essential oils of fresh leaves, stem, rhizomes and whole aromatic plants of *Amomum xanthophlebium* (Zingiberaceae) were obtained by hydrodistillation. Percentage yields of the leaf, stem and whole plant oils were 0.0032, 0.0074 and 0.0021% whereas the rhizome oil obtained was very little. Chemical components of each oil and their percentages were determined by Gas Chromatography x Gas Chromatography—Time-of-Flight Mass Spectrometry (GCxGC-TOFMS). Analysis of *A. xanthophlebium* oils showed that they were dominated by terpenes. Main components in the leaves were *allo*-aromadendrene (3.41%), (\pm)-globulol (2.58%) and rosifoliol (2.55%); stem, α -terpineol (4.25%), rosifoliol (2.41%) and bingpian (2.27%); rhizomes, viridiflorol (5.72%), (\pm)-globulol (5.23%) and α -cadinol (4.81%); whole plants, eucalyptol (4.11%), l- α -terpineol (2.88%) and rosifoliol (2.82%). The stem oil of *A. xanthophlebium* showed antibacterial activity against Gram-negative *Escherichia coli* and Gram-positive methicillin-resistant *Staphylococcus aureus* (MRSA) at the minimum inhibitory concentration of 80 mg/ml.

Keywords: Amomum xanthophlebium, essential oil, GCxGC-TOFMS

Pengenalan

Tumbuhan Zingiberaceae hidup subur dan bertaburan di seluruh kawasan tropika dan subtropika khususnya di kawasan Asia di mana pusat kepelbagaian mereka adalah wilayah Indo-Malaya. Dari 50 genus dan 1500 spesies Zingiberaceae yang dikenalpasti di dunia, sekurang-kurangnya 20 genus dan 300 spesies boleh ditemui di Malaysia [1]. Terdapat 13 genus Zingiberaceae dari kumpulan Alpinae di mana salah satunya adalah *Amomum* (tepus) [2]. Kebanyakan *Amomum* tumbuh bertaburan terutamanya di kawasan lembah dan lereng bukit bagi hutan tanah pamah

Masila et al: ANALISIS KROMATOGRAFI GAS x KROMATOGRAFI GAS-SPEKTROMETRI JISIM MASA-PENERBANGAN DAN AKTIVITI ANTIBAKTERIA MINYAK PATI *AMOMUM* XANTHOPHLEBIUM

yang gembur tanahnya [3]. Tumbuhan *Amomum* adalah agak tinggi dan sebahagian dari tumbuhan spesies tertentu tertanam di dalam tanah.

Tumbuhan *Amomum xanthophlebium* digunakan dalam masakan kari, merawat pening, penyakit cacing, sakit perut, cirit-birit dan penyakit yang berkaitan dengan cirit-birit [4]. Minyak pati daun *A. cannicarpum* memberi kesan yang baik terhadap yis *Candida albicans* dan kulat *Aspergillus fumigatus* [5] manakala minyak buahnya pula terhadap bakteria *Salmonella typhi, Pseudomonas aeruginosa* dan *Proteus vulgaris*, selain mampu melawan *C. albicans* dan *C. glabrata* [6]. Komposisi kimia minyak tumbuhan *Amomum* yang pernah dikaji termasuklah *A. cannicarpum*, *A. thyrsoideum*, *A. longilgulare*, *A. villosum*, *A. muricarpum*, *A. kwangsiense*, *A. schmidtti*, *A. xanthioides*, *A. tsao-ko*, *A. linguiforme* dan *A. testaceum* [7]. *Amomum linguiforme* dan *A. cannicarpum* mempunyai komponen utama metil chavikol dan β-pinena [8]. Kajian ini bertujuan menganalisis komposisi kimia minyak *A. xanthophlebium* dari bahagian daun, batang, rizom dan seluruh tumbuhan menggunakan KGxKG–SJMP serta menilai kesan minyak batang terhadap bakteria. Ia dapat menghasilkan maklumat mengenai kandungan kimia minyak serta kesan minyak terhadap bakteria penyebab penyakit.

Bahan dan Kaedah

Bahan tumbuhan

Bahagian daun, batang, rizom dan seluruh tumbuhan *Amomum xanthophlebium* segar di ambil dari Sungai Tekala, Semenyih, Selangor. Nama spesies tumbuhan disahkan oleh En. Shamsul Khamis, Institut Biosains, Universiti Putra Malaysia.

Penyulingan-air minyak pati

Setiap bahagian tumbuhan *Amomum xanthophlebium* dipotong dan dikisar dalam air. Bubur kisaran disuling 5-6 jam dengan alat-radas jenis-Clevenger. Minyak yang diperolehi dikeringkan dengan natrium sulfat kontang dan disimpan dalam botol kecil bertutup pada -18°C. Untuk analisis, minyak ini dilarutkan dalam diklorometana.

Kromatografi Gas × Kromatografi Gas-Spektrometri Jisim Masa-Penerbangan (KGxKG-SJMP)

Minyak pati dianalisis dengan alat KG×KG Agilent 6890N GC yang dilengkapi modulator terma LECO. Dua turus yang digunakan: Rtx-5MS (30 m, diameter dalam 0.25 mm, ketebalan filem 0.1 μm) dan Rtx-17 (1 m, diameter dalam 0.1 mm, ketebalan filem 0.1 μm). Program suhu ketuhar yang digunakan: bagi Rtx-5MS suhu mula 50°C selama 2 min, kemudian ditingkatkan pada 5°C/min ke 240°C dan kekal selama 5 min serta bagi Rtx-17 suhu mula 55°C selama 2 min, kemudian ditingkatkan pada 5°C/min ke 245°C dan kekal selama 5 min. Suhu suntikan 200°C; saiz suntikan 1 μl dengan nisbah pemecahan 50:1; gas pembawa He pada kadar aliran 1 ml/min dan tekanan 20 psi; suhu modulator 30°C offset dari oven utama; frekuensi modulasi 4 saat dengan masa denyut panas 0.8 saat.

Analisis Spektrometri Jisim (SJ) dijalankan dengan menggandingkan kepada SJ LECO Pegasus 4D–Masa-Penerbangan. Parameter operasi: hentaman elektron pada 70 eV; suhu sumber 200°C; julat imbasan jisim 50-500 U; kadar perolehan 200 spektrum/s.

Komponen dikenalpasti melalui perbandingan spektrum jisim mereka dengan pengkalan data spektrum jisim perisian NIST versi 2.0. Spektrum yang mempunyai kesamaan, kebalikan dan kebarangkalian melebihi 800, 800 dan 1000 dianggap mempunyai padanan yang baik [9].

Ujian Antibakteria

Teknik mikropencairan dilakukan bagi menentukan kepekatan minimum minyak pati batang segar *Amomum xanthophlebium* yang dapat merencatkan aktiviti bakteria [10]. Minyak disediakan dengan pencairan bersiri dua-kali mengikut kaedah Hussain et al. [10] dari 160 ke 10 mg/ml. Bakteria yang digunakan adalah Gram-negatif *Escherichia coli* serta Gram-positif *Staphylococcus aureus* dan *Staphylococcus aureus* rintang metisilin (SARM). Stok bakteria diperolehi dari Makmal Mikrobiologi, Pusat Pengajian Biosains dan Bioteknologi, Fakulti Sains dan Teknologi, Universiti Kebangsaan Malaysia. Setiap bakteria dicoret ke atas agar Mueller-Hinton (AMH) dalam piring petri dengan gelungan dawai pencoret steril (dari pemanasan pijar). Plat agar kemudian dieram 24 jam pada 37°C. Selepas itu, koloni tunggal bakteria dicungkil lalu dimasukkan ke dalam 10 ml kaldu nutrien dalam botol kaca, ditutup dan dieram dalam inkubator 24 jam pada 37°C. Larutan bakteria dan minyak pada 10⁷ sel/ml dan 160,

80, 40, 20, 10 mg/ml digunakan. Larutan kaldu nutrien (160 µl) dan 20 µl larutan minyak pada kepekatan berbezabeza ditambah satu demi satu ke dalam telaga U piring mikrotiter secara duplikat. Kemudian 20 µl inokulum bakteria dipipet masuk ke dalam setiap telaga U tersebut. Kawalan positif mengandungi 20 µl inokulum bakteria dan 180 µl kaldu nutrien manakala kawalan negatif mengandungi 20 µl larutan minyak dan 180 µl kaldu nutrien. Campuran dieram 18 jam pada 37°C. Kekeruhan setiap telaga diperhatikan bagi mendapatkan nilai kepekatan perencatan minimum (KPM). Ujian di atas diulangi dua kali lagi.

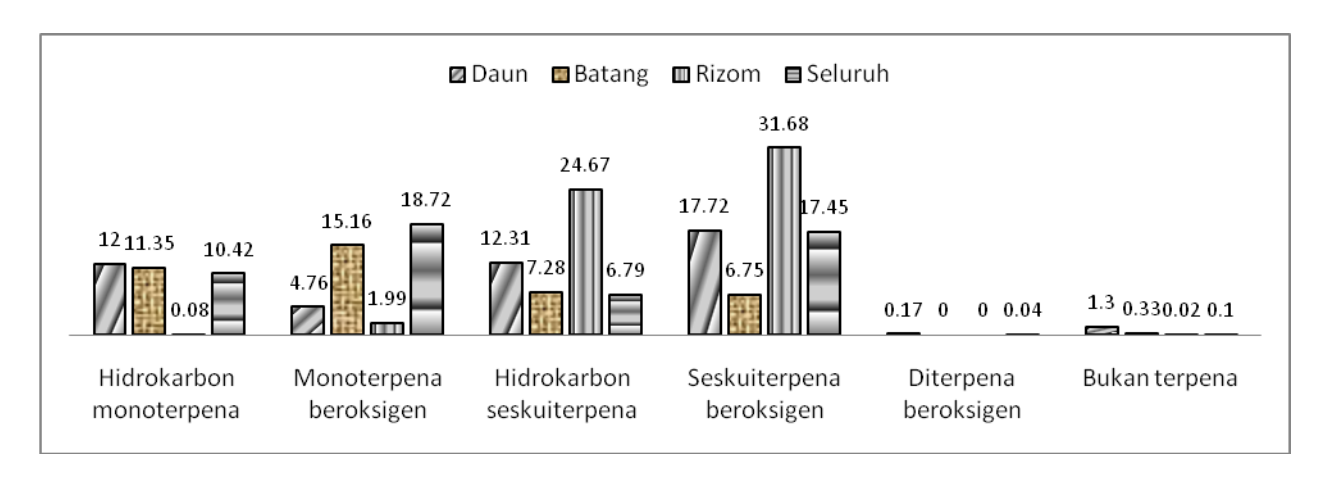
Hasil dan Perbincangan

Peratus hasil

Peratus minyak pati daun, batang dan seluruh tumbuhan *Amomum xanthophlebium* adalah 0.0032, 0.0074 dan 0.0021%. Amaun minyak rizom yang diperolehi adalah terlalu sedikit. Peratus minyak seluruh tumbuhan yang rendah dari daun serta batang adalah sesuai dengan hakikat bahawa batang bagi seluruh tumbuhan lebih berat dari daun dan rizom pula hampir tidak berminyak. Peratus di atas adalah jauh lebih rendah dari 0.03 dan 0.4% minyak daun segar *A. cannicarpum* [5] dan rizom segar *A. linguiforme* [8].

Analisis komposisi minyak pati

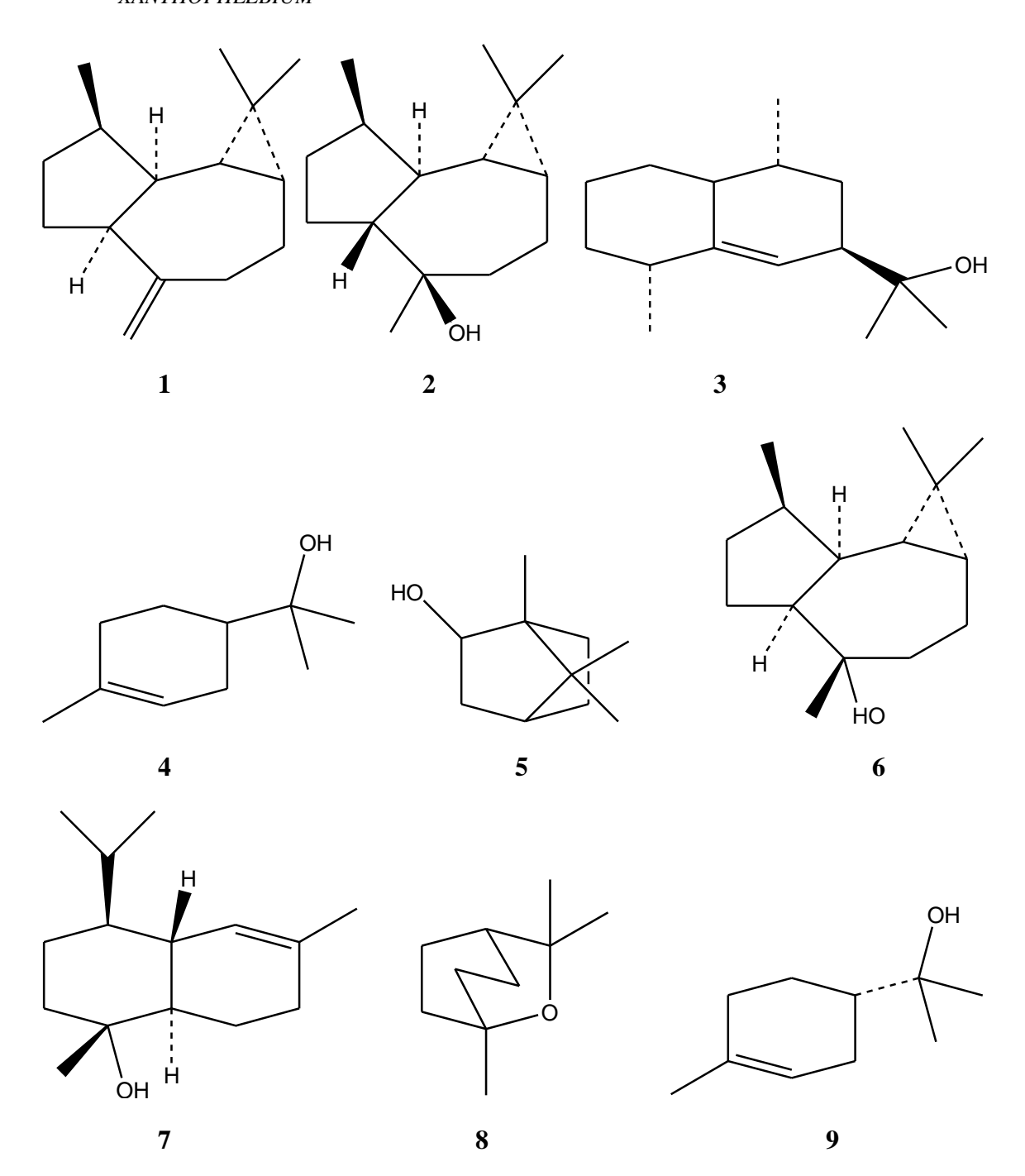
Semua 119 sebatian yang dapat dikenalpasti dari tumbuhan *Amomum xanthophlebium* yang melibatkan 115 terpena dan empat bukan terpena disenaraikan dalam Jadual 1. Jumlah peratus semua sebatian tersebut dalam minyak pati rizom adalah paling tinggi (58.44%) diikuti seluruh tumbuhan (53.52%), daun (48.26%) dan batang (40.87%). Komposisi minyak daun, batang, rizom dan seluruh tumbuhan bagi hidrokarbon monoterpena ialah 12.00, 11.35, 0.08 dan 10.42%; monoterpena beroksigen 4.76, 15.16, 1.99 dan 18.72%; hidrokarbon seskuiterpena 12.31, 7.28, 24.67 dan 6.79%; seskuiterpena beroksigen 17.72, 6.75, 31.68 dan 17.45%; diterpena beroksigen 0.17, 0.00, 0.00 dan 0.04%; serta bukan terpena 1.30, 0.33, 0.02 dan 0.10% (Rajah 1). Hanya rizom yang didominasi seskuiterpena (jumlah 56.35%) berbanding monoterpena 2.07% (tiada diterpena beroksigen dan ada 0.02% bukan terpena).



Rajah 1: Perbandingan peratusan lima kumpulan utama terpena dan satu kumpulan minor bukan terpena dalam minyak daun, batang, rizom dan seluruh tumbuhan segar *Amomum xanthophlebium*

Struktur sembilan sebatian utama *Amomum xanthophlebium* ditunjukkan dalam Rajah 2. Tiga sebatian utama dalam daun ialah *alo*-aromadendrena (1) (3.41%), (\pm)-globulol (2) (2.58%) dan rosifoliol (3) (2.55%); batang, α -terpineol (4) (4.25%), rosifoliol (3) (2.41%) dan bingpian (5) (2.27%); rizom, viridiflorol (6) (5.72%), (\pm)-globulol (2) (5.23%) dan α -kadinol (7) (4.81%); seluruh tumbuhan, eukaliptol (8) (4.11%), l- α -terpineol (9) (2.88%) dan rosifoliol (3) (2.82%). α -Kadinol (7) yang menduduki tempat ke-3 dalam rizom *A. xanthophlebium* juga berada pada kedudukan sama dalam minyak buah *A. cannicarpum* [6].

Masila et al: ANALISIS KROMATOGRAFI GAS x KROMATOGRAFI GAS—SPEKTROMETRI JISIM MASA-PENERBANGAN DAN AKTIVITI ANTIBAKTERIA MINYAK PATI AMOMUM XANTHOPHLEBIUM



Rajah 2: Sembilan sebatian utama dalam minyak daun, batang, rizom dan seluruh tumbuhan *Amomum xanthophlebium*

Analisis mendapati sebatian utama dalam setiap bahagian tumbuhan *Amomum xanthophlebium* adalah berbeza-beza. Rosifoliol (3) terdapat dalam tiga dari empat bahagian iaitu daun, batang dan seluruh tumbuhan. *alo*-Aromadendrena (1) yang pertama dalam daun hanya ke-19 dalam batang, tiada dalam rizom dan ke-13 dalam seluruh tumbuhan. α-Terpineol (4) pula merupakan pertama dalam batang tetapi dalam daun ke-16, dalam rizom ke-18 dan tidak wujud dalam seluruh tumbuhan. Dalam rizom, viridiflorol (6) yang pertama tetapi dalam daun ke-21, dalam batang ke-58 dan dalam seluruh tumbuhan ke-4. Akhir sekali, eukaliptol (8) yang pertama dalam seluruh tumbuhan menjadi ke-18 dalam daun, ke-5 dalam batang dan tidak wujud dalam rizom.

Jadual 1: Komposisi sebatian utama terpena dan minor bukan terpena yang wujud dalam minyak daun, batang, rizom dan seluruh tumbuhan segar *Amomum xanthophlebium*

Bil	Nama	Nombor Daftar CAS	Masa Penahanan ^a (s, min)	Minyak Daun (%)	Minyak Batang (%)	Minyak Rizom (%)	Minyak Seluruh Tumbuhan (%)
Hidr	okarbon monoterpena						
1	o-Simena	527-84-4	620, 0.750	1.28	-	-	1.43
2	Kosmena	460-01-5	780, 0.720	-	0.04	-	-
3	<i>p</i> -Menta-1,5,8-triena	21195-59-5	745, 0.750	-	0.03	-	-
4	1S-α-Pinena	7785-26-4	645, 0.800	-	0.31	-	-
5	α-Felandrena	99-83-2	665, 0.690	1.51	1.39	-	0.17
6	β-Felandrena	555-10-2	625, 0.870	0.77	-	-	-
7	α-Tujena	2867-05-02	500, 1.080	-	1.83	-	2.33
8	Kamfena	79-92-5	515, 0.660	0.32	0.43	-	0.33
9	β- <i>cis</i> -Osimena	3338-55-4	650, 0.710	0.51	0.13	-	0.75
10	Terpinolena	586-62-9	710, 0.720	0.36	0.50	-	-
11	3-Karena	13466-78-9	500, 0.670	1.14	-	-	-
12	β-Pinena	127-91-3	550, 0.660	1.91	-	-	2.40
13	Limonena	138-86-3	625, 0.840	2.54	-	-	-
14	γ-Terpinena	99-85-4	490, 0.710	0.01	-	-	0.29
15	Santolinatriena	2153-66-4	1035, 0.670	-	0.41	0.02	-
16	α -Pinena	2437-95-8	710, 0.720	1.59	0.49	0.06	-
17	2-Norpinena	4889-83-2	490, 0.890	-	0.91	-	-
18	β-Mirsena	123-35-3	570, 0.710	-	1.41	-	1.28
19	γ-Pironina	514-95-4	925, 0.830	-	0.45	-	-
20	1S-β-Pinena	18172-67-3	575, 0.950	-	0.78	-	-
21	Tujena	58037-87-9	550, 0.660	-	0.55	-	-
22	α-Terpinena	99-86-5	610, 0.680	-	0.95	-	-
23	1 <i>R</i> -α-Pinena	7785-70-8	495, 0.650	-	0.26	-	1.26
24	β- <i>trans</i> -Osimena	3779-61-1	655, 0.860	-	0.25	-	-
25	α,p-Dimetilstirena	1195-32-0	715, 0.760	0.06	0.23	-	0.18
	Peratus sub- jumlah			12.00	11.35	0.08	10.42
Mon	oterpena beroksigen						
26	3-Metil-6-metilena- oktana	74630-07-2	510, 0.680	-	0.01	-	-
27	Kuminal	122-03-2	925, 0.960	-	-	-	0.49
28	p-Simena-8-ol	1197-01-9	865, 1.200	0.05	0.06	-	1.76
29	6-Kamfenon	55659-42-2	725, 0.740	0.03	0.08	-	-
30	3-Nopinenon	16812-40-1	820 , 0.790	0.01	-	-	0.09
31	lS-Verbenon	1196-01-6	890, 0.840	-	0.08	-	-
32	Karvakrol	499-75-2	1015 , 1.490	0.02	-	-	-
33	Kuminol	536-60-7	995, 1.280	-	-	-	0.06

Masila et al: ANALISIS KROMATOGRAFI GAS x KROMATOGRAFI GAS—SPEKTROMETRI JISIM MASA-PENERBANGAN DAN AKTIVITI ANTIBAKTERIA MINYAK PATI AMOMUM XANTHOPHLEBIUM

34							
	Mirtenal	564-94-3	870, 0.770	_	-	_	0.07
35	2,6,6-Trimetil-3-	18358-53-7	815, 0.750	_	0.03	_	0.05
33		10330-33-7	015,0.750	_	0.03	_	0.03
	pinanon						
36	1-Pinokarveol	547-61-5	785, 0.850	0.19	-	-	-
37	β-Siklositral	432-25-7	895, 0.770	0.02		-	-
38	α-Pinena epoksida	1686-14-2	725, 0.700	0.12	0.08	_	0.64
39	α-Sitral	141-27-5	965, 0.870	0.07	0.44		0.99
						0.17	
40	Kamfor	21368-68-3	795, 0.740	-	-	0.17	-
41	trans-Karveol	1197-07-5	850, 0.860	-	0.30	-	-
42	<i>p</i> -Menta-1,5-dien-	19876-45-0	970, 1.120	-	0.01	-	0.03
	7-ol						
43	trans-2-Karen-4-ol	4017-82-7	945, 0.920	_	0.25	_	_
44	cis-Karveol	1197-06-4	900, 0.960	_	0.22		0.11
			,			-	
45	lS-cis-Verbenol	18881-04-4	790, 0.860	-	0.25	-	0.43
46	Mirtenol	515-00-4	875, 0.920	-	0.38	-	-
47	β-Sitral	106-26-3	925, 0.870	-	0.44	-	0.90
48	(+)-cis-Limonena	4680-24-4	775, 0.740	_	-	_	0.03
	oksida		,,,,,,,,,,				
49	α-Kamfolenal	4501 59 O					0.25
		4501-58-0	000 0000	-	-	-	0.35
50	Verbenol	473-67-6	800, 0.900	-	-	-	0.19
51	Bingpian	10385-78-1	825, 0.900	0.41	2.27	0.57	-
52	α-Terpineol	98-55-5	860, 1.090	1.34	4.25	0.97	_
53	Eukaliptol	470-82-6	630, 0.800	1.25	1.76	_	4.11
54	Kamfena hidrat	465-31-6		0.15	0.29		0.09
			800,0.800			-	
55	trans-Piperitol	16721-39-4	875, 0.840	0.06	0.77	0.04	0.69
56	cis-p-Ment-2-en-1-	29803-81-4	760, 0.880	0.25	-	-	0.65
	ol						
57	Sitrol	624-15-7	945, 1.050	0.04	-	0.06	0.61
58	Linalol	78-70-6	725, 0.910	0.44	0.60	0.18	0.86
59	ekso-Fenchol	22627-95-8	750, 0.800	0.19	0.32	-	0.21
	R (coroniol	106-24-1	0/15 /1 0/6/1	-	0.21	_	0.39
60	β-Geraniol		945, 0.960	-			
60 61	Isoborneol	124-76-5	815, 0.810	-	0.04	-	1.05
61	Isoborneol	124-76-5	815, 0.810		0.04	-	
	Isoborneol trans-p-Ment-2-en-			-		-	1.05
61 62	Isoborneol trans-p-Ment-2-en- 1-ol	124-76-5 29803-82-5	815 , 0.810 790 , 0.890	-	0.04 0.81	-	1.05
61 62 63	isoborneol trans-p-Ment-2-en- 1-ol l-4-Terpineol	124-76-5 29803-82-5 20126-76-5	815, 0.810 790, 0.890 845, 1.100	-	0.04	-	1.05 - 0.98
61 62 63 64	Isoborneol trans-p-Ment-2-en- 1-ol l-4-Terpineol l-α-Terpineol	124-76-5 29803-82-5 20126-76-5 10482-56-1	815 , 0.810 790 , 0.890 845 , 1.100 865, 0.960	-	0.04 0.81 1.07	-	1.05 - 0.98 2.88
61 62 63	isoborneol trans-p-Ment-2-en- 1-ol l-4-Terpineol	124-76-5 29803-82-5 20126-76-5	815, 0.810 790, 0.890 845, 1.100	-	0.04 0.81	-	1.05 - 0.98
61 62 63 64	Isoborneol trans-p-Ment-2-en- 1-ol l-4-Terpineol l-α-Terpineol	124-76-5 29803-82-5 20126-76-5 10482-56-1	815 , 0.810 790 , 0.890 845 , 1.100 865, 0.960	-	0.04 0.81 1.07	-	1.05 - 0.98 2.88
61 62 63 64 65 66	Isoborneol trans-p-Ment-2-en- 1-ol l-4-Terpineol l-α-Terpineol Linalol oksida D-Sitronelol	124-76-5 29803-82-5 20126-76-5 10482-56-1 5989-33-3 1117-61-9	815, 0.810 790, 0.890 845, 1.100 865, 0.960 710, 0.890 905, 0.980	- - -	0.04 0.81 1.07 0.03	-	1.05 - 0.98 2.88 0.01
61 62 63 64 65	Isoborneol trans-p-Ment-2-en- 1-ol l-4-Terpineol l-α-Terpineol Linalol oksida D-Sitronelol β-Sitronelol	124-76-5 29803-82-5 20126-76-5 10482-56-1 5989-33-3	815, 0.810 790, 0.890 845, 1.100 865, 0.960 710, 0.890	- - - - 0.11	0.04 0.81 1.07 0.03	-	1.05 - 0.98 2.88 0.01
61 62 63 64 65 66	Isoborneol trans-p-Ment-2-en- 1-ol l-4-Terpineol l-α-Terpineol Linalol oksida D-Sitronelol β-Sitronelol Peratus sub-	124-76-5 29803-82-5 20126-76-5 10482-56-1 5989-33-3 1117-61-9	815, 0.810 790, 0.890 845, 1.100 865, 0.960 710, 0.890 905, 0.980	- - - - 0.11	0.04 0.81 1.07 0.03 - 0.12	- - - -	1.05 - 0.98 2.88 0.01
61 62 63 64 65 66 67	Isoborneol trans-p-Ment-2-en- 1-ol l-4-Terpineol l-α-Terpineol Linalol oksida D-Sitronelol β-Sitronelol Peratus sub- jumlah	124-76-5 29803-82-5 20126-76-5 10482-56-1 5989-33-3 1117-61-9 106-22-9	815, 0.810 790, 0.890 845, 1.100 865, 0.960 710, 0.890 905, 0.980	- - - - 0.11	0.04 0.81 1.07 0.03	-	1.05 - 0.98 2.88 0.01
61 62 63 64 65 66 67	Isoborneol trans-p-Ment-2-en- 1-ol l-4-Terpineol l-α-Terpineol Linalol oksida D-Sitronelol β-Sitronelol Peratus sub- jumlah okarbon seskuiterpena	124-76-5 29803-82-5 20126-76-5 10482-56-1 5989-33-3 1117-61-9 106-22-9	815, 0.810 790, 0.890 845, 1.100 865, 0.960 710, 0.890 905, 0.980 910, 0.930	- - - 0.11 - 4.76	0.04 0.81 1.07 0.03 - 0.12 15.16	- - - - - - 1.99	1.05 - 0.98 2.88 0.01 - - 18.72
61 62 63 64 65 66 67 Hidr 68	Isoborneol trans-p-Ment-2-en- 1-ol l-4-Terpineol l-α-Terpineol Linalol oksida D-Sitronelol β-Sitronelol Peratus sub- jumlah okarbon seskuiterpena α-Kalakorena	124-76-5 29803-82-5 20126-76-5 10482-56-1 5989-33-3 1117-61-9 106-22-9	815, 0.810 790, 0.890 845, 1.100 865, 0.960 710, 0.890 905, 0.980 910, 0.930	- - - 0.11 - 4.76	0.04 0.81 1.07 0.03 - 0.12 15.16	- - - - - - 1.99	1.05 - 0.98 2.88 0.01 - - 18.72
61 62 63 64 65 66 67	Isoborneol trans-p-Ment-2-en- 1-ol l-4-Terpineol l-α-Terpineol Linalol oksida D-Sitronelol β-Sitronelol Peratus sub- jumlah okarbon seskuiterpena	124-76-5 29803-82-5 20126-76-5 10482-56-1 5989-33-3 1117-61-9 106-22-9	815, 0.810 790, 0.890 845, 1.100 865, 0.960 710, 0.890 905, 0.980 910, 0.930	- - - 0.11 - 4.76	0.04 0.81 1.07 0.03 - 0.12 15.16	- - - - - - 1.99	1.05 - 0.98 2.88 0.01 - - 18.72
61 62 63 64 65 66 67 Hidr 68	Isoborneol trans-p-Ment-2-en- 1-ol l-4-Terpineol l-α-Terpineol Linalol oksida D-Sitronelol β-Sitronelol Peratus sub- jumlah okarbon seskuiterpena α-Kalakorena Kalamenena	124-76-5 29803-82-5 20126-76-5 10482-56-1 5989-33-3 1117-61-9 106-22-9	815 , 0.810 790 , 0.890 845 , 1.100 865 , 0.960 710 , 0.890 905 , 0.980 910 , 0.930 1300 , 0.710 1275 , 0.750	- - - 0.11 - 4.76	0.04 0.81 1.07 0.03 - 0.12 15.16	- - - - - - 1.99	1.05 - 0.98 2.88 0.01 - - 18.72 0.03 0.55
61 62 63 64 65 66 67 Hidr 68 69	Isoborneol trans-p-Ment-2-en- 1-ol l-4-Terpineol l-α-Terpineol Linalol oksida D-Sitronelol β-Sitronelol Peratus sub- jumlah okarbon seskuiterpena α-Kalakorena	124-76-5 29803-82-5 20126-76-5 10482-56-1 5989-33-3 1117-61-9 106-22-9	815, 0.810 790, 0.890 845, 1.100 865, 0.960 710, 0.890 905, 0.980 910, 0.930	- - 0.11 - 4.76 0.07 1.46	0.04 0.81 1.07 0.03 - 0.12 15.16 0.02 0.23	- - - - - - 1.99	1.05 - 0.98 2.88 0.01 - - 18.72
61 62 63 64 65 66 67 Hidr 68 69 70	Isoborneol trans-p-Ment-2-en- 1-ol l-4-Terpineol l-α-Terpineol Linalol oksida D-Sitronelol β-Sitronelol Peratus sub- jumlah okarbon seskuiterpena α-Kalakorena Kalamenena α-Panasinsena	124-76-5 29803-82-5 20126-76-5 10482-56-1 5989-33-3 1117-61-9 106-22-9 21391-99-1 483-77-2 56633-28-4	815, 0.810 790, 0.890 845, 1.100 865, 0.960 710, 0.890 905, 0.980 910, 0.930 1300, 0.710 1275, 0.750 1170, 0660	- - 0.11 - 4.76 0.07 1.46	0.04 0.81 1.07 0.03 - 0.12 15.16 0.02 0.23	- - - - - - 1.99	1.05 - 0.98 2.88 0.01 - - 18.72 0.03 0.55
61 62 63 64 65 66 67 Hidr 68 69 70	Isoborneol trans-p-Ment-2-en- 1-ol l-4-Terpineol l-α-Terpineol Linalol oksida D-Sitronelol β-Sitronelol Peratus sub- jumlah okarbon seskuiterpena α-Kalakorena Kalamenena α-Panasinsena Kalarena	124-76-5 29803-82-5 20126-76-5 10482-56-1 5989-33-3 1117-61-9 106-22-9 21391-99-1 483-77-2 56633-28-4 17334-55-3	815, 0.810 790, 0.890 845, 1.100 865, 0.960 710, 0.890 905, 0.980 910, 0.930 1300, 0.710 1275, 0.750 1170, 0660 1165, 0.650	0.11 - 4.76 0.07 1.46	0.04 0.81 1.07 0.03 - 0.12 15.16 0.02 0.23 - 0.41	- - - - - - - - - - - - - - - - - - -	1.05 - 0.98 2.88 0.01 - - 18.72 0.03 0.55
61 62 63 64 65 66 67 Hidr 68 69 70	Isoborneol trans-p-Ment-2-en- 1-ol l-4-Terpineol l-α-Terpineol Linalol oksida D-Sitronelol β-Sitronelol Peratus sub- jumlah okarbon seskuiterpena α-Kalakorena Kalamenena α-Panasinsena Kalarena β-Bourbonena	124-76-5 29803-82-5 20126-76-5 10482-56-1 5989-33-3 1117-61-9 106-22-9 21391-99-1 483-77-2 56633-28-4 17334-55-3 5208-59-3	815, 0.810 790, 0.890 845, 1.100 865, 0.960 710, 0.890 905, 0.980 910, 0.930 1300, 0.710 1275, 0.750 1170, 0660 1165, 0.650 1110, 0.670	0.11 - 4.76 0.07 1.46 - 0.04	0.04 0.81 1.07 0.03 - 0.12 15.16 0.02 0.23 - 0.41	- - - - - - - - - - - - - - - - - - -	1.05 - 0.98 2.88 0.01 18.72 0.03 0.55 0.07
61 62 63 64 65 66 67 Hidr 68 69 70 71 72 73	Isoborneol trans-p-Ment-2-en- 1-ol l-4-Terpineol l-α-Terpineol Linalol oksida D-Sitronelol β-Sitronelol Peratus sub- jumlah okarbon seskuiterpena α-Kalakorena Kalamenena α-Panasinsena Kalarena β-Bourbonena Kariofilena	124-76-5 29803-82-5 20126-76-5 10482-56-1 5989-33-3 1117-61-9 106-22-9 21391-99-1 483-77-2 56633-28-4 17334-55-3 5208-59-3 87-44-5	815, 0.810 790, 0.890 845, 1.100 865, 0.960 710, 0.890 905, 0.980 910, 0.930 1300, 0.710 1275, 0.750 1170, 0660 1165, 0.650 1110, 0.670 1150, 0.680		0.04 0.81 1.07 0.03 - 0.12 15.16 0.02 0.23 - 0.41	1.99 0.06 2.34 - 0.36	1.05 - 0.98 2.88 0.01 18.72 0.03 0.55 0.07 0.90
61 62 63 64 65 66 67 Hidr 68 69 70	Isoborneol trans-p-Ment-2-en- 1-ol l-4-Terpineol l-α-Terpineol Linalol oksida D-Sitronelol β-Sitronelol Peratus sub- jumlah okarbon seskuiterpena α-Kalakorena Kalamenena α-Panasinsena Kalarena β-Bourbonena	124-76-5 29803-82-5 20126-76-5 10482-56-1 5989-33-3 1117-61-9 106-22-9 21391-99-1 483-77-2 56633-28-4 17334-55-3 5208-59-3	815, 0.810 790, 0.890 845, 1.100 865, 0.960 710, 0.890 905, 0.980 910, 0.930 1300, 0.710 1275, 0.750 1170, 0660 1165, 0.650 1110, 0.670 1150, 0.680 1195, 0.710	0.11 - 4.76 0.07 1.46 - 0.04	0.04 0.81 1.07 0.03 - 0.12 15.16 0.02 0.23 - 0.41	- - - - - - - - - - - - - - - - - - -	1.05 - 0.98 2.88 0.01 18.72 0.03 0.55 0.07
61 62 63 64 65 66 67 Hidr 68 69 70 71 72 73	Isoborneol trans-p-Ment-2-en- 1-ol l-4-Terpineol l-α-Terpineol Linalol oksida D-Sitronelol β-Sitronelol Peratus sub- jumlah okarbon seskuiterpena α-Kalakorena Kalamenena α-Panasinsena Kalarena β-Bourbonena Kariofilena	124-76-5 29803-82-5 20126-76-5 10482-56-1 5989-33-3 1117-61-9 106-22-9 21391-99-1 483-77-2 56633-28-4 17334-55-3 5208-59-3 87-44-5	815, 0.810 790, 0.890 845, 1.100 865, 0.960 710, 0.890 905, 0.980 910, 0.930 1300, 0.710 1275, 0.750 1170, 0660 1165, 0.650 1110, 0.670 1150, 0.680 1195, 0.710		0.04 0.81 1.07 0.03 - 0.12 15.16 0.02 0.23 - 0.41	1.99 0.06 2.34 - 0.36	1.05 - 0.98 2.88 0.01 18.72 0.03 0.55 0.07 0.90 1.93
61 62 63 64 65 66 67 Hidr 68 69 70 71 72 73 74 75	Isoborneol trans-p-Ment-2-en- 1-ol l-4-Terpineol l-α-Terpineol Linalol oksida D-Sitronelol β-Sitronelol Peratus sub- jumlah okarbon seskuiterpena α-Kalakorena Kalamenena α-Panasinsena Kalarena β-Bourbonena Kariofilena α-Kariofilena Isoledena	124-76-5 29803-82-5 20126-76-5 10482-56-1 5989-33-3 1117-61-9 106-22-9 21391-99-1 483-77-2 56633-28-4 17334-55-3 5208-59-3 87-44-5 6753-98-6 95910-36-4	815, 0.810 790, 0.890 845, 1.100 865, 0.960 710, 0.890 905, 0.980 910, 0.930 1300, 0.710 1275, 0.750 1170, 0660 1165, 0.650 1110, 0.670 1150, 0.680 1195, 0.710 1190, 0.660	- 0.11 - 4.76 0.07 1.46 - 0.04 0.53 0.80 0.29	0.04 0.81 1.07 0.03 - 0.12 15.16 0.02 0.23 - 0.41 - 1.55	1.99 0.06 2.34 - 0.36 - 3.26 4.55 0.32	1.05 - 0.98 2.88 0.01 18.72 0.03 0.55 0.07 - 0.90 1.93 0.12
61 62 63 64 65 66 67 Hidr 68 69 70 71 72 73 74 75 76	Isoborneol trans-p-Ment-2-en- 1-ol l-4-Terpineol l-α-Terpineol Linalol oksida D-Sitronelol β-Sitronelol Peratus sub- jumlah okarbon seskuiterpena α-Kalakorena Kalamenena α-Panasinsena Kalarena β-Bourbonena Kariofilena α-Kariofilena Isoledena alo-Aromadendrena	124-76-5 29803-82-5 20126-76-5 10482-56-1 5989-33-3 1117-61-9 106-22-9 21391-99-1 483-77-2 56633-28-4 17334-55-3 5208-59-3 87-44-5 6753-98-6 95910-36-4 25246-27-9	815, 0.810 790, 0.890 845, 1.100 865, 0.960 710, 0.890 905, 0.980 910, 0.930 1300, 0.710 1275, 0.750 1170, 0660 1165, 0.650 1110, 0.670 1150, 0.680 1195, 0.710 1190, 0.660 1175, 0.710	0.11 - 4.76 0.07 1.46 - 0.04 0.53 0.80 0.29 3.41	0.04 0.81 1.07 0.03 - 0.12 15.16 0.02 0.23 - 0.41 - 1.55 0.74	0.06 2.34 - 0.36 - 3.26 4.55 0.32	1.05 - 0.98 2.88 0.01 18.72 0.03 0.55 0.07 - 0.90 1.93 0.12 1.29
61 62 63 64 65 66 67 Hidr 68 69 70 71 72 73 74 75 76 77	Isoborneol trans-p-Ment-2-en- 1-ol l-4-Terpineol l-α-Terpineol Linalol oksida D-Sitronelol β-Sitronelol Peratus sub- jumlah okarbon seskuiterpena α-Kalakorena Kalamenena α-Panasinsena Kalarena β-Bourbonena Kariofilena α-Kariofilena Isoledena alo-Aromadendrena γ-Murolena	124-76-5 29803-82-5 20126-76-5 10482-56-1 5989-33-3 1117-61-9 106-22-9 21391-99-1 483-77-2 56633-28-4 17334-55-3 5208-59-3 87-44-5 6753-98-6 95910-36-4 25246-27-9 30021-74-0	815, 0.810 790, 0.890 845, 1.100 865, 0.960 710, 0.890 905, 0.980 910, 0.930 1300, 0.710 1275, 0.750 1170, 0660 1165, 0.650 1110, 0.670 1150, 0.680 1195, 0.710 1190, 0.660 1175, 0.710 1095, 0.660	0.11 - 4.76 0.07 1.46 - 0.04 0.53 0.80 0.29 3.41 1.04	0.04 0.81 1.07 0.03 - 0.12 15.16 0.02 0.23 - 0.41 - 1.55 0.74 1.07	1.99 0.06 2.34 - 0.36 - 3.26 4.55 0.32 - 1.33	1.05 - 0.98 2.88 0.01 - 18.72 0.03 0.55 0.07 - 0.90 1.93 0.12 1.29 0.19
61 62 63 64 65 66 67 Hidr 68 69 70 71 72 73 74 75 76	Isoborneol trans-p-Ment-2-en- 1-ol l-4-Terpineol l-α-Terpineol Linalol oksida D-Sitronelol Peratus sub- jumlah okarbon seskuiterpena α-Kalakorena Kalamenena α-Panasinsena Kalarena β-Bourbonena Kariofilena α-Kariofilena Isoledena alo-Aromadendrena γ-Murolena Dekahidro-1,1,7-	124-76-5 29803-82-5 20126-76-5 10482-56-1 5989-33-3 1117-61-9 106-22-9 21391-99-1 483-77-2 56633-28-4 17334-55-3 5208-59-3 87-44-5 6753-98-6 95910-36-4 25246-27-9	815, 0.810 790, 0.890 845, 1.100 865, 0.960 710, 0.890 905, 0.980 910, 0.930 1300, 0.710 1275, 0.750 1170, 0660 1165, 0.650 1110, 0.670 1150, 0.680 1195, 0.710 1190, 0.660 1175, 0.710	0.11 - 4.76 0.07 1.46 - 0.04 0.53 0.80 0.29 3.41	0.04 0.81 1.07 0.03 - 0.12 15.16 0.02 0.23 - 0.41 - 1.55 0.74	0.06 2.34 - 0.36 - 3.26 4.55 0.32	1.05 - 0.98 2.88 0.01 18.72 0.03 0.55 0.07 - 0.90 1.93 0.12 1.29
61 62 63 64 65 66 67 Hidr 68 69 70 71 72 73 74 75 76 77	Isoborneol trans-p-Ment-2-en- 1-ol l-4-Terpineol l-α-Terpineol Linalol oksida D-Sitronelol Peratus sub- jumlah okarbon seskuiterpena α-Kalakorena Kalamenena α-Panasinsena Kalarena β-Bourbonena Kariofilena α-Kariofilena Isoledena alo-Aromadendrena γ-Murolena Dekahidro-1,1,7- trimetil-4-metilena-	124-76-5 29803-82-5 20126-76-5 10482-56-1 5989-33-3 1117-61-9 106-22-9 21391-99-1 483-77-2 56633-28-4 17334-55-3 5208-59-3 87-44-5 6753-98-6 95910-36-4 25246-27-9 30021-74-0	815, 0.810 790, 0.890 845, 1.100 865, 0.960 710, 0.890 905, 0.980 910, 0.930 1300, 0.710 1275, 0.750 1170, 0660 1165, 0.650 1110, 0.670 1150, 0.680 1195, 0.710 1190, 0.660 1175, 0.710 1095, 0.660	0.11 - 4.76 0.07 1.46 - 0.04 0.53 0.80 0.29 3.41 1.04	0.04 0.81 1.07 0.03 - 0.12 15.16 0.02 0.23 - 0.41 - 1.55 0.74 1.07	1.99 0.06 2.34 - 0.36 - 3.26 4.55 0.32 - 1.33	1.05 - 0.98 2.88 0.01 - 18.72 0.03 0.55 0.07 - 0.90 1.93 0.12 1.29 0.19
61 62 63 64 65 66 67 Hidr 68 69 70 71 72 73 74 75 76 77	Isoborneol trans-p-Ment-2-en- 1-ol l-4-Terpineol l-α-Terpineol Linalol oksida D-Sitronelol Peratus sub- jumlah okarbon seskuiterpena α-Kalakorena Kalamenena α-Panasinsena Kalarena β-Bourbonena Kariofilena α-Kariofilena Isoledena alo-Aromadendrena γ-Murolena Dekahidro-1,1,7-	124-76-5 29803-82-5 20126-76-5 10482-56-1 5989-33-3 1117-61-9 106-22-9 21391-99-1 483-77-2 56633-28-4 17334-55-3 5208-59-3 87-44-5 6753-98-6 95910-36-4 25246-27-9 30021-74-0	815, 0.810 790, 0.890 845, 1.100 865, 0.960 710, 0.890 905, 0.980 910, 0.930 1300, 0.710 1275, 0.750 1170, 0660 1165, 0.650 1110, 0.670 1150, 0.680 1195, 0.710 1190, 0.660 1175, 0.710 1095, 0.660	0.11 - 4.76 0.07 1.46 - 0.04 0.53 0.80 0.29 3.41 1.04	0.04 0.81 1.07 0.03 - 0.12 15.16 0.02 0.23 - 0.41 - 1.55 0.74 1.07	1.99 0.06 2.34 - 0.36 - 3.26 4.55 0.32 - 1.33	1.05 - 0.98 2.88 0.01 - 18.72 0.03 0.55 0.07 - 0.90 1.93 0.12 1.29 0.19
61 62 63 64 65 66 67 Hidr 68 69 70 71 72 73 74 75 76 77	Isoborneol trans-p-Ment-2-en- 1-ol l-4-Terpineol l-α-Terpineol Linalol oksida D-Sitronelol β-Sitronelol Peratus sub- jumlah okarbon seskuiterpena α-Kalakorena Kalamenena α-Panasinsena Kalarena β-Bourbonena Kariofilena α-Kariofilena Isoledena alo-Aromadendrena γ-Murolena Dekahidro-1,1,7- trimetil-4-metilena- 1H-	124-76-5 29803-82-5 20126-76-5 10482-56-1 5989-33-3 1117-61-9 106-22-9 21391-99-1 483-77-2 56633-28-4 17334-55-3 5208-59-3 87-44-5 6753-98-6 95910-36-4 25246-27-9 30021-74-0	815, 0.810 790, 0.890 845, 1.100 865, 0.960 710, 0.890 905, 0.980 910, 0.930 1300, 0.710 1275, 0.750 1170, 0660 1165, 0.650 1110, 0.670 1150, 0.680 1195, 0.710 1190, 0.660 1175, 0.710 1095, 0.660	0.11 - 4.76 0.07 1.46 - 0.04 0.53 0.80 0.29 3.41 1.04	0.04 0.81 1.07 0.03 - 0.12 15.16 0.02 0.23 - 0.41 - 1.55 0.74 1.07	1.99 0.06 2.34 - 0.36 - 3.26 4.55 0.32 - 1.33	1.05 - 0.98 2.88 0.01 - 18.72 0.03 0.55 0.07 - 0.90 1.93 0.12 1.29 0.19
61 62 63 64 65 66 67 Hidr 68 69 70 71 72 73 74 75 76 77 78	Isoborneol trans-p-Ment-2-en- 1-ol l-4-Terpineol l-α-Terpineol Linalol oksida D-Sitronelol β-Sitronelol Peratus sub- jumlah okarbon seskuiterpena α-Kalakorena Kalamenena α-Panasinsena Kalarena β-Bourbonena Kariofilena a-Kariofilena Isoledena alo-Aromadendrena γ-Murolena Dekahidro-1,1,7- trimetil-4-metilena- 1H- sikloprop[e]azulena	124-76-5 29803-82-5 20126-76-5 10482-56-1 5989-33-3 1117-61-9 106-22-9 21391-99-1 483-77-2 56633-28-4 17334-55-3 5208-59-3 87-44-5 6753-98-6 95910-36-4 25246-27-9 30021-74-0 109119-91-7	815, 0.810 790, 0.890 845, 1.100 865, 0.960 710, 0.890 905, 0.980 910, 0.930 1300, 0.710 1275, 0.750 1170, 0660 1165, 0.650 1110, 0.670 1150, 0.680 1195, 0.710 1190, 0.660 1175, 0.710 1095, 0.660 1200, 0.690	0.11 - - - 0.07 1.46 - - 0.04 0.53 0.80 0.29 3.41 1.04 1.75	0.04 0.81 1.07 0.03 - 0.12 15.16 0.02 0.23 - 0.41 - 1.55 0.74 1.07	0.06 2.34 - 0.36 - 3.26 4.55 0.32 - 1.33 4.77	1.05 - 0.98 2.88 0.01 - 18.72 18.72 0.03 0.55 0.07 - 0.90 1.93 0.12 1.29 0.19 -
61 62 63 64 65 66 67 Hidr 68 69 70 71 72 73 74 75 76 77	Isoborneol trans-p-Ment-2-en- 1-ol l-4-Terpineol l-α-Terpineol Linalol oksida D-Sitronelol β-Sitronelol Peratus sub- jumlah okarbon seskuiterpena α-Kalakorena Kalamenena α-Panasinsena Kalarena β-Bourbonena Kariofilena α-Kariofilena Isoledena alo-Aromadendrena γ-Murolena Dekahidro-1,1,7- trimetil-4-metilena- 1H-	124-76-5 29803-82-5 20126-76-5 10482-56-1 5989-33-3 1117-61-9 106-22-9 21391-99-1 483-77-2 56633-28-4 17334-55-3 5208-59-3 87-44-5 6753-98-6 95910-36-4 25246-27-9 30021-74-0	815, 0.810 790, 0.890 845, 1.100 865, 0.960 710, 0.890 905, 0.980 910, 0.930 1300, 0.710 1275, 0.750 1170, 0660 1165, 0.650 1110, 0.670 1150, 0.680 1195, 0.710 1190, 0.660 1175, 0.710 1095, 0.660	0.11 - 4.76 0.07 1.46 - 0.04 0.53 0.80 0.29 3.41 1.04	0.04 0.81 1.07 0.03 - 0.12 15.16 0.02 0.23 - 0.41 - 1.55 0.74 1.07	1.99 0.06 2.34 - 0.36 - 3.26 4.55 0.32 - 1.33	1.05 - 0.98 2.88 0.01 - 18.72 0.03 0.55 0.07 - 0.90 1.93 0.12 1.29 0.19

81	α-Farnesena	502-61-4	1255, 0.840	2.05	_	_	0.38
82	β-Kubebena	13744-15-5	1285, 0.690	0.19	0.30	_	-
83	Eliksena	3242-08-8	1045, 0.670	0.05	0.12		0.01
84	Viridiflorena	21747-46-6	1245, 0.760	-	-	2.18	0.48
85	1-Etenil-1-metil-	110823-68-2	1115, 0.690	-	-	0.04	-
	2,4-bis(1-						
	metiletenil)-						
0.6	sikloheksana	220154.01.5	1245 0710		1.24	1.20	
86	1-Etenil-1-metil-	339154-91-5	1245, 0.710	-	1.34	1.30	-
	2,4-bis(1- metiletilidena)siklo-						
	heksana						
87	Germakrena D	23986-74-5	1230, 0.700	_	0.35	_	_
88	1,2,4aβ,5,6,8aβ-	31983-22-9	1290, 0.690	_	0.09	-	0.03
	Heksahidro-1β-						
	isopropil-4,7-						
	dimetilnaftalena						
89	γ-Kadinena	39029-41-9	1265, 0.690	-	-	-	0.16
90	2,7,10-	74645-98-0	965, 0.700	-	0.002	-	-
	Trimetildodekana Peratus sub-						
	jumlah			12.31	7.28	24.67	6.79
Sesku	iterpena beroksigen						
91	Ledena oksida	882187-44-2	1440, 0.820	0.51	0.11	-	0.30
92	β-Spatulenol	77171-55-2	1350, 0.700	1.85	0.84	3.80	1.86
93	trans,trans-	502-67-0	1510, 0.830	0.08	0.01	0.04	0.03
94	Farnesal (-)-9-Aristolena-10	174629-49-3	1520, 0.790			0.63	
74	β ,15-diol 6α , 7α -	174027-47-3	1320,0.770	_	_	0.03	_
	epoksida						
95	Humulena oksida II	19888-34-7	1380, 0.770	-	0.70	1.33	1.20
96	Oktahidro-7,7,8,8-	74842-43-6	1495, 0.830	-	0.02	-	-
	tetrametil-2,3b-						
	metano-3bH-						
	sikloprop[1,2]benz						
97	en-4-ol Spatulenol	6750-60-3	1410, 0.840	_			0.34
98	γ-Eudesmol	1209-71-8	1400, 0.840	-	-	2.19	-
99	α-Eudesmol	473-16-5	1330, 0.790	_	_	3.70	<u>-</u>
100	Viridiflorol	552-02-3	1325, 0.720	1.13	0.10	5.72	2.60
101	α-Kadinol	481-34-5	1425, 0.860	1.67	-	4.81	1.23
102	Dekahidro-1,1,4,7-	95975-84-1	1330, 0.730	1.03	-	-	0.44
	tetrametil-4aH-						
	sikloprop[e]azulen-						
102	4a-ol, Epiglobulol	00730 50 0	1440 0 700	1.06	1.50		0.60
103 104	Patchouli alkohol	88728-58-9 5986-55-0	1440 , 0.790 1435 , 0.750	1.96 1.38	1.52 0.14	0.36	0.60 0.12
104	(±)-Globulol	51371-47-2	1350, 0.730	2.58	0.14	5.23	2.30
106	trans-Farnesol	106-28-5	1495, 0.870	0.13	-	-	0. 08
107	Nerolidol	142-50-7	1320, 0.830	0.44	-	-	-
108	Kubenol	21284-22-0	1400, 0.770	0.34	0.26	-	0.27
109	Rosifoliol	63891-61-2	1370, 0.840	2.55	2.41	-	2.82
110	Elemol	639-99-6	1305, 0.820	-	-	0.40	-
111	d-Ledol	577-27-5	1360, 0.910	2.07	-	1.12	2.17
112 113	τ-Murolol Juniper kamfor	19912-62-0 473-04-1	1410, 0.850 1315, 0.750	-	0.23	2.35	0.90 0.19
113	Jumper Kannor	+/J-U4-1	1313,0./30	-	0.23	-	U.17
	Peratus sub-						
	jumlah			17.72	6.75	31.68	17.45

Masila et al: ANALISIS KROMATOGRAFI GAS x KROMATOGRAFI GAS-SPEKTROMETRI JISIM MASA-PENERBANGAN DAN AKTIVITI ANTIBAKTERIA MINYAK PATI *AMOMUM* XANTHOPHLEBIUM

Diter	pena beroksigen						
114	Isofitol	505-32-8	1705, 0.840	0.17	-	-	0.01
115	Fitol	150-86-7	1855, 0.810	-	-	-	0.03
	Jumlah			0.17	0.00	0.00	0.04
	Bukan terpena						
116	3,5-Dimetiloktana	15869-93-9	660, 0.700	0.02	-	0.02	0.03
117	p-Asetoksistirena	2628-16-2	935, 2.910	-	0.18	-	-
118	Benzilaseton	2550-26-7	930, 1.240	0.05	-	-	0.07
119	Eksalton	502-72-7	1655, 0.840	1.23	0.15	-	-
	Peratus sub-						
	jumlah			1.30	0.33	0.02	0.10
	Peratus jumlah			48.26	40.87	58.44	53.52

a = Masa penahanan pertama dan kedua adalah bagi turus primer dan sekunder

Aktiviti antibakteria

Untuk ujian antibakteria, dipilih kaedah kepekatan perencatan minumum (KPM) yang bermaksud kepekatan terendah bagi agen antibakteria (minyak pati) yang boleh menyebabkan perencatan kepada pertumbuhan bakteria. Kerana amaun yang mencukupi, hanya minyak batang segar *Amomum xanthophlebium* dijalankan ujian KPM. Tiga bakteria yang diuji adalah Gram-negatif *Escherichia coli* dan Gram-positif *Staphylococcus aureus*, *S. aureus* rintang metisilin (SARM). Pemerhatian terhadap kekeruhan di rekodkan dalam Jadual 2.

Jadual 2: Data kekeruhan dalam ujian antibakteria bagi minyak batang segar *Amomum xanthophlebium* di mana tanda √ bermaksud tidak keruh/cerah manakala tanda x bermaksud keruh

Bakteria	160 mg/ml	80 mg/ml	40 mg/ml	20 mg/ml	10 mg/ml
Escherichia	$\sqrt{}$	$\sqrt{}$	X	X	X
coli					
Staphylococcus	X	X	X	X	X
aureus					
SARM	$\sqrt{}$	$\sqrt{}$	X	X	X

Dari ujian yang dilakukan, didapati minyak batang segar *Amomum xanthophlebium* merencatkan *Escherichia coli* dan SARM pada KPM 80 mg/ml tetapi tidak menunjukkan sebarang perencatan terhadap *Staphylococcus aureus*. Kesan antibakteria yang lemah ini mungkin berpunca dari kehadiran hidrokarbon monoterpena dalam batang *A. xanthophlebium* (11.35%) [11]. Kebolehan minyak batang merencat SARM berbanding *S. aureus* menunjukkan kesan khusus dalam tindakannya terhadap bakteria. *Escherichia coli* (Enterobacteriaceae) boleh menyebabkan jangkitan pada bahagian perut. Penggunaan *A. xanthophlebium* segar secara tradisional dalam merawat jangkitan yang membawa kepada cirit-birit telah dapat dikaitkan secara saintifik dalam kajian ini.

Kesimpulan

Hidrokarbon seskuiterpena dan seskuiterpena beroksigen merupakan sebatian utama dalam minyak pati rizom segar *Amomum xanthophlebium*. Sebatian utama minyak daun adalah *alo*-aromadendrena, batang α -terpineol, rizom viridiflorol, dan seluruh tumbuhan eukaliptol. Aktiviti antibakteria minyak batang menunjukkan kesan terhadap SARM dan *Escherichia coli*.

Penghargaan

Pengarang pertama dan kedua ingin mengucapkan terima kasih kepada Bahagian Tajaan dan Biasiswa, Kementerian Pelajaran Malaysia kerana memberi peluang bagi mengikuti pengajian peringkat Sarjana Sains (Kimia) di Universiti Kebangsaan Malaysia. Kami juga ingin merakamkan penghargaan dan ucapan terima kasih kepada Kementerian Pengajian Tinggi dan Universiti Kebangsaan Malaysia ke atas pemberian peruntukan di bawah Skim Geran Penyelidikan Fundamental UKM-ST-06-FRGS0110-2009 dan Dana Operasi Universiti Penyelidikan UKM-OUP-KPB-31-156/2011 bagi membiayai kajian ini.

Rujukan

- 1. Habsah, M., Ali, A.M., Lajis, N.H., Sukari, M.A., Yap, Y.H., Kikuzaki, H., Nakatani, N. 2005. Antitumor promoting and cytotoxic constituents of *Etlingera elatior*. *Malaysian Journal of Medical Sciences*. 12(1): 6-12.
- 2. Zakaria, M.B. & Ibrahim, H. 1986. Phytochemical screening of some Malaysian species of Zingiberaceae. *Malaysian Journal of Science* 8: 125-128.
- 3. Takano, A., Hernawati & Tamin, R. 2001. Notes on *Globba* Linnaeus in Sumatra, W. Malaysia & Borneo: a new record of *Globba brachyanthera* var. *rubra* in Sumatra. *Folia Malaysiana* 2(1): 25-34.
- 4. Ibrahim, H. & Rahman, A.A. 1988. Several ginger plants (Zingiberaceae) of potential value. *Proceeding of the Seminar on Malaysian Traditional Medicine*, hlm. 159-161. Kuala Lumpur: IPT, University Malaya.
- 5. Mathew, J., Subulal, B., George, V., Dan, M. & Shiburaj, S. 2006. Chemical composition and antimicrobial activity of the leaf oil of *Amomum cannicarpum* (Wight) Bentham ex Baker. *Journal of Essential Oil Research* 18(1): 35-37.
- 6. Sabulal, B., Dan, M., Pradeep, N.S., Valsamma, R.K. & George V. 2006. Composition and antimicrobial activity of essential oil from the fruits of *Amomum cannicarpum*. *Acta Pharmaceutica* 56(4): 473–480.
- Sabulal, B., Dan, M., John J.A., Kurup, R., Pradeep, N.S., Valsamma, R.K. & George, V. 2006. Caryophyllenerich rhizome oil of *Zingiber nimmonii* from South India: chemical characterization and antimicrobial activity. *Phytochemistry* 67(22): 2469-2473.
- 8. Hazarika, A.K. & Nath, S.C. 1995. Methyl chavicol-the major component of the rhizome oil of *Amomum linguiforme* Benth. *Journal of Essential Oil Research* 7(3): 325-326.
- 9. Dallüge, J., van Stee, L.L.P., Xu, X., Williams, J., Beens, J., Vreuls, R.J.J. & Brinkman, U.A.T. 2002. Unravelling the composition of very complex samples by comprehensive gas chromatography coupled to time-of-flight mass spectrometry. cigarette smoke. *Journal of Chromatography*, A 974(1-2): 169-184.
- 10. Hussain, A.I., Anwar, F., Hussain Sherazi, S.T. & Przybylski, R. 2008. Chemical composition, antioxidant and antimicrobial activities of basil (*Ocimum basilicum*) essential oils depends on seasonal variations. *Food Chemistry* 108(3): 986-995.
- 11. Yaacob, K.B. 1988. Antimicrobial properties of essential oils. *Proceeding of the Seminar on Malaysian Traditional Medicine*, hlm. 125-129. Kuala Lumpur: IPT, University Malaya.



EXTRACTION OF Eu(III) IN MONAZITE FROM SOILS CONTAINING 'AMANG' COLLECTED FROM KG GAJAH EX-MINING AREA

(Pengekstrakan Eu(III) Dalam Monazit Daripada Tanih Mengandungi Amang Dari Kawasan Bekas Lombong Kg. Gajah)

Zaini Hamzah¹, Nor Monica Ahmad^{1*}, and Ahmad Saat²

¹Faculty of Applied Sciences, ²Institute of Science (IOS), Universiti Teknologi MARA (UiTM), 40450 Shah Alam, Selangor Darul Ehsan

*Corresponding author: normonica@gmail.com

Abstract

Malaysia was once a major tin exporting country. One of the by-products of the tin-mining activities is tin-tailing which known as 'amang' very rich in rare earth elements, especially the lanthanides which are present as a mixture of phosphate minerals, mainly as ilmenite, xenotime and monazite. In this study, Kg Gajah in Kinta Valley occupying the State of Perak was chosen as a study area, since this area used to be the largest mining area in the 60's and 70's. The soil samples were separated using wet separation technique followed by magnetic separation. The monazite was then digested using a mixture of HF/HNO₃ acids. The digested sample was extracted for its cerium content. The extraction behaviour of cerium in those samples has been investigated as a function of Cyanex 302 concentration in diluents and the time taken to reach the equilibrium. Extractant of bis(2,4,4-trimethylpentyl)-mono-thiophosphinic acid (Cyanex302) in n-heptane was used throughout the analysis. Aqueous phase from extraction was analyzed spectrometrically using Arsenazo (III) while organic phase was subjected to rotavapour followed by analysis by FTIR. The aim of this study is to have the best concentration for Cyanex302 in order to extract as much as possible of Europium and to confirm the transfer of Eu (III) to the Cyanex 302 as an extractant. Result from UV/VIS shows that 0.7 M is the best concentration of Cyanex 302 for the Eu (III) extraction from samples. Result from FTIR confirmed the structure of Cyanex302 has been replaced by Ce(IV).

Keywords: `Amang`, Rare earth elements (REE), Cyanex302, Arsenazo III

Abstrak

Malaysia pernah menjadi negara pengekspot timah yang utama. Salah satu dari hasil sampingan aktiviti lombong bijih timah ialah tahi bijih yang dikenali sebagai 'amang' yang kaya dengan unsur nadir bumi, terutamanya lantanid yang wujud sebagai campuran mineral fosfat, terutamanya ilminite, xenotime dan monazite. Di dalam kajian ini, Kg Gajah dalam kawasan Lembah Kinta di negeri Perak telah dipilih sebagai kawasan kajian, memandangkan kawasan ini pernah menjadi kawasan lombong timah terbesar dalam tahun 60an dan 70an. Sampel tanah diasingkan menggunakan teknik pemisahan basah dikuti dengan pemisahan magnet. Monozite kemudiannya dihadhamkan menggunakan campuran asid HF/HNO3. Sampel yang telah hadham telah diekstrak kandungan europium nya. Sifat pengekstrakan europium di dalam sample tersebut telah dikaji sebagai fungsi kepekatan Cyanex 302 di dalam pelarut dan juga masa yang diambil untuk mencapai keseimbangan. Pengekstrak bis(2,4,4-trimethylpentyl)-mono-thiophosphinic acid (Cyanex 302) dalam toluen telah digunakan sepanjang analysis. Fasa akuas dari pengektrakan ini telah dianalisis secara spektrometri menggunakan Arsenazo (III), manakala fasa organik telah dikeringkan menggunakan rotavapour sebelum dianalisis menggunakan spektrometer FTIR. Objektif kajian ini adalah untuk mendapatkan kepekatan terbaik bagi Cyanex 302 untuk mengekstrak sebanyak mungkin europim, dan memastikan pemindahan Eu ke dalam Cyanex 302. Hasil analisis UV/VIS menunjukan bahawa 0.7 M adalah merupakan kepekatan terbaik Cyanex 302 untuk ekstraksi Eu dari sampel. Hasil analisis FTIR mengesahkan bahawa struktur Cyanex 302 telah pun digantikan oleh Ce(IV).

Kata kunci: 'Amang', unsur nadir bumi, Cyanex 302, Arsenazo III

Introduction

Worobiec *et al*, [1] and Walsh [2] have reported that beach sand and rock is a mineral resources other than exmining area. However, former tin mining areas contained minerals which will be economically beneficial to the mineral industries. Tin ores were processed using a physical property (wet processing technique or smelting process) to recover the tin. 'Amang' is a widely accepted term in Malaysia for the heavy mineral rejects which remain after tin oxide (cassiterite) has been extracted from tin ore [3]. The remaining ('amang') were left there since not many people knew their uses. Nowaday, 'amang' is becoming more important since one can recover valuable heavy minerals from it. Some examples of heavy minerals are monazite ([Ce, La, Nd, Gd, Th] PO₄), zircon (ZrSiO₄), ilmenite (FeOTiO₂), xenotime (YPO₄) and struverite (Nb.Ta.TiO₂) which have various uses in minerals industries [4].

High grade (99.99%) europium oxide has important uses as red phosphor in television screen and in computer monitors, compact fluorescent light bulbs, X-ray and tomography scans, X-ray screen, high intensity mercury vapour lamps, neutron scintillations, charge particle detectors and optically read memory systems. Europhium is one of the least abundant of the rare earth elements, accounting for only 0.05-0.10% of the total rare earth content in its ores [5, 6].

Solvent extraction is generally used as the separation method for rare earth metals [7]. Extracting agents of industrial importance include tri-n-butyl phosphate, dimethyl heptyl methyl phosphonate, di (2-ethylhexyl) phosphoric acid, 2-ethylhexyl phosphoric acid mono 2-ethylhexyl ester, tetra decyl phosphoric acid and naphtenic acid [8]. Lanthanide elements are well chelated by phosphorous compounds such as phosphoric acid and phosphonic acid [9]. Cyanex302 consists of bis-(2,4,4-trimethylpentyl) mono-thiophosphinic acid, trisalkylphosphine oxide, bis-(2,4,4-trimethylpentyl) phosphinic acid, bis-(2,4,4-trimethylpentyl)-dithiophosphinic acid, and other unknown components. A lot of work has been done on rare earth ion extraction from hydrochloric acid, nitric acid and sulfuric acid media using Cyanex302 as and extractant [10].

The use of organic dyes for the spectrometric determination of actinides including uranium, in various materials has been reported to be simple and selective. Among these, the sodium salt of Arsenazo-III has been reported to be more sensitive than other chromogenic reagents this type, such as Arsenazo-1and thorane. In other words, by specifying the pH it is possible to use Arsenazo-III very selectively. It is a commercial product, equally soluble in both water and dilutes mineral acids [11]. Arsenazo-III is a dye that forms a colored complex with europium in an acidic solution at pH 3.

A portion of the minerals were then extracted for the europium content within the minerals and the analysis was done using UV/VIS and FTIR. The aim of this study is to study the effect of Cyanex302 concentration to the extraction of Eu(III) in monazite type minerals, to confirm the ion exchange mechanism in solvent extraction and to validate the method used for the extraction procedure.

Experimental

The spectrophotometric analysis was performed on a UV/VIS spectrophotometer Perkin Elmer Lambda 35. Hanna Instrument pH213 microprocessor pH meter calibrated daily with pH 4.0 and 7.0 buffer were used to measure the acidity of solution and pH of buffer. About 40 mg of monazite was digested using sand bath using a mixture of HF:HNO3 until the sample is turning to yellowish clear solution.. To make sure that the solutions are free from the undissolved particulates, it was then brought to the centrifuge for 2000 rpm within 7 minutes and filtered before diluted to 50.0 mL of volumetric flask. A 20.0 mL aliquot of prepared sample was pipette to the 100.0 mL of volumetric flask together with 10 mL of buffer, 10 mL NaCl and was top up with sodium citrate to the required volume for pH adjustment. Cyanex302 in n-heptane and toluene were used as extractants which were set at 0.1, 0.3, 0.4, 0.5, and 0.7 M for the organic phase. Sodium citrate and citric acid were used as a buffer while NaCl used to maintain the ionic strength of solution. Mixtures of organic and aqueous phases were shaken in the separating funnel for 5 minutes and allowed to reach the equilibrium within 5 minutes, 15 minutes and 30 minutes each. Then 0.05 % w/v of Arsenazo (III) was added to the aqueous phase for the spectrometry analysis by UV/VIS spectrometer.

Calibration

Working solution of europium was made by diluting the stock solution to the 0.1, 0.2, 0.3, 0.5, 0.7 and 0.8 for the calibration curve.

Recovery

A recovery test was performed using a known amount of analyte added to be sample and the analysis then performed and after the addition so that the amount received can be calculated [12, 13].

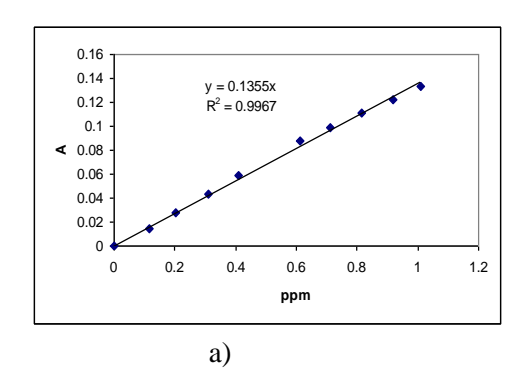
Extraction Eu(III) from Heavy Minerals

The pure europium was prepared in an aqueous phase and extracted using Cyanex302 diluted in toluene. Varying the concentrations of Cyanex302, we will find the best Cyanex302 concentration which extract most Eu(III) into the organic phase. The amount of Eu(III) extracted was measured by the concentration Eu(III) left in the aqueous phase. This concentration was determined using UV/Vis spectrometer by adding Arsenazo (III) into the aqueous phase to produce the colour which is related to the concentration of Eu(III) in the sample.

Results and Discussion

Calibration and Linearity

The standard solution was prepared in de-ionized water and buffer (citric acid/sodium citrate pH 2.2) to maintain pH ant 2.2 and 3 for toluene and n-heptane respectively. Figure 1a and 1b show the calibration curve for standard addition methods, respectively. The correlation coefficient for the calibration curve is 0.9967 while the correlation coefficient for the standard addition method is equal to 1 which is considered as a good linearity. Both curves can be used for estimating the concentration of Eu in the solution.



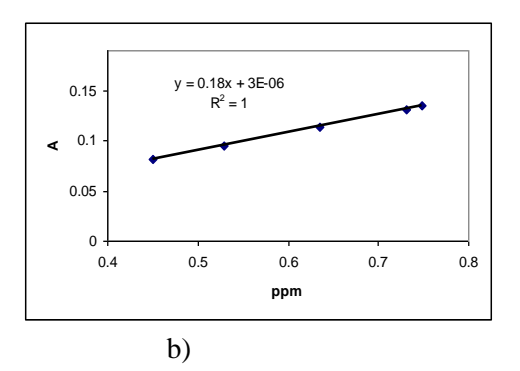


Figure 1: Linearity of the study represents by (a) Calibration curves and (b) Standard addition method

Recovery

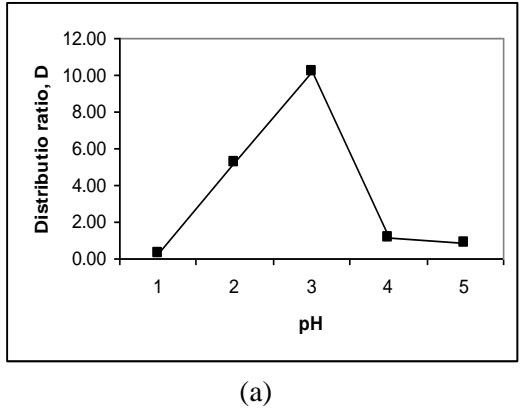
Table 1 show the recovery of the laboratory fortified blank and laboratory fortified matrix. Laboratory fortified blank gives recovery in the range of 100.00 to 108.57 percent. The recoveries of fortified matrix range from 82.30 to 110.45.

Eu (III) extraction: Extraction as a function of pH

Figure 2 shows the extraction of europium as a function of the pH. Figure 2(a) shows the extraction of different pH using n-heptane as Cyanex302 diluents. It can be seen that the highest distribution ratio which lead to the highest percent extraction is at pH 3. However for the extraction using toluene as diluent, the highest distribution ratio is at pH 2.2. This pH value agreed with Ohashi *et al*, [7] finding, that is at pH 2.2, it could extract higher amount of europium even though their study is using cloud point extraction by di(2-ethylhexyl)phosphoric acid and Triton X-100.

Table 1:	The percent recovery for laboratory fortified blank of sample spiked with
	standard europium

Spiking level (ppm)	Fortified Blank % Recovery	Fortified Matrix % Recovery
0.11	100.00	110.45
0.21	102.86	94.30
0.31	108.57	97.72
0.41	102.86	96.24
0.51	108.57	82.30



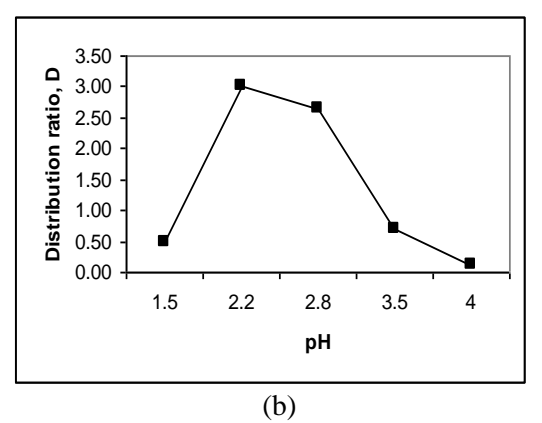
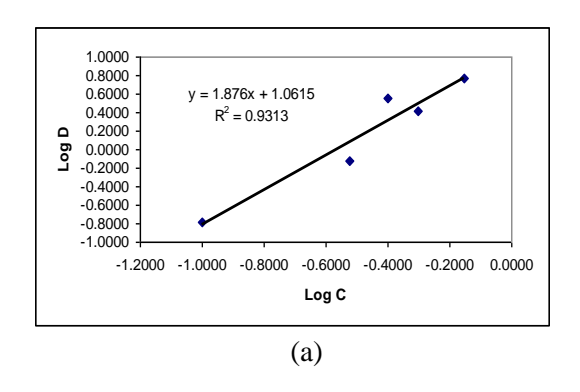
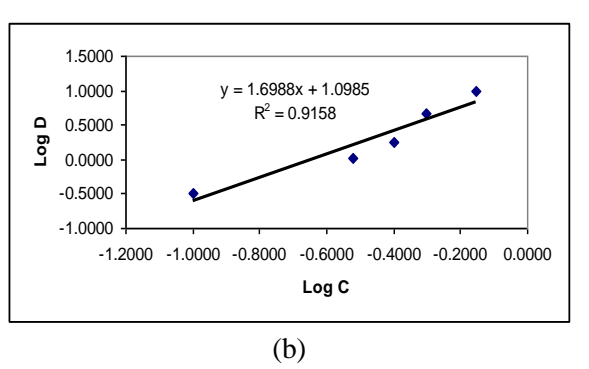


Figure 2: Effect of pH on the distribution ratio of Europium by (a) n-heptane (b) toluene

Nature of the extracted species

The nature of the extracted complex species was analyzed using the Log D versus Log C plots as suggested by Sarkar *et al*, [14, 15] and Ajgaonkar *et al*, [16]. In this study, the plot of log D versus log C as shown in Figure 3, show slopes of 1.876, 1.699 and 2.633 for 5, 15 and 30 minutes, respectively. However, the percent extraction was found greater in 15 minutes equilibrium time, thus indicating the best equilibrium time for europium extraction is 15 minutes.





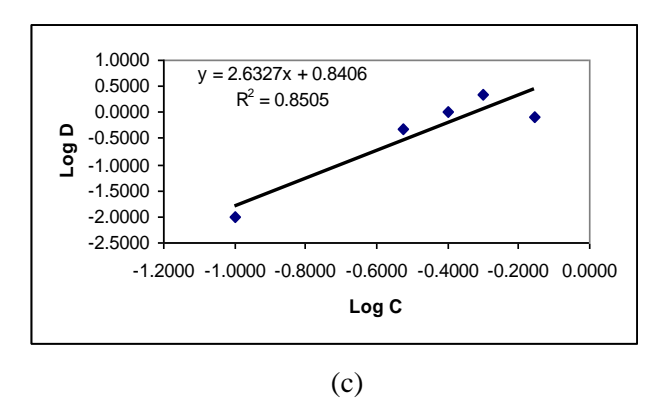


Figure 3: Plots of log D versus log C at various equilibrium time

The concentration of Cyanex302 were found to affect the amount of europium extracted from the aqueous phase. The higher the Cynex302 concentration, the more the europium ion will be transfered to the organic phase.

Concentration of	5 minutes	15 minutes	30 minutes	
extractant	(%)	(%)	(%)	
0.1 ppm	14.13	24.74	0.97	
0.3 ppm	43.00	51.12	33.10	
0.4 ppm	78.44	64.24	51.45	
0.5 ppm	72.56	82.35	67.96	
0.7 ppm	85.54	90.82	44.65	

Table 2: Effect of equilibrium time to the extraction of europium

Distribution coefficient of Eu(III) increases with the increase of concentration of the extractant [17]. In other study, it was found that a decrease in the concentration of Cyanex302 will give lower disribution ratio values [14, 15].

Extraction of Eu (III) from monazite samples

Table 3 shows the percent europium being extracted from two monazite samples (from Kg Gajah and Beh Minerals Sdn. Bhd., Perak) done in duplicates. It seems that the amount of europium extracted (in percent) from these monazites are comparable.

Table 3: Percent extraction of europium from duplicates samples

Sample	Amount Extracted (%)
Kg. Gajah 1	64.89
Kg. Gajah 2	62.20
Beh Minerals Sdn Bhd 1	50.03
Beh Minerals Sdn Bhd 2	57.78

Spectroscopy analysis

The replacement of other element by europium in Cyanex302 can be proved by analysis with IR spectroscopy as shown in Figures 4a and 4b. This is well agreed by Ramachandran *et al*, [18], Muhammad Idiris Saleh *et al*, [19], Francis *et al*, [20] Biswas *et al*, [21, 22].

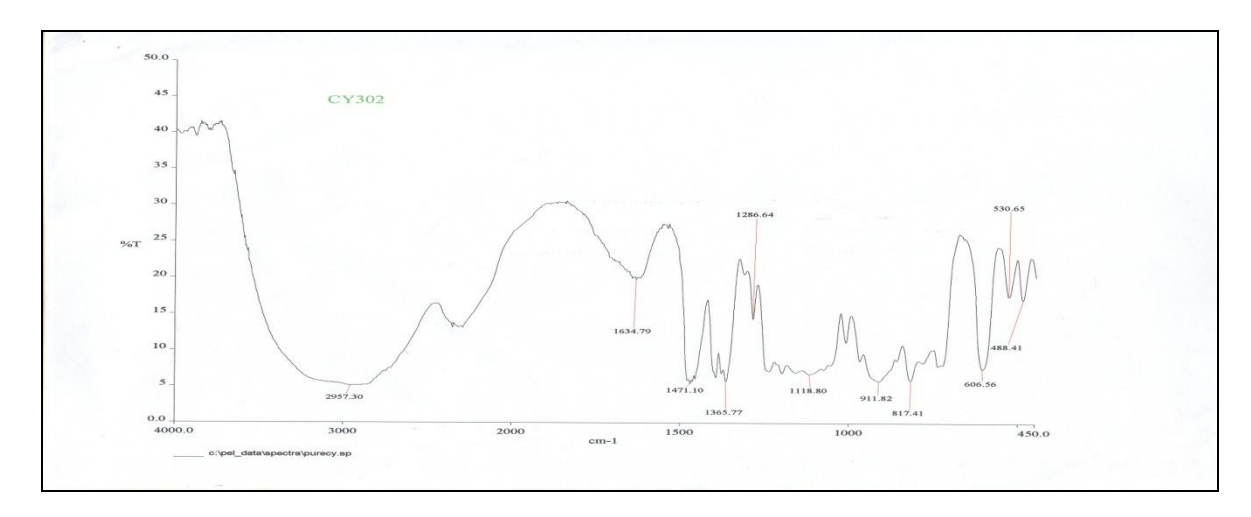


Figure 4a: FTIR spectrum of pure Cyanex302

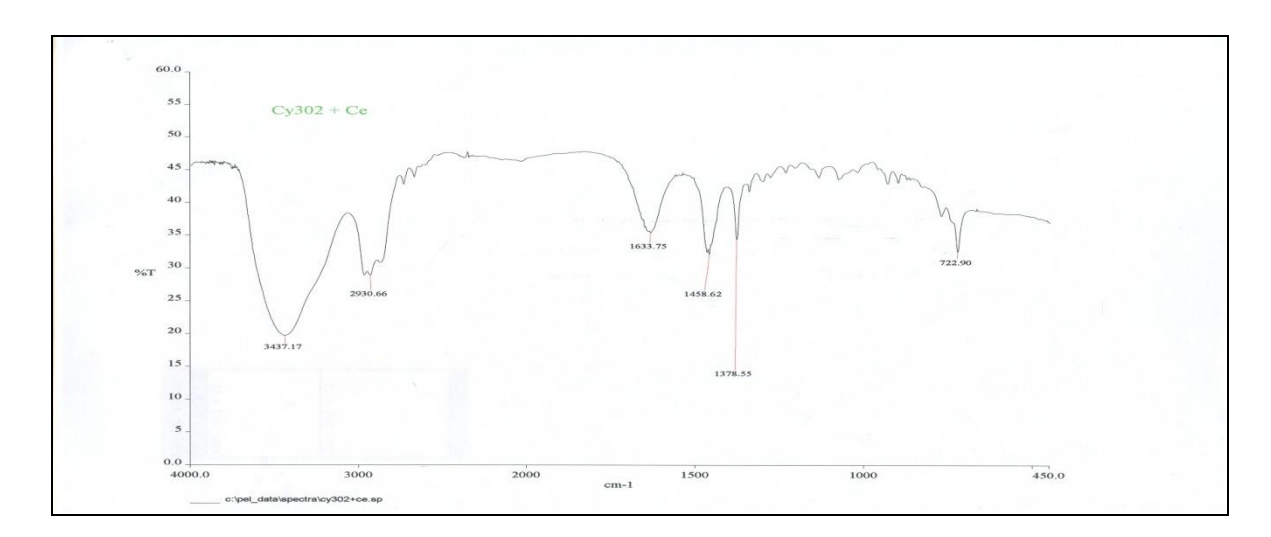


Figure 4b: FTIR spectrum of Eu-Cyanex302 complex

The IR spectra of europium complex with Cyanex302 and pure extractant were analyzed for a comparison. Cyanex302 spectrum shows two absorption bands at about 2950 cm⁻¹ and 2280 cm⁻¹ which indicates that the acids contains characteristics P(S)OH group. The bands at 750 and 905 cm⁻¹ indicate the P=S group and P-O stretching vibration in the P-O-H bond, respectively. In the spectra of Eu-Cyanex302 complex, the bands due to P(S)OH group are absent. These observations suggests when Cyanex302 molecule forms a complex with europium, the hydrogen atom of P-O-H is displaced by other ion [23].

Conclusion

Increasing the extractant concentrations will result in a better distribution ratio, D. It extracts more Eu(III) from monazite samples. The best concentration of Cyanex 302 for Eu(III) extraction in this study is 0.7 M at pH 2.2 for 15 minutes equilibrium time.

Acknowledgement

The authors would like to thank RMI (UiTM) and Faculty of Applied Sciences UiTM for the support given and MOSTI for funding this project under Science Fund (03-01-01-sf0084).

References

- 1. Worobiec, A., Stefaniak, E.A., Potgieter-Vermaak, S., Sawlowicz, Z., Spolnik, Z., Van Grieken, R. (2007). Characterisation of concentrates of heavy mineral sands by micro-Raman spectrometry and CC-SEM/EDX with HCA. *Applied Geochemistry*, **22**, 2078-2085
- 2. Walsh, J.A. (2007). The use of scanning electron microscope in the determination of the mineral composition of Ballachulish slate. *Materials Characterization*, **58**, 1095-1103.
- 3. Hu, S. J., Kandaiya, S. and T.S. Lee (1995). Studies of the radioactivity of amang effluent. *Applied Radiation and Isotopes*, **46**, 147-148.
- 4. Zaini Hamzah, Nor Monica Ahmad and Ahmad Saat (2009). Determination of heavy minerals in "amang" from Kampong Gajah ex-mining area. *The Malaysian J. Analytical Sciences*, **13(2)**, 184-203.
- 5. Morais C.A. and Ciminelli V.S.T. (1998). Recovery of europium from a rare earth chloride solution. *Hydrometallurgy* **49**, 167-177.
- 6. Morais C.A. and Ciminelli V.S.T. (1998). Recovery of europium by chemical reduction of a commercial solution of europium and gadolinium chloride. *Hydrometallurgy* **60**, 247-253.
- 7. Ohashi A., Hashimoto T., Imura H. and Ohashi K (2007). Cloud point extraction equilibrium of lanthanum (III), europium (III) and lutetium (III) using di(2-ethylhexyl)phosphoric acid and Triton X-100. *Talanta* **73**, 893-898.
- 8. Redling K (2006). Rare earth elements in agriculture with emphasis on animal husbandry. PhD thesis Ludwig-Maximilians-UniversitatMunchen, Germany.
- 9. Gracia Valls, R. Hrdlicka, A. Perutka, J. Havel, J. Deorka, N. V. Tavlarides, L. L. Munoz, M. and Valiente, M. (2001). Separation of rare earth elements by high performance liquid chromatography using a covalent modified silica gel column. *Analytica Chimica Acta*, **439**, 247-253.
- 10. Wu, D. Xiong, Y. Li, D. and Meng, S. (2005). Interfacial behavior of Ctanex302 and kinetics of lanthanum extraction. *Journal of Colloid and Interface Science*, 290, 235-240.
- 11. Khan, M. H. Warwick, P. and Evans, N. (2006). Spectrometric determination of uranium with arsenazo III in perchloric acid. *Chemosphere*, **61**, 1165-1169.
- 12. Gioia, M. G. Di Pietra, A. M. and Gatti, R. (2002). Validation of spectrometric method for determination of iron (III) impurities in dosage form. *Journal of Pharmaceutical and Biomedical Analysis*, **29**, 1159-1164.
- 13. Md. Pauzi Abdullah and Mohamad Nasir Othman (2007). Validation of an extraction technique based on Tributyl Phosphate for the determination of Pb(II) in water, *The Malaysian Journal of Analytical Sciences*, **11**(2), 361-369.
- 14. Sunil G.S. and Puroshattam M.D. (1999). Solvent extraction separation of antimony (III) and bismuth (III) with bis(2,4,4-trimethylpentyl) monothiophosphinic acid (Cyanex 302). *Separation and Purification Technology*, **15**, 131-138.
- 15. Sunil G.S. and Puroshattam M. D. (2000). Solvent extraction separation of Gold with Cyanex 302 as extractant. *Journal of the Chinese Chemical Society*, 47, 869-873.
- 16. Ajgaonkar, H.S. Puroshattam, M.D (1997). Solvent extraction separation of iron (III) and aluminium (III) from other elements with Cyanex 302. *Talanta*. **44**, 563-570.
- 17. Zhifeng Z, Hongfei L, Fuqiang G, Shulan M, Deqian L. (2008). Synergistic extraction and recovery of Cerium (IV) and Fluorin from sulfuric solutions with Cyanex 923 and di-2-ethylhexyl phosphoric acid. *Separation of Purification Technology*, **63**, 348-352.
- 18. Ramachandran Reddy, B. Rajesh Kumar, J. Phani Raja, K and Varada Reddy, A. (2004). Solvent extraction of Hf(IV) from acidic chloride solutions using Cyanex 302. *Minerals Engineering*, **17**, 939-942.

- 19. Muhammad Idiris Saleh, Md. Fazlul Bari, Bahruddin Saad. (2002), Solvent extraction of lanthanum(III) from acidic nitrate-acetato medium by Cyanex 272 in toluene. *Hydrometallurgy*, **63**, 75-84.
- 20. Tania F, Prasada Rao, T. Reddy, M.L.P. (2000). Cyanex 471X as extractant for the recovery of Hg(II) from industrial wastes. *Hydrometallurgy*, **57**, 263-268.
- 21. Biswas, R.K. and Begum, D.A. (1998). Solvent extraction of tetravalent titanium from chloride solution by di-2-ethylhexyl phosphoric acid in kerosene. *Hydrometallurgy*, **49**, 263-274.
- 22. Biswas, R.K. and Begum, D.A. (1998). Solvent extraction of Fe³⁺ from chloride solution by D2EHPA in kerosene *Hydrometallurgy*, 50, 153-163.
- 23. Reddy B. R, Kumar J. R. Raja K.P. and Reddy A. V (2004). Solvent extraction of Hf(IV) from acidic chloride solution using Cyanex302. *Minerals Engineering*, 17, 939-942.

Malaysian Journal of Analytical Sciences Vol 15 No 2 2011

		Page
1.	ASSESSMENT OF RADIATION HEALTH RISK IN CAMERON HIGHLANDS TEA PLANTATIONS (Risiko Penilaian Kesihatan di Ladang Teh Cameron Highlands) Zaini Hamzah, Seh Datul Riduan and Ahmad Saat	130
2.	KEGAGALAN CERUN DI BUKIT ANTARABANGSA, AMPANG, SELANGOR DAN HUBUNGANNYA DENGAN SIFAT FIZIK TANAH (Slope Failure at Bukit Antarabangsa, Ampang, Selangor, and Its Relationship to Physical Soil Properties) Muhammad Barzani Gasim, Sahibin Abd. Rahim, Mohd. Ekhwan Toriman dan Diyana Ishnin	138
-	SEDIMENTATION RATE AND CHRONOLOGY OF As AND Zn IN SEDIMENT OF A RECENT FORMER TIN MINING LAKE ESTIMATED USING Pb-210 DATING TECHNIQUE (Kadar Mendapan dan Kronologi As dan Zn dalam Sedimen Tasek Bekas Lombong Menggunakan Teknik Pentarikhan Pb-210) Zaharidah Abu Bakar, Ahmad Saat, Zaini Hamzah, Abdul Khalik Wood and Zaharuddin Ahmad	150
	MEASUREMENT OF ²²⁶ Ra, ²²⁸ Ra AND ⁴⁰ K IN SOIL IN DISTRICT OF KUALA KRAI USING GAMMA SPECTROMETRY (Pengukuran ²²⁶ Ra, ²²⁸ Ra dan ⁴⁰ K Di Dalam Taneh Daerah Kuala Krai Menggunakan Spektrometri Gama) Zaini Hamzah, Siti Afiqah Abdul Rahman, and Ahmad Saat	159
	DETERMINATION OF SIX PHTHALATES IN POLYPROPYLENE CONSUMER PRODUCTS BY SONICATION-ASSISTED EXTRACTION/GC-MS METHODS (Penentuan Enam Ftalat dalam Produk-Produk Konsumer Polipropilena dengan Kaedah Ekstraksi Bantuan-Sonikasi/GCMS) Chong Kian Wei, Loke Chui Fung and Michelle Pang	167
	DETERMINATION OF ORGANOPHOSPHORUS PESTICIDES USING MOLECULARLY IMPRINTED POLYMER SOLID PHASE EXTRACTION (Penentuan Pestisid Organofosforus Menggunakan Pengesktrakan Fasa Pepejal dengan Polimer Cap) Mohd Marsin Sanagi, Syairah Salleh, Wan Aini Wan Ibrahim, Ahmedy Abu Naim	175
	HEALTH STATUS OF RECREATIONAL BEACHES IN ISKANDAR DEVELOPMENT REGION, JOHOR, MALAYSIA (Status Kesihatan Pantai-Pantai Rekreasi di Wilayah Pembangunan Iskandar, Johor, Malaysia) Zaleha, K., Farah Diyana, M. F., Mohd Luthfi, O., Noorul Ain Falah, A., Ahmad Wafi, A.	184
გ -	THE EFFECTIVENESS OF SOOT REMOVAL TECHNIQUES FOR THE RECOVERY OF FINGERPRINTS	191

	(Keberkesanan Kaedah Penyingkiran Jelaga Bagi Memperoleh Kembali Cap Jari Pada Sisa Kebakaran Kaca Dalam Kes Bom Petrol) Umi Kalthom Ahmad, Yew Su Mei, Mohd Shahru Bahari, Ng Song Huat and Vijaya Kumar Paramasivam	
9.	RADIATION HAZARD FROM NATURAL RADIOACTIVITY IN THE SEDIMENT OF THE EAST COAST PENINSULAR MALAYSIA EXCLUSIVE ECONOMIC ZONE (EEZ) (Hazard Sinaran Dari Radionuklid Tabii Dalam Sedimen Di Zon Ekslusif Ekonomi (ZEE) Perairan Pantai Timur Semenanjung Malaysia) Yii Mei-Wo, Nurrul Assyikeen Md. Jaffary and Zaharudin Ahmad	202
	ANALYSIS OF ANIONIC POST-BLAST RESIDUES OF LOW EXPLOSIVES FROM SOIL SAMPLES OF FORENSIC INTEREST (Analisis Residu Pasca Letupan Anion Bagi Bahan Letupan Rendah Daripada Sampel Forensik Tanah) Umi Kalthom Ahmad, Ong Shin Tze, Muhammad Fauzi Ghazali, Yew Chong Hooi3, Mohd Koey Abdullah	213
11.	PHOTOLUMINESCENCE OF POROUS SILICON PREPARED BY CHEMICAL ETCHING METHOD (Fotoluminesen Poros Silikon Yang Disediakan Secara Punaran Kimia) Dwight Tham Jern Ee, Chan Kok Sheng and M.I.N. Isa	227
12.	DETERMINATION OF ORGANOPHOSPHORUS PESTICIDES BY DISPERSIVE LIQUID-LIQUID MICROEXTRACTION COUPLED WITH GAS CHROMATOGRAPHY-ELECTRON CAPTURE DETECTION (Penentuan Pestisid Organofosforus dengan Pengekstrakan Cecair-Cecair Serakan berganding dengan Kromatografi Gas-Pengesanan Penangkap Elektron) Mohd Marsin Sanagi, Siti Umairah Mokhtar, Mazidatul Akmam Miskam, Wan Aini Wan Ibrahim	232
13.	DEVELOPMENT AND VALIDATION OF RP-HPLC-UV/Vis METHOD FOR DETERMINATION OF PHENOLIC COMPOUNDS IN SEVERAL PERSONAL CARE PRODUCTS (Pembangunan dan Validasi Kaedah Fasa Berbalik-HPLC-UV/Vis untuk Penentuan Sebatian Fenolik dalam beberapa Produk Penjagaan Diri)	240
14.	COMPETITIVE METAL SORPTION AND DESORPTION ONTO Kappaphycus Alvarezii, SEAWEED WASTE BIOMASS (Persaingan Penjerapan dan Nyah-Penjerapan Logam Berat ke atas Sisa Rumpai Laut Kappaphycus alvarezii) Kang Oon Lee, Nazaruddin Ramli, Mamot Said, Musa Ahmad, Suhaimi Md Yasir, Arbakariya Ariff	252
15.	PENENTUAN ASID HIDROSIANIK (ANTI NUTRISI) DI DALAM BUAH NIPAH (Nypa fruticans) (Determination of Hydrocyanic Acid in Nipah Fruit (Nypa fruticans)) Mohd Zaidi Mat Satar, Mohd. Wahid Samsudin, Mohamed Rozali Othman	258
16.	DETERMINATION OF PLATINUM GROUP ELEMENTS IN TERRESTRIAL ROCKS USING NICKEL SULFIDE FIRE ASSAY ISOTOPE DILUTION ICP-MS (Penentuan Unsur Kumpulan Platinum Dalam Batuan Menggunakan Pencairan Isotop ICP-MS Assay Api Nikel Sulfida) B.S. Wee, M. Ebihara, A.K.H. Wood	265

ON GLASS FIRE DEBRIS IN PETROL BOMB CASES

	PEPTIDE SEPARATION BY CAPILLARY ELECTROPHORESIS WITH ULTRAVIOLET DETECTION: SOME SIMPLE APPROACHES TO ENHANCE DETECTION SENSITIVITY AND RESOLUTION (Pemisahan Peptida Oleh Elektroforesis Rerambut Dengan Pengesan Ultra-Lembayung: Pendekatan Mudah Untuk Meningkatkan Isyarat Pengesanan Dan Resolusi) L. Noumie Surugau	273
18.	DETERMINATION OF RADON ACTIVITY CONCENTRATION IN HOT SPRING AND SURFACE WATER USING GAMMA SPECTROMETRY TECHNIQUE (Penentuan Kepekatan Aktiviti Radon Di dalam Air Panasdan Air Permukaan Dengan Menggunakan Teknik Spektrometri Gama) Zaini Hamzah, Ahmad Saat, Mohammed Kassim	288
19.	SOURCES OF POLYCYCLIC AROMATIC HYDROCARBONS (PAHS) POLLUTION IN MARINE SEDIMENT FROM TUANKU ABDUL RAHMAN NATIONAL PARK, SABAH (Sumber Pencemaran Hidrokarbon Aromatik Polinuklear (PAH) Dalam Sedimen Marin Dari Taman Negara Tuanku Abdul Rahman, Sabah) Md Suhaimi Elias, Ab Khalik Wood, Zaleha Hashim, Mohd Suhaimi Hamzah, Shamsiah Ab Rahman, Nazaratul Ashifa Abdullah Salim	295



ASSESSMENT OF RADIATION HEALTH RISK IN CAMERON HIGHLANDS TEA PLANTATIONS

(Risiko Penilaian Kesihatan di Ladang Teh Cameron Highlands)

Zaini Hamzah¹, Seh Datul Riduan^{1*} and Ahmad Saat²

¹Faculty of Applied Sciences, ²Institute of Science, Universiti Teknologi MARA, 40450 Shah Alam, Selangor

*Corresponding author: sehdatulriduan@yahoo.com

Abstract

Exposure to the natural radiation is quite common except that the level varies from one place to another. The level of radiation will depend on the type of rocks and soil on that particular area, where the granitic rocks tend to contribute more to the background radiation. The present study was conducted in two of the Tea Plantations in Cameron Highlands, where it has been in operation for more than 50 years. The landscape is hilly type and the workers have to pluck the tea leaves manually. Practically, there are spending long hours in the plantation area. There were thirteen locations for soil sampling and surface dose in-situ measurement. Soil samples were taken back to the UiTM laboratory in Shah Alam for further analysis. Samples were clean, dried, ground and sieve to obtain homogenous samples before analysis. Samples were packed in a plastic container around 400 g, sealed and leave it for 3 weeks to allow radionuclides to reach secular equilibrium, before counting using gamma spectrometer with HPGe detector. The spectrum was analysed using gamma vision software to calculate the activity concentrations of ²²⁶Ra, ²²⁸Ra and ⁴⁰K. From the radium equivalent values, one can estimate the external hazard index, the absorb dose and cumulative effective dose received by the person who spend their time in the study area. The results show the external hazard index more than one for one of the tea plantation, but the cumulative effective dose is still below the recommended level.

Keywords: gamma spectrometer, radium equivalent, external hazard index, surface dose, intermediate igneous rock

Abstrak

Pendedahan kepada radionuklid semulajadi sentiasa ada kecuali kadar radiasi adalah berbeza daripada satu tempat kepada tempat yang lain. Kadar radiasi adalah bergantung kepada jenis batu dan tanah di sesuatu kawasan itu dimana batuan granit memberikan kadar bacaan radiasi yang tinggi. Kajian yang terbaru telah dijalankan di dua ladang teh bertempat di Cameron Highland yang telah beroperasi lebih daripada 50 tahun. Bentuk muka bumi yang berbukit dan para pekerja perlu memetik daun teh secara manual. Secara pratikalnya, mereka menghabiskan masa lebih lama di kawasan ladang. Tiga belas lokasi pengambilan sampel dan juga kadar dos di permukaan telah diambil di kawasan tersebut. Semua sampel telah dibawa ke makmal UiTM di Shah Alam untuk analisa seterusnya. Kesemua sampel tersebut telah dibersihkan, dikeringkan, disimpan dan diayak bagi menghasilkan sampel yang sebati sebelum dianalisa. Sampel telah dimasukkan kedalam bekas plastik dalam anggaran 400g sampel telah dimasukkan, kemudian ditutup dan disimpan selama 3 minggu bagi membiarkan sampel mencapai keseimbangan sekular. Spectrum telah dianalisa dengan menggunakan perisian GammaVision untuk mengira aktiviti kepekatan ²²⁶Ra, ²²⁸Ra dan ⁴⁰K. Daripada nilai keseimbangan radium, kadar serapan dan indeks radiasi berbahaya, dos serapan dan dos efektif terkumpul yang diterima oleh orang yang menghabiskan masa di kawasan kajian. Hasil kajian menunjukkan kadar serapan dan indeks radiasi berbahaya melebihi daripada satu di salah satu lokasi ladang teh tetapi dos efektif terkumpul masih dibawah tahap yang dicadangkan.

Kata kunci: spektrometer gamma, keseimbangan radium, index radiasi berbahaya, dos permukaan, batuan igneus pertengahan

Zaini Hamzah et al: ASSESSMENT OF RADIATION HEALTH RISK IN CAMERON HIGHLANDS TEA PLANTATIONS

Introduction

Radiation health risk now has been concern by public and they have a right know the hazard risks of the area there are visited. The natural radiation is contributed from the radionuclides materials that occur naturally from the earth crush also known as Naturally Occur Radionuclides Material (NORM). The high radiation of NORM was occurring at the location where the granite rock were enriching with radionuclides occur [1]. Soil is one of the major contributions of continuous radiation exposure to human and soil can be used as radiological indicator in environment [2]. The radioactivity in soil are primary comes from U, Th and their progenies and also from the natural K [3, 4]. The gamma radiation emit from ⁴⁰K, ²³⁸U, ²³²Th and their decays series represent the main external exposure to the environment [5]. NORM which also called as terrestrial background radiation is the main present of the external sources of irradiation to the human body [6]. These radionuclides can enter human body through ingestion of water and food, and inhalation of the air [7].

The major radionuclides that widely used for estimating the radiation health assessment are 226 Ra, 228 Ra and 40 K [8, 9, 10]. 226 Ra were come from series of 238 U which will decays to 222 Rn and 222 Rn are in gas state which can transfer trough the environment. 222 Rn is an alpha particle emitter and when 222 Rn enter human body through the air, it can initiate the cancer for example is lung cancer. 228 Ra represent the 232 Th and 40 K come from natural K that emit γ -rays to the environment.

The objective of this study is to determine the activity concentration of ^{226}Ra , ^{228}Ra and ^{40}K at tea plantation Cameron Highlands by using gamma rays spectrometer with HPGe detector. This study will also calculate the radium equivalent and then estimate the external hazard index of the study area. This study will give the information about the annual effective dose receive by the public and workers at the study area and also to provide baseline data for future assessment reference. The activity of ^{226}Ra , ^{228}Ra and ^{40}K was analyzed at γ -rays energy peak of 609 KeV for ^{226}Ra , 911 KeV for ^{228}Ra and ^{40}K at 1460 KeV[11].

Experimental

Samples collection and preparation

Cameron Highlands tea plantations areas were chosen to determine the health risk because of the usage of fertilizer and also as one of the tourism attraction. In order to determine NORM in soil, thirteen location of soil were taken at different slope with composite and profile of the soil taken. The samples was taken at two tea plantation place label as Plantation A and B. Table 1 shows the samples label at the study area and the position of the sampling point that was taken by using Global Positioning System (GPS) with elevation higher than 1100 m. There are 2 categories of samples taken which are composite soil samples and profile soils samples for all location by using hand auger. Composite samples consist of the top layer of the soil which about 10 cm from the surface of soil and profile soil samples was taken according to the depth of samples which is the samples was divided into 2 cm each for 20 cm depth soil. In-situ measurement of radiation dose was measured by using survey meter Model 2241 from LUDLUM Measurement Incorporations was taken for surface and 1 meter above the surface. All the samples were taken to the laboratory for oven dried at 60°C until constant weight achieve. Then the samples were grind to pass through 250 micron sieve. About 400 g of sample was kept and sealed in the plastic container and the samples were grounded for 3 weeks to let the samples achieve secular equilibrium before been measured using gamma rays spectrometer.

Measurement of ²²⁶Ra, ²²⁸Ra and ⁴⁰K

The samples was counted using gamma rays spectrometer with ORTEC® HPGe detector with resolution 1.84 keV, 25% relative efficiency at 1332 KeV 60Co gamma ray and couple to Multi Channel Analyser (MCA). Because of 226Ra is an alpha emitter the measurements of 226Ra are base on radon daughter which known as 214Bi and 214Pb [12]. 228Ra was measured based on activity of 228Ac by assuming secular equilibrium between parent and daughter. The efficiency calibration was made by using secondary standard made up by mixing UO₃ and KCl in the same container as samples and counted for 43200 second. Figure 1 shows the efficiency of the gamma rays spectrometer used for calculation of individual radionuclides activity in samples. Because of the energy of radionuclides interested is higher than 200 keV, equation (A) were used to calculate the detection efficiency at energy of each radionuclides.

Location	North	East	Elevation (m)
A1	4° 27.254"	101° 22.043"	1216
A2	4° 27.204"	101° 22.108"	1219
A3	4° 27.143"	101° 22.982"	1199
A4	4° 27.543"	101° 21.844"	1190
A5	4° 27.248"	101° 21.999"	1214
A6	4° 27.340"	101° 21.074"	1200
A7	4° 27.314"	101° 21.133"	1220
B1	4° 26.909"	101° 24.855"	1350
B2	4° 26.991"	101° 24.969"	1360
В3	4° 26.992"	101° 24.744"	1320
B4	4° 26.886"	101° 24.926"	1340
B5	4° 26.091"	101° 25.115"	1380
R6	4° 26.956"	101° 24.953"	1340

Table 1: Sample locations collection

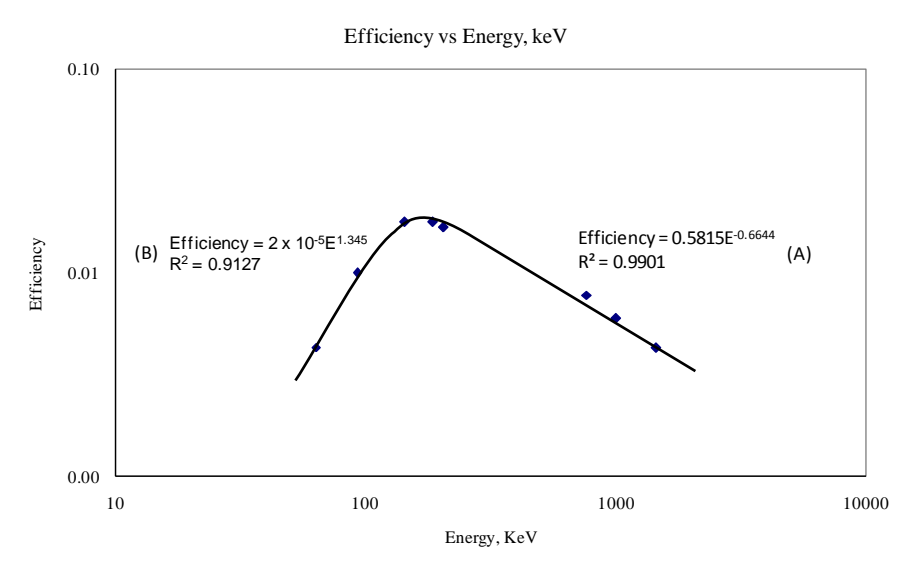


Figure 1: Efficiency Calibration using UO₃ and KCl by Gamma Rays Spectrometer

Energy peak 1461 keV for ⁴⁰K, 609 keV of ²¹⁴Bi for ²²⁶Ra and 911 keV for ²²⁸Ra were used for the laboratory measurement of activity concentration potassium, radium and thorium. The counting time for measuring each sample was 43200 second and the spectrum obtained was analyzed by using GammaVision software provided by ORTEC[®]. After the peak was analyzed, the activity per unit mass was calculated. The calculation of the individual radionuclides was calculated using the Equation (1),

$$A_{Ei} = \frac{N_{Ei}}{s_{E} \times t \times \gamma_{d} \times M_{S}} \tag{1}$$

Zaini Hamzah et al: ASSESSMENT OF RADIATION HEALTH RISK IN CAMERON HIGHLANDS TEA PLANTATIONS

 $A_{Ei} = Activity concentration (in Bq/kg)$

 N_{Ei} = Net peak area of a peak at energy E

 ε_E = Detection efficiency at energy E

t = Counting live time

 γ_d = Number of gammas per disintegration of this nuclide for a transition at energy E

 $M_s = \text{Mass in } kg \text{ of the measured sample}$

By considering Radium equivalent as external exposure that is widely used by the international parameter in radiological protection and radiological risk assessment is the effective equivalent dose which is originated by gamma emitters [13]. Radium equivalent was calculated using Equation (2) and absorbed dose rate Equation (3),

$$Ra_{eq} = C_{Ra} + 1.43C_{Th} + 0.07C_{K}$$
 (2)

$$D = 0.461C_{Ra} + 0.623C_{Th} + 0.0414C_{K}$$
 (3)

The external hazard index (H_{ex}) is an evaluation of potential hazards due to the radiological effect and it should be less than unity. The maximum value of H_{ex} is depending to the upper limit of Ra_{eq} which is 370 Bq/kg [6]. The H_{ex} can be calculated using equation (4) and annual effective dose Equation (5).

$$H_{ex} = \frac{c_{Ra}}{370} + \frac{c_{Th}}{259} + \frac{c_K}{4810} < 1 \tag{4}$$

Annual effective Dose(mSv.y⁻¹) = D (nGy/h) × 8760 (h/y) × 0.2 × 0.7(Sv/Gy) ×
$$10^{-6}$$
 (5)

C_{Ra}, C_{Th} and C_K are the activity concentrations of ²²⁶Ra, ²³²Th and ⁴⁰K in Bq/kg, respectively

Results and Discussion

The result from Table 2 shows that the activity of ²²⁶Ra, ²²⁸Ra and ⁴⁰K is higher than global average value provided by UNSCEAR 2008 report. Also the External Hazard Index is higher than unity for plantation B. This is because of different in location may result different activity concentration of radionuclides in soil [14, 15]. The ratio of ²²⁸Ra/²²⁶Ra in table 2 varied from 1.23 to 2.62. Ratios more than 1 concludes that ²²⁸Ra is more enriched in the soil compare to ²²⁶Ra may be due to the external sources that have not been identified.

Table 2: ²²⁶ Ra, ²	²⁸ Ra and ⁴⁰ K	of composite	soil samples
--	--------------------------------------	--------------	--------------

Location	²²⁶ Ra	±	²²⁸ Ra	±	⁴⁰ K	±	Ratio
	Bq/kg	±	Bq/kg		Bq/kg		228 Ra/ 226 Ra
A1	75.90	1.55	102.55	2.38	230.20	2.49	1.35
A2	65.97	1.42	80.99	2.11	84.91	4.34	1.23
A3	50.94	1.34	104.68	2.44	491.43	1.61	2.05
A4	54.66	1.27	105.04	2.35	329.17	1.96	1.92
A5	64.44	1.51	168.85	3.01	117.89	4.11	2.62
A6	80.58	1.76	132.68	2.75	219.43	2.77	1.65
A7	61.78	1.53	100.64	2.41	79.07	5.20	2.59
B1	117.28	2.10	202.21	3.48	282.00	7.05	1.72
B2	104.16	1.94	241.06	3.54	238.26	6.27	2.31
В3	118.72	1.98	201.55	4.31	203.09	6.21	1.70
B4	118.36	2.14	222.43	3.63	348.29	7.56	1.88
B5	137.08	2.18	233.96	3.77	407.35	8.11	1.71
B6	131.34	2.30	246.67	4.32	656.91	10.90	1.88

Table 3: Radiation surface doses in situ measurement

Location	Surface (μSv/h)	1 Meter Above Surface (μSv/h)
A1	0.30	0.23
A2	0.25	0.18
A3	0.25	0.19
A4	0.25	0.19
A5	0.28	0.19
A6	0.24	0.17
A7	0.23	0.16
B1	0.32	0.31
B2	0.36	0.32
В3	0.32	0.31
B4	0.34	0.31
B5	0.36	0.34
B6	0.34	0.29

Table 3 shows the radiation surface dose for study area on the surface and 1 meter above the surface. The higher radiation dose for surface and 1 meter above the surface is at location B2 and the lowest is at location A7. The Pearson correlation calculated shows that ²²⁶Ra and ²²⁸Ra has a strong correlation with surface dose measurement at surface and 1 meter above surface with correlation coefficient more than 0.88 but ⁴⁰K shows weak correlation with correlation coefficient 0.4 respectively.

Table 4 shows the calculated results for External Hazard Index, Radium Equivalent, Absorbed Dose Rate and Annual Effective Dose. This calculation is based on composite soil measurement.

Table 4: External Hazard Index, Radium Equivalent, Absorbed Dose Rate and Annual Effective Dose at tea
Plantation A and B

Location	Radium Equivalent	Absorbed Dose Rate	External Hazard	Annual Ef	fective Dose
	Bq/kg	nGy/h	Index	Public	Workers
A1	238.66	108.41	0.65	0.13	0.16
A2	187.74	84.39	0.51	0.10	0.12
A3	235.04	109.05	0.64	0.13	0.16
A4	227.91	104.27	0.62	0.13	0.15
A5	314.14	139.78	0.85	0.17	0.21
A6	285.67	128.89	0.78	0.16	0.19
A7	211.24	94.46	0.57	0.12	0.14
B1	426.17	191.72	1.16	0.24	0.28
B2	465.56	208.06	1.26	0.26	0.31
В3	421.15	188.70	1.14	0.23	0.28
B4	460.81	207.55	1.25	0.25	0.31
B5	500.16	225.81	1.36	0.28	0.33
B6	530.06	241.42	1.44	0.30	0.36

From the Table 4, location B6 has the highest calculation value for External Hazard Index, Radium Equivalent, Absorbed Dose Rate and Annual Effective Dose compared to others and the lowest is at location A2. Radium equivalent for plantation A is bellow limit but for plantation B, the value is exceed the upper limit for radium equivalent (370 Bq/kg) [8].

Zaini Hamzah et al: ASSESSMENT OF RADIATION HEALTH RISK IN CAMERON HIGHLANDS TEA PLANTATIONS

The External Hazard Index for location B is higher than unity and this is because the activity of the ²²⁶Ra and ²²⁸Ra is higher than recommendation value and the recommendation value is below than 1. Even through all the location is higher than recommendation value except for ⁴⁰K, external hazard index for location A still below unity. Only two location of ⁴⁰K that higher than recommendation value. According to the soil map of peninsular Malaysia, the soils at Cameron Highlands were originated as an intermediate igneous rock [16]. This explained the higher value of radionuclides in the soil. The higher value of External Hazard Index is maybe due to the location where igneous rocks were exist in Cameron Highland which make the activity concentration of ²²⁶Ra, ²²⁸Ra and ⁴⁰K is higher than global average value. The global average value for ²²⁶Ra, ²²⁸Ra and ⁴⁰K were set to be 32 Bq/kg, 45 Bq/kg and 412 Bq/kg [17]. The worldwide outdoor dose rates proposed by the UNSCEAR 2008 were 58 nGy/h but when compared with this study, there are 3 to 4 times higher than proposed value. Study by El-Arabi, 2007 on igneous rock give a higher value of external hazard index and annual dose above the global average value [18].

In this study, the annual effective doses are divided into two categories which are for worker doses and for public doses. For public it is well known that 0.2 occupancy fraction is for outdoor exposure in a year reported by UNSCEAR 2008. For workers, in my study area, the worker spend around 8 hour per day and 22 day per month in the tea plantation. They expose more to the radiation of the study area which is 2112 hour per year and for public is 1752 hour per year. Therefore for workers, the annual effective dose is higher than the public exposure but annual effective dose is still in the range proposed by the UNSCEAR 2008 is 0.3-1.0 mSv/y.

Activity profile for ²²⁶Ra, ²²⁸Ra and ⁴⁰K at Plantation A and B

Figures 2, 3 and 4 shows the activity profile for ²²⁶Ra, ²²⁸Ra and ⁴⁰K at plantation A and B. This profile shows the activity concentration behaviour in the soil and also can be used to monitor the change in concentration with depth. From Figure 2, it shows the profile for activity ²²⁶Ra in a depth of 20cm for location A and B. the similarities between these profiles is the activity of ²²⁶Ra show monotonic pattern trough the depth. There is no observable trend is shown at the study area depth profile. Range concentration of ²²⁶Ra for location A is 44.76-86.31 Bq/kg and Location B 70.20-142.89 Bq/kg. The mean concentration of A is 63.90 Bq/kg and B is 112.78 Bq/kg respectively.

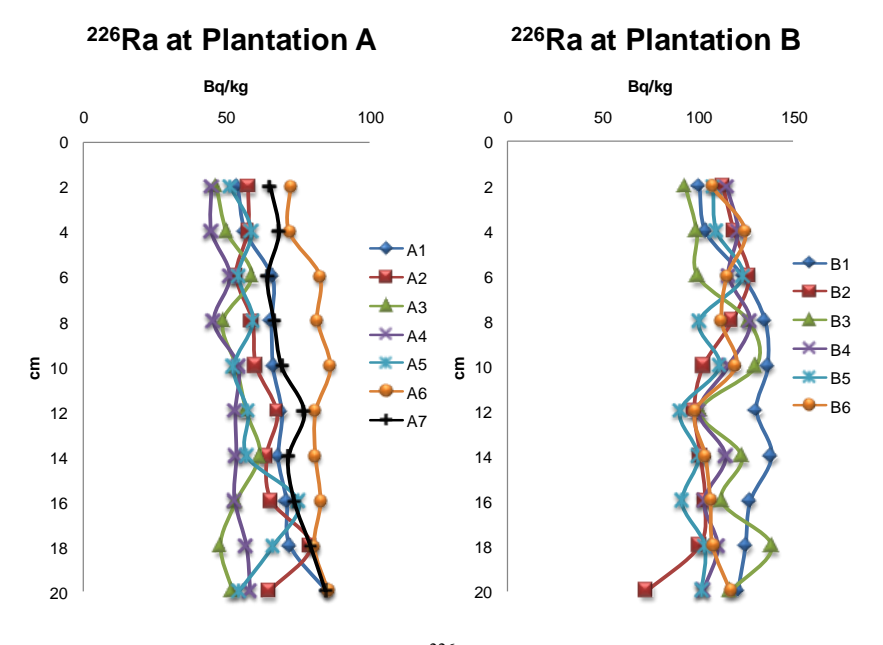


Figure 2: ²²⁶Ra profile

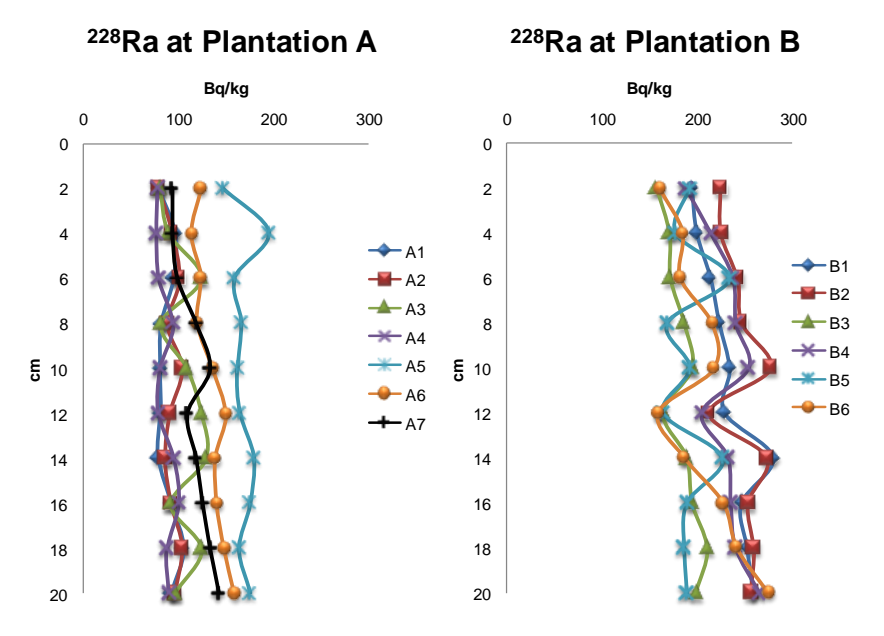


Figure 3: ²²⁸Ra profile

The activity profile for 228 Ra were also same as 226 Ra, there is no observable trend was shown in Figure 3. When compare between location A and B, the average activity concentration 228 Ra at B is higher than location A. The range concentration of 228 Ra is 77.04-195.53 Bq/kg for A and 157.11-280.11 Bq/kg for B. The mean concentration of 228 Ra is 113.55 Bq/kg for A and 217.41 Bq/kg for B respectively.

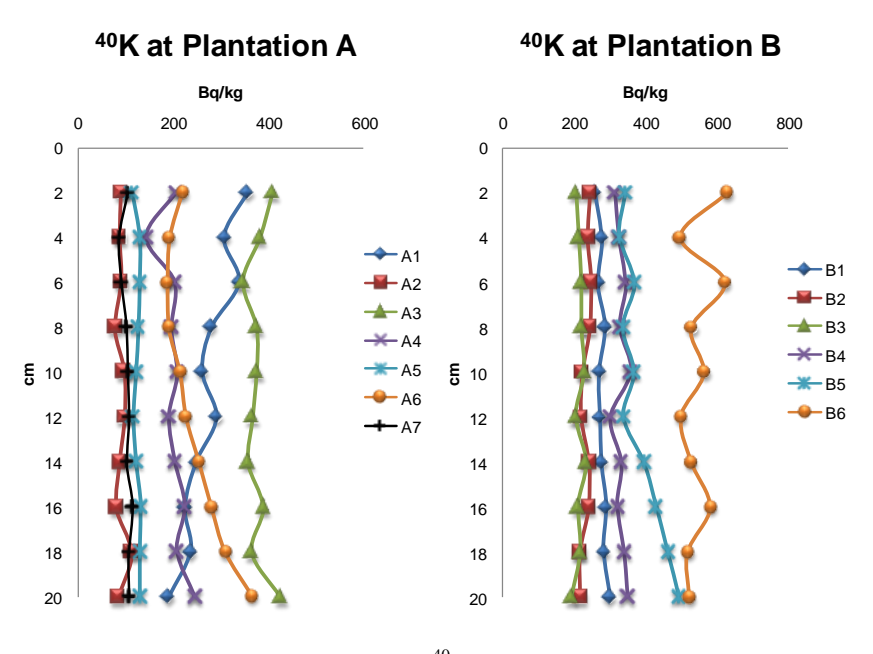


Figure 4: 40K profile

Zaini Hamzah et al: ASSESSMENT OF RADIATION HEALTH RISK IN CAMERON HIGHLANDS TEA PLANTATIONS

There is one locations profile for 40 K is increasing through the depth which is for location A6and B5. Also only one location is decreasing through the depth which is A1 .It seems that there is also no observable pattern for 40 K. The decreasing pattern at location A1 and B5 is maybe due to the external sources of K which is from fertilizer may occur which enrich the top layer and decreasing through the depth. The range concentration of 40 K for location A and B is 78.67-491.43 Bq/kg and 192.08-689.09 Bq/kg. Mean concentration is for A is 204.55 Bq/kg and B 337.31 Bq/kg respectively.

As overall estimation of the external hazard index of this study, the annual effective dose for public and workers is still in the range proposed by the UNSCEAR 2008 except for location B. This place is considered still under global average value.

Conclusion

In the present study the external hazard index (H_{ex}) for the study area is higher than unity for location B but the annual effective dose is still in the global average range for workers and public. The higher activity of NORM in the study area due to the location which is Cameron highlands is located at Titiwangsa range where the origin of the soil is intermediate igneous rock.

Acknowledgement

Thanks to District Officer of Cameron Highlands for giving permission doing research at Cameron Highlands. Also thanks to Institute of Science UiTM and Faculty of Applied Sciences UiTM for providing research facility and fund.

References

- 1. Abbady A., (2005). Assessment of the natural radioactivity and its radiological hazards in some Egyptian rock phosphates. Indian Journal of Pure and Applied Physics. 43(7): 489-493.
- Al-Hamarneh I.F. and Awadallah M.I., (2009). Soil radioactivity levels and radiation hazard assessment in the highlands of northern Jordan. Radiation Measurements. 44(1): 102-110.
- 3. Mehra R., Singh S., and Singh K., (2009). Analysis of ²²⁶Ra, ²³²Th and ⁴⁰K in soil samples for the assessment of the average effective dose. Indian Journal of Physics. 83(7): 1031-1037.
- 4. Singh S., Rani A., and Kumar Mahajan R., (2005). ²²⁶Ra, ²³²Th and ⁴⁰K analysis in soil samples from some areas of Punjab and Himachal Pradesh, India using gamma ray spectrometry. Radiation Measurements. 39(4): 431-439.
- 5. UNSCEAR, 2008. Sources and Effects of Ionizing Radiation. 1: 223-439.
- 6. Alaamer A., (2008). Assessment of human exposures to natural sources of radiation in soil of Riyadh, Saudi Arabia. Turkish Journal of Engineering & Environmental Sciences. 32(4): 229-234.
- 7. Alias M., Hamzah Z., Saat A., Omar M., and Z. T., (2005). Determination Of ²²⁶Ra, ²²⁸Ra And ⁴⁰K In Soil From Felda Jengka-15 Oil Palm Plantation. Malaysian Journal of Analytical Sciences. 9(1): 126 132.
- Alias M., Hamzah Z., Saat A., Omar M., and Wood A.K., (2008). An Assessment of Absorbed Dose And Radiation Hazard Index From Natural Radioactivity. Malaysian Journal of Analytical Sciences. 12(1): 195-204.
- 9. Banzi F.P., Kifanga L.D., and Bundala F.M., (2000). Natural radioactivity and radiation exposure at the Minjingu phosphate mine in Tanzania. Journal of Radiological Protection. 20: 41-51.
- 10. Msaki P. and Banzi F., (2000). Radioactivity in products derived from gypsum in Tanzania. Radiation protection dosimetry. 91(4): 409-412.
- 11. Hamzah Z., Ahmad S., Noor H., and Seh D., (2008). Surface Radiation Dose and Radionuclide Measurement in Ex-Tin Mining Area, Kg Gajah, Perak. The Malaysian Journal of Analytical Sciences. 12(2): 419-431.
- 12. El-Aydarous A., (2007). Gamma Radioactivity Levels and Their Corresponding External Exposure of Some Soil Samples from Taif Governorate, Saudi Arabia. Global Journal of Environmental Research. 1(2): 49-53.
- 13. Júnior J.A.S., Amaral R.S., Silva C.M., and Menezes R.S.C., (2010). Radium equivalent and annual effective dose from geological samples from Pedra Pernambuco Brazil. Radiation Measurements. 45(7): 861-864.
- 14. Wang Z., (2002). Natural radiation environment in China. International Congress Series. 1225: 39-46.
- 15. Martínez-Aguirre A., García-Orellana I., and García-León M., (1997). Transfer of natural radionuclides from soils to plants in a marsh enhanced by the operation of non-nuclear industries. Journal of Environmental Radioactivity. 35(2): 149-171.
- Division of Agriculture Ministry of Agriculture and Fisheries M., Generelized Soil Map Peninsular Malaysia 1970. 1970,
 Derectorat Pemetaan Negara, Malaysia No-137-1976: Kuala Lumpur.
- 17. UNCEAR, 2008. Sources and Effects of Ionizing Radiation. 1: 223-439.
- El-Arabi A.M., (2007). ²²⁶Ra, ²³²Th and ⁴⁰K concentrations in igneous rocks from eastern desert, Egypt and its radiological implications. Radiation Measurements. 42(1): 94-100.



KEGAGALAN CERUN DI BUKIT ANTARABANGSA, AMPANG, SELANGOR DAN HUBUNGANNYA DENGAN SIFAT FIZIK TANAH

(Slope Failure at Bukit Antarabangsa, Ampang, Selangor, and Its Relationship to Physical Soil Properties)

Muhammad Barzani Gasim^{1*}, Sahibin Abd. Rahim¹, Mohd. Ekhwan Toriman² dan Diyana Ishnin¹

 ¹Pusat Pengajian Sains Sekitaran dan Sumber Alam, Fakulti Sains dan Teknologi,
 ²Pusat Pengajian Sosial, Pembangunan & Sekitaran, Fakulti Sains Sosial dan Kemasyarakatan, Universiti Kebangsaan Malaysia,
 43600 UKM Bangi, Selangor, Malaysia

* Alamat email pengarang: dr.zani@ukm.my

Abstrak

Kegagalan cerun yang berlaku pada 6 Disember 2008 di Bukit Antarabangsa, Ampang, Selangor telah menyebabkan kematian dan kerosakan harta benda yang melibatkan lebih daripada 20 rumah penduduk telah ranap. Hujan lebat yang berlaku beberapa jam sebelum kegagalan cerun, telah meningkatkan ketepuan dan keplastikan tanah. Sebanyak 10 sampel tanah telah diambil secara rawak di cerun-cerun stabil dan gagal untuk menentukan sifat fizikal tanah, kadar penyusupan serta hubungannya dengan corak hujan. Tanah dianalisis berdasarkan sifat fiziknya, lima tahun (2005-2009) data hujan harian dianalisis untuk mendapatkan hubungannya dengan penyusupan air disetiap stesen persampelan. Kadar penyusupan diukur menggunakan infiltrometer "double rings". Hasil analisis sifat fizik tanah menunjukkan bahawa tekstur tanah didominasi oleh tanah berpasir yang mencatatkan peratusan kandungan pasir yang relatif tinggi. Nilai kadar serakan lempung adalah sederhana stabil sehingga sangat stabil atau berjulat daripada 0.013% sehingga 11.85%, kandungan organik antara 1.38 sehingga 2.74 %. Julat ruang rongga diantara 50.12% sehingga 62.31% dan purata tahap kekonduksian hidraulik diantara tahap 2 sehingga 5 atau agak perlahan sehingga pantas. Peratusan kestabilan agregat tanah berjulat dari 5.12 % sehingga 48.42%, nilai ini menunjukkan kekuatan relatif tekanan mekanik tanah adalah bernilai songsang terhadap peratusan kandungan air. Nilai keplastikan tanah berjulat tinggi sehingga sangat tinggi yang dicirikan dengan koloid yang tidak aktif. Taburan hujan bulanan berjulat daripada 38 mm hingga 427 mm. Kadar penyusupan semasa persampelan bernilai diantara 3.0 cm/jam hingga 7.0 cm/jam tetapi semasa kegagalan cerun dijangkakan berjulat diantara 10.94cm/jam sehingga 915.05cm/jam. Secara keseluruhan ditafsirkan bahawa sifat fizik tanah mempengaruhi kestabilan cerun, struktur tanah berpasir akan meningkatkan tahap keporosan tanah dan selanjutnya meningkatkan kadar penyusupan semasa hujan lebat dan akhirnya mencetuskan berlakunya kegagalan cerun.

Kata kunci: Bukit Antarabangsa, kadar penyusupan air, tanah berpasir, kegagalan cerun

Abstract

Slope failure which occurred on 6 December 2008 at Bukit Antarabangsa, Ampang Selangor has caused mortalities and loss of properties whereas more than 20 houses were flattened. Prior to slope failure, it was heavily downpoured for a few hours that increased the soil saturation and plasticity properties. A total of 10 soil samples were randomly taken from stable and unstable slopes to determine physical soil properties, infiltration rate and their relationship to rainfall pattern. Soils were analyzed in terms of their physical properties; five years (2005-2009) of daily rainfalls were analyzed to determine their relationship to infiltration rate at each sampling station. Infiltration rate is determined by using infiltrometer double ring. Analysis of physical soils properties shows that soil texture was dominated by sandy soil with relatively high percentage of sand. Values of clay dispersion coefficient were relatively stable to very stable from 0.013% to 11.85% and organic content from 1.38 % to 2.74 %. Range of porosity was from 50.12% to 62.31%, while the average levels of hydraulic conductivity was from level 2 to 5 or relatively slow to fast. Percentage of soil aggregate stability was from 5.12 % to 48.42 % and this value indicates that relative strength of soil mechanical pressure is inversely proportional to the percentage of water content. Soil plasticity value was high to very high but characterized by inactive colloids. Distribution of monthly rainfall was from 38 mm to 427mm. The infiltration rate during

Muhammad Barzani et al: KEGAGALAN CERUN DI BUKIT ANTARABANGSA, AMPANG, SELANGOR DAN HUBUNGANNYA DENGAN SIFAT FIZIK TANAH

sampling time was from 3.0 cm/hr to 7.0 cm/hr; but it was expected from 10.94cm/hr to 915.05 cm/hr during slope failures. Overall, it was interpreted that physical soil properties was closely interrelated with slope stability, structure of sandy soil will enhanced soil porosity stage and enhance the infiltration process during heavy rainfall, and finally triggering of slope failure.

Keywords: Bukit Antarabangsa, infiltration rate, sandy soil, slope failure

Pendahuluan

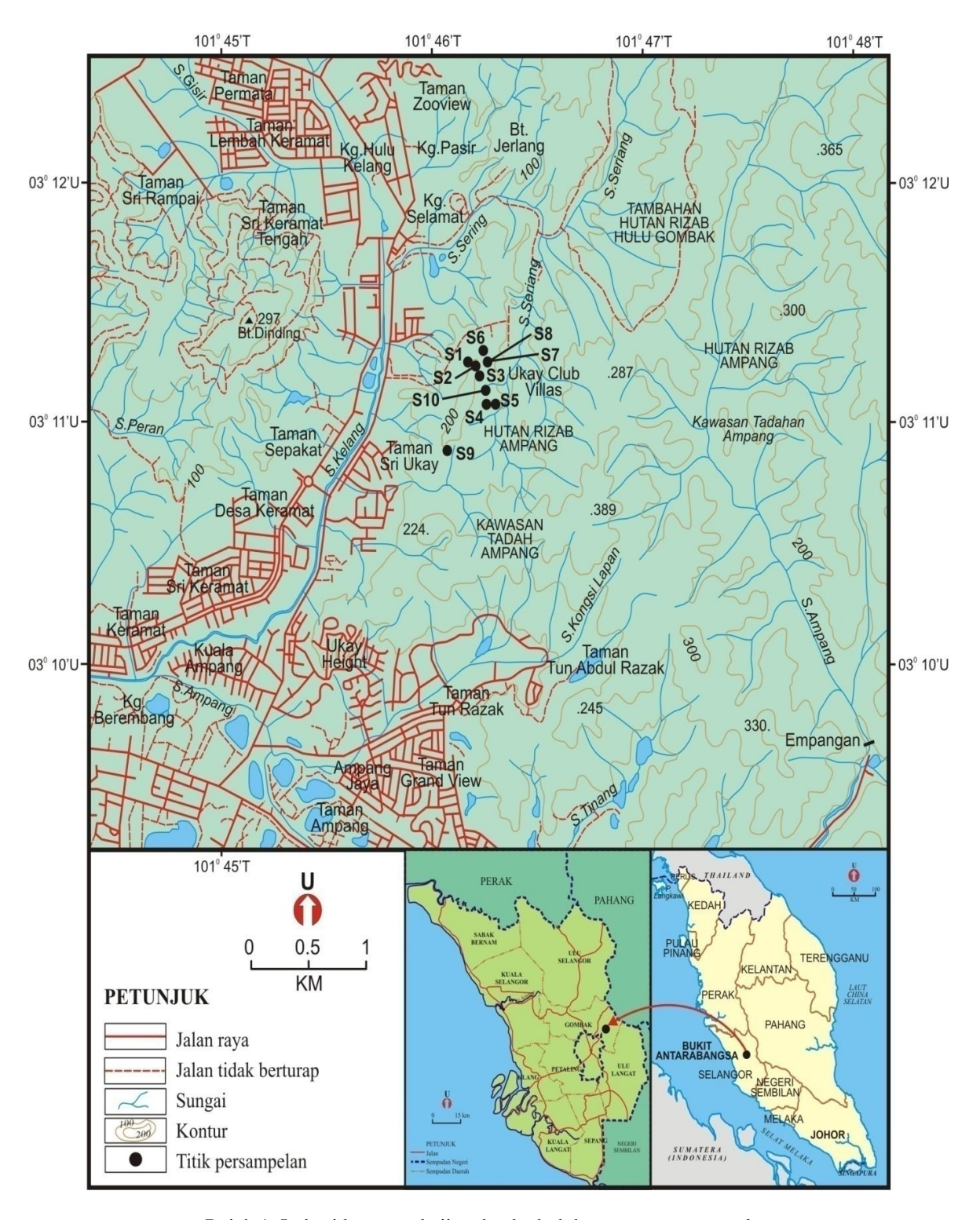
Bukit Antarabangsa, Hulu Klang, Selangor merupakan kawasan yang bertopografi berbukit bukau, dengan ketinggian di antara 133 hingga 203 meter di atas paras laut. Mempunyai longitud antara 101°46' T hingga 101°47' T dan latitud antara 03°10.8' U hingga 03°11.3' U (Rajah 1). Dicirikan oleh iklim yang panas dan lembab sepanjang tahun dan mempunyai jumlah hujan tahunan sebanyak 2500 sehingga 3000 mm.

Kegagalan cerun atau tepatnya tanah runtuh merupakan satu kejadian geologi yang melibatkan sebahagian besar pergerakan tanah, jatuhan batuan atau cantuman dari keduanya. Kebanyakkan runtuhan tanah bermula di lerenglereng cerun dan seringkali dicetus oleh air larian permukaan [1]. Runtuhan tanah berlaku mungkin secara berperingkat dan mungkin berlaku dengan pantas tanpa disedari sewaktu hujan lebat serta bergerak bersamanya bahan bumi yang menggelongsor mengikut tarikan graviti [2].

Menurut [3], air yang mengalir di permukaan akan sentiasa menyebabkan hakisan. Kadar hakisan semakin tinggi sekiranya tanah di sesuatu kawasan itu terletak di tempat yang tinggi dan curam seperti di lereng-lereng bukit. Pengaliran air yang teramat deras akan menghakis bunga tanah atau lapisan atas. Berkaitan dengan proses hakisan, runtuhan tanah juga akan berlaku di cerun bukit, terutamanya berlaku semasa hujan lebat. Proses kegagalan cerun menjadi satu masalah di kawasan di berbukit-bukau seperti Cameron Highlands, Fraser Hill, Genting Highlands di Pahang dan beberapa kawasan tanah tinggi di Malaysia.

Kebiasaannya kegagalan cerun atau tanah runtuh akan meragut nyawa manusia serta memusnahkan harta benda. Contohnya, beberapa kejadian tanah runtuh besar yang telah berlaku seperti di Highland Tower dan Taman Hillview di Hulu Kelang (Selangor), Gua Tempurung (Perak), Paya Terobong (Pulau Pinang), persimpangan lebuhraya NKVE, Bukit Lanjan serta beberapa kegagalan cerun bersaiz kecil dan sederhana. Fenomena ini seringkali dikaitkan dengan musim tengkujuh, di mana sejumlah curahan hujan yang tinggi bertindak sebagai pencetus kepada kegagalan cerun. Keadaan iklim tropika yang panas dan lembab ini juga turut menyebabkan proses luluhawa secara relatifnya adalah lebih tinggi berbanding kawasan beriklim lain [4]. Namun begitu, faktor-faktor lain seperti keadaan geologi, geomorfologi & struktur geologi akan berperanan dalam mempengaruhi corak pelemahan batuan [5]. Kawasan kajian yang terletak di Bukit Antarabangsa merupakan kawasan perumahan di lereng bukit di Ulu Klang, Selangor, Malaysia. Bukit Antarabangsa, Ampang adalah sebuah kawasan penempatan awam yang berprofil pertengahan ke tinggi. Namun begitu, penempatan yang dimajukan sebagai perumahan ini mempunyai keadaan muka bumi yang bercerun dan sama sekali tidak selamat dan tidak stabil untuk diduduki. Kebanyakan projek pembangunan di sekitar kawasan Bukit Antarabangsa terletak di kawasan cerun bukit.

Peristiwa tanah runtuh yang berlaku pada 6 Disember 2008 di Bukit Antarabangsa telah meranapkan 20 buah rumah dan mengorbankan sekurangnya lima orang penduduk dan lebih daripada 2,000 orang pula terpaksa dipindahkan ke tempat yang selamat. Kekuatan cerun yang tidak mampu mengawal dan menyokong kekuatan tapak bagi perumahan tersebut akibat. hujan yang berterusan, telah menyebabkan kawasan menjadi tidak stabil dan aliran air berlebihan ini telah menyusup ke bawah permukaan dan menjadikan bahan bumi di bawah permukaan semakin lemah. Ditambah pula, dengan keadaan cerun yang tidak stabil menyebabkan sejumlah bahan bumi bersama beberapa rumah penduduk yang terlibat runtuh di sepanjang cerun dan dilonggokkan ke beberapa ratus meter dari tempatnya yang asal. Menurut laporan [6], 13 Ogos 2008, menunjukkan bahawa kebanyakkan cerun di kawasan Bukit Antarabangsa berada pada kelas III, iaitu cerun yang berisiko tinggi kerana mempunyai kecerunan 26° - 35°. Objektif daripada kajian ini ialah: 1) Untuk menentukan sifat fizik tanah di kawasan kajian; 2) Untuk menentukan hubungan diantara curahujan dengan kadar penyusupan dan 3) Untuk mentafsirkan perkaitan diantara sifat fizik tanah, kadar penyusupan dan berlakunya tanah runtuh.



Rajah 1: Lokasi kawasan kajian dan kedudukan stesen persampelan

Kaedah Kajian

Sebanyak sepuluh pensampelan tanah telah dikutip dan pengukuran kadar penyusupan telah dilakukan selama dua kali kerja lapangan. Sampel tanah diambil 10 cm di bawah permukaan dengan menggunakan pengorek auger tangan. Di makmal sampel tanah di analisis untuk mendapatkan saiz butiran, serakan lempung, kandungan bahan organik, kekonduksian hidraulik, kestabilan agregat, keplastikan tanah dan sebagainya. Pengukuran kadar penyusupan dilakukan dengan menggunakan alat 'infiltrometer double rings'. Pengukuran dan pensampelan dilakukan di dua kawasan berbeza; kawasan yang mewakili cerun yang stabil dan yang mewakili kawasan cerun yang runtuh. Sampel tanah tersebut kemudiannya disimpan dalam beg plastik, dilabelkan, diikat dan dimasukkan dalam bekas yang kedap udara. Peta geologi bagi kawasan kajian diperoleh dari Jabatan Mineral dan Geosains Malaysia, untuk mendapatkan latarbelakang kepelbagaian batuan dan ciri geologi kawasan. Data hujan harian bagi tempoh tahun 2005 sehingga 2009 yang diperoleh dari Jabatan Kajicuaca Malaysia digunakan untuk membandingkan jumlah hujan semasa tanah runtuh dengan hari-hari yang lain. Nilai penyusupan semasa tanah runtuh ditafsirkan berdasarkan kiraan 10 hari jumlah hujan dibahagikan dengan 10 hari jumlah hujan semasa persampelan. Nilai ini kemudiannya didarabkan dengan nilai penyusupan semasa persampelan di lapangan yang menggunakan alat gegelang infiltrometer "Double Ring".

Hubungan di atas dapat disimpulkan berdasarkan formula di bawah:

Nilai penyusupan =
$$\frac{Jumlahhuja \ nsemasarun \ tuhan}{Jumlahhuja \ nsemasapen \ sampelan} \ x \ Nilai penyusupan \ semasa \ persampelan$$

Hasil dan Perbincangan

Hubungan Penyusupan dengan Kecerunan Cerun

Cerun merupakan permukaan tanah yang terdedah yang membentuk sudut tertentu terhadap satah ufuk. Kebiasaannya kegagalan cerun dikaitkan dengan keadaan cerun yang curam tetapi ini adalah tidak benar kerana terdapat banyak kes kegagalan cerun yang berlaku pada cerun yang landai [7]. Keadaan ini menunjukkan bahawa kestabilan sesuatu cerun bergantung kepada banyak faktor selain dari sudut kecondongannya. Menurut [8], kesan hujan ke atas kandungan air tanah bergantung kepada faktor seperti ciri-ciri tanah, topografi, jumlah dan keamatan hujan, litupan tumbuhan dan keadaan kandungan air tanah pada masa hujan.

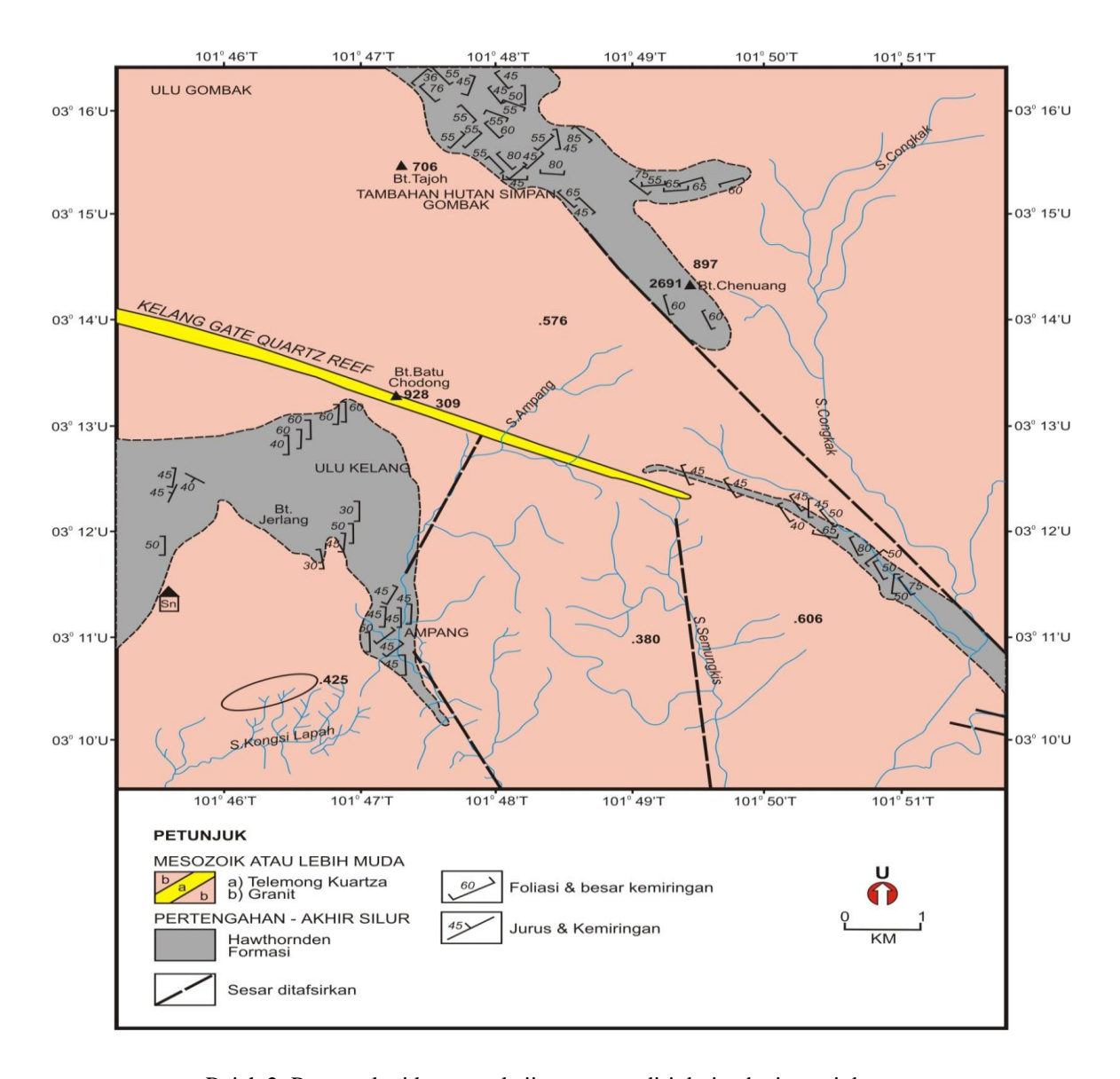
Kecerunan permukaan akan mempengaruhi kadar penyusupan air. Semakin landai cerun, semakin tinggi kadar penyusupan. Kadar penyusupan berkurangan jika kecerunan lebih daripada 2% kerana larian permukaan berlaku [9]. Kelajuan aliran yang bertambah akan menyebabkan hakisan. Kehadiran rumput akan mengurangkan masalah kelajuan aliran dan hentaman permukaan. Menurut [10], di cerun, air yang berada dalam tanah akan hilang melalui evapotranspirasi dan saliran yang bergerak perlahan melalui substrata.

Kestabilan cerun boleh diusahakan dengan litupan tumbuhan di atas permukaan cerun, tumbuhan akan membantu meningkatkan kandungan organisma pada tanah. Akar rumput yang reput pada tanah akan mengalami penguraian dan membantu dalam pengagregatan. Melalui proses ini, sistem struktur tanah akan diperbaiki dan meningkatkan kestabilannya. Penjerapan mineral akar rumput akan menggalakkan pemegangan nutrien pada tanah. Keadaan ini boleh mengelakkan kehilangan nutrien serta menggalakkan pertukaran kation pada tanah [11].

Geologi Kawasan Kajian

Mengikut [12] kawasan Bukit Antarabangsa (Kuala Lumpur dan sekitarnya) terdiri dari batuan Granite Banjaran Utama yang dikenali sebagai Granite Kuala Lumpur [13] berusia Trias yang mempunyai tipikal tekstur mega kristal. Sebahagian lagi kawasan terdiri daripada batuan skis yang dikenali sebagai Skis Hawthornden dan berusia Ordovisi-Silur [14]. Banjaran telerang kuarza wujud dalam kawasan granit yang mempunyai kedudukan BL-TD atau selari dengan beberapa set sesar mendatar ke kiri, yang dikenali sebagai Sesar Kuala-Lumpur (Rajah 2). Jurus sesar dan telerang ini telah memotong struktur rantau kawasan yang amnya hampir utara-selatan. Akibat daripada wujudnya kepelbagaian zon lemah dalam batuan granit dan skis telah menyebabkan berlakunya pergerakan cerun dalam bentuk kegagalan satah, kegagalan baji dan kegagalan terbalikan [15]. Kawasan perumahan di Bukit Antarabangsa

terletak dalam batuan granit yang berketinggian 143 m, kebanyakan batuan granit di kawasan ini terluluhawa dan sebahagian lagi didapati mengandungi beberapa set kekar dalam keadaan terbuka atau tertutup. Beberapa sistem saliran dikesan di bahagian hadapan cerun, kemudiannya bercantum membentuk alur dan akhirnya masuk ke Sungai Kongsi Lapan yang mengalir ke baratdaya (Rajah 2). Pembentukan zon-zon granit terluluhawa di kawasan ini dipercayai menerusi sistem kekar atau sesar yang wujud semasa penerobosan atau orogeni yang bertindak selepas itu.

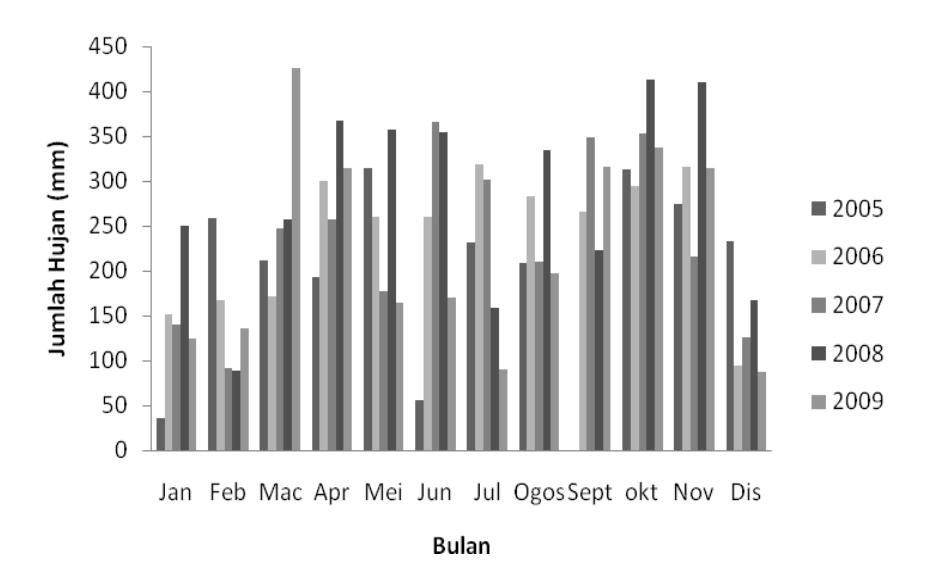


Rajah 2: Peta geologi kawasan kajian yang terdiri daripada tiga unit batuan

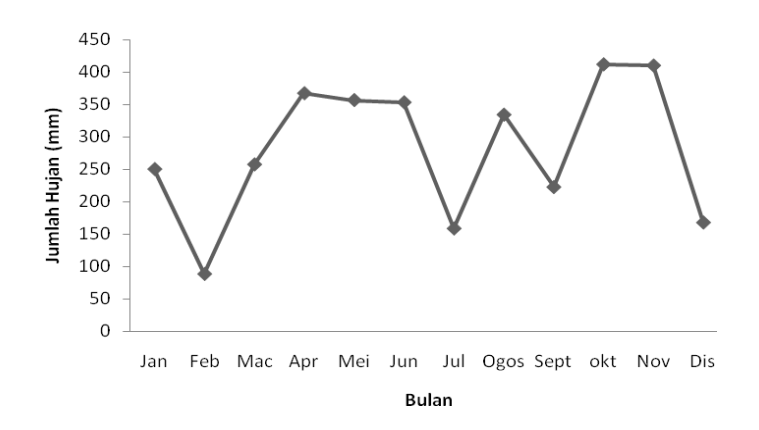
Hidrologi Kawasan Kajian

Berdasarkan analisis taburan hujan bulanan selama lima tahun (2005-2009), didapati bahawa curah hujan bulanan bagai kawasan kajian adalah berjulat daripada 38 sehingga 427 mm (Rajah 3). Berdasarkan pemerhatian di Rajah 3, didapati bahawa tren hujan bulanan di kawasan kajian mula menunjukkan kenaikan selepas tahun 2007 jika

dibandingkan dengan tahun-tahun sebelumnya. Hujan bulanan tertinggi tahun 2008 di kawasan kajian ialah Oktober - November, Mac sehingga September mencatatkan hujan yang sederhana lebat, sedangkan Disember sehingga Januari merupakan hujan bulanan yang terendah (Rajah 4).



Rajah 3: Taburan purata hujan bulanan selama 5 tahun (2005-2009)



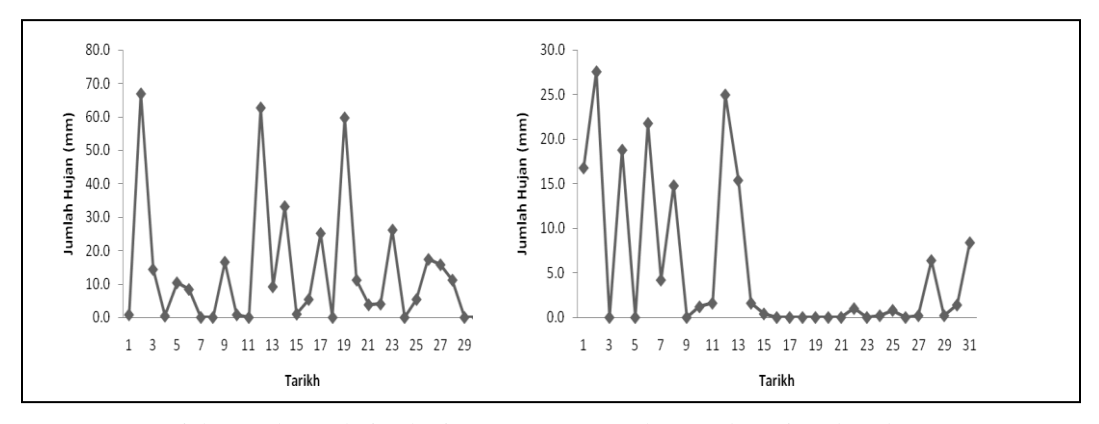
Rajah 4: Taburan hujan bulanan tahun 2008

Jumlah hujan selama 10 hari sebelum kejadian kegagalan cerun telah dikenalpasti iaitu sebanyak 112 mm (Jadual 1), atau hujan harian purata sebelum berlaku kegagalan cerun ialah 11.2mm. Secara relatif, jumlah hujan harian adalah relatif rendah, tetapi sifat tanah kawasan cepat menjadi tepu, kesan daripada kelebatan hujan pada bulanbulan sebelumnya. Jumlah hujan bulan Disember 2008 ialah 167.8 mm, jumlah ini jauh lebih kecil jika dibandingkan dengan jumlah hujan bulan November) iaitu sebanyak 410.4 mm. Tiga kemuncak hujan dicatatkan semasa November iaitu masing-masing 59, 63 dan 67 mm, sedangkan jumlah hujan tertinggi semasa Disember ialah 27.8 mm (Rajah 5). Berlakunya kegagalan cerun di Bukit Antarabangsa ialah dengan kelebatan 21.8mm pada pagi 6 Disember 2008 (Jadual 1, Rajah 5b).

Jadual 1: Cerapan hu	ian 10 hari sebelum	runtuhan (Nov/Des. 2008)

Tarikh	Jumlah Hujan(mm/hari)
1 al ikii	Julilali Hujali(Illili/IlaH)
27-Nov	15.8
28-Nov	11.2
29-Nov	0.0
30-Nov	0.0
1-Dec	16.8
2-Dec	27.6
3-Dec	0.0
4-Dec	18.8
5-Dec	0.0
6-Dec	21.8
Jumlah	112.0

Sumber: Jabatan Meteorologi Malaysia 2009



Rajah 5: Taburan hujan harian semasa November (a) dan Disember (b) 2008

Keputusan Sifat Fizik tanah

Duabelas parameter bagi analisis fiziko-kimia tanah telah dipilih dari 10 stesen pensampelan di kawasan kajian iaitu: ruang rongga, konduktiviti hidraulik, kadar penyusupan, koefisien serakan lempung, kandungan bahan organik, had atterberg terdiri dari had cecair, had plastik dan indeks keplastikan, taburan saiz partikel bagi pasir, lodak dan lempung serta tekstur tanah (Jadual 2 & 3).

Analisis makmal tersebut mendapati bahawa tanah yang dikaji mempunyai peratusan ruang rongga antara 50.12-62.31%, kandungan organik antara 1.38- 2.74 %, kekonduksian hidraulik antara 1-22.82 cmjam⁻¹, kadar penyusupan antara 5.4022-451.8072 cmjam⁻¹ dan koefisien serakan lempung antara 0.01-11.85%. Bagi had atterberg, had cecair adalah antara 56.6-71.8 %, had plastik antara 28.2-43.3 % dan indeks keplastikan antara 0.53-1.47. Hasil bagi tekstur tanah secara puratanya menunjukkan kandungan pasir dalam tanah yang dikaji berada pada julat di antara 55-97 %. Purata peratusan lempung pada tanah pula mencatatkan julat di antara 2-42 % iaitu kedua tertinggi selepas kandungan pasir dalam tanah. Kandungan lodak pula secara perbandingannya adalah sangat rendah dalam tanah dengan julat peratusan di antara 1-11%. Berdasarkan kepada pengkelasan Segitiga Ferret, tanah yang dianalisis berada dalam lingkungan kelas tanah lempung berpasir, loam lempung lodak, loam berpasir dan pasir, atau secara keseluruhannya kandungan utama adalah pasir atau berpasir (Rajah 6).

Muhammad Barzani et al: KEGAGALAN CERUN DI BUKIT ANTARABANGSA, AMPANG, SELANGOR DAN HUBUNGANNYA DENGAN SIFAT FIZIK TANAH

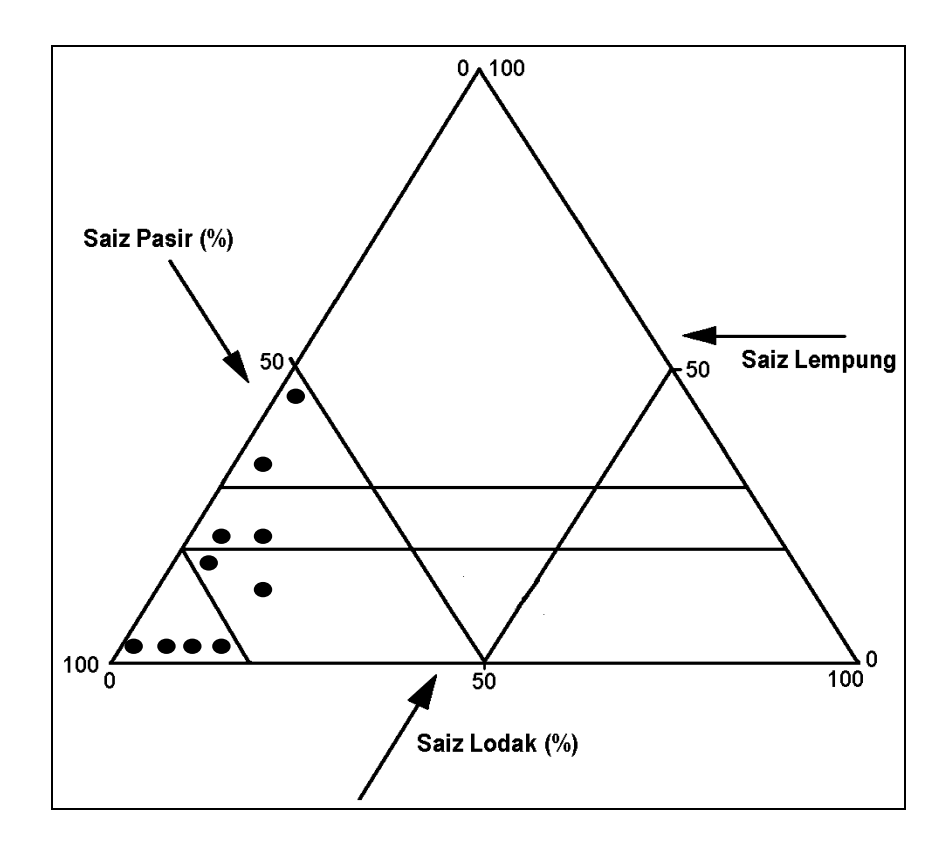
Jadual 2: Ringkasan hasil dari analisis fiziko-kimia tanah di kawasan kajian (St 1–St 5)

NO.	PARAMETER	UNIT	S1	S2	S3	S4	S5
Lokasi Cerapan			(G)	(G)	(G)	(S)	(S)
1	Ruang rongga	%	58.74	61.7	60.62	50.12	61.88
2	Kandungan bahan organik	%	1.80	1.77	1.54	2.74	2.57
3	Kekonduksian hidraulik	cmjam ⁻¹	2.6316	5.7427	4.8576	11.8313	22.8287
4	Kadar penyusupan	cmjam ⁻¹	7.2029	6.6026	7.2029	451.8072	451.8072
5	Koefisien serakan lempung	%	11.8477	0.1735	0.1865	1.4037	0.5189
	Had atterberg:						
6	Had cecair (LL)	%	63.5414	65.1012	62.0874	59.7867	60.6995
7	Had Plastik (PL)	%	36.4586	34.8988	37.9126	40.2133	39.3005
8	Indeks Keplastikan (IP)		0.6408	1.3803	1.2318	1.4788	0.7425
	Taburan Saiz Partikel						
9	Pasir	%	73	55	91	80	97
10	Lodak	%	5	3	7	2	1
11	Lempung	%	22	42	2	18	2
			Loam				
			lempung	Lempung			
12	Tekstur tanah		pasir	berpasir	Pasir	Pasir	Pasir

(G)-gagal (S)-stabil

Jadual 3: Ringkasan hasil dari analisis fiziko-kimia tanah di kawasan kajian (St 6-St 10)

NO.	PARAMETER	UNIT	S6	S7	S8	S9	S10
	Lokasi Cerapan		(S)	(G)	(G)	(S)	(S)
1	Ruang rongga	%	62.31	60.62	57.02	56.66	60.04
2	Kandungan bahan organik	%	1.38	1.55	2.09	1.62	1.70
3	Kekonduksian hidraulik	cmjam ⁻¹	2.7165	1.0741	6.4381	1.0000	3.6601
4	Kadar penyusupan	cmjam ⁻¹	110.4442	5.4022	5.4022	34.2137	13.8055
5	Koefisien serakan lempung	%	1.4181	3.8403	1.7262	0.5161	0.0135
	Had atterberg:						
6	Had cecair (LL)	%	62.4429	71.8102	56.8196	56.6465	60.6549
7	Had Plastik (PL)	%	37.5571	28.1898	43.1804	43.3535	39.3450
8	Indeks Keplastikan (IP)		1.3559	1.3408	0.5338	0.9773	1.1272
	Taburan Saiz Partikel						
9	Pasir	%	88	78	90	62	72
10	Lodak	%	11	6	8	4	5
11	Lempung	%	2	16	2	35	23
							Loam
				Loam		Lempung	lempung
12	Tekstur tanah		Pasir	Pasir	Pasir	berpasir	pasir

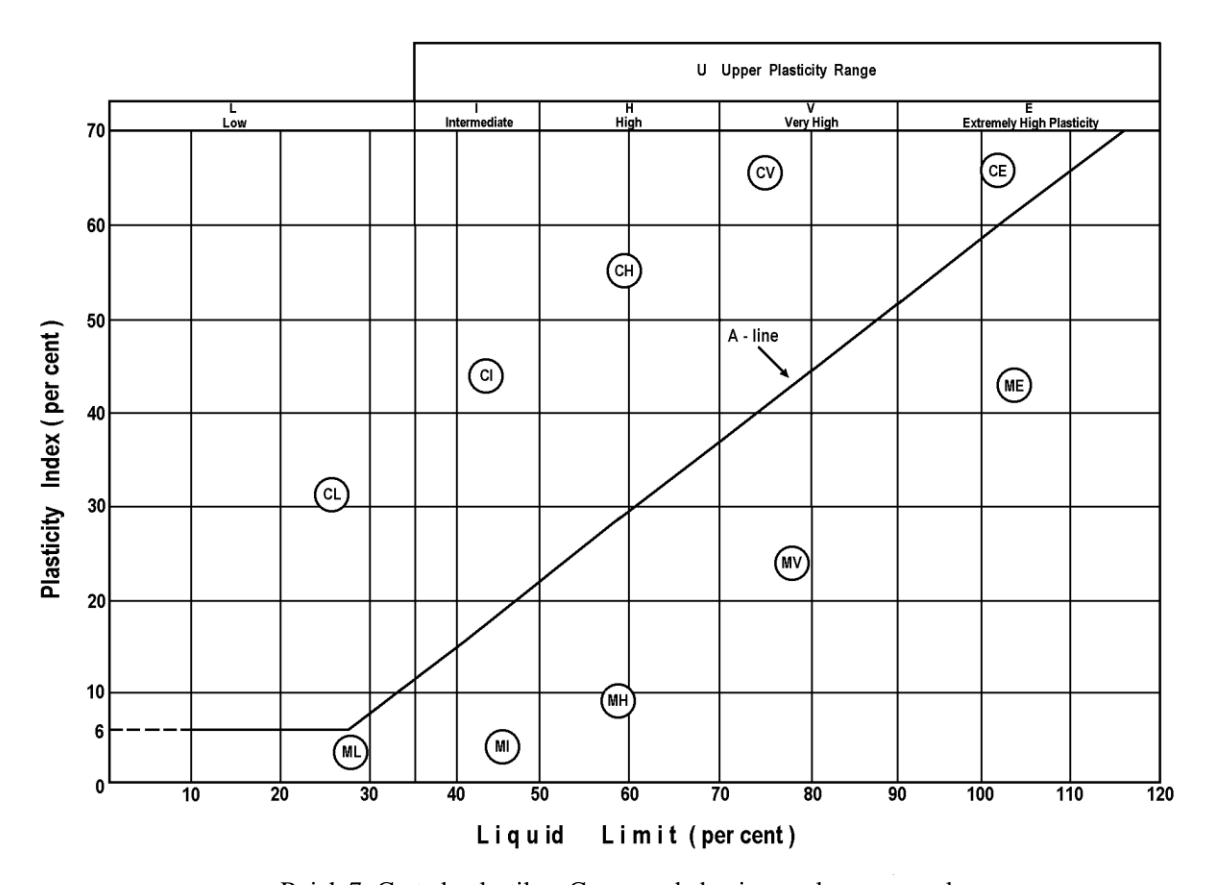


Rajah 6: Keputusan analisis saiz partikel di kawasan kajian

Had-had Atterberg

Hasil analisis makmal menunjukkan had plastik berada dalam julat 28.19% hingga 43.35% manakala had cecair berada dalam julat 56.65% hingga 71.81% (Jadual 2&3)). Berdasarkan pengelasan keplastikan tanah halus berdasarkan had cecair, didapati bahawa kesemua sampel tanah mempunyai keplastikan tinggi dan sangat tinggi. Had cecair bagi sampel tanah di stesen 7 adalah sangat tinggi, iaitu melebihi 70%. Manakala had cecair pada stesen yang lain adalah pada julat 50% hingga 65%.

Graf indeks keplastikan melawan had cecair diplotkan bagi mendapatkan carta keplastikan Casagrande bagi tanah kawasan kajian [16]. Rajah ini menerangkan sifat lempung atau sifat lodak dengan pemisahan garis A. Titik yang diplotkan di bawah garis A menunjukkan tanah jenis lodak manakala titik yang diplotkan di atas garis A menunjukkan tanah jenis lempung. Berdasarkan Rajah 7, didapati semua sampel tanah kawasan kajian adalah tanah jenis lodak dengan keplastikan tinggi (MH) dan sangat tinggi (MV).



Rajah 7: Carta keplastikan Casagrande bagi pengelasan sampel

Pengukuran Kekonduksian Hidraulik

Kekonduksian hidraulik boleh mencirikan sifat tanih, menurut Klute (1969), kekonduksian hidraulik menurun dengan cepat dengan menurunnya kadar kandungan air dalam tanih. Hasil analisis makmal (Jadual 4), didapati bahawa kekonduksian hidraulik bagi sampel 7 dan 9 adalah agak perlahan (0.5<K<2.0), sampel 1,2,3,6,10 adalah sederhana (2.0<K<6.25), manakala bagi sampel 8 dan 4 adalah agak cepat (6.25<K<12.50) dan sampel 5 adalah cepat (12.50<K<25.0).

Menurut Bouma dan Anderson (1971), kewujudan rongga dan alur dalam tanih akan menjadikan nilai kekonduksian hidraulik tinggi, walaupun ia menyumbang kepada pembahagian yang minima kepada keporosan tanih. Hasil analisis korelasi juga menunjukkan kekonduksian hidraulik mempunyai hubungan yang signifikan dengan peratus kandungan bahan organik (r= 0.829). Menurut Kohnke (1968), unsur kimia daripada pereputan organik mengambil tempat antara partikel lempung untuk membentuk agregat supaya meningkatkan kadar penyusupan dan ketelapan air pada tanih serta meminimumkan hakisan tanih.

Jadual 4: Pengelasan nilai kekonduksian hidraulik bagi semua stesen

Stesen	Nilai kekonduksian hidraulik	Julat kekonduksian hidraulik	Kelas	Tahap
1	2.6316	2.0 – 6.25	sederhana	4
2	5.7427	2.0 - 6.25	sederhana	4
3	4.8576	2.0 - 6.25	sederhana	4
4	11.8313	6.25 - 12.50	agak cepat	3
5	22.8287	12.50 - 25.0	cepat	2
6	2.7165	2.0 - 6.25	sederhana	4
7	1.0741	0.5 - 2.0	agak perlahan	5
8	6.4381	6.25 - 12.50	agak cepat	3
9	1.0000	0.5 - 2.0	agak perlahan	5
10	3.6601	2.0 - 6.25	sederhana	4

Hubungan signifikan juga ditunjukkan antara peratus kandungan bahan organik dan nilai kadar penyusupan menggunakan infiltrometer (r= 0.847). Menurut Stevenson (1994), bahan organik yang terbentuk di permukaan sisa tanih turut mempengaruhi pegangan air dengan mengurangkan penyejatan dan meningkatkan penyusupan air. Hasil analisis korelasi menunjukkan kekonduksian hidraulik mempunyai hubungan signifikan yang kuat dengan nilai kadar penyusupan menggunakan kaedah infiltrometer (r= 0.852). Manakala analisis korelasi antara ketumpatan kumin dan kekonduksian hidraulik, menunjukkan hubungan yang signifikan (r = -0.829).

Pengukuran Kadar Penyusupan

Nilai penyusupan semasa berlakunya tanah runtuh di Bukit Antarabangsa adalah ditafsirkan berdasarkan kiraan 10 hari jumlah hujan semasa runtuhan dibahagikan dengan 10 hari jumlah hujan semasa persampelan. Nilai ini kemudiannya didarabkan dengan nilai kadar penyusupan semasa persampelan di lapangan. Berdasarkan kiraan tersebut, maka nilai semasa persampelan dan semasa berlakunya kegagalan dapat diperoleh seperti dalam Jadual 5. Nilai purata penyusupan semasa kegagalan meningkat sekali ganda dibandingkan dengan nilai penyusupan semasa pensampelan, sedangkan stesen 4,5 dan 6 yang jauh lebih tinggi dibandingkan dengan stesen yang lain (Jadual 5). Ini menunjukkan bahawa proses penyusupan air berlaku lebih pantas sebelum berlakunya kegagalan, terlebih lagi yang berlaku di stesen 4.5 dan 6.

Jadual 5: Nilai penyusupan semasa persampelan dan berlakunya kegagalan

	Nilai penyusupan				
Stesen	Semasa persampelan(cm/jam)	Semasa kegagalan(cm/jam)			
1	7.2029	14.5882			
2	6.6026	13.3724			
3	7.2029	14.5882			
4	451.8072	915.0526			
5	451.8072	915.0526			
6	110.4442	223.6845			
7	5.4022	10.9412			
8	5.4022	10.9412			
9	34.2137	69.2936			
10	13.8055	27.9605			

Kesimpulan

Secara keseluruhannya, disimpulkan bahawa keadaan cerun di kawasan Bukit Antarabangsa dianggap kurang stabil disebabkan keadaan struktur geologinya yang lemah, seperti kawasan bertopografi tinggi, kemiringan cerun yang besar dan kandungan ketakselanjaran yang tinggi. Jumlah air hujan yang tinggi menyusup masuk ke dalam tanah melemahkan struktur tanah dan menyebabkan proses luluhawa yang aktif yang menghasilkan tanah berpasir. Peratus ruang rongga yang tinggi meningkatkan tahap keporosan tanah, meningkatkan lagi kadar penyusupan. Kestabilan agregat yang rendah disebabkan bahan organik yang rendah menyebabkan kurangnya tahap pegangan air dalam tanah. Manakala, kadar kandungan air dalam tanah juga mempengaruhi halaju hidraulik konduktivitinya. Keamatan hujan yang tinggi, menyebabkan meningkatnya kandungan air bawah tanah kesan daripada penyusupan yang pantas. Pengelasan keplastikan tanah berdasarkan had cecair, didapati bahawa kesemua sampel tanah mempunyai keplastikan tinggi dan sangat tinggi. Kadar penyusupan dan kekonduksian hidraulik yang tinggi di kawasan cerun yang selamat, menunjukkan adanya kecenderungan berlakunya runtuhan di masa hadapan, oleh yang demikian tindakan langkah keselamatan perlu dirancang dengan teliti.

Penghargaan

Penulis mengucapkan sekalung penghargaan kepada Universiti Kebangsaan Malaysia dan Kementerian Pengajian Tinggi bagi penganugerahan geran penyelidikan UKM-OUP-PI-25-114/2010 dan UKM-ST-06-FRGS0115-2009. Terima kasih juga kepada Fakulti Sains dan Teknologi bagi penggunaan kemudahan penyelidikan.

Rujukan

- 1. Syers J.K. & Rimmer D.L. 1994. *Soil science and sustainable land management in the tropics*. United Kingdom: Cab International. 77-78.
- 2. Fitzpatrick, E.A. 1974. An Introduction to Soil Science. New York: Longman Scientific and Technical. 255
- 3. Othman Yaacob & Shamshuddin Jusop. 1982. *Sains Tanah*. Kuala Lumpur: Dewan Bahasa dan Pustaka, Kementerian Pelajaran Malaysia. 402
- 4. Young, A. 1980. Tropical soils and soil survey. Cambridge University Press. 468
- 5. Muhammad Barzani Gasim & Brunotte, D.A. 1987. Structural Behavior of Crocker Formation and its implication to landslides. 9th Southeast Asian Geotechnical Conference, Bangkok, Thailand, 7-11 December 1987. 1-57-1-67.
- 6. BERNAMA. 2009. Dua kementerian selaras garis panduan pembangunan kawasan cerun. http://www.bernama.com/bernama/v5/bm/newsgeneral.php?id=432697[13 Ogos].
- 7. Marhana Abdul Latif. 2006. *Penentuan kestabilan cerun disebabkan oleh penyusupan hujan*. Laporan Projek Sarjana Muda. Universiti Teknologi Malaysia.
- 8. Herbel C.H. & Gile L.H. 1972. Field moisture regimes and morphology of some Arid-land soils in New Mexico. In. Bruce R.R., Flach K.W. & Taylor H.M. *Field Soil Water Regime*. Wisconson USA: Soil Science Society of America. 119–152.
- 9. Reynolds W.D. & Elrick D.E. 2005. Measurement and Characteristic of Soil Hydraulic Properties. Canada: CRC Press.
- 10. Miller D.E. 1973. Water retention and flow in layered soil profiles. In. Bruce R.R., Flach K.W & Taylor H.M (Edts). *Field Soil Water Regime*. 107-117. Wisconsin USA: Soil Science Society of America.
- 11. Shamshuddin Jusop. 1981. *Asas Sains Tanah.* Kuala Lumpur: Dewan Bahasa dan Pustaka, Kementerian Pelajaran Malaysia. 273
- 12. Ng, T.F. 1994. Microstructures of the deformed granites of the eastern Kuala Lumpur-Implication for mechanisms and temperatures of deformation. *Bull. Geo. Soc. Malaysia* 35: 47-59.
- 13. Tjia, H.D. 1972. Fault movement, reoriented stress field and subsidiary structures. Pacific Geology 5: 49-70.
- 14. Azman, A.Ghani. 2000. Chemical variation of muscovite from the Kuala Lumpur granite, Peninsular Malaysia. *Bull. Geo. Soc. Malaysia 44*: 117-124.
- 15. Tan Siang Fei & Tajul Anuar Jamaluddin. 2000. Geologi kejuruteraan kawasan Taman Bukit Utama, Ulu Kelang-Ampang. *Bull. Geo. Soc. Malaysia* 44: 55-58.
- 16. Kez'di A. 1974. Handbook of Soil Mechanic. Jil. 1: Soil Physics. New York: Elsevier Publishing Company.



SEDIMENTATION RATE AND CHRONOLOGY OF As AND Zn IN SEDIMENT OF A RECENT FORMER TIN MINING LAKE ESTIMATED USING Pb-210 DATING TECHNIQUE

(Kadar Mendapan dan Kronologi As dan Zn dalam Sedimen Tasek Bekas Lombong Menggunakan Teknik Pentarikhan Pb-210)

Zaharidah Abu Bakar¹, Ahmad Saat^{2*}, Zaini Hamzah¹, Abdul Khalik Wood³ and Zaharuddin Ahmad³

¹Faculty of Applied Sciences,
²Institute of Science,
Universiti Teknologi MARA, Malaysia, 40450 Shah Alam, Malaysia
³Malaysian Nuclear Agency,
43000 Bangi, Malaysia.

*Corresponding author: ahmad183@salam.uitm.edu.my

Abstract

Sedimentation in lake occurred through run-off from the land surface and settles on the bottom lake. Past mining activities might enhance sedimentation process in the former tin mining lakes either through natural or human activities. Former tin mining lakes were suspected to have high sedimentation rate due undisturbed environment for almost 50 years. To estimate sedimentation rate and metals contamination in this lake, Pb-210 dating technique was used. Two sediments cores were sampled using gravity corer from a former tin mining lake then analyzed using alpha-spectrometry and Neutron Activation Analysis (NAA). From this study, the results showed the sedimentation rate for sediment cores S1 and S2 are 0.26 cm y⁻¹ and 0.23 cmy⁻¹ respectively. According to sediment chronological sequences, high concentrations of As and Zn in the upper layer indicated that human activities contributed to these metals contamination in the lake sediment. Sedimentation rate and metals contamination possibly due to recent anthropogenic activities around the lake such as human settlement, farming and agricultures activities since the ceased of mining activities a few decades ago.

Keywords: Sedimentation, Pb-210, Former tin mining lake, Metals element

Abstrak

Pengenapan didalam tasik berlaku melalui aliran daripada permukaan tanah dan tenggelam ke dalam dasar tasik. Aktiviti aktiviti perlombongan yang lepas mugkin mempercepatkan proses pemgenapan di bekas tasik lombong bijih timah samada secara natural atau oleh aktiviti manusia. Bekas lombong bijih timah disyaki mempuyai kadar penenapan yang tinggi disebabkan persekitaran yang tidak terganggu untuk hampir selama 50 tahun. Untuk mengangar kadar pengenapan dan pencemaran logam di dalam tasik, kaedah pentarikhan Pb-210 telah digunakan. Kajian dilakukan di bekas tasik lombong bijih timah di daerah Kampung Gajah, Perak. Dua turus sediment diambil menggunakan turus persampelan graviti daripada tasik bekas lombong bijih timah dan dianalisa menggunakan spektrometri alpha dan Analisa Pengaktifan Neutron (NAA). Daripada kajian ini, keputusan menunjukkan kadar pengenapan untuk turus sediment S1 dan S2 masing – masing adalah 0.26 cm y⁻¹ dan 0.23 cm y⁻¹. Berdasarkan kepada turutan kronologi, kepekatan As dan Zn di lapisan atas sedimen menunjukkan aktiviti – aktiviti manusia menyumbangkan kepada pencemaran oleh metal ini didalam sedimen tasik. Kadar pemendapan dan pencemaran logam mungkin disebabkan oleh aktiviti – aktiviti antropogenik di sekiling tasik seperti penempatan manusia, penternakan dan pertanian sejak ditinggalkan beberapa dekad yang lepas.

Kata kunci: Mendapan, Pb-210, tasik lombong timah, unsur logam

Zaharidah Abu Bakar et al: SEDIMENTATION RATE AND CHRONOLOGY OF As AND Zn IN SEDIMENT OF A RECENT FORMER TIN MINING LAKE ESTIMATED USING Pb-210 DATING TECHNIQUE

Introduction

Over the past three decades, there has been an impressive increase in the volume and range of research on sedimentation. Accumulation of sediment in lakes facilitates us to obtain significant information to study about environmental changes [1, 2]. In Malaysia, a large number of former tin mining lakes have been abandoned for almost past 50 years. Lack of vegetation in abandoned mining lands render surface areas were directly exposed to rainfall impact and surface runoff. The effect of uncontrolled mining activities caused environmental problem such as deforestation and soil erosion that continue increasing the sedimentation rate [3]. Sedimentation profile also provides past evidence and rates of heavy metals contaminant deposition [4].

Pb-210 radiometric dating techniques introduced by Goldberg (1963) and expended to lake by Krishnaswami *et al.* (1971) has been used worldwide to reconstruct history of such recent sedimentation [5]. Pb-210 dating method has shown to be an ideal tracer for dating lake sediments deposited during the last 100 – 150 years which coincidence with period of environmental changes due to industrialization [6]. Conrad *et al.* (2007) recommended that Pb-210 dating method is a useful technique in investigation of changes in metals concentration on a decadal time scale. This is due to the fact that association of particles with Pb-210 making it a useful tracer for the fate of particle reactive contaminants such as trace metals.

Despite this useful potential, lack of Pb-210 dating method study has been applied in sediment of recent lakes in Malaysia. Thus this paper attempt to determined recent sedimentation rate, to reconstruct the sediment ages and metals input history using Pb-210 dating method.

Methodology

Study area

This study covers a former tin mining lake in Kampung Gajah area in the states of Perak, Malaysia that has been abandoned for more than 50 years. The lake is bordered within latitude 04°14.816" N - 04°15.107" N and longitude 101°2.889" E - 101°3.125" E. The total area of this lake is approximately 2.5 x 10⁵ m² and the volume of water is about 1.0 x 10⁷ m³. The deepest part of lake is about 10 m, receives seasonal water flow from an opening canal at the north-east that is connected to another lake used as a duck farm and flow out to the west of lake. Thus, there is a possibly of waste from other lakes enter the study area lake and flow out through other lakes to a nearest river. The study lake located 100 m from to the main road and around 1 km from residential areas. Although mining activities ceased long time ago, local peoples still used this area for growing cows and buffaloes, duck farming and fishing. Some fishes such as Temoleh (*Probarbus jullieni*), Lampan (*Puntius schwanenfeldii*), Tilapia Merah (*Oreochromis niloticus*), Catfish and Patin (*Pangasius sp*) are the main sources that essential to the diets and generating economies especially to the local peoples.

Samples collection

There are two points where sediment samples were collected, one at the middle of lake $(04^{\circ}14.928^{"} \text{ N}, 101^{\circ}03.043^{"}\text{E})$ and the edge of lake $(04^{\circ}14.854^{"} \text{ N}, 101^{\circ}03.134^{"}\text{ E})$. Sediment samples were collected using gravity corer sampling device (5 cm diameter, 40 cm long). Sediment cores were air dried for one week then sliced into 2 cm interval and oven dried at 60 °C until constant weight. The sediment cores showed light/dark-grey colour appearance. Sliced samples were ground and sieved in 450 μ m stainless steel sieves to the ensure homogeneity.

Pb-210 analysis

Total Pb-210 (Pb-210 $_{tot}$) was measured indirectly by determining the activity of its grandaughter, isotope Po-210. The Po-210 activity determined by alpha spectrometry is taken as a measurement of Pb-210 activity [2]. Pb-210 was assumed to be in radioactive equilibrium with Po-210 in the sediment samples. Chemical separation in analysis is controlled by Po-209 as internal standard [7].

About 2 g of sieved samples, standard and known amount of Po-209 tracer yield tracer were weighed and leached with HNO₃ and organic matter content digested with mixture of HNO₃ and H₂O₂ to get white residue. Remaining organic matter digested again using HCI and solution converted into 0.5M HCI medium. Residual solids were filtered and solution was treated with ascorbic acid to reduce Fe (II) to Fe (III) and prevent Fe deposition [8] and plated for 24 hours. Po-209 and Po-210 in solution then spontaneously deposited onto silver disc then counted using

alpha spectrometry. Po-210 and Po-209 emission from the disc releases alpha particles that have energy of 4843 keV and 5264 keV respectively were measured using alpha spectrometry with a 450 mm² area. Alpha radiations were then identified by EG & G ORTEC spectrometer using silicon surface barrier detectors with efficiency \geq 25%, energy ranged 0-10 meV and a multi-channel analyzer system. Energy resolution is \leq 20 keV (FWHM) with a detector – to – source spacing equal to the detector diameter. The outputs from the silicon detectors are amplified and transmitted through a multiplexer system into a computer based multi-channel analyzer. The system was calibrated using Mix Standard radioactive source. Samples activity and total uncertainties expressed in Becquerel per kilogram of dry weight (Bq kg¹ dry weight).

Pb-210 activity in a layer deposited at time, t in the past can be determined using the following equation:

Po-210 Activity (dpm) = Po-209 Added (dpm))
$$\times$$
 Po-209 Peak Area x *PDC* /(Po-210 Peak Area) (1)

where $PDC = e^{-\lambda \times \Delta t}$ is the plating date correction, with λ for Po-210 = 1.833 yr⁻¹, and Δt = date counted – date plated.

The Pb-210 activity concentration was calculated by dividing the activity of Po-210 to the mass of sample (Pb-210 Activity concentration (dpm g^{-1}) = Po-210 Activity (dpm) / Sample weight (g)). Supported Pb-210 activity at each site was determined as the average of the bottom segments that had exhibited a relatively constant activity indicative of the supported Pb-210 [9].

Metal analysis

For metal analysis, about 0.2~g of sieved samples and standard were weighed and sealed in small polyethylene vials for neutron activation analysis. The weighted samples and standards were irradiated in 750 kW TRIGA PUSPATI II nuclear reactor at Malaysian Nuclear Agency (MNA) with thermal neutron flux of $2~x10^{12}~n.cm^{-2}s^{-1}$. The irradiation time, decay time and measuring time used for metals analysis are given in Table 1.

Element Irradiation time Cooling Time (days) **Counting Time Distance from** (hours) (min) detector (cm) As 6 4 60 7 21 60 2 Zn 6

Table 1: Irradiation time, decay time and measuring time for metals analysis

Gamma emission were counted using Gamma spectrometer GEM series with HPGe Coaxial detector system (GEM-20180 model) equipped with multi-channel analyzer. The Canberra GEM series HPGe detector has the following specification: energy resolution of detector system is 1.88 keV and 25.4% relative efficiency at 1.33 MeV Co-60. Spectra were analyzed using GammaVision (version 6.01) and photopeak was selected based on interested element to be analyzed. Arsenic (As) and Zinc (Zn) were selected for metal analysis. For As and Zn the major photopeak at energy of 559 keV and 1116 keV were used for metals analysis. To ensure the accuracy of results, application of Certified Reference Materials (CRM) IAEA SOIL-7 and IAEA Sediment Lake-1 (SL-1), IAEA-368 (Pacific Ocean Lake), duplicate of samples and blank samples were also analyzed. Z - Score calculation was used as a measurement of acceptable variation of measured value of elements in the CRM from the certified value.

The Z-score is computed based on following equation:

$$Z = (X - C) / \sqrt{(U_x^2 + U_c^2)}$$
 (2)

where X is analytical result, C is certificate value, U_x is uncertainty of analytical result and U_c is the uncertainty of certificated value. For acceptance of the result, -2 < Z < 2 is anticipated while Z < -3 or Z > 3 is considered 'out of control' and need corrective action [10].

Results and Discussion

Data Verification

The quality of analyzed data for metal elements and radionuclides determined using IAEA SL-1 (Sediment Lake) and IAEA-368 (Pacific Ocean Sediment) and evaluated by Z-score is shown in Table 2. Replicate analyses of IAEA SL-1 and IAEA-368 confirm good agreement of Pb-210 activities determined with certified value . The result showed concentration of As, Zn and Pb-210 were agreed well with the certified values and the measured values in which the Z-score values lies within -2 < z < 2. Relative Percentage Difference (RPD) in CRM and analyzed samples were expressed as percentage (%) below than 10%. Relative Standard Deviation (RSD) was within 10% for both metals analyses and radionuclides. Blank samples did not indicate any significant contamination for the studied elements.

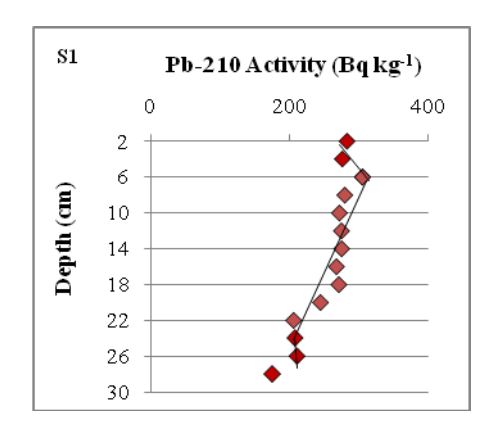
Table 2: Analytical value for sediment certified reference materials in comparison to certified reference values using NAA and Alpha spectrometry technique

Element	*As (μg g ⁻¹)	*Zn (μg g ⁻¹)	**Pb-210
Measured value	30.5±1.5	215.6±15.9	22.40±3.0
Certified value	27.5 ± 2.9	223±10	23.2 ± 3.7
Z-score	0.63	0.38	0.36
% RPD	7.17	3.31	3.42
% RSD	9.42	7.79	9.35

^{*}SL-1, **IAEA - 368

Core Profiles

Vertical profile of $Pb-210_{tot}$ activities in the sediment cores is shown in the Figure 1. $Pb-210_{tot}$ activities versus depth for S1 showed exponentially decline, with activity concentration 175.48-305.86 Bq kg⁻¹. The $Pb-210_{exc}$ varies from 6.07-106.24 Bq kg⁻¹. $Pb-210_{tot}$ activity concentration for S2 varies from 295.58-367.51 Bq kg⁻¹ with depth. $Pb-210_{tot}$ activities showed non linear decreased with the depth to a constant value. The $Pb-210_{exc}$ varies between 4.75-67.40 Bq kg¹.



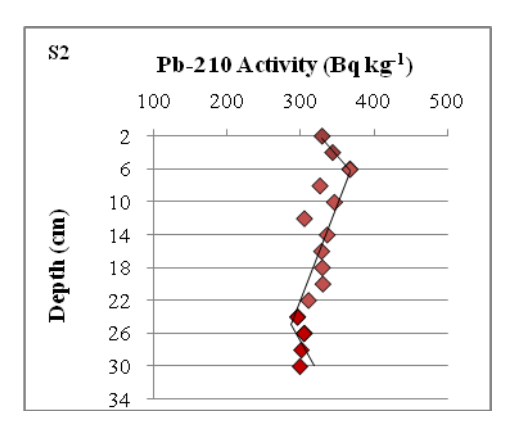


Figure 1: Pb-210_{tot} depth profiles in sediment cores

Pb-210_{exc} inventory was calculated as a sum of Pb-210_{exc} at all depths [14]. Inventory of Pb-210_{exc} in the core of S1 and S2 were estimated to be 16468 ± 128 Bq m⁻² and 7547 ± 87 Bq m⁻² is shown in Table 3. High inventory of Pb-210_{exc} at location S1 might be attributed to high deposition of materials and acted as pathway movement of sedimentary material [1]. Pb-210_{exc} inventory from atmospheric input alone is ca. 3000 - 4000 Bq m⁻² [11]. There is

no evidence of global atmospheric fallout due to atmospheric weapon testing reached Southeast Asia region [12]. Therefore, besides atmospheric input, the Pb-210 inventory may be due to surface run–off.

Location	Pb-210 _{exc} Inventory (Bq m ⁻²)	Sedimentation rate (cm y ⁻¹)	Flux (dpm cm ⁻² y ⁻¹)
S1	16468 ± 128	0.21 - 0.57	0.25
S2	7547 + 87	0.24 - 0.74	0.14

Table 3: Pb-210_{exc} inventory, sedimentation rate and flux in sediment cores

Pb-210_{exc} flux of the present study of in S1are similar to input of Pb-210_{exc} in sediments both of the Penang Island (5° N latitude) and Johor Strait (1° – 2° N latitude) (small difference in latitude) which are about 0.30 dpm cm⁻² y⁻¹ [13]. This finding consistence with Khalik *et al.* (2004) [13] and clearly confirmed that atmospheric origin seems the main source of Pb-210_{exc} supply. This is in contrast to location S2, where Pb-210_{exc} inventory is two times lower than the location S1. There is a possibility that Pb-210 has been diluted or due to mobilization process.

Sedimentation rate and dating model

Sedimentation within lake occurred through run-off from the land surface and settles on the bottom lake. Once Pb-210 deposited in the sediment, they are rapidly adsorb to fine grain materials and settled down to the bottom layer. Absorption of Pb-210 to the sediment lake has been assumed a uniform process and without of sediment redistribution. In present study, CRS model used to determine the sediment age and sedimentation rate within lake sediment by assuming sediment reworking (physical and biological) and diagenesis factors were neglected.

CRS model expressed as equation below:

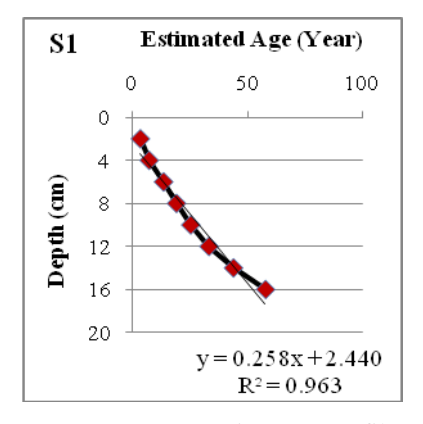
$$t = (1/\lambda) \ln (A_{(0)}/A_{(1)}) \tag{3}$$

where $A_{(0)}$ is total inventory of excess Pb-210 in the sediment column, $A_{(1)}$ is inventory of excess Pb-210 below depth x, λ is the decay constant of Pb-210 (0.693/22.3yr = 0.03114/yr) [6]. Mean sedimentation rate was determined from the slope of the least square fit for estimated age plotted versus depth.

Sedimentation rates in lake were found to vary 0.21-0.57 cm y^{-1} and 0.24-0.74 cm y^{-1} with mean sedimentation rate of sediment cores for location S1 and S2 are 0.26 and 0.23 cm y^{-1} respectively (Figure 2). Sedimentation rate determined only for the interval 2-16 and 2-18 cm depth core for S1 and S2 sediment cores. Below this depth, sediment has been dominated by soil or original base of lake. Area bordering former mining areas is left without vegetation and with different contour. Depending on the gradient of bank contour this will facilitated surface runoff of rainwater into the lake that carries along overburden that causes sedimentation at different rate. This may be could be reasonable explanation for dissimilarity of depth in the sediment. Location S1 located almost at the center of lake while S2 located away from the edge of lake but closest to the central of lake. Comparable sedimentation rate for both location could be explained possibly receiving constant water flow thus created thickness of sediment at the both location almost same and have better movement of water velocity with a little obstacle.

In comparison to study by Theng *et al.* (2003) [14] at the coastal water of Sabah, Malaysia showed low sedimentation rate at Sipitang which is 0.027 cm y^{-1} and high sedimentation rate at Teluk Kimanis which is 5.53 cm y^{1} as compared to the present study. Present study showed comparable sedimentation rate with Al - Oteibeh Lake, Syria which is 0.100 - 0.79 cm y^{-1} and Lago Verde crater lake, Mexico which is 0.09 - 0.23 cm y^{-1} [2, 15].

Zaharidah Abu Bakar et al: SEDIMENTATION RATE AND CHRONOLOGY OF As AND Zn IN SEDIMENT OF A RECENT FORMER TIN MINING LAKE ESTIMATED USING Pb-210 DATING TECHNIQUE



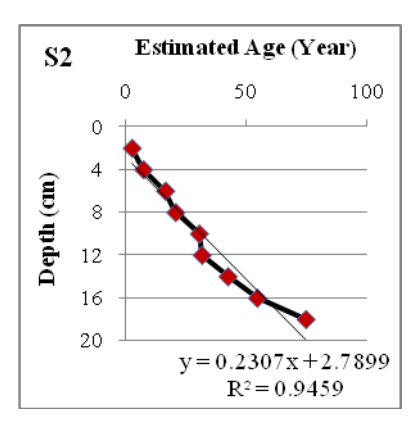


Figure 2: Profile of sedimentation rate in sediment cores

Sediment Chronology

Chronology of sediment was constructed using the CRS model. This is due to the fact that some sediment cores showed non–linear characteristics. Using CRS model, those non–linear features be interpreted by assuming a constant net rate of Pb-210_{exc} supply from the lake waters to the sediment [6]. Using the model, the supply of Pb-210_{exc} to the sediment surface is assumed constant and varying sedimentation rate between each depth. The model assumes no alteration after deposition of Pb-210, although terms of mixing and other diagenetic process can be incorporated into the calculation of dates [16]. The dating model for CRS calculation is expressed as in the equation 3. Depth profiles of Pb-210 activity and metals concentration were determined from same cores. Sediment depth converted to time based and used to date the sediment age then compare to metals contaminant within the period of time. The Pb-210 geochronology allowed the dating of sediments up to depth of 18 cm, corresponding to a period of ~ 40 years as showed in Table 4. Age of sediment core calculated using Pb-210 dating method yields reasonably precise date from ~1940 to present. S1 and S2 showed age of sediment nearly to each other. Age of sediment for core S1 and S2 showed sediment ages ranged 1940 to 2004 and 1939 – 2003 respectively.

Depth (cm) / Point	S1	S2
2	2004	2003
4	2000	1998
6	1994	1991
8	1990	1989
10	1984	1980
12	1978	1977
14	1970	1968
16	1959	1957
18	1940	1939

Table 4: Chronology of sediment age with function of depth

Depth profiles of anthropogenic metal elements concentration with age are showed in Figure 3 and Figure 4. Range of Arsenic (As) and Zinc (Zn) concentration with mean value for S1 and S2 showed in Table 5. Dating method showed small changes of sediment age within similar period and profile concentration of metals particularly were not same at each location. Constant concentration of As could be observed in the bottom sediment at both locations from year of $\sim 1939 - 1980$ possibly due to past mining activities. However, concentration of As increased beginning from year of ~ 1984 to a recent years possibly coincident with intensive development in the region of the

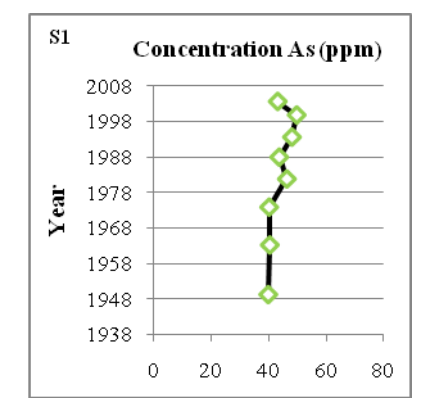
study area also increasing in industrialization and agriculture activities in late ~1990. Increasing of As concentration could be influence by atmospheric deposition as well as combustion, road construction and agricultural activities. Low concentration of As observed in the surface layer of sediment core S1 possibly caused by physical mixing during sampling or bioturbation by benthic microorganisms [17].

Concentration of As in the sediment lake is sensitive to redox changes as well as easily to distinguished either due to remobilization or loading changes [1]. Being a multiple oxidation state element, As is sensitive to redox changes condition in similar manner as Fe and Mn. Since as sensitive elements, As in the deeper sediment could be released into pore water via changes from As (V) to As (III) that is more mobile, soluble and toxic [18]. Some studies suggested high concentration of As at the upper layer could be affected by redox condition and adsorption of As onto Fe or Mn oxides particulate [2]. Thus, by considering of this factor, high concentration of As in the upper sediment core S2 could be possibly affected by redox condition.

	Location	S1	S2
As (ppm)	Range	39.88 – 49.55	33.41 – 104.77
	Mean	43.90	54.51
Zn (ppm)	Range	229.42 - 336.03	136.74 - 150.72
	Mean	266.64	143.68

Table 5: As and Zn concentration in sediment cores

Depth profile of Zn showed almost double concentration of Zn in the sediment core S1 as compared to S2. This is suggests that each location received different rate of metals input, since S1 being centrally location possibly acted as depocenter sedimentary material as mentioned earlier [19]. The other factor possibly due to different water flow rate causes precipitation of pollutants or variable pattern of sediment redistribution in the lake [15, 20]. Contrasting pattern was observed for S1 and S2 which lower at the recent years and vice versa for S2 as showed in Figure 4. Generally high concentration of As and Zn during the last few years possibly due to increasing use of fertilizer and pesticides in agriculture such as in some synthetic phosphorus fertilizer [20] and soil erosion due to human activities. Road construction and land development for housing areas as well as human settlement cause recent erosion in the study area and this coincide with the increase amount of metal introduced into the lake.



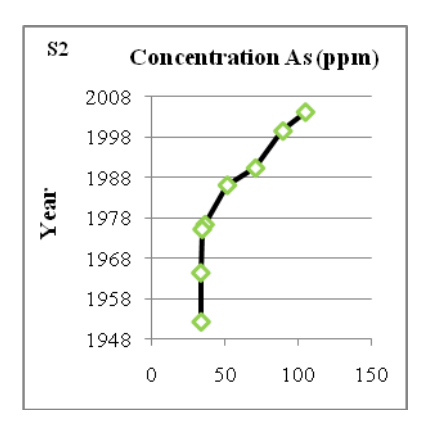
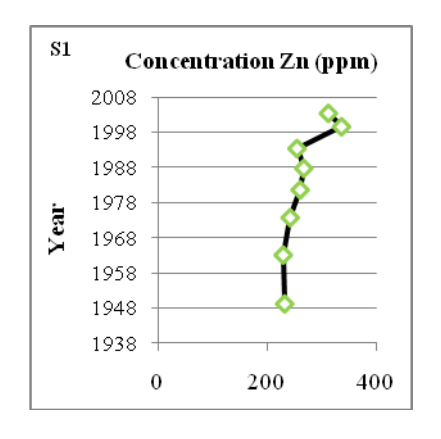


Figure 3: Profile of As concentration with respect to sediment age

Zaharidah Abu Bakar et al: SEDIMENTATION RATE AND CHRONOLOGY OF As AND Zn IN SEDIMENT OF A RECENT FORMER TIN MINING LAKE ESTIMATED USING Pb-210 DATING TECHNIQUE



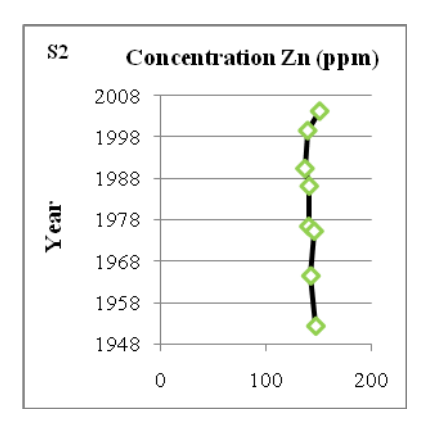


Figure 4: Profile of Zn concentration with respect to sediment age

Result of analysis showed As and Zn elements in sediment lake are good agreement with presence of these metal as earlier study by Ingham & Bradford (1960) [8] in the Geology of Kinta Valley. They were pointed out that As was found in contaminated tin-ore and removed by roasting and washing. The byproduct of As (arsenious oxide) sometimes collected for sale as an insecticide and weed killer. While, Zinc Sphalerite (ZnS) also found from several location in Kinta but there is no significant for economic value. The mineral was identified in a small quantity in limestone pipes.

Conclusion

Pb-210 dating method is applicable technique to establish recent sedimentation rate and sediment chronology in a former tin mining lake. Similar sedimentation rate showed constant flow rate of water yields same sedimentation rate at both locations. An attempt has been made to relate the metals pollution input with temporal changes in a former tin mining lake and chronology of metals input has been successfully determined. Increasing concentration of As and Zn in recent years possibly due to human activities around the lake area.

Acknowledgement

The authors gratefully acknowledge the financial support for this project from FRGS Research grant: 600 – IRDC/T/FRGS. 5/3/1333, UiTM and Malaysian Nuclear Agency (MNA).

References

- 1. Al-Masri, M.S., Aba, H., Khalil, H., and Al Hares, Z., (2002). Sedimentation Rates and Pollution History of a Dried Lake: Al-Oteibeh Lake. *J. Sc. Total Environmental.*, 293: 177-189.
- 2. An huh, C., Sheng C.K., Ling, W.C., and Mei, L.P. (1996). Lead- 210 and plutonium fallout in Taiwan as recorded at a subalpine lake, *J. of Southeast Asia Earth Sciences*., 14, 373-376.
- 3. Appleby, P.G., (2000) Radiometric dating of sediment records in European mountain lakes. J. *Limnol.*, 59: 1 14.
- 4. Balamurugan (1991). Tin Mining and Sediment Supply in Peninsular Malaysia with Special Reference to the Kelang River Basin. *J. The Environmentalist.*, 11: 281-291.
- 5. Binford, W. Michael., Kahl S. Jeffry, and Norton A. Stephen (1993). Interpretation of Pb-210 profile and verification of the CRS dating method in PIRLA project lake sediment cores. *J. Paleolimnology*, 9, 275-296.
- 6. Blais, M. J., Kalff, J., Cornett, R.J., and Evans, R. D., (1995). Evaluation of ²¹⁰Pb dating in lake sediments using stable Pb, *Ambrosia* pollen, and ¹³⁷Cs. *J. of Paleolimnology*, 13: 169 178.
- 7. Bonotto, D.M and Lima, J.L.N.D., (2006). Pb-210 derived chronology in sediment cores evidencing the anthropogenic occupation history at Corumbatai River basin, Brazil. *J. Environ Geol*, 50: 595-611.
- 8. Conrad, C. F., Fugate, D., Daus, J., Brause, C.J.C. and Kuehl, S.A., (2007). Assessment of the historical trace metals contamination of sediments in the Elizabeth River, Virginia. J. *Marine Bulletin.*, 54: 385 395.

- 9. Howarth, R.J., Evans, G., Croudace, I.W. and Chundy, A.B., (2005). Sources and timing of anthropogenic pollution in the Ensenada de San Simon (inner Ria de Vigo), Galicia, NW Spain: an application of mixture modeling and nonlinear optimization to recent sedimentation. *J. Science of the Total Environment*, 340: 149 176.
- 10. Ingham, F.T and Bradford, E.F., (1961). The Geology and Mineral Resources of the Kinta Valley, Perak. Federation of Malaya Ministry of Rural Development, Malaya., 286 304 pp.
- 11. Khalik A.W., Zaharudin, A. Noor, A.M.S., Rosnan, Y., and Carpenter, R., (2004). Metal diagenesis and transport in coastal sediments around Penang Island, Malaysia. *J. Nuclear and Related Technologies*, 1: 1 30.
- 12. Lima, A.L., Hubeny, J., Bradford, Reddy, C.M., King, J.W., Hughen, K.A., and Eglinton, T.I., (2005). High-resolution historical records from Pettaquamscutt River basin sediments: 1. Pb-210 and varve chronologies validate record of Cs-137 released by the Chernobyl accident. *J. Geochimica et Cosmochimica*, 69:1803-1812.
- 13. Li, A., Rockne, K.J., Starchio, N.C., Mills, W.J., Song, W., Ford, J.C., Buckley, D.R., (2006). Chronology of PBDE air deposition in the Great Lakes from sedimentary records. Final Report Great Lake Atmospheric Deposition Program Office Air and Radiation Division USEPA Region V. University of Illinois, Chicago.
- 14. Long, D.T., Giesy, J.P., Simpson, S.J. and Fett, J.D. Inland Lake sediment trends: Sediment analysis results for five Michigan Lakes. Environmental Isotope & Geochemical Laboratories, Michigan State University, Tech. Rep. 1999-2000.
- 15. Ruiz-Fernandez, A.C., Marcel, C.H., Paez-Osuna, F., Ghaleb, B. and Caballero, M., (2007). Pb-210 chronology and trace metal geochemistry at Los Tuxtlas, Mexico, as evidenced by a sedimentary record from the Lago Verde crater lake. *J. Quaternary Research*, 67: 181-192.
- 16. Ruiz-Fernandez, A,C., Paez-Osuna, F., Urrutia-Facugauchi, J., and Preda, M., (2005). Pb-210 geochronology of sediment accumulation rates in Mexico City Metropolitan Zone as recorded at Espajo de los Lirios lake sediment, J. *Catena*, 61: 31-48.
- 17. Sanchez Cabeza, J.A., Masque, P., Ani Rogolta, I., Merino, J., Alvisi, F., Palanques, A., Puig, P., (1999). Sediment Accumulation Rates in the Southern Barcelona Continental Margin (NW Mediterranean Sea) Derived from Pb-210 and Cs-137 Chronology. *J. Oceanography*, 44: 313 332.
- 18. Siong, W.B., Khalik, A.W., Hamzah, M.S., Rahman, S.A., Elias, M.S. and Salim, N.A.A., (2007). Certified reference materials for analytical quality control in Neutron Activation Analysis. *J. Malaysian Analytical Sc*, 11: 17-22
- 19. Schottler, S.P. and Engstrom, D.R., (2006). A chronological assessment of Lake Okeechobee (Florida) sediment using multiple dating markers. J. *Paleolimnol*, 36: 19 -36.
- 20. Theng, T.L., Zaharuddin, A., and Che Abd Rahim, M., (2003). Estimation of Sedimentation Rate Using Pb-210 and Po-210 at the Coastal Water of Sabah, Malaysia. *J. Radioanalytical and Nuclear Chemistry*, 1: 115 120.
- 21. Yang, H. and Rose, N., (2005). Trace element pollution records in some UK lake sediments, their history, influence factors and regional differences. J. *Environment International*, 31: 63–75.
- 22. Zaborska, A., Carroll, J., Papucci, C., Pempkowiak, J. (2007). Intercomparison of alpha and gamma spectrometry techniques used in Pb-210 geochronology. *J. Environment Radioactivity*, 93, 38-50.



MEASUREMENT OF ²²⁶Ra, ²²⁸Ra AND ⁴⁰K IN SOIL IN DISTRICT OF KUALA KRAI USING GAMMA SPECTROMETRY

(Pengukuran ²²⁶Ra, ²²⁸Ra dan ⁴⁰K Di Dalam Taneh Daerah Kuala Krai Menggunakan Spektrometri Gama)

Zaini Hamzah¹, Siti Afiqah Abdul Rahman^{1*}, and Ahmad Saat²

¹Faculty of Applied Sciences, ²Institute of Science, Universiti Teknologi MARA, 40450 Shah Alam, Selangor, Malaysia

*Corresponding author: siti_afiqah@ymail.com

Abstract

The granitic region is known to have high natural radionuclides content. The natural background of the area will be elevated and the exposure rate also will be higher as compared to other region. The present study is focusing on the presence of natural uranium isotopes using its progenies in soils belong to the river basin of the granitic region of Kuala Krai district, Malaysia. Granitic characteristics of the region were believed to produce significant concentrations of natural radionuclide such as uranium and thorium. This paper presents the results of measurement activity concentration 226 Ra, 228 Ra and 40 K in soil using Gamma Spectrometry to estimate activity concentration of radionuclides in fourteen soil samples collected from this study area. The range of activity concentration of 226 Ra, 228 Ra and 40 K is 40.2-264.0, 49.2-312.9 and 491.1-1184.2 Bq/kg respectively. These results were used to estimate the hazards index and annual exposure rate to the member of public.

Keywords: ²³⁸U activity concentration, granitic region, gamma spectrometer

Abstrak

Kawasan granatik telah diketahui mempunyai kandungan radionuklida tabii yang tinggi. Kadar sinaran latar kawasan tersebut juga akan tinggi dan kadar pendedahan terhadap manusia juga akan lebih tinggi berbanding dengan kawasan lain. Kajian ini memberikan fokus kepada pengesanan isotop uranium tabii menggunakan progeninya di dalam taneh yang di ambil dari kawasan granit di Daerah Kuala Krai, Malaysia. Sifat-sifat granitik kawasan ini dipercayai mempunyai kepekatan radionuklida tabii seperti uranium dan torium yang signifikan. Kertas kerja ini membentangkan hasil kajian pengukuran ²²⁶Ra, ²²⁸Ra dan ⁴⁰K di dalam taneh menggunakan spektrometri gama bagi menentukan kepekatan aktiviti radionuklida di dalam empat belas sampel taneh dari kawasan kajian. Julat pengukuran bagi ²²⁶Ra, ²²⁸Ra dan ⁴⁰K masing-masing 40.2-264.0, 49.2-312.9 dan 491.1-1184.2 Bq/kg. Keputusan ini telah digunakan untuk mengira indeks berbahaya dan kadar pendedahan tahunan terhadap penduduk setempat.

Kata kunci: Kepekatan aktiviti ²³⁸U, kawasan granit, spektrometer gama

Introduction

Kuala Krai is one of the districts in Kelantan and the second largest after Gua Musang District. Kuala Krai has an area of 2.329 km², bordering with Machang in the North and Gua Musang in the South, while the East is adjacent to the Terengganu and Jeli in the West. It is located on granites set which is an undifferentiated intrusive rock. It can be categorized into two sets which are coarse grain and fine grain. Coarse grain consists of pink granite, adamellite, diorite and granodiorite. Fine grain consists of rhyolite and dacite. Besides, there are lots of non-metallic mineral (clay, bell clay, kaolin, silica, barytes, serpentine, limestone, and dolomite), light metals in heavy minerals (e.g. ilmenite rutile) and other metals such as iron, manganese, chromium, copper, zinc, lead, gold and even uranium [1].

Information of distribution pattern of radionuclides in the soils is absolutely necessary in controlling radiation exposure level and can give some details or changes in the background on natural sources of radionuclides [2,3,4]. The natural radioactivity of soil and sediment depends on the soil and sediment formation and transport process that involving chemical and biochemical interactions that influence the distribution patterns of uranium, thorium and their decay products [5]. Although widely distributed, their concentration in the environment is believed to depend on the local geological conditions [6].

There were several studies on the measurement of radionuclides in Malaysia such as a few studies done by ESCAN (Environmental Studies using Conventional and Nuclear Techniques) group from UiTM. They have done studies on low level radionuclides in palm oil area in Jengka, Pahang, former tin mining area in Kg. Gajah, Perak and tourism beach areas on the peninsular side in Malaysia [7,8,9]. Those studies can be used as a guide as well as risk assessment to evaluate the possible exposure level to the natural radiation. However, until now, no similar study has been done in Kelantan, thus, this paper is aimed to set a baseline data for any possible environmental conditions which can be used for a future reference for any anthropogenic activities.

Measurement of ²²⁶Ra, ²²⁸Ra dan ⁴⁰K in soil using Gamma Spectrometer is reliable and preferably because it is an established method. Gamma Spectrometry is a convenience method with simple preparation procedure and simultaneously determined many radionuclides in a sample [10,11].

The objectives of the present study, are to measure the activity concentration of 226 Ra, 228 Ra dan 40 K in soil samples collected from district of Kuala Krai in Kelantan, to estimate the radium equivalent activity (Ra_{eq}), total absorbed dose rate (D), external hazard index (H_{ex}) and annual effective dose. The finding will be used as a baseline data in estimating the exposure to the background radiation for the Kelantan's population.

Method

Sampling site

The top soil samples were collected along Sungai Kelantan and its tributaries in the district of Kuala Krai. Figure 1 shows a map of sampling points in the study area, while Table 1 shows the coordinates of the sampling point obtained by using GPS.

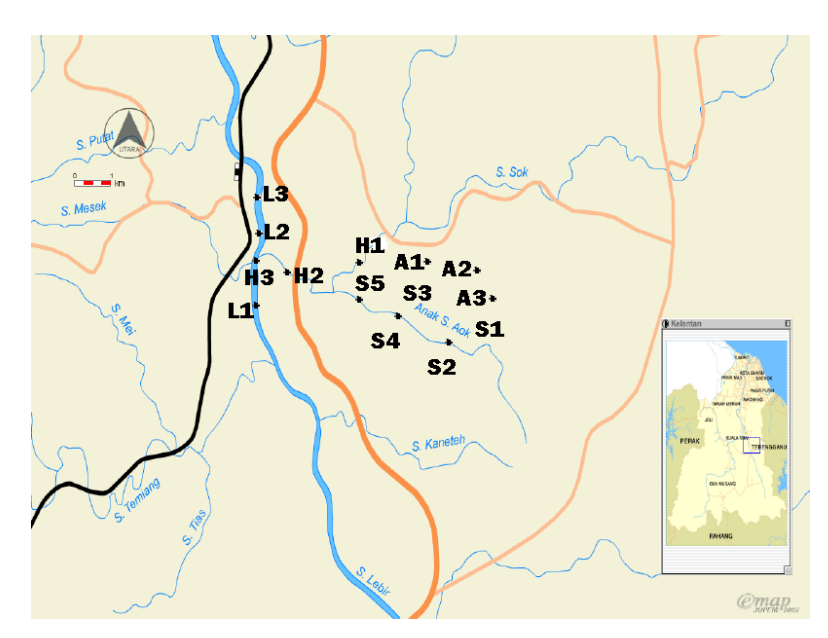


Figure 1: Maps of Sampling Points

Samples were collected at two types of locations, the one at hill and the other is along river. The area was chosen because of its potential of having uranium deposit and as well rich with other minerals. This area also is sitting on the granitic, giving another reason of choosing this area, because granitic rock usually has some amount of uranium deposit. The coordinates of the sampling points are given in the Table 1.

Sample Code	Location	Coordinates
A1		-
A2	Hilly area	N05°21.372', E102°17.554'
A3		N05°21.379', E102°17.339'
S1		N05°22.231', E102°15.042'
S2		N03 22.231 , E102 13.042
S3	Small river	NO5922 262' E102914 094'
S4		N05°22.262' , E102°14.984'
S5		N05°22.311', E102°15.184'
H1		N05°22.514', E102°16.605'
H2	Small river	N05°22.789', E102°16.186'
Н3		N05°22.486', E102°14.141'
L1		N05°22.133', E102°14.233'
L2	Main river	N05°22.680', E102°14.332'
L3		N05°23.253', E102°14.195'

Table 1: Sampling location, condition and the coordinates of the area.

Sampling and samples preparation

Soil samples were taken at 15 cm depth using hand auger at five different holes at each sampling point as to represent the location. All the stones, grass, root and the non-soil were taken out before transferred it into the plastic bags. The samples were then dried at 60° C until the constant mass. The dried samples were then ground using Agate bowl mill and sieved through 250 μ m aperture mesh to homogenize them. After that, those samples were transferred into 500 ml plastic container and sealed for at least three weeks to reach the secular between radium and the corresponding daughters.

Instrumentation

All measurements was performed with gamma spectrometer on an ORTEC coaxial HPGe detector having 1.85 keV energy resolution with a relative photo peak efficiency of 25%, at 1332 keV 60 Co gamma ray. The associated electronics consisted of a multi channel analyzer (MCA) allowing the determination of the uranium and thorium series radionuclide. For γ -analysis, the samples were placed directly over a coaxial HPGe detector. The sample counting time was 21600 seconds. The integrated counts for energy peaks of 226 Ra, 228 Ra and 40 K were analysed. Spectra analysis was done using Gamma Vision software. The efficiency calibration of the spectrometer was obtained using analytical grade UO₃ ore in KCl matrix prepared in UiTM laboratory [12].

Results and Discussion

Activity concentration of three radionuclides which are ²²⁶Ra, ²²⁸Ra and ⁴⁰K have been analyzed using gamma energy of 609, 911.2 and 1460 keV respectively. These energy peaks were chosen because of its high intensity which is 0.461, 0.29 and 0.107 respectively. Activity concentrations of ²²⁶Ra, ²²⁸Ra and ⁴⁰K in samples were calculated in Bq/kg. For this measurement, the Minimum Detectable Activity (MDA) was estimated to be about 1.5 Bq/kg [7].

Table 2 lists the activity concentrations of 226 Ra, 228 Ra and 40 K measured in 14 soil samples. The result shows a pattern whereby the hilly areas have the activity concentration of about two times higher than along the rivers. The activity concentration of 226 Ra (uranium series) is in the range of 143.4-264.0 Bq/kg at the hilly areas while 40.2-

Zaini Hamzah et al: MEASUREMENT OF ²²⁶Ra, ²²⁸Ra AND ⁴⁰K IN SOIL IN DISTRICT OF KUALA KRAI USING GAMMA SPECTROMETRY

182.1 Bq/kg along the river. It shows the hilly area has more uranium content in the soil, we need to do a thorough study in this area in order confirm that it has a potential uranium deposits.

Similarly with thorium series, the activity concentration of 228 Ra in the samples from the hilly area especially A1 and A3 also give higher value than others, i.e. 312.9 and 273.6 Bq/kg respectively. Generally, Th always presents with U in soil and give normal ratio about 1-3. Another sampling point that is H2 gives higher value of 284.4 Bq/kg. The ratio of 228 Ra/ 226 Ra shows that from this study area is in the range of 0.6-1.6.

Unlike ²²⁶Ra and ²²⁸Ra, the activity concentrations of ⁴⁰K show the highest value at H1 sampling point, with the value of 1184.2 Bq/kg. Activity concentration of ⁴⁰K does not give any effect on the concentration on uranium in soil, since ⁴⁰K does not belong to any uranium or thorium series. ⁴⁰K exists naturally and it can be elevated by the anthropogenic activities, such as fertilizer application in the agricultural area. Generally ⁴⁰K activity concentrations is higher in the samples collected along the river than the hilly area. This could be due to river system where it was flooded during the monsoon season and will deposits it potassium content along the river bank.

Sample Code	Activity	Activity	Activity	²²⁸ Ra/ ²²⁶ Ra
Sumpre Code	Concentration ²²⁶ Ra	Concentration ²²⁸ Ra	Concentration	ratio
	(Bq/kg)	(Bq/kg)	⁴⁰ K (Bq/kg)	Tutto
A1	264.0±16.2	312.9±17.7	649.5±25.5	1.2
A2	143.4±12.0	166.8±12.9	559.9±23.7	1.2
A3	251.1±15.8	273.6±16.5	491.1±22.2	1.2
S1	124.7±11.2	168.6±13.0	1005.4±31.7	1.1
S 2	159.6±12.6	192.6±13.9	932.8±30.5	1.4
S 3	120.6±11.0	160.0±12.6	988.6±31.4	1.3
S4	162.9±12.8	213.2±14.6	820.7±28.6	1.3
S5	130.5±11.4	199.1±14.1	646.1±25.4	1.5
H1	122.7±11.1	148.5±12.2	1184.2±34.4	1.2
H2	182.1±13.5	284.4±16.9	671.6±25.9	1.6
Н3	47.1±6.9	54.2±7.4	498.4±22.3	1.2
L1	122.7±11.1	71.7±8.5	671.0±25.9	0.6
L2	75.0±8.7	100.4±10.0	599.9±24.5	1.3
L3	40.2±6.3	49.2±7.0	650.4±25.5	1.2
*Malaysia				
average	67(38-94)	82(63-110)	310(170-430)	1.3
* Recommended	35	30	400	-
Value				

Table 2: Activity concentration of ²²⁶Ra, ²²⁸Ra and ⁴⁰K in soil samples

Table 3 shows the corresponding total absorbed dose rate (D), radium equivalent activity (Ra_{eq}), external hazard index (H_{ex}) and annual effective dose for each samples. The calculation was done using the reviewed equations below. The absorbed dose rate of gamma-rays is the estimate of amount of radiation receive or deposited onto human, therefore there is a need to calculate this value since there are villages along the rivers where the population are exposed to the gamma radiation. The radium equivalent activity and external hazard index are calculated to assess the radiological hazard index of soils. The annual effective dose is also higher than other places, thus it may affect the health of the human.

The contribution of natural radionuclides in absorbed dose rate is depending on the activity concentration of ²²⁶Ra (uranium series), ²²⁸Ra (thorium series) and ⁴⁰K. It is a total ionizing dose and is divided by the time it takes to deliver the dose. The high dose rate usually can cause more harm and damage to the human body than low dose

^{*}UNSCEAR (2008), in bracket is the range value

rates. The absorbed dose rate for area under investigation is tabulated in Table 3. The highest value of absorbed dose rate is from A1 and A3 which are 343.5 and 306.5 nGy/hr respectively. The value from this study is much higher than value found by Kurnaz [13], where the absorbed dose rate in air at Firtina Valley is ranging from 19.1 to 149.6 nGy/hr. It is also beyond the international recommended value which is 55 nGy/hr [14].

Absorbed Dose Rate =
$$0.461C_{Ra} + 0.623C_{Th} + 0.0414C_{K}$$
 (1)

Radium equivalent activity (Ra_{eq}) is a term of radiation hazard that is widely used to set a limit or regulatory regarding total activity of radionuclides. It is assumed that 370 Bq/kg of 226 Ra, 259 Bq/kg of 232 Th and 4810 Bq/kg of 40 K produce the same gamma-ray dose [15,16,17]. S3 shows the biggest value which is 761.4 Bq/kg suggested that total activity of radionuclides from this place are the highest among others. S5 and H2 also give slightly higher than the other places with 680.2 and 640.5 Bq/kg respectively. Thus, the exposure of radiation to human that lives around the area should be monitored as it can affect the health of people.

Radium equivalent =
$$C_{Ra} + 1.43C_{Th} + 0.077C_{K}$$
 (2)

External hazard index (H_{ex}) is another one of index that has been widely used to set a limit of exposure to human. The external hazard index is ranging from 0.43 to 2.02 with the highest value at points A1 and S1. It can be considered as a high value because the limit of external hazard index is 1.00, thus will affect the health of public or villagers around this area.

External Hazard Index =
$$C_{Ra}/370 + C_{Th}/259 + C_{K}/4810$$
 (3)

Annual effective dose is an estimate of the stochastic effect of radiation on human. It takes into account that people spend the times outdoor only 20% of the day, the dose received from natural radioactivity range from 0.09-0.42 mSv/yr.

Annual Effective Dose =
$$D (nGy/h) \times 8760 (h/year) \times 0.2 \times 0.7 (Sv/Gy) \times 10^{-6}$$
 (4)

Table 3: Sample codes as well as calculated absorbed dose rates, radium equivalent, external hazard index and Annual Effective Dose and In-situ surface dose.

Sample Code	D	Ra _{eq}	H _{ex}	Annual	In-situ	In-situ 1m
	(nGy/hr)	(Bq/kg)		Effective Dose	surface dose	above the
				(mSv/yr)	(µSv/hr)	ground dose
						(µSv/hr)
A1	343.5	443.2	2.06	0.25	0.58	0.57
A2	193.2	506.8	1.15	0.28	0.50	0.54
A3	306.5	425.5	1.84	0.24	0.55	0.54
S1	204.1	530.9	2.20	0.30	0.53	0.55
S2	232.2	465.0	1.37	0.26	0.49	0.46
S3	196.2	761.4	1.15	0.42	0.41	0.50
S4	241.9	425.1	1.43	0.24	0.57	0.56
S5	211.0	680.2	1.26	0.38	0.72	0.68
H1	198.1	426.3	1.15	0.24	0.46	0.60
H2	288.9	640.5	1.73	0.35	0.18	0.21
Н3	76.10	163.0	0.44	0.09	0.17	0.22
L1	129.0	276.9	0.75	0.16	0.39	0.34
L2	121.9	264.7	0.71	0.15	0.32	0.31
L3	76.10	160.7	0.43	0.09	0.38	0.39

A correlation study between annual effective doses with in-situ dose rate was carried out, as shown in **Figure 2**. There is no strong correlation between them as the points are scattered around and no trends are obtained. This indicates that the measured surface doses and annual effective doses are not correlated. It is also indicates that not only these three radionuclides that contribute to the radiation in the area but other radionuclides also exist and contribute to the surface dose rate.

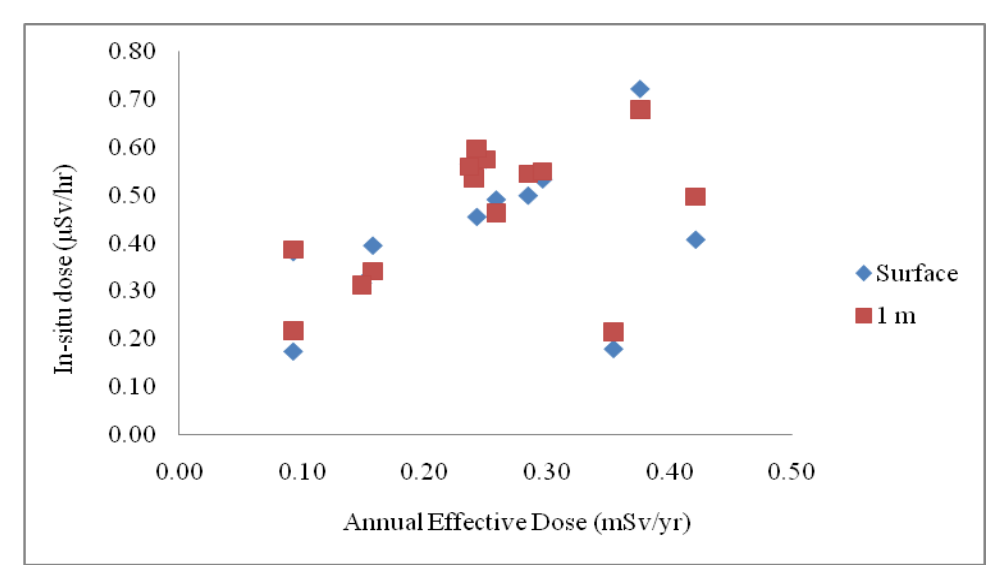


Figure 2: Correlation between Annual Effective Dose and in-situ dose measurements

Table 4 shows the comparison of the present study with the studies in Malaysia as well as in the whole world. Generally, most of the samples from the present study give values exceeded the international recommended value. It is slightly higher than the value obtained in Jengka, Pahang and beach areas. The value from Kg. Gajah, Perak, is higher than this study due to the former tin mining area with historical ore processing and smelting activities. Comparing to the world average, Kelantan area still on higher average level in terms of radiation level except for the annual effective dose.

Table 4: Comparison of the activity concentration of ²²⁶Ra, ²²⁸Ra and ⁴⁰K in soil samples as well as calculated absorbed dose rates, radium equivalent, external hazard index and absorbed dose rates with the literature.

Region		Concentration	D	Ra _{eq}	H _{ex}	AED	References	
Region	²²⁶ Ra	²²⁸ Ra	40 K	(nGy/hr)	(Bq/kg)	11 _{ex}	(mSv/yr)	References
Kuala Krai, Kelantan, Malaysia	40.2-264.0	49.2-312.9	491.1- 1184.2	76.1- 343.5	160.7- 761.4	0.43- 2.02	0.09- 0.42	Present study
Tourism Beach Areas, Malaysia	7.3-51.0	5.9-58.4	32-1293	9.05- 90.09	18.3- 189.3	0.05- 0.51	0.05- 0.55	Ahmad <i>et al.</i> , (2011)
Jengka 15, Pahang, Malaysia	16.6-22.1	22.4-33.8	55.5-243	25.76- 42.41	53.5- 91.4	0.16- 0.25	0.78x10 ⁻⁴ -1.42x10 ⁻⁴	Masitah Alias <i>et. al.</i> , (2008)
Kg. Gajah, Perak, Malaysia	199-12932	1215- 32330	21-9304	558.7- 35951.2	-	3.43- 220.36	-	Zaini Hamzah <i>et.</i> <i>al.</i> , (2008)

Turkey (Firtina	15.29-		105.35-	19.12-	44.92-	0.12-	0.0234-	Kurnaz et
Valley)	188.26	ı	1234.65	149.58	385.85	1.04	0.1834	al. (2007)
Kinta District, Perak, Malaysia	12-426	19-1377	19-2204	39-1039	52- 2227	-	-	Lee <i>et al.</i> (2009)
Burullus Lake, Eqypt	6.1-40	4.3-44.3	224-341	14.6- 51.6	30.1- 112.7	-	-	El-reefy <i>et al.</i> (2006)
Dhaka City, Bangladesh	21-43	34-81	402-750	ı	ı	ı	ı	Miah <i>et. al.</i> , (1998)
Aldama, Chihuahua, Mexico	44.6-460.5	41.9-77.0	807.5- 1766.2	220.4- 83.8 (nSv/hr)	ı	ı	0.44- 0.73	Sujo <i>et. al.</i> , (2004)
Inshaa, Cairo	5.3-7.7	10.7-17.0	152-202	-	-	-	-	Higgy & Pimpl, (1998)
*World Average Range	16-116	7-50	100-700	44	370	-	0.3-0.6	UNSCEAR (2000).

^{*}UNSCEAR (2000)

Conclusion

The environmental radioactivity monitoring of 14 soil samples from the region of having the potential uranium deposits showed high activity concentration of 226 Ra range from 40.2-264.0 Bq/kg. The activity concentration of 228 Ra ranges from 49.2-312.9 Bq/kg and activity concentration of 40 K 491.1-1184.2 Bq/kg, which are comparable with literature. This maybe attributed from the granitic region of that area that been believed to have a potential uranium deposit. From the activity concentration of these radionuclides, external hazard index (H_{ex}) of the area range is 0.43-2.02. This study can be used as the baseline data and can be used as reference data for monitoring any pollution for future study in that area or neighboring place.

Acknowledgement

We would like to thank Research Management Institute (RMI) of UiTM for providing grant through Excellence Fund and also Malaysian Nuclear Agency for providing facility for sample preparation.

References

- 1. Zaini Hamzah, Siti Afiqah Abdul Rahman, Ahmad Saat, Siti Shahrina Agos, Zaharuddin Ahmad, (2010). Measurement of ²²⁶Ra in River Water using Liquid Scintillation Counting Technique. *Journal of Nuclear and Related Technologies*. **7**: 12-23.
- 2. Miah, F.K., Roy, S., Touhiduzzaman, M. and Alam, B., (1998). Distribution of Radionuclides in Soil Sample in and around Dhaka City. *Applied Radiation & Isotopes*. **49**: 133-137.
- 3. A., El-Bahi, S.M., Ahmed, F., Abdel-Haleem, A.S., (2001). Natural Radioactivity and Radon Exhalation Rate of Soil in Southern Egypt. *Applied Radiation & Isotopes*. **55**: 873-879.
- 4. Chiozzi, P., Pasquale, V., Verdoya, M., (2002). Naturally Occurring Radioactivity at the Alps-Apennines Transition. *Radiation Measurement*. **35**: 147-154.
- 5. Myrick, T.F., Berven, B.A. and Haywood, F.F., (1983). Determination of Concentration of Selected Radionuclides in Suface Soil in the US. *Health Physics*. **58**: 417-418.
- 6. Tenniseen, A.C., (1994). Nature of earth materials. Printice-Hall, NJ07632: 333-334.
- 7. Ahmad Saat, Zaini Hamzah, Hamimah Jamaluddin, Husna Mardhiah Muda, (2011). Assessment of Outdoor Radiation Hazard of Natural Radionuclides in Tourism Beach Areas. Proceeding of 3rd International Symposium & Exhibition in Sustainable Energy & Environment,1-3 June 2011, Melaka, Malaysia. 123-127.
- 8. Masitah Alias, Zaini Hamzah, Ahmad Saat, Mohamat Omar, Abdul Khalik Wood, (2008). An Assessment of absorbed Dose and Radiation Hazard Index from Natural Radioactivity. *Malaysian Journal of Analytical Sciences*. **12**: 195-204.

Zaini Hamzah et al: MEASUREMENT OF ²²⁶Ra, ²²⁸Ra AND ⁴⁰K IN SOIL IN DISTRICT OF KUALA KRAI USING GAMMA SPECTROMETRY

- 9. Zaini Hamzah, Ahmad Saat, Noor Hayati Mashuri, Seh Datul Ridhuan, (2008). Surface Radiation Dose and Radionuclide Measurement in Ex-Tin Mining Area, K. Gajah, Perak. *Malaysian Journal of Analytical Sciences*. **12**: 419-431.
- 10. Saïdou, Bochud, F., Laedermann, J.P., Njock, M.G.K. and Froidevaux, P., (2008). A Comparison of Alpha and Gamma Spectrometry for Environmental Natural Radioactivity Surveys. *Applied Radiation & Isotopes.* **66**: 215-222.
- 11. Garcia-Talavera, M., (2003). Evaluation of the Suitability of Various γ Lines for the γ Spectrometric Determination of ²³⁸U in Environmental Samples. *Applied Radiation & Isotopes*. **59**: 165-173.
- 12. Ahmad Saat, Zaini Hamzah, Mohammad Fariz Yusop, Muhd Amiruddin Zainal, (2010). Experimental Determination of the HPGe Spectrometer Efficiency Calibration Curves for Various Sample Gometry for Gamma Energ from 50 keV to 2000 keV. *Progress of Physics Research in Malaysia*. 39-42.
- 13. Kurnaz, A., Küçükömeroğlu, B., Keser, R., Okumusoglu, N.T., Korkmaz, F., Karahan, G., and Çevik, U., (2007). Determination of Radioactivity Levels and Hazards of Soil and Sediment Samples in Firtina Valley (Rice, Turkey). *Applied Radiation & Isotopes*. **65**: 1281-1289.
- 14. UNCSEAR, United Nations Scientific Committee on the Effect of Atomic Radiation, (2000). Sources, effects and risk of Ionizing Radiation, United Nations, New York.
- 15. Beretka, J., Mathew, P.J., (1985). Natural Radioactivity of Australian Building Materials, Industrial Wastes and By-products. *Health Physics*. 48(1): 87-95.
- 16. Iqbal, M., Tufail, M., and Mirza, S.M., (2000). Measurement of Natural Radioactivity in Marble Found in Pakistan using a NaI(TI) Gamma-ray Spectrometer. *Journal of Environmental Radioactivity*. **51**: 255-265.
- 17. Lee, S.K., Wagiran, H., Ramli, A.T., Apriantoro, N.H., Wood, A.K., (2009). Radiological monitoring: terrestrial natural radionuclides in Kinta district, Perak, Malaysia. *Journal of Environmental Radioactivity*. **100**: 368-374.
- 18. El-Reefy, H.I., Sharshar, T., Zaghloul, R., and Badran, H.M., (2006). Distribution of Gamma-ray Emitting Radionuclides I the Environment of Burullus Lake: I. Soils and Vegetations. *Journal of Environmental Radioactivity*. **87:** 148-169.
- 19. Sujo, L.C., Cabrera, M.E.M., Villalba, L., Villalobos, M.R., Moye, E.T., León, M.G., Tenorio, R.G., Garcia, F.M., Peraza, E.F.H., Aroche, D.S., (2004). Uranium-238 and Thorium-232 Series Concentrations in Soil, Radon-222 indoor and Drinking Water Concentrations and Dose Assessment in the City of Aldama, Chihuahua, Mexico. *Journal of Environmental Radioactivity*. 77: 205-219.
- 20. Higgy, R.H., and Pimpl, M., (1998). Natural and Man-made Radioactivity in Soils and Plants Around the Research Reactor of Inshass. *Applied Radiation & Isotopes*. **49(12)**: 1709-1712.
- 21. UNCSEAR, United Nations Scientific Committee on the Effect of Atomic Radiation, (2008). Sources and Effects of Ionizing Radiation. Report to General Assembly with Scientific Annexes, United Nations, New York.
- 22. UNCSEAR, United Nations Scientific Committee on the Effect of Atomic Radiation, (1993). Exposure from Natural Sources of Radiation, United Nations, New York.
- 23. Huy, N.Q. and Luyen, T.V., (2004). A Method to Determine ²³⁸U Activity in Environmental Soil Samples by Using 63.3-keV-photopeak-gamma HPGe Spectrometer. *Applied Radiation & Isotopes*. **61**: 1419-1424.



DETERMINATION OF SIX PHTHALATES IN POLYPROPYLENE CONSUMER PRODUCTS BY SONICATION-ASSISTED EXTRACTION/GC-MS METHODS

(Penentuan Enam Ftalat dalam Produk-Produk Konsumer Polipropilena dengan Kaedah Ekstraksi Bantuan-Sonikasi/GCMS)

Chong Kian Wei*, Loke Chui Fung and Michelle Pang

Chemistry and Biology Division, School of Arts and Science, Tunku Abdul Rahman College, Jalan Genting Kelang, Setapak, 53300 Kuala Lumpur, Malaysia

*Corresponding author: chongkw@mail.tarc.edu.my

Abstract

Studies on determination of six kinds of phthalates, i.e. dimethyl phthalate (DMP), diethyl phthalate (DEP), dibutyl phthalate (DBP), benzyl butyl phthalate (BBP), di-(2-ethylhexyl) phthalate (DEHP), and di-n-octyl phthalate (DnOP), in three kinds of plastic containers for food use, including food container, instant noodle cup and snack container, by gas chromatography in combination with mass spectrometry detector (GC-MS) in electronic ionization mode with selected-ion monitoring (SIM) acquisition method (GC-MS(EI-SIM)) have been carried out. Extraction, clean-up and analysis methods have been developed and optimized. Determination of samples were performed after sonication-assisted extraction with 1:9 toluene and dichloromethane, clean-up with Bio-Beads S-X8 gel-permeation column and analyzed by GC-MS methods. The characteristic ions, 163, 194 for DMP; 149, 177, 222 for DEP; 149, 233, 251 for DBP; 91, 149, 206 for BBP; 149, 176, 193 for DEHP; 149, 167, 279 for DNOP were chosen for quantitative studies. These techniques are possible to detect phthalates at the level of 1-70 mg/kg. The overall recoveries were 79.2-91.1% with relative standard deviation (R.S.D.) values at 3.1-11.3%. Only DEHP was detected in the studied samples.

Keywords: Phthalates; Polypropylene Products; Sonication-assisted extraction; GC-MS (EI-SIM); Recoveries

Abstrak

Pengajian penentuan enam jenis ftalat, iaitu dimetil ftalat (DMP), dietil ftalat (DEP), dibutil ftalat (DBP), benzyl butyl ftalat (BBP), di-(2-ethylhexyl) ftalat (DEHP), dan di-n-oktil ftalat (DnOP), dalam tiga jenis bekas plastik untuk kegunaan makanan, termasuk bekas makanan, cawan mee segera dan bekas makanan ringan, dengan menggunakan kromatografi gas bergabung dengan pengesan spektrometer jism (GC-MS) dalam mod pengionan elektronik bersama-sama kaedah pengambilalihan (GC-MS (EI-SIM)) pemantauan ion-selektif (SIM) telah dilakukan. Kaedah ekstraksi, pembersihan dan analisis telah dibangunkan dan dioptimumkan. Penentuan sampel dijalankan setelah ekstraksi bantuan-sonikasi dengan menggunakan pelarut toluena dan diklorometana 1:9, pembersihan dengan turus perembesan-gel S-X8 Bio-Beads dan dianalisis dengan kaedah GC-MS. Ciri ionion, 163, 194 untuk DMP, 149, 177, 222 untuk DEP, 149, 233, 251 untuk DBP, 91, 149, 206 untuk BBP, 149, 176, 193 untuk DEHP, 149, 167, 279 untuk DNOP telah dipilih untuk kajian secara kuantitatif. Teknik ini boleh mengesan ftalat pada paras 1-70 mg/kg. Pemulihan keseluruhan adalah 79.2-91.1% dengan nilai sisihan piawai relatif (SPR) sebanyak 3.1-11.3%. Hanya DEHP dikesan pada sampel yang dikaji.

Kata kunci: ftalat; produk polipropilena; exstraksi bantuan-sonikasi; GC-MS(EI-SIM); Pemulihan

Introduction

Nowadays people are easily exposed to phthalates (phthalic acid esters, PAEs) particularly infant. Besides having carcinogenic and estrogenic effects to human, some of the phthalates are toxic and able to induce asthma [1]. The exposure mainly due to the characteristic of phthalates, which is not chemically bound to the polymeric material, therefore; can leach to the environment. Infants have the highest tendency to expose to phthalates because they tend

Chong Kian Wei et al: DETERMINATION OF SIX PHTHALATES IN POLYPROPYLENE CONSUMER PRODUCTS BY SONICATION-ASSISTED EXTRACTION/GC-MS METHODS

to put their toys or pacifiers, which may contain phthalates into their mouth. Phthalates in toys which are specifically designed to be chewed by infant may leach into their saliva and then ingested into their stomach. Although the leached phthalates in the saliva are low, the amount is high enough to cause adverse effects to the infant such as liver, reproductive tract and kidney disorders. Cancer is the adverse effect for more serious cases [2]. Due to these effects, many countries in Europe such as Austria, Denmark, Finnish, Greece and Danish had banned the use of phthalates additives in various soft PVC toys and childcare products for children under three years old at the end of the 1990s. Other countries such as Finnish and Danish had stipulated a permissible limit for each relevant phthalates in these products, which should not more than 0.05% [3,4]. Phthalates are widely used as plasticizers in the manufacturing of plastics especially for food packaging. It was suspected to be the endocrine disrupter agents and has estrogen-like structure which is able to displace the estrogen activity [5]. This will further affect the hormone growth and produce breast cancer cells. Human beings have high possibility to be exposed to phthalate esters since these compounds are widely used in the production of agricultural, industrial and household detergents. Dibutyl phthalate (DBP) tends to impair androgen-dependent development for the male reproductive system [6] and inhibits the production of testosterone. This phthalate can be rapidly absorbed into the systemic circulation and spread through the body in a short time. Mono-2-ethylhexyl phthalate, which is one of the urinary metabolites, was detected in the urine content of the workers, who were exposed to high concentration of diethyl phthalate (DEP), dibutylphthalate (DBP), and di(2-ethylhexyl) phthalate (DEHP) mono-2-ethylhexyl phthalate in several PVC production factories. This causes the workers have lower concentration of testosterone compared to the other normal individuals [7]. The US Food and Drug Administration's Center for Devices and Radiological Health and Health Canada have reported the risk assessment of DEHP that migrated from PVC medical devices in hospitalized patients [8].

The analysis of polymer can be considered as two-stage procedure which includes the extraction of the additives from the polymer followed by their identification and quantification. Conventionally, additives in polymer samples are extracted by Soxhlet liquid extraction method. The disadvantages of this method are large volume of solvent and bigger amount of sample are required, long extraction time, contamination and loss of some of the analytes in the preconcentration steps [9]. During the last few years, several methods were proposed for the determination of phthalates by gas chromatography (GC) and high performance liquid chromatography (HPLC) preceded by different preconcentration techniques such as liquid-liquid extraction (LLE), solid-phase extraction (SPE), and solid-phase microextraction (SPME) [10]. SPME has important advantages over conventional extraction techniques because it is solvent free, fast, portable and easy to be used. However, the fiber used in this method has limited life time due to the fragility and degradation. Therefore, liquid-phase microextraction (LPME) is developed as an alternative extraction technique, which uses only a few microliters of organic solvent. The advantages of using LPME are fast, inexpensive and involving very simple equipments [11]. Supercritical Fluid Extraction (SFE) is a relatively new sample preparation method. An additional advantage of SFE is its selective extraction which can be performed by changing conditions, temperature and density of the fluid [9] with the condition that the liquid solvent must be compatible with the analyte. Gel permeation chromatography (GPC), which is able to separate the macromolecules from the smaller molecules with the use of porous gels or rigid inorganic packing particles is gaining attention recently. According to Kostanski et al. [12], GPC could reproducibly and accurately provide molecular weight distribution and molecular weight averages for linear homo- and uniform composition copolymers under a proper calibration.

In this paper, the studies of gas chromatography in combination with mass spectrometry detector (MSD) for the determination of six kinds of phthalates, i.e. dimethyl phthalate (DMP), diethyl phthalate (DEP), dibutyl phthalate (DBP), benzyl butyl phthalate (BBP), di-(2-ethylhexyl) phthalate (DEHP), and di-n-octyl phthalate (DnOP), in plastic products for food use have been reported. A gel permeation chromatography technique was developed, which was able to separate the phthalates from the dissolved polymer. Three kinds of plastic containers for food use, including food container, instant noodle cup and snack container were tested. Approximate two to three characteristic ions of each phthalate were selected for quantitative studies. The method was evaluated by investigating the accuracy and precision of the spiked samples and the developed method was applied for the determination of phthalates in three kinds of real samples.

Experimental

Apparatus and chemicals

A Model U-2000 UV/Vis spectrophotometer (Hitachi, Japan) was used for photometric measurements. A Spectrum 100 fourier transform infrared (FTIR) (Perkin Elmer, USA) coupled with attenuated total Reflectance (ATR) was used to identify the sample material. The concentration of phthalates was measured using a gas chromatograph (Model 7890A, Agilent Technologies. Inc., USA) equipped with mass spectrometer (Model 5975C), automatic liquid sampler (Model 7683B) and Enhanced Chemstation software (version E.02.00.493). An ultrasonic sonicator (JAC Ultrasonic 2010, Kodo-Tech Research Co. Ltd) was used in sample extraction.

DMP, DEP and DBP with purity of 99% were purchased from ACROS organic-New Jersey, USA. DEHP (99%), DnOP (99%), BBP (98%) and amorphous polypropylene were purchased from ALDRICH Chemistry USA. Analytical grade dichloromethane and toluene were purchased from Fisher Chemicals and SYSTERM®ChemAR and used after undergone distillation. Bio-Beads S-X8 (200-400 mesh size) was purchased from Bio-Rad Laboratories Inc., USA. Chromatographic glass column was purchased from PLT Scientific Private Limited, Malaysia.

Standards and spiked samples

Standards were prepared in a mixture of toluene and dichloromethane at the ratio of 1:9. The stock mixture solution of the six phthalates standards at concentration of 6000 mg/L was prepared and stored at 4 °C. Suitable working solutions with concentration in the range of 5-35 mg/L were prepared from the stock solution to establish the calibration curves. The calibration curves were plotted by peak area versus concentration. Standards with single phthalate at 5 mg/L were prepared for determination of the retention volume of each phthalate. Three batches of 2 g of polypropylene pellets, previously shown to be free from the target compounds, were spiked with 1-3 mg each of the phthalates for recovery testing.

Determination of retention volume

50 g of S-X8 Bio-Beads was soaked in dichloromethane for overnight before packed into a 700 mm x 25 mm i.d. chromatographic glass column as specified in EPA method 3640A [13]. The retention volumes of polypropylene and each of the phthalates were determined by eluting the 100 mL of spiked solution containing 2 g of polypropylene and 0.01 g of phthalate through the chromatographic glass column containing S-X8 Bio-Beads at 3.125 mL/min using 1:9 ratio of toluene and dichloromethane. Every 10 mL of the eluate was collected and the content of the phthalate in each eluate was determined using UV/Vis spectrophotometer at the range of 190-350 nm. Eluted polypropylene was determined by evaporating the excess solvent on the aluminium foil before weighed with balance. Increase weight of the aluminium foil was used as an indication that the polypropylene has been eluted from the column.

Extraction and Clean Up

To avoid phthalates contamination, all glassware used in the study was washed with acetone and rinsed with dichloromethane before dried at 120 °C for overnight. To ensure the efficiency of extraction of the phthalates, samples were cut with scissors into small pieces. Approximately 2 g of each sample was weighed accurately and transferred to a glass bottle containing 100 mL of 1:9 ratio of toluene and dichloromethane. The extraction was carried out by sonication at 60 °C until the plastic sample was fully dissolved. The clean-up of the extract was carried out using a chromatographic glass column containing 50 g of Bio-Beads S-X8. The first 100 mL of the eluate was discarded and the following 150 mL was collected for analysis of phthalates using GC-MS. All blanks, spiked samples and real samples were undergone similar extraction and analysis procedures. The recovery test was repeated three times for each spiked concentration. Before extraction was carried out, all real samples were analyzed by FTIR-ATR to determine the sample material.

Data acquisition and analysis conditions

An overview of GC-MS parameters used in the analysis of phthalates in this study was given in Table 1. The phthalates were separated in a 60 m x 0.25 mm, 0.25 μ m, DB-5MS, capillary column (Agilent Technologies) with a carrier gas of ultrapure helium at constant flow rate of 1.0 mL/min. The splitless mode was selected for sample injection and the injector temperature was maintained at 300 °C. The GC oven temperature was programmed with

an initial temperature at 100 °C for 1 min, then ramped at 20 °C /min to 300 °C and then held at 300 °C for 20 min. The mass spectrometer was operated in electron impact (EI) mode and in the optimum condition based on the automatic tuning result. The transfer line, ion source and quadrupole mass analyser temperatures were maintained at 325, 230, 150 °C. A solvent delay time of 6.0 min was selected. The phthalates were determined in both full scan (TIC) and selected ion monitoring (SIM) modes. The presence of the phthalates in the samples and standards was confirmed by the mass spectra obtained from the full scan acquisition mode in the range of 50-600 (m/z). SIM mode signal, which was generated by monitoring two to three fragment ions, was used for quantitative determination of the phthalates in the samples and standards. The monitored ions were as follows with the numbers in brackets were used for identification: DMP: 163, (194); DEP: 149, (177), (222); DBP: 149, (233), (251); BBP: (91), (149), 206; DEHP: 149, (176), 193; DnOP: (149), (167), 279. Enhanced Chemstation software was used for control, operation and data acquisition. The method detection limit for each phthalate was calculated from six replicated measurements of a low concentration spiked standard solution according to the Analytical Detection Limit Guidance from Wisconsin Department of Natural Resources [14].

Results and Discussion

Optimization of clean-up procedure

Dissolved polypropylene in the sample needs to be removed before it can be analyzed using GC-MS. This is because polypropylene, which is a macromolecule with high boiling point, tends to deposit in the injector port liner and can cause carry-over contamination to the second analysis. Consequently, sample clean-up is required to remove the dissolved polypropylene from the sample extract. In this study, polypropylene sample containing phthalates were dissolved in 1:9 ratio of toluene and dichloromethane before eluted through a chromatographic glass column containing Bio-Beads SX-8. The collected eluate was injected directly into GC column for further separation and analysis.

Table 1: Gas chromatographic and mass spectrometric parameters used for analysis of phthalates in three kinds of plastic containers for food use

Parameter	
Injector Port	Splitless Mode
Injection Volume	1μL
Injection Port Temperature	300 °C
Carrier gas-helium flow	1.0 ml min ⁻¹
Column (capillary column)	DB-5MS (5% phenyl, 95% dimethylsiloxane)
Column Diameter	$60m\times0.25mm\times0.25~\mu m$ film thickness
Oven temperature program	$100~^{\circ}\text{C}$ for 1 min then $20~^{\circ}\text{C}$ min $^{-1}$ to $300~^{\circ}\text{C}$ for 20 min
Transfer line temperature	325 °C
Ion Source Temperature	230 °C
Quadrupole Temperature	150 °C
Electron energy	69.922 eV
Ionisation current	34.610
Electronic multiplier potential	1270.588 V

Swollen Bio-Beads powder in dichloromethane was packed into the chromatographic column under pressure produced by vacuum pump. Packed column was cleaned with excessive dichloromethane to remove excessive styrene, which was remained in the Bio-Beads powder during the manufacturing. The eluent in the column was replaced to 1:9 ratio toluene and dichloromethane before a spiked phthalate solution was introduced into the

column. The eluate was collected at approximately 3.125 mL/min and the content of phthalate in the eluate was detected using UV/Vis spectrophotometer. The obtained retention volumes were shown in Table 2. As was shown in Table 2, phthalates, which have higher molecular weight, were eluted from the column earlier than the lower molecular weight phthalates. DMP, which has the lowest molecular weight among these phthalates, was collected in 210 to 220 mL fraction, whereas; DEHP and DnOP, which have the highest molecular weight, were collected in 180 to 190 mL fraction. Poplypropylene was collected in 30 to 80 mL fraction. Therefore, based on this result, first 100 mL of eluate eluted from the clean-up column was discarded and the following 150 mL of the eluate was collected for GC-MS analysis.

Sample	Molecular Weight (g/mol)	Retention Volume (ml)
DMP	194.18	210-220
DEP	222.09	190-200
DBP	278.15	190-210
BBP	312.14	180-220
DEHP	390.28	180-190
DnOP	390.28	180-190
Polypropylene	-	30-80

Table 2: The retention volumes of each phthalate

Optimum of data acquisition for GC-MS analysis

Scan mode was used in the GC-MS analysis of the six kinds of phthalates. Retention times and mass spectra of the standards were used to identify the detected phthalates. Figure 1 and 2 are the chromatograms of the full scan mode (TIC) and selected ion mode (SIM) of a mixture of standard of DMP, DEP, DBP, BBP, DEHP and DnOP at 25 mg/L. As shown in these two figures, six kinds of phthalates were well separated by the GC column used in this study. The sensitivities of detecting phthalates were high in SIM mode, which is attributed to the clear baseline obtained in SIM mode chromatogram (Figure 2). The first three phthalates; DMP, DEP and DBP have higher sensitivity than the last three phthalates; BBP, DEHP and DnOP. This could be attributed to some of BBP, DEHP and DnOP, which are less volatile with higher molecular weight compared to the DMP, DEP and DBP, might have deposited somewhere in the GC-MS analysis system or undergone improper fragmentation in the ion source.

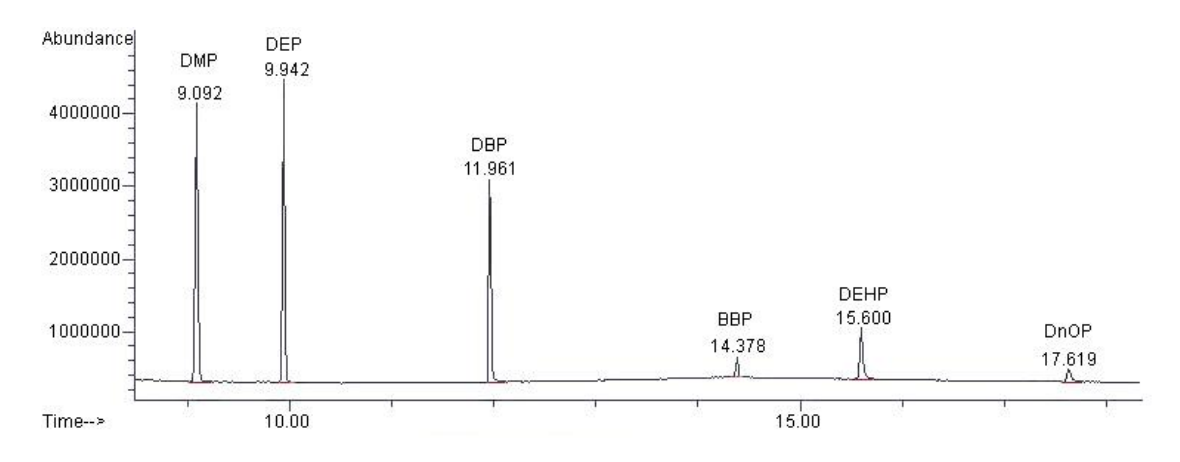


Figure 1: The total ion chromatogram of six phthalates at the concentration of 25 mg/L obtained by full-scan mode (TIC).

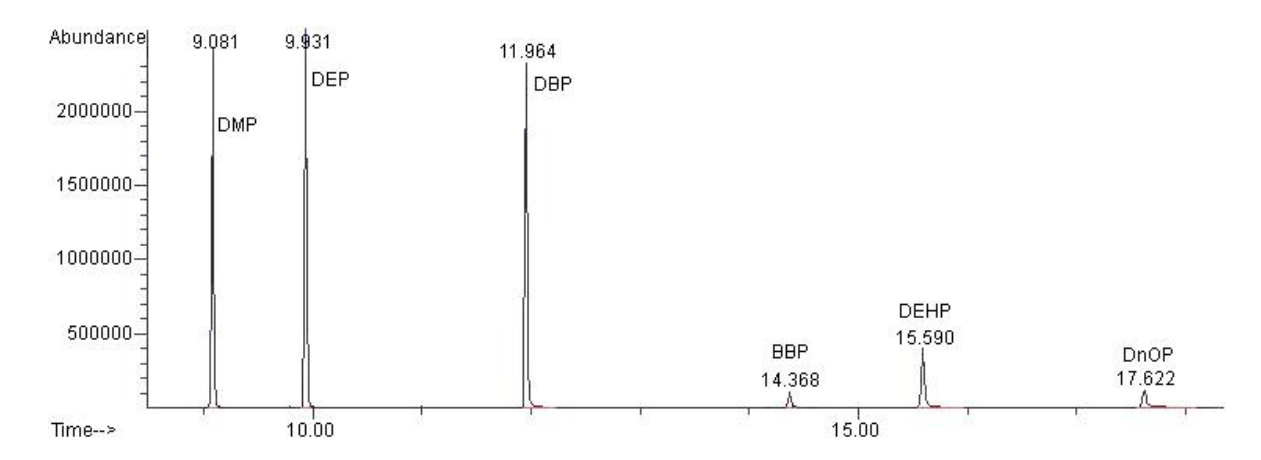


Figure 2: The total ion chromatogram of six phthalates at the concentration of 25 mg/L obtained by selected-ion monitoring (SIM) mode.

Method evaluation

Spiked samples were tested to evaluate the developed method. The developed method was possible to detect phthalates at the level of 1.0-70.0 mg/kg. As shown in Table 3, the recovery data are all within 79.2-91.1% with R.S.D. values at 3.1-11.3%, suggesting that only small quantity of phthalates was lost during the clean-up process.

Real samples

The developed analytical procedure was applied to three real samples of plastic products for food use, i.e. food container, instant noodle cup and snack container, which were bought from the market randomly. All these three samples were scanned with FTIR-ATR to ascertain these samples were made from polypropylene polymer by comparing the IR spectra obtained with the pure polypropylene spectrum. Six kinds of phthalates, i.e. DMP, DEP, DBP, BBP, DEHP and DnOP, were screened and determined by GC-MS-SIM methods. The retention times and mass spectra were used for compound identification, whereas; peak area generated in SIM mode was used for peak quantification using external standard calibration method. The obtained results were listed in Table 4. All of the three examined samples were found to contain DEHP and free from other five phthalates. The detected levels of DEHP in food container and instant noodle cup were complied with the European Community (EC) DEHP maximum permissible level in plastic material, which is not more than 0.1% [15], whereas; DEHP in the snack container is slightly higher than this limit.

Table of the second parameters and the second parameters								
	10 ppm		20ppm		30ppm		Average	RSDp
Compound	Recovery (%)	RSD (%)	Recovery (%)	RSD (%)	Recovery (%)	RSD (%)	Recovery	(%)
DMP	71.9	6.3	92.9	3.9	72.6	4.3	79.2	5.0
DEP	79.7	2.5	97.1	2.4	96.4	4.3	91.1	3.2
DBP	98.8	2.1	90.7	3.4	74.5	15.0	88.0	8.9
DEHP	91.2	1.3	81.8	12.6	86.4	14.9	86.5	11.3
BBP	78.7	1.5	75.3	11.5	97.6	4.5	83.8	7.2
DnOP	92.9	0.1	97.2	4.5	83.1	2.8	91.1	3.1

Table 3: Average recovery and relative standard deviation for each phthalates

Note: RSDp represents Pooled Relative Standard Deviation

Table 4: Determination of phthalates in three kinds of sample by GC-MS-SIM method

Phthalate compound	Detected phthalate level in sample (%)					
•	Food Container	Instant Noodle Cup	Snack Container			
DMP	ND	ND	ND			
DEP	ND	ND	ND			
DBP	ND	ND	ND			
BBP	ND	ND	ND			
DEHP	0.083	0.097	0.127			
DnOP	ND	ND	ND			

Note: ND represents not detected.

Conclusion

A method for the determination of phthalates in plastic product for food use samples utilizing gel permeation chromatographic clean-up procedure in combination with GC-MS-SIM method was developed. All six phthalates, i.e. DMP, DEP, DBP, BBP, DEHP and DnOP were separated well within 20 min in DB-5MS column without significant interference from the sample matrix. The clean-up with gel permeation chromatography was developed and the retention volumes of each phthalate and polypropylene were determined. First 100 mL eluate, which contained polypropylene, was discarded and the following 150 mL portion was collected for determining of the phthalates content. The developed method was possible to detect phthalates at the level of 1.0-70.0 mg/kg. The overall recoveries are all within 79.2-91.1% with R.S.D. values at 3.1-11.3%. All of the three examined samples were found to contain DEHP but free from other five phthalates.

Acknowledgement

The authors would like to thank Tunku Abdul Rahman College for supporting this research.

References

- 1. Larsen, S.T., Hansen, J.S., Hansen, E.W., Clausen, P.A., and Nielsen, G.D. (2007). Airway inflammation and adjuvants effect after repeated airborne exposures to di-(2-ethylhexyl) phthalate and ovalbumin in BALB/c mice. *Toxicology*, 235, 119-129.
- 2. Ema, M. and Miyawaki, E. (2001). Adverse effects on development of the reproductive system in male offspring of rats given monobutyl phthalate, a metabolite of dibutyl phthalate, during late pregnanacy. *Reproductive Toxicology*, 15, 189-194.
- 3. Gangi, J.D. (1999). Phthalates in PVC medical products from 12 countries. Greenpeace USA. pp:1-12.
- 4. Rastogi, S.C., Jensen, G.H., and Worsoe, I.M. (2003). Compliance testing of phthalates in toys. National Environmental Research Institute Ministry of the Environment. pp:11-12.
- 5. Nakajin, S., Shinoda, S., Ohno, S., Nakazawa, H., and Makino, T. (2001). Effect of phthalate esters and alkylphenols on steroidogenesis in human adrenocorticol H295R cells. *Environmental Toxicology and Pharmacology*. 10, 103-110.
- 6. Foster, P.M.D., Cattley, R.C., and Mylchreest, E. (2000). Effects of Di-n-butyl Phthalate (DBP) on Male Reproductive Development in the Rat: Implications for Human Risk Assessment. *Food and Chemical Toxicology*. 38, 97-99.
- 7. Hines, C.J., Hopf, N.B., Deddens, J.A., Silva, M.J., and Calafat, A.M. (2009). Estimated daily intake of phthalates in occupationally exposed groups. *Journal of exposure Science and environmental Epidemiology*, 1-9.

Chong Kian Wei et al: DETERMINATION OF SIX PHTHALATES IN POLYPROPYLENE CONSUMER PRODUCTS BY SONICATION-ASSISTED EXTRACTION/GC-MS METHODS

- 8. Ito, R., Seshimo, F., Miura, N., Kawaguchi, M., Saito, K., and Nakazawa, H. (2005). High-through put determination of mono-and di(2-ethylhexyl) phthalate migration from PVC tubing to drugs using liquid chromatography–tandem mass spectrometry. *Journal of Pharmaceutical and Biomedical Analysis*. 39, 1036-1041
- 9. Marin, M.L., Jimenez, A., Lopez, J., and Vilaplane, J. (1996). Analysis of poly(vinyl chloride) additives by supercritical fluid extraction and gas chromatography. *Journal of Chromatography A*. 750, 183-190.
- 10. Shen, H.Y. (2005). Simultaneous screening and determination eight phthalates in plastic products for food use by sonication-assisted extraction/GC–MS methods. *Talanta*. 66, 734–739.
- 11. Farahani, H., Norouzi, P., Dinarvand, R., and Ganjali, M.R. (2007). Development of dispersive liquid—liquid microextraction combined with Gas chromatography—mass spectrometry as a simple, rapid and highly Sensitive method for the determination of phthalate Esters in water samples. *Journal of Chromatography A.* 1172, 105-112.
- 12. Kostanski, L.K., Keller, D.M., Hamielec, A.E. (2004). Size-exclusion chromatography-a review of calibration methodologies. *Biochemical and Biophysical Methods*. 58, 159-186.
- 13. EPA method 3640A, Gel-permeation cleanup. 1994, USEPA, Washington DC, pp. 1-24.
- 14. Ripp, J. (1996). Analytical Detection Limit Guidance & Laboratory Guide for Calculating Analytical Detection Limits, Wisconsin Department of Natural Resources, Madison, WI 53707.
- 15. Official Journal of the European Communities (2002). Commission Directive 2002/72/EC of 6 August 2002 relating to plastic materials and articles intended to come into contact with foodstuffs. Official Journal of the European Communities.



DETERMINATION OF ORGANOPHOSPHORUS PESTICIDES USING MOLECULARLY IMPRINTED POLYMER SOLID PHASE EXTRACTION

(Penentuan Pestisid Organofosforus Menggunakan Pengesktrakan Fasa Pepeal dengan Polimer Cap)

Mohd Marsin Sanagi^{1,2}*, Syairah Salleh², Wan Aini Wan Ibrahim^{1,2}, Ahmedy Abu Naim¹

¹IbnuSina Institute for Fundamental Science Studies, Nanotechnology Research Alliance, ²Department of Chemistry, Faculty of Science, UniversitiTeknologi Malaysia, 81310 UTM JohorBahru, Johor, Malaysia

*Corresponding author: marsin@kimia.fs.utm.my

Abstract

Molecularly imprinted polymer solid phase extraction (MIP-SPE) method has been developed for the determination of organophosphorus pesticides (OPPs) in water samples. The MIP was prepared by thermo-polymerization method using methacrylic acid (MAA) as functional monomer, ethylene glycol dimethacrylate (EGDMA) as crosslinker, acetonitrile as porogenic solvent and quinalphos as the template molecule. The three OPPs (diazinon, quinalphos and chlorpyrifos) were selected as target analytes as they are widely used in agriculture sector. Various parameters affecting the extraction efficiency of the imprinted polymers have been evaluated to optimize the selective preconcentration of OPPs from aqueous samples. The characteristics of the MIP-SPE method were validated by high performance liquid chromatography (HPLC). The accuracy and selectivity of the MIP-SPE process developed were verified using non-imprinted polymer solid phase extraction (NIP-SPE) and a commercial C_{18} -SPE was used for comparison. The recoveries of the target analytes obtained using the MIPs as the solid phase sorbent ranged from 83% to 98% (RSDs 1.05 - 1.98%; n=3) for water sample. The developed MIP-SPE method demonstrates that it could be applied for the determination of OPPs in water samples.

Keywords: Organophosphorus pesticides, Molecularly imprinted polymer, Solid phase extraction

Abstrak

Pengesktrakan fasa pepejal polimer cap molekul (MIP-SPE) telah dibangunkan bagi penentuan racun organofosforus (OPPs) dalam sampel air. MIP telah disediakan dengan kaedah pempolimeran terma menggunakan asid metakrilik (MAA) sebagai monomer berfungsi, etilina glikol dimetakrilik (EGDMA) sebagai rantai silang, asetonitril sebagai pelarut porogen dan kuinalfos sebagai molekul templat. Tiga OPPs (diazinon, kuinalfos dan klorpirifos) dipilih sebagai analit sasaran kerana ia digunakan secara meluas dalam sektor pertanian. Pelbagai parameter yang mempengaruhi kecekapan pengekstrakan polimer cap telah dinilai bagi mengoptimumkan pra-pemekatan bagi sebatian OPPs dalam sampel akueus. Kaedah MIP-SPE telah disahkan menggunakan kromatografi cecair prestasi tinggi (HPLC).Ketelitian sertak etepatan kaedah MIP-SPE telah digunakan menggunakan pengesktrakan fasa pepejal polimer bukan cap (NIP-SPE) dan komersial C₁₈-SPE telah digunakan sebagai perbandingan. Peratus pengembalian yang diperolehi bagi sasaran analit menggunakan MIP sebagai penyerap fasa pepejal adalah dalam lingkungan 83% hingga 98% (sisihan piawai relatif, RSD 1.05 hingga 1.98%) bagi sampel air. Kaedah MIP-SPE yang telah dibangunkan terbukti boleh digunakan untuk penentuan OPPs dalam sampel air.

Kata kunci: Racun organofosforus, Polimer cap molekul, Pengekstrakan fasa pepejal

Introduction

Molecularly imprinted polymers (MIPs) are crosslinked polymers with specific recognition sites complementary in term of size, shape and functionality, to the template molecule, involving an interaction mechanism based on molecular recognition [1]. In recent years, the development of MIPs for solid phase extraction (SPE) has been

extensively reported since it provides good selectivity as separation materials [2-4]. These applications deal with the selective enrichment and sample clean-up of traces of organic compounds from aqueous samples (such as tap, river and waste waters) or for the purifications of extracts resulting from the treatment of solid samples (such as soil or sediment).

Organophosphorus pesticides (OPPs) are important compounds to be analyzed because over the last few years' pesticide contamination of drinking water and agricultural products has become a major concern and the number of pesticide has been steadily increasing [5]. They are widely used in agriculture and animal production for the control of various insects. Hence, it is of great interest to develop new MIP-SPE that usesOPP as a template for the determination of OPPs. In this work MIP-SPE was developed using quinalphos as a template, methacrylic acid as a functional group and ethylene glycol dimethacrylate as a cross linker by non-covalent imprinting through bulk polymerization method. The target analytes with structures similar to quinalphos, namely diazinon and chlorpyrifoswere considered in this study(Figure 1). The extraction efficiency of the MIP-SPE of OPPs from environmental water samples was evaluated using HPLC and analytical parameters of the method, linearity, detection limits and repeatability were established. The method was validated and successfully applied to determined OPPs compounds from environmental water samples.

Figure 1: Structures of target analytes

Experimental

Preparation of molecularly imprinted polymers with bulk methods

Polymer preparation has been described in detail in our previous study [6]. In the procedure, 1mmol of template (quinalphos) and 4mmol of MAA were dissolved in 6 mL of porogenic solvents (acetonitrile) in a glass polymerization test tube. After oscillating for 15 min, ethylene glycol dimethacrylate (EGDMA, 20 mmol) as cross-linker and2,2'-Azobisisobutyronitrile (AIBN, 50 mg) as initiator were added into the solution. The test tube was placed on ice and purged with nitrogen for 15min. The glass tube was sealed under vacuum and placed in water bath at 60°C for 24 h. The bulk polymers obtained was crushed, ground and sieve through 75 µm sieve. The polymer particles obtained were washed with 10% acetic acid methanol solution until quinalphos template could not be detected by UV spectrophotometry. The extracted particles were then washed with methanol to remove residual acetic acid. Finally, the collected particles were dried at 55 °C in an oven under vacuum for 12h. Non-imprinted polymers were prepared in the same manner, but without the addition of the template molecule.

Molecularly imprinted polymer solid phase extraction procedure

Dry imprinted and non-imprinted polymer particles (100g each)were packed into empty cartridge (3 mL) with glass-wool frit at each end. The cartridges were conditioned with methanol (10 mL) and 5 mL of deionized water from a MilliQwater system from Thermo Scientific (Barnstead, MA, USA). For each cartridge, 10 mL of OPPs mixture-spiked river water sample (0.1 mgL⁻¹ for each) was passed through each cartridge at 1 mLmin⁻¹ using a vacuum system. The extract was cleaned up by 5 mL of acetonitrile-water mixture (3:7, v/v) to eliminate molecules retained by non-specific adsorption to the polymer, followed by 10 min drying of cartridge was operated by vacuum in order to remove the residuals solvent. The extractwasthen eluted with a 5 mL of methanol-acetic acid (95:5, v/v) mixture solution. Finally, the obtained extract solution was blown under nitrogen and re-dissolved with 0.2 mL of acetonitrile for HPLC analysis.

C₁₈SPE

Two C_{18} cartridges from Sigma Aldrich were conditioned with 10 mL of methanol and 5 mL of MilliQwater. For each cartridge, 10 mL of OPPs-spiked river water sample were loaded on the cartridge. OPPs were washed with 5 mL of acetonitrile-water mixture (3:7, v/v) and subsequently eluted using 5 mL of methanol. The extracts were evaporated to dryness and re-dissolved in 0.2 mL of acetonitrile for HPLC analysis.

Sample Preparation

The river water sample was obtained from a river running across the UTM Johor Bahrucampus. The samples were kept refrigerated at 2-5°C prior to analysis to minimize degradation. The samples were filtered using 0.45 µm filter paper from Whatman(NJ, USA) to ensure the samples were free from particles that might block the SPE cartridge and HPLC system.

Results and Discussion

Characterization of Imprinted polymer

Characterization was performed by Fourier transform infrared (FTIR) spectroscopy to observe the functional absorption of certain groups in MIP before and after washing stage and also NIP by using the KBr pellet method (Figure 2). A C=O stretching vibration occurs in the region 1700 -1750 cm⁻¹ because of the cross-linked polymerization of EDMA and MAA, and repeated EDMA as cross-linking unit was carried out. The absorbance peaks for all spectrawere almost identical except for the intensity of the peak at 3600-3400 cm⁻¹ for O-H band, where the peak intensity for MIP before washing was lower than that for MIP after washing, but it was similar tothat for NIP. A possible reason for this phenomenon is that the template molecule (quinalphos) was assembled with monomer (MAA) via hydrogen bonding with hydroxyl group in monomer during the preparation of MIP before washing. The proposed interaction is illustrated in Figure 3. However, after the template removal, a strong and broad stretching vibration absorbance peak of hydroxyl group from monomer was observed clearly due to the absence of any hydrogen bond disruption which is in agreement with a study reported byBrune*et al.*, (1999) [7]. The difference in intensity indicates that the template has been leached out.

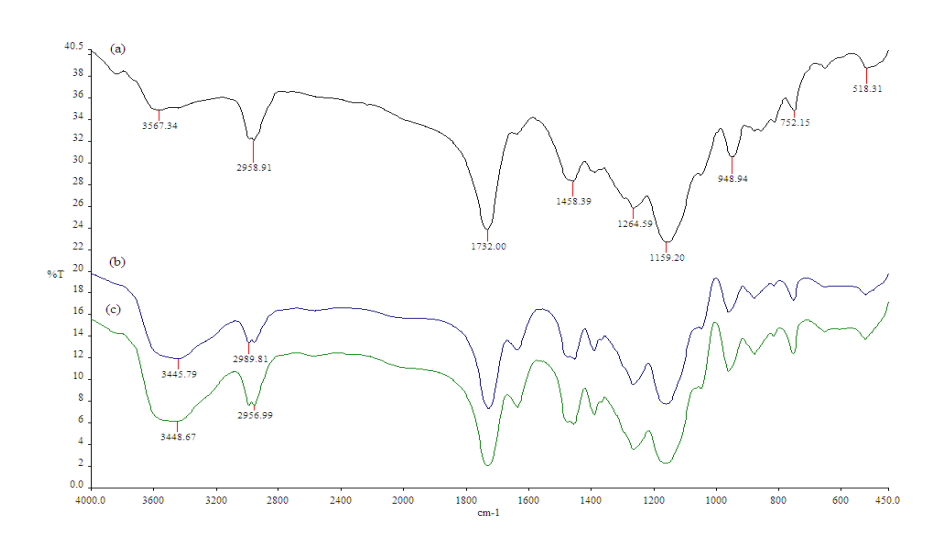


Figure 2: FTIR spectra of MIP (a) before washing, (b) after washing, (c) NIP.

Mohd Marsin Sanagi et al: DETERMINATION OF ORGANOPHOSPHORUS PESTICIDES USING MOLECULARLY IMPRINTED POLYMER SOLID PHASE EXTRACTION

Figure 3: Proposed interaction between monomer (methacrylic acid) and template (quinalphos).

Scanning electron microscopy (SEM) was used to determine the surface morphology and image of the MIP. Figure 4 shows SEM micrographs of MIP at various magnifications which generally shows rough MIP surface with irregular pores.

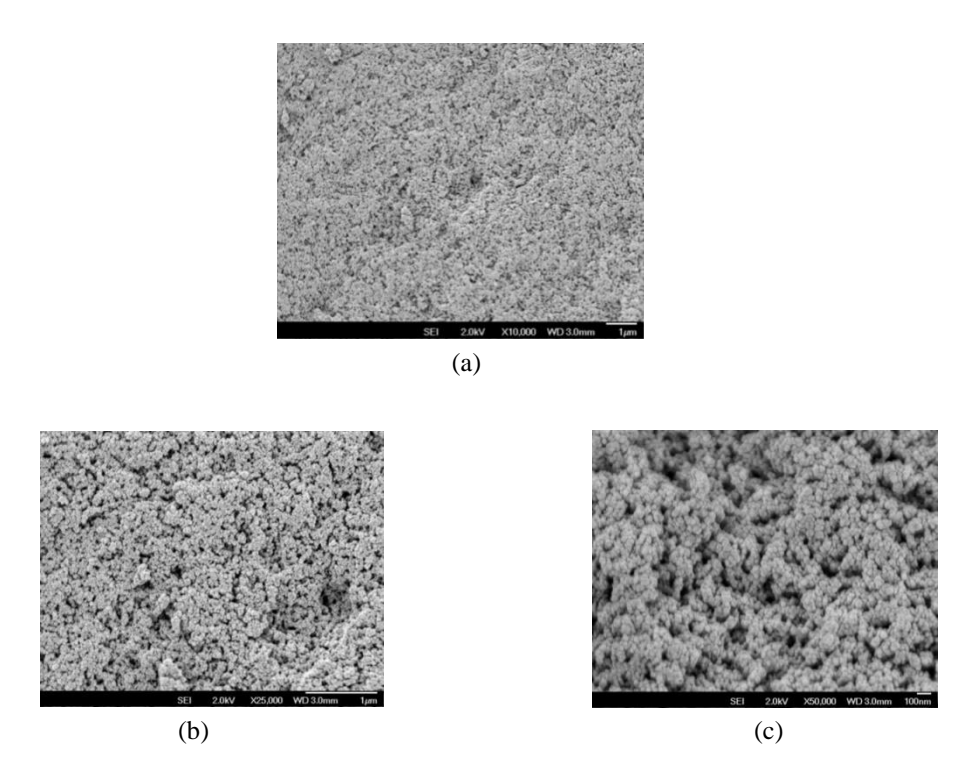


Figure 4: The SEM images of MIP at different magnifications: (a) × 10,000, (b) ×25,000 and (c) ×50,000

Optimization of MIP-SPE procedure

In order to evaluate the imprinting affect and applicability of the MIPs for the extraction and determination of trace quinalphos, the MIP-SPE process was optimized by evaluating the washing solvent, volume of loading sample, andthe composition and volume of the eluting solvent to achieve good sensitivity and precision of this method.

Washing solvent

Thetype of the washing solution plays a vital role on the selectivity of the MIPs in order to maximize the specific interaction between analyte and binding site and to simultaneously discard matrix component in the polymer by decrease the non-specific interaction at binding site [8]. Samples (10 mL) containing 0.1 mgL⁻¹ quinalphos dissolved in water were loaded onto the cartridgesand washed with various solvent tested and eluted with10 mL of methanol-acetic acid (9:1, v/v) mixture solution. The concentration recoveries were determined by HPLC.

Since recognition is often best in the porogen solvent used in polymerization of the MIP [9], it was decided that acetonitrile (ACN)should be used as washing solvent in combination with water. Figure 5 shows the effect of washing with various percentage of acetonitrile in the acetonitrile-water mixtures (10, 20, 30, 40 and 50 %) on the recovery of quinalphos. The results showed that washing solvent containing up to 20% acetonitrile in mixture had no significant effect on theretention of quinalphos on both MIP and NIP cartridges. However, with increased acetonitrile in the washing solutions of 30%, the recovery of quinalphos in NIP cartridge was markedly decreased to 37.6%, while the recovery of quinalphos by the MIP cartridges was essentially not reduced (96.7% recovery). This indicates that the presence of specific interactions taking place in the binding sites. However, higher portions of acetonitrile in mixture solvent of >40% led to a large decrease of quinalphos retention both on the MIP and NIP cartridges due to the disruption of specific interactions between the analytes and binding sites. In this study, therefore, a mixture of acetonitrile-water 30:70% v/v was selected as washing solution.

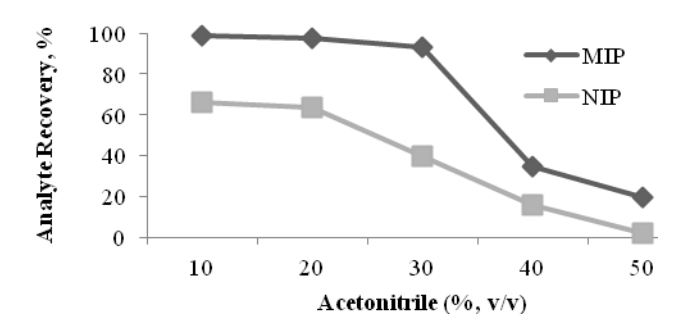


Figure 5: Recovery of quinalphos with different acetonitrile percentages in washing solvent for MIP-SPE and NIP-SPE.

Elution solvent and volume

Samples (10 mL)containing 0.1 mgL⁻¹ quinalphos dissolved in water were loaded onto the cartridges, washed with 5 mL mixture of 30% acetonitrile in water, and eluted with different percentages of acetic acid in methanol (1, 5, and 10%). The concentration of the quinalphos was determined with HPLC at 200 nm wavelength of detection. Methanol was used as eluentsince it has the properties of having stronger hydrogen bond and the easy permeability of analyte in methanol that may induce efficient elution. The addition of a small percentage of acetic acid (1 to10%)in the mixture was applied in order to overcome strong interactions between analyte and the MIP and thus enhancing the enrichment factor.

In this experiment, pure methanol (0% acetic acid) was tested in order to confirm that acetic acid played an important role in desorbing quinalphos from the MIP in elution solvent. The results showed thatthe addition of acetic acid increased the analyte recovery and themost likely explanation was that acetic acid competed with

quinalphos for the functional group in the binding sites (Figure 6). However, solvent with relatively high percentage (10%) of acetic acid apparently tend to decrease the analyte recovery. Thus, 5% of acetic acid in methanol was selected as optimal elution solvent for the following study.

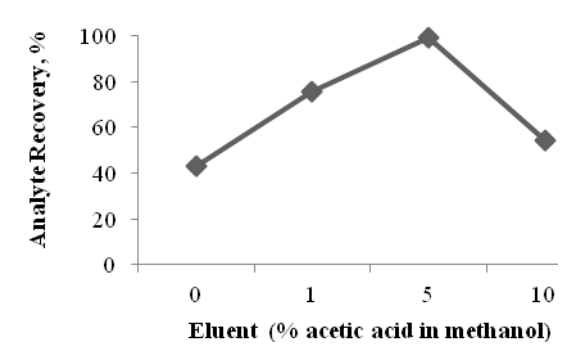


Figure 6: Recovery of eluting solvent for MIP-SPE experiment.

In order to determine the optimum eluting volume, 5 mL of water sample spiked with 1 mgL⁻¹ quinalphos was percolated through MIP-SPE, and a different volumes (3, 6, 10 and 15 mL) of a mixture of methanol with 5% acetic acid were applied as eluting solvent and the elutes were analyzed by HPLC. The results showed thatincreasing solvent volume from 3 mL to 10 mL increased the recovery of selected analyte extracted (Figure 7). However, the analyte recoverystarted to decreased when 15 mL of elution solvent was used. The use of 10 mL solvent volume showed highest recovery of quinalphos. Thus, 10 mL of methanol with 5% acetic acid was selected as the eluting solvent.

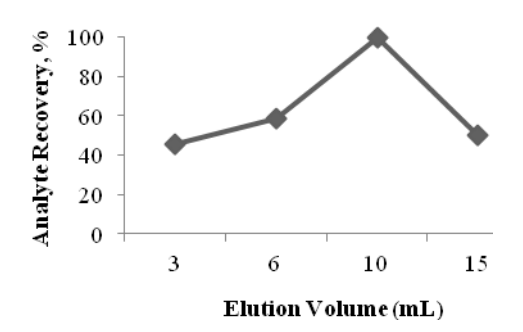


Figure 7: Recovery of different volume of eluting solvent for MIP-SPE

Experiment of the sample volume

In order to determine the optimum loading volume, experiments were carried out on using various sample volumes ranging from 5 mL to 50 mL and the extraction efficiency was investigated. It was found that the examined sample volumes, 5 mL, 10 mL, 15 mL, 25 mL and 50 mL, gave analyte recoveries of 61%, 92%, 45%, 29% and 16% respectively (Figure 8). It was noted that the highest recovery was observed when sample volume was at 10 mL.Hence, 10 mL was selected as the optimal sample volume.

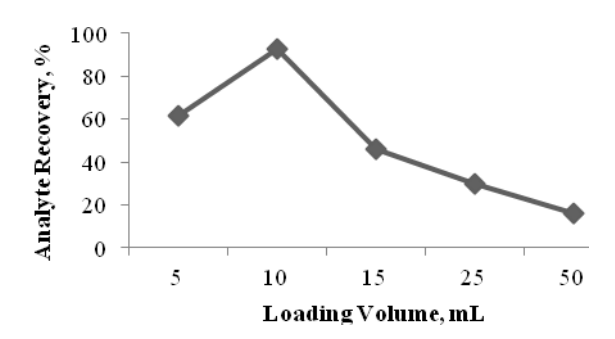


Figure 8: Analyte recovery for different loading volume of sample MIP-SPE.

Determination of Organophosphorus Pesticides with HPLC

Determination of organophosphoros pesticides (quinalphos, diazinon, and chlorpyrifos) was carried out using HPLC-UV as described in the procedure. The mobile phase consisted of acetonitrile-water (6:4, v/v) and the flow rate of the mobile phase was 0.4 mLmin⁻¹. The oven temperature was set at 60°C, the injection volume was 0.5 μ L, and all compounds were detected at 200 nm. The method performance was evaluated by determination of linearity, sensitivity, repeatability, and accuracy of the method.

The linearity of calibration curves were obtained by the determination of the peak areas from analysis of 0.005 mgL⁻¹ to 0.15 mgL⁻¹ of each analyte and the all *r*-values were 0.999 (Table 1). The limit of detection (LOD), defined as the lowest analyte concentration with a signal-to-noise ratio of 3, were also investigated through the detection of spiked MilliQwater at serial concentrations. The results showed that the LODs were between 0.0063 mgL⁻¹ to 0.0076 mgL⁻¹, which indicated that this method could be used to detect the analytes in polluted water samples.

Analytes	Correlation, r	Linear range (mgL ⁻¹)	LOD (µgL ⁻¹)	LOQ (µgL ⁻¹)	RSD (n=3)
Quinalphos	0.994	0.01-0.15	6.67	20.22	1.96
Diazinon	0.997	0.01-0.15	7.62	23.08	2.44
Chlorpyrifos	0.995	0.01-0.15	6.33	19.27	1.89

Table 1: Validation parameters for Molecularly Imprinted Polymer Solid Phase Extraction

Determination of OPPs in spiked water sample

The developed MIP-SPE method was applied for the enrichment of OPPs in river water samplesto demonstrate the applicability and reliability of this method. However, no target analyte was detected which suggested that there was no detectable OPPs in the river water sample. Thus, to assess matrix effects, river water samples were spiked and the extracted performance was evaluated. Figure 9 shows HPLC tracings of the OPPs in river water before and after spiking at 0.1 mgL⁻¹. The results suggested that the matrix effect on MIP-SPE for river water sampleswas negligible.

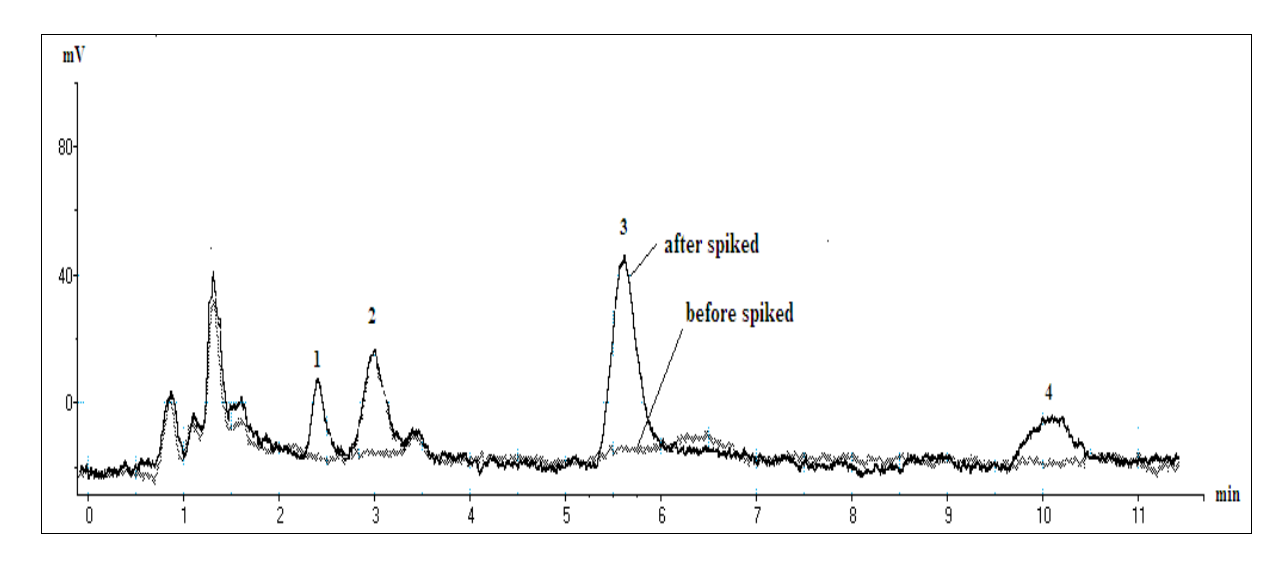


Figure 9: Chromatograms of river water sample before (grey line) and after spiked with 0.1 mgL⁻¹ of each analyte (black line). (1) diazinon, (2) hexaconazole (internal standard), (c) quinalphos, (d) chlorpyrifos.

Table 2: Recoveries (%) and precision (RSD) of OPPs in water san	nples spiked with 0.1 mgL ⁻¹ .
--	---

OPPs	MIP-	SPE	NIP-	SPE	C ₁₈ SPE		
	Recovery RSD		RSD Recovery RSD		Recovery RS		
	(%)	(n=3)	(%)	(n=3)	(%)	(n=3)	
Quinalphos	98.71	1.05	68.87	2.05	59.34	3.47	
Diazinon	90.25	1.39	65.75	2.67	57.59	1.50	
Chlorpyrifos	83.14	1.98	53.79	2.51	56.62	2.70	

The analyte recoveries obtained using MIPs as the solid phase sorbent for quinalphos, diazinon and chlorpyrifos were in the range between 83% and 98% for water sample (Table 2). The RSD values of the target analytes were excellent with values of <2%. However, the analyte recoveries obtained using NIP as the solid phase sorbent for target analytes in water sample were significantly lower with values only between 68% and 53%. Meanwhile, the extraction recoveries by using $C_{18}SPE$ as sorbent were below than 59% for all spiked OPPs compounds.

Comparison of the results from the enrichment methods studied (MIP-SPE, NIP-SPE, or C_{18} SPE) clearly demonstrated the advantage of using molecularly imprinted polymers as selective sorbents for the determination of OPPs in water samples.

Conclusion

In this work, aquinalphos imprinted polymer was prepared by bulk polymerization using MAA, EDMA, and acetonitrile as functional monomer, cross linker, and porogen solvent, respectively. The imprinted polymers showed good selectivity and enrichment efficiency over non-imprinted polymer and commercial SPE-C₁₈. The MIP polymer used as adsorbents in SPE coupled with HPLC was successfully applied for the enrichment and analysis of OPPs in river water samples. High analyte recoveries (83-98%) and precision (1.05-1.98%) for the OPPs proved that the method was valid for the analysis of target analyte in water sample.

Acknowledgement

The authors would like to thank Universiti Teknologi Malaysia for facilitations and the Ministry of Higher Education Malaysia (MOHE) for financial support through Fundamental Research Grant Scheme Vote number 78477 and studentship for Syairah Salleh.

References

- 1. Pichon, V. and Hugon, F.C. (2008). Role of Molecularly Imprinted Polymer for Selective Determination of EnvironmentalPollutants—A Review. *Anal. Chim. Act.* **622**, 49.
- 2. Gomes, R. and Augusto F. (2006). Sol-Gel Molecular Imprinted Ormosil for Solid-Phase Extraction of Methylxanthines. *J. Chromatogr A.* **1114**.216–23.
- 3. Liu, H.Y., Wang, M.M., Liu, S.B., and Chen, Y. (2006). Chromatographic Characterization and Solid-Phase Extraction on Diniconazole-Imprinted Polymers Stationary Phase. *React. Funct. Polym.* **66**. 579–83.
- 4. Baggiani C, Baravalle P, Giraudi G, and Tozzi C. (2007). Molecularly Imprinted Solid-Phase Extraction Method for the High Performance Liquid Chromatographic Analysis of Fungicide Pyrimethanil in Wine. *J Chromatogr.* A1141.158-64.
- 5. Raharjo, Y., Sanagi, M.M., Wan Ibrahim, W.A., Abu Naim, A., and Aboul-Enein, H.Y. (2009). Application of Continual Injection LPME Method Coupled with Liquid Chromatography to the Analysis of Organophosphorus Pesticides. *J. Sep. Sci.* 32. 623.
- 6. Sanagi, M. M., Salleh, S., Wan Ibrahim, W.A., and Naim, A. A. (2010). Molecularly imprinted polymers for solid phase extraction of orghanophosphorus pesticides. *J. Fundamental Sci.*, 6. 27-30.
- 7. Brune, B. J., Koehler, J. A., Smith, P. J. and Payne, G. F. (1999). Correlation between adsorption and small molecule hydrogen bonding. *Langmuir*. 15. 3989
- 8. He, C.Y., Long, Y.Y., Pan, J.L., Li, K.A., and Liu, F. (2007). Application of Molecularly Imprinted Polymers to Solid-Phase Extraction of Analytes from Real Samples. *J. Biochem. Biophys. Methods.* **70.** 133.
- Sellergren, B. (1999). Polymer and Template-Related Factors Influencing the Efficiency in Molecularly Imprinted Solid-Phase Extractions. Trends Anal. Chem. 18.164.



HEALTH STATUS OF RECREATIONAL BEACHES IN ISKANDAR DEVELOPMENT REGION, JOHOR, MALAYSIA

(Status Kesihatan Pantai-Pantai Rekreasi di Wilayah Pembangunan Iskandar, Johor, Malaysia)

Zaleha, K.*, Farah Diyana, M. F., Mohd Luthfi, O., Noorul Ain Falah, A., Ahmad Wafi, A.

Institute of Tropical Aquaculture, Universiti Malaysia Terengganu, 21030, Kuala Terengganu, Terengganu, Malaysia.

*Corresponding author:zaleha@umt.edu.my

Abstract

This study aims to evaluate the health status of recreational beaches in Wilayah Iskandar development area Johor. The nematode/copepod ratio may be used as useful tool for assessing the environmental quality of the beaches. The meiobenthos samples were collected using a PVC corer at three stations at intertidal zone along beaches in Wilayah Iskandar. Four sampling sessions were conducted in March, April, May and June 2009 during low tide. Physico-chemical parameters including salinity, pH, dissolved oxygen and temperature were measured *in situ* at each station using YSI multi probe MPS 556 and sediment samples were collected for chlorophyll *a* analysis. The chlorophyll-a concentrations were determined based on the spectrophotometric method using 665 nm wavelength. The ratio showed a wide variability between stations with highest values recorded at Station 3 (2.25 to 131.1) and lowest at Station 2 (0.99 to 15.53). The overall ratio of nematode/copepod could be related to the increase of potentially polluted area along the beaches such as at Station 3. The presence of pre-diapause copepod which is able to survive **in** the environment condition stress becomes a good indicator for the health status of beaches in Wilayah Iskandar development area.

Keywords: Iskandar Development Region, beach, nematode/copepod, ratio, meiobenthos

Abstrak

Kajian ini dilakukan untuk menilai status kesihatan pantai-pantai rekreasi di kawasan Wilayah Pembangunan Iskandar. Nisbah nematod/kopepod boleh digunakan sebagai alat yang berguna untuk menilai kualiti persekitaran pantai-pantai tersebut. Sampel meiobentos diambil dengan menggunakan tiub pengorek PVC pada tiga stesen di zon pasang surut sepanjang pantai-pantai di Wilayah Iskandar. Empat sesi penyampelan telah dilakukan pada bulan Mac, April, Mei dan Jun 2009 semasa air surut penuh. Parameter fizikokimia termasuk kemasinan, pH, oksigen terlarut dan suhu diukur secara *in situ* di setiap stesen dengan menggunakan YSI multi probe MPS 556 dan sampel sedimen diambil untuk analisis klorofil *a.* Kepekatan klorofil-a ditentukan berdasarkan kaedah spektrofotometrik menggunakan gelombang 665 nm. Nisbah tersebut menunjukkan kepelbagaian yang tinggi di antara stesen-stesen dengan nilai yang tertinggi dicatatkan di Stesen 3 (2.25 to 131.1) dan nilai terendah di Stesen 2 (0.99 to 15.53). Keseluruhan nisbah nematod/kopepod berkemungkinan berkait rapat dengan peningkatan kawasan yang berpotensi tercemar di sepanjang pantai tersebut contohnya seperti di Stesen 3. Kehadiran kopepod di peringkat *'pre-diapause'* yang mampu hidup dalam keadaan tekanan persekitaran dapat dijadikan penunjuk yang baik untuk status kesihatan pantai-pantai di kawasan Wilayah Pembangunan Iskandar, Johor.

Kata kunci: Wilayah Pembangunan Iskandar, pantai, nisbah nematod/kopepod, meiobenthos

Introduction

Tourism and recreational activities have been known to represent disturbances and been linked to pollution and industrialization that may affect spatial heterogeneity, structure and dynamics of natural community [1]. The impacts caused directly by recreational activities are becoming important environmental issues [2]. To date, most tourism-impact studies have been mainly focused on changes in abundance and diversity of large macrobenthos, loss of individual species or decreasing populations of shore birds, whereas smaller animals were largely neglected

Zaleha et al: HEALTH STATUS OF RECREATIONAL BEACHES IN ISKANDAR DEVELOPMENT REGION, JOHOR, MALAYSIA

[3,4]. However, Kennedy and Jacoby (1999) indicated the meiobenthos are more diverse than any other marine benthic component and moreover as an excellent indicator of marine environmental quality [5]. At present, many studies have been carried out on the use of meiobenthos as biological indicators and they have been widely used as tools for environmental monitoring. The use of meiobenthos as tools in monitoring environmental changes has been discussed by several authors in previous studies [6,7,8].

Raffaelli and Mason (1981) were the first who proposed the use of nematode to copepod ratio as a tool for biomonitoring [9]. They showed that the overall ratio of nematode/copepod increased with increasing degree of pollution. Recently, the nematode/copepod ratio is suggested as a potentially useful for biomonitoring habitats and it has been use as an indicator of pollution in harbour ecosystems [10]. However, the validity of this technique subsequently argued by several authors that it is not universally applicable to all habitats [11,12]. Lambshead (1984) concluded that the ratio is unreliable due to the difficulties in separating the effects of pollution on the ratio from the effects of other environmental variables [12]. The present study was carried out to examine the nematode/copepod ratio and the spatial distribution of the meiobenthic communities in determining the health status of recreational beaches in Wilayah Iskandar development area, Johor.

Experimental

Study area

Facing the Johor Straits, the recreational beaches in Wilayah Iskandar development area, Johor Bharu is one of the most famous tourist attractions of Johor. It covers an area of approximately 450-acre (1.8 km²). Three stations (Figure 1) were chosen for the study area. Station 1 (01°27′23.44″N, 102°42′49.0″E) which is close to War Memorial in the lower part of the bay consisted of white medium sand on the beach. Station 2 (01°27′54.34,″N 103°43′47.20″E) is about 2 km away from Station 1 is covered with scattered patches of seagrass beds and macroalgae, *Padina sp.* The sediment textures primarily consist of coarse sand in the uppermost beach. Station 3 (01°28′38.78″N, 103°43′16.64″E) is situated near to the boats and ferries parking spot with medium sand and hard clay sediment.

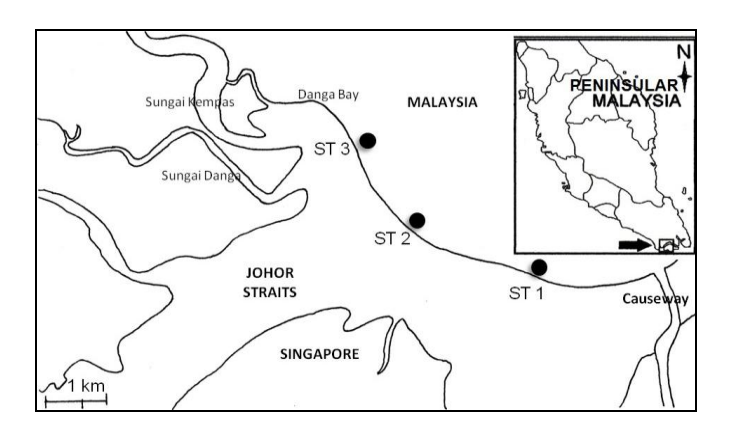


Figure 1: Map of sampling stations at Wilayah Iskandar development area

Sampling

Sampling sessions were carried out in intertidal zone at Lido beach (March, April, May and June 2008) during low tide. At each site, the meiobenthos samples were collected by inserting the PVC hand core with 3.4 cm of inner diameter on the sediment down to 10 cm depth [13]. Five replicates of sediment samples were collected at three quadrates (Q1, Q2, Q3) along a transect laid from uppermost to the low tide level of the beach. Q1, Q2, and Q3 are located at the upper, middle and lower level of the beach. Core samples were then transferred into labelled plastic bags and immediately fixed with 10% buffered formaldehyde [14].

An additional sediment samples at each sampling station were taken and brought back to the laboratory for chlorophyll *a* analysis. Environmental parameters of the overlying water such as temperature, salinity, dissolved oxygen concentration and pH were measured *in situ* at each station using YSI 556 Multi-probe meter.

In the laboratory, meiobenthos was extracted from the sediment using decantation method [14]. The samples were sieved with a $63 \mu m$ sieve and all the organisms specimens were preserved in labeled bottles containing 5% neutralized formalin mixed with Rose Bengal stain. Samples of meiobenthos were sorted and enumerated into different taxa under a stereo microscope.

Chlorophyll-a concentration was determined using spectrophotometric method [15]. The sediment of 2.5 cm section were weighed, thawed and placed in a screw cap dark glass bottle with addition of 20 ml of 100% acetone at 4°C in the dark for 24 hours for the complete pigment extraction. Then 3 ml of clarified extract were added to the cuvette, measured at 665 nm using Perkin Elmer Spectrophotometer. A drop of 0.1 N HCI were added and re-read at 665 nm after 2 min. The concentration of chlorophyll *a* in the extract solvent was calculated using the equations [16].

Data analysis

The density of meiobenthos was expressed as number of individuals (N) per unit area (10 cm²) based on the mean of five replicate cores. Analysis of similarities one-way ANOSIM was used to test the significant differences between multivariate groups of samples from different sampling stations. The similarity matrices for cluster and MDS analysis was generated using Bray-Curtis similarity of a square-root transformed data. All univariate indices and multivariate measures were performed using the PRIMER (Plymouth Routines in Multivariate Ecological Research) software v5 package [17]. The nematode to copepod ratio (N:C ratio) was calculated by dividing the number of nematodes in a sample by the number of copepods [9]. It was calculated as mean of all N:C values found in the sedimentary environments at each sampling location.

Results and Discussion

The environmental parameters of sampling stations are shown in Table 1. Temperature and pH showed small variations between the three beaches at Wilayah Iskandar development area. Low dissolved oxygen of overlying water was noted at certain area at Station 3 (3.66 mg/L). The water quality at these areas was observed to be in poor conditions as the area was polluted by oil and grease from the boat activities near to the beaches. Low concentration of chlorophyll-a in the sediment at the area also showed the worse environmental conditions and almost totals absence of other groups of meiobenthos. Less water circulation resulting less dilution of contaminant, thus increase the effect of pollution to the area.

Environmental parameters	Station 1	Station 2	Station 3
Salinity (psu)	20.57 ± 2.63	18.66±7.32	8.54 ± 8.2
Temperature (°C)	28.74±1.14	29.63±0.64	28.51±1.3
pH	7.57±0.32	7.58 ± 0.2	7.32 ± 0.47
Dissolved oxygen (mg/L)	7.47±3.34	6.5 ± 1.62	3.66 ± 1.1
Chlorophyll-a (mg m ⁻³)	0.14±0.05	0.55±0.13	0.05 ± 0.06

Table 1: Environmental parameters at each sampling station in Wilayah Iskandar.

Five taxa were recorded from the meiobenthic samples in Wilayah Iskandar development area beaches; Nematoda, Harpacticoida, Oligochaeta, Polychaeta and Isopoda (Figure 2). At all sampling stations, nematodes were the most abundant taxon with a mean density ranged from 54.03 to 263.8 ind.10 cm⁻². They numerically dominated all stations, accounting for 68% of the total meiobenthos (Figure 3). Polychaetes were the second dominant group at

Zaleha et al: HEALTH STATUS OF RECREATIONAL BEACHES IN ISKANDAR DEVELOPMENT REGION, JOHOR, MALAYSIA

Station 1 (13.4 to 76.7 ind.10cm⁻²), accounting for 9% of the total meiobenthos while harpacticoid copepod for 8%. Higher average total meiobenthos densities were noted at Station 2 (141.7 to 444.2 ind.10 cm⁻²) followed by Station 1 (183.5 to 325.5 ind.10cm⁻²) while Station 3 recorded lowest values (69 to 192.4 ind.10cm⁻²). Only pollution-tolerant taxa as polychaetes and nematodes recorded high in density at Station 3 [18]. The low values of density if compared to other studies [19,20,21] and the dominance of pollutant-tolerant group such as nematodes and polychaetes [22,23,24,25] suggest the existence of pollution at the recreational beaches.

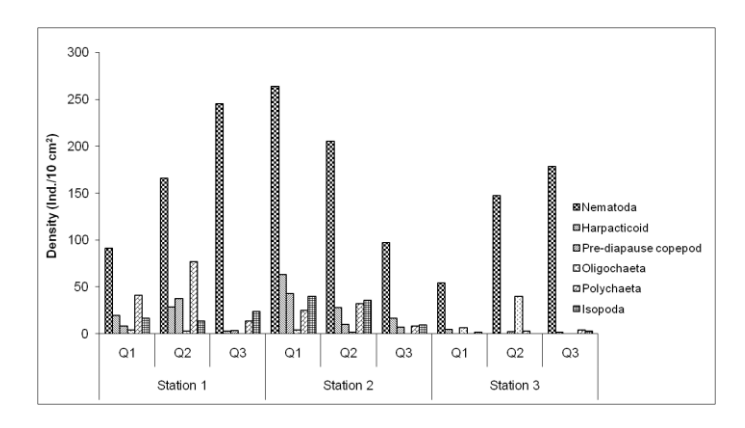


Figure 2: Mean density (Ind.10cm⁻²) of meiobenthic taxa at the three sampling stations

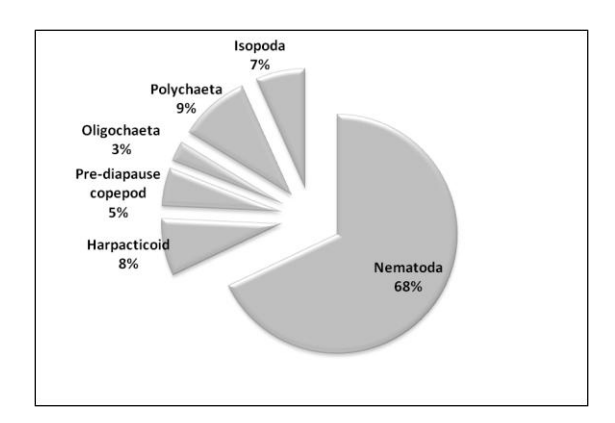


Figure 3: Composition of meiobenthos group at three sampling stations

Gheskiere *et. al* (2005) reported that tourism related activities are particularly affecting the sandy beach meiobenthos in the upper beach zone [26]. The lowest density of meiobenthos (Figure 2) as shown in the upper beach zone (Q1) (Station 1 and Station 3) was found to correlate to such disturbances. Effects of tourist at upper beaches are characterized by a lower percentage of total organic matter (% TOM), lower densities and diversities of meiobenthos compared to non-tourists locations. The one-way ANOSIM tests showed that the meiobenthic communities at sampling stations differed significantly between stations (R: 0.29, P: 0.04) but no significant differences was found between the tide levels (R: 0.05, P: 0.3). The MDS ordination plot of meiobenthic community did not show any clear trend across samples (Figure 4). However, the samples from Station 3 showed high dispersion in the plot, indicating high variability in the structure of their communities. The multivariate approach is important for description of heavily stressed communities characterized by high variability in their structure and low

number of counted individuals [27]. Caswell and Cohen (1991) hypothesized that disturbance might induce higher spatial variability in assemblages due to community stress [28]. Warwick and Clarke (1993) have also consistently recorded increased variability among replicates from several benthic communities (meio- as well as macrobenthos) exposed to increasing disturbance levels [27].

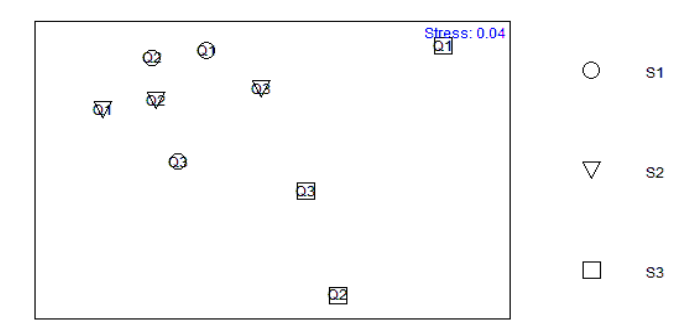


Figure 4: MDS ordination plot based on meiobenthos density at three sampling stations

Values of the nematode/copepod ratio of each station at Wilayah Iskandar development beach are presented in Table 2. The ratio showed a wide variability between stations with highest values were recorded at Station 3 (11.8 to 101.7) and lowest at Station 2 (2.5 to 5.4). The high ratio at Station 3 (>100) could indicate that the area has been polluted. Station 1 and Station 2 recorded lower (<100), than that was proposed by Raffaeli and Mason (1981) for gross polluted situations [9]. Among the two dominant groups of meiobenthos, copepods are more sensitive to environmental stress than nematodes, so that high nematode/copepod ratios might be indicative of pollution situations with higher nematodes density. The ratio increases with organic pollution [29].

The overall ratio which is larger than 100 clearly suggest that the beaches are considerably polluted. Human activities such as recreational boating contribute to the decline in harpacticoids and meiobenthos abundances. Many studies have reported that marine copepods are known to be sensitive to oil and other pollutants [30,31]. The harpacticoid copepod density may provide a useful indicator that can be used in interpreting the health of the ecosystem. The depletion in their densities may reveal the stress or alteration of the health of their habitat.

Table 2: Values of nematode/copepod ratio and densities of nematodes and harpacticoid copepods (Ind/10cm²) at three sampling stations

Station	Station 1			Station 2			Station 3		
Q	Q1	Q2	Q3	Q1	Q2	Q3	Q1	Q2	Q3
N	91	166	245	264	105	97	54	147	178
C	28	66	7	106	38	24	5	3	2
N:C	3.22	2.51	37.26	2.5	5.4	4.11	11.81	50.72	101.7

The presence of pre-diapause copepods was noted at the three beaches of Wilayah Iskandar development with the mean density ranged from 2.2 to 42.8 ind.10cm⁻² (Figure 2). The behavioural response of copepods to undergo this pre-diapause stage at sampling stations is suggested to be due to their response towards environmental stress in their habitat. It is an adaptation of copepods to survive or avoid stressful and unfavourable environmental conditions [32]. Stressed benthic environment as a result of low water quality at the beaches might trigger their occurrence. This dormant copepod has the potential to become a useful tool for environmental parameters indicator and their existence may indicate environmental stress condition in ecosystems. Dale *et. al* (1999) reported that dinoflagellate

Zaleha et al: HEALTH STATUS OF RECREATIONAL BEACHES IN ISKANDAR DEVELOPMENT REGION, JOHOR, MALAYSIA

cysts can be useful indicators of the development or presence of eutrophication in recent marine environments [33]. Their surveys can give early warning of the presence of toxic species in a given area [34].

Conclusion

Within meiobenthos, nematodes and harpacticoids are the important group to be used as a tool for environmental monitoring to determine the health status of recreational beaches. The nematode/copepod ratio and the presence of pre-diapause copepod at the sampling stations indicated that the recreational beaches of Wilayah Iskandar could be under exposure of contaminant from human activities.

References

- 1. Dronkers, J., and de Vries, I., 1999. Integrated coastal management: the challenge of trans-disciplinarity. Journal of Coastal Conservation, 5: 97–102.
- 2. Schlacher, T.A., Schoeman, D.S., Dugan, J., Lastra, M., Jones, A., Scapini, F., and McLachlan, A., 2008. Sandy beach ecosystems: key features, management challenges, climate change impacts, and sampling issues. Marine Ecology, 29: 70–90.
- 3. Chandrasekara, W. U., and Frid, C. L. J. 1996. Effects of human trampling on tidalflat infauna. Aquatic Conservation: Marine and Freshwater Ecosystems, 6: 299–311.
- 4. Lafferty, K. D. 2001. Birds at a Southern California beach: seasonality, habitat use and disturbance by human activity. Biodiversity and Conservation, 10: 1949–1962.
- 5. Kennedy, A.D. and Jacoby, C.A. 1999. Biological indicators of marine environmental health: Meiofauna- A neglected benthic component?. Environmental Monitoring and Assessment, 54: 47-68.
- 6. Moens, T. and Vincx, M. 2000. Temperature and salinity constraints on the life cycle of two brackish-water nematode species, Journal of Experimental Marine Biology and Ecology, 243: 115–135.
- 7. Kim, D. and Shirayama, Y. 2001. Respiration rates of free-living marine nematodes in the subtidal coarse-sand habitat of Otsuchi Bay, northeastern Honshu, Japan. Zoological Science, 18: 969-973
- 8. Sutherland, T.F., Levings, C.D., Petersen, S.A., Poon, P. and Piercey, B. 2007. The use of meiofauna as an indicator of benthic organic enrichment associated with salmonid aquaculture. Marine Pollution Bulletin, 54: 1249-1261.
- 9. Raffaelli, D.G. and Mason, C.F.1981. Pollution monitoring with meiofauna using the ratio of nematodes to copepods. Marine Pollution Bulletin, 12: 158-163.
- 10. Moreno, M., Vezzulli, L., Marin, V., Laconi, P., Albertelli, G., and Fabiano, M. 2008. The use of meiofauna diversity as an indicator of pollution in harbours. International Council for the Exploration of the Sea. Published by Oxford Journals.
- 11. Coull B. C., Hicks G. R. F., and Wells J. B. J. 1981. Nematode-copepod ratios for monitoring pollution: a rebuttal. Marine Pollution Bulletin, 12:378–381
- 12. Lambshead P. J. D. 1984. The nematode–copepod ratio. Some anomalous results from the Firth of Clyde. Marine Pollution Bulletin, 15: 256–259
- 13. Monthum, Y., and Aryuthaka, C. 2006. Spatial distribution of meiobenthic community in Tha Len seagrass bed, Krabi Province, Thailand. Coastal Marine Science, 30(1): 146-153.
- 14. McIntyre, A.D., and R.M. Warwick, 1984. Meiofauna Techniques. Pages 217-244 in A.D. McIntyre, and N.A. Holme, editors, Methods for the Study of Marine Brnthos. IBP Handbook 16 Oxford: Blackwell Scientific Publications.
- 15. Lorenzen, C.J. and Jeffrey, S.W. 1980. Determination of chlorophyll in seawater. UNESCO Technical Papers Marine Science. 35. 20 p.
- 16. Lorenzen, C.J. 1967. Determination of chlorophyll and phaeopigments: spectrometric equations. Limnology Oceanography, 12: 343–346.
- 17. Clarke, K. R., and Gorley, R.N. 2006. Primer v6 user manual. Primer-E Ltd., Plymouth Marine Laboratory, Plymouth, UK.
- 18. Paggy, A.C., Ocon, C., Tangorra, M., and Rodrigues-Capitulo, A. 2006. Response of the zoobenthos community along the dispersion plume of a highly polluted stream in the receiving waters of a large river (Rio de la Plata, Argentina). Hydrobiologia, 568:1-14
- 19. Pinto, T.K.O. and Santos, P.J.P. 2006. Meiofauna community structure variability in a Brazillian tropical sandy beach. Atlântica, Rio Grande, 28(2): 117-127

- 20. Albuquerque, E.F., Pinto, A.P.B., Perez, A.A.Q. and Veloso, V.G. 2007. Spatial and temporal changes in interstitial meiofauna on a sandy ocean beach of South America. Brazillian Journal of Oceanography, 55(2): 121-131
- 21. Rodriguez, J.G., Lopez, J. and Jaramillo, E. 2001. Community structure of the intertidal meiofauna along a gradient of morphodynamic sandy beach types in southern Chile. Revista Chilera de Historia Natural, 74: 885–897.
- 22. Millward, R.N., and Grant, A. 1995. Assessing the impact of copper on nematode communities from a chronically metal-enriched estuary using pollution-induced community tolerance. Marine Pollution Bulletin, 30: 701-706
- 23. Lampadariou, N., Austen, M.C., Robertson, N. and Vlachonis, G. 1997. Analysis of meiobenthic community structure in relation to pollution and disturbance in Iraklion Harbour, Greece. Vie Milieu, 47: 9-24
- 24. Schratzberger, M., Rees, H.L. and Boyd, S.E. 2000. Effects of simulated deposition of dredge material on structure on nematode assemblages the role of contamination. Marine Biology. 137: 613-62
- Gyedu-Ababio, T.K. and Baird, D. 2006. Response of meiofauna and nematode communities to increased levels of contaminants in a laboratory microcosm experiment. Ecotoxicology Environmental Safety,63: 443-450
- 26. Gheskiere, T., Vincx, M., Weslawski, J.M., Scapini, F. and Degraer, S. 2005. Meiofauna as descriptor of tourism-induced changes at sandy beaches. Marine Environmental Research, 60: 245–265



THE EFFECTIVENESS OF SOOT REMOVAL TECHNIQUES FOR THE RECOVERY OF FINGERPRINTS ON GLASS FIRE DEBRIS IN PETROL BOMB CASES

(Keberkesanan Kaedah Penyingkiran Jelaga Bagi Memperoleh Kembali Cap Jari Pada Sisa Kebakaran Kaca Dalam Kes Bom Petrol)

Umi Kalthom Ahmad¹, Yew Su Mei¹, Mohd Shahru Bahari¹, Ng Song Huat² and Vijaya Kumar Paramasivam³

¹Department of Chemistry,
Faculty of Science, Universiti Teknologi Malaysia,
81310 UTM Skudai, Johor Darul Ta'zim
²PDRM Forensic Laboratory,
8 1/2 mile, Jalan Cheras/Kajang,
43200 Cheras, Selangor.
³Makmal Penyiasatan Kebakaran,
Balai Bomba & Penyelamat, Senawang,
70450 Senawang, Negeri Sembilan.

Abstract

The increased use of petrol bombs as an act of vengence in Malaysia has heightened awareness for the need of research relating physical evidence found at the crime scene to the perpetrator of the crime. A study was therefore carried out to assess the effectiveness of soot removal techniques on glass fire debris without affecting the fingerprints found on the evidence. Soot was removed using three methods which were brushing, 2% NaOH solution and tape lifting. Depending on the visibility of prints recovered, prints which were visible after soot removal were lifted directly while prints that were not visible were subjected to enhancement. Glass microscope slides were used in laboratory experiment and subjected to control burn for the formation of soot. Soot was later removed following enhancement of the prints over time (within 1 day, within 2 days and after 2 days). While in simulated petrol bomb ground experiment, petrol bombs were hurled in glass bottles and the fragments were collected. Favorable results were obtained in varying degrees using each soot removal methods. In laboratory testing, brushing and 2 % NaOH solution revealed fingerprints that were visible after removal of excess soot and were lifted directly. As for tape lifting technique, some prints were visible and were successfully lifted while those that were not visible were subjected to superglue fuming for effective fingerprint identification.

Keywords: Soot removal, Glass, Petrol bomb, Brushing, NaOH wash solution (2%), Tape lifting

Abstrak

Penggunaan bom petrol sebagai alat untuk membalas dendam yang semakin meningkat di Malaysia telah menimbulkan kesedaran untuk kajian mengenai bahan bukti fizikal di tempat kejadian yang dapat dikaitkan dengan penjenayah. Maka, satu kajian telah dilakukan untuk menilai keberkesanan teknik penyingkiran jelaga pada kaca tanpa merosakkan cap jari yang berada pada bahan bukti. Jelaga disingkirkan dengan menggunakan tiga kaedah, iaitu memberus, larutan NaOH 2 % dan pengangkat pita. Bergantung kepada ketampakan cap jari yang ditimbulkan, cap jari yang tampak selepas penyingkiran jelaga akan diangkat terus manakala cap jari yang tidak tampak akan ditimbulkan. Sisip kaca mikroskop telah digunakan dalam uji kaji makmal dan dibakar dalam pembakaran terkawal untuk pembentukan jelaga. Jelaga disingkirkan dan diikuti dengan penimbulan cap jari dalam tempoh tertentu (dalam masa 1 hari, dalam masa 2 hari dan selepas 2 hari). Manakala dalam simulasi bom petrol, bom petrol yang terisi dalam botol kaca telah dilontar dan fragmen-fragmennya dikutip. Keputusan yang memuaskan diperoleh pada tahap yang berbeza menggunakan setiap jenis kaedah penyingkiran jelaga. Dalam uji kaji makmal, kaedah memberus dan larutan NaOH 2 % telah menimbulkan cap jari yang tampak selepas menyingkirkan jelaga yang berlebihan dan direkod terus. Dalam kaedah pengangkat pita, sebahagian cap jari adalah tampak dan berjaya direkod manakala sebahagian cap jari yang tidak tampak diproses dengan kaedah pewasapan superglue untuk penimbulan cap jari.

Umi Kalthom Ahmad et al: THE EFFECTIVENESS OF SOOT REMOVAL TECHNIQUES FOR THE RECOVERY OF FINGERPRINTS ON GLASS FIRE DEBRIS IN PETROL BOMB CASES

Kata kunci: Penyingkiran jelaga kaca, bom petrol, memberus, larutan cuci NaOH 2%, pengangkat pita

Introduction

Arson is a crime that may be defined as the willful and malicious burning of other people's properties or burning one's own properties for some improper purposes [1]. Unlike other crimes, fire will not burn and destroy the particular target at the fire scene but destroy whatever is in its path [2]. One of the aspects in arson investigation involves chemical analysis of the collected fire debris resulting from the fire [2, 3, 4]. In chemical analysis, the chemist will deal with extraction, isolation and analysis of the target compound that could be used to accelerate a fire that was set intentionally [5]. The search for evidence of any accelerant used at the scene is a difficult task because the volume of accelerant used is very little and accelerants contain volatiles which evaporate quickly [2].

Molotov cocktail, also known as petrol bomb or fire bomb, is relatively easy to be constructed and is used by arsonist in order to set a fire. Molotov cocktail is not a bomb as popularized by media but an incendiary device where a mechanical explosion occurs when the bottle with a burning wick is thrown and, upon impact the bottle breaks and permits the fuel to spread or splatter [6].

Latent fingerprints consist of a variety of inorganic and organic substances which mainly composed of five basic components i.e., water, skin oils, proteins, salts and contaminants [4]. These components are mainly secreted by eccrine gland and sebaceous gland as fingers and palm were contaminated with secretions from sebaceous glands which mainly consist of oily components though eccrine glands were primarily located at such parts [7, 8]. The fingerprint recovered from glass fragments of petrol bomb would have greater evidential value because this can link the suspect with the bottle that has been thrown [9]. However, fingerprints are one of the evidences that may be overlooked by the fire investigators because they have a misconception that fingerprints are unlikely to be recovered from associated fire damaged evidence [7, 10]. Many of them, including the arsonists assumed that the evidences will be destroyed by the fire.

Several researches regarding soot removal processes have been developed aimed at removing soot that covered the underneath fingerprint and revealed that fingerprints could still be recovered. The most effective method for soot removal and development of marks depended on the type of matrices where prints are deposited [7, 10, and 11]. Ultra high frequency sonication as a method to removed soot had been carried out by Shelef *et al.* [12] with 34 % recovery rate. Spawn [13] had demonstrated the used of running water and tape lifting method to remove soot from household objects. Application of 1% and 2% sodium hydroxide (NaOH) wash solution onto glass surfaces to remove soot was done by Stow and McGurry [9] with successful recovery of fingerprints. They also recommended the use of NaOH solution as soak to loose the soot. Bradshaw *et al.* [10] found that tape lifting was the most effective method to remove soot on nonporous surface and Absorene on porous surface for latent fingerprints. Soot was also found to be successfully removed from larger areas such as window and wall by using latex in recent researches [14, 15].

As there is a significant increment of petrol bomb cases in Malaysia especially when sensitive issues that caused civil unrest in society occurred and lack of research regarding recovery of fingerprints from fire damaged evidence being reported, an initial study was therefore carried out to determine the most suitable method for removal of soot and recovery of fingerprints from glass surfaces.

Experimental

Materials and Chemical Reagents

The materials and chemical reagents used in this study were soft fingerprint brush, fingerprint lifting tape, superglue fuming cabinet, retort stand, forceps, tray, magnifying lamp, Polilight PL500 (Rofin, Australia), Acetone (QRëC, Pulau Pinang), Sodium hydroxide pellet (MERCK, Germany), superglue, Small particles reagent (SPR) 100 (Sirchie, USA), SPR400UV (Sirchie, USA), black fingerprint powder (SPEX Forensics, USA), fluorescent fingerprint powder (Lightning Powder Company, USA), petrol, beer glass bottles, glass microscope slides and cotton cloth (Good Morning towel).

Methodology

The method used was adapted from the work of Stow and McGurry [9]. The quality of finger marks recovered were rated according to Table 1.

Table 1 Fingerprint rating scale

Scale	Description
0	No visible ridges
1	Poor quality
2	Reasonable quality or partial print
3	Good quality, clear ridges

Laboratory Experimentation

The experiment was carried out in laboratory using glass microscope slides to cover every eventuality that may occur in actual cases. The following were the possible conditions for:

i. Unburned glass

- Clear unburned glass containing uncontaminated fingerprint.
- Unburned glass containing uncontaminated fingerprint that have been contaminated with accelerant after being placed onto glass surface.
- Unburned glass containing accelerant contaminated fingerprint.
- Unburned glass containing uncontaminated fingerprint on accelerant contaminated glass surface.

ii. Burned glass

- Burned glass containing uncontaminated fingerprint.
- Burned glass containing uncontaminated fingerprint which have been contaminated with accelerant after being placed onto glass surface
- Burned glass containing accelerant contaminated fingerprint
- Burned glass containing uncontaminated fingerprint on accelerant contaminated glass surface

Fingerprint was deposited onto nine glass slides for each type of glass condition. These samples were divided into 3 sets. The attempt of removing soot and recovering the fingerprint was conducted within 1 day for the first set, within 2 days for the second set and after 2 days for third set.

Powder dusting method, superglue fuming method and SPR method were carried out on recovery of fingerprint from unburned glass slides. For uncontaminated print on unburned glass slide, fingerprint was placed on glass and recovered directly. While for glass slide containing uncontaminated fingerprint which has been contaminated with accelerant after being placed onto glass surface, the glass slide which has been placed with fingerprint was doused with accelerant. The glass slide was left to dry in a fume-cupboard for 30 minutes before the recovery of print was done. As for uncontaminated fingerprint on accelerant contaminated glass surface, clean glass slide was firstly doused with accelerant and was left to dry in fume-cupboard for 30 minutes. The print was then placed onto the glass surface. Lastly, for glass containing accelerant contaminated fingerprint, finger bearing accelerant was placed on the glass before recovery of print was carried out.

In burned condition, each type of the fingerprint was applied to the glass slides individually and subjected to control burning. A sheet of towel (5 cm x 10 cm) was placed in a metal tray and filled with 3 mL of accelerant. The slides were then suspended over the metal tray using retort stand and the accelerant was ignited in a fume cupboard (Figure 1). After soot was formed on the glass, the soot was removed by brushing method, using sodium hydroxide wash solution (2 %) and tape lifting method. Once the soot was removed, the slides were subjected to latent

fingerprint examination. The quality of fingerprint mark on the glass was assessed if the print was visible after removal of soot. Development of fingerprint was carried out for print which was not visible by superglue fuming method. Further enhancement was carried out by using combination of fluorescent SPR and fluorescent powder and viewed under UV source from Polilight for prints which were difficult to see. Prints developed were assessed and photographed.

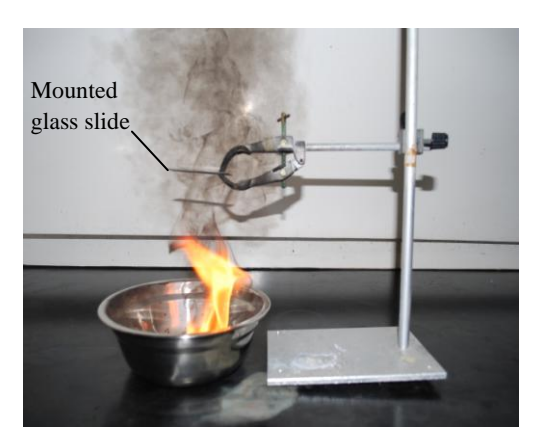


Figure 1: Experimental set-up of control burning in laboratory experiment

Ground Experiment

The throwing of petrol bomb was conducted to assess the practicability of each soot removal method in real petrol bomb cases. The experiment was conducted at Headquarters of Fire and Rescue Department Negeri Selangor at Bukit Jelutong, Shah Alam. Petrol bomb was hurled by fireman under close supervision of police officers from Bomb Disposal Unit and PDRM Forensic Laboratory, Cheras.

The beer glass bottles were initially cleaned thoroughly with soap and water followed by using acetone. A volume of 250 mL accelerants was then funneled into each bottle using gloves followed by insertion of towel wick (11 cm X 31 cm). Prints were deposited onto the glass bottles at the position where the bottles will be held, both on the body and neck of the bottle and the locations of the deposited prints were marked and outlined. The site of petrol bomb throw was cleaned thoroughly prior to ignition. The wick was then ignited and petrol bomb hurled to the explosion site. The fire was then allowed to extinguish naturally. All glass fragments from the broken glass bottle were collected using forceps, stored in a card box and transported back to laboratory for analysis.

The samples collected were subjected to brushing method, NaOH wash solution (2 %) and tape lifting method for glass fragments which were covered with soot. Each type of soot removal method consisted of 9 samples with 3 in a set. One set of the samples were subjected to soot removal process within a day after collection. This process was repeated within 2 days and after 2 days for the other two sample sets. Once the soot was removed, the fragments were subjected to latent fingerprint examination under magnifying lamp. Enhancement was carried out for prints which were not visible under normal condition using superglue fuming method. Further enhancement was carried out by using combination of fluorescent SPR and fluorescent powder and viewed under UV source using Polilight for prints which were difficult to see using similar procedures as in laboratory experiment. The prints developed were thus recorded, assessed and photographed.

Soot Removal Method

In brushing method, excess soot covered on glass was removed using soft brush by brushing gently [16]. For samples subjected to NaOH wash solution (2 %), the solution was applied by using a plastic bottle wash. The

sample was immersed into the solution if the sample was small in size [9]. As for tape lifting method, the adhesive tape was applied to the soot covered glass surface gently to remove excess soot. This step was repeated until print was visible or soot was completely removed [16].

Results and Discussion

Fingerprint Quality Score

Images of print which corresponded to the scores on scale 0 to 3 are shown in Figure 2. The assessment of print quality was subjective and relied on consistent visual scoring by the examiner.

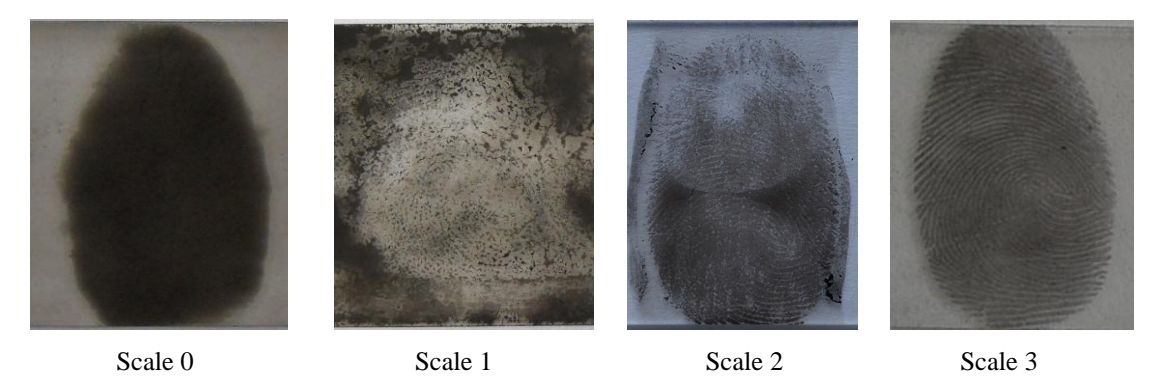


Figure 2: Fingerprint quality with scale 0 to 3 according to the clarity of the fingerprint marks

Laboratory Experimentation

Unburned Condition

The quality of fingerprints developed by powder dusting, superglue fuming and SPR method is shown in Table 2. SPR was found to be the most effective method in developing types of fingerprint. Powder dusting and superglue fuming method on the other hand, were the least effective methods because fingerprint marks could only be developed from uncontaminated samples and samples treated with petrol.

Table 2: Fingerprint quality of different glass condition developed within 24 hours in unburned condition using fingerprint development method

Glass condition	Fingerprint quality					
	Powder dusting	Superglue fuming	SPR			
Uncontaminated fingerprint	3	3	3			
Petrol contaminated fingerprint	3	3	3			
Uncontaminated fingerprint doused with petrol	3	3	3			
Uncontaminated fingerprint on petrol contaminated surface	3	3	2			

The results of this work is in close agreement with that reported by Stow and McGurry [9] with successful development of petrol contaminated fingerprint and uncontaminated fingerprint doused with petrol using SPR and powder dusting method.

Burned Condition

Table 3 showed the fingerprint quality of soot covered sample. The most effective soot removal method is brushing method that gave clear fingerprints (score 3) being recovered, followed by tape lifting method and lastly, NaOH wash solution (2 %). It was found that visible prints were recovered after removal of excess soot covered on glass surface using brushing and NaOH was solution (2 %).

Table 3: Fingerprint quality of different glass condition recovered within 24 hours in burned condition using soot removal method

Glass condition			
_	Brushing	NaOH wash solution (2 %)	Tape lifting
Uncontaminated fingerprint burned with petrol	3	3	3
Petrol contaminated fingerprint	3	2	2
Uncontaminated fingerprint doused with petrol	3	1	3
Uncontaminated fingerprint on petrol contaminated surface	3	2	2

Persistency of Fingerprint

Unburned Condition

The fingerprint were intact throughout the tested period and the overall success rates of fingerprint developed under unburned condition decreased to 75 % on the third day after preparation. The rate of success in development of print is shown in Figure 3. Based on the types of fingerprint which were able to be developed by each method, both superglue fuming method and SPR method gave 100 % success up to 3 days after preparation while powder dusting method has a success rate of 75 % on the third day after preparation. It was reported that fingerprint washed with petrol were successfully developed with 80 % to 90 % and 50 % to 60 % success up to 5 days after preparation using SPR and superglue method [17]. Compared to this study, both methods gave 100 % success on the first day in the test which is similar with the results obtained in this experiment.

Burned Condition

The success rate of fingerprint recovered for each soot removal method throughout 3 days period were decreased (Figure 4). Brushing and NaOH wash solution (2 %) have success rate of 91.67 % and tape lifting method has 83.33 % success rate after 2 days preparation. The overall fingerprint mark recovery success rate in this condition is 100 % for first two days and 75 % for the third day.

Most types of fingerprint which were able to recover by each method remained intact and able to be recovered after 2 days preparation except for uncontaminated fingerprint doused with petrol. As only good quality fingerprint marks were tested in this study, the success rate of fingerprint marks recovered from brushing and NaOH wash solution (2 %) within 1 day were both 100 % compared to 100 % and 75 % success rate respectively in the test conducted by Stow and McGurry [9] in recovery of fingerprint from good quality donor and from poor quality donor.

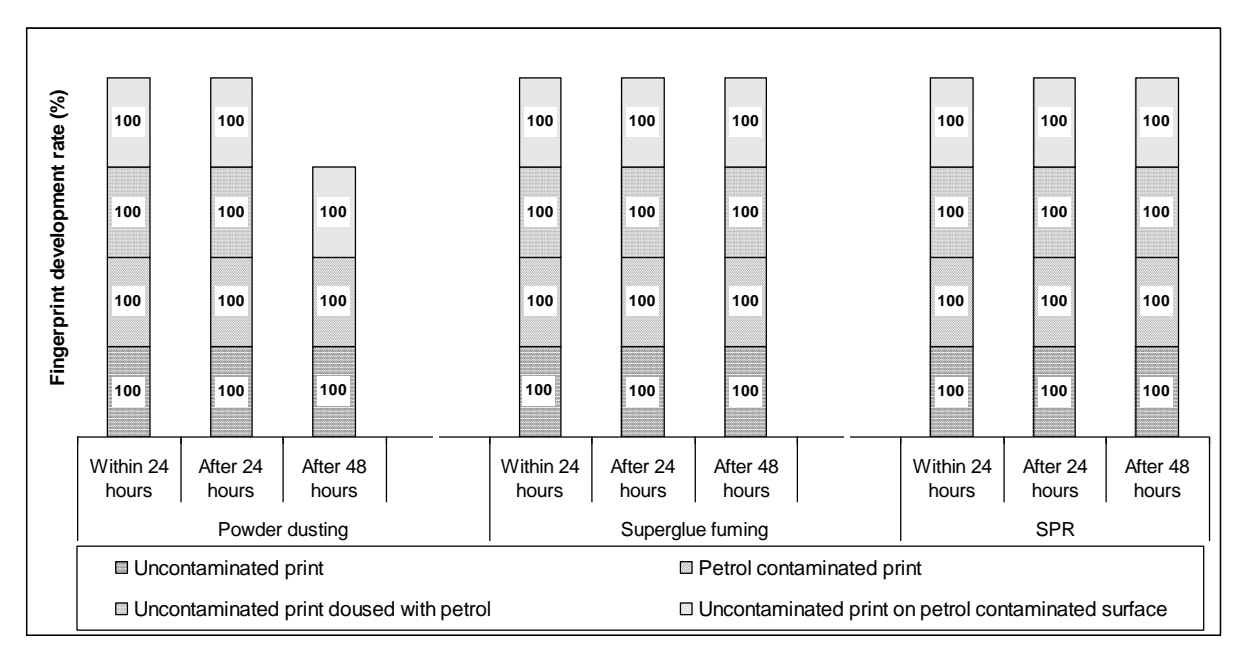


Figure 3: Development rate of different fingerprint types under unburned condition over 3 days period. (Test were conducted in triplicate for each type of fingerprint in each period)

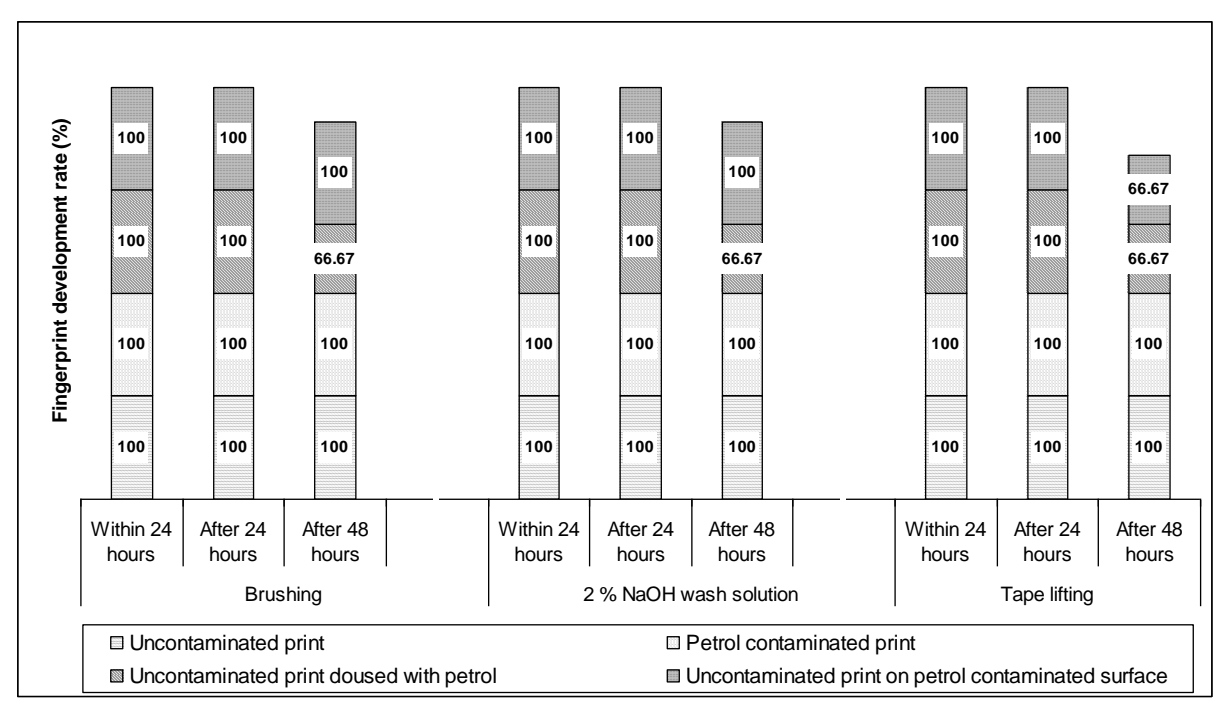


Figure 4: Recovery rate of different fingerprint types under burned condition over 3 days period. (Test were conducted in triplicate for each type of fingerprint in each period)

Ground Experiment

A total of 27 bottles were exploded in this stage and 27 bottles were broken into fragments as the bottles were thrown against a cement wall. Among 27 broken bottles, 26 of the bottles were burned and soot was formed on these bottles. The number of fragments collected from each bottle varied from 1 to 65 pieces. Total fragments collected in whole experiment were 1133 pieces which consisted of 663 pieces of soot covered fragments. All of the fragments were examined for the presence of fingerprint and 58 fingerprints were recovered from soot covered fragments.

Furthermore, fingerprint with score 0 was not accounted for in this stage because the exact number of score 0 fingerprint mark could not be determine. There were two possibilities to explain this finding; either there was no fingerprint deposited by on the fragment or the fingerprint on the glass surface was destroyed.

Soot Covered Fragments

The soot removal methods discuss here were conducted on glass fragments recovered from petrol bomb. Prints were successfully recovered using brushing, NaOH solution (2 %) and tape lifting method (Figure 5). Similar to laboratory experiments, most of the fingerprint marks recovered using each soot removal method were visible after removal of excess soot. The exposure of fingerprint to heat and fire has led to fusion of soot to the ridges thus the fingerprint was revealed when excess soot was removed [10, 13]. The recovery of prints from sample B3 was unsuccessful while no soot covered fragments were recovered from sample T2 because sample T2 was not burned.

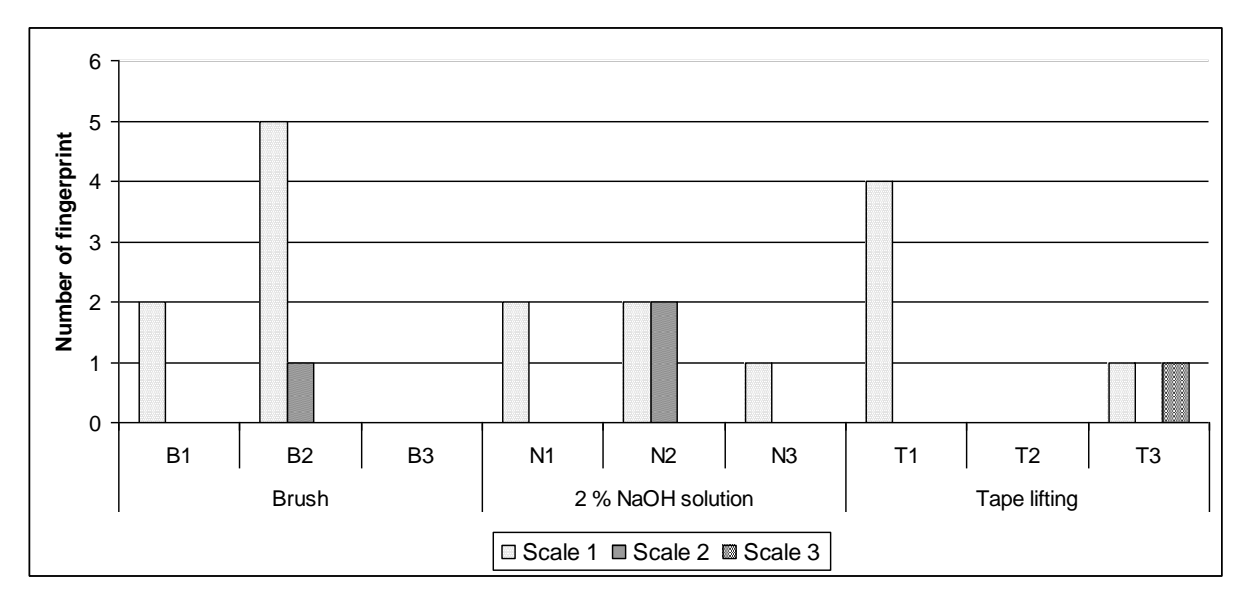


Figure 5: Number of fingerprints recovered in each fingerprint quality by brushing (B), NaOH wash solution (N) and tape lifting (T).

Removal of soot by brushing method is an easy and simple method because the extensive soot on glass surface can be removed easily with light brushing action. The use of NaOH wash solution (2 %) also success in removing excess soot covered on glass fragments and revealed the fingerprint mark underneath it. Some fragments with extensive soot were also subjected to soak in the solution as recommended by Stow and McGurry [9] but no fingerprint marks were recovered from such fragments. Heavy application of NaOH solution (2 %) was found to disrupt the fingerprints [9]. Selection of this method should be used with caution because the used of this solution

will have detrimental effect to DNA [10, 16]. It was also observed that white deposits formed on the glass surface which had been treated with this solution when the sample was left overnight.

In the use of tape lifting method to remove soot result recovery of fingerprint mark, it was only visible when examine at oblique angle. Prints were attempted to develop by superglue fuming method but the fingerprints were still not visible when view at parallel angle. Enhancement of fingerprints was carried using combination of fluorescent SPR suspension and fluorescent powder and the samples were viewed using light source at specific wavelength. Best contrast of fingerprint marks was obtained when viewed under UV light.

Tape lifting method was found to be the most effective method among the three although brushing is the most effective in laboratory experiment. Fragments that had been treated using brushing and NaOH wash solution (2 %) methods were further processed using tape lifting method. The combination of brushing and NaOH solution (2 %) with tape lifting method increased the recovery of fingerprint. Combination of brushing with tape lifting increases the recovery of fingerprint marks while combination of NaOH solution (2 %) with tape lifting increases the recovery of fingerprint marks from three to seven fingerprint marks. Combinations of such methods were also suggested by Bradshaw *et al.* [10].

Persistency of Fingerprint

Figure 6 shows the number of fingerprint recovered from soot covered fragments in the 3 days period. Fingerprints were also unsuccessfully recovered from sample B3, B6, N7, M3 and M6. For sample B5, B9, N4 and T2, there was no recovery of soot covered fragments from these samples.

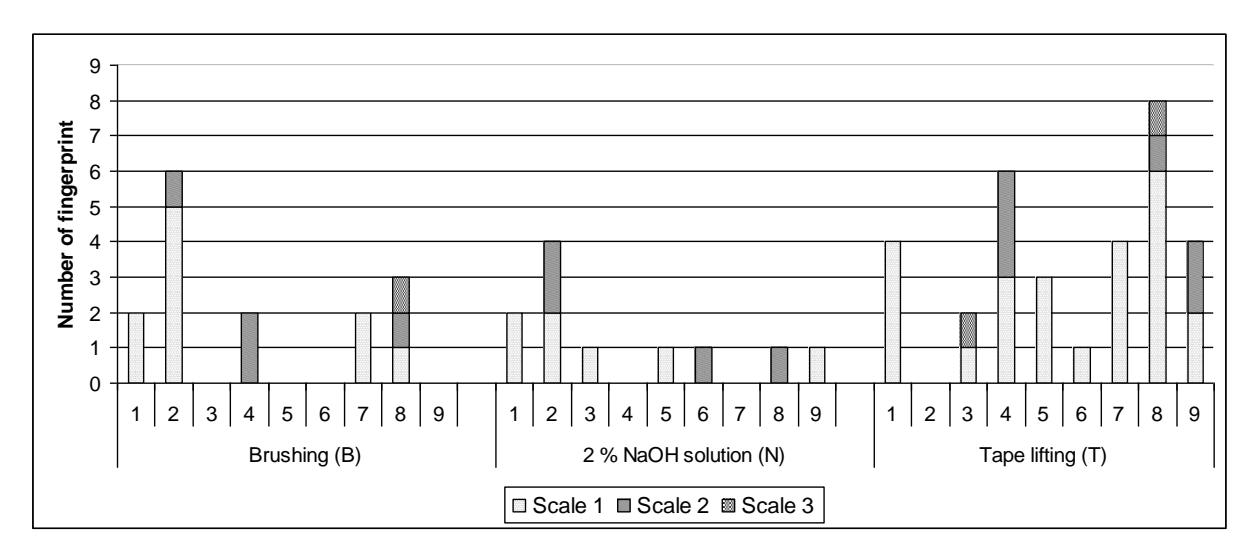


Figure 6. Number of fingerprint mark recovered from soot covered fragments

Comparison between Laboratory Experiment and Ground Experiment

Compared to recovery of fingerprint in laboratory experiment which was in controlled environment, recovery of fingerprint from glass fragments in ground experiment was more difficult. In laboratory experiment, glass slides were suspended at a fixed distance from the heat source. Hence, the heat received by all the samples was consistent. While in the simulated petrol bomb scene, the fragments were scattered over a range of distance from the point of origin with heavily soot covered fragments to a distance where non soot covered fragments were located. The chances to recover fingerprint from soot covered fragments located near to the seat of fire was lower as it was the hottest area where the fingerprint will be destroyed by heat. In addition, the exposure time of fragments to heat also

Umi Kalthom Ahmad et al: THE EFFECTIVENESS OF SOOT REMOVAL TECHNIQUES FOR THE RECOVERY OF FINGERPRINTS ON GLASS FIRE DEBRIS IN PETROL BOMB CASES

affect the recovery of fingerprint as the physical and chemical properties of fingerprint will be affected by such exposures [10, 11, 13]. However, the temperature of fire and exposure time of sample to fire in each experiment was not obtained in this study. Furthermore, safety gloves were worn during hurling of petrol bomb due to safety consideration. This may smudge the prints initially planted on the glass bottle and possibly removal of some prints.

The condition of soot covered glass fragment obtained from simulated scene varies too. Some of the fragments were contaminated with dirt and some fragments heavily contaminated with oil which causes the recovery of fingerprint marks becomes more difficult. Furthermore, the outer side of glass bottle that impacted the cement floor could contribute to destruction of fingerprints upon contact with the cement floor. As the glass surfaces were only suspended over the accelerant in laboratory experiment, no contamination of oil were found on glass surfaces.

Conclusion

This work has showed that it is possible to recover fingerprints from soot covered glass fragments from petrol bombs over a three days period of storage in laboratory using brushing, NaOH wash solution (2 %) and tape lifting method. All the methods used show successful recovery to varying degree with tape lifting method as the most effective method in soot removal process for recovery of prints from soot covered fragments. This method can also be used in combination with brushing and NaOH wash solution (2 %). For non soot covered fragments, recovery of fingerprint marks using superglue fuming method follow by examination under light source at specific wavelength proved successful in recovery of prints from uncontaminated fragments.

Acknowledgement

Thanks are due to the Department of Chemistry, Faculty of Science, UTM for research facilities and Forensic Laboratory of Royal Malaysia Police for technical support. Special thank goes to the Fire and Rescue Team of Headquarters, Fire and Rescue Department, Selangor and Bomb Disposal Unit, Bukit Aman for their assistance in the petrol bombs explosion.

References

- 1. Fisher, B. A. J. (1992). *Techniques of Crime Scene Investigation*. (5th ed.) New York: Elsevier Science Publishing Co., Inc.
- 2. Stewart, G. B. (2006). Crime Scene Investigation: Arson. United States of America: Thomson Gale.
- 3. Midkiff, C. R. (1982). Arson and Explosion Investigation. In Saferstein, R. (Ed.) *Forensic Science Handbook* (pp. 222-237). New Jersey: Prentice-Hall Inc.
- 4. DeHaan, J. D. (2007). *Kirk's Fire Investigation*. (6th ed.) Upper Saddle River, New Jersey. Pearson Education Inc.
- 5. Almirall, J. R., and Furton, K. G. (2004). Characterization of Background and Pyrolysis Products that may Interfere with the Forensic Analysis of Fire Debris. *J. Anal. Appl. Pyrolysis*. 71, 51-67.
- 6. Bordie, T. G. (1973). Bomb and Bombings: A Handbook to Detection, Disposal and Investigation for Police and Fire Departments. United States of America: Charles C Thomas.
- Deans, J. (2006). Recovery of Fingerprints from Fire Scenes and Associated Evidence. Sci. Justice. 46(3), 153-168.
- 8. Asano, K. G., Bayne, C. K. and Buchanan, M. V. (2002). Chemical composition of fingerprints for gender determination. *J. Forensic Sci.* 247, 805-807.
- 9. Stow, K. M., and McGurry, J. (2006). The Recovery of Finger Marks from Soot-covered Glass Fire Debris. *Sci. Justice*. 46(1), 3-14.
- 10. Bradshaw, G., Bleay, S., Deans, J. and NicDaeid, N. (2008). Recovery of Fingerprints from Arson Scenes: Part 1- Latent Fingerprints. *J. For. Ident.* 58(1), 54-82.
- 11. Moore, J., Bleay, S., Deans, J. and NicDaied, N. (2008). Recovery of Fingerprints from Arson Scences: Part 2-Fingerprints in Blood. *J. For. Ident.* 58(1), 83-108
- 12. Shelef, R., Levy, A., Rhima, I., Tsaroom, S. and Elkayam, R. (1996). Recovery of Latent Fingerprints from Soot-Covered Incendiarized Glass Surfaces. *J. For. Ident.* 46b (5), 565-569.
- 13. Spawn, M. A. (2004). Effects of Fire on Fingerprint Evidence. Minutiae. 79, 4-6.

- 14. Larkin, T. P. B., Marsh, N. P. and Larrigan, P. M. (2008). Using Liquid Latex to Remove Soot to Facilitate Fingerprint and Bloodstain Examinations: A Case Study. *J. For. Ident.* 58(5), 540-550.
- 15. Clutter, S. W., Bailey, R., Everly, J. C. and Mercer, K. (2009). The Use of Liquid Latex for Soot Removal from Fire Scenes and Attempted Fingerprint Development with Ninhydrin. *J. Forensic Sci.* 54(6), 1332-1335.
- 16. Bleay, S. M., Bradshaw, G. and Moore, J. E. (2006). *Fingerprint Development and Imaging Newsletter: Special Edition*. United Kingdom: Home Office Scientific Development Branch.
- 17. Shelef, R., Levy, A., Rhima, I., Tsaroom, S. and Elkayam, R. (1996). Development of Latent Fingerprints from Unignited Incendiary Bottles. *J. For. Ident.* 46a (5), 557-560.



RADIATION HAZARD FROM NATURAL RADIOACTIVITY IN THE SEDIMENT OF THE EAST COAST PENINSULAR MALAYSIA EXCLUSIVE ECONOMIC ZONE (EEZ)

(Hazard Sinaran Dari Radionuklid Tabii Dalam Sedimen Di Zon Ekslusif Ekonomi (ZEE) Perairan Pantai Timur Semenanjung Malaysia)

Yii Mei-Wo*, Nurrul Assyikeen Md. Jaffary and Zaharudin Ahmad

Waste And Environmental Technology Division Malaysian Nuclear Agency 43000 Kajang, Malaysia

*Corresponding author: yii@nuclearmalaysia.gov.my

Abstract

Sixteen marine sediment cores from selected locations within the EEZ were collected for determination of NORM concentrations. The samples were dried, finely ground, sealed in a container and stored for more than 30 days to establish secular equilibrium between 226 Ra and 228 Ra and their respective radioactive progenies. They were counted and quantified using high-purity germanium (HPGe) detector coupled to spectrometer at respective progeny energy peak. Three calculated parameters from NORM concentrations, i.e. the Radium equivalent (Ra_{eq}), Representative level index ($I_{\gamma\tau}$), External hazard index (H_{ex}) are ranged between 68.6-210.5 Bq/kg (mean 143.1 ± 27.7 Bq/kg), 0.50-1.54 (mean 1.04 ± 0.20) and 0.19-0.57 (mean 0.39 ± 0.07 Bq/kg), respectively. This is well below the recommended limit value of 370 Bq/kg (for Ra_{eq}) and unity (for H_{ex}). It is also slightly less than the background level radiation from soil in Peninsular Malaysia, $I_{\gamma\tau} \sim 1.5$. Therefore, the additional radiation exposure to peoples handling the samples is small, when compared to the background radiation received by them. The data is discussed and compared with those given in the literature.

Keywords: EEZ, sediment, radium equivalent activity, representative level index, external hazard index.

Abstrak

Enam belas turus sedimen dari lokasi terpilih dalam ZEE telah diambil untuk pengukuran kepekatan NORM. Sampel tersebut dikeringkan, dikisar halus, dilakri dalam bekas dan disimpan untuk tempoh melebihi 30 hari bagi mencapai keseimbangan sekular antara 226 Ra dan 228 Ra bersama progeni radioaktif mereka. Mereka diukur dan dikuantitikan pada puncak tenaga progeni masing-masing dengan menggunakan pengesan germanium lampau tulin yang disambung kepada spektrometer. Tiga parameter kiraan dari kepekatan NORM iaitu, Radium setaraan (Ra_{eq}), Indeks tahap perwakilan ($I_{\gamma r}$), Indeks hazard luaran (H_{ex}) adalah masing-masing dalam julat 68.6-210.5 Bq/kg (purata 143.1 ± 27.7 Bq/kg), 0.50-1.54 (purata 1.04 ± 0.20) dan 0.19-0.57 (purata 0.39 ± 0.07 Bq/kg). Nilai tersebut adalah di bawah had yang dicadangkan iaitu 370 Bq/kg (untuk Ra_{eq}) dan uniti (bagi H_{ex}). Ia juga kurang berbanding tahap sinaran latar belakang dari tanah di Semenanjung Malaysia, $I_{\gamma r} \sim 1.5$. Oleh itu, pendedahan sinaran tambahan kepada orang yang mengendalikan sampel adalah kecil jika dibandingkan dengan sinaran latar belakang yang diterima oleh mereka. Data keputusan akan dibincang dan dibanding dengan nilai dari rujukan.

Kata kunci: ZEE, sedimen, radium setaraan, indeks tahap perwakilan, indeks hazard luaran.

Introduction

Two prominent sources of external radiation are cosmic rays and terrestrial gamma rays. Cosmic rays are mostly been shielded off by the ozone and contribute less radiation hazard to human beings. Meanwhile, the primary source of terrestrial radiation received by humans is from the store of natural radioactivity in earth crust, which derives essentially from ⁴⁰K and the progenies of ²³⁸U and ²³²Th decay series such as radium, radon, actinium, protactinium, lead and polonium. These progenies first appear in the lithosphere level, deposited on the soil surface, then washed

Yii Mei-Wo et al: RADIATION HAZARD FROM NATURAL RADIOACTIVITY IN THE SEDIMENT OF THE EAST COAST PENINSULAR MALAYSIA EXCLUSIVE ECONOMIC ZONE (EEZ)

and drained through rivers transport and finally end up in the estuary and entering the marine environment. It also has gone through several pathways such as weathering, erosion, fallout, rainwater and human activities [1, 2, 3, 4].

When the marine sediments were excavated for study, the researchers whose working environment was surrounded by these sediment samples daily are exposed to additional radiation from these natural radioactivities. Therefore, the radiation hazards to these people are of interests in order to ensure that no additional doses are imposed on to them. Among those, radium-226 (²²⁶Ra, uranium series progeny), radium-228 (²²⁸Ra, thorium series progeny) and potassium-40 (⁴⁰K) are at most concern due to theirs high solubility and mobility as well as emitting gamma energies. In most literatures, radiation hazards were calculated from the specific activity of these three radionuclides [5, 6, 7, 8].

Koide *et al.* (1973) [9] specified that the radioactivity of the progenies from the natural decay series in the marine environment may not necessary be in equilibrium with it parents. Two main sources of marine radioactivities are coming from the weathering and mineral recycling of the terrestrial rocks. In other word, sediment in the coastal is mainly contributed from materials on terrestrial. Baseline information on the spatial variation of radionuclide concentration in the environment is necessary to evaluate any change induced by humans in the future [10]. In addition, these data are required to trace the movement of radionuclides from original source into environmental and biological systems [11].

In coastal areas and on the continental shelf, it is reasonable to assume that the sediments have a range of concentration of natural radionuclides similar to that of terrestrial rocks, and the radioactive equilibrium is maintained. The concentrations of ²²⁶Ra, ²²⁸Ra and ⁴⁰K on terrestrial especially in the areas of Peninsular Malaysia had been widely reported [12, 13, 14, 15, 16]. Several studies on NORM and their progenies had also been reported on the Malaysian marine ecosystems [17, 18] but none specify on the radiation hazard.

The main scope of this work is to determine the additional radiation hazards received by the researchers while carry out they daily routine. This enable a dosimetric evaluation for hazard to these people were estimated. Additionally, these data will indirectly give a brief idea of the radiation levels in the surrounding area on terrestrial at East Coast Peninsular Malaysia.

Experimental

Sampling, preparation and measurement

The east coast of Peninsular Malaysia Exclusive Economic Zone, EEZ was the designated area for this study. Samples were collected during sampling expedition on board the K.L. PAUS (owned by the Malaysian Fisheries Institute) from June 11th to 30th, 2008. A total of thirty locations had been identified to be sampling site. Location and sampling dates are as given in Table 1 while Fig. 1 marks the location of each sampling points. The samplings were done systematically according to a grid within Malaysian EEZ which covers shallow coastal, near-shore and off shore zones of the east coast of Peninsular Malaysia. Physical and chemical parameters such as salinity, temperature and dissolved oxygen (DO) of the water column were also measured as supporting parameters (Table 1).

The core sediments were collected using a 12 cm diameter multicorer device and sliced into 2 cm sections at site and sealed in a pre-weighted HDPE container. During sampling expedition, some of the cores showed thorough vertical mixing of fine and sandy mud, however, some cores are too short (< 20 cm) and while others are too sandy (as illustrated in Fig. 1) and all these cores are not processed for analysis. Only good sediment cores (sixteen in total) with enough length and low sand content (marked • close circle as in Fig.1) were processed and analyzed.

Inside the laboratory, all these selected core samples were dried at 60°C for minimum 72 hours until they reached a constant mass, then ground to pass through a 200 mesh sieve for radiochemical analysis. Samples were transferred into 200 mL marinelli beaker, sealed with thick PVC tape to inhibit radon from escaping. All samples were stored for a period in excessive of 30 days [5, 19] to establish secular equilibrium between ²²⁶Ra and ²²⁸Ra and their respective radioactive progeny prior to gamma counting.

Table 1: Surrounding physical conditions and coordinates of sampling locations

Station	Date	Latitude	Longitude	Water depth (m)	Surface Seawater temp.(°C)	Distance from shore (nautical miles)
SF01	18.06.08	06° 13.99' N	102° 19.00' E	13.0	30.87	2.7
SF02	17.06.08	06° 50.04' N	102° 47.04' E	46.5	30.51	50
SF03	17.06.08	07° 05.03' N	103° 04.99' E	50.0	30.32	73
SF04	17.06.08	07° 25.98' N	103° 26.01' E	61.0	30.03	100
SF05	16.06.08	06° 56.09' N	103° 56.04' E	52.0	30.01	108
SF06	16.06.08	06° 42.14' N	103° 35.17' E	52.0	30.13	80
SF07	16.06.08	06° 10.00' N	103° 01.00' E	45.0	30.25	40
SF08	18.06.08	05° 52.10' N	102° 51.92' E	34.0	30.41	15
SF09	20.06.08	05° 22.06' N	102° 21.97' E	47.0	28.98	14
SF10	14.06.08	05° 48.20' N	103° 48.98' E	55.0	30.27	48
SF11	14.06.08	06° 06.16' N	104° 09.11' E	72.0	30.04	75
SF12	14.06.08	06° 32.01' N	104° 22.11' E	59.0	29.58	101
SF13	13.06.08	06° 16.98' N	105° 16.99' E	55.0	29.87	139
SF14	13.06.08	05° 57.15' N	104° 58.13' E	56.0	29.63	115
SF15	12.06.08	05° 29.08' N	104° 29.02' E	60.7	29.62	80
SF16	12.06.08	05° 18.50' N	104° 12.60' E	60.0	29.65	56
SF17	20.06.08	04° 54.12' N	103° 42.98' E	54.0	29.93	17
SF18	11.06.08	04° 28.14' N	103° 49.98' E	40.0	29.79	20
SF19	22.06.08	03° 37.07' N	103° 41.08' E	23.0	29.50	15
SF20	22.06.08	03° 55.10' N	104° 00.05′ E	50.0	29.74	40
SF21	23.06.08	04° 22.16' N	104° 22.07' E	65.0	29.63	52
SF22	23.06.08	04° 44.19' N	104° 38.44′ E	66.0	29.63	70
SF23	12.06.08	05° 08.10' N	105° 12.90' E	67.2	29.89	109
SF24	23.06.08	03° 32.08' N	104° 36.00' E	62.0	29.75	70

SF25	24.06.08	03° 09.14' N	104° 09.04′ E	41.0	29.03	42	_
SF26	26.06.08	02° 56.13' N	103° 49.97' E	20.0	29.44	24	
SF27	24.06.08	02° 16.94' N	104° 16.97' E	30.0	29.21	19.5	
SF28	24.06.08	02° 39.18' N	104° 38.91′ E	58.0	29.30	47	
SF29	25.06.08	02° 00.55' N	104° 41.97' E	46.0	29.73	35	
SF30	25.06.08	01° 48.04' N	104° 15.03' E	14.0	29.47	4.5	

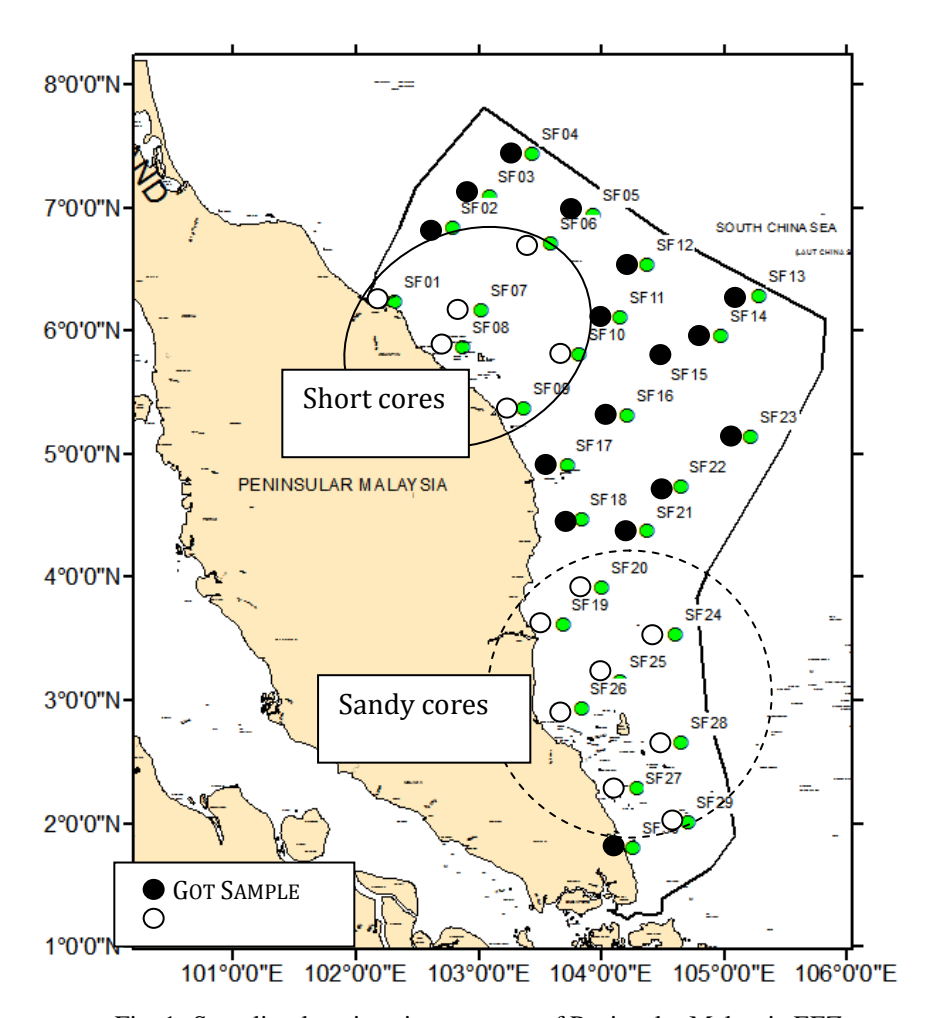


Fig. 1: Sampling locations in east coast of Peninsular Malaysia EEZ

All samples were counted for 86,400 seconds using HPGe spectrometer and corrected to the date of sampling. Counting times were long enough to ensure a 2σ counting error of less than 10%. The energy peaks used are the same as reported by Yii *et al.* 2009 [20].

Counting System

The high-purity germanium (HPGe) detector was characterized to provide 25% efficiency and 1.8 keV at FWHM for the 1332 keV gamma-ray line of ⁶⁰Co. It was calibrated using procedures as reported earlier by Yii *et al.* 2009 [20].

The radioactivity concentrations in the environmental samples were calculated using equation as reported by Yang *et al.* (2005) [5] and Chen *et al.* (2005) [21]. The minimum detectable activity (MDA) for both ²²⁶Ra and ²²⁸Ra was quantified at 2 Bq/kg per dry weight (dry wt.), while ⁴⁰K was quantified at 5 Bq/kg after considering the size and the counting time of the sample.

Results and Discussion

Surrounding physical conditions at sampling locations were summarized in Table 1. All the values of samples are found to be greater than the minimum detectable activity (MDA). From the measurement, it found that the concentrations of naturally occurring radionuclides vary significantly from place to place as their presence in the marine environment depends on their physical, chemical and geochemical properties and the pertinent environment in the biological process [22]. In total, from all sediment cores, the concentration of 226 Ra is ranged between 16-46 Bq/kg with a mean value of 30 ± 6 Bq/kg; the activity of 228 Ra varies from 28 to 87 Bq/kg with a mean value of 56 \pm 11 Bq/kg; and that of 40 K from 171 to 690 Bq/kg with a mean of 420 ± 90 Bq/kg. The activity concentrations of radionuclides in most cores are quite uniform suggesting that there is thorough vertical mixing of sediment throughout the core. However, the activity concentrations in some cores appear to be higher when compared to other stations. The large area of sampling, i.e. EEZ could be the reason why the concentrations are not uniformly distributed.

Calculation of radiological effects

The most widely used radiation hazard index is called the radium equivalent activity, Ra_{eq} . The radium equivalent activity is a weighted sum of activities of the ^{226}Ra (^{238}U), ^{228}Ra (^{232}Th) and ^{40}K radionuclides based on the assumption that ^{226}Ra , 259 Bq/kg of ^{228}Ra and 4810 Bq/kg of ^{40}K produce the same gamma ray dose rate [5, 8, 23]. Radium equivalent activity can be calculated from the following relation:

$$Ra_{eq} = A_{Ra} + 1.43 A_{Th} + 0.077 A_{K}$$
 (1) [24]

where A_{Ra} , A_{Th} , A_K are the activity concentration of ^{226}Ra , $^{232}Th(^{228}Ra)$ and ^{40}K , respectively. To be non-hazardous, the Ra_{eq} should not exceed a maximum of 370 Bq/kg [25].

Another radiation hazard index called the representative level index, I_{yr}, is defined from the following formula [26].

$$I_{\gamma r} = \frac{1}{150 \, Bq \, / \, kg} A_{Ra} + \frac{1}{100 \, Bq \, / \, kg} A_{Th} + \frac{1}{1500 \, Bq \, / \, kg} A_{K} \tag{2}$$

where A_{Ra} , A_{Th} , A_{K} having the same meaning as in Eq. (1).

External hazard index (H_{ex}) is another assumption that enables to evaluate the additional radiological hazard of natural gamma-radiation to the workers whose deal and surrounded by the sediments daily. The calculation was performed using equation as reported by Yang *et al.* (2005) [5] and Nabil *et al.* (2010) [6].

$$H_{ex} = \frac{Q_U}{370} + \frac{Q_{Th}}{259} + \frac{Q_K}{4810} \le 1 \tag{3}$$

where Q_U , Q_{Th} , and Q_K are the activity concentrations of $^{238}U(^{226}Ra)$, $^{232}Th(^{228}Ra)$ and ^{40}K , respectively.

The Radium equivalent activity (Ra_{eq}), Representative level index ($I_{\gamma r}$), External hazard index (H_{ex}) for each individual 2 cm layer section sediment of the core had been calculated from the NORM activity and shown as in Figs. 2 – 4 and summarized in Table 2.

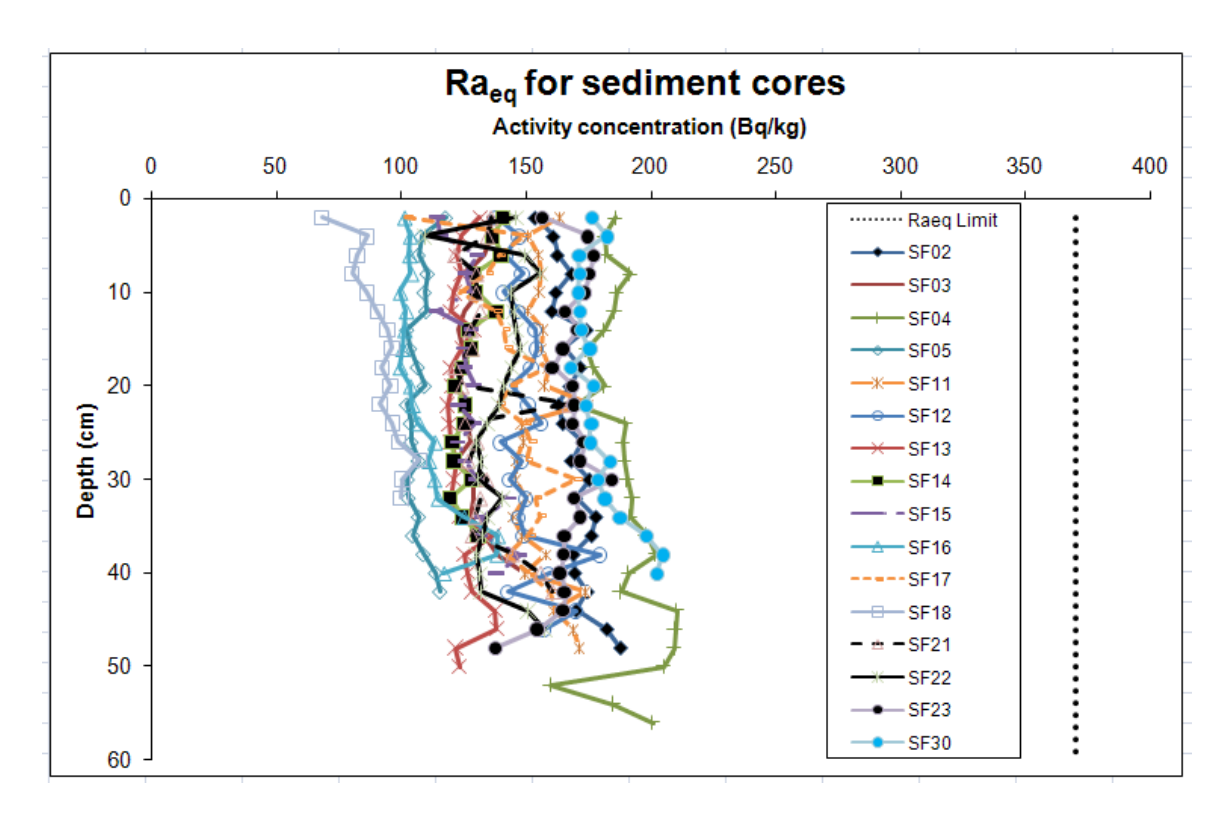


Fig. 2: Radium Equivalent in core sediment from east coast of Peninsular Malaysia EEZ

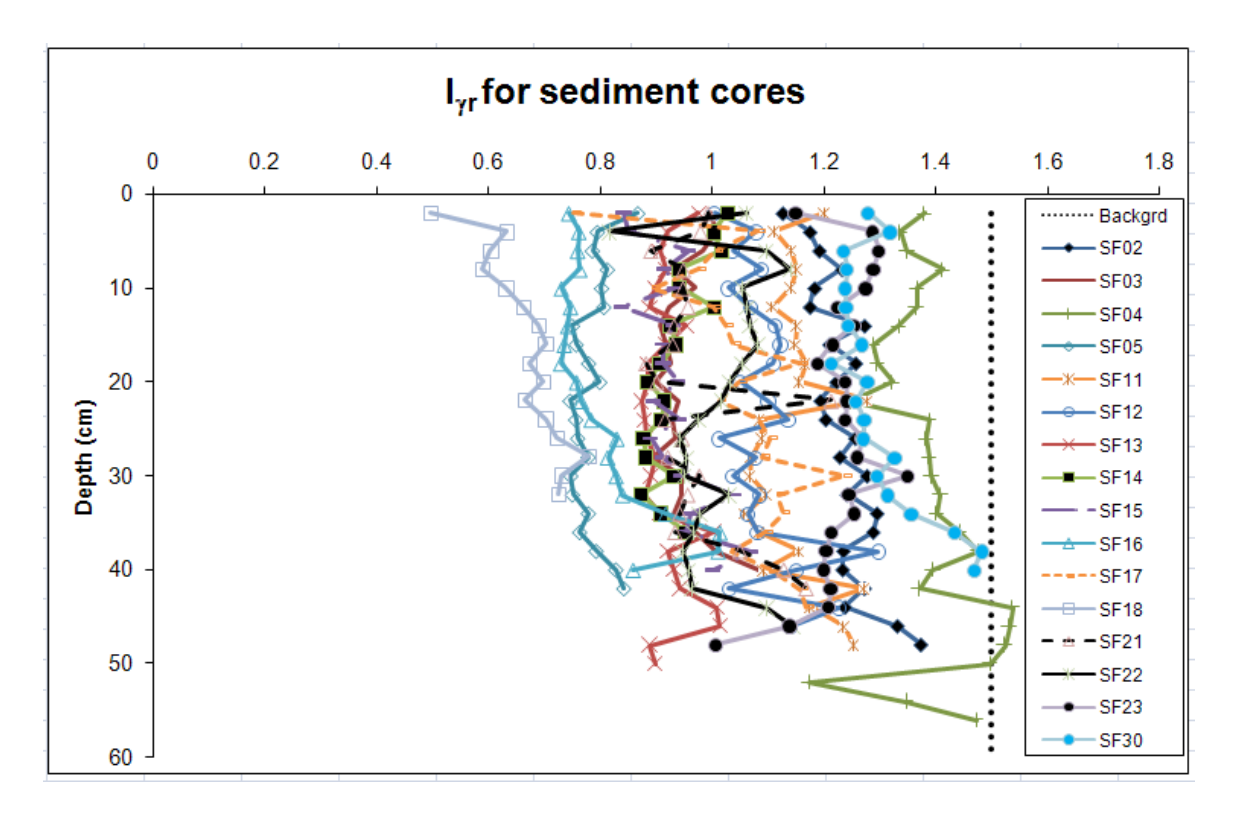


Fig. 3: Representative Level Index in core sediment from east coast of Peninsular Malaysia EEZ

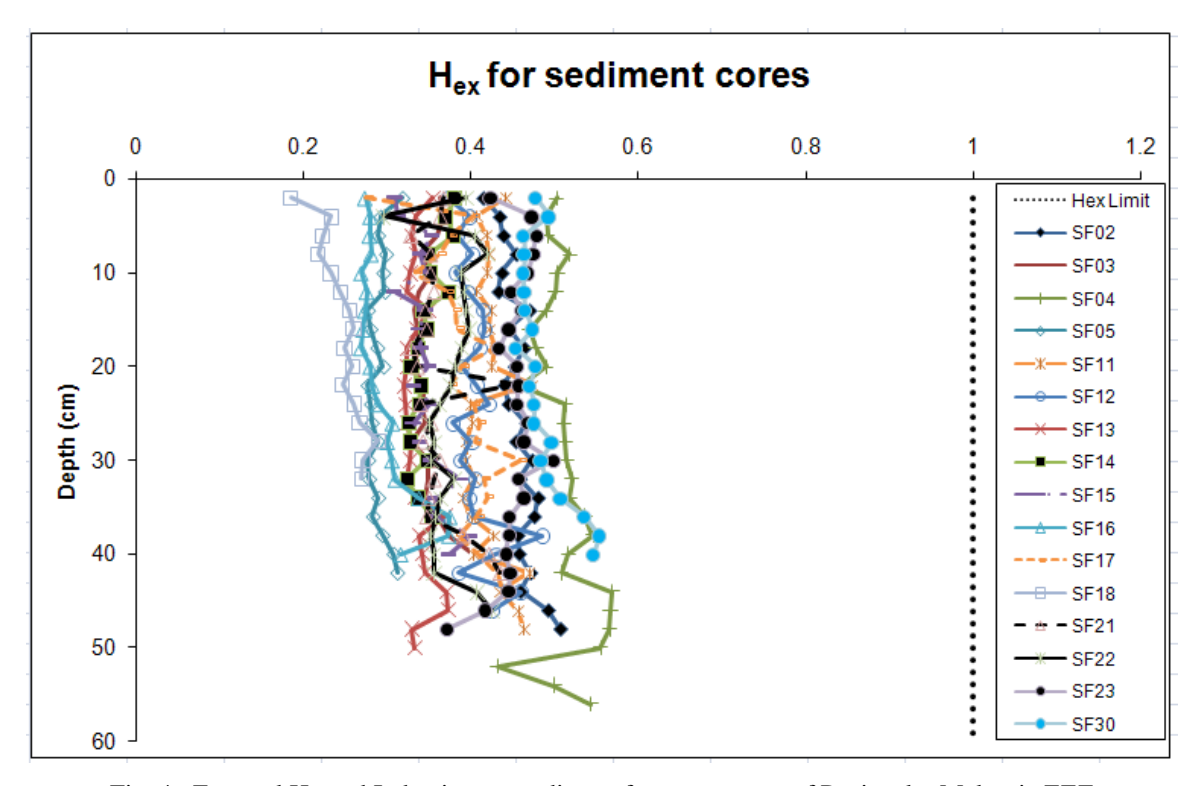


Fig. 4: External Hazard Index in core sediment from east coast of Peninsular Malaysia EEZ

Table 2:	Ra.a.	I	Har	in	the east	coast	Peninsular	Malays	sia EEZ	sediment cores

Station	Ra _{eq} , (I	Bq/kg)	I	уг	Н	H _{ex}		
Station	Range	Mean	Range	Mean	Range	Mean		
SF 02	153.6 – 187.8	169.4 ± 7.6	1.13 – 1.37	1.24 ± 0.05	0.41 - 0.51	0.46 ± 0.02		
SF 03	121.9 – 149.4	129.7 ± 6.6	0.89 - 1.08	0.95 ± 0.05	0.33 - 0.40	0.35 ± 0.02		
SF 04	160.0 - 210.5	189.4 ± 11.9	1.17 – 1.54	1.39 ± 0.08	0.43 - 0.57	0.51 ± 0.03		
SF 05	102.5 – 118.0	107.7 ± 4.4	0.75 - 0.87	0.79 ± 0.03	0.28 - 0.32	0.29 ± 0.01		
SF 11	144.9 – 175.0	156.3 ± 8.9	1.06 - 1.28	1.15 ± 0.06	0.39 - 0.47	0.42 ± 0.02		
SF 12	138.0 – 179.7	150.5 ± 9.6	1.00 - 1.30	1.09 ± 0.07	0.37 - 0.49	0.41 ± 0.03		
SF 13	118.6 – 138.1	124.8 ± 5.8	0.87 - 1.01	0.92 ± 0.04	0.32 - 0.37	0.34 ± 0.02		
SF 14	120.0 - 140.9	128.7 ± 6.6	0.87 - 1.03	0.93 ± 0.05	0.32 - 0.38	0.35 ± 0.02		
SF 15	114.3 – 147.7	128.1 ± 8.5	0.84 - 1.07	0.93 ± 0.06	0.31 - 0.40	0.35 ± 0.02		
SF 16	99.6 – 138.6	110.1 ± 11.8	0.73 - 1.01	0.81 ± 0.09	0.27 - 0.37	0.30 ± 0.03		
SF 17	101.5 – 169.8	145.6 ± 14.3	0.75 - 1.24	1.06 ± 0.10	0.27 - 0.46	0.39 ± 0.04		
SF 18	68.6 - 107.2	91.8 ± 9.3	0.50 - 0.78	0.67 ± 0.07	0.19 - 0.29	0.25 ± 0.03		
SF 21	121.9 – 167.4	134.6 ± 12.4	0.88 - 1.21	0.98 ± 0.09	0.33 - 0.45	0.36 ± 0.03		
SF 22	109.4 – 157.6	139.3 ± 10.6	0.82 - 1.14	1.02 ± 0.08	0.30 - 0.43	0.38 ± 0.03		
SF 23	137.9 – 184.4	167.2 ± 9.0	1.01 – 1.35	1.23 ± 0.07	0.37 - 0.50	0.45 ± 0.02		
SF 30	167.9 – 204.8	180.0 ± 10.6	1.21 – 1.48	1.30 ± 0.08	0.45 - 0.55	0.49 ± 0.03		
*Overall	68.6 – 210.5	143.1 ± 27.7	0.50 - 1.54	1.04 ± 0.20	0.19 - 0.57	0.39 ± 0.07		

^{*}Overall value given was the range and average mean for all reported sediment cores

From the data, it is obvious that for each sediment section of the cores, the calculated value for that of radium equivalent activity and external hazard index are well below the recommended value, showing that the sediment samples does not necessary adding extra radiation hazards to the workers even though they are surrounded by these samples daily. Meanwhile, calculated representative level index ($I_{\gamma r} \sim 1.0$) was also less than the background level ($I_{\gamma r} \sim 1.5$) in Peninsular Malaysia's soil. In all cores, only layer 42 – 44 cm of the SF 04 core sediment having values slightly more than that of the background level.

From the pictorials in Figs. 2-4, we can conclude that the hazard index is low especially when dealing with sediments from stations SF 05, SF 16 and SF 18. Whilst, stations SF 04 and SF 30 are contributing more radiation hazards compared to the sediments from other locations.

The results for the radium equivalent activity, representative level index, and external hazard index of the present work and other studies are compared in Table 3. It is found that , in general, the value of Ra_{eq} , $I_{\gamma r}$ and H_{ex} calculated for the sediments in this study is comparable to those reported elsewhere and less than recommended figures,

indicating that the hazard of radiation exposure for the workers whose handle the samples are less when compared to the Peninsular Malaysia's background radiation received by them.

Table 3: Comparison of Ra_{eq} , I_{yr} , H_{ex} of the present work and other studies.

Country	Sample	Ra _{eq} (Bq/kg)	$\mathbf{I}_{ m \gamma r}$	H _{ex}	References
Egypt	Beach sand	182.0	1.3ª	0.5ª	Ref. [27]
Egypt	Nile island's soil	152.9	1.3	0.4^{a}	Ref. [8]
Brazil	Soil	147.8 ^a	1.1 ^a	0.4^{a}	Ref. [28]
India	Soil	86.7 ^a	0.6^{a}	0.2^{a}	Ref. [7]
Thailand	Soil	204.6 ^a	1.4 ^a	0.6^{a}	Ref. [12]
Malaysia (Peninsula)	Soil	208.1 ^a	1.5 ^a	0.6^{a}	Ref. [12]
World average	Soil	118.5 ^a	0.9^{a}	0.3^{a}	Ref. [29]
World average	Soil	129.7 ^a	1.0^{a}	0.4^{a}	Ref. [12]
Red Sea	Sediment	32.4 ^a	0.2^{a}	0.1 ^a	Ref. [22]
South China Sea (Sarawak)	Sediment	101.6 ^a	0.7^{a}	0.3	Ref. [20]
South China & Sulu Sea (Sabah)	Sediment	64.7ª	0.5 ^a	0.2	Ref. [20]
Peninsular EEZ	Sediment	143.1	1.0	0.4	Present work

^aCalculated by the author using data given in the reference.

Conclusion

Core sediments from stations SF 04 and SF 30 are contributing more radiation hazards whiles core sediments from stations SF 05, SF 16 and SF 18 are contributing less radiation hazards than most of the average cores. Overall, the Radium equivalent activity (Ra_{eq}), Representative level index ($I_{\gamma r}$), External hazard index (H_{ex}) is ranged between 68.6 – 210.5 Bq/kg (mean 143.1 ± 27.7 Bq/kg), 0.50 – 1.54 (mean 1.04 ± 0.20) and 0.19 – 0.57 (mean 0.39 ± 0.07 Bq/kg), respectively. This value is less than the recommended limit value of 370 Bq/kg (for Ra_{eq}) and unity (for H_{ex}). It is also slightly less than the background level radiation from soil in Peninsular Malaysia, $I_{\gamma r} \sim$ 1.5. Therefore, the additional radiation exposure to the workers while handling the samples is small, as compared to the background radiation received by them.

Acknowledgement

The authors would like to express their special appreciations to the Ministry of Science, Technology & Innovation Malaysia for providing research funding under e-ScienceFund research grant (04-03-01-SF0020). The authors

would also like to thank the captain and crews of the K.L. PAUS and the Department of Fisheries for their support and assistance during sampling expeditions. We would also like to express our gratitude to Universiti Kebangsaan Malaysia (UKM), Universiti Malaysia Terengganu (UMT) for support throughout this study. Last but not least, the thanks to the personnel of Radiochemistry and Environment Group for their constant support in this study.

References

- 1. Ahmad-Taufek, A. R., Ahmad-Termizi, R. & Abdul-Khalik, W. (2004). Analysis of The Concentration of Natural Radionuclides in rivers in Kota Tinggi District, Malaysia. *Journal of Nuclear and Related Technologies* 1, 41 52.
- 2. Akram, M., Qureshi, R. M., Ahmad, N., Solaija, T. J., Mashiatullah, A., Ayub, M. A. & Irshad, S. (2004). Determination of Natural and Artificial Radionuclides in Seawater and Sediments off Gwadar Coast, Arabian Sea. *The Nucleus* 41, 19 25.
- 3. Myrick, T. E., Berven, B. A. & Haywood, F. F. (1983). Determination of concentrations of selected radionuclides in surface soil in the U.S. *Health Physics* 45, 631 642.
- 4. Nagaya, Y. & Saiki, M. (1967). Accumulation of radionuclides in coastal sediments of Japan (I). Fallout radionuclides in some coastal sediments in 1964–1965. *Journal of Radiation Research* 81, 37 43.
- 5. Yang, Y. X., Wu, X. M., Jiang, Z. Y., Wang, W. X., Lu, J. G., Lin, J., Wang, L. M. & Hsia, Y. F. (2005). Radioactivity concentrations in soils of the Xiazhuang granite area. China, *Applied Radiation Isotopes* 63, 255 259.
- 6. Nabil, M. H., Tetsuo, I., Masahiro, H., Atsuyuki, S., Shinji, T., Masahiro, F. & Sarata, K. S. (2010). Assessment of the natural radioactivity using two techniques for the measurement of radionuclide concentration in building materials used in Japan. *Journal of Radioanalytical and Nuclear Chemistry* 283, 15 21.
- Narayana, Y., Somashekarappa, H. M., Narunakara, N., Avadhani, D. N., Mahesh, H. M. & Siddappa, K. (2001). Natural radioactivity in the soil samples of coastal Karnataka of South India. *Health Physics* 80, 24 33.
- 8. Ahmed, N. K. & El-Arabi, A. G. M. (2005). Natural radioactivity in farm soil and phosphate fertilizer and its environmental implications in Qena governorate, Upper Egypt. *Journal of Environmental Radioactivity* 84, 51 64.
- 9. Koide, M., Bruland, K. W. & Goldberg, E. D. (1973). Th-228/Th-232 and Pb-210 geochronologies in marine and lake sediment. *Geochimica et Cosmochimica Acta* 37, 1171 1187.
- 10. Meriwether, J. R., Beck, J. N., Keeley, D. F., Langley, M. P., Thompson, R. H. & Young, J. C. (1958). Radionuclides in Louisiana soils. *Journal of Environmental Quality* 17, 562 568.
- 11. Osburn, W. S. (1965). Primordial Radionuclides: Their distribution, movement, and possible effect within terrestrial ecosystems. *Health Physics* 11, 1275 1295.
- 12. UNSCEAR (2000). Sources, Effects and Risks of Ionizing Radiation. Report to the General Assembly, with scientific annexes, United Nations, New York.
- 13. Malaysian Nuclear Agency (2006). Laporan Kemajuan Kontrak Perkhidmatan Penyelidikan Sinaran di Malaysia, Progress Report, Bangi, Malaysia. (in Malays)
- 14. Omar, M., Ibrahim, M. Y., Hassan, A., Lau, H. M. & Ahmad, Z. (1990). Enhanced Radium Level in Tin Mining Areas in Malaysia. In: Proceedings of an International Conference on High Levels of Natural Radiation. M. Sohrabi, J.U. Ahmad and S.A. Durrani (eds.). 3 7 Nov 1990, Ramsar, Islamic Republic of Iran. 191 195.
- 15. Yahaya, R., Che-Rosli, C. M., Yasir, M. S., Amran, A. M., Ismail, B. & Sukiman, S. (1997). Analysis of Fallout and Naturally Occuring Radioancitve Elements in Selangor. *Malaysia Journal Analytical Sciences*, 3, 237 241.
- 16. Yasir, M. S., Amran, A. M., Farhana, I., Siti-Qalila, M. T. & Mohd-Rashidan, Z. A. (2006). Analisis ²³⁸U, ²³²Th, ²²⁶Ra dan ⁴⁰K dalam Sampel Amang, Tanah dan Air di Dengkil, Selangor Menggunakan Spektrometri Gama. *Malaysia Journal Analytical Sciences*, 10, 35 40.
- 17. Zal U'yun, W. M, Zaharudin, A., Abdul-Kadir, I., Yii, M. W., Norfaizal, M., Jalal, S., Kamarozaman, I., Khairul-Nizam, R. & Maziah, M. (2005). Kajian Awal ke Atas Taburan Radionuklid Tabii Di Perairan Pantai Timur Semenanjung Malaysia. *Malaysia Journal Analytical Sciences*, 9, 325 337.
- 18. Zal U'yun, W. M., Mohamed, C. A. R., Yii, M. W., Zaharudin, A., Kamaruzaman, I. & Abdul-Kadir, I. (2010). Vertical inventories and fluxes of ²¹⁰Pb, ²²⁸Ra and ²²⁶Ra at southern South China Sea and Malacca Straits. *Journal of Radioanalytical and Nuclear Chemistry*, 286, 107 113.

- 19. Dowdall, M. & O'Dea, J. (2002). ²²⁶Ra/²³⁸U disequilibrium in an upland organic soil exhibiting elevated natural radioactivity. *Journal of Environmental Radioactivity* 59, 91 104.
- 20. Yii, M. W., Zaharudin, A. & Abdul-Kadir, I. (2009). Distribution of naturally occurring radionuclides activity concentration in East Malaysian marine sediment. *Applied Radiation Isotopes* 67, 630 635.
- 21. Chen, S. B., Zhu, Y. G. & Hu, Q. H. (2005). Soil to plant transfer of ²³⁸U, ²²⁶Ra and ²³²Th on a uranium mining-impacted soil from southeastern China. *Journal of Environmental Radioactivity* 82, 223 236.
- 22. Sam, A. K., Ahamed, M. M. O., EI-Khangi, F. A., El-Nigumi, Y. O. & Holm, E. (1998). Radioactivity levels in the Red Sea Coastal Environment of Sudan. *Marine Pollution Bulletin* 36, 19 26.
- 23. Stranden, E. (1979). A simple method for measuring the radon diffusion coefficient and exhalation rate from building materials. *Health Physics* 37, 242 244.
- 24. Berekta, J. & Mathew, P. J. (1985). Natural radioactivity of Australian building materials waste and by-products. *Health Physics* 48, 87 95.
- 25. UNSCEAR (1982). Ionizing Radiation: Sources and Biological Effects. United Nations, New York.
- 26. Alam, M. N., Chowdhury, M. I., Kamal, M., Ghose, S. & Ismail, M. N. (1999). The ²²⁶Ra, ²³²Th and ⁴⁰K activities in beach sand minerals and beach soils of Cox's Bazar, Bangladesh. *Journal of Environmental Radioactivity* 46, 243 250.
- 27. Seddeek, M. K., Badran, H. M., Sharshar, T. & Elnimr, T. (2005). Characteristics, spatial distribution and vertical profile of gamma-ray emitting radionuclides in the coastal environment of North Sinai. *Journal of Environmental Radioactivity* 84, 21 50.
- 28. Malanca, A., Pessina, V. & Dallara, G. (1993). Assessment of the natural radioactivity in the Brazilian state of Rio Grande do Norte. *Health Physics* 65, 298 302.
- 29. UNSCEAR (1993). Sources, Effects and Risks of Ionizing Radiation. Report to the General Assembly, with scientific annexes, United Nations, New York.



ANALYSIS OF ANIONIC POST-BLAST RESIDUES OF LOW EXPLOSIVES FROM SOIL SAMPLES OF FORENSIC INTEREST

(Analisis Residu Pasca Letupan Anion Bagi Bahan Letupan Rendah Daripada Sampel Forensik Tanah)

Umi Kalthom Ahmad¹, Ong Shin Tze¹, Muhammad Fauzi Ghazali², Yew Chong Hooi³, Mohd Koey Abdullah³

¹Department of Chemistry,
Faculty of Science, Universiti Teknologi Malaysia,
81310 UTM Skudai, Johor Darul Ta'zim

²Criminalistics Section,
Forensic Division, Department of Chemistry Malaysia,
Jalan Sultan, 46661 Petaling Jaya, Selangor.

³PDRM Forensic Laboratory,
8 1/2 mile, Jalan Cheras/Kajang, 43200 Cheras, Selangor.

Abstract

The growing threats and terrorist activities in recent years have urged the need for rapid and accurate forensic investigation on post-blast samples. The analysis of explosives and their degradation products in soils are important to enable forensic scientist to identify the explosives used in the bombing and establish possible links to their likely origin. Anions of interest for post-blast identification of low explosives were detected and identified using ion chromatography (IC). IC separations of five anions (Cl⁻, NO₂⁻, NO₃⁻, SO₄²⁻, SCN⁻) employed a Metrosep Anion Dual 2 column with carbonate eluent. The anions were separated within 17 minutes. Sampling of post blast residues was carried out in Rompin, Pahang. The post-blast explosive residues were extracted from soil samples collected at the seat of three simulated explosion points. The homemade explosives comprised of black powder of various amounts (100 g, 150 g and 200 g) packed in small plastic sauce bottles. In black powder standard, three anions (Cl⁻, NO₃⁻, SO₄²⁻) were identified. However, low amounts of nitrite (NO₂⁻) were found present in post-blast soil samples. The amounts of anions were generally found to be decreased with decreasing amount of black powder explosive used. The anions analysis was indicative that nitrates were being used as one of the black powder explosive ingredients.

Keywords: Anions, homemade low explosives, ion chromatography, black powder, post-blast soil samples

Abstrak

Ancaman dan aktiviti pengganas yang berleluasa sejak beberapa tahun kebelakangan ini telah membangkitkan keperluan untuk siasatan forensik yang segera dan tepat terhadap sampel sisa letupan. Analisis terhadap bahan letupan dan produk degradasi dalam tanah adalah penting untuk saintis forensik mengenalpasti bahan letupan yang telah digunakan dalam aktiviti letupan dan seterusnya mengaitkan hubungan yang mungkin terhadap sumber asalnya. Anion yang penting dalam pengenalpastian bahan letupan telah dikesan melalui ion kromatografi (IC). Pemisahan IC bagi lima jenis anion (Cl⁻, NO₂⁻, NO₃⁻, SCN⁻) melibatkan penggunaan turus Metrosep Anion Dual 2 dengan eluen karbonat. Anion ini telah dipisahkan dalam masa 16 minit. Persampelan sisa bahan letupan telah dijalankan di Rompin, Pahang. Sisa bahan letupan ini telah diekstrak dari sampel tanah yang dikumpul daripada tempat letupan simulasi. Bahan letupan buatan sendiri terdiri daripada pelbagai amaun (100 g, 150 g dan 200 g) serbuk hitam yang dimampat dalam botol plastik sos yang kecil. Dalam serbuk hitam piawai, tiga anion (Cl⁻, NO₃⁻, SO₄²) telah dikenalpasti. Namun, nitrit (NO₂⁻) telah ditemui dalam sampel tanah pasca letupan. Kandungan ion didapati menurun dengan pengurangan amaun serbuk hitam yang diguna. Analisis anion ini menunjukkan bahawa nitrat telah digunakan sebagai salah satu ramuan dalam bahan letupan serbuk hitam.

Kata kunci: Anion, bahan letupan buatan sendiri, kromatografi ion, serbuk hitam, sampel tanah pasca letupan

Umi Kalthom Ahmad et al: ANALYSIS OF ANIONIC POST-BLAST RESIDUES OF LOW EXPLOSIVES FROM SOIL SAMPLES OF FORENSIC INTEREST

Introduction

In the last decade, terrorism has emerged as an international disaster threat that can be widespread to any particular region within the world. The bombings that occurred in Bali on the 12 October 2002 have brought a great impact to the world especially towards the nation of Australia where two bombs exploded almost simultaneously in a night club district on the tourist island Kuta, killing 202 people, most of whom were Australians [1]. On 9 September 2004, another massive bomb took place in front of the Australian Embassy in Jakarta, Indonesia, resulting in ten dead victims and over 180 injured. The explosion was later identified as a car bomb, driven by a suicide bomber [2]. The subsequent bombing occurred on 7 July 2005 where a series of coordinated suicide bombs exploded on London's public transport system, killing 56 people and 700 were injured [3]. A very recent terrorist attack took place in Jakarta, Indonesia on 17 July 2009 where high explosive bombs exploded in two luxury hotels, resulting in the death of nine people and approximately 40 wounded [4]. In Malaysia, only a few cases relating to homemade explosive bombings have been reported. Two thieves attempted to break open an automated teller machine (ATM) in CIMB bank in Puchong with a homemade explosive device made of fireworks. The ATM machine and part of the ceiling were damaged but they did not get the money [5].

Explosions often present complex and difficult circumstances to investigate. Normally, these incidents are committed at the convenience of a perpetrator who has thoroughly planned the criminal act and has left the crime scene long before any official investigation is launched. Furthermore, proving commission of the offense is more difficult because of the extensive destruction that frequently dominates the crime scene. The contribution of a forensic scientist is only one aspect of a comprehensive and difficult investigative process that must establish a motive, the modus operandi, and a suspect [6].

In general, explosives are classified as high and low explosives, according to the type and velocity of the reaction involved. High explosives as detonating charges, are subdivided into two groups, primary and secondary explosives, according to their function in the explosion. The primary explosives, which include lead azide and lead styphnate, are used to start the explosion as in the blasting cap [7]. Secondary explosives, which include nitroaromatics and nitramines are common at military sites than primary explosives. If the explosive decomposition reaction moves through the charge faster than the speed of sound in the unreacted medium, it is termed as detonation. However, if it moves slower, it is termed as deflagration [8]. All high explosives and blasting agents detonate when properly initiated, whereas low explosives or black powder deflagrate. Low explosives are normally known as propellants as they undergo deflagration slowly at rate of 1000 feet per second [6]. Gun powder or black powder and smokeless powder are some of the typical low explosives known. There are many compositions of black powder with the common form containing a mechanical mixture of potassium or sodium nitrate with sulphur and finely ground charcoal [9].

Ion chromatographic (IC) analysis is an important tool for forensic explosives investigation. A large proportion of improvised explosive devices used in bombing incidents in the United States used low explosives such as black powder or homemade mixtures. These types of bombs leave significant amount of inorganic residues upon deflagration [10].

The growing threat, unlawful intention and sophisticated criminal or terrorism activities committed using energetic materials in recent years have generated the need for fast and accurate investigation techniques for evaluating vital clues left at the crime scene. The post-blast analysis of trace amounts of explosives is particularly difficult because traces are usually trapped in or deposited on various debris materials. Identifying unknown explosives requires the ability to quantitatively determine a large number of inorganic and organic materials. Thus, analysis of explosives and their post-blast residues in soil is of great important to enable the forensic scientist to identify the explosives that were used in the bombing and eventually help to find links to their likely origin. Knowing the explosive compounds and materials subsequently leads to tracing and identifying the perpetrators involved in the bombing activities. Limited studies have reported on the analysis of post-blast residues using several analytical techniques [10-16]. The objective of the study was to analyze selected anions of interest in post-blast residues using IC.

Experimental

Apparatus and Chemicals

Standard solutions of inorganic anions Cl⁻, NO₂⁻ and SO₄²⁻ were purchased as 1000 ppm stock solutions (Merck, Darmstadt, Germany) and were diluted as required using deionized water. The remaining inorganic anion standard solutions (NO₃⁻ and SCN⁻) were prepared from potassium nitrate and potassium thiocyanate (Fisher Scientific, Malaysia). For the bicarbonate eluent used for anionic analysis, the chemicals were solid analytical grade sodium bicarbonate and sodium hydrogen carbonate (Merck, Darmstadt). Water treated with Barnstead Nanopure ultrapure water purification system was used to prepare standard solutions and eluent.

Sampling

The sampling exercise was conducted at the sea shore of Pantai Wecando, Kampung Jawa, Rompin in collaboration with Post Blast Investigation (PBI) team of Forensic Laboratory from Royal Malaysia Police. To imitate real post-blast conditions, three black powder explosives of different amount (100 g, 150 g and 200 g) placed in separate document bags were deflagrated under controlled conditions. The explosives were loaded in three separate ketchup sauce plastic containers of the same size and thickness. Each plastic container was then inserted into a nylon document bag $(25.0 \times 38.0 \times 8.0 \text{ cm})$ filled with polystyrene foam.

Three points on the ground were set as the point of explosion of the homemade bomb. The blast points were labeled as Point A, B and C respectively and the direction was determined using a compass. Each point was subdivided into four grids and labeled as A1 to A4, B1 to B4 and C1 to C4 respectively. The sampling grid was marked with red masking tape at every 5 m with a metal tag positioned on the ground to produce an area size of 25 m² in each grid. Figure 1 illustrates the schematic diagram of the sampling grid and the blast points. The distance from Point A to B and C was 11.18 m respectively.

The soil collection method in the study was performed as reported by Radtke *et al.* [17] with slight modification. The soil control samples from each point of explosion were collected before each explosion. At each grid, a stainless steel spade was used to collect 100 g samples from the top 1 inch of soil. Each detonation point was sampled four times, once from each grid. The samples from each point of detonation were placed into three separate snap-seal plastic bags and homogenized by hands.

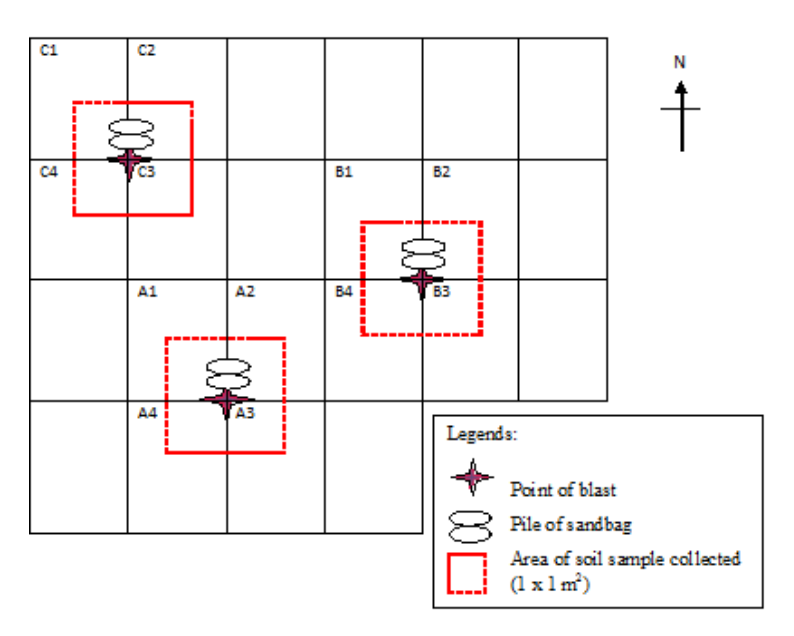


Figure 1: Schematic diagram of the sampling grid and the points of blast.

Umi Kalthom Ahmad et al: ANALYSIS OF ANIONIC POST-BLAST RESIDUES OF LOW EXPLOSIVES FROM SOIL SAMPLES OF FORENSIC INTEREST

The homemade bombs and explosion exercise were prepared and conducted by PBI team. After each blast, all the fragments found were first tagged with red flags. The document bag and plastic container fragments as well as the cotton and polystyrene foams were then photographed and collected. Four moderately contaminated areas within each point of detonation were selected based on visible soil discoloration. The soil samples were collected within an area size of 1 m² and to the depth of 1 to 2 inches using stainless steel spade and stored into snap-seal plastic bags and labeled accordingly. The pH of the soil samples collected was measured on-site using universal pH indicator strips (Merck, Darmstadt). The samples collected were taken to the laboratory for chemical analysis.

Soil Extraction

The soil sample extraction was performed using Johns *et al.* [11] method. All soils were air dried at room temperature prior for extraction. The samples were not exposed to direct sunlight. A 0.8 g sample of soil was added to 8 mL of deionized water in a 15 mL Falcon tube. The mixture was gently shaken, sonicated for 40 mins and centrifuged at 3500 rpm for 5 mins. The supernatant produced was passed through a cleaned 0.45 µm disc syringe filter. The extraction procedures were repeated three times for each sample of soil to produce three batches of soil extracts. The extracted solutions were diluted 500X using deionized water. The control soil samples from Point A, B and C were labeled as A-CS, B-CS and C-CS respectively. The soil samples containing post-blast residues from Point A, B and C were labeled as A-PBS, B-PBS and C-PBS respectively. The extracted samples were kept under refrigeration at 4°C.

Analysis of Black Powder Standard

The black powder control sample used in the study was provided by PBI team. The unexploded control sample was observed and examined microscopically under low magnification and then weighed. The sample was ground into fine powdered form using mortar and pestle. A 0.1 g of black powder was added to 10 mL of deionized water. The mixture was vortexed, filtered and diluted $600 \times \text{using}$ deionized water. The diluted standard solution was kept under refrigeration at 4°C .

Instrumentation

The IC analyses were conducted using a Metrohm Advance IC system (Metrohm Ltd, Herisau, Switzerland) equipped with a modular system comprising of the eluent 11 system, 830 interface, 819 detector, 820 separation center, 818 pump, 833 liquid handling unit. For anionic separation, the column used was Metrosep Anion Dual 2 with dimension of 75 mm \times 4.6 mm I.D. and particle size of 6.0 μ m. The guard column used was Metrosep C2 Guard for anion exchanger column. The pump was operated at a flow rate of 0.8 mL/min. The eluent used was 1.3 mM Na₂CO₃ and 2.0 mM NaHCO₃.

Preparation and Separation of Standard Solutions

A single stock standard solution (100 ppm) containing a mixture of all ions of interest (Cl⁻, NO₂⁻, NO₃⁻, SO₄²⁻ and SCN⁻) were prepared by adding 1 mL standard solution of each ion with 45 mL of deionized water. After sonication for 10 mins, 5 mL of the solution was then added to 45 mL deionized water to produce 10 ppm anionic standard solution. A serial dilution (1 - 5 ppm) was prepared from the 10 ppm standard solution. Each solution was sonicated, filtered through 0.45 μ m disc syringe filter and degassed. All standard solutions were stored in screwed-top glass bottle and kept under refrigeration at 4°C. The anion mixed standard solutions of 1 – 5 ppm were separated by IC to reveal analyte peak areas that were used to produce an anion calibration graph.

Limits of Detection (LOD)

The LODs of each ion were evaluated by diluting 1 ppm standard solution of anions containing a mixture of all ions with deionized water and separated in IC method under Metrohm Anion Dual 2. The lowest detectable concentration for each ion was noted based on the signal-to-noise ratio of 2:1.

Results and Discussion

IC Separation of Standards

In this study, inorganic homemade explosive device containing black powder was used to conduct a simulated explosion. The ionic species originated from the fuel and oxidizer of the explosive material was deposited at the surface of blast seat as a result of chemical reaction occurred during the explosion. Thus, some of the typical

components of black powder explosives and their probable decomposition products or by-products were identified as the ions of interest for the analyses of post-blast residues from soil sample extracts.

A set of target analytes comprising five anions (Cl⁻, NO₂⁻, NO₃⁻, SO₄²⁻ and SCN⁻) was selected as the indicator ions for identification of the homemade inorganic explosive. In the IC separation, two different flow rates were tested in this study. By using a flow rate of 1.0 mL/min, only four peaks were obtained where by the NO₂⁻ and Cl⁻ were found to coelute. Therefore, acceptable separation was achieved at a flow rate of 0.8 mL/min in which the five ions of interest present in the standard solution were well separated within 16 minutes (Figure 2).

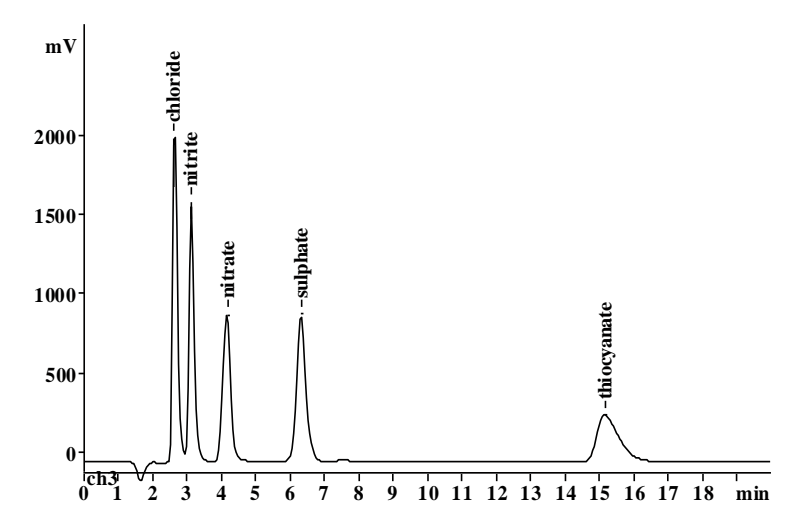


Figure 2: Separation of 5 ppm anion standard solution by IC. Conditions: a Metrohm Anion Dual 2 column (75 mm x 4.6 mm I.D.), flow rate of 0.8 mL/min, an injection volume of 20 μ L, column temperature at 28 °C, bicarbonate eluent, suppressed conductivity detection.

Method Validation and Repeatability

A calibration plot for anions was generated to determine the concentration of the analyte ions in the post-blast soil residues. Five different concentrations (1–5 ppm) of standard solutions were used under the same chromatographic condition. The correlation coefficients (r^2) and detection limits (LOD) are listed in Table 1. From the table, the $r^2 > 0.93$ proved good linearity of the present method. The LOD of each analyte ions were determined and compared against previous studies. The LOD for anionic species ranged from 0.1 - 100 ppb. The results reveal a reduction in LOD for Cl⁻ and NO₃⁻ compared to the study done by Johns *et al.* [11]. The differences in LOD obtained from the present study and the earlier study [9] may be due to variation in the IC system as well as the columns used.

Table 1: The detection limits (LODs) and correlation coefficient (r ²) of the anions obtained in the stu
--

Analyta	Limit of Dete	ction (LOD) (ppb)	Correlation coefficient (r ²)
Analyte	This study	Previous study ^a	Correlation coefficient (1)
Cl-	1.8	2.2	0.9831
NO2-	9.5	4.4	0.9926
NO3-	0.1	5.4	0.9326
$\mathrm{SO_4}^{2}$	27	3.1	0.9779
SCN-	100	5.5	0.9984

^a The value was compared against the LOD from Johns et al. [9]

^bNR- Not reported

A good chromatographic analysis of explosive residues should include reproducible retention time, minimal interferences and the ability to separate each ion present in the post-blast residues [12]. To determine the repeatability of the method, three replicate injections were performed using a standard mixture containing the anions of interest. Each sample was injected into the IC system three times consecutively and also at intervals of three days to examine the within-day and day-to-day variations of the retention time during the separation of analyte ions. The retention time, resolution and relative standard deviation (RSD) were summarized in Table 2. The results show that the RSD for retention time for the selected anions evaluated within-day were less than 0.25 % For day-to-day variation, the RSD were less than 2.86 %. Based on the data, the variation of retention time was larger for day-to-day compared to that of within-day. The resolution factor (R_s) of 1.0 or greater represents complete separation. In this study, the R_s of anions separation was evaluated and calculated in which all values are greater than 1.0. Therefore, the inorganic ions were completely separated by IC.

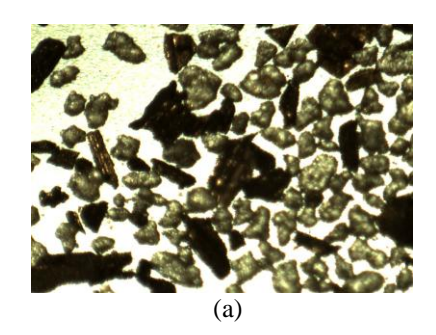
Table 2: The mean retention time, resolution and relative standard deviations of anions obtained using IC system for evaluation of within-day and day-to-day variations.

Analyte	Within-day (n=3)			Day-to-day (n=6)		
	Mean Retention Time (min)	*R_s	RSD (%)	Mean Retention Time (min)	*R_s	RSD (%)
Cl	2.6		0.00	2.7		1.49
NO_2^-	3.1	1.17	0.00	3.2	1.21	1.89
NO_3^-	4.1	1.88	0.25	4.2	1.89	0.96
SO_4^{2}	6.3	2.73	0.00	6.4	2.82	2.86
SCN^{-}	15.4	7.81	0.13	16.1	7.97	2.85

R_s - Resolution

Analysis of Black Powder Standard

The black powder standard was examined microscopically under low magnification. Figure 3a shows appearance of black powder under 20-fold magnification. The sample was observed to consist of a mixture of small crystal-like particles and grayish black irregular shape particles. Such observation was consistent with the raw material of black powder, which contains a mixture of nitrate salt as main compound and carbon source. When examined under 30-fold magnification, it was possible to see traces of fine powder (Figure 3b).



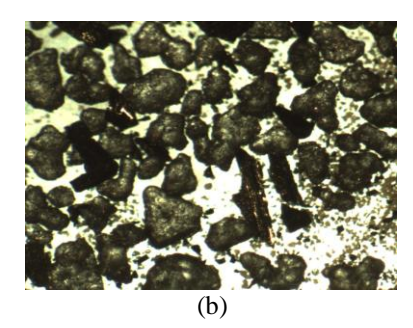


Figure 3: Appearance of black powder at (a) 20 x magnification and (b) 30 x magnification.

The particles of the black powder standard observed under microscope were measured and tabulated in Table 3. For small crystal-like particles (nitrate salt), the mean grain size measured was 6.3 μ m. As for the grayish black irregular shape particles (carbon), the mean grain size was 11.8 μ m. The particle size of homemade black powder standard obtained in this study was compared with that of commercial black powder known as sulfurless fine grain gunpowder (SFG). The SFG was graded according to its grain size. For example, SFG 12 contains particles of size 1.40 mm. As the grading numerical increases, the gunpowder becomes finer by having smaller grains. In the work reported by Kosanke *et al.* [18], the carbon presented in commercial black powder was less than 20 μ m. Under scanning electron microscope (SEM), the sizes of black powder particles fall in the range of 10 – 15 μ m [19]. Thus, the grain size of homemade black powder measured in the present study was similar to that of commercial black powder.

Type of particle	Largest grain	Smallest grain	Ratio
	(µm)	(µm)	(Largest: smallest)
Crystal-like	9.50	3.10	3.06
Gravish-black	18 00	5 60	3 21

Table 3: Particle sizes of homemade black powder standard.

A study done by Brown and Rugunanan [20] reported the effect of particle sizes of KNO $_3$ and charcoal contain in black powder to the burning rates. By varying the sizes of both particles, a maximum burning rate (0.95 \pm 0.01 cm/s) was observed at a mean charcoal particle size of approximately 25 μ m and the burning rates generally decreased with increasing charcoal particle size. As for KNO $_3$, a maximum burning rate (0.83 \pm 0.01 cm/s) occurred when particle-size ranged from 0 to 53 μ m was tested. The results suggested that variation of the particle size of charcoal had a greater effect on the burning rate than that of varying the KNO $_3$ particle size.

The ground black powder was extracted using deionized water and separated by IC to identify the inorganic ions present in the explosives. Black powder which consists of KNO₃, charcoal and sulfur may produce anions such as NO₂-, NO₃-, SO₄-2-, SCN- on the aqueous extract [10]. Figure 4 shows the chromatogram of black powder standard where the anions were well separated by IC within 7 mins. NO₃- constituted the major anion and small amounts of Cl⁻ and SO₄-2- were detected. From the IC separation of black powder, it was conclusive that nitrate salt was used as an important ingredient in the black powder explosive. The detection of Cl⁻ suggests that chloride salt may have been used as an additive in the explosive material.

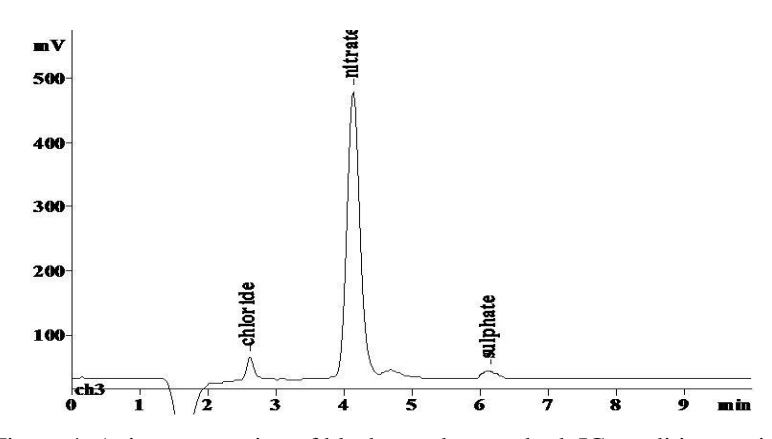


Figure 4: Anions separation of black powder standard. IC conditions as in Figure 2.

Umi Kalthom Ahmad et al: ANALYSIS OF ANIONIC POST-BLAST RESIDUES OF LOW EXPLOSIVES FROM SOIL SAMPLES OF FORENSIC INTEREST

The 10 % aqueous extract of black powder (0.1 g/ 10.0 mL) were separated by IC and the concentrations of ions present in the raw material were calculate. Table 4 shows the concentration (μ g/g) of ions detected in the black powder standard. The quantitative analysis of black powder standard gives assistance to the further analysis of postblast residues in determining the nature and possible composition profile of the sample.

Table 4: The amount of ionic analytes detected in black powder standard.

Analyte	Mean concentration (μg/g)±SD	Percentage of ionic analyte composition (%)
Cl	6484.8±80.7	4.32
NO_2^-	ND	0
NO_3	139732.1±250.2	93.00
$NO_3^ SO_4^{2-}$	4020.1±59.6	2.68
SCN ⁻	ND	0

SD - Standard deviation based on triplicate extraction

ND - Not detected

The typical composition of black powder is 75 % KNO₃, 15 % charcoal and 10 % sulfur. However, many variations to that ratio have been identified and reported, in which most of the differences are insignificant [18, 21]. In this study, the homemade black powder contained 93 – 95 % of nitrate salt and only 2.68 % of sulphate as the ionic analyte content. There were small amounts of Cl⁻ (4.32 %) present in the explosive which suggest the use of chloride salt as an additive. The percentage of analyte comprises the black powder standard varied to that of the typical composition of black powder. This may be due to the dissociation or decomposition of these ions in the aqueous extract which could not be recovered and detected using IC. Apart from that, the differences in percentage of analytes in black powder composition may be due to the homemade recipe in which additives and analyte substitutes were incorporated in the explosive mixture.

Analysis of Post-blast Residues

In this study, soil sample size of 0.8 g which showed the best extraction efficiency was applied to the identification of homemade inorganic explosives in the pre-blast and post-blast residues. The blank sample containing deionized water was separated by IC for each batch of sample. Any ions present in the blank were deducted in further analysis.

Soil Analysis at Explosion Point A

At point A explosion site, 200 g of homemade explosives were compacted in the plastic container placed in the document bag. The soil samples were collected before and after the explosion to determine the amount of explosive residues present in the samples. The 10% aqueous extract (0.8 g/8.0 mL) of blank soil collected before the explosion (A-CS) shows the presence of significant amount of Cl^- as well as NO_3^- and $SO_4^{2^-}$ (both in low amounts) as the background ions in the soil matrix (Figure 5a). After the explosion, the soil sample (A-PBS) surrounded within the blast seat at point A was collected and separated by IC. Figure 5b shows the chromatogram of the anions analysis of A-PBS. Cl^- , NO_2^- , NO_3^- and $SO_4^{2^-}$ were detected in the post-blast residues.

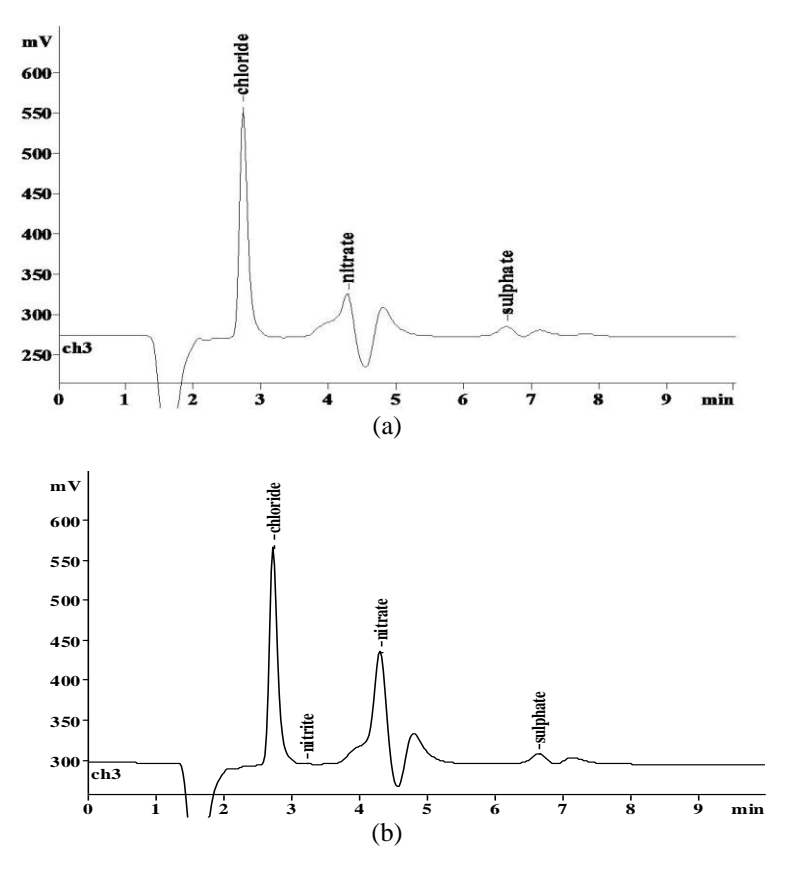
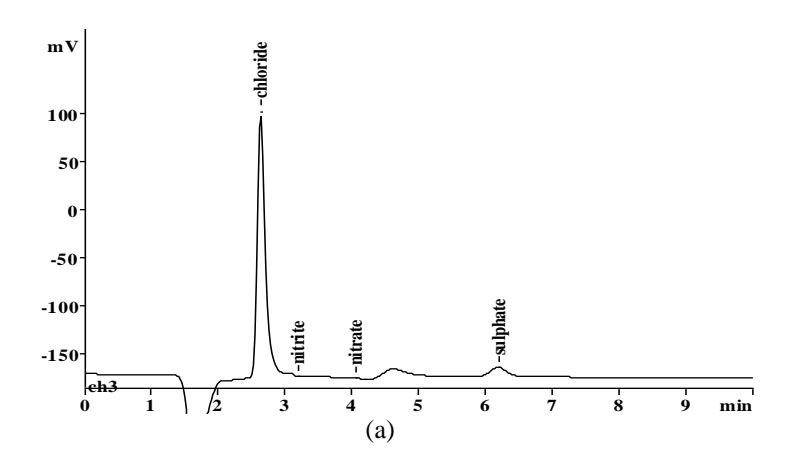


Figure 5: Anions separation of soils collected from blast seat A for (a) pre-blast soil extract and (b) post-blast soil extract. IC conditions as in Figure 2.

Soil Analysis at Explosion Point B

At point B explosion site, 150 g of homemade explosives were employed and deflagrated. As at explosion Point A, soil samples were collected before and after the explosion to determine the amount of explosive residues present in the soil sample. The aqueous extract of blank soil collected before the explosion (B-CS) revealed the presence of Cl $_1$, NO $_2$, NO $_3$ and SO $_4$ as the background ions (Figure 6a). The analysis of post-blast soil (B-PBS) is illustrated in Figure 6b. Based on the chromatogram, Cl $_1$, NO $_2$, NO $_3$ and SO $_4$ were detected in the post-blast residues.



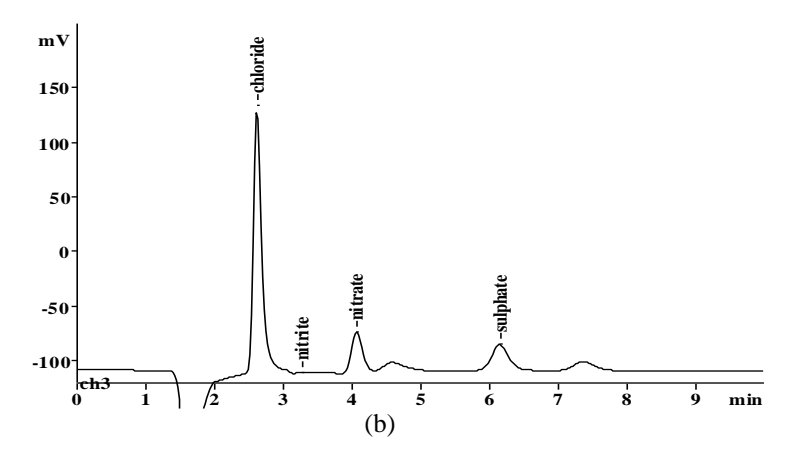
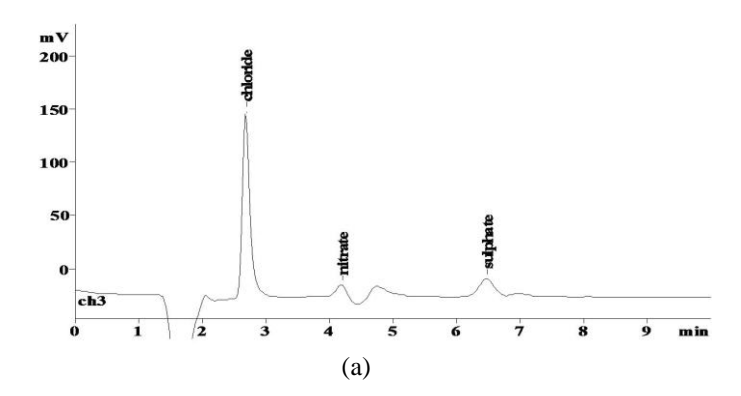


Figure 6: Anions separation of soils collected from blast seat B for (a) pre-blast soil extract and (b) post-blast soil extract. IC conditions as in Figure 2.

Soil Analysis at Explosion Point C

As explosion point C, 100 g of homemade low explosives was deflagrated. Similar to soil sampling at blast points A and B, the soil samples were collected before and after the explosion to determine the amount of explosive residues present in the soil sample. The background ions present in the pre-blast soil (C-CS) were identified by IC. From the anions chromatogram, Cl^- , NO_3^- and $SO_4^{2^-}$ were detected in the blank soil (Figure 7a). Figure 7b shows the anion analysis of post-blast soil (C-PBS) in which significant amount of Cl^- , NO_3^- , as well as low amounts of NO_2^- and $SO_4^{2^-}$ were detected in post-blast residues.



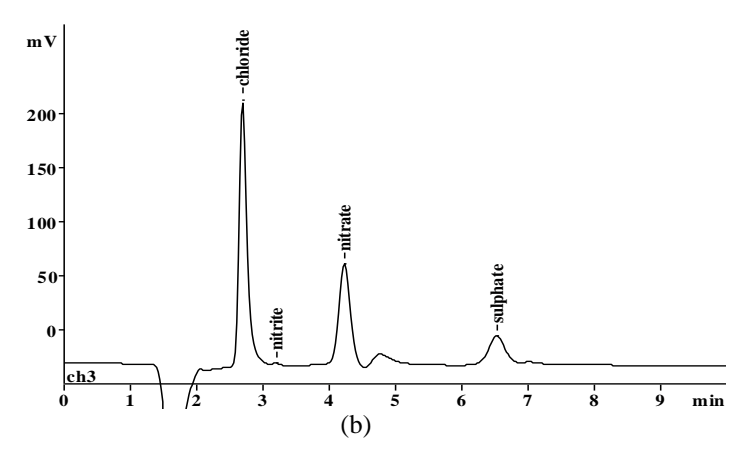


Figure 7: Anions separation of soils collected from blast seat C for (a) pre-blast soil extract and (b) post-blast soil extract. IC conditions as in Figure 2.

Post-Blast Identification of Homemade Inorganic Explosives

IC has been successfully applied to post-blast residues for identification of explosives-related ions [10-13]. The detection of explosives residue after a bombing may be possible as the explosive material is not completely consumed during an explosion. The relative concentration of the ions in the residues was different from their relative concentration in the unconsumed explosive. This complication has lead to the difficulty in interpretation of IC results for post-explosion samples. The productions of additional ions resulted from chemical reaction occurred during explosion further complicated the possibility in relating the composition profile of the original explosion used. Therefore, it was considered unsafe or inaccurate in the attempt of identifying the type or composition of the original explosive on the basis of IC results for the residues [17]. By considering the weaknesses and difficulties encountered in IC interpretation of explosive materials, a different approach was made in the present study to evaluate the percentage of explosives deposited and left behind at the bombing scene.

Table 5 shows the concentration of analyte ions detected in these samples. The amounts of ions detected in the post-blast residues were compared against the amount of ions present in the unburned black powder. Based on the study, percentage of these ions remained in post-blast soils were calculated. In all three samples, 86 - 99 % of Cl⁻ was detectable in post-explosion residues. Most of the NO_3^- were decomposed or dispersed away from the crater to the bombing fragments as only 11 - 16 % of the ions remained in the post-blast soils. By comparing the amount of $SO_4^{2^-}$ detected in unconsumed black powder, higher amount of the same ion was identified in the sample A. This trend was inconsistent for sample B and C as only 95 - 99 % of $SO_4^{2^-}$ was identified in the post-blast soils. The presence of $SO_4^{2^-}$ could have originated from sulfur fuel used as one of the ingredients in the homemade explosive.

The large amount of NO₃⁻ detected in the unconsumed black powder as well as the post-blast residue support the use of nitrate-containing explosive. However, large amount of Cl⁻ produced in the explosion could not serve as evidence for the original presence of chlorate-based mixture. This was due to the fact that large amount of Cl⁻ was found to be present in pre-blast soil samples, which may interfere the IC analysis or overload the chromatographic column [9]. In this study, the presence of Cl⁻ detected in unconsumed black powder may be originated from chloride salt which was used as an additive in the homemade explosive. In addition to Cl⁻, NO₃⁻ and SO₄²⁻ which were originally present in black powder, NO₂⁻ formed in the combustion was also identified in the present study. The formation of NO₂⁻ in post-explosion residue was probably due to the reduction of nitrate incorporated in the original explosive (Equation 1). However, its amount varies depending on several factors such as burn rates and the heat of the blast [10].

$$KNO_3 \longrightarrow K^+ + NO_2^- + \frac{1}{2}O_2$$
 (1)

Umi Kalthom Ahmad et al: ANALYSIS OF ANIONIC POST-BLAST RESIDUES OF LOW EXPLOSIVES FROM SOIL SAMPLES OF FORENSIC INTEREST

In the second approach, a study was conducted to evaluate the correlation between the concentration of analyte ions detected and the amount of explosives used. A 3-dimensional (3-D) bar graph was drawn to illustrate the relationship between these variables (Figure 8). From the graph, the mean concentration of each analyte ions detected from the post-blast residues of soil samples show gradual decrease with the reduction in amount of explosives used in the simulated explosion.

Overall, the post-explosion residues showed the presence of chloride, nitrite, nitrate and sulphate in this study. These ions were consistent with the presence of nitrate salt oxidizer, carbon and sulfur fuel in the homemade inorganic explosive used. Besides, the partial identification of these ions can be related to the reactants and products of Equation 2 [10].

$$KNO_{3} + KClO_{4} + S + C + C_{6}H_{5}CO_{2}Na + NH_{2}C(NH)NHCN \longrightarrow NO_{2}^{-} + Cl^{-} + SO_{4}^{-2} + HS^{-} + SCN^{-} + OCN^{-} + HCO_{3}^{-} + K^{+} + Na^{+}$$
(2)

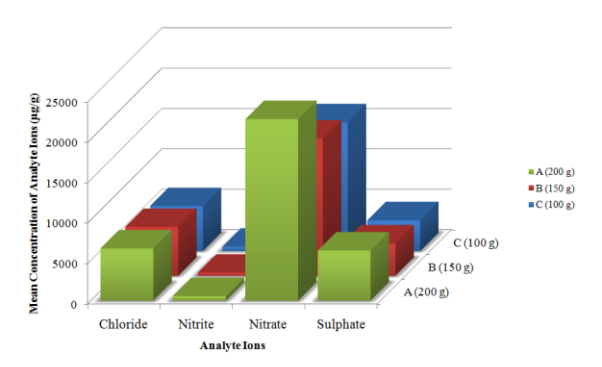


Figure 8: The relationship between the amount of explosives used and the mean concentration of analyte ions detected from post-blast residues of soil samples.

Table 5: Summarized data for the mean concentration of analyte ions calculated in relation to the amount of explosives used for the simulated explosion and percentage of analyte ions remained in post-blast residues.

	Plack powder	Post-blast residues A (200 g)		
Analyte	Black powder standard	Amount of analytes	Percentage resided in soil (%)	RSD (%)
Cl	6484.8±80.7	6477.6±615.5	99.89	11.68
NO_2^-	ND	576.5±41.5		
NO_3	139732.1±250.2	22498.2±1240.8	16.10	7.55
SO ₄ ²	4020.1±59.6	3814.8±616.5	94.90	11.92

SD – Standard deviation based on triplicate extractions.

ND – Not detected

	Dlook povedor	Post-blast residues B (150 g)			
Analyte	Black powder standard	Amount of analytes	Percentage resided in soil (%)	RSD (%)	
Cl	6484.8±80.7	6072.1±442.2	93.64	8.54	
NO_2^-	ND	404.4±6.4			
NO_3^-	139732.1±250.2	17025.8±1080.0	12.18	8.73	
SO_4^{2-}	4020.1±59.6	4017.1±393.8	99.92	11.77	

SD - Standard deviation based on triplicate extractions.

ND – Not detected

		Post-blast residues C (100 g)			
		Amount of analytes	Percentage resided in soil (%)	RSD (%)	
Cl	6484.8±80.7	5578.5±356.9	86.02	7.29	
NO_2^-	ND	556.4±5.0			
NO_3	139732.1±250.2	15964.6±1888.5	11.43	16.46	
SO_4^{2-}	4020.1±59.6	3828.2±150.5	95.23	3.46	

SD - Standard deviation based on triplicate extractions.

ND – Not detected

Conclusion

IC has been successfully applied in post-blast identification of homemade inorganic explosives. In this study, IC analysis of soil collected at the seat of blast has successfully been carried out and strongly indicated that a low explosive containing KNO₃ has been employed in the explosion. By noting the presence of Cl⁻, NO₂⁻, NO₃⁻ and SO₄²⁻, it can be concluded that the explosive contained nitrate salt, which is a strong evidence for the use of black powder explosive in the improvised explosive device.

Acknowledgement

The authors would like to acknowledge Forensic Laboratory of Royal Malaysia Police for much helpful arrangement during the sampling and all the police officers from Maktab Teknik PDRM Muar who assisted us throughout the sampling exercise. Thanks are also due to The Department of Chemistry, Faculty of Science UTM for research facilities and Budget Mini 2009 of Ministry of Higher Education for funding Ong's Master study.

References

- 1. Royds, D., Lewism S. W. and Taylor, A. M. (2005). A Case Study in Forensic Chemistry: The Bali Bombings. *Forensic Chemical Analysis*. 67 (2): 262-268.
- 2. Jakarta hotel blasts kill 8, wound 50 (2009, July 17). *The Star*. Retrieved June 8, 2010, from http://thestar.com.my/news/story.asp?file=/2009/7/17/nation/20090717095 051&sec=nation
- 3. Rose, G. (2009). Who Cares for Which Dead and How? British Newspaper Reporting of the Bombings in London, July 2005. *Geoforum* 40. (1): 46-54.
- 4. Karishma Vaswani (2009, July 17). Fatal blasts hit Jakarta hotels. *BBC News*. Retrieved June 8, 2010, from http://news.bbc.co.uk/2/hi/asia-pacific/8155084.stm
- 5. Thieves blow up ATM with fireworks bomb (2008, October 14). *The Star.* Retrieved July 8, 2010, from http://thestar.com.my/news/story.asp?file=/2008/10/14/nation/ 2270584&sec=nation

Umi Kalthom Ahmad et al: ANALYSIS OF ANIONIC POST-BLAST RESIDUES OF LOW EXPLOSIVES FROM SOIL SAMPLES OF FORENSIC INTEREST

- 6. Saferstein, R. (2007). *Criminalistics: An Introduction to Forensic Science*. (9th Ed.) New Jersey: Person Prentice Hall.
- 7. Moore, D. S. (2007). Recent Advances in Trace Explosives Detection Instrument. Sens Imaging 8: 9-38.
- 8. Martin, R. J., Reza, A. and Anderson, L. W. (2000). What is An Explosion? A Case History of An Investigation for the Insurance Industry. *J. Loss Prevention in the Process Industries* 13: 491-497.
- 9. Yinon, J. and Zitrin, S. (1993). *Modern Methods and Applications in Analysis of Explosives*. Chichester: John Wiley and Son.
- 10. McCord, B. R., Hargadon, K. A., Hall, K. E. and Burmeister, S. G. (1994). Forensic Analysis of Explosives Using Ion Chromatographic Methods. *Anal. Chem. Acta* 288: 43-56.
- 11. Johns C., Shellie, R.A., Potter, O. G., O'Reilly, J. W., Hutchinson, J. P., Guijt, R. M., Breadmore, M. C., Hilder, E. F., Dicinoski, G. W. and Haddad, P. R. (2008). Identification of Homemade Inorganic Explosives by Ion Chromatographic Analysis of Post-blast Residues. *J. Chromatogr. A.* 1182 (2): 205-214.
- 12. Hargadon, K. A. and McCord, B. R. (1992). Explosive Residue Analysis by Capillary Electrophoresis and Ion Chromatography. *J. Chromatogr.* 602: 241-247.
- 13. Miller, M. L., Doyle, J. M., Lee, R. A. and Gillette, R. (2001). Analysis of Anions by Capillary Electrophoresis and Ion Chromatography for Forensic Applications. *Forensic Sci. Comm.* 3 (2):21-29.
- 14. Ahmad, U.K. and Kiu, K.H. (2007). Solid Phase Microextraction-Gas Chromatography for the Analysis of Explosives in Post Blast Water Samples, *Jurnal Teknologi*, 46(C), 59-74.
- 15. Ahmad, U.K., Rajendran, S, Lee. L.W. and Yew, C.H. (2008). Forensic Analysis of High Explosives Residues in Post-Blast Water Samples Employing Solid Phase Extraction for Analyte Preconcentration. *Malays. J. Anal. Sci.* 12(2): 367-374.
- 16. Ahmad, U.K., Lee, W.L. and Yew, C.H. (2011). Direct Immersion Solid Phase Microextraction for the Forensic Determination of Nitro Explosives in Post-Blast Water Samples. *Health Environ. J.* 2 (1):27-37.
- 17. Radtke, C. W., Gianotto, D. and Roberto, F. F. (2002). Effects of Particulate Explosives on Estimating Contamination at a Historical Explosives Testing Area. *Chemosphere* 46: 3-9.
- 18. Kosanke, B. J., Sturman, B., Kosanke, K., Maltitz, I. V., Shimizu, T., Kubota, N., Jennings-White, C. & Chapman, D. (2004). *Pyrotechnic Chemistry: Pyrotechnic Literature Series No. 4*. Whitewater: Journal of Pyrotechnics Inc.
- 19. Trifilieff, O. and Wines, T. H. (2009). Black Powder Removal from Transmission Pipelines. *Pipeline Rehabilitation and Maintenance Conference*. January 19-21, 2009. Manama, Bahrain: 1-12.
- 20. Brown, M. E. and Rugunanan, R. A. (1989). A Temperature-Profile Study of the Combustion of Black Powder and its Constituent Binary Mixtures. *Propellants, Explosives, Pyrotechnics* 14: 69-75.
- 21. Beveridge A. (1998). Forensic Investigation of Explosions. London: Taylor & Francis Ltd.
- 22. Kuila, D. K., Chakrabortty, A., Sharma, S. P. and Lahiri, S. C. (2006). Composition Profile of Low Explosives from Cases in India. *Forensic Sci. Int.* 159: 127-131



PHOTOLUMINESCENCE OF POROUS SILICON PREPARED BY CHEMICAL ETCHING METHOD

(Fotoluminesen Poros Silikon Yang Disediakan Secara Punaran Kimia)

Dwight Tham Jern Ee, Chan Kok Sheng and M.I.N. Isa*

Department of Physics, Faculty Science and Technology Universiti Malaysia Terengganu, 21030 Kuala Terengganu, Terengganu, Malaysia

*Corresponding author: ikmar_isa@umt.edu.my

Abstract

Recently, porous silicon (PS) was intensely studied by researcher due to its photoluminescence (PL), which has potential application in optoelectronic devices and sensor. In this work, the PS was prepared by chemical etching of p-type silicon wafer where the etchant consist of mixture of hydrofluoric acid (HF) and nitric acid (HNO₃). The PS was characterized by Scanning Electron Microscope (SEM) and Photoluminescence Spectrometer. The porosity of the PS was in the range of (49-80) % and it is dependent on etching time. The peak of the PL ranges from 636 nm to 640 nm and the intensity of PL increase proportionally with the etching time. Band gap energy of PS was higher than silicon (1.11 eV) which is from 1.93 eV to 1.95 eV and the blue shift of the PL peak observed as the porosity increases.

Keywords: Porous Silicon, Chemical Etching, Photoluminescence

Abstrak

Baru-baru ini, penyelidikan poros silicon (PS) telah dijalankan dengan ketara atas sebab kebolehannya mengeluarkan fotoluminesen (PL) yang menjadikan PS berpotensi dalam aplikasi optoelektronik dan sensor. Dalam penyelidikan ini, PS dihasilkan dengan mengunakan cara punaran kimia atas silicon wafer jenis-p, dimana kandungan bahan punar itu terdiri daripada campuran asid hidrofluorik (HF) dan asid nitrik (HNO₃). PS telah dicirikan dengan mengunakan mikroskop imbasan electron (SEM) dan spektrometer fotoluminesen. Poros yang dihasilkan atas PS adalah dalam julat (49-80) % dan ia bersandar dengan masa punaran. Puncak PL berjulat dari 636 nm ke 640 nm dan keamatan PL meningkat secara bekadaran dengan masa punaran. Tenaga jurang jalur PS lebih tinggi daripada silicon (1.11 eV) iaitu dari 1.93 eV ke 1.95 eV dan anjakan biru di puncak PL dapat dilihat apabila keporosan PS meningkat.

Kata kunci: Silikon Poros, Punaran Kimia, Fotoluminesen

Introduction

Recently, porous silicon (PS) was intensely studied by researchers since it was reported for visible photoluminescence by Canham in 1990. According to Canham, porous silicon has potential application in optoelectronic and sensor [1]. Generally, there are two methods used to produce porous silicon namely electrochemical etching and chemical etching in the HF based solution. The difference between both method is chemical etching is performed etching without using external bias, which can be considered as a localized electrochemical process started chemically [2]. The etchant consist of HF and HNO₃ are used in the etching process. In chemical etching, anode and cathode site are formed on the etched surface which caused the local current to flow on the surface during the etching process. The oxidation process at the anode is proposed to be the dissolution of Si which forms Si²⁺ and Si⁴⁺, while the cathode reaction is a complex reduction of H⁺ which the hole injection process happened on the Si surfaces.[2,3]. Photoluminescence (PL) is a spontaneous emission of light from a material under optical excitation. The PL Spectrum produced by the material is able to be used to characterize the electrical parameters [4]. In this work, the PS was prepared by chemical etching method then the photoluminescence property, porosity and surface morphology were studied.

Experimental

The porous silicon was fabricated by using the light doped p-type silicon wafer, where the dopant was boron. The wafers were cleaned by using solvent clean method to remove oil and organic residue that is on its surface. In the cleaning process two solvents were needed which is acetone and ethanol. For acetone, it will leave it own residue; therefore, ethanol is used to clean off the acetone residue [5]. Then, the silicon wafers were dipped in the prepared etching solutions which contain concentrated hydrofluoric acid (48%) and nitric acid (65%).

The etching time was fixed with the interval of 5 minutes. Five PS samples were prepared. After the etching, slow evaporation drying method was used to reduce the crack of the formed porous silicon by rinsing the sample with ethanol [6]. Then the sample is dried in the fume hood.

The PS surface was observed by using SEM and the elemental analysis on the surface of PS was analyzed by using Energy Dispersive Spectroscopy (EDS). The porosity of the PS was measured by using gravimetric method of the sample. Besides, the photoluminescence of the PS was characterized in the range of 500 nm to 800 nm by using photoluminescence spectroscopy system, model Jobin Yvon HR 800 UV. Then, from the PL spectrum, the energy gap was determined by equation (1):

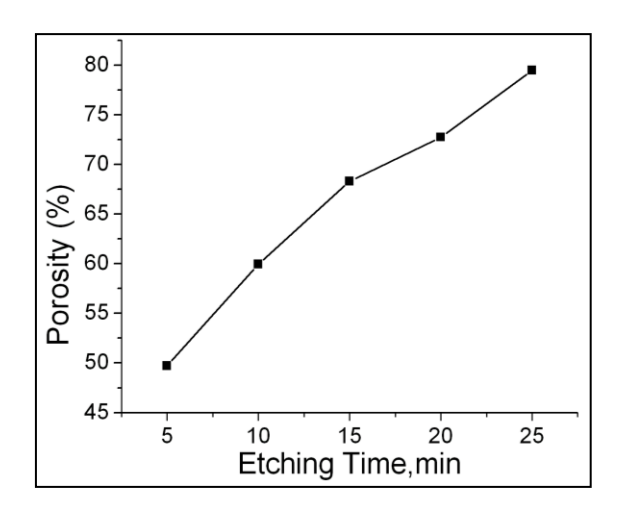
$$E_{gap} = \frac{hc}{\lambda} \tag{1}$$

where E_{gap} is energy gap of the PS, h is Planck constant, c is the speed of light and λ is the peak wavelength of the photoluminescence.

Results and Discussion

Porosity by Gravimetric Method

The weight of the sample, before and after etching was measured to determine the weight loss and the porosity of the sample. The obtained porosity, (%) shows that it was dependent on the etching time as depicted in Figure 1. The porosity of the PS produced by the chemical etching method is in the range between (49-80) %. Besides, the etching rate shows a gradual decrease with time. This might be due to the hindrance of the bubble produced during the etching process. As bubble formed on the sample surface, it reduces the surface area for etching process for a short moment before the bubble released from the sample surface. [7]



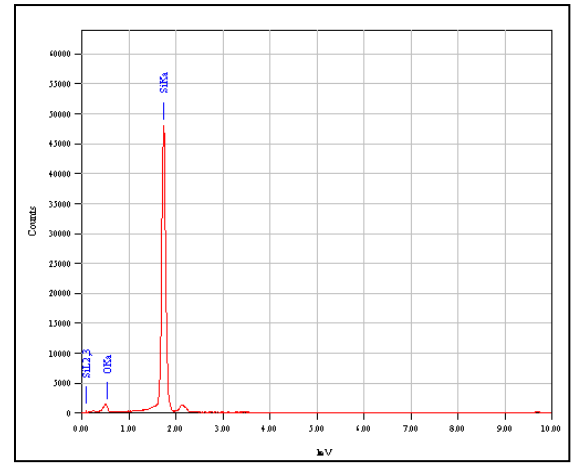


Figure 1: The Porosity of PS versus Etching Time

Figure 2: The EDS spectra for PS

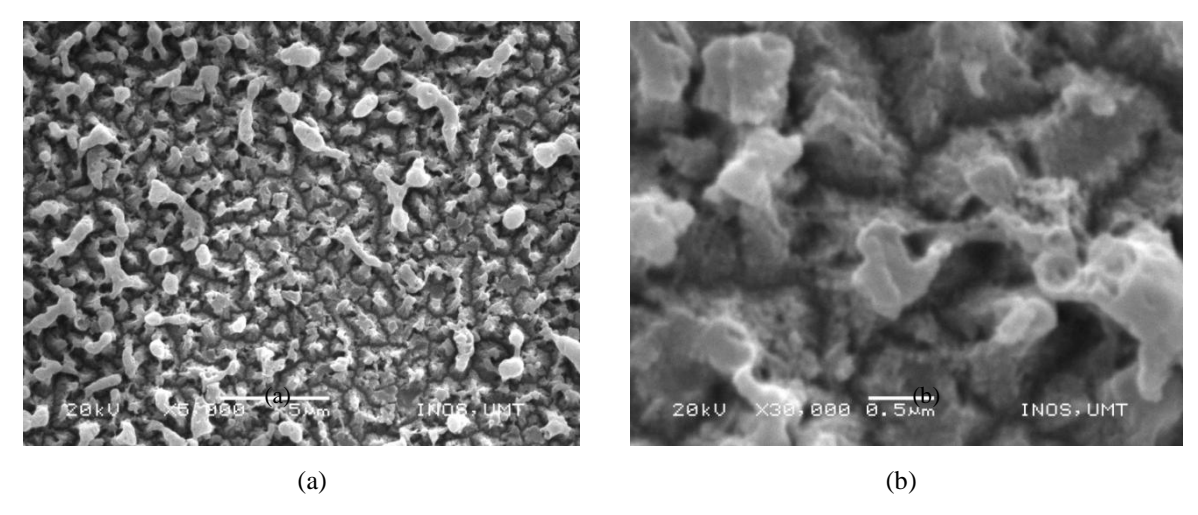


Figure 3: SEM images of PS prepared at 5 minutes of etching time with magnification of (a) $\times 5000$ and (b) $\times 30000$

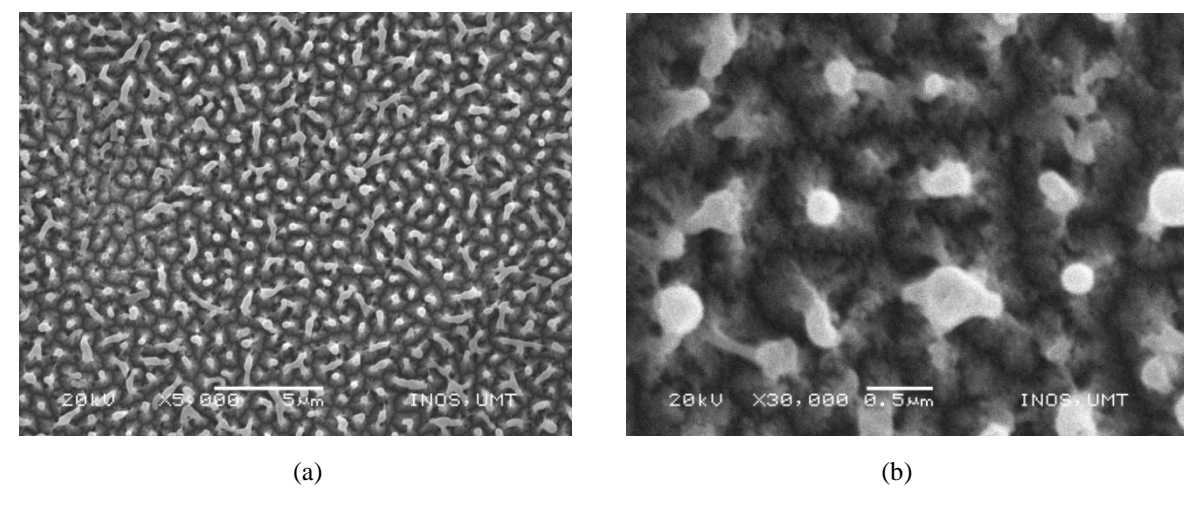


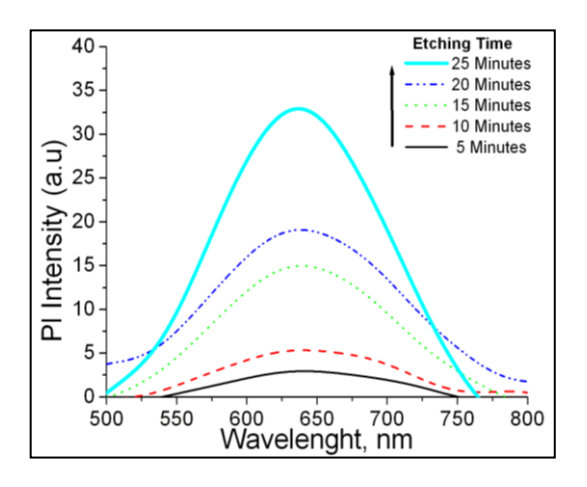
Figure 4: SEM images of PS prepared at 5 minutes of etching time with magnification of (a) $\times 5000$ and (b) $\times 30000$

Surfaces investigation by SEM and EDS

The surface of the PS was investigated by using SEM, where it shows that after the chemical etching process, there is an obvious increase in surface area due to the formation of crystallites and pore population. The surface morphology of the PS after 5 minutes etching time as shown in Figure 3 was mixture of anisotropic crystallites and pores population. Such morphology was due to the frequent attacked of HF acid at the grain boundary. The superficial anisotropic crystallites are residue of etched layer. While in Figure 4, it depicts that, the surface morphology after 25 minutes etching time has smaller crystallites and pore population. The small crystallites are in cylindrical columnar shape as shown in figure 4b. The elemental analysis on the surface of the PS was performed by EDS. Figure 2 shows that the PS surface only consist of silicon and oxygen, for it can be concluded that most of the surface species of the PS contain Si-O bonds.

The Photoluminescence Properties and Energy gap by Photoluminescence Spectroscopy

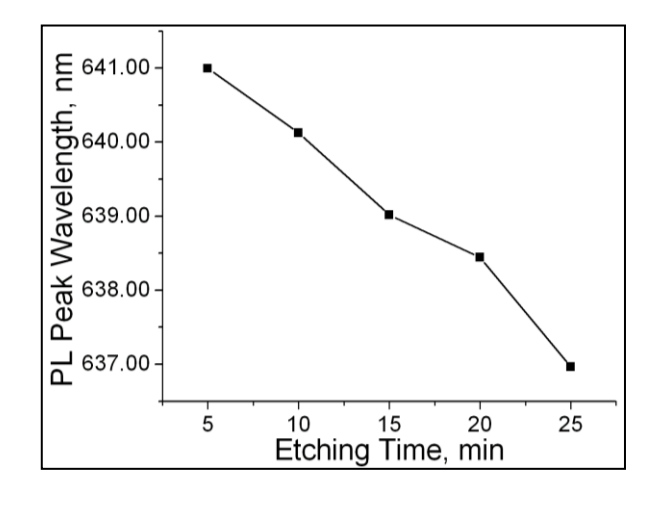
The PL Spectrum, was obtained when the excitation wavelength is shorter than the emission wavelength. This is because shorter wavelength has higher energy to cause photoluminescence. The PS produced is able to illuminate visible light which fall in the range (636-640) nm as can be seen in Figure 5. Hence, orange red luminescence was observed from the PS. The PS is able to illuminate light because of the surface states and the quantum confinement that developed on the PS after the etching process.[1,8] From Figure 5 and Figure 6, it shows that the PL intensity increase with etching time. This is because PL intensity is affected by porosity or the total volume of crystallites on the surface of PS [9]. The information obtained from Figure 5 is used in plotting Figure 6 and Figure 7, so that it is able to show a better relationship between all parameters. A slight blue shift can be seen in the Figure 5 and Figure 7 as the etching time increase. This effect is due to the decrease of the cylindrical crystallites size and the pore population [10]. The energy gap was then calculated using equation 1 and plotted in Figure 8. The PS energy gap is definitely having higher energy gaps compare to Silicon (1.11eV) and it increases from (1.93 - 1.95)eV as etching time and porosity increased.



35-(n 30-E 25-10-45 50 55 60 65 70 75 80 Porosity, %

Figure 5: The Photoluminescence Spectrum of the Porosity

Figure 6: Relationship between PL Peak Intensity and PS



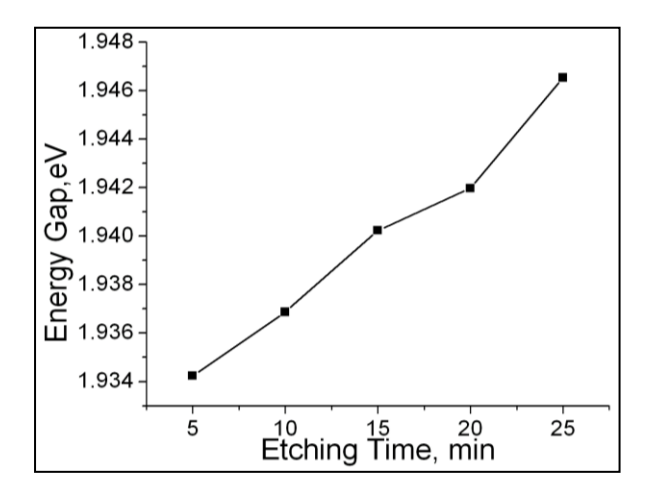


Figure 7: PL Peak wavelength against Etching Time.

Figure 8: PS Energy Gap against Porosity

Conclusion

In conclusion, the PS has been successfully fabricated by chemical etching. The results obtain form chemical etching PS, show the effect of different etching time on the morphology, porosity, PL spectrum and energy gaps of the PS. The porosity formed by this method increases with etching time are in the range of (49-80) %. The crystallite size decreases with etching time, hence this behavior contributes to the blue shift and the increase of energy gaps. The PL produced by the PS is in orange red light.

Acknowledgement

The authors would like to thank Physical Sciences Department of University Malaysia Terengganu for the helps and financial support of this work.

References

- 1. Canham, L.T. 1990. Silicon quantum wire array fabricated by electrochemical and chemical dissolution of wafers. Applied Physics Letter 57:1046-1048
- 2. Lemus, R.G., Rodriguez, C.H., Hander, F.B. and Duart, J.M.M. 2002. Anodic and optical characterisation of stain-etched porous silicon antireflection coatings Solar Energy Materials & Solar Cell 72:495-501
- 3. Shih, S., Jung, K. H., Hsieh, T. Y., Sarathy, J., Campbell, J. C., Kwong, D. L. 1992. Photoluminescence and formation mechanism of chemically etched silicon. Applied Physics Letters 60:1863
- 4. Gfroerer, T.H. 2000. Photoluminescenc in Analysis of Surfaces and Interfaces. In Encyclopedia of Analytical Chemistry, ed. R.A. Meyer, pp 9209-9231. Chichester: John Wiley & Sons Ltd.
- 5. Kern, W. 1993. Overview and Evolution of Semiconductor Wafer Contamination and Cleaning Technology. In Handbook of Semiconductor Wafer Cleaning Technology, ed. W. Kern, pp 3-57. Park Ridge, New Jersey: Noyes Publishing.
- 6. Canham, L.T. 1997. 'Drying of porous silicon', in Properties of Porous Silicon, Institution of Engineering and Technology, London:43.
- 7. Lehmann, V., Foll, H. 1990. Formation Mechanism and Properties of Electrochemically Etched Trenches in n-Type Silicon. Journal of the Electrochemical Society .137:653-658
- 8. Lehmann, V., Gosele, U. 1991. Porous silicon formation: A quantum wire effect. Applied Physics Letters 58:856-858
- 9. Kim, D.-A., Shim, J.-H., Cho, N.-H. 2004. PL and EL features of p-type porous silicon prepared by electrochemical anodic etching. Applied Surface Science. 234:256-261
- 10. Gelloz,B. 1997. Possible explanation of the contradictory results on the porous silicon photoluminescence evolution after low temperature treatments. Applied Surface Science. 108:449-454.



DETERMINATION OF ORGANOPHOSPHORUS PESTICIDES BY DISPERSIVE LIQUID-LIQUID MICROEXTRACTION COUPLED WITH GAS CHROMATOGRAPHY-ELECTRON CAPTURE DETECTION

(Penentuan Pestisid Organofosforus dengan Pengekstrakan Cecair-Cecair Serakan berganding dengan Kromatografi Gas-Pengesanan Penangkap Elektron)

Mohd Marsin Sanagi^{1,2*}, Siti Umairah Mokhtar¹, Mazidatul Akmam Miskam¹, Wan Aini Wan Ibrahim^{1,2}

¹Department of Chemistry, Faculty of Science, Universiti Teknologi Malaysia, 81310 UTM Johor Bahru, Johor, Malaysia ²Ibnu Sina Institute for Fundamental Science Studies, Nanotechnology Research Alliance, UniversitiTeknologi Malaysia, 81310 UTM Johor Bahru, Johor, Malaysia

*Corresponding author: marsin@kimia.fs.utm.my

Abstract

A simple, rapid and sensitive method termed as dispersive liquid–liquid microextraction (DLLME) combined with gas chromatography-electron capture detector (GC-ECD) was developed for the determination of selected organophosphorus pesticides (OPPs) namely chlorpyrifos, dimethoate and diazinon in water sample. In this method, a mixture of carbon disulfide, CS_2 (extraction solvent) and methanol (disperser solvent) was rapidly injected using syringe into the 5.00 mL water sample to form a cloudy solution where the OPPs were extracted into the fine droplets of extraction solvent. Upon centrifugation for 3 min at 3500 rpm, the fine droplets were sedimented at the bottom of the centrifuge tube. Sedimented phase (1 μ L) was injected into the GC-ECD for separation and determination of OPPs. Important extraction parameters, such as type of disperser solvent, volume of extraction solvent and volume of disperser solvent were investigated. The optimized conditions for DLLME of the selected OPPs were methanol as disperser solvent, 30 μ L of extraction solvent (CS₂) and 1.0 mL of disperser solvent (methanol). Under the optimum extraction conditions, the method showed good linearity in the range of 0.1 to 1.0 μ g/mL with correlation coefficient (r^2), in the range of 0.9976 to 0.9994 and low limits of detection (LOD) between 0.047 and 0.201 μ g/mL. The proposed method provided acceptable recoveries (72.67- 144%) with good RSDs ranging from 2.74% to 7.48%. This method was successfully applied to the determination of OPPs in water samples obtained from a golf course and chlorpyrifos and diazinon were detected at concentration 0.18 μ g/mL and 0.07 μ g/mL, respectively.

Keywords: Dispersive liquid—liquid microextraction; GC-ECD; Organophosphorus pesticides

Abstrak

Satu kaedah yang mudah, cepat dan peka yang dikenali sebagai pengekstrakan cecair-cecair serakan (DLLME) yang digandingkan dengan kromatografi gas-pengesanan penangkap electron (GC-ECD) telah dibangunkan bagi penentuan pestisid organofosforus (OPPs) terpilih, iaitu kloropirifos, dimetoat dan diazinon dalam sampel air. Dalam kaedah ini, satu campuran karbon disulfide CS₂ (pelarut pengekstrakan) dan methanol (pelarut serakan) disuntik dengan cepat menggunakan picagari ke dalam sampel air 5.00 mL untuk membentuk larutan keruh di mana OPPs terekstrak ke dalam butiran halus pelarut pengekstrakan. Setelah pengemparan selama 3 min pada 3500 rpm, butiran halus itu termendak di dasar tabung pengemparan. Fasa termendak (1 1 μL) disuntik ke dalam GC-ECD) bagi pemisahan dan penentuan OPPs.Parameter pengesktrakan yang penting termasuk jenis pelarut serakan, isipadu pelarut pengekstrakan dan isipadu pelarut serakan telah dikaji. Keadaan optimum DLLME bagiOPPs terpilih ialah methanol sebagai pelarut serakan, 30 μL pelarut pengekstrakan (CS₂) dan 1.0 mL pelarut serakan (metanol). Di bawah keadaan optimum, kaedah ini menunjukkan kelinearan baik dalamjulat 0.1 hingga 1.0 μg/mL dengan koefisien korelasi(r²), dalam julatdari 0.9976 hingga 0.9994 dan had pengesanan(LOD) di antara 0.047 dan 0.201 μg/mL. Kaedah yang dicadangkan ini memberi pulangan yang baik (72.67- 144%) dengan sisihan piawai relatif (RSD) yang baik di

Mohd Marsin Sanagi et al: DETERMINATION OF ORGANOPHOSPHORUS PESTICIDES BY DISPERSIVE LIQUID-LIQUID MICROEXTRACTION COUPLED WITH GAS CHROMATOGRAPHY-ELECTRON CAPTURE DETECTION

antara 2.74% dan 7.48%. Kaedah ini telah berjaya diaplikasikan dalam pengesanan OPPs dalam sampel air yang diperolehi dari padang golf. Klopirifos dan diazinon telah dikesan masing-masing pada kepekatan 0.18 µg/mL dan 0.07 µg/mL.

Kata kunci: Pengekstrakan cecair-cecair serakan; GC-ECD; Pestisid organofosforus

Introduction

According to the status list of all active pesticide substances on the European Union (EU) market, more than 1100 pesticides are currently registered [1]. The pesticides industry is made up of companies, both multinational and local companies that are involved in manufacturing, formulating or trading activities. The majority of pesticides are imported as technical materials, which are then blended, diluted or formulated. Pesticides are widely used for agricultural activities due to their relatively low price and high effective ability to control pests, weeds, and diseases [2]. The increasing production of pesticides for agricultural and non-agricultural purposes has caused the pollution of air, soil, ground, and surface water which involves a serious risk to the environment and as well as human health due to either direct exposure or through residues in food and drinking water [3].

Organophosphorus pesticides (OPPs) are widely used in many countries for agriculture and pests control. OPPs (phorate, diazinon, disolfotane, methyl parathion, sumithion, chloropyrifos, malathion, fenthion, profenphose, ethion, phosalone, azinphose-methyl) are widely found in water resources. These pesticides are commonly use on golf courses in order to maintain the quality of the turfs. As the result, the caddies and green keepers often experience health problems due to the exposure to the evaporated chemicals and contaminated soil. In additions, the golfers themselves breathe in the toxins as they walk the course before the newly sprayed pesticides could settledown. The need for accurate determination of pesticides at the trace levels in the environmental samples is therefore obvious. With the improvement of self-safeguard consciousness and the development in analytical instruments, levels of pesticides in vegetables and fruitsare currently regulated by international and national organizations [4] and maximum residue levels (MRLs) have been established in many countries [5].

Sample preparation is normally required to isolate and concentrate compounds of interest from the sample matrix, before analysis [6]. Ultimately, the concentration of target compounds is enhanced (enrichment) and the presence of matrix components is reduced (sample clean up). In order to achieve a low detection limit, an enrichment step should be conducted prior to analysis [7].

Classical liquid-liquid extraction is considered to be a time-consuming and multistage operation, where problems of emulsion formation obstruct automation [8]. The demand for automation in analytical liquid-liquid extraction (LLE) combines with a small amount or elimination of solvent has led to recent development of dispersive liquid-liquid extraction (DLLME). DLLME was first reported by Asadi and his co-workers in 2006 [1]. It is a novel liquid-phase microextraction technique which is based on a ternary component solvent system in which extraction solvent and disperser solvent are rapidly injected into the aqueous sample in a conical test tubeusing a syringe. The mixture is then shaken and a cloudy solution is usually formed in the test tube. After centrifugation, the fine particles of extraction solvent were sedimented in the bottom in the conical test tube. The resultant sedimented phase is taken with a microsyringe and injected into GC for analysis [1,9-10]. DLLME is a miniaturized LLE that uses microliter volumes of extraction solvent. The advantages of DLLME method are the simplicity of operation, rapidity, low cost, high-recovery, high enrichment factor, and environmental benignity, with wide application prospects in trace analysis.

In this work, DLLME was used for the extraction of OPPs namelychlorpyrifos, dimethoate and diazinon in water sample. The objectives of this study are to determine the effect of selection solvents, disperser solvents, volume of extraction solvent and volume of disperser solvents and to apply the optimum DLLME conditions in the analysis of OPPs in water sample.

Experimental

Chemicals and Reagents

The selected OPPs used in this research namely dimethoate, diazinon and chlorpyrifos(Figure 1) were analytical grade from Sigma-Aldrich (USA). Carbon disulfide used as an extraction solvent while methanol as a disperser solvent was purchased from Fluka, Switzerland. Doubly-distilled water used for preparation of aqueous solution at

least $18M\Omega$ was purified by Nano ultra-pure water system (Barnstead, USA). The standard stock solutions of 1000 ppm of the analytes were prepared in acetonitrile and were stored in fridge prior usage. The working standard solutions of lower concentrations were prepared by diluting standard stock solution with acetonitrile.

Figure 1: Structures of selected organophosphorus pesticides.

GC-ECD Conditions

A Perkin Elmer XL gas chromatography (GC) equipped with an electron capture detector (ECD) (San Jose, United State) was employed for the analysis of pesticides. High purity of nitrogen gas use as carrier gas and make up gas. Ultra pure helium passes through a molecular sieve trap and oxygen trap was used as the carrier gas at constant velocity of 2.3 mL/min. The injection port was held at 250° C and used in the splitless mode. Separation was carried out on a DB-5 capillary column, 30 m x 0.25 mm with 0.25 μ m film thickness which also known as Ultra 2. The oven temperature programmed as follows: initial 150° C (held 2 min) and then ramped at 4° C min⁻¹ to 220° C, held for 1 min and finally ramped at rate of 10° C/min to 275° C and held for 5 min. The ECD temperature was maintained at 300° C.

Dispersive Liquid Liquid Microextraction Procedure

A 5 mL of doubly-distilled water was placed in a 10 mL screw cap glass test tube with conical bottom and spike the selected OPPs. Methanol (1 mL), as disperser solvent and 45.0 μ L carbon disulfide (as extraction solvent) were injected rapidly into the sample solution by using a 1 mL syringe and the mixture was gently shaken. A cloudy solution (water/methanol/carbon disulfide) was formed in the test tube. In this step, the OPPs in water sample were extracted into the fine droplets of carbon disulfide. The mixture was then centrifuged for 3 min at 3500 rpm. After this process the dispersed fine droplets of carbon disulfide were sedimented in the bottom of test tube. Sedimented phase (1 μ L) was withdrawn using 1 μ L micro syringe (zero dead volume, cone tip needle) and injected into GC-ECD.

Sample Preparation

The optimum conditions for DLLME were applied for the analysis of water sample collected near the golf courses. The water sample was filtered through $0.45~\mu m$ Whatman nylon filter membrane to remove adhering particles and the sample was stored in refrigerator prior to use.

Results and Discussion

Optimization of Extraction Conditions

In order to optimize the DLLME of OPPs from water samples, analytical factors that potentially affect sample were studied. The parameters involved were the selection of disperser solvent, volume of disperser solvent and volume of extraction solvent.

Selection of Disperser Solvent

In this research, two different disperser solvents were evaluated which are acetonitrile and methanol (Figure 2). Disperser solvent is soluble in extraction solvent and should be miscible in water, thus enabling the extraction solvent to be dispersed as fine particles in aqueous phase to form a cloudy solution (water/disperser solvent/extraction solvent). In such a case, the surface area between extraction solvent and aqueous phase (sample) can be definitely large, thus increasing the extraction efficiency [1]. The key point for the selection of disperser solvent is the miscibility in both the extraction solvent and the aqueous sample [11]. Therefore, methanol and acetonitrile were selected for this purpose of this study.

Figure 2 shows a series of sample solution was studied by using 1 mL of methanol, and acetonitrile containing carbon disulfide (as extraction solvent). According to the figure, methanol gave the highest peak area compared to acetonitrile. Thus, this indicates that methanol have high extraction efficiency to extract the compound from aqueous sample and was employed in the subsequent experiments.

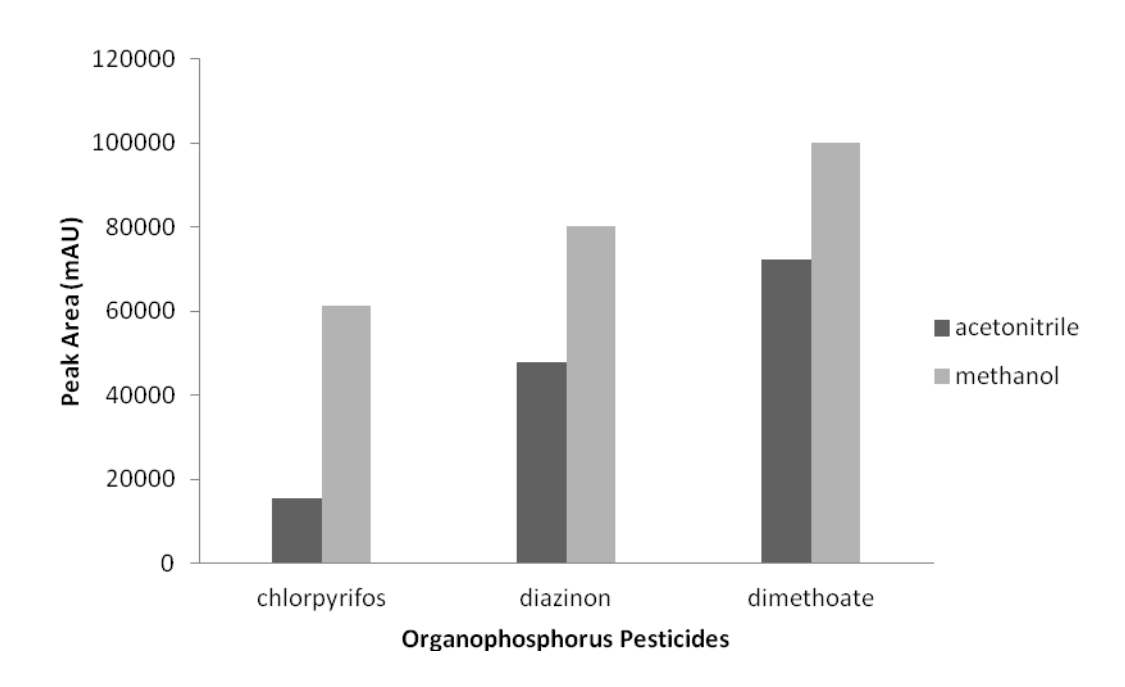


Figure 2: Selection of disperser solvent for each OPPs studied.

Effect of Extraction Solvent Volume

The extraction solvent volume has great effects on the enrichment factor. With the increase of the extraction solvent volume, the final organic phase obtained by centrifugation is increased, resulting in a decrease of the concentration of the target analyte in organic phase.

In this research, the extraction solvent was fixed to carbon disulfide since other chlorinated solvent could damage the instrument. In order to examine that effect, different volumes of carbon disulfide were examined between 30, 45 and 60 μ L. As depicted in Figure 3, as the volume of extraction solvent increased, the peak area decreased significantly. 30 μ L of extraction solvent gave the highest peak area and providehigh enrichment factor and high sensitivity for the determination of OPPs. Therefore, 30 μ L of carbon disulfide was chosen as optimum condition and utilized through out the subsequent experiments.

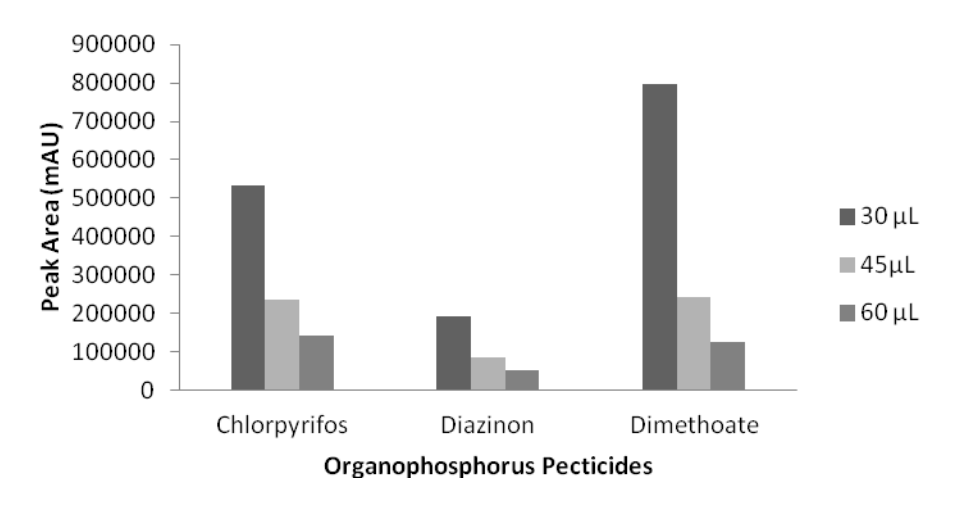


Figure 3: Effect of extraction solvent volume on the DLLME of OPPs.

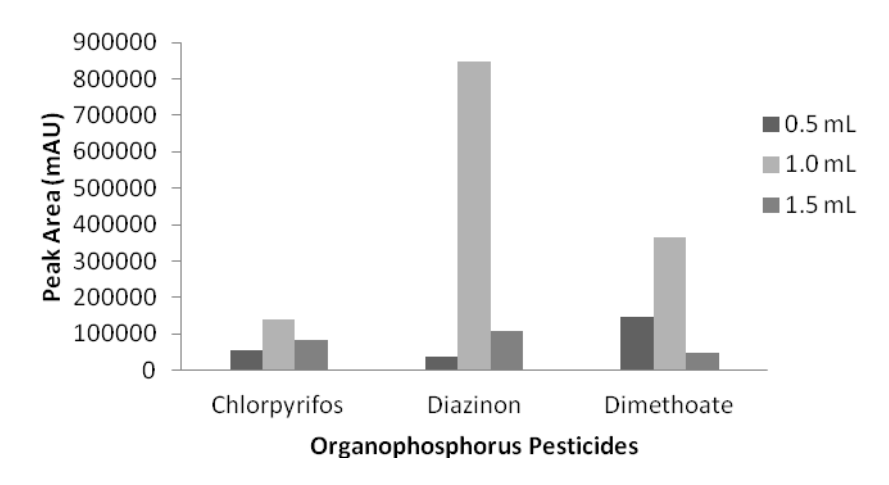


Figure 4: Effect of disperser solvent volume on the DLLME of OPPs.

Effect of Disperser Solvent Volume

To evaluate the effect of the dispersive solvent to enrichment factor, the volume of methanol was varied between 0.5 to 1.5 mL. As depicted in Figure 4, the peak area increased when the volume of methanol was increased to 1.0 mL. However, when the volume of the disperser solvent was increased to 1.5 mL, the peak area decreased. This result may be attributed to the increased solubility of the extraction solvent in the water as the volume of methanol increased. Thus, 1.0 mL of methanol was chosen as optimum and employed to all subsequent experiments.

Method Validation

For validation of the DLLME method, optimized conditions (methanol as disperser solvent with volume of 1.0 mL, and volume of extraction solvent (CS₂): 30 μ L) were used for the extraction of OPPs using DLLME. The correlation coefficient (r²), limit of detection (LOD) and limit of quantification (LOQ) of each pesticide are shown in Table 1. LOD represents the lowest concentration that can be detected by GC-ECD, which gives a signal-to-noise ratio of 3. Meanwhile, LOQ is known as the concentration of pesticides that produces a peak ten times higher than the noise level corresponding to signal to noise of S/N = 10.The LODs of the pesticideswere found to be 0.095 μ g/mL for chlorpyrifos,0.266 μ g/mL for diazinon and 0.085 μ g/mL for dimethoate. The LOQs of the pesticides ranged from 0.283 μ g/mL to 0.888 μ g/mL.

Table 1: Correlation coefficients, LOD and LOQ of selected OPPs using DLLME combined with GC-ECD.

OPPs studied	Correlation coefficient, r^2	LOD (µg/mL)	LOQ (μg/mL)
Chlorpyrifos	0.9994	0.095	0.318
Diazinon	0.9976	0.266	0.886
Dimethoate	0.9987	0.085	0.283

Real Sample Analysis

In order to investigate the applicability of the proposed trace enrichment microextraction method, the selected water sample was studied. The optimum conditions obtained in the optimization of DLLME was then applied to the determination of OPPs in water sample.

The water sample without spiking was analyzed in triplicate by the proposed method and the representative chromatograms can be seen in Figure 5. As depicted in the chromatogram, it can be seen that chlorpyrifos and diazinon were detected in the water sample with concentration of 0.18 μ g/mL and 0.07 μ g/mL respectively. This indicates that the selected OPPs were used in the area for the sample collection.

To study the recoveries of the OPPs in the real sample, the water sample was spiked with $1.5 \,\mu\text{g/mL}$ of each OPPs. The recoveries were calculated for triplicate samples. Table 2 shows the relative recoveries of the spiked samples respectively. In general, the relative recovery ranged between 72% to 144% with RSD less than 8 %.In spiked technique, high recoveries in analysis of samples usually correspond to high accuracy. The relative recovery is calculated from percentage of standard pesticides spiked expected area by comparison with standard solution of pesticides at the same level.

Table 2: Percent recovery and relative standard deviation (RSD) of spiked water sample by DLLME

Analyte	Recovery (%)	RSD (%)	
Chlorpyrifos	72.67	2.74	
Diazinon	144	7.48	
Dimethoate	79	5.64	



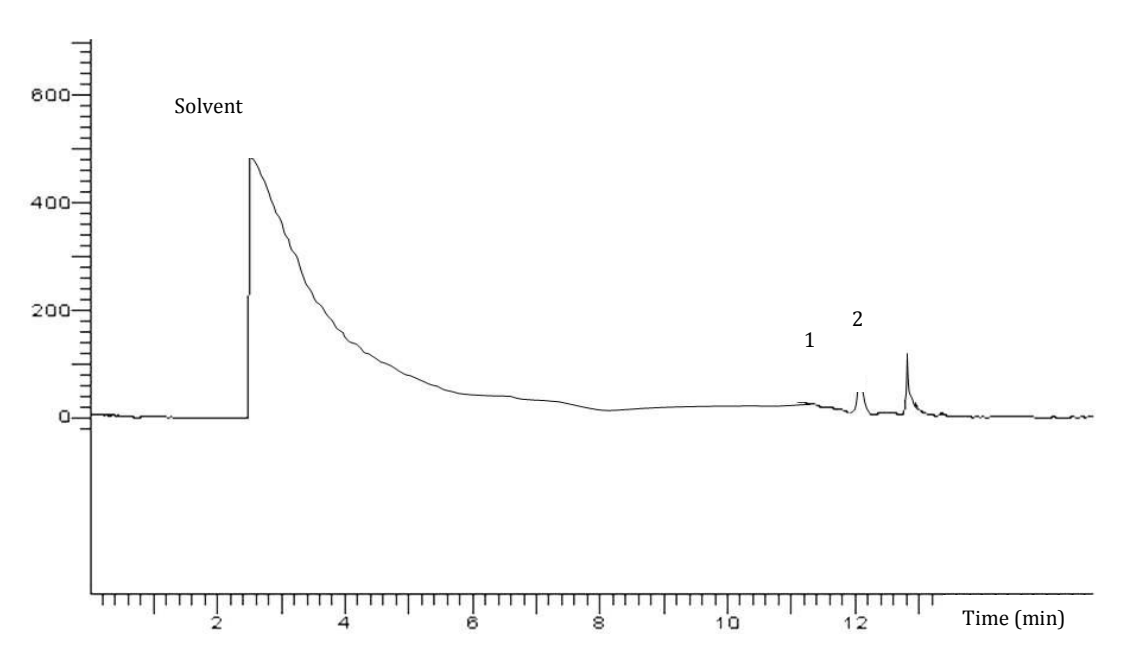


Figure 5: GC-ECD chromatogram of OPPs in water sample obtained by DLLME under optimized conditions. Peaks: (1) chlorpyrifos, (2) diazinon.

Conclusion

A method based on DLLME coupled with GC-ECD was developed for the determination of OPPs in water sample. The LOD was between 0.085 μ g/mL and0.266 μ g/mL while the LOQ was between 0.283 μ g/mL and0.886 μ gm/L. The recovery was in the range 72.67-144%. The relative standard deviations were in the range of 2.74-7.48%. The method has the merits of simplicity, low cost, and relatively short time for equilibrium extraction.

Acknowledgement

The authors are grateful to UniversitiTeknologi Malaysia for the facilitations and Ministry of Science, Technology and Innovation (MOSTI) Malaysia and the Ministry of Higher Education (MOHE) Malaysia for financial supports through research grant vote number 78477.

References

- 1. Fu, L., Liu, X., Hu, J., Zhao, X., Wang, H., Wang, X., (2009). Application of Dispersive Liquid Liquid Microextraction for the Analysis of Triazophos and Carbaryl Pesticides in Water and Fruit Juice Samples. *Anal. Chim. Acta*, **632**, 289-295.
- 2. Zang, X.H., Wu, Q.H., Zhang, M.Y., Xi, G.H., Wang, Z. (2009). Developments of Dispersive Liquid –Liquid Microextraction Technique. *Chin. J. Anal. Chem.* 37, 161-168.
- 3. Wan, H.B., Wong, M.K., Mok, C.Y. (1996). Pesticides in Golf Course Waters Associated with Golf Course Runoff. *Environ. Contamin. Toxicol.*, *56*, 205-209.
- 4. Wan Ibrahim, W.A., Farhani, H., Sanagi, M.M. and Aboul-Enein, H.Y. (2010). Solid phase microextraction using new sol-gel hybridpolydimethylsiloxane-2-hydroxymethyl-18-crown-6-coated fiber fordetermination of organophosphorous pesticides. *J. Chromatogr. A.* **1217**, 4890–4897.

Mohd Marsin Sanagi et al: DETERMINATION OF ORGANOPHOSPHORUS PESTICIDES BY DISPERSIVE LIQUID-LIQUID MICROEXTRACTION COUPLED WITH GAS CHROMATOGRAPHY-ELECTRON CAPTURE DETECTION

- 5. Zhao, E., Zhao, W., Han, L., Jiang, S. and Zhou, Z. (2007). Application of Dispersive Liquid Liquid Microextraction for the Analysis of organophosphorus Pesticides in Watermelon and Cucumber. *J. Chromatogr. A.***1175**, 137-140.
- 6. Xu, H., Liao, Y.and Yao, J. (2007). Development of a Novel Ultrasound-assisted Headspace Liquid-phase Microextraction and its Application to the Analysis of Chlorophenols in Real Aqueous Samples. *J. Chromatogr.* A. 1167, 1-8.
- 7. Liu, X.; Chen. X.; Yang, S. and Wang, X. (2007). Comparison of Continuous-flow Microextraction and Static Liquid-phase Microextraction for the Determination of *p*-toluidine in *Chlamydomonasreinhardtii.J. Sep. Sci.* 30, 2506-2512.
- 8. Sanagi, M.M., See, H.H., Wan Ibrahim, W.A. and Abu Naim, A. (2007). Determination of pesticides in water by cone-shaped membrane protectedliquid phase microextraction prior to micro-liquid chromatography. *J. Chromatogr. A*, **1152**, 215–219.
- 9. Huan, Z.X, Hua, W.Q., Yue, Z.M., Hong, X.G.and Zhi, W. (2009). Developments of Dispersive Liquid-Liquid Microextraction Technique. *Chin. J. Anal. Chem.* **37(2)**, 161-168.
- 10. Xiong, J. and Hu, B. (2008). Comparison of Hollow Fiber Liquid Phase Microextraction and Dispersive Liquid-Liquid Microextraction for the Determination of Organosulfur Pesticides in Environmental and Beverages Samples by Gas Chromatography with Flame Photometric Detection. *J. Chromatogr. A.* **1193**, 7-18.
- 11. Liu, Y., Ercheng, Z., Wentao, Z., Haixiang, G. and Zhiqiang, Z.(2009). Determination of Four Heterocyclic Insecticides by Ionic Liquid Dispersive Liquid–Liquid Microextraction in Water Samples. *J. Chromatogr.* A.1216, 885–891.



DEVELOPMENT AND VALIDATION OF RP-HPLC-UV/Vis METHOD FOR DETERMINATION OF PHENOLIC COMPOUNDS IN SEVERAL PERSONAL CARE PRODUCTS

(Pembangunan dan Validasi Kaedah Fasa Berbalik-HPLC-UV/Vis untuk Penentuan Sebatian Fenolik dalam beberapa Produk Penjagaan Diri)

Mohammed Akkbik, Zaini Bin Assim*, Fasihuddin B. Ahmad

Department of Chemistry, Faculty of Resource Science and Technology, Universiti Malaysia Sarawak, 94300 Kota Samarahan, Sarawak, Malaysia

*Corresponding author: zaini@frst.unimas.my

Abstract

A HPLC method with ultraviolet-visible spectrophotometry detection has been optimized and validated for the simultaneous determination of phenolic compounds, such as butylated hydroxyanisole (BHA) and butylated hydroxytoluene (BHT) as antioxidants, and octyl methylcinnamate (OMC) as UVB-filter in several personal care products. The dynamic range was between 1 to 250 mg/L with relative standard deviation less than 0.25%, (n=4). Limit of detection for BHA, BHT and OMC were 0.196, 0.170 and 0.478 mg/L, respectively. While limit of quantification for BHA, BHT and OMC were 0.593, 0.515 and 1.448 mg/L, respectively. The recovery for BHA, BHT and OMC ranged from 92.1-105.9%, 83.2-108.9% and 87.3-103.7%, respectively. The concentration ranges of BHA, BHT and OMC in 12 commercial personal care samples were 0.13-4.85, 0.16-2.30 and 0.12-65.5 mg/g, respectively. The concentrations of phenolic compounds in these personal care samples were below than maximum allowable concentration in personal care formulation i.e 0.0004 – 10 mg/g, 0.002 – 5 mg/g and up to 100 mg/g for BHA, BHT and OMC, respectively.

Keywords: Phenolic compounds, personal care products, RP-HPLC-UV/Vis, optimization and validation method.

Abstrak

Kaedah kromatografi cecair prestasi tinggi (KCPT) dengan pengesan spektrometri ultralembayung-boleh nampak telah dioptimumkan dan divalidasi untuk penentuan serentak sebatian fenolik seperti hidroksianisol terbutil (BHA) dan hidroksitoluena terbutil (BHT) sebagai antioksida, dan oktil metilsinamat (OMC) sebagai penapis-UVB dalam beberapa produk penjagaan diri. Julat dinamik adalah antara 1 ke 250 mg/L dengan sisihan piawai relatif kurang dari 0.25% (n=4). Had pengesanan untuk BHA, BHT dan OMC adalah 0.196, 0.170 dan 0.478 mg/L, masing-masingnya. Manakala had penentuan kuantitatif untuk BHA, BHT dan OMC adalah 0.593, 0.515 and 1.448 mg/L, masing-masingnya. Perolehan semula untuk BHA, BHT dan OMC adalah dalam julat dari 92.1-105.9%, 83.2-108.9% dan 87.3-103.7%, masing-masingya. Kepekatan BHA, BHT dan OMC dalam 12 sampel penjagaan diri komersial adalah dalam julat 0.13-4.85, 0.16-2.30 dan 0.12-65.5 mg/g, masing-masingnya. Kepekatan sebatian fenolik dalam sampel penjagaan diri adalah di bawah kepekatan maksimum dibenarkan dalam formulasi produk penjagaan diri iaitu 0.0004 – 10 mg/g, 0.002 – 5 mg/g dan hingga 100 mg/g untuk BHA, BHT dan OMC, masing-masingnya.

Kata kunci: Sebatian fenolik, produk penjagaan diri, RP-HPLC-UV/Vis, pengoptimaan dan validasi kaedah.

Introduction

Phenolic compounds such as butylated hydroxyanisole (BHA), butylated hydroxytoluene (BHT) and octyl methylcinnamate (OMC) (see Figure 1) are active constituents in personal care products [1,2].

Zaini Assim et al: DEVELOPMENT AND VALIDATION OF RP-HPLC-UV/Vis METHOD FOR DETERMINATION OF PHENOLIC COMPOUNDS IN SEVERAL PERSONAL CARE PRODUCTS

Figure 1: Structures of common phenolic compounds in personal care products.

BHA and BHT are added individually or in combination to prevent oxidative rancidity in personal care products [3], while OMC is used to absorbs UV-light between 280-320 mm to protect the skin from sunburn [2]. The amount of BHA and BHT in personal care formulation depends on the amount of sensitive compounds, such as α -hydroxy acids, ceramides, lipids, vitamins, oils and others, that are susceptible to oxidation by atmospheric oxygen to form unstable peroxide radicals [4,5]. BHA and BHT prevents the oxidation by inhibiting reactions promoted by oxygen and thus the formation of ketones and aldehydes that can give a products unpleasant smell and rancidity can be avoided [5]. Antioxidants prevent cosmetic formulations from peroxide radical because of their ability to neutralize those radicals through the transfer of hydrogen to this radical and stabilizing the antioxidant by resonance [6,7]. On the other hand, the amount of OMC added depend on type of product and part of body it applied [2,8,9,10,11]. Reversed phase HPLC with UV/vis detector (RP-HPLC-UV/Vis) is an important technique for phenolic compounds analysis because it have strong chromophores that absorb light in the wavelength region from 200 to 800 nm [12]. Application of RP-HPLC-UV/Vis in analysis of phenolic antioxidents such as BHA, BHT and OMC have been reported by several researchers [2, 5, 13]. The objective of this study is to determine the optimum analytical condition and validate the method for a simulataneous qualitative and quantitative analysis of phenolic compounds as well as to develop an analytical method evaluation and quality control of phenolic compounds by RP-HPLC-UV/Vis in personal care products.

Materials and Methods

Personal care samples

Four types of personal care products, namely sun cream, milk lotion, hair gel and hair oil were purchased from several local supermarkets in Kuching, Sarawak, Malaysia. Three commercial brands were collected for each type of personal care product.

Chemicals

The organic solvents (n-hexane, methanol, ethanol and acetonitrile) used for the analysis of phenolic compounds were of analytical grade (99.99% purity) from Merck (Darmstadt, Germany). Reverse-osmosis type quality water was used for analysis. BHA, BHT and OMC with purity 96%, 99.8% and 98%, respectively, were purchased from ACROS-ORGANICS (New Jersey, USA).

Preparation of standard solution

A 5000 mg/L stock solution of BHA, BHT and OMC in acetonitrile was prepared by weighing 1250 mg each of BHA, BHT and OMC in the flask and diluted with 100 mL acetonitrile. The mixture was shaken until a homogenous and clear solution was formed. Acetonitrile was then added to a final volume of 250 mL. The stock solution was covered with aluminum foil and stored in a freezer (4°C) and away from light for a maximum of one month. Prior to analysis, standard working solutions were prepared by diluting appropriate amounts of the stock solutions in acetonitrile.

Extraction procedure

Extraction of BHA, BHT and OMC from personal care samples was performed using reflux method according to the procedure described by Capitan-Vallvey et al. [4,5] with slight modification. Briefly, 0.1 to 1 g of personal care samples were accurately weighed in the 100 mL capacity round bottom flask. Prior to extraction, 25 mL n-hexane was added to the samples in order to remove lipids, fatty acids and volatile oils, and followed by addition of 15 mL acetonitrile. The sample was extracted under reflux for 30 minutes at 70°C with stirring. Extraction was performed

in triplicates. The mixture was transferred to separatory funnel and two layers, that are n-hexane and acetonitrile phases were formed. The n-hexane phase was repartitioned for two or three times using 10 mL of acetonitrile and shake vigorously. The n-hexane phase was removed and acetonitrile phase was collected. The acetonitrile phase (extract) was concentrated using a vacuum rotary evaporator at 45° C. The residue was redissolved with 10 mL of acetonitrile and filtered by membrane filter (Millipore, 0.5μ m x 45 mm), then transferred into a 25 mL volumetric flask. It was diluted to 25 mL with acetonitrile.

High performance liquid chromatography (HPLC) analysis

The quantitative and qualitative analysis of phenolic compounds was performed on a Shimadzu HPLC system model LC-20AT equipped with four pumps and Shimadzu SPD-20 AV UV/Vis detector. Exactly 50 μ L samples was injected and the chromatographic separation was performed on a RP-C₁₈ Metacil (5 μ m) ODS column, 4.6 mm×250 mm. The analytical condition for HPLC analysis was according to Saad et al. [14] with a slight modification by using 280 nm as maximum wave length (λ_{max}), mobile phase system consisting of acetonitrile (phase A) and (water/acetic acid, 99:1, v/v) (phase B) and flow rate 0.8 ml/min. The resolution factor was calculated according to the equation used by Song & Wang [15].

Results and Discussion

Optimization of HPLC condition

Determination of the optimum wave length by spectrophotometer UV/Vis

The UV spectrum of BHA, BHT and OMC exhibited maximum absorption at 290, 275and 300 nm, respectively. The UV/Vis detector of RP-HPLC was fixed at 280 nm as maximum wave length (λ_{max}) for simultaneous determination.

Effect of the pH of mobile phase on resolution factor (R_s)

The pH is an important parameter to be optimized as it affects the ionization of phenolic compounds. Separation of BHA, BHT and OMC are sensitive to the pH because at low pH values BHA, BHT and OMC are ionized due to increase of protonation in mobile phase [14,16,17,18]. The analytical conditions for analysis of BHA, BHT and OMC were based on conditions recommended by Saad et al. [14], where a mixture of phase A (acetonitrile) with phase B (water:acetic acid) act as mobile phase with 280 nm as maximum wave length and 0.8 mL/min as flow rate of mobile phase. The pH was optimized by varying the percentage of acetic acid in order to adjust pH of the phase B of mobile phase at pH 3, 3.2, 3.5, 4 and 7. Decreasing pH value increases the separation and ionization of BHA, BHT and OMC, particularly between BHT and OMC. Figure 2 shows the effect of pH on the resolution factor (R_s) between BHT and OMC by varying the percentage of acetic acid in phase B of mobile phase from 0% to 2% (see Table 1).

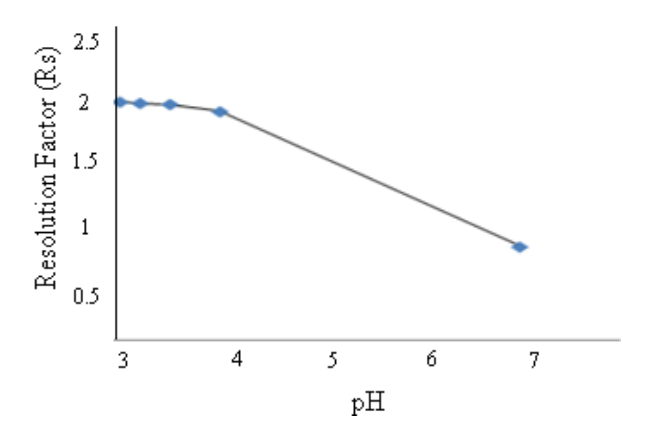


Figure 2: Variation of resolution factor between BHT and OMC at different pH values of phase B of mobile phase.

Zaini Assim et al: DEVELOPMENT AND VALIDATION OF RP-HPLC-UV/Vis METHOD FOR DETERMINATION OF PHENOLIC COMPOUNDS IN SEVERAL PERSONAL CARE PRODUCTS

Table 1: Effect of acetic acid percentage in phase (B) on pH, resolution factors and total analysis time.

Acetic acid concentration (%, v/v)	0	0.5	1	1.5	2
pH value	7.0	4.0	3.5	3.2	3.0
Resolution factors (R _s)	0.79	1.92	1.98	1.99	2.00
Total time to elutes the analytes (min)	8.5	6.0	5.5	5.3	5.3

It was observed that the resolution factor (R_s) particularly for separation between BHT and OMC depended on the pH values of phase B of mobile phase. Mixture of water:acetic acid (99:1; v/v) of phase B as buffer solution at pH 3.5 was chosen after a compromise between resolution factors (R_s : 1.98 > 1.5) and total elution time to completely separated BHA, BHT and OMC were 5.5 minutes. BHA, BHT and OMC were eluted earlier at pH 3.5 compared to those at pH 4 and 7 (see Figures 3). The resolution factor was also better at pH 3.5 (R_s : 1.98 > 1.5) compared to pH 4 (R_s : 1.92 > 1.5) and pH 7 (R_s : 0.79 < 1.5).

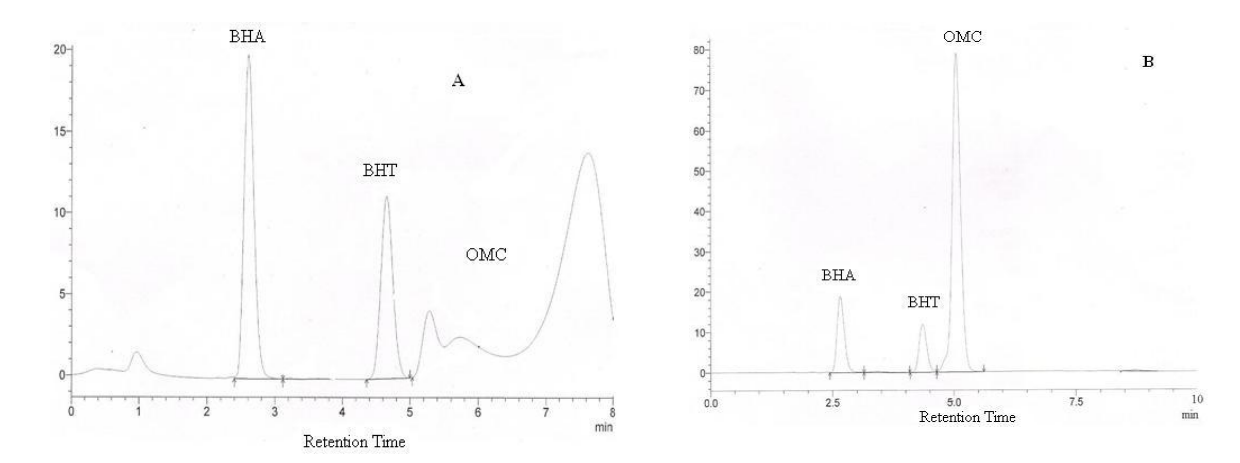


Figure 3: Chromatogram of BHA, BHT and OMC analyzed using RP-HPLC-UV/Vis at λ_{max} = 280 nm, (A: pH 7, Rs: 0.79 < 1.5 and B: pH 3.5, Rs: 1.98 > 1.5).

Effect the flow rate of mobile phase on retention time

Flow rate of mobile phase has important effect on retention time, peak area and little effect on separation for BHA, BHT and OMC. Table 2 shows gradient scaling of flow rates from 0.1 mL/min to 1.25 ml/min using RP-HPLC-UV/Vis.

Effect of mobile phase composition on retention time

The optimum composition of mobile phase for RPHPLC-UV/Vis analysis was determined by comparing the influence of different binary mixtures on retention times of BHA, BHT and OMC. Several mobile phase systems for RP-HPLC-UV/Vis analysis with detection at maximum wave length (λ_{max}) of 280 nm and flow rate of mobile phase at 0.8 mL/min were tested. These mobile phase systems were acetonitrile with water:acetic acid (99:1; v/v) (system A)[14,19], acetonitrile with methanol (system B) [16,20], ethanol with mixture of water:acetic acid (99:1; v/v)

(system C) [4,11] and acetonitrile with ethanol (system D) [21]. Figure 4 shows that better separation of BHA, BHT and OMC was achieved by using acetonitrile with mixture of water:acetic acid (99:1; v/v) as mobile phase.

Table 2: The retention times of BHA, BHT and OMC at different flow rate of mobile phase.

Flow rate	Retention time of BHA	Retention time of BHT	Retention time of OMC
(mL/min)	(minutes)	(minutes)	(minutes)
0.10	21.18	34.93	40.69
0.15	13.98	22.81	26.48
0.20	10.53	16.89	19.49
0.25	8.59	14.49	16.99
0.30	7.02	11.22	12.94
0.35	5.90	9.09	10.44
0.40	5.34	8.86	9.93
0.45	4.97	8.08	8.92
0.50	4.3	6.74	7.74
0.55	3.82	6.05	6.95
0.60	3.49	5.51	6.33
0.65	3.21	5.03	5.79
0.70	3.03	5.03	5.85
0.75	2.82	4.60	5.33
0.80	2.65	4.35	5.05
0.85	2.35	3.79	4.37
0.90	2.33	3.72	4.29
0.95	2.22	3.63	4.19
1.00	2.09	3.29	3.79
1.05	1.97	3.06	3.62
1.10	1.92	3.05	3.58
1.15	1.87	3.01	3.56
1.20	1.81	2.94	3.48
1.25	1.72	2.85	3.29

Validation method

The validation studies for BHA, BHT and OMC using RP-HPLC-UV/Vis were performed under the following optimized condition: maximum wave length at 280 nm, flow rate of mobile phase at 0.8 mL/min and mobile phase system consists of a mixture phase A (acetonitrile) with phase B (water:acetic acid; 99:1; v/v) with ratio (90A:10B; v/v). The analysis under this optimized condition was completed in approximately 8 minutes.

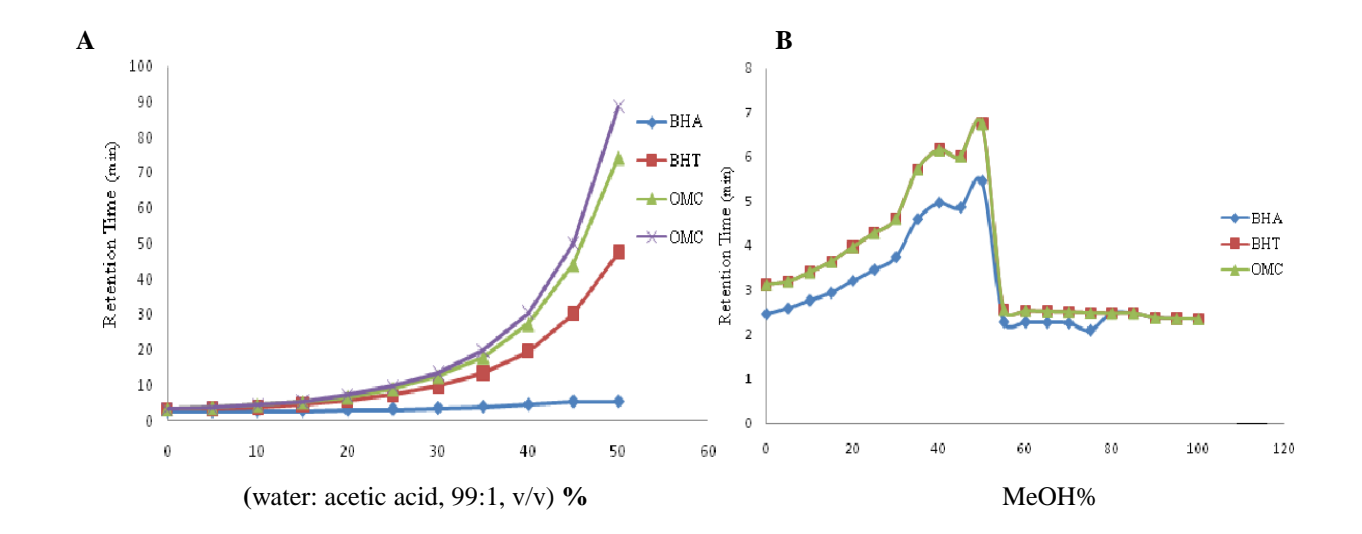
Linearity, limit of detection (LOD) and limit of quantification (LOQ)

Eight standards solution of BHA, BHT and OMC in acetonitrile with concentrations of 1, 10, 25, 50, 75, 100, 125 and 250 mg/L were prepared. The calibration curves were obtained by plotting the peak area of chromatograms for BHA, BHT and OMC against the concentration (see Figure 5) in four replicates (n=4). Correlation coefficients (R²) were 0.999 for all standards. Table 3 shows the results of analytical method validation obtained from the calibration curves of BHA, BHT and OMC analyzed on RP-HPLC-UV/Vis.

LOD for BHA and BHT by RP-HPLC-UV/Vis at 0.196 and 0.170 mg/L, respectively. These ranges were lower compared to those reported by Capitan-Vallvey et al. [5], Saad et al. [14] Campos & Figueiredo-Toledo [22] and Perrin & Meyer [23]. While, LOD for OMC by RP-HPLC-UV/Vis obtained in this study was 0.478 mg/L and this was lower compared to those reported by Chawla & Mrig [2], Salvador & Chisvert [11], Orsi et al. [16] and

Zaini Assim et al: DEVELOPMENT AND VALIDATION OF RP-HPLC-UV/Vis METHOD FOR DETERMINATION OF PHENOLIC COMPOUNDS IN SEVERAL PERSONAL CARE PRODUCTS

Mazonakis et al. [24]. Thus, the LOD for BHA, BHT and OMC obtained in this study have been improved than those reported by previous studies due to the application of efficient mobile phase and detection system.



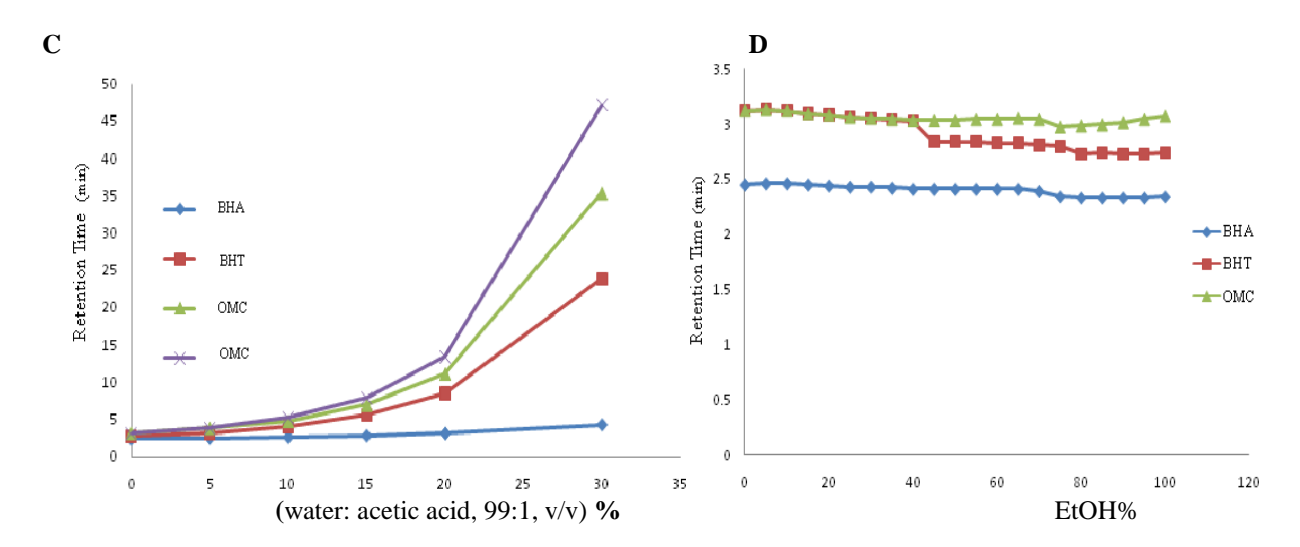


Figure 4: Effect of mobile phase composition on retention time of BHA, BHT and OMC.

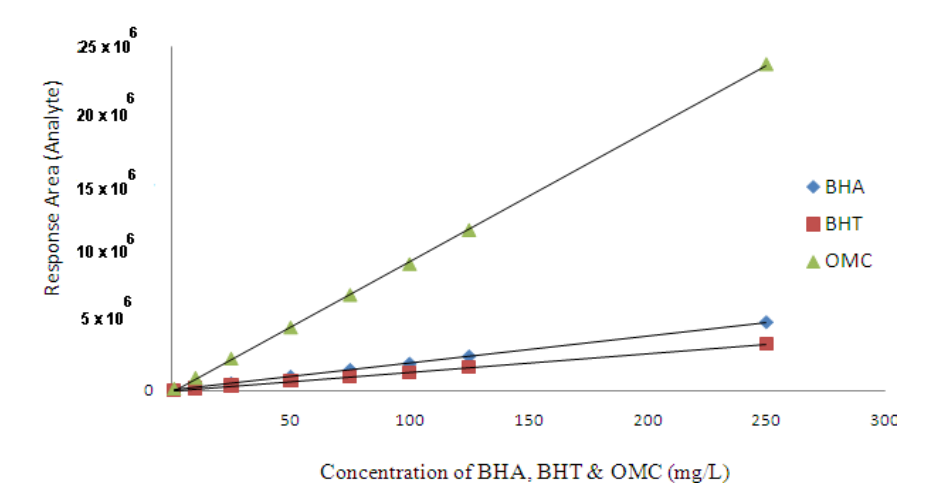


Figure 5: Calibration curves for BH, BHT and OMC analysed on RP-HPLC-UV/Vis at λ_{max} =280 nm, 0.8 ml/min and (water: acetic acid, 99:1, v/v) as mobile phase.

Table 3: Validation of analytical method for BHA, BHT and OMC by RP-HPLC-UV/Vis.

Compound	R.T	Calibration	\mathbb{R}^2	RSD	LOD	LOQ
_	(min)	Equation		%	(mg/L)	(mg/L)
BHA	2.60	y=19673x + 2579	0.999	0.18	0.196	0.593
BHT	4.35	y = 13410x - 5551	0.999	0.17	0.170	0.515
OMC	4.95	y = 95019x - 14004	0.999	0.25	0.478	1.448

Comparison with LOD reported in literatures:

Phenolic	LOD (mg/L)								
compounds	[2]	[5]	[11]	[14]	[16]	[22]	[23]	[24]	
BHA	-	1.8	-	0.5	-	0.6	-	-	
BHT	-	2.1	-	0.5	-	2.7	-	-	
OMC	1.38	-	0.9	-	0.8	-	0.478	1.11	

Recovery efficiency and Method Performance

The relative recoveries for phenolic compounds were determined by using the external standard addition method at four spiking levels of 1, 5, 10 and 25 mg/L by comparing with a standard chromatogram of similar concentration. Mean recoveries for each spiking level were determined three times with four replicates representing at each time (see Table 4).

Table 4: Results of recovery study for BHA, BHT and OMC by RP-HPLC-UV/Vis at λ_{max} = 280 nm.

	Relative Recovery (%, n=12)							
Spiked	BHA	RSD	BHT	RSD	OMC	RSD		
(mg/L)		%		%		%		
1	105.9	2.64	108.9	7.69	103.7	2.53		
5	102.3	3.72	102.8	4.02	94.6	1.95		
10	99.7	1.65	95.9	3.13	93.3	1.45		
25	92.1	1.18	83.2	2.24	87.3	1.27		

Zaini Assim et al: DEVELOPMENT AND VALIDATION OF RP-HPLC-UV/Vis METHOD FOR DETERMINATION OF PHENOLIC COMPOUNDS IN SEVERAL PERSONAL CARE PRODUCTS

Recoveries of BHA and BHT were in the range of 92.1-105.9% and 83.2-108.9%, respectively. These recovery efficiencies are comparable to those reported by Saad et al. [14] which ranged between 96.7-101.2 and 73.9-94.6%, respectively, by using the similar external standard addition method. The recovery of OMC in this study was in the range of 87.3-103.7%. This is comparable to those reported by Mazonakis et al. [24] which ranged between 87.6-101.3%.

Real samples Analysis

Four types of personal care products such as sunscreen cream, milk lotion, hair gel and hair oil with three different samples for each type were analyzed for their BHA, BHT and OMC content. These samples were analyzed three times with four replicates for each time. The results for analysis of real samples using the optimized RP-HPLC-UV/Vis method are presented in Tables 5, 6, 7 and 8.

Table 5 shows that concentration ranges of BHA and BHT in three different commercial products of sunscreen cream, namely Aiken, Nivea and Gervenne ranged between 1.82-4.85 and 1.01-1.33 mg/g, respectively. These range were higher than those reported by Yang et al. [3]. While, the concentration of BHT in these sunscreen products was lower than concentration of BHT in other sunscreen products as reported by Capitan-Vallvey et al. [4]. On other hand, the concentration range of OMC in these sunscreen products (16.23-65.50 mg/g) was lower compared to those reported by Chawla & Mrig [2], Wang & Chen [8], Chisvert et al. [9, 25] and Orsi et al. [16].

Table 5: Concentration of BHA, BHT and OMC in sunscreen samples determined by RP-HPLC-UV/Vis at λ_{max} = 280 nm.

Commercial	Country	Phenolic		Mean Concentration (mg/g)				
Name	of	Compound	(1)	(2)	(3)	Average	RSD	
	Origin	S	(n=4)	(n=4)	(n=4)	(mg/g)	%	
Aiken	Malaysia	BHA	4.80±0.10	4.90±0.07	4.90±0.05	4.85	1.50	
		BHT	1.30 ± 0.06	1.40 ± 0.07	1.28 ± 0.03	1.33	3.88	
		OMC	62.10 ± 0.60	65.9 ± 0.41	68.5 ± 0.51	65.5	0.77	
Nivea	Thailand	BHA	3.31 ± 0.09	3.03 ± 0.08	3.43 ± 0.07	3.26	2.43	
		BHT	1.16 ± 0.06	1.03 ± 0.04	0.85 ± 0.04	1.01	4.47	
		OMC	27.68 ± 0.4	30.72 ± 0.3	25.48 ± 0.6	27.96	1.58	
Gervenne	Malaysia	BHA	1.93 ± 0.08	1.81±0.06	1.72 ± 0.08	1.82	3.92	
	•	BHT	n.d	n.d	n.d	n.d	n.d	
		OMC	16.66±0.4	14.61±0.5	17.43 ± 0.4	16.23	2.68	

Comparison:

Concentration (mg/g) reported in literatures Phenolic [2] [3] [4] [8] [16] [25] [9] This study compounds BHA 0.003-0.026 1.82-4.85 n.d **BHT** 0.408 0.006 2.263 n.d 1.01-1.33 **OMC** 18.3-8\0.1 19.5-90.5 20-74 5.8-77.8 56.12-16.23-65.50 91.02

n.d: not detected or below detection limit.

Table 6 shows that concentration ranges of BHA and BHT in three different commercial products of milk lotion, namely Nivea, New Trendy and Garnier (2.74-4.50 and 0.73-2.30 mg/g, respectively) were higher compared to concentration of BHA and BHT in other milk lotion products reported by Yang et al. [3], Capitan-Vallvey et al. [4,5] and Tsai & Lee [26]. The concentration range of OMC in these milk lotion samples (8.99-17.00 mg/g) was lower

compared with concentration of OMC in milk lotion products reported by Salvador & Chisvert [11] and Mazonakis et al. [24].

Table 6: Concentration of BHA, BHT and OMC in Milk lotion samples using RP-HPLC-UV/Vis at λ_{max} = 280 nm.

Commercial	Country	Phenolic		Mean Concentration (mg/g)				
Name	of	Compounds	(1)	(2)	(3)	Average	RSD	
	Origin		(n=4)	(n=4)	(n=4)	(mg/g)	%	
Nivea	Thailand	BHA	4.51±0.12	4.46±0.05	4.55±0.04	4.50	1.57	
		BHT	1.96 ± 0.09	2.58 ± 0.07	2.37 ± 0.06	2.30	3.21	
		OMC	13.4 ± 0.26	12.5 ± 0.17	15.6 ± 0.21	13.83	1.55	
New Trendy	Malaysia	BHA	3.92 ± 0.15	4.15 ± 0.11	4.42 ± 0.09	4.16	2.82	
		BHT	n.d	n.d	n.d	n.d	n.d	
		OMC	7.82 ± 0.38	8.68 ± 0.32	10.48 ± 0.31	8.99	3.79	
Garnier	Indonesia	BHA	2.96 ± 0.09	2.47 ± 0.10	2.79 ± 0.09	2.74	3.32	
		BHT	0.64 ± 0.03	0.83 ± 0.02	0.71 ± 0.03	0.73	3.26	
		OMC	20.41 ± 0.38	16.64±0.30	15.13±0.30	17.0	1.86	

Comparison:

Concentration (mg/g) reported in literatures Phenolic [3] **[4]** [5] [11] [23] [25] This study compounds BHA n.d 0.017 n.d n.d 2.74-4.50 BHT 0.610 0.408 n.d - 2.30n.d n.d **OMC** 30.2-74.1 70-75 8.99-17.00

n.d: not detected or below detection limit.

Table 7 shows concentration ranges of BHA and BHT in three different hair gel products, namely De Boy, Beyond and Elite were in the range between 1.28-1.51 and 0.16-0.22 mg/g, respectively. Yang et al. [3] and Garcia-Jimenez et al. [27] reported that BHA and BHT was not detected in several hair gel products analysed. While, the concentration of OMC in these hair gel samples was in the range of 0.12-0.84 mg/g. OMC was not detected in hair care products screened by Gao & Bedell [28].

Table 7: Concentration of BHA, BHT and OMC in hair gel samples determined by RP-HPLC-UV/Vis at λ_{max} = 280nm.

Commercial	Country of	Phenolic		Mean Cor	centration (m	ıg/g)	
Name	Origin	Compounds	(1)	(2)	(3)	Average	RSD
			(n=4)	(n=4)	(n=4)	(mg/g)	%
De Boy	Malaysia	BHA	1.23±0.05	1.27±0.04	1.33±0.04	1.28	3.14
		BHT	0.17 ± 0.01	0.24 ± 0.01	0.26 ± 0.01	0.22	3.40
		OMC	0.11 ± 0.01	0.15 ± 0.01	0.12 ± 0.01	0.13	4.52
Beyond	Malaysia	BHA	1.28 ± 0.04	1.36 ± 0.06	1.49 ± 0.05	1.38	3.37
		BHT	0.13 ± 0.01	0.19 ± 0.01	0.16 ± 0.01	0.16	4.05
		OMC	0.31 ± 0.01	0.24 ± 0.01	0.36 ± 0.02	0.30	3.48
Elite	Malaysia	BHA	1.42 ± 0.06	1.48 ± 0.03	1.63 ± 0.04	1.51	2.76
		BHT	0.17 ± 0.01	0.11 ± 0.01	0.23 ± 0.01	0.17	4.48
		OMC	0.81 ± 0.03	0.93 ± 0.02	0.79 ± 0.02	0.84	2.69

Zaini Assim et al: DEVELOPMENT AND VALIDATION OF RP-HPLC-UV/Vis METHOD FOR DETERMINATION OF PHENOLIC COMPOUNDS IN SEVERAL PERSONAL CARE PRODUCTS

Comparison:		Concentration (mg	/g) reported in lite	eratures	
Phenolic compound	[3]	[26]	[27]	This study	
BHA	n.d	n.d	-	1.28-1.51 mg/g	
BHT	n.d	n.d	-	0.16-0.22 mg/g	
OMC	-	-	n.d	0.12-0.84 mg/g	

n.d: not detected or below detection limit.

Table 8: Concentration of BHA, BHT and OMC in hair oil samples determined by RP-HPLC-UV/Vis at λ_{max} = 280nm.

Commercial	Country	Phenolic		Mean Conce	entration (mg	g/g)	
Name	of	Compounds	(1)	(2)	(3)	Average	RSD
	Origin		(n=4)	(n=4)	(n=4)	(mg/mL)	%
Elite	Malaysia	BHA	3.96±0.04	3.93±0.03	3.85±0.05	3.89	1.06
		BHT	0.89 ± 0.02	0.87 ± 0.02	0.84 ± 0.01	0.87	2.11
		OMC	0.83 ± 0.02	0.82 ± 0.01	0.80 ± 0.01	0.82	1.37
Gervenne	Malaysia	BHA	0.11 ± 0.01	0.12 ± 0.01	0.15 ± 0.01	0.13	4.66
		BHT	1.44 ± 0.05	1.61 ± 0.05	1.57 ± 0.06	1.54	3.25
		OMC	3.42 ± 0.06	3.29 ± 0.07	3.48 ± 0.05	3.40	1.75
Johnsons	Philippines	BHA	0.34 ± 0.01	0.29 ± 0.01	0.26 ± 0.01	0.30	3.40
		BHT	0.19 ± 0.01	0.22 ± 0.01	0.14 ± 0.01	0.18	4.13
		OMC	0.51 ± 0.02	0.63 ± 0.01	0.56 ± 0.01	0.57	2.19

Comparison:

	Concentration (mg/g) reported in literatures				
Phenolic	[4]	[5]	[28]	This study	
compounds					
BHA	0.031	n.d	-	0.13-3.89	
BHT	0.100	0.659	-	0.18-1.54	
OMC	-	-	n.d		

Conclusion

A convenient and rapid RP-HPLC-UV/Vis has been developed for the estimation of common phenolic compounds in several types of personal care products. The optimum parameters that can be used are as follows; binary mixture of phase A (acetonitrile) and phase B (water /acetic acid, 99:1, v/v) as mobile phase with the elution ratio (90 A: 10 B, v/v) with the analysis time (8 minutes), pH 3.5 of phase B (using acetic acid for adjust it), 0.8 mL/min flow rate of 0.8 mL/min and maximum detector wave length at 280 nm. The method is fast, accurate, sensitive, provide excellent recoveries, convenient and effective for the simultaneous quantification of phenolic compounds for routine analysis in quality control of commercial cosmetic products. The developed method can be used to fingerprint the relevant phenolic compounds markers present in personal care products under optimum parameters. This method can be applied to analyze the phenolic compounds in commercial cosmetic and food products.

Acknowledgement

The authors wish to thank Syrian Ministry of Higher Education for a scholarship given to Mohd Akkbik and Department of Chemistry, Faculty of Resource Science and Technology, UNIMAS for research facilities for this study.

References

- 1. Tsai, T.F., Lee, M.R. (2008). Determination of antioxidants and preservatives in cosmetics by SPME combined with GC–MS. *Chromatographia*, 67: 425-431.
- Chawla, H.M., Mrig, S. (2009). Simultaneous quantitative estimation of oxybenzone and 2-ethylhexyl-4-methoxycinnamate in sunscreen formulations by second order derivative spectrophotometry. *Journal of Analytical Chemistry*, 64(6): 585–592.
- 3. Yang, T.J., Tsai, F.J., Chen, C.Y., Yang, T.C.C. & Lee, M.R. (2010). Determination of additives in cosmetics by supercritical fluid extraction on-line headspace solid-phase microextraction combined with gas chromatography—mass spectrometry. *Journal of Analytical Chemistry for Anti-Counterfeiting Trade Agreement*, 668:188-194.
- 4. Capitan-Vallvey, L. F., Valencia, M. C., Nicolas, E. A. (2002). Flow-through sensor for determination of butylated hydroxytoluene in cosmetics. *Analytical Letters*, 35(1): 65-81.
- 5. Capitan-Vallvey, L. F., Valencia, M. C., Nicolas, E. A. (2004). Solid-phase ultraviolet absorbance spectrophotometric multisensor for the simultaneous determination of butylated hydroxytoluene and co-existing antioxidants. *Journal of Analytical Chemistry for Anti-Counterfeiting Trade Agreement*, 503: 179-186.
- 6. Porat, Y., Abramowitz, A., Gazit, E. (2006). Inhibition of amyloid fibril formation by polyphenols: Structural similarity and aromatic interactions as a common inhibition mechanism. *Chemical Biology and Drug Design*, 67: 27–37.
- 7. Stockmann, H., Schwarz, K., Huynh, T. (2000). The influence of various emulsifiers on the partitioning and antioxidant activity of hydroxybenzoic acids and their derivatives in oil-in-water emulsions. *Journal of Surfactants and Detergents*, 77(5): 535-542.
- 8. Wang, S.P., Chen, W.J. (2000). Determination of *p*-aminobenzoates and cinnamate in cosmetic matrix by supercritical fluid extraction and micellar electrokinetic capillary chromatography. *Journal of Analytical Chemistry for Anti-Counterfeiting Trade Agreement*, 416: 157-167.
- Chisvert, A., Salvador, A., Pascual-Marti, M.C. (2001). Simultaneous determination of oxybenzone and 2ethylhexyl 4-methoxycinnamate in sunscreen formulations by flow injection-isodifferential derivative ultraviolet spectrometry. *Journal of Analytical Chemistry for Anti-Counterfeiting Trade Agreement*, 428: 183-190.
- 10. Dutra, E.A., Oliveira, D.A.G.D., Kedor-Hackmann, E.R.M., Santoro, M.L.R.M. (2004). Determination of sun protection factor (SPF) of sunscreens by ultraviolet spectrophotometry. *Brazilian Journal of Pharmaceutical Sciences*, 40(3): 381-385.
- 11. Salvador, A., Chisvert, A. (2005). An environmentally friendly (green) reversed-phase liquid chromatography method for UV filters determination in cosmetics. *Journal of Analytical Chemistry for Anti-Counterfeiting Trade Agreement*, 537: 15-24.
- 12. Venkatesh, G., Majid, M. I. A., Ramanathan, S., Mansor, S. M., Nair, N. K., Croft, S. L., Navaratnam, V. (2008). Optimization and validation of RP-HPLC-UV method with solid-phase extraction for determination of buparvaquone in human and rabbit plasma: application to pharmacokinetic study. *Biomedical Chromatography*, 22: 535–541.
- 13. Lee, M. R., Lin, C. Y., Li, Z. G., Tsai, T. F. (2006). Simultaneous analysis of antioxidants and preservatives in cosmetics by supercritical fluid extraction combined with liquid chromatography–mass spectrometry. *Journal of Chromatography A*, 1120: 244-251.
- 14. Saad, B., Sing, Y.Y., Nawi, M. A., Hashim, N., Ali, A. M., Saleh, M. I., Ahmad, K. (2007). Determination of synthetic phenolic antioxidants in food items using reversed-phase HPLC. *Food Chemistry*, 105: 389–394.
- 15. Song, D., Wang, J. 2003. Modified resolution factor for asymmetrical peaks in chromatographic separation. *Journal of Pharmaceutical and Biomedical Analysis*, 32: 1105-1112.
- 16. Orsi, D.D., Giannini, G., Gagliardi, L., Porra, R., Berri, S., Bolasco, A., Carpani, I., Tonelli, D. (2006). Simple extraction and HPLC determination of UV-A and UV-B filters in Sunscreen. *Chromatographia*, 64: 9-10.
- 17. Fang, F., Jing-Ming, L., Qiu-Hong, P., Wei-Dong, H. (2007). Determination of red wine flavonoids by HPLC and effect of aging. *Food Chemistry*, 101: 428–433.
- 18. Neungnapa, R., Jia, Z., Xuewu, D., Bao, Y., Jianrong, L., Yueming, J. (2008). Effects of various temperatures and pH values on the extraction yield of phenolics from litchi fruit pericarp tissue and the antioxidant activity of the extracted anthocyanins. *International Journal of Molecular Sciences*, 21:105-116.

Zaini Assim et al: DEVELOPMENT AND VALIDATION OF RP-HPLC-UV/Vis METHOD FOR DETERMINATION OF PHENOLIC COMPOUNDS IN SEVERAL PERSONAL CARE PRODUCTS

- 19. Dondi, D., Albini, A., Serpone, N. (2006). Interactions between different solar UVB/UVA filters contained in commercial suncreams and consequent loss of UV protection. *The Royal Society of Chemistry and Owner Societies*, 5: 835-843.
- 20. Perrin, C., Meyer, L. (2003). Simultaneous determination of ascorbyl palmitate and nine phenolic antioxidants in vegetable oils and edible fats by HPLC. *Journal of the American Oils Chemist's Society*, 80 (2): 115 -118.
- 21. Tsuji, S., Nakano, M., Terada, H., Tamura, Y., Tonogal, Y. (2005). Determination and confirmation of five phenolic antioxidants in foods by LC/MS and GC/MS. *Japanese Society of Food Hygienically*, 46(3): 63-71.
- 22. Campos, G.C.M.D., Toledo, M.C.F. (2000). Determination of BHA, BHT and TBHQ in fats and oils by high performance liquid chromatography. *Brazilian Journal of Food Technology*, 3: 65-71.
- 23. Perrin, C., Meyer, L. (2002). Quantification of synthetic phenolic antioxidants in dry foods by reversed-phase HPLC with photodiode array detection. *Food Chemistry*, 77: 93–100.
- 24. Mazonakis, N.E., Karathanassi, P.H., Panagiotopoulos, D.P., Hamosfakidi, P.G., Melissos, D.A. (2002). Cleaning validation in the toiletries industry. *Journal of Analytical Chemistry for Anti-Counterfeiting Trade Agreement*, 467: 261-266.
- 25. Chisvert, A., Pascual-Marti, M.C., Salvador, A. (2001b). Determination of UV-filters in sunscreens by HPLC. *Journal of Analytical Chemistry*, 369: 638–641.
- 26. Tsai, T. F., Lee, M. R. (2008). Determination of antioxidants and preservatives in cosmetics by SPME combined with GC-MS. *Chromatographia*, 67: 425-431.
- 27. Garcia-Jimenez, J.F., Valencia, M.C., Capitan-Vallvey, L.F. (2007). Simultaneous determination of antioxidants, preservatives and sweetener additives in food and cosmetics by flow injection analysis coupled to a monolithic column. *Journal of Analytical Chemistry for Anti-Counterfeiting Trade Agreement*, 594: 226-233.
- 28. Gao, T., Bedell, A. (2001). Ultraviolet damage on natural gray hair and its photoprotection. *Journal of Cosmetic Science*, 52: 103-118.
- 29. Fent, K., Kunz, P.Y., Zenker, A., Rapp, M. (2009). A tentative environmental risk assessment of the UV-filters 3-(4-methylbenzylidene-camphor) 2-ethyl-hexyl-4-trimethoxycinnamate, benzophenone-3, benzophenone-4 and 3-benzylidene camphor. *Marine Environmental Research*, 10: 1016-1018.



COMPETITIVE METAL SORPTION AND DESORPTION ONTO Kappaphycus Alvarezii, SEAWEED WASTE BIOMASS

(Persaingan Penjerapan dan Nyah-Penjerapan Logam Berat ke atas Sisa Rumpai Laut Kappaphycus alvarezii)

Kang Oon Lee¹, Nazaruddin Ramli^{1*}, Mamot Said¹, Musa Ahmad¹, Suhaimi Md Yasir², Arbakariya Ariff³

¹School of Chemical Sciences and Food Technology, Faculty of Science and Technology, Universiti Kebangsaan Malaysia, 43600 UKM Bangi, Selangor, Malaysia; ²School of Sciences and Technology, Universiti Malaysia Sabah, Sabah, Malaysia; ³Faculty of Biotechnology and Biomolecular Science, Universiti Putra Malaysia, Serdang, Selangor, Malaysia.

*Corresponding author: naza@ukm.my

Abstract

Competitive metal sorption and desorption onto $Kappaphycus\ alvarezii$ waste biomass were investigated. Metal sorption capacities were 0.82 mg Cr(III)/g, 0.73 mg Ni(II)/g, 0.67 mg Cd(II)/g, 0.65 mg Cu(II)/g and 0.64 mg Zn(II)/g in multi metal system. Whereas, desorption efficiencies were 66.08%, 71.50% and 80.44% using 0.1M HNO₃, 0.1M HCl and 0.1M H₂SO₄, respectively. The metal sorption sequence were Cr(III) > Ni(II) > Cd(II) > Cu(II) > Zn(II), while metal desorption sequence were Cd(II) > Zn(II) > Ni(II) > Cr(III). Fourier transformed infrared spectroscopy (FTIR) technique was used to characterize the seaweed waste biomass. FTIR analysis shown that carbonyl (-C-O) and nitrile (-C=N) groups interact with the metal ions. The experiments result revealed that $Kappaphycus\ alvarezii$ waste biomass represent an attractive candidate to remove multi metal ions.

Keywords: Sorption, Desorption, Kappaphycus alvarezii

Abstrak

Persaingan penjerapan dan nyah-penjerapan logam berat ke atas sisa rumpai laut $Kappaphycus\ alvarezii$ telah dikaji. Kapasiti penjerapan mencatat $0.82\ mg\ Cr(III)/g,\ 0.73\ mg\ Ni(II)/g,\ 0.67\ mg\ Cd(II)/g,\ 0.65\ mg\ Cu(II)/g\ dan\ 0.64\ mg\ Zn(II)/g\ dalam sistem campuran logam berat. Sementara itu, kapasiti nyah-penjerapan masing-masing mencatat <math>66.08\%$, 71.50% dan 80.44% menggunakan $0.1M\ HNO_3$, $0.1M\ HCl$ dan $0.1M\ H_2SO_4$. Penjerapan logam berat mengikut turutan Cr(III) > Ni(II) > Cd(II) > Cu(II) > Zn(II). Selain itu, nyah-penjerapan logam berat mengikut turutan Cd(II) > Zn(II) > Cu(II) > Ni(II) > Cr(III). Teknik spektroskopi inframerah transformasi Fourier (FTIR) telah digunakan dalam mencirikan sisa rumpai laut. Analisa FTIR menunjukkan kumpulan karbonil (-C-O) dan nitrile (-C=N) berinteraksi dengan logam berat. Hasil kajian mendapati sisa rumpai laut $Kappaphycus\ alvarezii\ mempunyai\ keberkesanan tinggi dalam menyingkirkan campuran logam berat.$

Kata kunci: penjerapan, nyah-penjerapan, Kappaphycus alvarezii

Introduction

Heavy metals are derived from various industrial activities viz. mining, tanning, smelting and electroplating [1]. Heavy metals are toxic, non-biodegradable and tend to accumulate in environment [2]. In recent years, heavy metals such as copper, cadmium and chromium are detected at elevated levels and pose a serious threat to environment [3]. Therefore, appropriate technologies are required to remove these metals to acceptable limits before discharging them into the environment.

Kang Onn Lee et al: COMPETITIVE METAL SORPTION AND DESORPTION ONTO Kappaphycus Alvarezii, SEAWEED WASTE BIOMASS

New search technologies have been directed attention to biosorption process, with numerous biological material exhibit excellent biosorption capacities [4]. Among them, seaweed biomass have been proved to be the most efficient metal sorbent and examined in numerous biosorption studies [5]. Seaweed biomass such as *Sargassum* sp. and *Ulva* sp. have been shown to be effective and reliable metal sorbent to remove individual metal ions, such as Pb(II), Cu(II), Cd(II), and Zn(II) [4]. However, *Kappaphycus alvarezii* waste biomass have not been investigated as metal sorbent to remove metal ions.

Kappaphycus alvarezii is reliable and abundance waste biomass obtains from carrageenan extaction process. This waste biomass is rich in lignocellulosic material and its contain various chemical groups that able to interact with metal ions. Furthermore, this waste biomass is non-toxic, inert and ready to use in biosorption process [6].

In practice, various metal ions are encountered in wastewaters, and it is potentially impact the biosorption behavior: synergistic, antagonistic or non-interactive [2]. However, limited information is available to elucidate the competitive biosorption behavior [7]. It is important to provide better understanding to its application for real wastewater treatment.

In this work, competitive metal sorption onto *Kappaphycus alvarezii* waste biomass was investigated and their selectivity and competitive effect were compared with non-competitive metal system. Desorption using mineral acids $(0.1 \text{M} \text{ HCl}, 0.1 \text{ M} \text{ HNO}_3 \text{ and } 0.1 \text{ M} \text{ H}_2\text{SO}_4)$ were conducted. FTIR analyses were conducted to elucidate biosorption mechanisms.

Experimental

Seaweed waste biomass preparation

Kappaphycus alvarezii waste biomass was prepared in the laboratory using a common industrial process. The seaweed biomass was extracted with aqueous solution at 60° C for 6 hr. Then, the seaweed waste biomass was filtered using filter paper (Whatman No 2). The seaweed waste biomass was washed with distilled water and dried at 60° C for 24 hr. The dried seaweed waste biomass was ground in a blender and stored in a desiccator.

Metal solution preparation

The stock Cu(II), Cd(II), Cr(III), Ni(II) and Zn(II) solutions (1000 mg/L) were prepared by dissolving the metal nitrates (Merck) in deionised water. The metal solutions (10 mg/L) containing single and multi metal ions were prepared by diluting the stock solutions with deionised water. The metal solutions was adjusted to pH 3 by using 0.1 M NaOH.

FT-IR analysis

The untreated and Cr(III)-treated seaweed waste biomass samples were analysed using Fourier transform infrared spectroscopy. The seaweed waste biomass samples were encapsulated in KBr at a ratio of 1: 100. The IR spectra were collected using a Perkin Elmer spectrometer within the range 400--4000 cm⁻¹.

Biosorption experiment

Biosorption experiments were conducted by batch method using in shake flasks. Seaweed waste biomass (0.5 g) was added to a flask containing 50 ml mixed metal solution. The samples were agitated on a rotary shaker at 300 rpm for 3 hr. The samples were filtered using filter paper (Whatman No. 2), and the metal concentrations were measured using an AAS (PerkinElmer, USA).

The metal sorption capacities were calculated using the following equation:

$$Qm = (C_0 - C_s).V / M \tag{1}$$

where, Q_m (mg/g) is the amount of metal adsorbed, V(L) is the volume of the solution, M (g) is the mass of the biomass, and C_0 (mg/L) and C_e , (mg/L) are the initial and equilibrium concentrations of metal ions, respectively.

Desorption experiment

Desorption experiments were conducted in shake flasks. Multi metal treated seaweed waste biomass (0.5 g) was added to separate flask containing 50 ml of eluenting solutions (0.1M HCl, 0.1 M HNO₃ or 0.1 M H₂SO₄). The samples were agitated on a rotary shaker at 300 rpm for 1 hr. The samples were filtered using filter paper (Whatman No. 2), and the metal concentrations were measured using an AAS (PerkinElmer, USA).

Results and Discussion

FT-IR analysis

The FTIR analyses were conducted to identify characteristic functional groups and their possible interactions with metal ions.

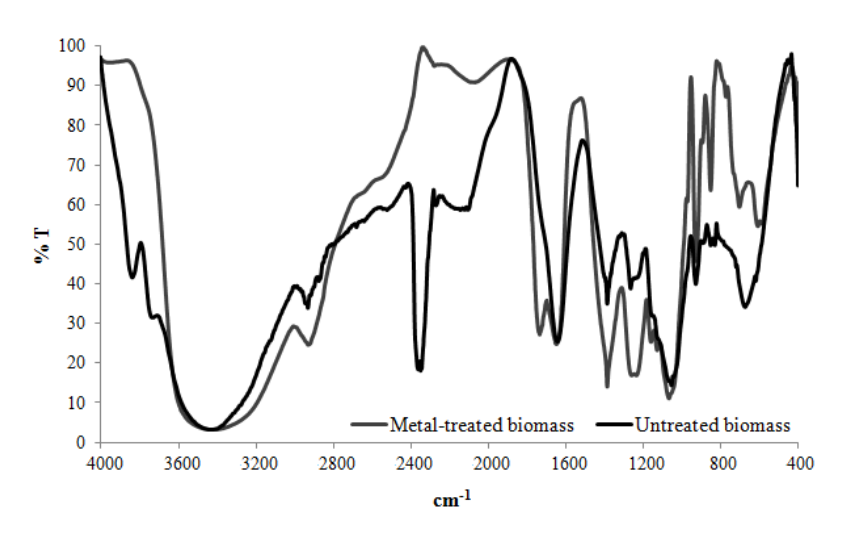


Figure 1: The untreated and metal-treated Kappaphycus alvarezii waste biomass FTIR spectra

The FTIR spectrum indicated several intense characteristic bands related with functional groups presented in the seaweed waste biomass. The absorption peaks at 3420 cm^{-1} (-OH or -NH groups), 2930 and 1385 cm⁻¹ (-CH₃ groups), 2350 cm⁻¹ (-C \equiv N groups), 1646 and 1240 cm⁻¹ (-COOH groups) and 1050 cm⁻¹ (-C-O groups).

Table 1 displays the main vibration frequencies and functional groups responsible to metals sorption. It is observed that some vibration frequencies change after treated with metal ions.

Table 1: IR vibration wavenumber and functional groups observed on Kappaphycus alvarezii					
waste biomass					

Wavenur	nber (cm ⁻¹)	
Unloaded biomass Metal-loaded biomass		Functional groups
3430	3430	-OH and -NH stretching
2930	2930	-CH ₃ stretching
2350	_	-C≡N stretching
_	1730	-C=O stretching
1640	1645	-COO stretching
1385	1385	-CH ₃ bending
1240	1235	-C-O stretching
1065	1065	-C-O stretching

The absorption peak at 1640 and 1240 cm⁻¹ corresponds to the –COO groups shifted to 1645 and 1235 cm⁻¹, indicating that –COO groups are involved in biosorption process. The peak at 2350 cm⁻¹ corresponds to the $-C\equiv N$ groups disappeared, suggesting that $-C\equiv N$ groups are involved in biosorption process. A new peak at 1730 cm⁻¹ corresponds to the –C=O groups appeared, suggesting that –C=O groups oxidize to –C=O groups during biosorption process. However, the adsorption peaks around 2930, 1385 and 1065 cm⁻¹ does not change, indicate that –CH₃ and –OH does not involved in biosorption process.

The significant changes in the vibrational frequencies implicate that–CO, —COOH and −C≡N groups interacted with metal ions through ion exchange and complexation reactions.

Biosorption experiment

Metal sorption experiments were conducted in single metal system, and their selectivity and competitive effect were investigated in multi metals system. Metal sorption capacities were 0.82~Cu(II)/g, 0.83~mg~Cd~(II)/g, 0.86~mg~Cr(III)/g, 0.76~mg~Ni(II)/g and 0.84~mg~Zn~(II)/g in single metal systems, and 0.65~Cu(II)/g, 0.67~mg~Cd~(II)/g, 0.82~mg~Cr(III)/g, 0.73~mg~Ni(II)/g and 0.64~mg~Zn~(II)/g in multi metals system (Table 2). The metal sorption capacities was lower in multi metal system. This confirm that metal competition was occurred and caused antagonistic effect on biosorption process.

Cr(III) was favorably adsorbed on seaweed waste biomass over Cu(II), Cd(II), Ni(II) and Zn(II) in single and multimetal systems. This confirms that Cr (III) bind more selective to seaweed waste biomass than other metal ions. However, it was difficult to find a common rule to determine how metal properties exactly affect the binding strength of metal ions to seaweed waste biomass [8].

In general, the binding strength increased with (1) increases in the ionic radius and decreases in the charge, (2) decreases in the hydrated radius and increases in the charge, or (3) decreases in the electronegativity [8].

	Meta sorption capacities (mg/g)				
Metal ion	Singel metal system	Muti metals system			
Cu	0.82	0.65			
Cd	0.83	0.67			
Cr	0.86	0.82			
Ni	0.75	0.73			
Zn	0.84	0.64			

Table 2: Biosorption capacities (mg/g)

The metals sorption sequence were Cr(III) > Zn(II) > Cd(II) > Ni in single metal system, and Cr(III) > Ni(II) > Cd(II) > Cd(I

It is obvious that different selectivity in multi metals system were diverse, and thus predictions on sorption selectivity should based on result obtained in multi metals system [9].

Desorption

Biosorption studies can be complemented with desorption to recover the metal retained and reuse the biomass. The desorption experiment were conducted using three different eluenting solutions. Hydrochloric, nitric and sulphuric acid were choose because mineral acids are the most feasible eluenting agents [10].

It is observed that $0.1M\ H_2SO_4$ is a better eluenting agent than $0.1M\ HCl$ and $0.1M\ HNO_3$, although complete desorption were not achieve (Table 3). In practice, complete desorption is difficult to achieve in multi metal system [10].

In general, carbonyl and nitrile groups in seaweed waste biomass become protonated in acidic condition and does not attract the positively charged metal ions [11]. Meanwhile, some polysaccharides and mineral dissolve in acidic solution, and seaweed waste biomass become more fragile and loss its weight [12].

Metal desorption percentage (%) 0.1 M HCl 0.1 M HNO₃ 0.1 M H₂SO₄ Metal ion Cu 65.76 64.64 80.22 Cd 85.74 74.55 94.33 Ni 64.44 61.37 74.38 Zn 79.23 71.96 83.36 69.93 62.35 57.89 Cr

Table 3: Desorption percentage (%)

The metal desorption sequence were Cd(II) > Zn(II) > Ni(II) > Ni(II) > Cr(III). This revealed that desorption level were related to the affinity of metal to seaweed waste biomass [10]. In general, metal with higher affinity were more difficult to desorbs, and thus retain into seaweed waste biomass. Cr(III) was the least desorbed from seaweed waste biomass. Cd(II), Ni(II) and Zn(II) are retain through electrostatic interactions, whereas Cu(II) and Cr(II) are retain through covalent interactions [13].

Conclusion

In this work, competitive metal sorption and desorption onto $Kappaphycus\ alvarezii$ waste biomass were investigated. The metal sorption sequence were Cr(III) > Ni(II) > Cd(II) > Cu(II) > Zn(II), while metal desorption sequence were Cd(II) > Zn(II) > Cu(II) > Ni(II) > Cr(III).

Acknowledgement

This work was financially supported by a Research University Grant from UKM-GUP-NBT-08-27-104.

References

- 1. Yalcin, E., Cavusoglu, K., Maras, M., Biyikoglu, M., 2008. Biosorption of lead(II) and copper (II) metals ions on Cladophora glomerata (L.) Kuitz. (Chlorophyta) Algae: Effect of algal surface modification. Acta Chim. Slov. 55, 228-232.
- 2. Xue, Y.J., Hou, H.B., Zhu, S.J., 2009. Competitive adsorption of copper(II), cadmium(II), lead(II) and zinc(II) onto basic oxygen furnace slag. J. Hazard Mater. 162(1), 391-401.
- 3. Garcia–Sanchez, A., Alastuey, A., Querol, X., 1999. Heavy metal sorption by different minerals: application to the remediation of polluted soils. Sci. Total Environ. 242, 179-188.
- 4. Sag, Y., Kutsal, T., 2001. Recent Trends in the Biosorption of Heavy Metals: A Review. Biotechnol. Bioprocess Eng. 6, 376-385.
- Pagnelli, F., Petrangeli, M.P., Toro, L., Trifoni, M., Veglio, F., 2000. Biosorption of metal ions on Arthrobacter sp.: Biomass characterization and biosorption modeling. Environ. Sci. Technol. 34, 2773-2778.
- 6. Figueirai, M.M., Volesky, B., Ciminelli, V.S.T., Felicity, Roddick, A., 2000. Biosorption of metals in brown seaweed biomass. Wat. Res. **34**, 196-204.
- 7. Wang, S. B., Terdkiatburana, T., Tadé, M.O., 2008. Adsorption of Cu(II), Pb(II) and humic acid on natural zeolite tuff in single and binary systems. Sep. Pur. Techno. **62**(1), 64-70.
- 8. Song, H. P., Li, X. G., Sun, J. S., Yin, X. H., Wang, Y. H., Wu, Z. Z., 2007. Biosorption Equilibrium and Kinetics of Au(III) and Cu(II) on Magnetotactic Bacteria. Chin. J. Chem. Eng. **15**(6), 847-854.
- 9. Wilke, A., Buchhloz, R., Bunke, G., 2006. Selective biosorption of heavy metals by algae. Environ. Biotechnol. 2 (2), 47-56.

Kang Onn Lee et al: COMPETITIVE METAL SORPTION AND DESORPTION ONTO *Kappaphycus Alvarezii*, SEAWEED WASTE BIOMASS

- 10. Diniz, V., Volesky, B., 2006. Desorption of lanthanum, europium and ytterbium from Sargassum. Sep. Pur. Techno. **50**, 71-76.
- 11. Wankasi, D., Horsfall, M. Jnr., Spiff, A. I., 2005. Desorption of Pb2+ and Cu2+ from Nipa palm (Nypa fruticans Wurmb) biomass. Afr. J. Biotechnol. **4** (9), 923-927.
- 12. Kuyucak, N., Volesky, B., 1989. Desorption of cobalt-laden algal biosorbent. Biotechnol. Bioeng. 33, 815-822.
- 13. Fontes and Gomes, 2003. Simultaneous competitive adsorption of heavy metals by the mineral matrix of tropical soils. Appl. Geochem. **18** (6), 795-804.



PENENTUAN ASID HIDROSIANIK (ANTI NUTRISI) DI DALAM BUAH NIPAH (Nypa fruticans)

(Determination of Hydrocyanic Acid in Nipah Fruit (Nypa fruticans))

Mohd Zaidi Mat Satar, Mohd. Wahid Samsudin, Mohamed Rozali Othman*

Pusat Pengajian Sains Kimia dan Teknologi Makanan, Fakulti Sains dan Teknologi, Universiti Kebangsaan Malaysia, 43600 Bangi, Selangor, Malaysia.

*Corresponding author: rozali@ukm.my

Abstrak

Kajian tentang kandungan anti-nutrisi asid hidrosianik telah dijalankan ke atas buah nipah (*Nypa fruticans*). Analisis melibatkan sampel sabut, biji buah dan air nira *Nypa fruticans* yang diambil daripada tiga lokasi berbeza di Semenanjung Malaysia iaitu di Seberang Perak (Perak), Merchang (Terengganu) dan Kuala Sanglang (Perlis). Kaedah penitratan alkali secara kuantitatif telah digunakan bagi menentukan kandungan asid hidrosianik di dalam setiap sampel. Hasil kajian menunjukkan kandungan asid hidrosianik bagi sabut adalah yang tertinggi di antara ketiga-tiga lokasi persampelan diikuti dengan sampel biji buah dan air nira. Kandungan asid hidrosianik di kesemua lokasi berada dalam julat 0.03-0.06, 0.03-0.05 dan 0.02-0.03 mg/100 g masing-masing untuk sabut, biji buah dan air nira. Ujian statistik ANOVA satu hala (pada aras keyakinan 95%) menunjukkan bahawa terdapat perbezaan yang bererti (p<0.05) di antara lokasi persampelan dan kandungan asid hidrosianik bagi sampel sabut sahaja.

Kata kunci: Nypa fruticans, asid hidrosianik, sabut, biji buah, air nira

Abstract

A study on hydrocyanic acid (antinutrition) content in nipah (*Nypa fruticans*) plant components have been carried out. Analysis involve a sample of husk, seed and sap of *Nypa fruticans* collected from three different sampling location located at Seberang Perak (Perak), Merchang (Terengganu) and Kuala Sanglang (Perlis). A quantitative alkaline titration method was used to determine the content of hydrocyanic acid in all samples. Study carried out has proved that husk of *Nypa fruticans* fruit has higher content of hydrocyanic acid at all sampling location followed by seed and sap. Hydrocyanic content at all sampling location ranged from 0.03-0.06, 0.03-0.05 and 0.02-0.03 mg/100 g for husk, seed and sap of *Nypa fruticans* respectively. Statistical test carried out using one way ANOVA (at 95% confidential level) signify that the different of sampling location and hydrocyanic acid content is significant (p<0.05) for husk of *Nypa fruticans* only.

Keywords: Nypa fruticans, hydrocyanic acid, husk, seed, nira sap

Pendahuluan

Terdapat beberapa kajian yang membuktikan bahawa buah yang kurang dikenali sebenarnya mempunyai potensi untuk dieksploitasikan bagi tujuan sumber makanan kepada manusia berdasarkan kandungan nutrisinya yang berguna [1]. Contohnya, spesies *Nypa fruticans* yang tumbuh subur di Malaysia. Spesies ini adalah satu-satunya spesies pokok palma yang tergolong dalam genus nypa. Air nira daripada batang pokok ini boleh digunakan untuk menghasilkan tuak, cuka dan juga gula [2]. Bagi tujuan perubatan pula, *Nypa fruticans* digunakan sebagai penawar kepada penyakit gigi dan sakit kepala [3], disamping itu juga telah dilaporkan bahawa banyak bahagian pada pokok nipah boleh digunakan bagi tujuan perubatan [4].

Pandangan daripada orang ramai membuktikan bahawa air nira nipah sememangnya mempunyai khasiat yang tersendiri dan digunakan dalam pelbagai tujuan terutamanya bagi tujuan perubatan. Malah, air nira nipah telah

diperakui mempunyai potensi yang tinggi dalam mempertingkatkan tenaga fizikal dan tahap stamina badan. Cuka yang terhasil melalui air nira nipah yang telah diperam selama 40 hari pula dipercayai bukan sahaja dapat digunakan dalam masakan, malah dapat digunakan sebagai ubat bagi penyakit seperti kencing manis, darah tinggi, gout dan batu karang.

Kajian terhadap bahan makanan yang kurang kepentingannya adalah sangat penting untuk mengatasi penyakit yang disebabkan oleh pengambilan nutrisi kerana manusia kini sedang berhadapan dengan masalah kekurangan zat makanan disebabkan oleh pembangunan negara dan meningkatnya jumlah penyakit yang berbahaya akibat daripada kekurangan zat makanan [5]. Pendekatan mengenai pengambilan makanan yang seimbang sangat berguna bagi mengatasi masalah kekurangan zat makanan.

Antinutrisi asid hidrosianik yang terdapat di dalam tumbuhan seperti buah-buahan terhasil melalui kehadiran glikosid sianogenik yang terhasil melalui proses sianogenesis. Sianogenesis merupakan suatu proses di mana beberapa bahagian pada tumbuhan menghasilkan asid sianohidrik (HCN), yang juga dikenali sebagai asid prussik [6 - 8]. Di dalam kebanyakan kes, hidrolisis akan diakhiri dengan penghasilan gula dan sianohidrin oleh β-glukosidase (Rajah 1). Ini seterusnya akan menghasilkan asid hidrosianik dan hasil sampingan sama ada keton atau aldehid [9]. Hidupan boleh terdedah kepada sianida sama ada menerusi udara, air minuman dan juga makanan [10].

$$\begin{array}{c|c}
R & OGI \\
R & C
\end{array}$$

$$\begin{array}{c}
R & OH \\
R & C
\end{array}$$

$$\begin{array}{c}
R & C
\end{array}$$

$$\begin{array}{c}
C & + HCN \\
R & C
\end{array}$$
sianohidrin

Rajah 1 Penghasilan HCN melalui tumbuhan sianogenik

Asid hidrosianik merupakan sebatian kimia yang tidak berwarna dan sangat beracun. Hidrogen sianida adalah asid lemah dengan pKa 9.2 dan boleh mengion di dalam larutan air menjadi anion sianida CN⁻. Hidrogen sianida di dalam bentuk cecair dipanggil asid hidrosianik manakala garam bagi hidrogen sianida dikenali sebagai sianida. Asid hidrosianik juga boleh dikesan di dalam makanan seharian manusia di mana ia bertindak sebagai antinutrisi yang boleh mengganggu penyerapan nutrisi di dalam tubuh badan. Kebanyakan asid hidrosianik dikesan di dalam buahbuahan yang mempunyai liang seperti ceri, aprikot, epal dan lain-lain. Liang-liang ini mempunyai sianohidrin dalam jumlah yang kecil seperti mandelonitril dan amigladin yang akan merembeskan asid hidrosianik secara perlahanlahan [10, 11]. Sekitar 100 g biji epal mempunyai kira-kira 10 mg asid hidrosianik.

Asid hidrosianik merupakan bahan toksik bagi kebanyakan organisma hidup disebabkan keupayaannya bergabung dengan logam (Fe²⁺, Mn²⁺ dan Cu²⁺) iaitu kumpulan berfungsi bagi kebanyakan enzim. Keadaan ini akan menghalang kebanyakan proses seperti penurunan oksigen di dalam respirasi rantaian cytocrom, pengangkutan elektron semasa fotosintesis dan aktiviti enzim seperti katalase dan oksidase [12, 13].

Walaupun buah nipah atau *Nypa fruticans* tidak begitu dikenali ramai, namun terdapat ramai juga pengguna yang begitu menggemari buah nipah disebabkan air nira yang dihasilkan daripada spesies ini. Ini mungkin disebabkan ia boleh digunakan dalam pelbagai tujuan dan kepentingan terutamaya dari segi kesihatan. Kajian tentang antinutrisi atau toksik di dalam makanan ini perlu dilakukan kerana produk ini sudah mula mendapat perhatian ramai. Antaranya adalah dengan mengkaji kandungan asid hidrosianik yang terdapat pada spesies *Nypa fruticans* ini.

Bahan dan Kaedah

Kesemua sampel diambil di kawasan tanaman pokok nipah (*Nypa fruticans*) di kawasan darat. Persampelan dilakukan ke atas tiga lokasi iaitu di Seberang Perak, Perak, Merchang, Terengganu dan Kuala Sanglang, Perlis.

Kesemua sampel dibawa balik ke makmal untuk dianalisis. Warna, rupabentuk buah, kulit dan isi buah *Nypa fruticans* dicatat. Air nira dipastikan berada di dalam keadaan yang sejuk atau beku. Sabut dan biji buah *Nypa fruticans* kemudiannya akan diasingkan dan dikeringkan di udara selama 24 jam dan seterusnya akan dikisar halus dengan menggunakan pengisar elektrik. Sampel yang dikisar disimpan di dalam balang pengontangan sebelum analisis seterusnya dijalankan. Air nira dimasukkan ke dalam peti sejuk supaya sentiasa beku. Ini bagi memastikan kualiti air nira ini tidak terjejas.

Penentuan asid hidrosianik (toksik)

Asid hidrosianik ditentukan mengikut kaedah penitratan alkali [14]. Kira-kira 14 g sampel direndam bersama 200 ml air di dalam kelalang penyulingan selama dua jam. Sampel air nira diandaikan mempunyai ketumpatan sebanyak 1 g/L. Proses penyulingan kemudiannya dilakukan sehingga kira-kira 150-200 ml hasil sulingan diperoleh dan dikutip dalam 2.5% (w/v) larutan natrium hidroksida. Seterusnya, 8 ml 5% kalium iodida dimasukkan ke dalam 100 ml hasil sulingan dan dititrat dengan 0.02 M larutan argentum nitrat menggunakan mikroburet. Takat akhir ditentukan melalui kekeruhan larutan yang berkekalan.

Keputusan dan Perbincangan

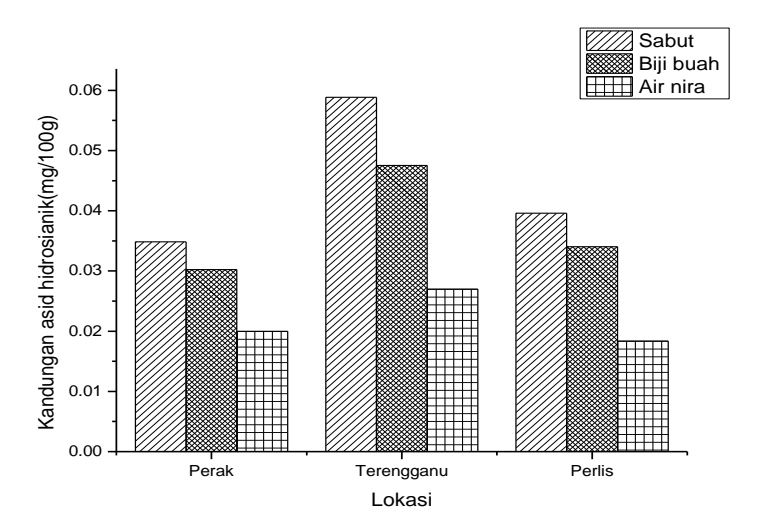
Kandungan asid hidrosianik di semua lokasi

Terdapat perbezaan kandungan asid hidrosianik di antara sampel sabut, biji buah dan air nira *Nypa fruticans*. Secara keseluruhannya, kandungan asid hidrosianik di dalam setiap sampel di setiap lokasi persampelan adalah mengikut urutan sabut>biji buah>air nira. Kandungan asid hidrosianik di dalam setiap sampel berada dalam julat 0.03-0.06 mg/100 g. Tahap asid hidrosianik di dalam setiap sampel sabut dan biji buah adalah masih rendah sekiranya dibandingkan dengan kajian yang dilakukan oleh penyelidik lain sebelum ini [15]. Manakala kandungan asid hidrosianik di dalam biji buah pula berada diparas yang rendah berbanding 36 mg/100 g, iaitu paras asid hidrosianik dianggap berbahaya untuk manusia [15]. Kandungan asid hidrosianik di dalam setiap sampel diringkaskan seperti di dalam Jadual 1 dan Rajah 2.

Jadual 1:	Kandungan asid	hidrosianik di	dalam sampel	l sabut, biji t	ouah dan air	nira Nypa fruticans
						Jr J

Sampel	Lokasi	Kandungan HCN (mg/100 g)
Sabut	Perak	0.035 ± 0.010
	Terengganu	0.058 ± 0.019
	Perlis	0.040 ± 0.002
Biji buah	Perak	0.030 ± 0.004
	Terengganu	0.048 ± 0.012
	Perlis	0.034 ± 0.009
Air nira	Perak	0.010 ± 0.007
	Terengganu	0.027 ± 0.007
	Perlis	0.018 ± 0.009

Kandungan asid hidrosianik di dalam sampel sabut adalah tertinggi di Terengganu diikuti dengan Perlis dan Perak iaitu masing-masing sebanyak 0.058 ± 0.019 , 0.040 ± 0.002 dan 0.035 ± 0.010 mg/100g (Jadual 1). Terengganu juga mencatatkan kandungan asid hidrosianik tertinggi bagi sampel biji buah iaitu sebanyak 0.048 ± 0.012 mg/100 g manakala Perak dan Perlis mencatatkan kandungan asid hidrosianik yang hampir sama di dalam sampel biji buah iaitu sebanyak 0.030 ± 0.004 dan 0.034 ± 0.009 mg/100 g. Dengan membuat andaian bahawa ketumpatan air nira adalah 1 g/L, kandungan asid hidrosianik bagi sampel air nira pula adalah mengikut urutan Terengganu > Perak > Perlis.



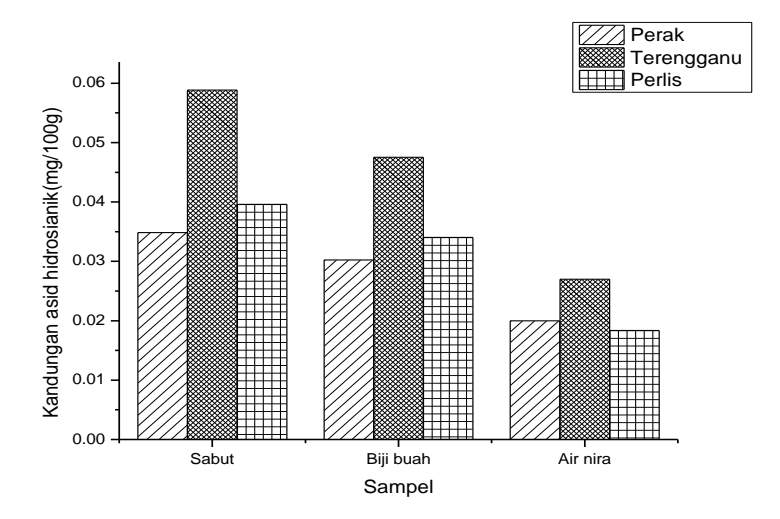
Rajah 2: Kandungan asid hidrosianik di dalam sampel sabut, biji buah dan air nira Nypa fruticans

Perbezaan kandungan asid hidrosianik di dalam setiap sampel pada Nypa fruticans menunjukkan bahawa sampel daripada Nypa fruticans menghasilkan glikosid sianogenik, yang mana apabila ia dihidrolisis dengan enzim tertentu, ia akan menghasilkan asid hidrosianik atau lebih dikenali sebagai asid prussik [6] Namun begitu, perbezaan kandungan asid hidrosianik adalah mungkin disebabkan kadar penghasilan sianohidrin seperti mandelonitril atau amigladin pada setiap liang-liang permukaan sampel [10, 11]. Kehadiran asid hidrosianik di dalam setiap sampel Nypa fruticans ini menunjukkan bahawa sampel Nypa fruticans adalah tumbuhan sianoporik iaitu tumbuhan yang merembeskan asid hidrosianik apabila tisu-tisu tumbuhan ini hancur atau terganggu [16]. Kandungan asid hidrosianik yang rendah di dalam setiap sampel Nypa fruticans membawa maksud bahawa ia tidak memudaratkan pengguna. Selain daripada asid fitik, oksalat dan tannin yang dikategorikan sebagai toksik di dalam makanan, asid hidrosianik juga dianggap sebagai toksik kerana ia mampu menjadi perencat kepada sistem respirasi di dalam tubuh badan. Kandungan asid hidrosianik yang tinggi di dalam nutrisi makanan adalah berbahaya kepada manusia. Kajian lalu [17 - 20], menyatakan bahawa had bagi sianida di dalam nutrisi sama ada dalam bentuk sintetik atau organik boleh menyebabkan perubahan drastik dalam penambahan berat badan, pengambilan nutrien, aktiviti enzim di dalam hati dan kepekatan tiosianat di dalam serum dan urin menerusi kajiannya terhadap tikus dan hamster. Keadaan ini sama sekali juga bakal memberi kesan kepada manusia sekiranya tahap asid hidrosianik di dalam makanan adalah tinggi.

Perbandingan kandungan asid hidrosianik

Perbandingan kandungan asid hidrosianik di dalam sabut di setiap lokasi

Perbandingan kandungan asid hidrosianik di dalam sabut ditunjukkan seperti dalam Rajah 3. Berdasarkan Rajah 3, sampel sabut di lokasi Terengganu mencatatkan kandungan asid hidrosianik tertinggi iaitu sebanyak 0.058 ± 0.019 mg/100 g diikuti sampel dari Perlis dan Perak masing-masing sebanyak 0.040 ± 0.002 dan 0.035 ± 0.010 mg/100 g. Ujian statistik ANOVA satu hala (pada aras keyakinan 95%) menunjukkan bahawa terdapat perbezaan yang bererti antara lokasi persampelan dan kandungan asid hidrosianik di dalam sabut (p<0.05). Ini menunjukkan bahawa terdapat perbezaan yang bererti antara lokasi dan kandungan asid hidrosianik di dalam sabut.



Rajah 3: Perbandingan kandungan asid hidrosianik di dalam sampel sabut, biji buah dan air nira di setiap lokasi persampelan

Perbezaan kandungan asid hidrosianik di dalam sabut *Nypa fruticans* mungkin disebabkan pengaruh jenis tanah pada tanaman *Nypa fruticans*. *Nypa fruticans* merupakan tumbuhan paya bakau yang kebanyakannya hidup di paya bakau. Di dalam kajian ini, persampelan di setiap lokasi dilakukan di kawasan daratan. Maka, perbezaan kandungan asid hidrosianik mungkin disebabkan oleh tahap kelembapan air atau tahap kandungan karbon organik di dalam tanah di lokasi persampelan.

Perbandingan kandungan asid hidrosianik di dalam biji buah di setiap lokasi

Perbandingan kandungan asid hidrosianik di dalam sampel biji buah ditunjukkan di dalam Rajah 3. Didapati sampel daripada Terengganu mencatatkan kandungan asid hidrosianik tertinggi iaitu sebanyak 0.048 ± 0.012 mg/100 g manakala sampel dari Perlis dan Perak masing-masing sebanyak 0.034 ± 0.009 dan 0.030 ± 0.004 mg/100 g. Ujian statistik ANOVA satu hala (pada aras keyakinan 95%) menunjukkan bahawa tidak terdapat perbezaan yang bererti antara lokasi persampelan dan kandungan asid hidrosianik di dalam biji buah (p>0.05). Ini menunjukkan bahawa tidak terdapat perbezaan yang bererti antara lokasi dan kandungan asid hidrosianik di dalam sabut. Selain daripada faktor kelembapan tanah dah karbon organik di dalam tanah, faktor usia buah juga kemungkinan menyumbang kepada perbezaan kandungan asid hidrosianik di dalam sampel biji buah. Buah nipah mengambil masa kira-kira empat bulan untuk matang. Usia buah yang berlainan menjadi faktor terhadap berbezanya struktur dalaman tisu pada tumbuhan. Asid hidrosianik hanya akan terhasil seandainya tisu tumbuhan terganggu atau hancur [16]. Bagi tumbuhan yang masih sempurna atau tidak berlaku kerosakan terhadap tisunya, enzim degradatif akan terpisah dengan glikosid sianogenik. Oleh itu, sedikit asid hidrosianik akan terkumpul di dalam sel seterusnya akan meruap dan terbebas ke udara [16]. Keadaan ini mungkin berlaku semasa kerja makmal dilakukan.

Perbandingan kandungan asid hidrosianik di dalam air nira di setiap lokasi

Perbandingan kandungan asid hidrosianik di dalam sampel air nira ditunjukkan di dalam Rajah 3. Kajian mendapati bahawa kandungan asid hidrosianik di dalam air nira adalah yang terendah berbanding sampel buah dan biji *Nypa fruticans*. Kandungan asid hidrosianik tertinggi di dalam sampel air nira adalah di lokasi Terengganu iaitu sebanyak 0.027 ± 0.007 mg/100 g diikuti dengan lokasi Perlis dan Perak masing-masing sebanyak 0.018 ± 0.009 dan 0.010 ± 0.007 mg/100 g. Ujian statistik ANOVA satu hala (pada aras keyakinan 95%) menunjukkan bahawa tidak terdapat perbezaan yang bererti antara lokasi persampelan dan kandungan asid hidrosianik di dalam air nira (p>0.05). Ini menunjukkan bahawa tidak terdapat perbezaan yang bererti antara lokasi dan kandungan asid hidrosianik di dalam air nira. Kandungan asid hidrosianik yang rendah di dalam air nira berbanding sampel lain memberi gambaran

bahawa medium cecair memberi kesan yang kurang baik terhadap penguraian enzim glikosida oleh enzim yang terdapat di dalam air nira. Keadaan ini akan mengurangkan penghasilan asid hidrosianik apabila sel-sel sudah musnah. Faktor yang perlu diambil kira dalam menentukan toksik di dalam sesuatu subjek adalah saiz dan jenis subjek itu, kelajuan menghadam makanan, jenis makanan dan kehadiran enzim penguraian pada tumbuhan dan juga pada sistem penghadaman [16]. Selain daripada itu, kandungan asid hidrosianik yang tidak berbahaya di dalam air nira mencadangkan bahawa air nira tidak mendatangkan bahaya kepada pengguna. Had pengambilan maksimum asid hidrosianik yang telah dicadangkan untuk manusia adalah di antara 0.5-3.5 mg/kg berat badan [21].

Kesimpulan

Asid hidrosianik di dalam setiap sampel berada dalam julat yang rendah dan tidak akan memudaratkan kesihatan pengguna. Asid hidrosianik juga menjadi parameter penting dalam menentukan kandungan toksik di dalam makanan. Lokasi persampelan memberikan perbezaan yang bererti terhadap kandungan asid hidrosianik di dalam sampel sabut sahaja. Kandungan asid hidrosianik di dalam buah nipah ini boleh memberi maklumat penting dalam mempelbagaikan penggunaan berasaskan buah nipah.

Penghargaan

Setinggi-tinggi penghargaan kepada pihak Universiti Kebangsaan Malaysia di atas bantuan melalui geran UKM-ST-06-FRGS0148-2010.

Rujukan

- 1. Temple, V.J. 1998. *Lesser known plant foods in Nutritional quality of plants food*. Post Harvest Res. Unit, Dept. of Biochem, University of Benin, Benin City. 245-274.
- 2. Kelvin, K.P., Dennis, H. M. dan Morgany, T. 2001. A guide to mangroves of Singapore. Raffles museum of Biodiversity Research. National University of Singapore.
- 3. Miah, M. D., Ahmed, R. dan Islam, S. J. 2003. *Indigenous management practices of golpata (Nypa fruticans) in local plantations in Southern Bangladesh*. Institute of Forestry and Environmental Sciences, University of Chittagong. 47: 185–190.
- 4. Bandaranayake, W. M. 1998. Traditional and medicinal uses of mangroves. *Mangroves and Salt Marshes*. 2: 133-148.
- 5. FAO. 1997. Preventing micronutrient malnutrition: a guide to food based dietary approaches. Washington: FAO & ILSI.
- 6. Harborne, J.B. 1972. Cyanogenic glucosides and their function. In: Phytochemical ecology. Academic Press, London.
- 7. Harborne, J.B. 1986. Recent Advances in Chemical Ecology. *Nat. Prod. Rep.* 324-344.
- 8. Harborne, J.B. 1993. *Plant toxins and their effects on animals. In: Introduction to Ecological Biochemistry*. Academic Press, London.
- 9. Francisco, I. A. dan Pinotti, M. H. P. 2000. Cyanogenic glycosides in plants. *Brazilian Archives of Biology and Technology*. 43: 487-492.
- 10. Vetter, J. 2000. Plant cyanogenic glycosides. J. Tox. 38: 11-36.
- 11. Jones, D. A. 1998. Why are so many food plants cyanogenic. *Phytochemistry*. 47: 155-162.
- 12. Cheeke, P.R. 1995. Endogenous toxins and mycotoxin in forage grasses and their effects on livestock. *J. Ani. Sci.* 73, 909-918.
- 13. McMahon, J.M., White, W.L.B. dan Sayre, R.T. 1995. Cyanogenesis in cassava (*Manihot esculenta Crantz*). *J. Exp. Bot.* 46: 731-741.
- 14. A.O.A.C. 1975. Official methods of analysis (11th ed). Association of analytical chemists. Washington D.C.
- 15. Osabor, V. N., Egbung, G. E. dan Okafor, P. C. 2008. Chemical Profile of *Nypa fruticans* from Cross River Estuary, South Eastern Nigeria. *Pakistan Journal of Nutrition*. 7: 146-150.
- 16. Conn E. E. 1969. Cyanogenetic glycosides. Ag. Food Chem. 17:519.
- 17. Tewe, O.O., Job, T. A., Loosli, J. K. dan Oyenuga, V. A. 1976. Cassava diets and performance of rats over two reproductive cycles. *Nig. J. Anim. Prod.* 3: 67-73.
- 18. Frake, R. A. dan Sharma, E. P. 1986. Comparative metabolism of linamarin and amaygdalin in harvester. *Food Chem. Toxicol.* 24: 417- 420.

- 19. Aletor, V. A. dan Fetuga, B. L. 1988. Dietary interaction of lima bean (*Phaseolus lunatus*) trypsin inhibitor, haemagglutinin and cyanide: I. Effect on growth performance, nitrogen utilization and physiopathology in growing rats. *J. Anim. Physiol. Anim. Nutr.* 60: 113-122.
- 20. Aletor, V. A. 1993. Cyanide in garri. 1. Distribution of total, free and bound hydrocyanic acid (HCN) in commercial garri, and the effect of fermentation time on its residual cyanide content. *Int. J. Food Sci. Nutr.* 44: 281-287.
- 21. Montgomery, R. D. 1969. Cyanogens. In toxic constituents of plant foodstuffs, I. E Liener (ed.). Academic Press



DETERMINATION OF PLATINUM GROUP ELEMENTS IN TERRESTRIAL ROCKS USING NICKEL SULFIDE FIRE ASSAY ISOTOPE DILUTION ICP-MS

(Penentuan Unsur Kumpulan Platinum Dalam Batuan Menggunakan Pencairan Isotop ICP-MS Assay Api Nikel Sulfida)

B.S. Wee^{1,2}, M. Ebihara², A.K.H. Wood¹

¹Malaysian Nuclear Agency, Bangi, 43000 Kajang, Selangor, Malaysia. ²Tokyo Metropolitan University, Minami-ohsawa 1-1, Hachioji-shi, 192-0397 Tokyo, Japan.

Abstract

Platinum group elements (PGE: Ru, Rh, Pd, Os, Ir, Pt) are highly siderophile elements (HSE) and their abundances in terrestrial rocks are low (~ ppb). This group of elements is important for understanding of geochemical processes, essential in mineral exploration, environmental studies, and identification of impact craters. Determination of PGE is very challenging and a reliable analytical technique is required to obtain high quality data. This study aims to utilize the fire assay isotope dilution inductively coupled plasma mass spectrometry (ICP-MS) for the determination of platinum group elements in terrestrial rock samples (WPR-1, WMG-1, and UMT-1). The nickel sulfide fire assay is applied to preconcentrate PGE from terrestrial rocks. All samples (about 0.2-0.5 g) were spiked with enriched isotopes (except Rh) prior to fire assay procedure in order to achieve isotope equilibrium. The NiS beads obtained were dissolved in HCl and the residue containing PGE was then dissolved prior to ICP-MS measurement. Isotopic ratios of PGE were measured and concentrations were calculated using the isotope dilution equation. The recoveries are in the range of 60 - 85% for all PGE except Os, which is prone not to be quantitatively collected due to the formation of OsO4. However, the lost of analytes does not affect the accuracy of the data obtained once the equilibrium between elements in samples and spikes is established. Actually, an excellent agreement between our data and literature values was confirmed for Os data. The measurement of PGE using ICP-MS requires correction from monoatomic and polyatomic ions having the same mass-to-charge ratio as those of analytes of interest. Instrument memory effect is evident in Os measurements and flushing with HCl and TMSC were adequate to reduce the memory effect. Low sample blanks (< 12 pg/g) and detection limits (< 15 pg/g) were achieved. In conclusion, the present method is able to determine PGE with reasonable accuracy despite of small sample size and is very favorable for application to terrestrial samples.

Keywords: platinum group elements, terrestrial rocks, fire assay, isotope dilution, ICP-MS

Abstrak

Unsur-unsur kumpulan Platinum (PGE: Ru, Rh, Pd, Os, Ir, Pt) adalah unsur-unsur yang cenderung untuk berkumpul dalam logam dan kepekatan unsur-unsur ini dalam batuan adalah rendah (~ ppb). Unsur-unsur ini adalah penting dalam kajian proses geokimia, penerokaan mineral, kajian alam sekitar, dan mengenalpasti kawah impak. Penentuan PGE adalah mencabar dan teknik analisis yang baik diperlukan untuk mendapatkan keputusan yang bermutu. Kajian ini adalah bertujuan untuk menggunakan teknik assay api isotop pencairan dengan plasma gandingan aruhan spectrometer jisim (ICP-MS) dalam penentuan PGE dalam sampel batuan (WPR-1, WMG-1, and UMT-1). Kaedah assay api adalah digunakan untuk pemekatan PGE dari batuan. Semua sample (kira-kira 0.2 – 0.5 g) ditambah dengan isotop diperkaya (kecuali Rh) sebelum menjalani kaedah assay api supaya keseimbangan isotop boleh dicapai. Manik NiS yang diperolehi itu dicairkan dalam HCl dan mendakan yang mengandungi PGE itu dilarutkan sebelum penentuan dengan ICP-MS. Nisbah isotop PGE diukur dan kepekatan dikira menggunakan persamaan isotop pencairan. Julat pemerolehan semula adalah 60 – 85% untuk PGE kecuali Os disebabkan oleh pembentukan OsO₄ yang susah untuk dikumpul secara kuantitatif. Akan tetapi, kehilangan analit tidak menjejaskan kejituan keputusan yang diperolehi selepas keseimbangan isotop dalam sample dicapai. Sebenarnya, keputusan Os yang diperolehi itu adalah bersetuju dengan nilai dalam penerbitan. Pengukuran PGE menggunakan ICP-MS memerlukan pembetulan dari segi ion monoatomik dan poliatomik yang mempunyai nisbah jisim-kepada-caj yang serupa dengan analit. Kesan ingatan alat adalah

Wee et al: DETERMINATION OF PLATINUM GROUP ELEMENTS IN TERRESTRIAL ROCKS USING NICKEL SULFIDE FIRE ASSAY ISOTOPE DILUTION ICP-MS

ketara dalam pengukuran Os dan pencucian dengan HCl dan TMSC adalah memadai untuk mengurangkan kesan ingatan. Sample kosong (< 12 pg/g) dan had pengesanan (< 15 pg/g) yang rendah telah dicapai. Dalam kesimpulan, kaedah ini dapat mengukur PGE dengan kejituan yang berpatutan untuk size sampel yang kecil dan adalah sesuai untuk digunakan untuk sampel batuan.

Kata kunci: unsur kumpulan platinum, batuan, assay api, pencairan isotop, ICP-MS

Introduction

Platinum group elements (PGE: Ru, Rh, Pd, Os, Ir, Pt) are noble metals with low abundances in Earth's crust [1]. These elements are useful in geochemical studies such as discussion on planetesimal accretion, late veneer hypothesis, and identification of impactors. Determinations of PGE are rather challenging and do require sensitive analytical methods to obtain reliable data. Preconcentration/decomposition techniques are necessary to separate PGE from their matrices before measurement could be performed. For geological samples, nickel sulfide fire assay is a suitable method for PGE preconcentration in order to provide good sensitivity for measurement. The advantage of this method is that all PGE are collected into nickel sulfide beads.

Isotope dilution (ID) is a method suitable to obtain reliable data for elemental analysis except for monoisotopic elements. Unknown sample is added with enriched isotope of an element and quantitative determination of elemental concentration is based on the measurement of isotopic ratio of element in a sample [2]. The use of isotope dilution technique is able to eliminate the problem of recovery after sample processing and results are precise and accurate [3]. Generally, determinations of isotopic ratios are performed using mass spectrometry. This study aims to utilize the fire assay isotope dilution inductively coupled plasma mass spectrometry (ICP-MS) for the determination of platinum group elements in terrestrial rock samples (WPR-1, WMG-1, and UMT-1).

Experimental

In this experiment three terrestrial rock samples namely UMT-1, WMG-1 and WPR-1 were analyzed and are listed below:

- 1. UMT-1 is the ultramafic ore tailings containing high concentrations of PGEs.
- 2. WMG-1 is the mineralized gabbro from Wellgreen Complex, Yukon Territory, Canada.
- 3. WPR-1 is the altered peridotite.

These samples were obtained from CANMET (Canada) with certified values for Ru, Rh, Pd, Ir and Pt. In addition, proposed values were given to Os while Re is not reported for these standard reference materials.

In this study, quantifications of PGE in rock samples were performed using isotope dilution method except for Rh. Solutions containing enriched isotopes of PGE as indicated in Table 1 were used. All chemicals used in this study were of analytical grade. Fire assay requires mixture of sodium carbonate as basic reagent while silica and sodium tetraborate as acidic reagent. Nickel and sulfur are added to the flux in a 5:3 ratio, which act as collector for PGE. Little amount of flour is added to provide a reducing condition. Figure 1 shows the procedure for nickel sulfide fire assay for PGE determinations. About 0.2-0.5 g sample were used and blanks were also included in this procedure. The sample is mixed to the flux in a crucible and subjected to heating in a furnace to about 850°C for about 20 minutes and then 1000°C for about 20 minutes. After that, the crucible was taken out from the furnace and allows it to cool. Once the crucible has cooled, nickel sulfide beads were obtained from the slag by cracking the crucible. The nickel sulfide beads were ground using a nickel mortar. Then, the powder was transferred to a 100 ml beaker and adds 30 ml deionized (DI) water and 30 ml 12M HCl. Heat the solution on a hotplate for a few hours until no effervescent. After the solution had cooled, pass the solution through a vacuum-filter fitted with cellulose filter disc. Collect the PGE containing residue and dilute in 1.5 ml 12M HCl and 1.5 ml H_2O_2 (30%). Heat the solution to about 100°C until no effervescent. Once the residue has dissolved, transfer the solution and internal standards (In, Tl, Bi) were added to make up to 15 ml of measurement solution in 10% HCl.

Ni-S Fire Assay (PGE)

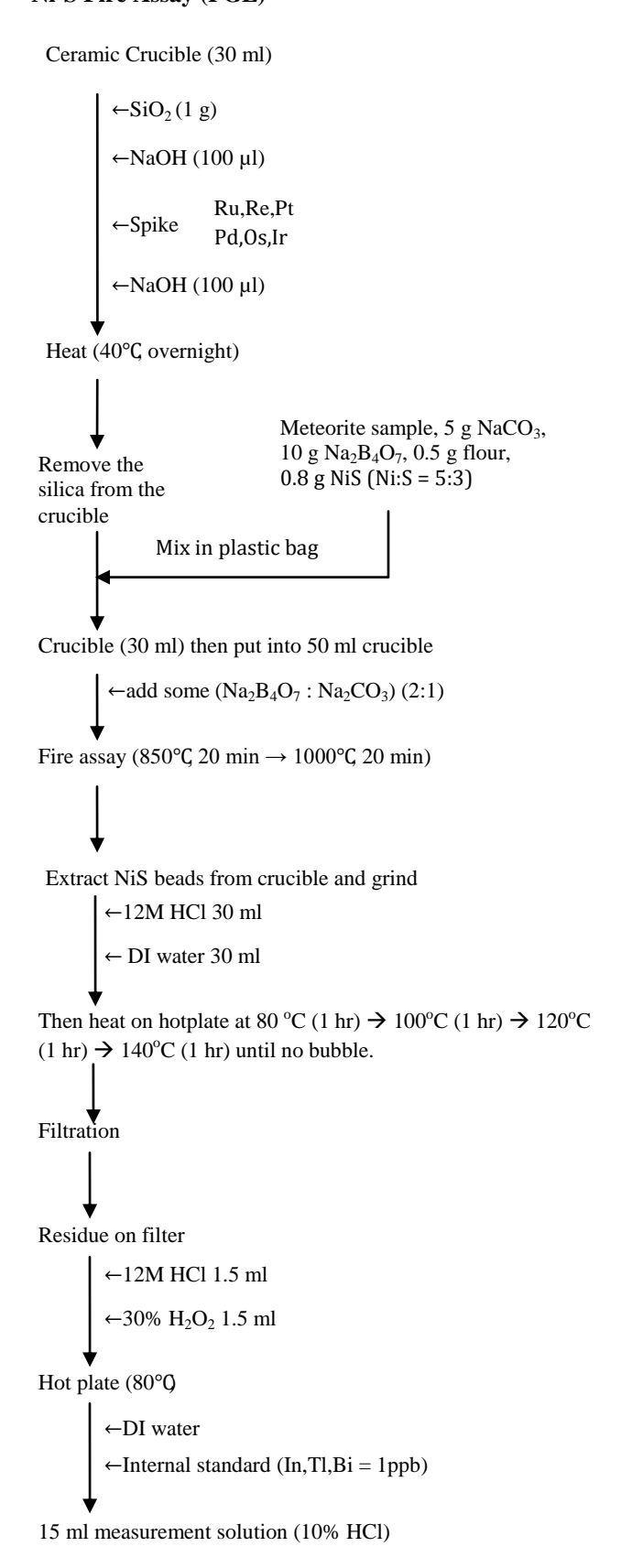


Figure 1: Fire assay procedure for PGE preconcentration.

267

	1	1
Enriched	Natural	Spike
Isotopes	abundances (%)	abundances (%)
⁹⁹ Ru	12.76	97.69
¹⁰⁵ Pd	22.33	97.00
¹⁸⁹ Os	16.15	95.26
¹⁹¹ Ir	37.30	98.23
¹⁹⁶ Pt	25.24	94.57

Table 1: Enriched isotopes for PGE determinations rock samples.

The VG PlasmaQuad 3 (Fision Instruments, UK) was used to determine the PGE isotopes in the solution samples. The instrument was optimized by using a monitoring solution containing 115 In (10 ppb) to obtain count rates of about 7 to 10×10^5 cps. All sample solutions were added with 1 ppb of 115 In, 205 Tl and 209 Bi as internal standards. Detail operating condition for PGE determination using ICP-MS is presented in Table 2. Scanning for each isotope was done using peak jump mode and repeated five times for each sample. Count rates obtained for these 115 In, 205 Tl and 209 Bi are about $3-4\times10^4$ cps. About 5 to 6 samples were measured in each run to avoid instrument instability due to prolong measuring time.

Table 2: ICP-MS operating condition during PGE measurement.

Plasma incident power	1360 W	Detection mode	Peak jumping
Cooling gas	14 l/min	Sweeps	250
Auxiliary gas	1.25 l/min	Repeat integration	5
Nebulizer gas	0.90 l/min	Dwell time per isotope	1000 μs
Points per peak	5	Acquisition time	50 s

Results and Discussion

ICP-MS measurement of PGE

For isotope dilution method, the following isotopic ratios were determined: 99 Ru/ 100 Ru, 99 Ru/ 101 Ru, 99 Ru/ 102 Ru, 105 Pd/ 106 Pd, 105 Pd/ 108 Pd, 189 Os/ 189 Os, 189 Os/ 190 Os, 191 Ir/ 193 Ir, 194 Pt/ 196 Pt, and 195 Pt/ 196 Pt. For 103 Rh, external calibration with internal standards (In and Tl) were used for quantification. Low mass PGE isotopes are normalized to 115 In while high mass PGE are normalized to 205 Tl. Standard solutions in the range of 0.1 – 15 ppb were used for external calibration for all PGE and to monitor the recovery of each element by calculating the difference between isotope dilution data.

Instrument mass fractionation during measurement was monitor using isotopic ratios of standard solutions of low and high concentrations as presented in Table 3. The deviations of isotopic ratios between standard solutions and literature values were ranged from 0.3% (191 Ir/ 193 Ir) to 6.3% (99 Ru/ 102 Ru). The measured mean ratios were independent of concentrations with relative standard deviations between 0.6% and 2.4%, which correspond to the linearity of ICP-MS at large concentration range. At low concentrations (0.10 ppb and 0.15 ppb), data show slightly more variable due to random error at low count rates.

Table 3: Measured isotope ratios in standard solutions containing PGE. Literature values were from [4].

Concentration	⁹⁹ Ru/ ¹⁰⁰ Ru	⁹⁹ Ru/ ¹⁰¹ Ru	⁹⁹ Ru/ ¹⁰² Ru	¹⁰⁵ Pd/ ¹⁰⁶ Pd	¹⁰⁵ Pd/ ¹⁰⁸ Pd
0.10 ppb	1.003 ± 0.090	0.713 ± 0.041	0.378 ± 0.023	0.828 ± 0.034	0.805 ± 0.024
0.15 ppb	1.002 ± 0.046	0.716 ± 0.028	0.384 ± 0.012	0.804 ± 0.020	0.792 ± 0.022
10 ppb	0.992 ± 0.007	0.705 ± 0.002	0.375 ± 0.002	0.807 ± 0.004	0.801 ± 0.002
15 ppb	0.990 ± 0.006	0.701 ± 0.004	0.372 ± 0.003	0.806 ± 0.002	0.799 ± 0.002
Average	0.997 ± 0.006	0.709 ± 0.006	0.377 ± 0.004	0.811 ± 0.010	0.799 ± 0.005
Literature	1.013	0.748	0.404	0.817	0.844
Average/Literature	0.984	0.948	0.933	0.993	0.947
Concentration	$^{189}{\rm Os}/^{188}{\rm Os}$	¹⁸⁹ Os/ ¹⁹⁰ Os	$^{191}{ m Ir}/^{193}{ m Ir}$	¹⁹⁴ Pt/ ¹⁹⁶ Pt	¹⁹⁵ Pt/ ¹⁹⁶ Pt
0.10 ppb	1.199 ± 0.074	0.606 ± 0.019	0.608 ± 0.017	1.314 ± 0.074	1.380 ± 0.044
0.15 ppb	1.247 ± 0.028	0.617 ± 0.015	0.595 ± 0.012	1.315 ± 0.052	1.317 ± 0.058
10 ppb	1.237 ± 0.007	0.607 ± 0.003	0.594 ± 0.003	1.251 ± 0.005	1.318 ± 0.007
15 ppb	1.234 ± 0.002	0.610 ± 0.001	0.590 ± 0.002	1.256 ± 0.002	1.310 ± 0.005
Average	1.229 ± 0.018	0.610 ± 0.004	0.597 ± 0.007	1.284 ± 0.031	1.331 ± 0.028
Literature	1.220	0.615	0.595	1.306	1.340
Average/Literature	1.007	0.992	1.003	0.983	0.993

Interference in PGE measurements

Interferences from monoatomic and polyatomic ions were monitored using single standard solution of Cd, Cu, Hg, Hf, Mo, Ni, Ta, W, Zn and Zr during sample analysis. Corrections of interferences were performed for all samples and blanks using common spreadsheet program. The measurement of 100 Ru requires correction for 100 Mo in the range of 20-60%, 101 Ru requires correction of 1-33%, and 102 Ru requires correction of 1-48%. For 106 Pd, 108 Pd, 190 Os and 198 Pt, their interference corrections are less than 10%.

Instrument memory effect

During the course of measurements, background counts were monitored by measuring blank solution 10% HCl before each sample. Generally, background counts for lower mass PGE (99 Ru to 108 Pd) were below 50 cps while at higher mass PGE (188 Os to 196 Pt) were below 80 cps. Instrument memory effect is evident for Os especially after measurement of standard solutions of high concentrations (10-15 ppb). For sample solutions, Os count rates were generally below 5000 cps in most cases and memory effects were reduced to background level of 30-50 cps after about 15-20 minutes washing using dilute TMSC followed by 5% HCl. For other PGE no memory effects were observed.

Procedure blank and detection limits

A procedure blank was included for each batch of analysis for blank correction. For procedure blank, PGE concentrations are given as pg/g assuming 1:1 dilution factor. Data from the procedure blank showed that contributions of PGE from chemical reagents were in pg/g order (Table 4). Platinum and Pd show higher

Wee et al: DETERMINATION OF PLATINUM GROUP ELEMENTS IN TERRESTRIAL ROCKS USING NICKEL SULFIDE FIRE ASSAY ISOTOPE DILUTION ICP-MS

concentrations than other PGE elements in procedure blanks measured in this study. Similar observations were reported by Ravizza and Pyle [5] that such variability may be caused by contamination. In most cases, contribution from blank is below 1%.

Detection limits were estimated based on three times standard deviation from previous four runs. Platinum and Pd show higher detection limits than other member of the PGE. Similar observation was reported by Ravizza and Pyle [5] that Pt data are more variable possibly due to contamination. From the low procedure blank and detection limits, the current procedure is able to cater for the analysis of rock samples in this study.

Table 4: NiS fire assay procedure blank (concentrations in pg/g). Detection limit (DL) is 3σ of blank.

Run	Os	Ir	Ru	Pt	Rh	Pd
Mean	2.1	1.7	4.3	9.6	2.6	11.8
±	1.2	0.7	1.2	4.6	2.6	4.7
DL	3.7	2.2	3.7	13.7	7.9	14.0

Determinations of PGE in UMT-1, WMG-1 and WPR-1

Results from the measurement of the rock samples are presented in Tables 5a to 5c. Most of the results were found to be within error of the certified values [6] of these rock samples. For Os, our data were in good agreement with non-certified values. In the case of Pt, uncertainty for UMT-1 was about 29%, which is higher than those of WMG-1 and WPR-1. Variation of Pt value in UMT-1 maybe due to heterogeneity or 'nugget effect' commonly found in PGE analysis. For other PGEs, uncertainties are less than 5% in WMG-1 and WPR-1 whereas uncertainties in UMT-1 are about 12% or less. The use of isotope dilution gives good reproducibility for PGE analysis even though the sample size is less than 1 g in this study.

The recovery (calculated using data of external calibration and isotope dilution) of PGE using fire assay method shows that more than 50 - 80% of the PGE are collected into NiS bead except for Os. The volatile OsO_4 escapes during the dilution of NiS bead causing the recovery of Os to be lower than 10%. The recovery of Pt in WPR-1 is rather low (14%) which may be due to loss of NiS beads during crushing or filtration. However, the use of isotope dilution is able to give good results disregard of the recovery of PGE in NiS beads. Isotope ratios are not affected by loss of analytes during NiS beads digestion. For the determination of Rh, correction of recovery was done by taking average between Ru and Pd due to their similar masses.

Table 5a: PGE concentrations in UMT-1 (n = 6)

Elements	Measured	±	Certified	±	Recovery (%)
Os	8.89	1.07	8		6.9
Ir	10.1	1.2	8.8	0.6	61
Ru	10.9	0.5	10.9	1.5	73
Rh	10.4	0.8	9.5	1.1	69
Pt	129	38	129	5	60
Pd	111	5	106	3	65

Table 5b: PGE concentrations in WMG-1 (n = 3)

Elements	Measured	±	Certified	±	Recovery (%)
Os	26.8	0.6	24		5.0
Ir	53.4	0.9	46	4	65
Ru	30.7	0.7	35	5	70
Rh	26.1	0.7	26	2	67
Pt	726	98	731	36	63
Pd	392	9	382	11	64

Table 5c: PGE concentrations in WPR-1 (n = 3)

Elements	Measured	±	Certified	±	Recovery (%)
Os	16.6	0.6	13		7.2
Ir	16.7	0.4	13.5	1.8	83
Ru	23.6	0.7	22	4	56
Rh	11.8	2.2	13.4	0.9	53
Pt	322	49	285	11	14
Pd	251	13	235	9	51

Conclusion

This study showed that the use of NiS fire assay with isotope dilution ICP-MS is very suitable for analysis of PGE in geological sample. Good accuracy and precision could be achieved using this method even for small sample size (0.2 - 0.5 g). Besides, the low procedure blanks of this method are favorable for various geological samples with low PGE contents.

Acknowledgement

One of the authors (B.S.W) would like to thank the MEXT of Japan for a graduate scholarship and the Malaysian Nuclear Agency for a study leave.

References

- 1. K.H. Wedepohl (1995). The composition of the continental crust. *Geochim. Cosmochim. Acta* **59**, 1217 1232.
- 2. R.L. Watters Jr., K.R. Eherhardt, E.S. Beary, and J.D. Fassett (1997). Protocol for isotope dilution using inductively coupled plasma-mass spectrometry (ICP-MS) for the determination of inorganic elements. *Metrologia* **34**, 87 96.
- 3. A.A. van Heuzen, T. Hoekstra, and B. van Wingerden (1989). Precision and accuracy attainable with isotope dilution analysis applied to inductively coupled plasma mass spectrometry: theory and experiments. *J. Anal. Atomic Spec.* **4**, 483 489.
- 4. J.R. De Laeter, J.K. Böhlke, P. De Bièvre, H. Hidaka, H.S. Peiser, K.J.R. Rosman, and P.D.P. Taylor (2003). Atomic weights of the elements: Review 2000. *Pure Appl. Chem.* **75**, 683 800.

Wee et al: DETERMINATION OF PLATINUM GROUP ELEMENTS IN TERRESTRIAL ROCKS USING NICKEL SULFIDE FIRE ASSAY ISOTOPE DILUTION ICP-MS

- 5. G. Ravizza, and D. Pyle (1997). PGE and Os isotopic analyses of single sample aliquots with NiS fire assay preconcentration. *Chem. Geol.* **141**, 251 268.
- 6. T. Meisel, and J. Moser (2004). Reference materials for geochemical PGE analysis: new analytical data for Ru, Rh, Pd, Os, Ir, Pt and Re by isotope dilution ICP-MS in 11 geological reference materials. *Chem. Geol.* **208**, 319 338.



PEPTIDE SEPARATION BY CAPILLARY ELECTROPHORESIS WITH ULTRAVIOLET DETECTION: SOME SIMPLE APPROACHES TO ENHANCE DETECTION SENSITIVITY AND RESOLUTION

(Pemisahan Peptida Oleh Elektroforesis Rerambut Dengan Pengesan Ultra-Lembayung: Pendekatan Mudah Untuk Meningkatkan Isyarat Pengesanan Dan Resolusi)

L. Noumie Surugau

Industrial Chemistry Program, School of Science and Technology, Universiti Malaysia Sabah, Locked Bag 2073, 88999 Kota Kinabalu, Sabah, Malaysia.

*Corresponding author: lnoumie@ums.edu.my

Abstract

Capillary electrophoresis (CE) is one of the leading separation technologies for analysis of water-soluble analytes. CE has many advantages over the more established methods such as liquid chromatography and gel electrophoresis particularly in rapid analysis, require very little sample, use less or no toxic organic solvent, high peak efficiency and ease of automation. Despite the many attractive advantages of CE, CE users continue to seek improvements particularly on detection sensitivity, resolution and selectivity. This paper presented several simple approaches to improve detection sensitivity using simple sample preconcentration called field-enhanced sample injection (FESI) and chromatographic-based ZipTip C₁₈ pre-concentrator. Also, some improvements in the resolution of complex peptides mixture when using two strategies namely, capillary coating and manipulation of the hydrophobicity of peptides using perfluorinated acids as background electrolyte (BGE), which have anionic conjugate base forms with hydrophobic character. As test compounds, standard peptide mixture and proteins digests were used for these studies. The results showed that FESI has significantly enhanced the detection signal of peptide standards and bovine serum albumin (BSA) tryptic digests. As for the use of ZipTip C₁₈ pre-concentrator, selective enhancement in detection signal was particularly notable on the late migrating peptides. Coating the capillary proved to have little changes on the CE of peptides when used in conjunction with acidic BGE. Electropherograms of BSA tryptic peptides in pentafluoropropionic acid (PFPA) and heptafluorobutyric acid (HFBA) showed interesting profile, with notable resolution improvement for peptides with close similarity in electrophoretic mobilities.

Keywords: Capillary electrophoresis, peptide, protein digests, pre-concentration, detection sensitivity, resolution.

Abstrak

Elektroforesis rerambut (CE) merupakan salah satu teknologi pemisahan terkini untuk analisis analit boleh-larut air. CE mempunyai banyak kelebihan berbanding dengan kaedah-kaedah yang lebih terkenal seperti kromatografi cecair dan elektroforesis jel, antaranya ialah analisis yang pantas, memerlukan sampel yang amat sedikit, menggunakan amat kurang atau tiada langsung pelarut organik toksik, keberkesanan puncak yang tinggi dan automasi yang mudah. Walaupun mempunyai banyak kelebihan-kelebihan yang menarik, namun pengguna-pengguna CE masih berusaha untuk menambahbaik kaedah ini terutamanya dari segi kepekaan pengesanan, resolusi dan selektiviti. Kertaskerja ini melaporkan beberapa pendekatan-pendekatan mudah untuk meningkatkan kepekaan pengesanan dengan menggunakan kaedah pra-pemekatan mudah yang dipanggil suntikan sampel medan-diperkuat (FESI) dan pra-pemekat berasaskan kromatografi ZipTip C₁₈. Juga, beberapa kaedah penambahbaikan resolusi campuran peptida yang kompleks dengan menggunakan dua strategi yang dipanggil penyalutan rerambut dan manipulasi ciri hidropobisiti peptida dengan mengunakan asid-asid perfluorin sebagai elektrolit latarbelakang (BGE). Asid-asid perfluorin membentuk bes konjugat anionik yang memberikan ciri hidropobik kepada BGE. Sebatian peptida piawai dan hasil hadaman beberapa protein telah digunakan sebagai sebatian ujian dalam kajian ini. Hasil kajian menunjukkan bahawa kaedah FESI dapat meningkatkan isyarat pengesanan sebatian sebatian peptida piawai dan hasil hadaman BSA dengan berkesan. Bagi penggunaan pra-pemekat ZipTip C₁₈ pula, peningkatan secara selektif ke atas isyarat pengesanan dapat

L. Noumie Surugau: PEPTIDE SEPARATION BY CAPILLARY ELECTROPHORESIS WITH ULTRAVIOLET DETECTION: SOME SIMPLE APPROACHES TO ENHANCE DETECTION SENSITIVITY AND RESOLUTION

diperhatikan terutamanya pada peptida yang termigrasi lewat. Menyalut rerambut menunjukkan perubahan yang sedikit ke atas CE peptida apabila digunakan bersama dengan BGE berasid. Elektroferogram-elektroferogram peptida triptik BSA dalam asid pentafluoropropionik dan asid heptafluorobutirik sebagai BGE menunjukkan corak yang menarik, di mana peningkatan resolusi peptida yang mempunyai mobiliti elektroforetik yang hampir sama adalah jelas kelihatan.

Kata kunci: Elektroforesis rerambut, peptida, hasil penghadaman protein, pra-pemekatan, kepekaan pengesanan, resolusi.

Introduction

Peptides represent a large and complex group of biomolecules playing variable and vitally important roles in a living organism. Peptides act, among others, as hormones, neutrotransmitters, immunomodulators, coenzymes or enzyme inhibitors, drugs, toxins and antibiotics. Peptide and protein assays in biological samples are increasingly important in the diagnosis and treatment of a number of diseases. The importance of peptides in proteomics is ever increasing, since both the structure and function of many proteins are identified via their peptide fragments [1,2].

Traditionally, peptides have been analyzed by high-performance liquid chromatography (HPLC); CE is becoming rapidly accepted as complementary to this method. CE has several advantages over HPLC, including rapid analysis time, high separation efficiency, requires very little sample amount and eliminates the use of toxic solvents and handling their waste. CE, both CE-ultraviolet (CE-UV) and CE-mass spectrometry (CE-MS) has been utilized for the separation and characterization of peptides. This is reflected in the large number of publications on CE of peptides in various samples. For instance, peptides in human serum [3], polypeptides in urine and cerebrospinal fluid [4] and body fluid [5], Amadori compounds [6], plasma [7], to name a few of the recent publications.

In CE, the narrow bore capillary allows injection of 2 - 10 nL normally, which is very convenient for analysis of biological sample. Paradoxically, this advantage leads to major drawbacks [8]. Most commercial CE detectors rely on on-column UV absorption, therefore, the optical pathlength (Equation 1) is essentially equal to the internal diameter (i.d.) of the capillary; which is normally $50 - 100 \, \mu m$.

$$A = \varepsilon l_{p}C \tag{1}$$

where A is absorbance, ε is the molar absorption coefficient, C the sample concentration, and l_p the optical pathlength.

This poses a severe limitation on account of the Beer-Lambert Law. The concentration limit of detection (CLOD) in CE, which typically ranges from 10^{-5} to 10^{-6} M, is thus poorer than HPLC. Unfortunately, protein concentrations in biological samples (e.g. blood, plasma, cells) can be in the sub-micromolar range. At these concentrations, tryptic fragments represented in the peptide map are undetectable by the conventional CE with UV absorbance detection. Over the years, several techniques have been developed for improving detection sensitivity in CE. These improvement efforts can be grouped into two areas: CE detection technology and sample pre-concentration. On detection sensitivity, attempts were aimed at lengthening the detection pathlength l_p such as Z-shaped cells [8,9], bubble-shaped cells [10] or multi-reflection detection cells [11] and rectangular CE [12]. This technology produces the best sensitivity enhancement (by one order of magnitude), but decreases resolution and remains expensive. Other attempts have aimed to improve the performance of other detection schemes such as MS [13,14], laser-induced fluorescence (LIF) with derivatization [15] and without derivatization [16], electrochemical [17] and chemiluminescene [18]. MS is universal with very high detection sensitivity for peptides but is expensive and requires complex instrumentation. LIF detectors are more sensitive than UV but not as flexible as UV detectors, e.g. they require specific derivatization reagents among other limitations. As for electrochemical and chemiluminescene detection schemes, their applications are still limited in peptides and proteins.

A simpler and more straightforward technique of improving the detection sensitivity in CE-UV is sample pre-concentration. There are two mechanisms of sample pre-concentration: electrophoretic-based and chromatographic-based. In this report, sample pre-concentration using field-enhanced sample injection (FESI) and chromatographic-based using commercial ZipTip C₁₈ pre-concentrator are described. FESI pre-concentration is based on the

difference between the velocity of the analyte in the sample plug and the velocity in the running buffer. The stacking process occurs when the injection part of the capillary is still in the sample vial, which is during the injection using voltage. Then, the focusing process occurs after replacing the sample vial with the buffer vial and during the start of the CE run. This is very simple to perform in any CE analysis: a small plug of water (or any solution with lower conductivity than the BGE is injected into the capillary after filling it with BGE, then sample injection is performed using electrokinetic injection. The chromatographic-based pre-concentrator ZipTip C₁₈ tips are commonly used for sample clean-up. At the same time, it also pre-concentrates the analyte into a small sample volume. Details of the extraction and pre-concentration procedures are given in the methodology section.

Interaction between analyte and inner capillary wall is detrimental to CE. The small diffusion coefficients of proteins, of the order of 10⁻¹⁰ m² s⁻¹ compared to 10⁻⁸ m² s⁻¹ for small molecules such as peptides, should in theory give peak efficiencies of the order of 10⁶ theoretical plates. However, these values are not achieved experimentally, and in many cases peak tailing is seen to occur. This is a result of strong electrostatic interactions between regions of net positive charge density on the protein or peptide surface with negatively charged capillary inner wall. In the current study, therefore, the inner wall of the bare fused silica capillary was coated with a coating solution commercially available from Target Discovery (Palo Alto, CA, USA) called UltraTrol™. The exact properties of the coating solution are not available due to intellectual property factors, but according to the manufacturer it is a class of linear polyacrylamide, N-substituted acrylamide co-polymers for the control of electroomostic force and electroosmotic flow (EOF). The solution is used to pre-coat the bare fused silica capillary and not added into the BGE, therefore no alteration occurs to the viscosity or ionic strength of the BGE. Because it alters the EOF, it is expected to affect the electrophoretic mobilities of the analyte. Manipulation of the intrinsic electrophoretic mobilities of analytes would offer an opportunity to enhance their selectivity and thus improve resolution.

Another effort carried out to improve the peptide resolution in this study is ion interaction strategy. CE separations are based on differences in analyte charge-to-size ratios. In theory, therefore, positively charged peptides of the same molecular size and charge, differing only in hydrophobicity, would not be separated by CE. Thus, selectivity of CE separations can only be optimized based on other characteristics, such as their hydrophobicity [19]. In cases where resolution of peptides is poor due to close similarity in electrophoretic mobility arising from there being little difference in charge and/or size, manipulating their hydrophobicity could be an alternative to optimize their separation. In reversed-phase-liquid chromatography (RP-LC) the process of ion-pairing has been widely utilized to enhance selectivity for the separation of analytes with similar hydrophobicity. The most widely used anionic ion-pairing reagents for RP-LC of peptides were perfluorinated carboxylic acids, such as trifluoroacetic acid (TFA) and its higher homologues such as pentafluoropropionic acid (PFPA) and heptafluorobutyric acid (HFBA) [20, 21]. Thus, in the current study, PFBA and HFBA were employed as separation buffers (to replace phosphate buffer) to investigate if they would affect the resolution of peaks in the complex peptide mixture of a BSA digest.

Experimental

Chemicals and materials

Acetonitrile (ACN), trifluoroacetic acid (TFA), phosphoric acid, 85 % (w/v), HPLC-grade water, peptide standards mixture (P2693), bovine serum albumin (BSA), TPCK-treated trypsin [EC 3.4.21.4], 4-dimethylaminopyridine (DMAP), HFBA, PFPA and lithium hydroxide were purchased from Sigma-Aldrich (Poole, UK). The six-protein mixture digest (P/N 161088) was obtained from LC Packings, Dionex Co. (Amsterdam, The Netherlands); ammonium bicarbonate was bought from BDH Laboratory Supplies (Poole, UK); ZipTip C₁₈ pipette tips were obtained from Millipore Ltd. (Watford, UK); and UltraTrolTM dynamic pre-coating (ULHN-02841-6905-SM0010) was bought from Target Discovery Inc. (Palo Alto, CA, USA). Fused-silica capillaries were obtained from Composite Metal Services Ltd. (Ilkely, UK). All reagents were of analytical grade; BSA, protein digests and peptide standards were used without any further purification.

Apparatus and procedures

CE-UV analyses were performed in 50 cm, 50 μ m i.d. and 365 μ m o.d. uncoated fused-silica capillary on a Beckman P/ACE MDQ system (Beckman-Coulter, High Wycombe, UK) equipped with a UV diode array detector. The UV absorbance scan range from 190 to 300 nm took place at 10 cm from outlet end through a window created by removal of 1 cm of polyimide coating. The polyimide coating was also removed 2-3 mm from both ends to

L. Noumie Surugau: PEPTIDE SEPARATION BY CAPILLARY ELECTROPHORESIS WITH ULTRAVIOLET DETECTION: SOME SIMPLE APPROACHES TO ENHANCE DETECTION SENSITIVITY AND RESOLUTION

minimize adsorption of the positively charge peptides on the coating [22]. For a new capillary, it was conditioned by rinsing with solutions in the following order: (i) MeOH (5 min), (ii) HPLC water (30 min) (iii) 1 M HCl (30 min), (iv) HPLC water (30 min), (v) 1 M NaOH (30 min), (vi) HPLC water (30 min) and (vii) BGE (30 - 60 min). For used but still good capillary, it was conditioned with 0.1 M NaOH (15 - 30 min), HPLC-grade water (30 min) and then BGE (30 - 40 min) prior to analysis. In between runs, capillary was rinsed with running buffer for 2 - 5 min. Re-conditioning of the capillary was performed again if the reproducibility of migration time and peak area was poor. Separation was carried out using applied voltage of +15 - 30 kV. Temperatures of samples compartment and capillary during analysis were set constant at 25° C. All analyses were carried out in triplicate or more. Other experimental details are described in Results and Discussion.

Preparation of buffer, standard and sample solutions

Except for the II-CE experiments, the BGE was 80 mM phosphate buffer which was prepared from a concentrated phosphoric acid 85 % (w/v). Similarly, the 80 mM PFBA and 80 mM HFPA buffers were prepared from concentrated PFBA and HFPA, respectively. In all cases the pH of the BGEs were adjusted to 2.3 with 1.0 M LiOH. Meanwhile, the digestion buffer was 50 mM ammonium bicarbonate, pH 7.8, prepared from ammonium bicarbonate salt. The final pH of each buffer was measured using a Corning ion analyzer 150 (Halstead, UK). All buffers were sonicated for 20 min or more, filtered through a 0.2 μ m microfilter (Sartorius, Göttingen, Germany) prior to use. A stock solution of nine peptide standards (P2693) (containing 25 μ g of each peptide) was prepared by adding 450 μ L HPLC-grade water and 50 μ L of 0.1 % TFA into the mixture vial to give 50 μ g mL⁻¹ each peptide. Further dilution into 10% BGE was carried out to obtain solution with the concentration of 5.0 μ g mL⁻¹ each peptide. The six-protein mixture digest working solution of 1.0 pmol μ L⁻¹ was prepared by adding 100 μ L 0.05 % TFA in HPLC-grade water into the vial containing 100 pmol each protein. All solutions were prepared in HPLC-grade water.

Protein digestion procedures

About 0.5 mg of BSA or six-protein mixture was dissolved in 0.5 mL digestion buffer. TPCK-treated trypsin was added to the BSA digestion solution at a substrate-to-enzyme ratio of 1:20 to 1:50. The digestion vial was then incubated in a water bath at 37° C for 18 h. Phosphoric acid (0.5 mL, 1.0 M) was added into the digest to terminate the proteolysis and acidify the digest solution. The mixture was then centrifuged at 5,500 g for 10 - 15 min to obtain a clear solution. $100 \,\mu$ L of the clear solution were diluted with $20 \,\mu$ L phosphate BGE and made up to $200 \,\mu$ L with HPLC-grade water to give a final concentration of $250 \,\mu$ g mL⁻¹ total peptides. If necessary, further dilution was carried out to obtain more diluted digest samples. The samples were analyzed immediately.

Sample pre-concentration procedures

Procedures for the FESI stacking experiments were as previously reported by Monton and Terabe [27]. The procedures were as follows: (i) capillary was filled with BGE (20 psi, 2 min), (ii) injection of water plug (0.5 psi, 5 -7 s), (iii) sample injection using voltage (electrokinetic injection) (+5 - +7 kV, 5 - 10 s), (iv) injection of BGE (0.5 psi, 5 s), (v) separation (+25 - +30 kV, until analysis completed).

ZipTip C₁₈

Procedures for ZipTip C_{18} pre-concentration were as recommended by Millipore Corp. (UK). For this experiment, a 10 μ L pipette (Eppendorf UK, Cambridge, UK) was used, where the ZipTip C_{18} pre-concentrator was assembled on the pipette as a tip. The solutions used were: (i) wetting solution (A): 100 % ACN; (ii) equilibration (B) and washing (C) solutions: 0.1 % TFA; (iii) elution solution (D): 0.1 % TFA in 50:50 (v/v) ACN:H₂O. Three processes were involved namely, (i) equilibrium, (ii) binding and washing, and (iii) elution. Prior to use, the ZipTip tip was conditioned by rinsing with solution A twice, then rinsed three times with solution B. For binding, the sample solution was aspirated from and dispensed into its original tube 15 times. Then, the ZipTip tip was rinsed with solution C, also 15 times. To elute the bound analytes, the ZipTip tip was rinsed by aspirating and dispensing 4 μ L solution D into a sample tube 15 times. The pre-concentrated sample was then analysed with CE.

Dynamic coating procedures

Procedures for application of the UltraTrol dynamic pre-coating were as recommended by the manufacturer (Target Discovery Inc., USA).

Ion interaction CE (II-CE)

The procedures were similar to those in other CE analyses, but 80 mM phosphate (pH 2.3) buffer was replaced by PFBA or HFPA at similar concentration and pH.

Results and Discussion

FESI pre-concentration

Initially the capillary is filled with BGE, followed by a hydrodynamic injection of a short plug of water, which guarantees the presence of a sufficiently long zone of low conductivity [23]. At low pH, the electroosmosis is limited, which means that the plug of water stays at the injection end. Injection of a BGE plug after the sample injection aids this process and prevents expulsion of any of the water plug due to Joule heating and expansion of the capillary contents. Being positively charged, the peptides that enter the capillary rapidly move to the front of the water plug. At this point they encounter a lower electric field and slowed down immediately, a process that literally stacks the peptides at the front of the water plug/BGE interface. After substituting the sample vial with a BGE vial at the inlet, the CE voltage is turned on, and the focused analytes separate according to their electrophoretic mobility. The electropherograms of FESI stacking and non-FESI (i.e. using normal pressure injection) of peptide standard mixture and BSA tryptic digest are shown in Figures 1A and 1B, respectively.

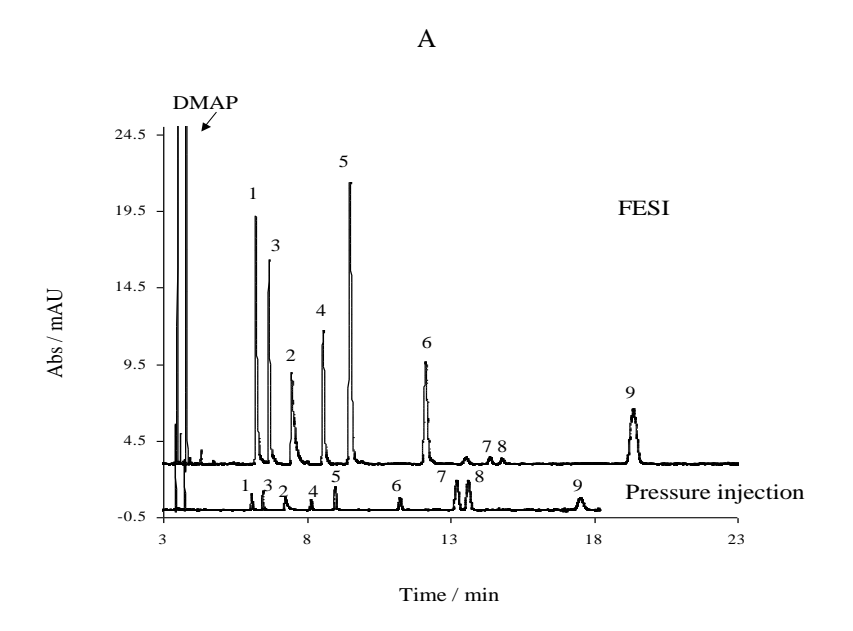
Figure 1A showed significant increased in the detection signal (i.e. UV absorbance) of the peptides. The injected sample volume in the non-FESI was approximately 6.0 nL, which corresponds to 29 pg each peptide. In the FESI method, the electric field across the capillary under applied voltage would not be uniform due to the water plug at the injection end, and calculation of the injected amount using the formula for electrokinetic injection (Equation 2) would not be accurate.

$$Q = \frac{1}{4}(\mu_{\rm ep} + \mu_{\rm eo})\pi D^2 E_{\rm ini} C t_{\rm ini}$$
 (2)

where, Q is the amount injected, μ_{ep} and μ_{eo} are electrophoretic and electroosmotic mobilities, respectively, E_{inj} is the field strength across the injection zone, D is the capillary internal diameter, C is the solute concentration and t_{inj} is the injection duration.

The amount of sample loaded by electrokinetic injection was, therefore, using approximated by peak area comparison [24]. Using bradykinin (peak 1) as a basis, the peak area when using FESI was 35.5 times bigger relative to that obtained by typical pressure injection, which is equivalent to 210 nl of injected sample solution. As described in Introduction, narrow bore capillary allows injection of 2 - 10 nL normally using pressure injection. It is shown here that FESI method allows much larger injection of sample which ultimately produce enhanced detection signal. The effect of FESI was evaluated by direct comparison of peak height in FESI and non-FESI electropherograms of the test peptides. Table 1 shows the reproducibility (expressed as % relative standard deviation, % RSD) of migration time and, peak height, corrected peak area (PA) and sensitivity enhancement factor (SEF) of the peptide mixture for the FESI studies.

As seen in Table 1, % RSD of migration time increases on descending the column which most probably due to the decrease of electrophoretic mobility, and therefore greater susceptibility to EOF variations from run to run. Previous researchers also noted high variations in FESI which caused difficulty in quantification [25]. On the basis of the present data, peak height has better reproducibility than peak area. According to Ledger *et al.* [25], this is because peak height is less influenced by migration time and integration errors. Thus, the SEF was expressed in term of peak height.



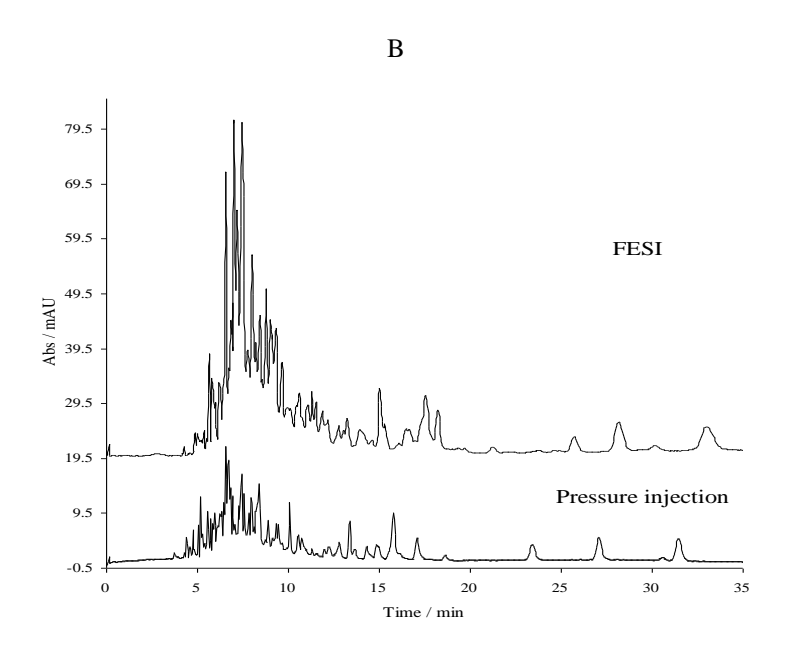


Figure 1: CE electropherograms of FESI vs. non-FESI of peptide standards (A) and BSA tryptic digest (B) in 80 mM phosphate buffer adjusted to pH 2.3 with 1.0 M LiOH. A: Inj.: +5 kV, 60 s (FESI); 0.5 psi, 5 s (non-FESI); voltage / current: +25 kV / 58.6 μ A.; sample conc.: 5.0 μ g mL⁻¹ each peptide with 10 mM DMAP in 10 % phosphate buffer. Peak identifications: 1, bradykinin; 2, substance P; 3, bradykinin F1-5; 4, arg⁸-vasopressin; 5, *Luteinizing-hormone-releasing hormone* (LHRH); 6, bombesin; 7, leu-enkephalin; 8, met-enkephalin; 9, oxytocin. B: Inj.: +5 kV, 5 s (FESI); 0.5 psi, 5s (non-FESI); voltage / current: +30 kV / 56.0 μ A; sample conc.: 250 μ g mL⁻¹ BSA digest; Capillary: 40 × 50 cm, 50 μ m i.d. UV detection at 190 nm; data rate: 16 Hz.

Except the enkephalins (peaks 7 and 8), the peak heights of all the peptides were increased significantly with SEF_{height} values up to 19. Apart from the marker, DMAP, bradykinin (peak 1) was the most enhanced, followed by LHRH (peak 5), substance P (peak 2) and \arg^8 -vasopressin (peak 4). The amount of sample loaded into the capillary using electrokinetic injection is theoretically determined by the electrophoretic mobility, μ_{ep} , of the peptides. The higher the value of μ_{ep} , the greater is the loading. This explains the highest SEF for DMAP: although it has a single charge of +1 (protonated amino group), it has the highest mobility because it has the smallest mass and size. Peptides with high charge-to-size ratios have high velocity under the applied voltage and therefore high amounts are transported into the water plug.

Table 1: % RSDs of migration time, $t_{\rm m}$, peak height, corrected peak area, PA and SEF_{height} of the test peptides and DMAP. For peak identification, refer to Figure 1.

Analyte		$\mathrm{SEF}_{\mathrm{height}}$		
	$t_{ m m}$	peak height	corr. PA	
DMAP	0.37	0.86	6.5	22
1	0.46	7.0	15.7	19
2	0.53	1.8	16.6	8
3	0.48	22	17.8	13
4	0.83	4.3	17.1	13
5	0.90	2.2	16.7	15
6	1.0	3.5	14.2	11
7	1.1	9.9	22.2	0.3
8	1.1	12.8	29.6	0.3
9	1.5	5.0	12.4	5

 $^{^{1}}$ SEF_{height} = $\frac{\text{peak height (FESI)}}{\text{peak height (pressure inj.)}}$

To test the viability of this method on more complex peptide mixtures, BSA and six-protein mixture tryptic digests were used as samples. BSA is a large protein with 607 amino acid units and a molecular mass of 66.2 kDa. Based on the ExPASy Proteomics Tools [26], digestion with trypsin would be expected to produce 75 peptide fragments. The non-FESI electropherogram in Figure 1(B) was obtained from \sim 6.0 nl of 50 μ g mL⁻¹ digest solution, which equivalents to 3.8 μ M BSA. The concentration of the resultant BSA tryptic fragments should be to a first approximation 3.8 μ M. As with the peptide standards, it was suspected that a normal stacking also occurred during the hydrodynamic injection due to the difference in conductivity of the sample plug and BGE inside the CE column. The electropherogram obtained using the FESI method was based on electrokinetic injection of +5 kV for 60 s, from a sample volume of 200 μ l. To ensure high loading, the injection time was considerably longer than in the previous

L. Noumie Surugau: PEPTIDE SEPARATION BY CAPILLARY ELECTROPHORESIS WITH ULTRAVIOLET DETECTION: SOME SIMPLE APPROACHES TO ENHANCE DETECTION SENSITIVITY AND RESOLUTION

study with the peptide standards. The results showed that detection signals for most of the tryptic peptides in BSA were improved significantly. For closer inspection, the electropherograms have been expanded and displayed in two parts as shown in Figure 2.

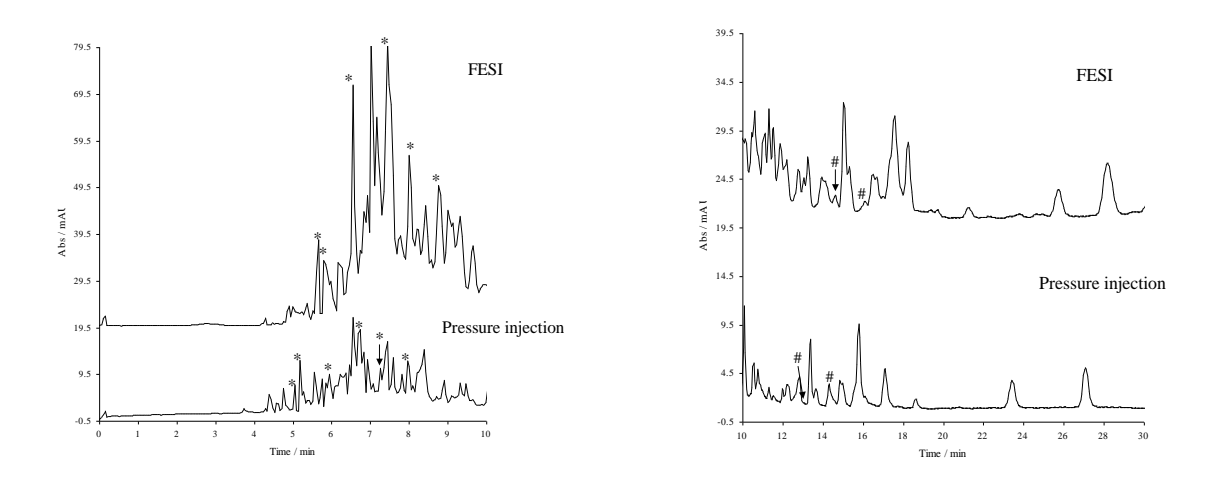
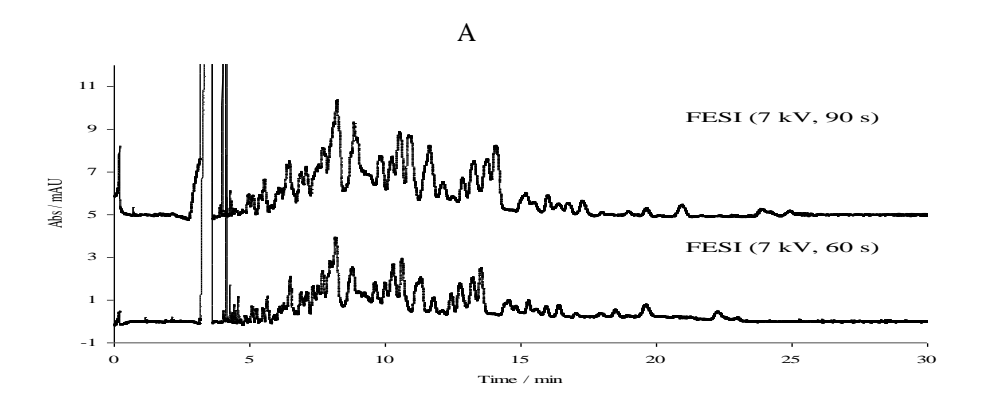


Figure 2: Expanded electropherograms of Figure 1(B). Enhanced (*) and not enhanced signal (#). Experimental conditions are as described in Figure 1.

Examining the pattern of the peaks in Figure 2, some interesting observations are revealed concerning signal enhancement. The peaks marked with (*) were enhanced exceptionally strongly in FESI, whilst peaks marked with (#) were not enhanced at all in FESI. Whilst there is partial correlation with mobility, insofar as peaks in the first set of the electropherogram and those in the latter set, more subtle effects are required to explain the details. It may be in part due to the way mobilities of differently charged species vary with ionic strength, since ionic strength is low in the water plug. Other possible factors are the pH values in the sample solution and in the water plug; the latter will change rapidly during the electrokinetic injection process, but initially will be neutral and thus quite different from that in the BGE.

Similar investigations were carried out using a more complex sample i.e. a mixture of peptides resulted from the tryptic digestion of a solution containing six different protein standards. The solution consisted of 1.0 pmol each cytochrome c (11 kDa), lysozyme (14 kDa), alcohol dehydrogenase (37 kDa), bovine serum albumin (69 kDa), apotransferrin (78 kDa) and beta-galactosidase (135 kDa). The number of the resultant tryptic peptide fragments are not exactly known but they are estimated to be hundreds. Their electropherograms obtained using FESI and pressure injection are shown in Figure 3.

The huge early migrating peaks seen here are likely to arise from salts in the sample solution because no sample pre-treatment was performed. The peaks shown in the figure correspond to $\sim 0.5~\mu M$ peptides in the injection solution. Since there was very little signal for the sample using pressure injection, consistent with the extremely low peptide concentrations, huge enhancements in detection sensitivity were achieved using the FESI method. Comparing electropherograms where the electrokinetic injection time was increased from 60 s to 90 s at the same applied voltage, the pattern remains almost identical and there is additional enhancement of peak heights and areas. However, the widths of some of the peaks are increased and resolution decreased.



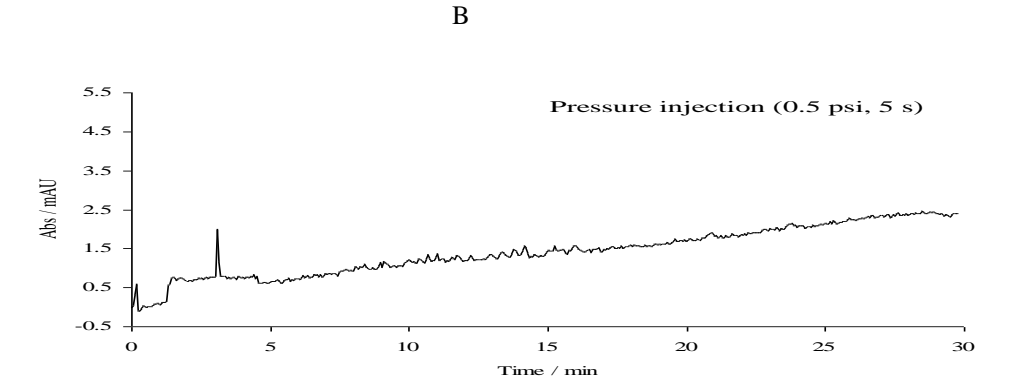


Figure 3: CE electropherograms of FESI (A) vs. non-FESI (B) of six-protein mixture tryptic digest. Sample conc.: peptides from 0.5 μ M each protein; inj.: 5.0 kV, 90 s and 60 s (FESI); 0.5 psi, 5 s (pressure); voltage / current: 25 kV / 58.6 μ A. Other experimental conditions details are as described in Figure 1.

ZipTip C₁₈ pre-concentrator

ZipTip C_{18} tips are commonly used for sample clean-up. At the same time, it also pre-concentrates the analyte into a small sample volume. An electropherogram of a BSA tryptic digest after pre-concentration with ZipTip C_{18} is presented in Figure 4.

The sample was injected using pressure. The electropherogram here corresponds to 5.9 nl of the pre-concentrated sample. Comparing this figure and Figure 1(B), the enhancement in detection signal was not as great as in the FESI method, particularly for the small peaks at the front. However, detection enhancement in the later migrating peaks was significantly higher. In Figure 1(B), the later migrating peaks were generally low and very broad. In Figure 4, most of them are sharper peaks. The explanation for this observation is almost certainly due to positive discrimination by the ZipTip C_{18} material for the more hydrophobic peptides.

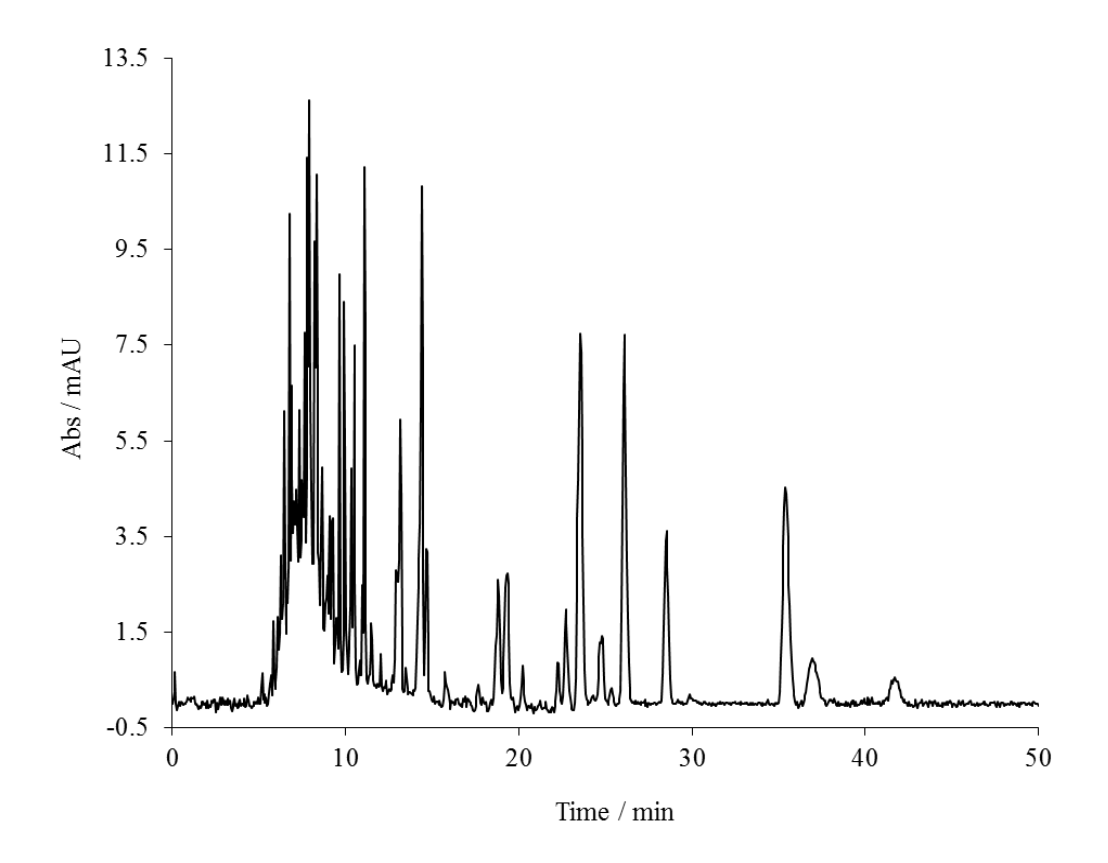
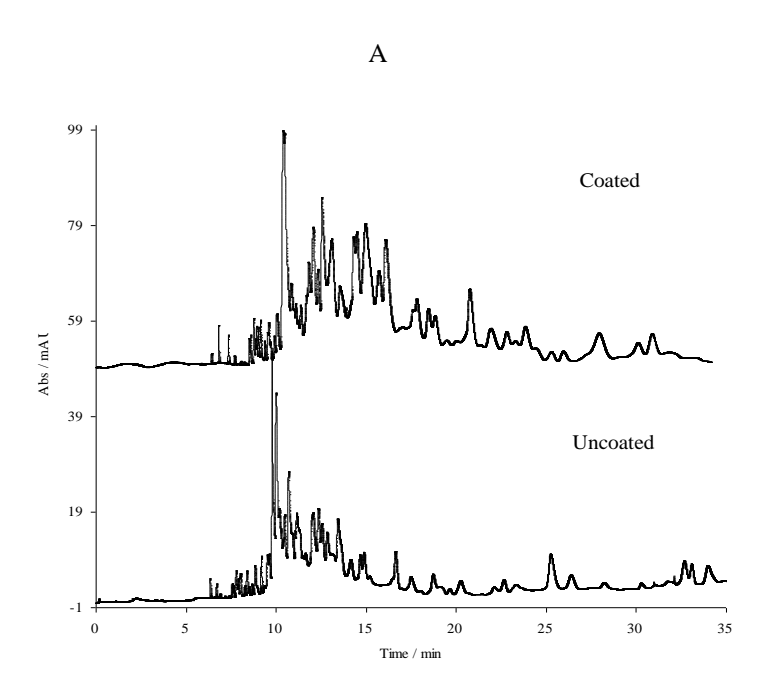


Figure 4: Electropherogram of BSA tryptic digest after pre-concentration using ZipTip C_{18} . Experimental conditions are similar as in Figure 1.

Coated capillary

In this study, the capillary was coated with commercial polyacrylamide polymer to control the EOF. Having the inner wall of the capillary coated, peak efficiency should be better due to elimination of wall-peptide interactions, and improvement in resolution is possible. It was investigated in this study if this is the case by comparing CE separations of the BSA tryptic digest in uncoated and coated capillaries, using the same phosphate BGE (pH 2.3). The electropherogram, along with an expanded electropherogram for better inspection, are shown in Figure 5. This figure shows that peak efficiencies of some of the peaks in the coated capillary were slightly better than in the uncoated one. Also, some improvement in the resolution was observed, particularly in the early peaks (Figure 5B), which suggests may be due to complete suppression of wall interaction with the highly cationic peptides. In general, however, there is relatively very little difference in the performance of the coated and uncoated capillaries. The fact that the BGE is acidic (pH 2.3), wall-peptide interaction is less pronounced due to insignificant ionization of the silanol inner wall in the uncoated fused silica capillary. Thus, the little difference between the electropherograms in Figure 5A. It would be interesting to try out this coating material in used conjunction with BGE at high pH. Another observation worth reporting here is that peptides in the uncoated capillary migrate slightly faster than in the coated one, consistent with the small amount of EOF in the former case.



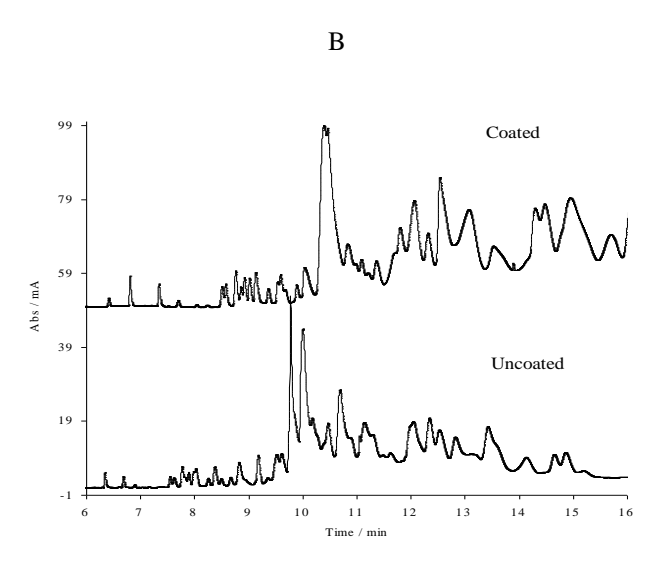
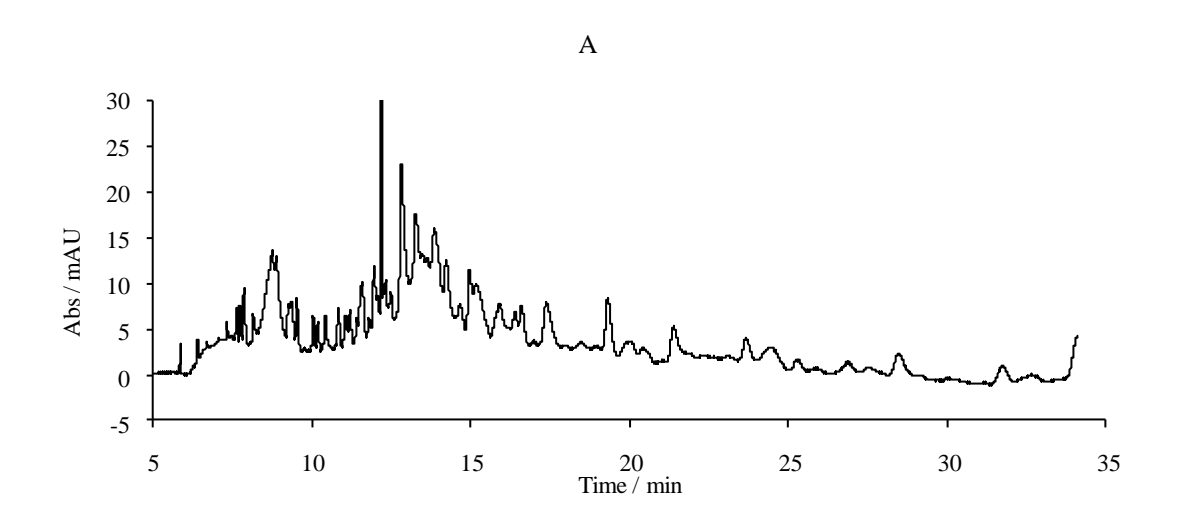


Figure 5: Normal (A) and expanded electropherograms (B) of BSA tryptic digest in uncoated and coated capillary. Sample conc.: $50.0~\mu g~mL^{-1}$; inj.: 0.5~psi, 5~s. Voltage / current: 20~kV / $45.2~\mu A$ (uncoated), 20~kV / $39.3~\mu A$ (coated). Other experimental conditions are as described in Figure 1.



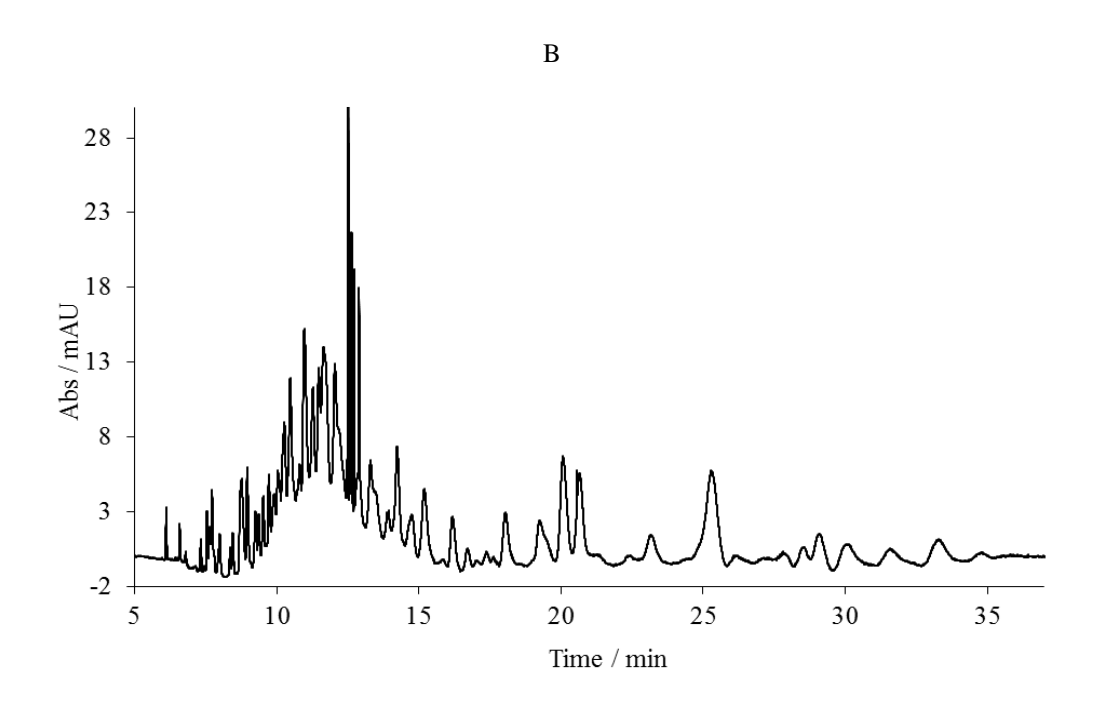


Figure 6: Electropherograms of BSA tryptic digest in 80 mM PFPA BGE (A) and 80 mM HFPA (B). BGE: 80 mM PFPA and HFPA adjusted to pH 2.3 with 1 M LiOH. Sample conc.: $50.0~\mu g~mL^{-1}$; inj.: 0.5~psi, 5~s. Voltage / current, +25~kV / $56.5~\mu A$. Other experimental details are similar to Figure 1.

Ion interaction-CE

In the previous electropherograms of the BSA tryptic digest (Fig. 1A), the peaks in the middle (10-16 min) were mostly not fully resolved. This may implies that there are a large number of peptides with almost similar mobilities. In this experiment, phosphate buffer was replaced with PFPA or HFBA, perfluorinated acids which have low pK_a values and anionic conjugate base forms having some hydrophobic character. These more hydrophobic anions were expected to show ion-pair interactions with the cationic peptides [27], modifying their migration times and changing the profile of the electropherogram. It was hoped that this would also improve the resolution. The concentrations of the perfluorinated acids were kept the same as phosphoric acid (80 mM), as were the pH values (2.3). The same basic solution, 1 M LiOH, was used to adjust the pH. The electropherogram obtained with PFPA and HFBA is shown in Figure 6A and B, respectively.

It should be noted that the current is almost the same as that obtained in the phosphate BGE, i.e. $56.5~\mu A$ as compared to $58.6~\mu A$ for the same applied voltage of 25~kV. This implies that ionic concentrations are similar in the two BGEs. Comparing Figures 1(B) and 6(A), differences between these two electropherograms can be easily seen. Some of the unresolved peaks in the middle are now further resolved with better peak shape. Similarly, in HFPA (Figure 6(B), significant improvements in the resolution and peak efficiencies were observed here. The explanation for this may be hydrophobic interaction between the hydrophobic amino acids in the peptides and the perfluorinated anions. Manipulation in the degree of ion-ion/hydrophobic interactions of these peptides appears to have resulted in improved efficiency in the CE, and thus the observed improvement in the peak resolution. Because anions of HFBA are more hydrophobic than in PFPA, the effects would be expected to be greater with HFBA. Similar observations were reported by Popa *et al.* [27] in CE resolution of synthetic peptides when phosphoric acid in the buffer was replaced by perfluorinated acids. They also observed further improvements in resolution in HFBA compared to in PFBA.

Conclusions

Detection sensitivity, resolution and peak effeciency have all been improved by one or other of the different strategies explored in this study. FESI offers the benefits of simplicity, and can be done on-line with minimal adaptation of the CE conditions: it is simple to inject a water plug prior to the sample, and to use electrokinetic rather than pressure injection. The detection sensitivity for species which are charged at the sample pH was shown to be substantially enhanced using this approach, while uncharged species are not injected and not amplified. Use of the commercial ZipTip C_{18} tips gave very good results for the late-migrating peptides, and generally provided benefits for improving the quality of the CE separation of peptides. This is due to a combination of desalting and selective retention of hydrophobic species on the C_{18} stationary phase in the ZipTip. Coating the capillary made little changes in the electropherograms, thus offers no benefit to CE of peptides at low pH. Ionic interaction CE was found to cause interesting changes in the peptide separation. This is the first time such experiments have been carried out on a protein digest. The use of HFBA was found to offer most promise in sharpening the peaks.

Acknowledgement

The author is grateful to Universiti Malaysia Sabah for the financial support.

References

- 1. Washburn, M.P., Wolters, D., Yates III, J.R. 2001. Large-scale analysis of the yeast proteome by multidimensional protein identification technology. *Nat. Biotechnol.* **19**: 242-248.
- 2. Wittke, S., Fliser, D., Haubitz, M., Bartel, S., Krebs, R., Hausadel, F., Hillmann, M., Golovko, I., Koester, P., Haller, H., Kaiser, T., Mischak, H., Weissinger, E.M. 2003. Determination of peptides and proteins in human urine with capillary electrophoresis—mass spectrometry, a suitable tool for the establishment of new diagnostic markers. *J. Chromatogr. A* **1013**(1-2): 173-181.
- 3. Sassi, A.P., Andell III, F., Bitter, H.-M., Brown, M.P.S., Chapman, R.G., Espiritu, J. Greenquist, A.C., Guyon, I., Horchi-Alegre, M., Stults, K.L., Wainright, A., Heller, J.C., Stults, J.T. 2005. An automated, sheathless capillary electrophoresis-mass spectrometry platform for discovery of biomarkers in human serum. *Electrophoresis* 26(7-8): 1500-1512.

L. Noumie Surugau: PEPTIDE SEPARATION BY CAPILLARY ELECTROPHORESIS WITH ULTRAVIOLET DETECTION: SOME SIMPLE APPROACHES TO ENHANCE DETECTION SENSITIVITY AND RESOLUTION

- 4. Wittke, S., Mischak, H., Walden, M., Kolch, W., Rädler, T., Wiedemann, K. 2005. Discovery of biomarkers in human urine and cerebrospinal fluid by capillary electrophoresis coupled to mass spectrometry: Towards new diagnostic and therapeutic approaches. *Electrophoresis* 26(7-8): 1476-1487.
- 5. Kaiser, T., Wittke, S., Just, I., Krebs, R., Bartel, S., Fliser, D., Mischak, H., Weissinger, E.M. 2004. Capillary electrophoresis coupled to mass spectrometer for automated and robust polypeptide determination in body fluids for clinical use. *Electrophoresis* **25**(13): 2044-2055.
- 6. Hau, J., Devaud, S., Blank, I. 2005. Detection of Amadori compounds by capillary electrophoresis coupled to tandem mass spectrometry. *Electrophoresis* **26**(13): 2077-2083.
- 7. Ullsten, S., Zuberovic, A., Wetterhall, M., Hardenborg, E., Markides, K.E., Berquist, J. 2004. A polyamine coating for enhanced capillary electrophoresis-electrospray ionization-mass spectrometry of proteins and peptides. *Electrophoresis* **25**(13): 2090-2099.
- 8. Moring, S.E., Reel, R.T., van Soest, R.E.J., Lauer, H.H. 1993. Optical improvements of a Z-shaped cell for high-sensitivity UV absorbance detection in capillary electrophoresis. *Anal. Chem.* **65**(23): 3454-3459.
- 9. Chervet, J.P., Van Soest, R.E.J., Ursem, M. 1991. Z-shaped flow cell for UV detection in capillary electrophoresis. *J. Chromatogr. A* **543**: 439-449.
- 10. Heiger, D. N. 1992. High Performance Capillary Electrophoresis. Hewlett-Packard, USA. pp. 100-101.
- 11. Wang, T., Aiken, J.H., Huie, C.W., Hartwick, R.A. 1991. Nanoliter-scale multireflection cell for absorption detection in capillary electrophoresis. *Anal. Chem.* **63**(14): 1372-1376.
- 12. Cifuentes, A., Rodriguez, M.A., Garcia-Montelongo, J. F. 1996. Rectangular capillary electrophoresis: study of some dispersive effects. *J. Chromatogr. A* **737**(2): 243-253.
- 13. Stutz, H. 2005. Advances in the analysis of proteins and peptides by capillary electrophoresis with matrix-assisted laser desorption/ionization and electrospray-mass spectrometry detection. *Electrophoresis* **26**(7-8): 1254-1290.
- 14. Simpson, D. C., Smith, R.D. 2005. Combining capillary electrophoresis with mass spectrometry for applications in proteomics. *Electrophoresis* **26**(7-8): 1291-1305.
- 15. Timperman, A.T., Oldenburg, K.E., Sweedler, J.V. 1995. Native fluorescence detection and spectral differentiation of peptides containing tryptophan and tyrosine in capillary electrophoresis. *Anal. Chem.* **67**(19): 3421-3426.
- 16. Tong, W., Yeung, E.S. 1996. Determination of insulin in single pancreatic cells by capillary electrophoresis and laser-induced native fluorescence. *J. Chromatogr. B: Biomed. Sci. Appl.* **685**(1): 35-40.
- 17. Voegel, P.D., Baldwin, R.P. 1997. Electrochemical detection in capillary electrophoresis. *Electrophoresis* **18**(12): 2267-2278.
- 18. Staller, T.D., Sepaniak, M.J. 1997. Chemiluminescence detection in capillary electrophoresis. *Electrophoresis* **189**(12-13): 2291-2296.
- 19. Grossman, P.D., Wilson, K.J., Petrie, G., Lauer, H.J. 1988. Effect of buffer pH and peptide composition on the selectivity of peptide separations by capillary zone electrophoresis. *Anal. Biochem.* **173**(2): 265-270.
- 20. Popa, T.V., Mant, C.T., Hodges, R.S. 2004. Capillary electrophoresis of cationic random coil peptide standards: Effect of anionic ion-pairing reagents and comparison with reversed-phase chromatography. *Electrophoresis* **25**(9): 1219-1229.
- 21. Mant, C.T., Hodges, R.S. 1991. *High-Performance Liquid Chromatography of Peptides and Proteins: Separation, Analysis and Conformation*, CRC Press, Boca Raton, FL.
- 22. Ensing, K., de Boer, T., Schreuder, N., de Zeeuw, R. 1999. Separation and identification of neuropeptide Y, two of its fragments and their degradation products using capillary electrophoresis—mass spectrometry. *J. Chromatogr. B: Biomed. Sci. Appl.* **727**(1-2): 53-61.
- 23. Zhang, C.-X., Thormann, W. 1996. Head-Column Field-Amplified Sample Stacking in Binary System Capillary Electrophoresis: A Robust Approach Providing over 1000-Fold Sensitivity Enhancement. *Anal. Chem.* **68**(15): 2523-2532.
- 24. Monton, M. R. N., Terabe, S. 2004. Field-enhanced sample injection for high-sensitivity analysis of peptides and proteins in capillary electrophoresis—mass spectrometry. *J. Chromatogr.* **1032**(1-2): 203-211.
- 25. Ledger, R., Tucker, I.G., Walker, G.F. 2002. Quantitative capillary electrophoresis assay for the proteolytic stability of luteinizing hormone-releasing hormones. *J. Chromatogr. B* **769**(2): 235-242.
- 26. http://www.expasy.org/tools/peptidecutter/.

27. Popa, T.V., Mant, C.T., Hodges, R.S. 2006. Ion-interaction–capillary zone electrophoresis of cationic proteomic peptide standards. *J. Chromatogr. A* **1111**(2): 192-199.



DETERMINATION OF RADON ACTIVITY CONCENTRATION IN HOT SPRING AND SURFACE WATER USING GAMMA SPECTROMETRY TECHNIQUE

(Penentuan Kepekatan Aktiviti Radon Di dalam Air Panas dan Air Permukaan Dengan Menggunakan Teknik Spektrometri Gama)

Zaini Hamzah¹, Ahmad Saat², Mohammed Kassim^{*1}

¹Faculty of Applied Sciences, ²International Education Centre (INTEC), UniversitiTeknologi MARA, KampusSeksyen 17, 40200 Shah Alam, Malaysia

*Corresponding author: mohammed_kassim84@yahoo.com

Abstract

Naturally occurring radionuclides in water such as, ²²²Rn which emit gamma radiation through its decaying process could reach to human. Water samples were chosen to present ground and surface water. The groundwater samples were collected from, Perak, Selangor, Kelantan and Sembilan. The surface water samples were collected from Perak, Kelantan, and Pahang. In this study, the surface doses rate measurements were done in-situ using LUDLUM rate meter, and the radioactivity concentration levels were done by counting the water samples using gamma spectrometer with HPGe detector. The activities are ranged from (0.29-1.41 Bq/l).

Keywords: Radon, Gamma spectrometry, Surface water, Groundwater

Abstrak Yang berlaku secara semulajadi radionuklid di dalam air seperti, ²²²Rn yang mengeluarkan radiasi gamma melalui proses mereput dapat sampai kepada manusia. Sampel air telah dipilih untuk membentangkan air bawah tanah dan permukaan. Sampel air bawah tanah telah dikutip dari, Perak, Selangor, Kelantan dan Sembilan. Sampel air permukaan telah dikumpulkan dari Perak, Kelantan, dan Pahang. Dalam kajian ini, pengukuran kadar dos permukaan telah dijalankan di-situ dengan menggunakan meter kadar LUDLUM, dan tahap kepekatan radioaktif telah dilakukan dengan mengira sampel air yang menggunakan spektrometer gamma dengan pengesan HPGe. Aktiviti-aktiviti adalah dari (0,29-1,41 Bq/l).

Kata kunci: Radon, Spektrometri Gamma, Air Permukaan, Air Tanah

Introduction

In the last two decades, there has been a great deal of awareness about the health risks from exposure to radon radioactive gas and its decay products. Large-scale radon surveys have been carried out in Europe and in the United States, more than that have been conducted in any country in the World. However, the study of radon has been increasingly growing throughout the world [1]. The main issue was the monitoring of radon gas in air inside dwellings. Over the last century more emphasis has been placed on measuring ²²²Rn levels in soils. This is due to the fact that most of the radon in dwellings comes from the underground soil [2]. Nowadays, there are many problems concern the people not only in Malaysia but around the world. One of the problems is radionuclides in water. Radionuclides are isotopes which have the ability to produce radiation. Radiation is produced when elements with an unstable atomic structure undergo decay into another element. Radiation is all around us, every minute of every day. Some radiation is essential to life, such as heat and light from the sun. As used in medicine, radiation helps us to diagnose and treat diseases and to save lives [3]. But other radiation such as radon isotopes, and its decay products of uranium and thorium, can be quite harmful to human beings. The radionuclides in water are member of three natural radioactive series, which are the uranium series, thorium series, and the actinium series [4].

The isotopes in the uranium decay series that may pose a health risk because of their presence in water are ²²⁶Ra and ²²²Rn [5]. The human population typically is exposed to radiation from water, both by ingestion and inhalation. These radiations arise from the uranium and thorium decay series. This paper is focused on radon in water which is a radioactive inert gas produced by the alpha-decay of ²²⁶Ra in the ²³⁸U series with a half-life of 3.84 days. Since ²²²Rn occurs naturally in soil and rocks, it is virtually omnipresent on earth. It accounts for more than 50% of the total dose from all sources of ionizing radiation absorbed by the population [6]. Since ²²²Rn readily dissolves in water under pressure, groundwater is another source of radon. High concentration of ²²²Rn may cause concern about its effects on health. Either drinking groundwater or breathing can give rise to exposure of humans to its radiation and may result in cancer deaths [7]. The aim of this paper is measuring ²²²Rn in hot spring and surface water using gamma spectrometry technique.

Experimental

Samples of hot spring water were collected from Perak, Selangor, Kelantan, and Nigeria Sembilan. Because of springs of hot mineral water is very attractive to the external and internal tourism industries, and many people are going there as patients, visitors, and tourists to spend the holidays, and even consumption from the people who live there. However, hot spring water contains many useful elements, such as, calcium, iron, magnesium...etc. also contains natural radioactive isotopes, such as, uranium, radium and radon's progeny (²¹⁴Bi and ²¹⁴Pb). Visitors to the bath houses of these springs are unaware that they can breathe ²²²Rn emanated from the surrounding hot spring water or be exposed to hazardous radiation emitted from radionuclides in the hot mineral water [8]. However, samples of natural water were collected from Kelantan, Perak, and Pahang.

Radiation doses were measured (in-situ) at the selected points at the surface and 1 meter height. The measurements were conducted using LUDLUM rate meter. During collect the water samples, many parameters have been measured to check the quality of the water using (HYDROLAB, model DS5, USA). The sampling points were determined by using a global positioning system (GPS). Then, samples were transferred into plastic containers carefully because radon is a gas and it can be escape from water to air.

In the laboratory, the pH of the water samples was controlled using nitric acid to stabilize the water, then the samples were divided to two portions (filtered and unfiltered water), to determine dissolve and suspended radon in water. For the filtration, membrane filter 0.45 µm was used because it seems the best filter to remove the suspended materials in the water. Sample preparation was done by filling the water sample (filtered and unfiltered) to the Marinelli beaker 500mL until it is full. The beaker was weighted and sealed using silicon glue [9] to avoid the leakage of radon from water. The beakers were kept for a month, to allow the equilibrium between ²²²Rn and its progeny to reach. When radon is measured in water sample, usually waits until equilibrium is reached where the disintegration rate of the radionuclides is the same and this depends on the half-life of the radionuclide. However, in this study, equilibrium happens after 6-7 radon decays. Therefore, samples were kept for a month because of the half-life of radon is almost 4 days.

Results and Discussion

The measurement was done by gamma spectrometer with a high-purity germanium detector (HPGe) of high resolution. This advanced spectrometer consists of an HPGe detector of resolution 1.84 keV at 1.33 MeV. The samples were counted for 12 hours (43200s) which found to be enough to get good statistical peaks. However, the calibration of gamma spectrometry was done using standard contained UO₃ to cover energy from 63 until 1001 keV mixed with KCl to present the energy 1460 for ⁴⁰K, and it is not necessary to have large number of gamma lines above 400 keV to obtain good calibration; two points are enough to have good fit with low uncertainty.

Table 1.	Sampling	noints an	d Survey	meter reading
rabic r.	Samping	pomis an	a buive,	meter reading

Location	Latitude	Longitude	Surface Dose	1 Meter Dose
KST	$05^{\circ} 21.253$	102° 14.532'	0.122	0.137
KSM	$05^{0} 06.042$	$102^{0} 20.959$	0.150	0.135
KKKB	$02^{0} 55.814$	101° 51.355'	0.131	0.121
TNKSS	$04^{0} 31.121$	$102^{0} 30.497$	0.134	0.124
TNKK	$04^{0} 31.222$	$102^{0} 28.624$	0.230	0.125
TNSTB	$04^{0}\ 26.926$	$102^{0} 28.996$	0.080	0.109
KGLL	$04^{0}\ 22.500$	101° 03.200'	0.096	0.088
KGSR	$04^{0}\ 27.170$	101° 04.090'	0.131	0.114
KGSK2L	$04^{0}\ 23.730$	101° 03.960'	0.132	0.122
HSP	$02^{0} 37.891$	$102^{0} 03.321$	0.232	0.164
HSSSHL1	$03^{0}05.448$	101° 47.670°	0.124	0.103
HSSSHL2	$03^{0}08.353$	101° 50.170°	0.124	0.100
HSSK	$03^{0} 59.688$	101° 23.612'	0.138	0.119
HSTB	05° 16.590'	$102^{0} 02.595$	NONE	NONE

Table 2: Water Quality Parameters

Code	Temperature	DO	Conductivity	pН	Salinity	TDS	Turbidity
	(°C)	(mg/L)	(μS·cm ⁻¹)		(mg/L)	(mg/L)	(NTU)
HSP	39.8	5.32	0.2440	7.80	0.12	0.17	8.9
HSSSHL1	42.0	7.60	0.2651	8.67	0.13	0.17	3.3
HSSSHL2	50.0	2.40	0.0509	8.82	0.01	0.03	3.4
HSSK	90.0	2.33	0.1957	8.93	0.09	0.13	0.0
HSTB	N.R	7.40	0.2922	8.93	0.14	0.12	0.0
KST	30.0	3.00	0.0435	7.20	0.01	0.03	802.0
KSM	28.0	2.60	0.0452	7.40	0.01	0.03	842.0
KKKB	25.0	9.20	0.0290	7.10	0.00	0.02	125.0
TNKSS	25.7	2.96	0.0599	6.78	0.02	0.04	21.2
TNKK	27.3	2.12	0.0430	7.16	0.01	0.03	13.9
TNSTB	27.6	1.90	0.0301	7.06	0.00	0.02	33.1
KGLL	28.0	4.35	0.1045	7.04	0.03	0.07	0.0
KGSR	25.3	4.73	0.0233	6.20	0.00	0.02	9.5
KGSK2L	27.6	1.20	0.0589	6.18	0.02	0.09	0.0

Previous studies used the energy 609 keV to obtained ²²²Rn activity concentration due to no inference with other radionuclides in this energy and the contribution of the intensity to the total intensity of gamma-radiation is almost 50%. However, for other peaks for ²¹⁴Bi such as, 934 keV, 1120 keV, and 1764 keV lines impose weak intensities. On the other hands, germanium detectors have lower efficiency in high energies which can cause non-detectable counting rates and they give activities with significantly uncertainties. For those difficulties, the calculation of ²²²Rn activities using 934, 1120, and 1764 keV might result in poor precision and accuracy, therefore, ²²²Rn activity was calculated from the energy 609 keV only. The peak 352 keV for ²¹⁴Pb was not considered due to the interference between ²¹¹Bi and ²¹⁴Pb in the same energy.

However, in this study, there is strong inversely correlation between radon activity concentration in hot springs water and conductivity, TDS, and salinity for both unfiltered and filtered samples, and there is inversely correlation between radon activity concentrations in filtered samples only and the temperature. The rest of the parameters, there is very weak correlation with radon activity concentration in hot springs samples which can be ignored in some

Mohammed Kassim et al: DETERMINATION OF RADON ACTIVITY CONCENTRATION IN HOT SPRING AND SURFACE WATER USING GAMMA SPECTROMETRY TECHNIQUE

cases. Moreover, the Table showed that conductivity has significant correlation with many parameters, which are, temperature, dissolved oxygen, salinity, TDS, and turbidity. On the other hand, TDS has significant inversely correlation with temperature, dissolved oxygen, turbidity and salinity. Finally salinity has significant inversely correlation with turbidity, temperature, and dissolved oxygen.

Salinity is an indicator of the concentration of the amount of dissolved salts, including calcium, magnesium, sodium and potassium) [10]. For the conductivity which can be defined as "the ability of water to carry an electric current" [10], which is proportional to the concentration of ions [10]. In this study, hot springs samples were more salinity than other types of water including rivers and lakes therefore, the correlation between conductivity and salinity in hot springs could be considered normal because specific conductivity is higher in saline systems than in non-saline systems [10]. On the other hand, study was done by [11] showed that radon activity concentration was unrelated to salinity. However, in low salinity environments radium is strongly adsorbed on surfaces, where as radon is dissolved and migrates with the fluid. In groundwater, there is correlation between salinity and radium because of competition between radium and cations for adsorption sites on solids [12], and increases in salinity tend to increase ²²⁶Ra activity concentration in groundwater; because of ion-exchange mechanisms a greater partition of the exchangeable radium in pore water than on surface exchanges sites at higher salinities [11].

However, there is strong inversely correlation between radon activity concentration in surface water and salinity only for both unfiltered and filtered samples, for the rest of the parameters, there is no significant correlation with radon activity concentration in surface water. However, conductivity has significant correlation with DO, TDS, and salinity. Salinity has significant inversely correlation with DO.

Table 3: Radon activity concentrations

Sample No.	Location	State	Type of water	²²² Rn (Bq/L) Unfiltered	²²² Rn (Bq/L) Filtered (F)
				(U)	, ,
1,2	KST	Kelantan	River	0.99 ± 0.07	0.51 ± 0.05
3,4	KSM	Kelantan	River	1.11 ± 0.07	0.99 ± 0.07
5,6	KKKB	Kelantan	River	1.41 ± 0.08	0.76 ± 0.06
7.8	TNKSS	Pahang	River	0.35 ± 0.04	0.32 ± 0.04
9,10	TNKK	Pahang	River	1.05 ± 0.07	0.92 ± 0.06
11,12	TNSTB	Pahang	River	0.47 ± 0.05	0.38 ± 0.04
13,14	KGLL	Perak	Lake	0.39 ± 0.04	0.29 ± 0.04
15,16	KGSR	Perak	Lake	1.27 ± 0.08	0.66 ± 0.06
17,18	KGSK2L	Perak	Lake	0.40 ± 0.04	0.30 ± 0.04
19,20	HSP	Nigeria Sembilan	Hot Spring	1.12 ± 0.06	1.08 ± 0.05
21.22	HSSSHL1	Selangor	Hot Spring	0.50 ± 0.05	0.41 ± 0.03
23,24	HSSSHL2	Selangor	Hot Spring	0.61 ± 0.05	0.51 ± 0.05
25,26	HSSK	Perak	Hot Spring	0.82 ± 0.08	0.53 ± 0.07
27,28	HSTB	Kelantan	Hot Spring	0.63 ± 0.06	0.50 ± 0.05

Table 4: Pearson correlation coefficient, between radon activity concentration in hot spring samples and water quality parameters

	Rn (U)	Rn (F)	Tem.	DO	Cond.	pН	Sal.	TDS
Temp.	-0.14	-0.74	1			•		
DO	-0.08	-0.47		1				
Cond.	-0.71	-0.72	-0.79	-0.84	1			
pН	-0.14	-0.05	0.15	-0.15	0.02	1		
Sal.	-0.73	-0.78	-0.58	-0.72	0.98	0.01	1	
TDS	-0.61	-0.63	-0.75	-0.77	0.84	-0.02	0.83	1
Tur.	-0.17	-0.26	-0.71	-0.05	-0.77	-0.01	-0.72	-0.78

Table 5: Pearson correlation coefficient, between radon activity concentration in surface samples and water quality parameters

	Rn (U)	Rn (F)	Tem.	DO	Cond.	pН	Sal.	TDS
Temp.	-0.07	-0.04	1					
DO	0.31	-0.14	-0.10	1				
Cond.	-0.15	-0.16	0.06	-0.66	1			
pН	0.04	0.02	-0.11	-0.13	-0.22	1		
Ŝal.	-0.74	-0.59	0.04	-0.65	0.76	-0.01	1	
TDS	-0.18	-0.21	0.04	-0.25	0.55	-0.09	0.42	1
Tur.	0.12	0.16	0.05	-0.15	-0.13	0.04	-0.23	-0.22

However, high radon content in hot spring can be due to the leakage of the gas, and alpha-recoil transfer of the radon nuclide, from the uranium [13 and 14], and due to discharge from granite rocks [15]. As the literature indicated, natural radionuclide concentrations in environmental samples can be very different due to geographical, geological factors, the time of sampling as well as on the location, and temperature this may cause different results in different studies [16 and 17]. Radon activity concentration in hot spring samples did not excess the limit for radon in water, which is 11 Bq/l that proposed by USEPA. However, the results were comparable to the previous study done by [16 and 18].

In surface water radon is not a major concern, due to there is no groundwater contribution to the river water or aeration of river water can decrease radon concentrations very fast because of escape radon from water into atmosphere [19]. On the other hand, once the radionuclides are entered in water, their behavior is very hard to estimate, and every river, and lake it has its own characteristic this might be different from place to place. Radon content in surface water might be affected by several factors, such as the geology of the area, and bottom sediments [18 and 20]. Most of the radionuclides that transport to the surface water can be attach to sediments on the bottom. The process of interaction of dissolved radionuclides in water with suspended solids has been investigated by many researchers. However, the bottom sediments in surfaces water (rivers, and lakes) could be considered as sinks, where as the radionuclides interact with suspended materials and migrate to the sediments [21]. Low ²²²Rn activity concentrations were found in all locations and did not excess the maximum level for ²²²Rn in water this was proposed by USEPA 1999, and activity concentrations of ²²²Rn in filtered water samples are slightly lower than unfiltered water samples, due to removal of non-dissolve suspended solid from water, which contains a small amount of radionuclides. However, the results obtained from rivers in this study were compared with the reported values from other countries around the world and it was observed that the measured activity concentrations of ²²²Rn water were lower and almost similar than many literatures, [18 and 20].

Conclusion

We have found that the radon levels in hot spring water and surface water are range from (0.29-1.41 Bq/l) which is within acceptable values, but the concentration of radon is different at studied sites. The differences are possibly due to different origins, depths and pathways of the out flowing water. Surface radiation dose measured at 1m above the surface are in range between $0.088 - 0.137 \,\mu Sv/hr$ for all the locations, and for the surface are range between 0.096-

Mohammed Kassim et al: DETERMINATION OF RADON ACTIVITY CONCENTRATION IN HOT SPRING AND SURFACE WATER USING GAMMA SPECTROMETRY TECHNIQUE

 $0.232~\mu Sv/hr$. The global range for surface radiation dose is $0.079-0.13~\mu Sv/hr$. Therefore, it can be concluded that the surface radiation dose are more than the global range at selected sites.

Acknowledgement

The authors would like to thank Universiti Teknologi MARA Malaysia for providing grant to carry out this study, and students for their participation in collect the samples.

References

- 1. Pillay, M.S. Talha M.Z, (2003): Drinking water Quality Issues; Water and Drainage Conference in Kuala Lumpur
- 2. Durrani, S.A., 1999. "Radon concentration values in the field: correlation with underlying geology". *Radiat. Meas.* 31, 271-276.
- 3. Karr, J., Mannusen, J., McKnight, D., Naiman, R., Stanford, J., (1995), Freshwater Ecosystems and their Management. *A National Initiative; Science, Vol. 270, 27*
- 4. Oyvind S. Bruland1, Thora J. Jonasdottir2, Darrell R. Fisher3 and Roy H. Larsen, 2008, "Ra²²³: From Radiochemical Development to Clinical Applications in Targeted Cancer Therapy", *Current Radiopharmaceuticals*, 1, 203
- 5. Duenas, C., Fernandez, M.C, Liger, E., Carretero, J., 1997, "Natural radioactivity levels in bottled water in Spain" *Water Res.* 318-1919-1924.
- 6. United Nations Scientific Committee on the Effects of Atomic Radiation (UNSCEAR), 1995, Sources and Effects of Ionizing Radiation. United Nations, New York.
- 7. US Environmental Protection Agency (USEPA), 1999," Health risk reduction and cost analysis for radon in drinking water" *Federal Register 64-38*, 9559, (Washington, DC).
- 8. S. A. Saqan, M. K. Kullab, A. M. Ismail, 2000," Radionuclides in hot mineral spring waters in Jordan" *Journal of Environmental Radioactivity* 52 -99-107
- 9. P. P. Parekh, A. Bari, T. M. Semkow, M. A. Torres, 2002" A new method for sealing containers with liquid samples for radioactivity measurements" *Journal of Radio-analytical and Nuclear Chemistry*, Vol. 253, No. 2-321-5
- 10. United Nations Environment Programme GEMS/Water Programme, 2006," water quality for ecosystem and human health" ISBN 92-95039-10-6, p 16
- 11. Sebastien Lamontagne, Corinne Le Gal La Salle, Gary J. Hancock, Ian T. Webster, Craig T. Simmons, Andrew J. Love, Julianne James-Smith, Anthony J. Smith, Jochen Kampf, Howard J. Fallow field, 2008,"Radium and radio radioisotopes in regional groundwater, intertidal groundwater, and seawater in the Adelaide Coastal Waters Study area: Implications for the evaluation of submarine groundwater discharge" *Marine Chemistry* 109-318-336
- 12. R.M.R. Almeida, D.C. Lauria, A.C. Ferreira, O. Sracek, 2004," Groundwater radon, radium and uranium concentrations in Regiao dos Lagos, Rio de Janeiro State, Brazil" *Journal of Environmental Radioactivity* 73-323
- 13. C. Rodenas, J. Gómez, J. Soto, F. Maraver, 2008,"Natural radioactivity of spring water used as spas in Spain" *Journal of Radioanalytical and Nuclear Chemistry, Vol. 277, No.3 625–630*
- 14. David S. Vinson, Avner Vengosh, Daniella Hirschfeld, Gary S. Dwyer, 2009," Relationships between radium and radon occurrence and hydrochemistry in fresh groundwater from fractured crystalline rocks, North Carolina (USA)" *Chemical Geology 260 -159–171*
- 15. A. Horvath, L.O. Bohus, F. Urbani, G. Marx, A. Piroth, E.D. Greaves, 2000,"Radon concentrations in hot spring waters in northern Venezuela" *Journal of Environmental Radioactivity* 47-127-133
- 16. Daryoush Shahbazi-Gahrouei, Mohsen Saeb, 2008,"Dose assessment and radioactivity of the mineral water resources of Dimeh springs in the Chaharmahal and Bakhtiari Province, Iran" *NUKLEONIKA* 531-31-34
- 17. Walter D'Alessandro, Fabio Vita, 2003, "Groundwater radon measurements in the Mt. Etna area" *Journal of Environmental Radioactivity* 65 187–201
- 18. I. Yigitoglu, F. Öner, H. A. Yalim, A. Akkurt, A. Okur and A. Özkan, 2010,"Radon concentrations in water in the region of Tokat city in Turkey" *Oxford Journals Mathematics & Physical Sciences &* Medicine Radiation Protection Dosimetry Volume *142*, *Issue2-4 Pp.* 358-362

- 19. A. F. Maged, 2009,"Estimating the radon concentration in water and indoor air" *Environ Monit Assess* 152-195-201
- 20. M.S. Al-Masri, R. Blackburn, 1999,"Radon-222 and related activities in surface waters of the English Lake District" *Applied Radiation and Isotopes 50-1137-1143*
- 21. Luigi Monte, Patrick Boyer, John E. Brittain, Lars Hakanson, Samuel Lepicard, Jim T. Smith,2005,"Review and assessment of models for predicting the migration of radionuclides through rivers" *Journal of Environmental Radioactivity* 79-273–296



SOURCES OF POLYCYCLIC AROMATIC HYDROCARBONS (PAHS) POLLUTION IN MARINE SEDIMENT FROM TUANKU ABDUL RAHMAN NATIONAL PARK, SABAH

(Sumber Pencemaran Hidrokarbon Aromatik Polinuklear (PAH) Dalam Sedimen Marin Dari Taman Negara Tuanku Abdul Rahman, Sabah)

Md Suhaimi Elias*, Ab Khalik Wood, Zaleha Hashim, Mohd Suhaimi Hamzah, Shamsiah Ab Rahman, Nazaratul Ashifa Abdullah Salim

Analytical Chemistry Application Group, Waste and Environmental Technology Division, Malaysian Nuclear Agency, Bangi, 43000 Kajang, Selangor, Malaysia

*Corresponding author: mdsuhaimi@nuclearmalaysia.gov.my

Abstract

The concentrations of parent and alkyl Polycyclic Aromatic Hydrocarbons (PAHs) in marine sediment samples collected from Tuanku Abdul Rahman National Park, Sabah were determined by using GCMS. The ratio of anthracene to anthracene plus phenanthrane, fluorenthane to fluorenthane plus pyrene, benz[a]anthracene to benz[a]anthracene plus chrysene and indeno[1,2,3-cd]pyrene to indeno[1,2,3-cd]pyrene plus benzo[g,h,i]perylene, compounds were used to identify the sources of PAHs pollution. The total concentration of parent and alkyl PAHs are ranged from 121.7 to 191.5 ng/g dry weight. The concentrations of PAHs pollution in sediments were categorised as a moderate polluted. The ratio values of PAHs compound indicate the origin source of PAHs pollutions in marine sediment sample of Tuanku Abdul Rahman National Park were originated from fossil fuel combustion (pyrolytic).

Keywords: PAHs, national park, pollution source, sediment

Abstrak

Pengukuran kepekatan sebatian hidrokarbon polisiklik aromatik alkil dan induk di dalam sample sedimen marin yang diambil dari Taman Negara Tuanku Abdul Rahman dilakukan dengan menggunakan peralatan GCMS. Penentuan sumber pencemaran PAH ditentukan dengan menggunakan penilaian nisbah sebatian antrasena terhadap antrasena campur fenantrena, fluorantena terhadap fluorantena campur piren, benz[a]antrasena terhadap benz[a]antrasena campur krisena dan indeno[1,2,3-cd]piren terhadap indeno[1,2,3-cd]piren campur benzo[g,h,i]perilena. Jumlah kepekatan sebatian PAH alkil dan induk berada dalam julat 121.7 hingga 191.5 ng/g berat kering. Kepekatan PAH di dalam sedimen dikatogerikan sebagai sederhana tercemar. Nilai nisbah sebatian PAH menunjukan sumber pencemaran PAH di dalam sedimen marin Taman Negara Tuanku Abdul Rahman berasal daripada pembakaran minyak fosil (pirolitik).

Kata kunci: PAH, taman negara, sumber pencemaran, sedimen

Introduction

Polycyclic aromatic hydrocarbons (PAHs) are a class of organic priority pollutants, ubiquitous in the aquatic ecosystems, resistance to biodegradation and show adverse health effects (carcinogenic activity) depending on the molecular weight and structure [Hoffman et al., 1984] [1-5]. PAH can be introduced into the marine environment by various ways such as oil spill, forest fire, combustion of petrol and diesel, coal combustion [3,5-7], urban runoff, domestic and industrial wastewater discharges [4, 6].

Source of PAH pollution can be categorized into two groups; (1) pyrolytic and (2) petrogenic. Pyrolytic PAHs are generated through incomplete combustion of organic matter such as coal, petroleum and wood combustion, industrial operation and power plant using fossil fuels. Petrogenic PAHs are derived from crude oil and petroleum product such as kerosene gasoline, diesel fuel, lubricating oil and asphalt. Petrogenic PAHs are emitted directly to

marine environment through oil spills and routine operation of tankers (e.g. discharge of ballast water) [8]. Source of PAH pollution can be identify by using isomer pair ratios such as anthracene/ (anthracene+phenanthrene); indeno[1,2,3-cd]pyrene/ (indeno[1,2,3-cd]pyrene + benzo[g,h,I]perylene); benz[a]anthracene/ (benz[a]anthracene + chrysene) and fluoranthene/ (fluoranthene + pyrene) [5,9].

Study on PAHs pollution at Tuanku Abdul Rahman national park and others marine park of Sabah are still limited. In this present study, organic contamination (PAHs) was selected because they are important due to carcinogenic and toxicity to the human health and also for baseline data and/or information. The goal of this work was to determine the concentrations of PAH compound in the sediment and to identify the possible source of these compounds whether from anthropogenic or natural processes.

Methodology

Sampling Location

Eleven sampling locations were selected at Tuanku Abdul Rahman National Park of Sabah as shown in Figure 1. The sediment samples were collected using a Ponar grab sampler, and they were transferred into glass bottles with aluminium caps using a stainless steel spatula. The marine sediment samples were stored in glass bottles and stored at below 5°C before analysis. The sampling station coordinates of Tuanku Abdul Rahman National Park were shown in Table 1. 5.0 gram of wet sediment sample was dried in oven at 105°C until constant weight. The percentage of water content in sediment sample and PAHs concentrations in dry weight unit were calculated as described in Reference Method in Marine Pollution Studies No.20 [10].

Station	Latitude	Longitude	Water depth (m)
TAR 1	6° 01.308' N	116° 04.416' E	27.2
TAR 2	6° 02.248' N	116° 02.915' E	33.5
TAR 3	6° 02.634' N	116° 01.371' E	44.5
TAR 4	6° 02.548' N	116° 00.498' E	34.7
TAR 5	5° 58.409' N	116° 02.235' E	31.3
TAR 6	6° 00.015' N	116° 01.834' E	27.0.
TAR 7	5° 58.419' N	116° 02.240' E	21.6
TAR 8	5° 57.648' N	116°01.969' E	11.2
TAR 9	5° 57.253' N	115° 59.407' E	32.0
TAR 10	5° 58.301' N	115° 59.381' E	36.1
TAR 11	5° 58.039' N	116° 00.401' E	30.0

Table 1: Sampling stations and coordinates of Tuanku Abdul Rahman National Park, Sabah

Soxhlet extraction of marine sediment sample

20 g wet sediment samples were weighted in a glass beaker where about 30 g of Na_2SO_4 was added to the sediment sample, mix together for a homogenous. Sample was added into the soxhlet apparatus and spike with two internal standard for aliphatic fraction (n-octadecene- $5\mu g/l$) and PAHs fraction (orto-terphenyl- $5\mu g/l$) for recovery assessment. The sample was soxhlet extracted using 250 ml (50:50 v/v) mixture of dichloromethane (DCM) and hexane (analar grade). After 12 hours extraction, the extracted samples were dry up until 1ml by using rotary evaporator. 8.0g of silica gel and 8.0g of alumina were deactivated with 0.16 ml and 0.4 ml deionzed water, respectively. Silica gel and alumina were filling up into silica-alumina column (20mm diameter and 150 mm height). 1ml of extracted sample was fractioned into subfraction using silica-alumina column. Copper granules were used to remove sulphur from the extract, which was then passed through a silica/alumina chromatographic column. Then 30 ml of hexane was eluted pass through into the silica-alumina column to elute aliphatic compounds ($C_{12} - C_{34}$) fraction (F1). Forty (40) ml mixture of DCM and hexane (50:50 v/v) was used to elute the PAHs for fractionation 2 (F2) and followed by 40 ml of hexane-DCM (20:80) for fractionation 3 (F3). The eluent from fractionation 2 and 3 (F2 and F3) was collected and concentrated to a few ml in a rotary evaporator. After that the

concentrated samples were transferred into a vial, and reduced to 1 ml under a gentle nitrogen gas stream. The final solution F2 and F3 were analyzed by GC-MS to determine the aromatic hydrocarbon compounds quantitatively.

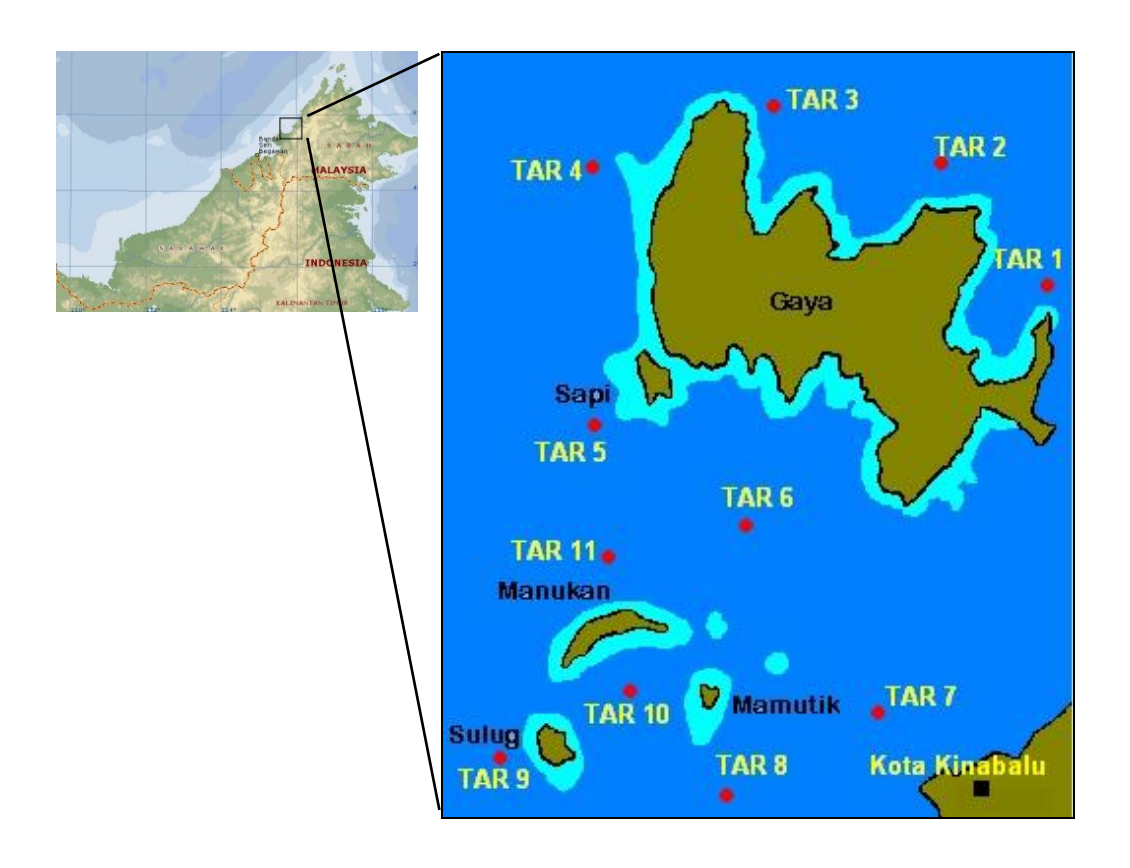


Fig. 1: Sampling stations of Tuanku Abdul Rahman National Park of Sabah

Gas Chromatography-Mass Spectrometry (GC-MS) analysis

The PAHs compounds were analyzed by GC-MS (Shimadzu QP5050A model) using selected ion monitoring (SIM) mode. A 30 m x 0.25 mm x 0.25 µm ZB1 fused silica capillary column (Phenomenex) was used to identify them. Helium was used as carrier gas with a flow-rate of 3 ml/min. The initial injection and interface temperature of GC-MS was setup at 70°C and 270°C respectively. The column temperature was started at 70 °C, held for 2 min, then increased at 15 °C/ min up to 300°C and the temperature will be maintained at 300°C for 12 minutes. The PAH analysis took about 1 h to be complete to identification and quantification of the alkyl and parent PAHs base on ion fragmentation and retention time compared to of that the external PAHs standard. The alkyl PAHs such as 1-methyl naphthalene, 1-ethyl naphthalene, 2,3,6-trimethyl naphthalene, 2-methyl phenanthrene , 1-methyl phenanthrene, 3,6-dimethyl phenanthrene, 1-methyl pyrene and 17 parent aromatic hydrocarbons analyzed namely; naphthalene, acenaphthylene, acenaphthene, fluorene, phenanthrene, anthracene, fluoranthene, pyrene, chrysene, perylene, benz[a]anthracene, benzo[b]fluoranthene, benzo[k]fluoranthene, benzo[a]pyrene, indeno[1,2,3-cd)-pyrene, dibenz[a,h]anthracene, and benzo[g,h,i]perylene.

Results and Discussion

Tuanku Abdul Rahman National Park consists of Sapi, Manukan, Mamutik, Sulug and Gaya Island. Twenty-four species of parent and alkyl PAH compounds were measured by using GCMS for source identification of PAHs pollution. The analysed PAHs compound from sediment samples of Tuanku Abdul Rahman National Park were shown in Table 2 and total parent and alkyl PAHs concentrations of each station were shown in Figure 2 (Bar

graph). The total (Σ) concentration of parent and alkyl PAHs compound are ranged from 121.7 to 191.5 ng/g dry weight. The PAH concentrations could be characterized as low, moderate, high and very high ones when the Σ PAHs were 0–100, 100–1000, 1000–5000, and more than 5000 ng/g, respectively [11]. PAHs pollution of Tuanku Abdul Rahman National Park sediments were categorize as a moderate pollution due to their PAH concentration within the range 121.7 to 191.5 ng/g dry weight as shown in Figure 2.

Based on the PAH isomer pair ratio measurement compiled by Yunker et al., [9]; Anth/(Anth+Phen) ratio less than 0.1 indicates source of PAH dominance of petroleum and ratio higher than 0.1 indicates dominance of combustion; Fl/(Fl+Py) ratio less then 0.4 shown petroleum source, 0.4 to 0.5 petroleum combustion (pyrolytic) and more than 0.5 combustion of coal, grasses and wood; B[a]A/B[a]A+Chry ratio less than 0.2 petroleum source, 0.2 to 0.35 petroleum and combustion and more than 0.35 combustion source; and IP/IP+BghiP ratio less than 0.2 petroleum, 0.2 to 0.5 petroleum combustion and more than 0.5 combustion of coal, grasses and wood.

Isomer pair ratio of Anth/(Anth+Phen) of Tuanku Abdul Rahman National Park sediment ranged from 0.66 to 0.73 as shown in Table 2. These indicated the source of PAHs pollution is originated from the combustion. The ratio of Benz[a]Anthracene to Benz[a]Anthracene + chrycene (B[a]A/B[a]A+Chry) shown four of the stations (TAR 01, TAR 04, TAR05 and TAR11) was not calculated due to not detected of the Benz[a]Anthracene compound of that stations. However, the ratio of B[a]A/(B[a]A+Chry) for other stations are ranged from 0.54 to 0.60, which indicated the source of PAHs pollution from combustion. Most isomer pair ratio values of IP/(IP+BghiP) in all stations are 0.41 except for TAR 04, TAR 05 and TAR 10. TAR 04 and TAR 05 stations were not calculated due to not detected of Indeno(1,2,3-cd)pyrene and the ratio for TAR 10 is 1.0 due to not detected of Benzo[g,h,i]perylene compound. According to Yunker et al., [9] the IP/(IP+BghiP) values of 0.20 to 0.50 indicate the source of PAH pollution from petroleum combustion (pyrolytic). The Fl/(Fl+py) ratios in all station ranged from 0.45 to 0.47, these clearly indicated the source of PAH pollution in Tuanku Abdul Rahman National Park was originated from petroleum combustion (pyrolytic).

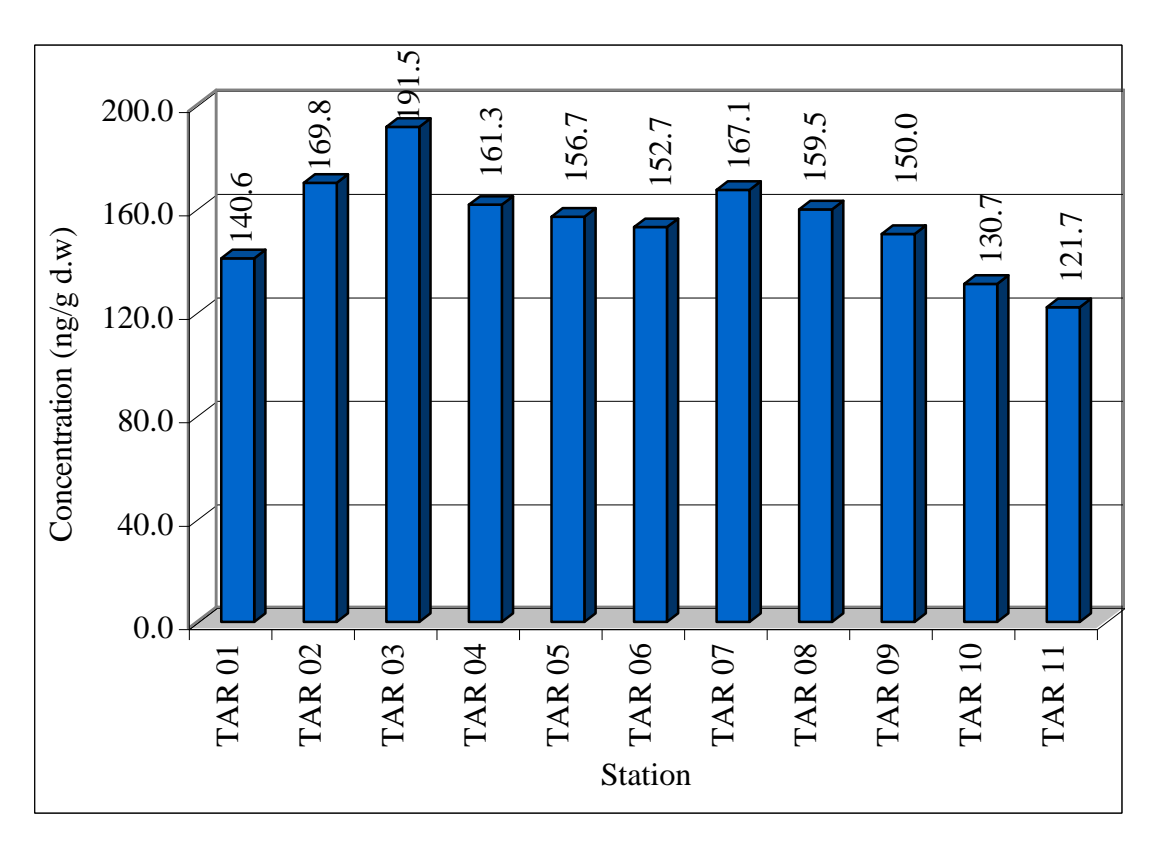


Fig 2: Total parent and alkyl **PAHs** conce ntratio n of Tuank u Abdul Rahm an Natio nal.Pa rk, Sabah.

Table 2: Parent and alkyl PAHs concentration (ng/g d.w) in marine sediment samples collected from Tuanku Abdul Rahman National Park, Sabah

C1		Star	tion	
Compound	TAR 01	TAR 02	TAR 03	TAR 04
Naphthalene	7.85 ± 0.86	6.47 ± 0.72	8.23 ± 0.90	9.35 ± 1.02
1-Methyl Naphthalene	6.18 ± 0.08	5.76 ± 0.08	7.23 ± 0.09	7.99 ± 0.10
1-Ethyl Naphthalene	2.85 ± 0.08	2.82 ± 0.08	3.74 ± 0.10	3.66 ± 0.10
2,3,6 -Trimethyl Naphthalene	2.50 ± 0.02	2.47 ± 0.02	3.12 ± 0.02	3.12 ± 0.02
Acenaphthylene	n.d	4.35 ± 0.12	5.61 ± 0.16	5.69 ± 0.16
Fluorene	7.02 ± 0.13	7.05 ± 0.13	8.98 ± 0.17	8.81 ± 0.17
Acenaphthene	2.26 ± 0.10	2.23 ± 0.09	3.49 ± 0.15	3.12 ± 0.13
Phenanthrene	5.71 ± 0.34	5.17 ± 0.31	6.98 ± 0.42	6.78 ± 0.41
Anthracene	12.25 ± 2.07	12.23 ± 2.07	13.72 ± 2.33	14.23 ± 2.41
2-Methyl Phenanthrene	7.37 ± 1.16	6.94 ± 1.08	8.23 ± 1.29	8.40 ± 1.32
1-Methyl Phenanthrene	1.66 ± 0.32	1.53 ± 0.28	1.87 ± 0.36	2.03 ± 0.37
3,6-Dimethyl Phenanthrene	5.35 ± 1.74	5.29 ± 1.71	6.98 ± 2.26	6.50 ± 2.10
Fluoranthene	5.59 ± 0.16	5.99 ± 0.17	8.35 ± 0.24	7.32 ± 0.20
Pyrene	6.66 ± 0.37	6.82 ± 0.37	9.73 ± 0.53	8.54 ± 0.47
1-Methyl Pyrene	4.99 ± 0.60	5.05 ± 0.61	5.74 ± 0.68	n.d
Perylene	14.03 ± 5.46	14.34 ± 5.58	14.84 ± 5.77	15.99 ± 6.24
Chrysene	13.32 ± 2.53	16.81 ± 3.19	15.34 ± 2.91	15.31 ± 2.91
Benz[a]anthracene	n.d	19.51 ± 2.93	20.70 ± 3.11	n.d
Benzo[b]fluoranthene	5.02 ± 0.80	4.96 ± 0.08	5.26 ± 0.85	5.72 ± 0.91
Benzo[k]fluoranthene	3.04 ± 0.33	3.01 ± 0.33	3.19 ± 0.35	3.47 ± 0.39
Benzo[a]pyrene	4.64 ± 0.69	4.58 ± 0.69	4.86 ± 0.74	5.28 ± 0.80
Indeno [1,2,3-cd)pyrene	4.64 ± 1.43	4.58 ± 1.43	4.86 ± 1.52	n.d
Dibenz[a,h]anthracene	4.16 ± 2.10	4.11 ± 2.05	4.36 ± 2.20	4.74 ± 2.35
Benzo[g,h,i]perylene	2.71 ± 0.14	2.68 ± 0.14	2.84 ± 0.14	3.09 ± 0.16
∑Parent and Alkyl PAH	140.6	169.8	191.5	161.3
Anth/(Anth+Phen) ratio	0.68	0.70	0.66	0.68
Fl/(Fl+Py) ratio	0.46	0.47	0.46	0.46
B[a]A/(B[a]A + Chry) ratio	n.c	0.54	0.57	n.c
IP/(IP+BghiP) ratio	0.41	0.41	0.41	n.c

n.d-below detection limit; n.c-not calculated. Anth = Anthracene; Phen = Phenanthrene; Fl = Fluoranthene; Py = Pyrene; B[a]A=Benz[a]anthracene; Chry = Chrysene; IP=Indeno[1,2,3-cd]pyrene; BghiP=Benzo[g,h,I]perylene.

Continued Table 2:

G 1		Sta	tion	
Compound -	TAR 05	TAR 06	TAR 07	TAR 08
Naphthalene	6.88 ± 0.76	7.07 ± 0.78	5.95 ± 0.65	5.79 ± 0.64
1-Methyl Naphthalene	6.00 ± 0.08	5.31 ± 0.07	4.05 ± 0.05	3.98 ± 0.05
1-Ethyl Naphthalene	3.50 ± 0.09	2.78 ± 0.08	2.53 ± 0.07	2.53 ± 0.07
2,3,6 -Trimethyl Naphthalene	3.25 ± 0.02	2.53 ± 0.02	2.53 ± 0.02	2.29 ± 0.01
Acenaphthylene	5.38 ± 0.15	4.67 ± 0.13	4.68 ± 0.13	4.46 ± 0.13
Fluorene	8.88 ± 0.17	7.58 ± 0.14	7.59 ± 0.14	7.24 ± 0.14
Acenaphthene	3.50 ± 0.15	2.40 ± 0.10	n.d	n.d
Phenanthrene	6.75 ± 0.41	5.43 ± 0.32	5.57 ± 0.34	5.19 ± 0.31
Anthracene	13.63 ± 2.31	13.14 ± 2.23	13.03 ± 2.21	12.42 ± 2.11
2-Methyl Phenanthrene	8.13 ± 1.27	7.58 ± 1.19	7.97 ± 1.26	7.36 ± 1.16
1-Methyl Phenanthrene	1.88 ± 0.36	1.77 ± 0.34	1.77 ± 0.34	1.81 ± 0.34
3,6-Dimethyl Phenanthrene	6.75 ± 2.20	5.94 ± 1.91	5.82 ± 1.87	5.43 ± 1.74
Fluoranthene	7.38 ± 0.21	6.44 ± 0.18	6.33 ± 0.18	5.91 ± 0.17
Pyrene	9.13 ± 0.50	7.45 ± 0.41	7.09 ± 0.39	6.87 ± 0.38
1-Methyl Pyrene	5.50 ± 0.66	5.31 ± 0.64	5.44 ± 0.65	5.19 ± 0.62
Perylene	14.76 ± 5.77	n.d	14.93 ± 5.81	14.47 ± 5.66
Chrysene	13.76 ± 2.62	13.90 ± 2.64	13.92 ± 2.64	13.27 ± 2.53
Benz[a]anthracene	n.d	20.97 ± 3.15	21.00 ± 3.15	20.02 ± 3.00
Benzo[b]fluoranthene	5.28 ± 0.85	5.33 ± 0.85	5.34 ± 0.85	5.09 ± 0.81
Benzo[k]fluoranthene	3.20 ± 0.35	3.23 ± 0.35	3.24 ± 0.35	3.09 ± 0.34
Benzo[a]pyrene	4.88 ± 0.74	4.93 ± 0.74	4.93 ± 0.74	4.70 ± 0.71
Indeno [1,2,3-cd)pyrene	n.d	4.93 ± 1.52	4.93 ± 1.52	4.70 ± 1.46
Dibenz[a,h]anthracene	4.38 ± 2.20	n.d	4.43 ± 2.20	4.22 ± 2.10
Benzo[g,h,i]perylene	2.85 ± 0.15	2.88 ± 0.15	2.88 ± 0.15	2.75 ± 0.14
∑Parent and Alkyl PAH	156.7	152.7	167.1	159.5
Anth/(Anth+Phen) ratio	0.67	0.71	0.70	0.71
Fl/(Fl+Py) ratio	0.45	0.46	0.47	0.46
B[a]A/(B[a]A +Chry) ratio	n.c	0.60	0.60	0.60
IP/(IP+BghiP) ratio	n.c	0.41	0.41	0.41

 $n.d-below \ detection \ limit; \ n.c-not \ calculated. \ Anth=Anthracene; \ Phen=Phenanthrene; \ Fl=Fluoranthene; \ Py=Pyrene; \ B[a]A=Benz[a]anthracene; \ Chry=Chrysene; \ IP=Indeno[1,2,3-cd]pyrene; \ BghiP=Benzo[g,h,I]perylene.$

Continued Table 2:

Community		Station	
Compound	TAR 09	TAR 10	TAR 11
Naphthalene	5.72 ± 0.63	5.30 ± 0.58	5.19 ± 0.57
1-Methyl Naphthalene	3.93 ± 0.05	3.89 ± 0.05	3.77 ± 0.05
1-Ethyl Naphthalene	2.50 ± 0.07	2.36 ± 0.06	2.36 ± 0.06
2,3,6 -Trimethyl Naphthalene	2.26 ± 0.01	2.24 ± 0.01	2.24 ± 0.01
Acenaphthylene	4.41 ± 0.12	4.36 ± 0.12	4.36 ± 0.12
Fluorene	n.d	n.d	n.d
Acenaphthene	n.d	2.12 ± 0.09	n.d
Phenanthrene	5.12 ± 0.31	4.71 ± 0.28	4.60 ± 0.28
Anthracene	12.38 ± 2.11	12.25 ± 2.09	12.27 ± 2.09
2-Methyl Phenanthrene	7.38 ± 1.16	6.95 ± 1.10	6.84 ± 1.07
1-Methyl Phenanthrene	1.67 ± 0.32	1.53 ± 0.28	1.53 ± 0.28
3,6-Dimethyl Phenanthrene	5.36 ± 1.74	5.30 ± 1.71	5.31 ± 1.71
Fluoranthene	5.83 ± 0.16	5.54 ± 0.15	5.54 ± 0.15
Pyrene	6.79 ± 0.37	6.48 ± 0.36	6.49 ± 0.36
1-Methyl Pyrene	5.00 ± 0.60	n.d	n.d
Perylene	14.05 ± 5.50	13.90 ± 5.42	13.92 ± 5.42
Chrysene	13.10 ± 2.49	12.96 ± 2.47	12.97 ± 2.47
Benz[a]anthracene	19.77 ± 2.97	19.56 ± 2.94	n.d
Benzo[b]fluoranthene	5.02 ± 0.80	4.97 ± 0.80	4.98 ± 0.80
Benzo[k]fluoranthene	3.05 ± 0.33	3.02 ± 0.33	3.02 ± 0.33
Benzo[a]pyrene	4.64 ± 0.69	4.59 ± 0.69	4.60 ± 0.69
Indeno [1,2,3-cd)pyrene	4.64 ± 1.43	4.59 ± 1.43	4.60 ± 1.43
Dibenz[a,h]anthracene	4.17 ± 2.10	4.12 ± 2.05	4.13 ± 2.05
Benzo[g,h,i]perylene	2.71 ± 0.14	n.d	2.69 ± 0.14
∑Parent and Alkyl PAH	150.0	130.7	121.7
Anth/(Anth+Phen) ratio	0.71	0.72	0.73
Fl/(Fl+Py) ratio	0.46	0.46	0.46
B[a]A/(B[a]A + Chry) ratio	0.60	0.60	n.c
IP/(IP+BghiP) ratio	0.41	1.00	0.41

 $n.d-below \ detection \ limit; \ n.c-not \ calculated. \ Anth=Anthracene; \ Phen=Phenanthrene; \ Fl=Fluoranthene; \ Py=Pyrene; \ B[a]A=Benz[a]anthracene; \ Chry=Chrysene; \ IP=Indeno[1,2,3-cd]pyrene; \ BghiP=Benzo[g,h,I]perylene.$

Conclusion

The Σ concentration of parent and alkyl PAHs compound in marine sediment samples collected from Tuanku Abdul Rahman National Park are ranged from 121.7 to 191.5 ng/g dry weight. The PAHs pollution of Tuanku Abdul Rahman National Park can be categorized as moderately polluted with total parent and alkyl PAHs from 100-1000 ng/g dry weight.

Based on isomer pairs ratios of PAHs compounds, with the ratio value of Anth/Anth+Phen, Fl/Fl+Py, IP/(IP+BghiP) and B[a]A/B[a]A +Chry in all station clearly indicate, the source of PAHs pollution in marine sediment sample of Tunku Abdul Rahman National Park areas were dominated by petroleum combustion (pyrolytic). The source of PAHs pollution from petroleum combustion probably originated from combustion of diesel and gasoline (petrol) from vehicle engine.

Acknowledgement

Authors would like to thank the Ministry of Science, Technology & Innovation Malaysia (MOSTI) for financial support under Sciencefund research grant (04-03-01-SF0026). The authors would also like to express their gratitude to the Sabah Parks for their support and assistance throughout implementation of this project. Lastly, the authors would also dedicate their thanks to the personnel of Analytical Chemistry Application Group for their assistance and analysis of sample.

References

- 1. Hoffman, E.J., Mills, G.L., Latimer, J.S., Quinn, J.G., (1984). Urban runoff as a source of polycyclic aromatic hydrocarbons to coastal waters. Environmental Science and Technology 18, 580-87.
- 2. Pruell, R.J., Quinn, J.G., (1985). Geochemistry of organic contaminants in Narragansett Bay sediments. Estuarine Coastal and Shelf Science 21, 295-312.
- 3. Viguri, J., Verde, J., and Irabien, A., (2002). Environmental assessment of polycyclic aromatic hydrocarbons (PAHs) in surface sediments of the Santander Bay, Northern Spain. Chemosphere 48. 157–165.
- 4. Tsapakis, M., Stephanou, E. G., and Karakassis, I. (2003). Evaluation of atmospheric transport as a nonpoint source of polycyclic aromatic hydrocarbons in marine sediments of the Eastern Mediterranean. Marine Chemistry 80. 283–298.
- 5. Md Suhaimi Elias, Ab. Khalik Wood, Zaleha Hashim, Wee Boon Siong, Mohd Suhaimi. (2007) Polycyclic Aromatic Hydrocarbon (PAH) Contamination in the Sediments of East Coast Peninsular Malaysia The Malaysian Journal of Analytical Sciences, Vol 11, No 1: 70-75.
- 6. Witt, G., Trost, E., (1999). Polycyclic aromatic hydrocarbons (PAHs) in sediments of the Baltic sea and of the German coastal waters. Chemosphere 38 (7), 1603–1614.
- 7. Li, J., Zhang, G., Li, X.D., Qi, S.H., Liu, G.Q., Peng, X.Z. (2006). Source seasonality of polycyclic aromatic hydrocarbons (PAHs) in a subtropical city, Guangzhou, South China Science of the Total Environment. 355. 145–155.
- 8. Boonyatumanond, R., Wattayakorn, G., Togo, A., Takada, H. (2006). Distribution and origins of polycyclic aromatic hydrocarbons (PAHs) in riverine, estuarine, and marine sediments in Thailand. Marine Pollution Bulletin. 52, 942 956.
- 9. Yunker, M.B., Macdonald, R.W., Vingarzan, R., Mitchell, R.H., Goyette, D.S., Stephanie, (2002). PAHs in the Fraser River basin: a critical appraisal of PAH ratios as indicators of PAH source and composition. Organic Geochemistry 33, 489 515.
- 10. Reference Method in Marine Pollution Studies No.20. Determination of Petroleum Hydrocarbon in Sediment. (1992) United Nation Environment Programme.
- 11. Baumard, P., Budzinski, H. and Garrigues, P. (1998). Polycyclic Aromatic Hydrocarbons (PAHs) in Sediments and Mussels of the Weastern Mediterranean Sea. Environ. Toxicol. Chem. 17, 765 776.